TECHNICAL REPORT
TR-2201-AMP

NAVAL TOTAL ASSET VISIBILITY (NTAV) PRECISION ASSET LOCATION (PAL)
System Tests on the SS Curtiss

by

Steven J. Gunderson
Mary F. Canfield
Geoffery Dann
Daniel J. McCambridge

January 2004

REPORT DOCUMENTATION PAGE			*Form Approved* OMB No. 0704-0811

The public reporting burden for this collection of information is estimated to average 1 hour per response, including the time for reviewing instructions, searching existing data sources, gathering and maintaining the data needed, and completing and reviewing the collection of information. Send comments regarding this burden estimate or any other aspect of this collection of information, including suggestions for reducing the burden to Department of Defense, Washington Headquarters Services, Directorate for Information Operations and Reports (0704-0188), 1215 Jefferson Davis Highway, Suite 1204, Arlington, VA 22202-4302. Respondents should be aware that notwithstanding any other provision of law, no person shall be subject to any penalty for failing to comply with a collection of information, it if does not display a currently valid OMB control number.

PLEASE DO NOT RETURN YOUR FORM TO THE ABOVE ADDRESS.

1. REPORT DATE *(DD-MM-YYYY)* January 2004	2. REPORT TYPE Final	3. DATES COVERED *(From – To)* 1 Oct 1997 – 30 Sep 2001

4. TITLE AND SUBTITLE	5a. CONTRACT NUMBER
NAVAL TOTAL ASSET VISIBILITY (NTAV) **PRECISION ASSET LOCATION (PAL) –** **System Tests on the SS Curtiss**	5b. GRANT NUMBER
	5c. PROGRAM ELEMENT NUMBER
6. AUTHOR(S) Steven J. Gunderson, Mary F. Canfield, Geoffrey Dann, and Daniel J. McCambridge	5d. PROJECT NUMBER
	5e. TASK NUMBER
	5f. WORK UNIT NUMBER

7. PERFORMING ORGANIZATION NAME(S) AND ADDRESSES Naval Facilities Engineering Service Center 1100 23rd Avenue Port Hueneme, California 93043-4370	8. PERFORMING ORGANIZATION REPORT NUMBER **TR-2201-AMP**
9. SPONSORING/MONITORING AGENCY NAME(S) AND ADDRESS(ES) Chief of Naval Research Office of Naval Research, Code 33 800 North Quincy Street Arlington, VA 22217-5660	10. SPONSOR/MONITORS ACRONYM (S)
	11. SPONSOR/MONITOR'S REPORT NUMBER(S)

12. DISTRIBUTION/AVAILABILITY STATEMENT
Approved for public release; distribution is unlimited.

13. SUPPLEMENTARY NOTES

14. ABSTRACT

Two precision asset location (PAL) systems were tested on the SS Curtiss in Port Hueneme, California. The two systems were a commercial-off-the-shelf direct sequence spread spectrum (DSSS) system from WhereNet, Inc., and a prototype ulta-wideband (UWB) system from Multi-Spectral Solutions, Inc. (MSSI). The objective was to evaluate the two technologies for operation in high multipath shipboard environments.

Testing was performed in open cargo spaces (worst-case multipath) and partially loaded cargo spaces (blockage). A reference laser surveying system was installed for comparison and accuracy tests were conducted over a cargo space. Both systems operated in the open-space shipboard environment and to each vendor's specified accuracy. Each system's accuracy decreased during blockage experiments.

The University of Southern California's UltRa Lab characterized the SS Curtiss shipboard environment and found it had delay spreads on the order of 3 μsec, far exceeding the 10 to 300 ns delay spreads of office and industrial environments. Multipath nulls were also measured, with some as deep as 30 to 40 dB.

15. SUBJECT TERMS
Automatic Identification Technology (AIT); Radio Frequency Identification (RFID); Real-Time Location System (RTLS); Total Asset Visibility (TAV); Ultra-Wideband (UWB); Precision Asset Location (PAL); Autonomous Manifesting (AM); Aether Wire & Location (AW&L); Multi-Spectral Solutions Inc. (MSSI); WhereNet

16. SECURITY CLASSIFICATION OF:			17. LIMITATION OF ABSTRACT	18 NUMBER OF PAGES	19a. NAME OF RESPONSIBLE PERSON Steve Gunderson, Dan McCambridge
a. REPORT	b. ABSTRACT	c. THIS PAGE			
U	U	U	U	250	19b. TELEPHONE NUMBER *(include area code)* (805) 982-1262, (805) 982-1296

This page left blank.

Executive Summary

The Naval Facilities Engineering Service Center (NFESC) conducted a test of two precision asset location (PAL) systems on the SS Curtiss in Port Hueneme, California. The two systems were:

- WhereNet, commercial-off-the-shelf (COTS), direct sequence spread spectrum (DSSS)
- Multi-Spectral Solutions Inc. (MSSI), prototype, ultra-wideband (UWB)

The WhereNet system operated in the unlicensed 2.45 GHz band and had an advertised 10-foot accuracy.   The MSSI system operated in "L" band at 1.5 GHz and had a specified 1-foot accuracy outdoors. Both systems used a 'beacon' architecture where tags radiate short transmissions, which were picked up by a group of receivers. Signal first arrival times were measured and location was calculated by hyperbolic equations, much the same as global positioning system (GPS). Both systems were selected as "best-of-breed."

The systems were tested in a shipboard environment in an empty cargo hold. It presented the worst-case multipath environment. The objectives of the test were:

- Do DSSS and UWB work in shipboard environments?
- Do they have dropouts and dead zones resulting from multipath?
- What are the resulting accuracies?

- What are the effects of blockage by containers?
- What are the optimum tag and antenna locations?

Both systems worked in the empty ship's hold. The WhereNet system required their recommended 8 antenna configuration to read without frequent partial reads experienced with 4 antennas. The MSSI UWB system worked with 4 antennas. Both systems worked within the vendor's advertised/estimated accuracy in the empty cargo holds. WhereNet specified 10 feet for 67% of reads (one standard deviation) and MSSI estimated accuracy to a few feet in the ship. The root mean square (RMS) (67%) accuracy of the systems were:

> WhereNet   6 feet
> MSSI   2 – 5 feet

The WhereNet "Y" axis error followed tag location over the "Y" axis. This was due to virtual images of antennas in the bulkheads behind the "Y" axis antennas, causing the antennas to appear further outside the test box for some readings. WhereNet used omni-directional antennas that received reflected signals from front and rear. MSSI used corner antennas that did not receive signals from the sides or rear.

Both systems had reduced accuracy during the second week container blockage experiments. This was expected by the vendors as line-of-sight to antennas was blocked by containers. A surprising finding was that the WhereNet system accuracy increased in the aisleway between double high-stacked containers. This may have been due to the system bi-laterating with only two antennas at opposite ends of the aisle. Another surprising finding was the MSSI system located a tag surrounded by containers on three sides. UWB signals may have diffracted around container edges and through large cracks between containers. Further testing is needed to confirm these observations.

Ships present an adverse and difficult radio frequency (RF) environment and best available PAL technologies need further development and testing.

This page left blank.

Table of Contents

Table of Contents (continued)

List of Figures

List of Figures (continued)

List of Figures (continued)

List of Figures (continued)

This page left blank

List of Acronyms

A/D   Analog-to-Digital
AIT   Automatic Indentification Technology
AM   Autonomous Manifesting
AOA   Angle of Arrival
APC   American Power Corporation
ANSI   American National Standards Institute
ASIC   Application Specific Integrated Circuit
ASK   Amplitude Shift Keying
ATP   Advanced Technology Program
AV   Asset Visibility
AWT   Advanced Warfighting Technology

BAA   Broad Agency Announcement
BSA/LSA   Beach/Logistic Support Area
BWRC   Berkeley Wireless Research Center

CHM   Cargo Health Monitoring
COTS   Commercial off the Shelf
C++   "C" Programming Language, Object Oriented

dB   Deci (1/10th) Bell
dBm   Deci (1/10th) Bell relative to 1 mili-Watt
DARPA   Defense Advanced Research Project Agency
DLA   Defense Logistics Agency
DLL   Dynamic Linked Library
DOD   Department of Defense
DOE   Department of Energy
DTOA   Differential Time of Arrival
DSP   Digital Signal Processor
DSSS   Direct Sequence Spread Spectrum
DXF   Data Exchange Format (AutoCAD's)

EMC   Electromagnetic Compatibility
EMI   Electromagnetic Interference
EMW   Expeditionary Maneuver Warfare
ESRI   Environmental System Research Institute
EST   Eastern Standard Time

FCC   Federal Communication Commission
Fedex   Federal Express
FEP   Front End Processor
FHSS   Frequency Hopping Spread Spectrum
FM   Frequency Modulation
Fwd   Forward

GAO   General Accounting Office
GFI   Government Furnished Information
GIS   Geographic Information System
GMT   Greenwich Mean Time

List of Acronyms (continued)

GHz   Giga (Billion) Hertz (cycles per second)
GPS   Global Positioning System
GUL   General Use Laboratory

HA/DR   Humanitarian Assistance Disaster Reflief
HERO   Hazards of Electromagnetic Radiation on Ordinance
HMMWV   High Mobility Multi-Wheeled Vehicle

IBM   International Business Machines
ID   Identification
IEEF   Institute of Electrical and Electronic Engineers
IFFT   Inverse Fast Fourier Transform
INCITS   International Committee for Information Technology Standards
IR   Infrastructure Reduction
ISM   Industrial Scientific Medical
ISO   International Standard Organization

LAN   Local Area Network
LNA   Low Noise Amplifier
Loran   Long Range Navigation

mW   Mili (1/1000) Watt
MARAD   Maritime Administration
MB   Million Bytes
MEMS   Micro Electro Mechanical Systems
MHz   Mega (Million) Hertz (cycles per second)
MITLA   Micro-Electronics Technology in Logistics Applications
MPF   Maritime Preposition Force
MSSI   Multi-Spectral Solutions, Inc.
MRC   Major Regional Crises
MTMC   Military Traffic Management Command
MURI   Multidisciplinary University Research Initiative

NAVSEA   Naval Sea Systems Command
NEO   Non-Combatant Evacuation Operation
NFESC   Naval Facilities Engineering Service Center
NGI   Next Generation Internet
NIST   National Institute of Standards and Technology
NPRM   Notice of Proposed Rule Making
NTAV   Naval Total Asset Visibility

OFDM   Orthogonal Frequency Division Multiplexing
OMFTS   Operational Maneuver From the Sea
ONR   Office of Naval Research
OOK   On-Off Keying
OTH   Over the Horizon

PAD   PulsON™ Application Demonstrator
PAL   Precision Asset Location

List of Acronyms (continued)

PCI	Personal Computer Interface
PCMCIA	Personal Computer Memory Card International Association
PDA	Personal Digital Assistant
PNNL	Pacific Northwest National Laboratory
PST	Pacific Standard Time
RAM	Random Access Memory
R&D	Research and Development
R&O	Report and Order
RDT&E	Research, Development, Test, and Evaluation
RF	Radio Frequency
RFID	Radio Frequency Identification
RMS	Root Mean Square
RO/RO	Roll On/Roll Off
RTLS	Real Time Location System
RTOA	Relative Time of Arrival
R/W	Read and Write
SAW	Surface Acoustic Wave
SBIR	Small Business Innovative Research
SDK	System Development Kit
SIXCON	Fuel Tank Module
SPAWAR	Space and Naval Warfare Systems Command
SQL	System Query Language
SSC	SPAWAR Systems Center
Stbd	Starboard
STOM	Ship to Objective Maneuver
T&E	Test and Evaluation
TAV	Total Asset Visibility
TCP-IP	Transmission Control Protocol / Internet Protocol
TDC	Time Domain Corporation
TDR	Time Domain Reflectometer
TI	Texas Instruments
TRANSCOM	U.S. Transportation Command
UHF	Ultra-High Frequency
USC	University of Southern California
UPS	Uninterruptible Power Supply
UPS	United Parcel Service
UWB	Ultra-Wideband
VA	Volt Amp
VAC	Volts Alternating Current
VC	Venture Capital
WPAN	Wireless Personal Area Network
3rd MAW	3rd Marine Air Wing

This page left blank

1.0 INTRODUCTION

The Office of Naval Research (ONR) tasked the Naval Facilities Engineering Service Center (NFESC), Port Hueneme, California, under the Naval Total Asset Visibility (NTAV) project, to investigate, identify, and develop technologies to fill gaps in emerging Total Asset Visibility (TAV) systems. The objective was to support the emerging concepts of Operational Maneuver From the Sea (OMFTS) and Seabasing. These concepts require the ability to rapidly locate and track items within ships for just-in-time delivery directly to units ashore, bypassing logistics build-up areas.

The NTAV project focused on two primary capabilities: Precision Asset Location (PAL) in a shipboard environment and Autonomous Manifesting (AM) of cargo containers. NFESC surveyed and identified candidate technologies and tested two representative PAL systems on a cargo ship. Both PAL systems operated in the high multipath environment of an empty cargo hold, but experienced difficulty accurately locating tags in a partially loaded cargo hold due to line-of-sight antenna blockage.

The University of Southern California (USC) under ONR 313 Marine Corps 6.1 research grant tested the RF environment characteristics on the cargo ship. It had long delay spreads of 2-3 μsec (-20 dB), exceeding the design parameters of the test systems.

1.1 Background

1.1.1 Office of Naval Research NTAV Project

ONR funded this 6.3 Exploratory Development under Program Element 060212N. Dr. Phillip Abraham, ONR Code 33 was the Program Sponsor. NFESC was the Performing Activity. The Amphibious and Expeditionary Department was the Program Manager and Principal Investigator. The Shore Facilities Department provided Project Lead, and the Energy and Utilities Department provided testing support.

The NTAV project had three sub-projects:

- Precision Asset Location
- Autonomous Manifesting
- Cargo Health Monitoring

Precision Asset Location (PAL) focused on locating items over longer ranges: outside, in large spaces and on ships, 100s to 1,000s of feet. Autonomous Manifesting (AM) focused on automatically manifesting containers, or shorter ranges, 10s of feet. Cargo Health Monitoring (CHM) focused on tracking cargo environmental history and status, immediate contact for shock, temperature, and humidity.

A fourth sub-project was identified for start in the following fiscal year:

- Infrastructure Reduction

Infrastructure Reduction (IR) was originally included in AM as a way to communicate between tags within containers, but was separated to highlight its ability to support PAL, AM, and CHM. The focus of IR is to have a fully wireless architecture without dedicated readers. IR leveraged work performed by Defense Advanced Research Project Agency's (DARPA) Next Generation Internet (NGI) program.

1.1.2 Operational Need

Desert Storm. The reference event for most current logistics efforts was Desert Shield/Desert Storm. Desert Storm saw a massive mobilization in the first Major Regional Crises (MRC) since Vietnam. U.S. Transportation Command (TRANSCOM) shipped 40,000 ISO containers to the theater. Over 25,000 of those containers had to be opened to determine their contents as paper manifests were inaccurate and easily lost. The lack of confidence in the logistics system resulted in 2-3 times overshipment, and with the misplaced and lost materiel, resulted in losses of $3 billion per GAO Report B-246015, Dec 1991 [1].

The fundamental difference between Vietnam and Desert Storm was during Vietnam cargo was shipped as breakbulk and could be easily inspected to determine what it was. During Desert Storm, most cargo was shipped in ISO containers, which hid the cargo, preventing it from being easily inspected. Manifests then became the primary means for determining container contents, with no easy secondary backup means - visual inspection.

OMFTS/STOM/EMW. Following Desert Storm, the Navy and Marine Corps developed concepts to eliminate the need for logistics buildups ashore. The ideas were described in documents "From the Sea," [2] "Forward from the Sea,"[3] "Operational Maneuver from the Sea" (OMFTS) [4] "Ship-to-Objective Maneuver" (STOM) [5], and "Expeditionary Maneuver Warfare" (EMW) [6]. The objective is to keep Naval forces over-the-horizon (OTH) out of view and reach of shore weapons in order to maximize surprise and maneuver. Forces, weapons, and supplies will be delivered directly from the ship to the objective passing over the littoral region and mines.

Current Maritime Preposition Force (MPF) methods use Beach/Logistic Support Areas (BSA/LSA) to stage supplies for delivery to forward operational forces. This forms a two-step supply process, increasing delivery time and providing a concentrated area within reach of adversaries. BSA/LSAs are needed because of administrative loads to maximize cargo loads. This requires ships to be offloaded and supplies organized for issue. Conversely, MPF ships are tightly loaded in reverse offload sequence for contingency type, e.g., NEO, HA/DR. This works well if the right MPF ship is near by the type of contingency it is loaded for. If the contingency changes, thus the offload sequence, a MPF ship will "churn" its cargo for a different offload sequence. This can possibly "knot" the ship, slowing offload.

Actual ship loads can have up to 40% stow error compared to stow plans. This results from a variety of factors including broken cranes, ramps, elevators, and vehicles. A change in placement of one item can cascade throughout a ship. Ships must be reinventoried after loading to identify actual stow locations. This is required to recalculate trim and stability. Stow databases are then manually updated with actual cargo locations. Manual reinventory is impractical if a MPF ship churns its cargo preparing for offload.

Seabasing addresses the limitations of the above approaches by providing selective offload and just-in-time delivery. BSA/LSAs will not be needed to reorganize supplies for issue, it will be done on ship. The Navy has new LHD-1 class ships for seabases. Smart packaging and Auto ID tags with read/write technology has been identified as necessary technologies to support seabasing. Automatic tracking is needed to speed planning and provide management control over material. The goal is to be able to identify a specific item, on a specific pallet, in a specific container, and in a specific storeroom.

During Desert Storm, several carriers continuously launched aircraft with two or less weapons, and sometimes none. Carriers have 32 magazines over 8 decks and various staging areas to store weapons and components. Even mess areas are used for assembly and staging. Locating and assembling weapon components can require up to 9 hours. Suitable weapons were often offloaded from returned aircraft and could have been loaded on other aircraft. If weapons and their components were found and assembled in 30 minutes or less, the aircraft would leave with full loads, making aircraft carriers more lethal.

Shipboard Environment. The shipboard environment is nearly all metal construction. This provides a highly reflective environment for RF waves. Ships can be equated to caverns with long reverberation times. Communication at a distance can be difficult because the reverberation is greater than the original signal. Many items aboard ships are likewise metal including containers, vehicles, and weapons. These items can further reflect, but more importantly block RF signals.

The consequence of the highly reflective all-metal construction is that strong reflections can interfere with direct signals, nearly canceling them at locations. These multipath nulls can be quite deep, up to 30 – 40 dB, or 1,000 – 10,000 fold decrease in power. Figure 1 shows a multipath null for a narrow band RF signal for different antenna heights above a storeroom floor at two different separations, 5 and 10 m. The multipath null is much less pronounced at less separation – 5 m than 10 m. The deeper null indicates that the direct and reflect signals have nearly identical magnitudes, thus more completely canceled.
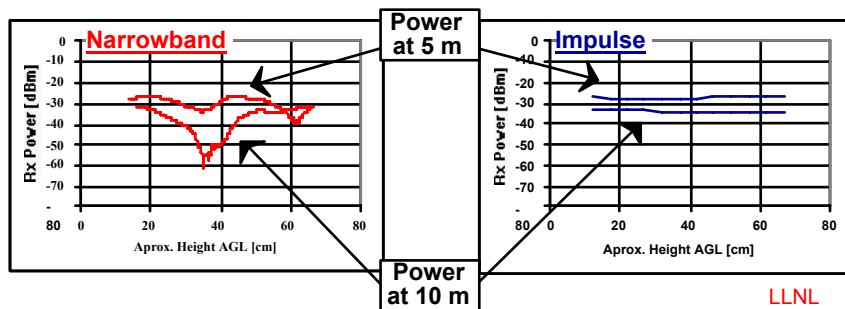
Figure 1. Narrowband RF multipath null compared to impulse.

An impulse waveform is included for comparison. The impulse waveform does not exhibit the same nulls, thus is much less susceptible to multipath. The narrowband signal is more susceptible to multipath because of its sinusoidal characteristic and regular structure. Impulse waveforms do not have the same sinusoidal structure. Multipath nulls produce greater attenuation, which can result in an inability to communicate. Nulls can be counteracted by placing antennas closer together, overcoming the attenuation.

Early radio frequency identification (RFID) systems used narrowband RF that was susceptible to multipath nulls. The nulls produced dead zones resulting in misreads, limiting the ability of these systems to accurately inventory ships. More readers can be used, providing shorter distances, at increased cost. Narrowband RFID systems have not been used in ships with success.

Ships also have significant electromagnetic issues. Electromagnetic interference (EMI) and electromagnetic compatibility (EMC) with existing shipboard radios and radars is mandatory. New systems cannot interfere with existing systems (EMI). The converse is true, new systems must be able to operate when existing systems are operating (EMC). Shipboard radars and radios can be quite powerful providing significant energy levels in spaces and topside.

RF systems must also follow hazards of electromagnetic radiation on ordnance (HERO) requirements if they are used on or around ordnance. HERO limits radiated power levels to prevent damaging weapon electronics, triggering action, and even detonation. Many RFID systems operate at Federal Communication Commission (FCC) Part 15 unlicensed power levels on the order of a milliwatt (1/1000 watt) radiated power and are possibly HERO compliant. Some RFID systems have higher power levels and may not be permitted around ordnance. HERO must be followed.

<u>Seabasing and MPF Operational Issues.</u> The primary operational issues for RFID aboard ship are:

- Location Accuracy
- Misreads
- Blocking

For location accuracy, item size determines the required accuracy. Ten feet may be acceptable for containers and vehicles, whereas 1 foot may be needed for individual items and pallets. Within "arms reach," or 2 to 3 feet is an adequate rule. Vehicle orientation can require greater accuracy, possibly 1 foot. Vehicle orientation is needed for ship stowing to determine whether vehicles are parked straight in or backed in to rapidly drive off vehicles (and trailers). The Marine Corps also "nests" cargo, placing items on or within other items, e.g., placing a SIXCON tank with fuel on the back of a HMMWV. One foot accuracy may be needed for nesting. Robotics and automated material handling requires at least 1 foot or even inches. The most common identified objective is 1 foot.

Misreads equate to inventory errors and are unacceptable. Confidence in the system can be reduced and manual methods resorted. This happens with barcodes. Marines still use manual checks as they do not trust barcodes, using both at the same time. Misreads can be caused by dead spots resulting from multipath. More readers can be used, reducing the effects of multipath, but at an increased cost. Logistics systems try to achieve high accuracy and misreads is an important issue.

Blocking is another cause of misreads. It is caused by one item blocking and/or reflecting RF propagation to another item. It is the hardest to overcome as material and cargo is stacked, optimizing loading. Containers provide the worst case for blockage because of their size, metal construction, and close stacking proximity. Blockage can prevent the RFID readers locate items and possibly read them. Readers can be placed in locations to avoid blockage, and possibly minimize multipath, but again with increased expense. Processes and procedures, together with smart sequence algorithms can overcome the effects of blockage. A possible algorithm may be: "I could locate/hear it before, but another item has been placed alongside or on top of it, so it must still be there."

<u>The Four BIG Questions.</u> Four major questions have been identified for asset visibility systems:

- What do I have?   AV
- Where is my stuff?   PAL
- What is in the box?   AM
- What is its condition/history?   CHM

The ONR NTAV program follows these questions. The first question, "What do I have?" has been addressed and solved by prior Government Research & Development (R&D) and commercial products. It was not part of the NTAV project. The second through fourth questions were part of the NTAV project. The second question, "Where is my stuff?" was the focus of classified Government R&D and now significant commercial activity. NTAV focused on testing and evaluating the best available commercial-off-the-shelf (COTS) and developmental PAL systems in a shipboard environment.

The third question "What is in the box?" is the most difficult and gets at the core of the problems in Desert Storm. It also has immediate application for Marine Corps task organization and unit deployment. Numerous companies, including UPS, Fedex, IBM, and TI have tried to solve AM, without success. It is a difficult problem and new approaches and technologies were sought. It has been called the "Holy Grail of Logistics." NTAV identified a DARPA technology, which may solve AM. It is still being developed and tested (Appendix B).

The fourth question, "What is its condition/history?" is the focus of active commercial, Government, and national laboratory development. Many sensors are being developed for the food industry. MicroElectroMechanical Systems (MEMS) technology, with its ability to miniaturize sensors, is another approach being employed for complex systems. The objective is to imbed small inexpensive sensors directly into items. NTAV did not invest heavily into CHM because of the extensive commercial and Government development, much of it focused on food, medical supplies, vehicles, and weapons.

NTAV focused on the hard problems not solved by prior or current efforts, primarily PAL and AM. Unique Naval applications, particularly shipboard asset visibility, which present relatively small markets, will likely not be solved by commercial industry. Industry requires market sizes of at least $1 billion to pursue active investment and development. The general rule of thumb is that a new start company requires at least $100 million of investment capital to enter a market with a product. Shipboard applications may attract commercial interest as the commercial transportation and shipping industry represents more than $0.5 trillion annually in the United States alone.

Now over 12 years after Desert Storm, many of the asset visibility problems are still not solved. Active commercial and Government development in asset visibility and RFID systems followed Desert Storm. The objective was to produce a fully automatic, hands off, asset visibility and tracking capability to operate in crises situations. None of the available commercial systems fully address the needs and questions. Technologies did not mature in expected time frames. The rule of thumb for technology development is 10 years from concept to prototypes, 20 years to commercialization, and 30 years to mass acceptance. The Internet was no exception. New technologies still not in the commercial marketplace may be needed to solve asset visibility problems. NTAV sought these technologies.

1.1.3 Prior Development

MITLA. Shortly after Desert Storm, DoD established the Micro-Electronics Technology in Logistics Applications (MITLA) working group to study and develop asset visibility technologies to address the problems discovered during Desert Storm. The MITLA working group included members from the Army, Navy, Air Force, Marine Corps, TRANSCOM, Defense Logistics Agency (DLA), and Military Traffic Management Command (MTMC). They surveyed a broad range of commercial automatic identification technology (AIT) including barcodes and then available passive RFID tags. None of the available optical and passive RF (read only) technologies provided enough memory to electronically record manifests and attach them to containers. They required external databases, which could be separated from containers, resulting in the same problems.

The MITLA working group awarded a Small Business Innovative Research (SBIR) contract to Savi Technology. Savi developed an active two-way RFID system that allowed more complete records to be recorded in tags rather than simple ID numbers that needed to be tied to external databases; and the ability to remotely Read and Write (R/W) tag information. They developed larger memory tags that could hold complete container manifests. Savi tags became DoD's standard RFID technology.

The Savi tags were based on analog cell phone technology and operated in unlicensed FCC Part 15 bands of 315 MHz and 433 MHz. Radiated power was on the order of 1 mW. They used narrowband frequency modulation (FM) and were susceptible to multipath nulls. Savi tags had high parts count and high costs. They did not use application specific integrated circuit (ASCI) technology to reduced costs. Batteries and packaging were the primary cost drivers. Savi tags were too expensive, $35 to $250 each.

Figure 2 shows the original Savi components, Ty tag, hand-held interrogator and "satellite" interrogator. They were intended to work in warehouses. Figure 3 shows the ruggedized tags and interrogators developed for MITLA for mounting on containers and outdoor use.

Figure 2. Original Savi components.

Figure 3. Ruggedized Savi components.

Marine Corps AWT R&D. The Marine Corps Advanced Warfighting Technology (AWT) invested R&D to develop new ruggedized tags and interrogators for expeditionary field use in the BSA/LSA. A series of components were developed based on the MITLA/Savi technology to fill gaps needed for Marine Corps expeditionary application.

A lower cost package tag, a "Radio Label" or "Radel" was developed. It was based on the Ty tag, and cost $20 versus $35. It had a flat bent slot antenna to reduce profile. It was popular with the medical community for tracking supplies. Figure 4 shows the Radel.

A 128 Kbyte Manifest tag was developed with database capability and GPS interface. It was intended to be mounted on containers and connected to an interior interrogator for automatically manifesting containers. A local tag database capability was added to reduce needing to read a whole tag database, saving battery life, and reducing transmission time for short inquiries, e.g. "Do you have NSN xxxxxx?" Figure 5 shows the Manifest tag with GPS receiver attached.

A rapidly deployable solar powered wireless interrogator was developed for field use. Earlier Savi interrogators required cables to connect interrogators. Cables are impractical in sandy beach areas as they are difficult to deploy and easily broken by vehicles. A 900-MHz wireless LAN was added to replace the cables and components were mounted on heavy lighting tripods. Figure 6 shows the rapidly deployable interrogator, with interrogator, wireless LAN (second interrogator housing), solar panels, and tripod.

Figure 4. Savi Radio Label.

Figure 5. Manifest Tag with GPS receiver.

Figure 6. Wireless interrogator.

Figure 7. Savi System with tracking software.

Figure 7 shows the Savi system with tracking software and graphical display. The Savi system could approximate item location by signal strength measurements between readers. Using 200- to 300-foot spacing between interrogators, accuracy was on the order of 100s of feet. Multipath, blockage, and antenna orientation can affect amplitude, thus affecting accuracy. The Savi system could tell if an item was nearby, but not where it was. Savi experimented with acoustic location without success.

A demonstration of AWT developed Savi components was held in Port Hueneme in November 1994. The scenario was a simulated ship off load to a staging area. Wireless interrogators were placed along roads between the ship and the staging area, and manifest tags with GPS were placed on containers. The wireless interrogators fed the tracking software. Containers were tracked and inventoried as they moved from ship to staging area.

Automatic container manifesting was also tried. A hand-held interrogator was placed inside a container to read package tags. The interrogator was connected to the externally mounted Manifest tag with GPS and read by wireless interrogators and displayed with the Savi tracking software. Containers were successfully manifested in isolation. Automatic manifesting failed when containers were adjacent. Items located in adjacent containers were also read, but it was not possible to determine if an item was inside a container, or in an adjacent container, or outside a container. ISO containers have wood, not metal floors, and RF leaked between containers. It is difficult to bound interrogation due to RF leakage. Other approaches were identified and tried, including higher RF frequencies, directional antennas, magnetic portal readers, and acoustics. They all failed for various reasons.

Many other companies have developed RFID systems. The major objective was to reduce cost and to break the $1 tag cost barrier. Single chip designs were developed by Amtech, TI, Micron, IBM, Intermec and others in an attempt to reduce cost. Bar code and passive RF are still dominant players over active R/W systems. All of these systems address the first question, "What do I have?"

The next generation RFID systems address the second question: "Where is my stuff?" The primary economic driver for these systems is reducing time to locate items, eliminating lost time, and reducing time to manufacture. Order of magnitude improvements are possible, greatly reducing operations cost, time, and inventory. NTAV started its investigations with these technologies and systems.

1.2 Commercial Product/Market Survey

The NTAV team surveyed commercial and developmental PAL systems and technologies. Ultra-wideband (UWB) RF was identified in 1999 as a candidate PAL technology because of its ability to measure distance with high accuracy. Two long standing developers of UWB systems were visited in September 1999, Time Domain Corporation (TDC) and Multi-Spectral Solutions, Inc. (MSSI). The NATV team also attended the September 1999 Ultra-Wideband Conference in Washington, D.C. (http://www.uwb.org).

A survey of commercial PAL systems was performed and two vendors with direct sequence spread spectrum (DSSS) systems were identified. A Broad Agency Announcement (BAA) was advertised in November 1999 and responses received, evaluated, and awarded. Two commercial analog PAL systems were identified, but the Army and Naval Sea Systems Command (NAVSEA) evaluated them for inventory control applications and we did not duplicate their efforts. A demonstration of an analog PAL system was performed on a ship, with similar multipath null and leakage problems as a Savi system.

The technical approaches fell into five broad categories: Analog, Digital, Hybrid, Emerging, and Advanced.

Analog systems measure signal strength, angle of arrival, phase, or combinations. Signal strength was used by the Savi system. Angle of Arrival (AOA) requires complex antennas for measurement, but can determine location with two antennas. Phase can measure distance quite accurately and is used in laser rangefinders. Multipath and reflections can affect all three techniques, limiting the usefulness of analog to open areas without obstructions or reflecting surfaces. Analog systems are used in aeronautical navigation and long-range navigation (Loran) systems. Analog is relatively simple and has been used for many decades. It, however, has limited accuracy and has been largely replaced by digital techniques. NTAV did not test analog approaches.

Digital systems measure time of flight of radio or light, much the same as radar. Two approaches are used: Relative time of arrival (RTOA) and differential time of arrival (DTOA). Both approaches require at least three antennas to determine location in two dimensions. RTOA uses transmitter/receivers (transceivers) that receive a transmitted signal, then amplify and return it. Transceivers echo a response, much like radar, and distance is calculated from time of flight. It is the easiest of digital approaches as each distance is individually measured, reducing ambiguity. The primary disadvantage with RTOA is that tagged items have receivers that are always on, decreasing battery life.

DTOA measures the difference in arrival times from transmitters to receivers. Global positioning systems (GPS) use DTOA. Satellites with synchronized atomic clocks transmit precision timed signals that are received by GPS receivers, which then calculate position. PAL systems invert this architecture, transmitting from a tag, and received by a group of receivers, which measure arrival times and calculate position. The advantage of the inverted architecture is eliminating receivers on tagged items, greatly increasing battery life. Digital systems are more expensive than analog systems because of increased complexity. Digital systems, however, follow Moore's Law, with dramatic cost reduction and performance improvements over time. NTAV tested digital approaches.

Various hybrid approaches were proposed, combining RF, acoustical, and optical. One approach used RF to signal a tag to flash a light that would be picked up by imaging optical sensors. Another system received high power ultrasonic pulses from speakers and responded by RF creating a RTOA system with acoustics. Acoustic and optical systems are subject to blockage and background interference. RF has the advantage of being able to pass through dielectric materials (wood, paper, plastic, etc.)

providing a way to read when other phenomenon, acoustic or light, are blocked. No optical or acoustic system has been successfully fielded because of blockage.

Another (analog) hybrid system combined passive RFID with phase measurement to determine distance. It would form a RTOA architecture, without needing tag receivers. This system was not developed in time for the NTAV tests. It was based on a commercial passive RFID system with modifications to extend range and frequency hopping spread spectrum (FHSS) to combat multipath. It was developed for the Army for asset tracking in ranges to find high value equipment after exercises. The objective was long-range detection from helicopters flying over an area and achieved 700-foot range.

Another (digital) passive system was identified after the NTAV tests were performed. It uses DSSS with passive surface acoustic save (SAW) tags to from a RTOA architecture, without needing tag receivers. Tags were the size of credit cards or 3 1/2-inch floppy disks. No tag battery was needed but readers transmit power levels were 4 watts and may not be HERO compliant.

Emerging and advanced systems focused on UWB because of its ability to accurately measure distance. A UWB location system had been developed for the Army for tracking vehicles in ranges. It had high accuracy, < 1 foot over 1.2 miles. It was a RTOA system, not requiring cables, but was not suitable for tagging applications with small tags. A DTOA version for tagging based on the RTOA system was proposed and accepted for development and testing.

An advanced UWB system being developed by DARPA was identified. It had a high accuracy, 1-inch, but had very short range – 30 feet. Its range was too short for PAL in ships and BSA/LSAs, but was adequate for AM and ISO containers. IR may be addressed with its wireless self-networking. A longer-range version, 90 feet, is in development and may be suitable for PAL. It was not available for NTAV shipboard tests. Appendix B describes the technology and container testing. The DARPA UWB technology may combine all three areas: PAL, AM, and IR into one architecture and technology.

Other UWB technologies were reviewed from other vendors, but none had working PAL systems. NTAV presented at the ONR Workshop on Ultrawideband Communications at the Berkeley Wireless Research Center (BWRC) on 17 May 2000 [7]. Following that brief, USC and BWRC joined in an Army Multidisciplinary University Research Initiative (MURI) proposal for UWB. The objective was asset location with single-chip design. USC and BWRC were selected for award.

Also following that conference, Time Domain Corporation (TDC) also started UWB asset visibility development and teamed with General Electric (GE) on a National Institute of Standards and Technology (NIST) Advanced Technology Program (ATP) proposal. GE and TDSI were selected for award on their proposal. The general consensus at the ONR UWB workshop was that asset visibility is UWB's natural application because of its ability to measure distance accurately.

The major reason UWB is considered an emerging technology is that the FCC recently approved unlicensed Part 15 Subpart F operation of UWB on February 14, 2002 [8]. Key application areas include imaging, vehicular radars, and short-range communication and measurement. Asset visibility (AV) is not expressly allowed, but asset visibility is on the FCC's list of UWB applications [9] [10]. Asset visibility is considered to fall under imaging.

Few unlicensed UWB devices have been approved under new Part 15 Subpart F rules. One of the first approved UWB devices is a commercial version of the UWB PAL system NTAV tested [11].

Table 1 summarizes the NTAV technology survey.

Table 1. NTAV Technology Survey

Approach	Vendor	Technology	Description	Application
Analog	Savi	Analog Cell Phone FM Transceiver Amplitude Measurement 315 & 433 MHz, 1 mW	MITLA read/write tag 100s of ft accuracy	Asset visibility
	RF Code Spider	Discrete Components AM Beacon Amplitude Zones 303.8 MHz, 1 uW	Asset control Weapons tracking HERO certified 20 ft accuracy	PAL
	Sovereign PalTrack	Radio Remote Control AM Beacon Amplitude Triangulation 418/433 MHz, 0.1 mW	Asset visibility 10-20 ft accuracy	PAL
	Company Alpha	RF Phase Locked Loop Phase Measurement	RF location system	PAL
Digital	Pinpoint	ASIC / DSP DSSS Transceiver RTOA 2.5 & 5.8 GHz, 1 W	Real time location System for hospitals 6 ft accuracy	PAL
	WhereNet	ASIC / Gate Array / DSP DSSS Beacon DTOA 2.5 GHz, 1 mW	Real time location System for industrial 10 ft accuracy	PAL
	i-Ray	SAW / DSP DSSS Passive RTOA 915 MHz, 4 W	Passive RTLS 3D 100 ft range 2 ft accuracy	PAL
Hybrid	Company Beta	RFID + Optical Sensor Flashing Light / Sensor Optical Triangulation Light & RF	Optical location system	PAL
	Company Gamma	Acoustic + RFID Ultrasonic Transceiver RTOA 40 KHz Sound + RFID	Acoustic location system	PAL
	Pacific Northwest National Lab (PNNL)	Passive RFID Phase Measurement RTOA 915 MHz/2.5 GHz 1–7 W	Passive RF location Passive tags 700 ft range	PAL
Emerging	Multi-Spectral Solutions Inc. (MSSI)	Microwave, Tunnel Diode UWB Transceiver & Beacon RTOA & DTOA 1.5 GHz, 0.25 W peak	Exercise tracking 3D 1.2 mile range outdoors <1 ft outdoor accuracy	PAL
	Time Domain Corporation & General Electric	SiGe Custom Chip UWB 1-2 GHz	Hospital LAN & location NIST ATP, 2001 start	PAL
Advanced	AetherWire & Location	UWB, Single Chip UWB Doublets RTOA 0.1 - 1.0 GHz	DARPA localizers 3D/self-networking 30 ft range 1 in accuracy	AM, PAL & IR
	USC & BRWC	UWB, Single Chip	MURI, FY02 start	PAL & AM

1.3 Objectives

1.3.1 Expanded NTAV Program Objective

The NTAV project initially selected two UWB technologies, one emerging and the other advanced, for proof of concept demonstrations. The technology selections were based on the project being funded by ONR 6.3 Exploratory Development. Mid program, NTAV's scope was expanded to include formal testing and evaluation (T&E) rather than just demonstrations. A commercial digital PAL system was added for test to baseline the current state-of-the-art. Two technologies were compared: DSSS and UWB.

Testing was broken into two major phases:

- Phase 1   Open Space: Worst Case Multipath
- Phase 2   Loaded Ship: Worst Case Blockage

The ONR seabasing project used the Phase 1 testing as an early opportunity to try PAL systems aboard a ship in preparation for the Phase 2 tests. The ONR seabasing project was the transition customer for NTAV and would be the lead on the Phase 2 testing as part of their development and testing. An extension to the Phase 1 testing with limited blockage and vehicle orientation tests was added for the Seabasing project. It gave them hands-on experience with the test systems in a loaded ship environment.

ONR Code 313, as part of the Marine Corps 6.1 Basic Research, funded Dr. Robert Scholtz and students at USC, to do UWB characterizations of RF environments. USC preformed open space tests following the Phase 1 test. The empty ship provided an opportunity they would not normally had. Most of their previous characterizations were office environments. The ship provided a Naval environment.

1.3.2 Test Objectives

NTAV's testing was set up as structured accuracy tests over an open area. The test systems were compared to a reference laser surveying system, tags moved over a mapped grid, measurements automatically recorded, and error calculated. The objective was to answer the following questions:

- Do DSSS and UWB work in shipboard environments?
- Are there dropouts and dead zones resulting from multipath?
- What are the resulting accuracies?

The seabasing partial blockage tests were conducted more as a demonstration, without exhaustive mapping. The same test systems were used and containers were loaded into the empty cargo space. Tags were placed on containers and read. Tags and antennas were moved to investigate blockage behavior. The objective was to get hands-on experience of the behavior of the systems in a loaded space.

- What are the effects of blockage by containers?
- What are the optimum tag and antenna locations?

1.4 Scope

The NTAV tests were part of a technology exploration in an ONR 6.3 Exploratory Development program. DSSS and UWB were evaluated in a shipboard environment. The focus was on basic accuracy and the ability to address multipath, not specific system performance. The NTAV test was not a competitive test between vendors. The purpose was Research, Development, Test, & Evaluation (RDT&E) to identify candidate technologies for possible application aboard ships.

This page left blank.

2.0   TEST

2.1   System Identification

Two state-of-the-art systems, representing two technologies, DSSS and UWB, were selected for testing. WhereNet was selected for DSSS and MSSI was selected for UWB. Analog PAL systems were not selected as other Government laboratories either had, or were in the process of testing them. Pinpoint's DSSS system was tested by NAVSEA aboard a ship and we did not want to duplicate their efforts. AetherWire's system did not have enough range for PAL and was selected for AM.

2.1.1   WhereNet

WhereNet was a COTS real time location system (RTLS). It was based on classified Department of Energy (DOE) work in the early 1990s to track weapons. Ford Motor Company was their largest customer with extensive installations in Ford manufacturing plants. WhereNet had an advertised 250-foot indoor/700-foot outdoor range and 10-foot accuracy.

WhereNet operated in unlicensed 2.45 GHz Industrial Scientific Medical (ISM) band at 1 mW peak power. Its DSSS waveform was 30 Mchips per second with 60-MHz bandwidth. It used 511 chips/bit for 27 dB processing gain. The WhereNet receivers used fast analog to digital (A/D) converters with custom 17 Gops/sec digital signal processor per antenna. The digital processors found first arrival and rejected multipath. Most of the system's cost was in the receiver/processor due to the digital signal processors.

WhereNet was a DTOA beacon architecture to eliminate tag receivers and increase tag battery life. It had a star architecture with antennas feeding a central receiver/processor. Receiver antennas used two circularly polarized helical antennas side by side for additional diversity and down converted signals from 2.4 GHz to 160 MHz for running over coax cables. Coax cable lengths were measured by time domain reflectometer (TDR) and time synchronization was maintained in the central receiver. Figure 8 shows the WhereNet components and Figure 9 shows the WhereNet architecture.

2.1.2   Multi-Spectral Solutions, Inc. (MSSI)

The MSSI system was a developmental UWB system based on an Army range tracking system. The Army's system was developed for tracking vehicles and robots. It used an RTOA architecture with transceivers to eliminate wires and cables, and battery operation was not a primary consideration. The RTOA system had long range, 1.2 miles, and high accuracy, <1 foot outdoors. A DTOA beacon architecture version was developed for NTAV to minimize tag power requirement and increase battery life.

The MSSI system operated at 1.5 GHz with 250 mW peak power. It was not approved to operate in the United States as it fell in the GPS L2 band. Its UWB waveform was a wavelet of several cycles, with 27% fractional bandwidth, or 400 MHz. MSSI receivers used tunnel diode detectors, with constant false alarm rate (CFAR) bias loops, for leading edge detection. Antennas were vertically polarized fat dipoles and corner reflectors. Resolution and accuracy was expected to be about 1-foot outdoors, and degrade in a shipboard environment to a few feet.

The MSSI system used distributed receivers with a daisy chain LAN architecture between receivers. System clock and digital signals with tag response and time heard were transmitted over the RS-422 LAN. The receivers synchronized their internal 100 MHz clocks to a 10 MHz LAN master clock. The receiver time clock offsets were determined by a reference tag placed at a known location. Figure 10 shows the MSSI components and Figure 11 shows the MSSI architecture. Table 2 summarizes both systems characteristics.

Figure 8. WhereNet components.
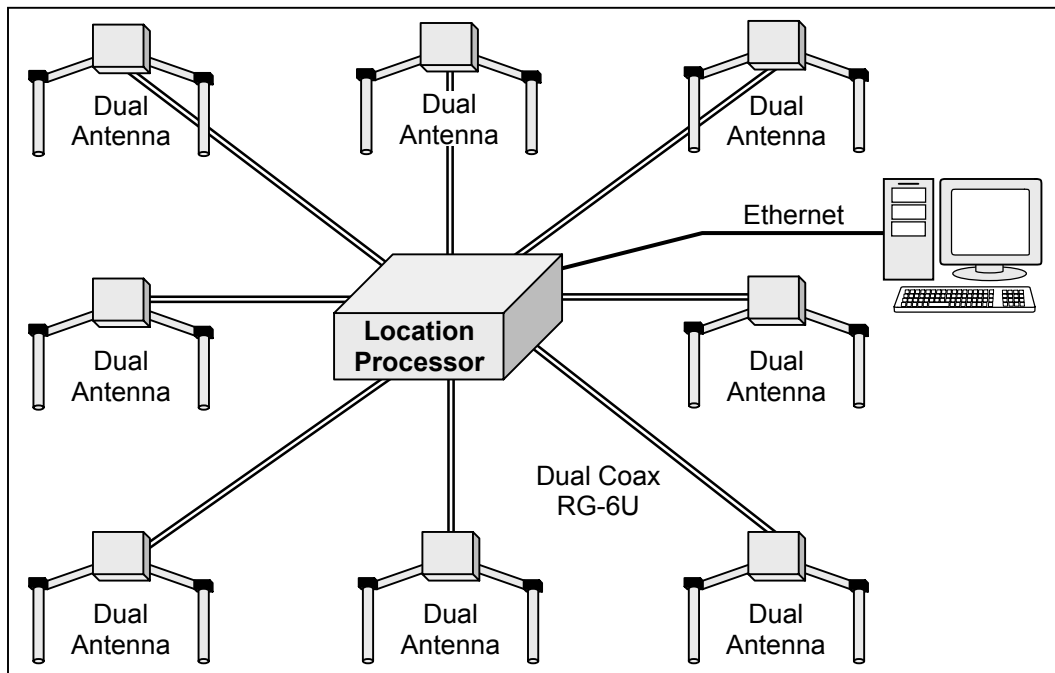
Figure 9. WhereNet architecture.

Figure 10. MSSI components.

Precision **A**sset **G**eolocation
System Block Diagram

RF Receiver &
Timing Pulse
Processor *

RF Receiver &
Timing Pulse
Processor *

RF Receiver &
Timing Pulse
Processor *

RF Receiver &
Timing Pulse
Processor *

RF Receiver &
Timing Pulse
Processor *

Tag

Tag

Tag

Tag-0
*

Tag

Tag

Tag

RS422 Serial Data Link and
Timing Reference Clock

* Known Locations

Base Control
Unit

RS232
Serial Data Link
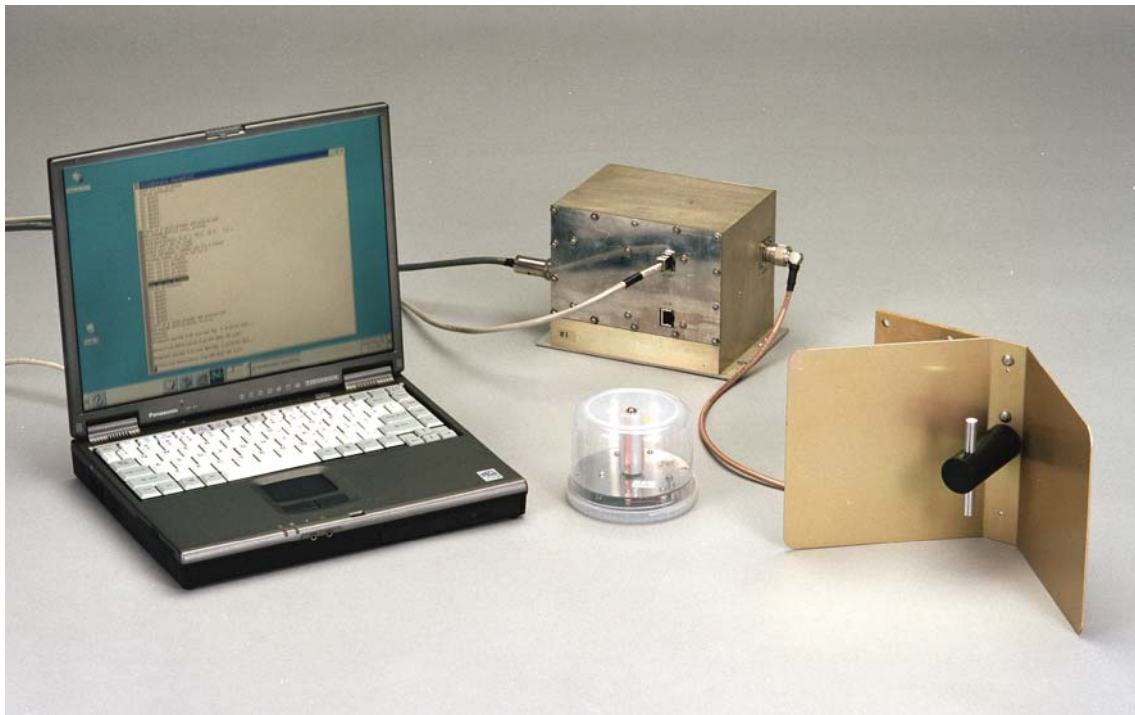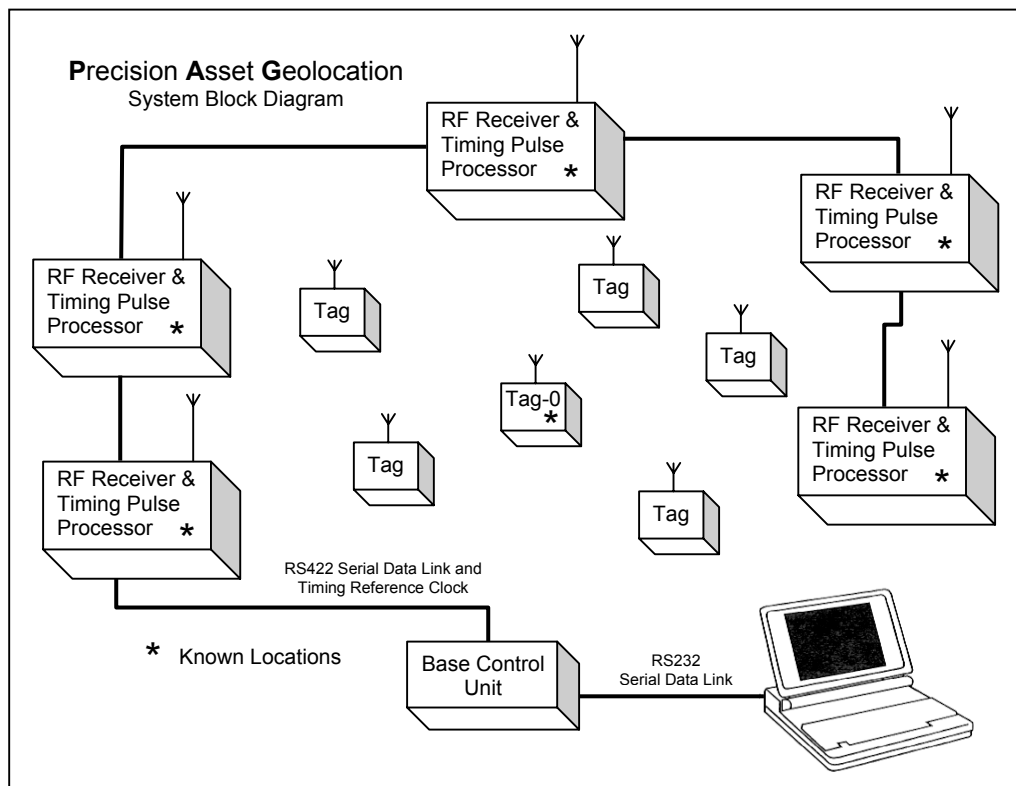
Figure 11. MSSI architecture.

Table 2. Test System Specifications and Characteristics

Characteristic	WhereNet	MSSI
Category	Digital	Emerging
Availability	COTS	Developmental
FCC Approval	Unlicensed operation ISM II Band	Not approved to operate in U.S. GPS L2 Band
Waveform	Direct sequence spread spectrum (DSSS), 30 Mchips/sec, 511 chips/bit 33 ft / chip, 17 Kft / Bit	Ultra-wide band (UWB) wavelet 27% fractional bandwidth 4 ft / Pulse
Architecture	DTOA beacon Central receiver / star	DTOA beacon Distributed receivers on LAN
Frequency	2.45 GHz	1.5 GHz
Bandwidth	60 MHz	400 MHz
Transmit Power	1 mW, 0 dBm	250 mW peak, 24 dBm
Receiver	Fast analog to digital (A/D) converter 17 Gops/sec digital signal processor 27 dB processing gain (below noise) First arrival 1/6 Chip Resolution = 5.5 nsec = 5.5 ft	Microwave components Tunnel diode detector CFAR bias loop (above noise) Integrating leading edge detection 2 nsec resolution = 2 ft
Antennas	Dual helical Circular polarized Preamplifier and down converted to 160 MHz for dual coax 8 antennas required indoors	Fat dipole corner reflector Vertical polarized Receiver/detector located with antenna 4 antennas required indoors
Calibration	Measured antenna locations Measured cable lengths, TDR	Measured antenna locations Reference rag in known location
Cable Length	Coax 2,000 ft, 4,000 ft with amplifier	LAN cable length = 150 ft
Range & Accuracy	700 ft outdoors, 250 ft indoors 10 ft accuracy indoors/outdoors 2D, assumes 4 ft tag height	1.2 mi outdoors, 250 ft indoors 1 ft outdoors, est. 3 ft shipboard 2D and 3D (with 5th antenna)
System Capacity	10,000s of tags in 40,000 sq ft 10% air capacity 120-150 tags / sec	Not specified Error correction, redundant transmissions, minor skewing
Tag	2½" X 2½" X 1", 6.25 cu in. Application specific integrated circuit "F" plane antenna, circular polarized 4 tag sub-blinks per tag read 32 bit tag ID (4 billion) 3-5 yr battery life at 10 blinks/min Fixed tag ID & adj blink rate	4¼" dia, 3¼" high, 46 cu in. Discrete and integrated circuitry Fat dipole on ground plane single polarized 1 tag transmit/tag read 255 IDs, 40 bits, 2 data fld & qty 3 hr battery life (feasibility demo) Fixed tag ID & blink rate
Software	WhereSoft locate & container Graphical user interface (GUI) SQL and streaming interfaces NT4.0, Microsoft SQL 7.0 data base	MSSI – Linux command line Plain ASCII Text config files ASCII File & RS-232 data stream Red Hat Linux 6.2
Cost	$12K controller, $4K / channel $35K / 8 channel – antennas $35 / tag: driven by ASIC and battery Software: $25K + 25K	$8.5K / receiver – antenna $42.5K / 5 antennas (prototype) $750 / tag (prototype) Software: N/A

2.1.3   Technology Comparison

Both systems were DTOA systems with digital time measurement. They measured distance at the speed of light where 1 foot = 1 nsec. Hyperbolic equations were used to calculate location, the same as GPS. Three receivers must have direct RF propagation to locate tags.

DSSS. The WhereNet DSSS system operated like a GPS system in reverse. It measured time, chips and phase. Phase was used for greater accuracy and compensated for the lack of bandwidth. DSSS used digital signal processing (DSP) and detection. RF waveforms were converted to digital data through an Analog to Digital (A/D) converter and the DSP correlated chip sequences to bits. DSSS allowed the signal to be below the noise level. This is achieved by processing gain, by correlating and averaging over a long period. The theoretical amount of processing gain is directly related to the number of chips per bit. WhereNet had theoretical 27 dB processing gain from its 511 chips/bit. Transmit power was 0 dBm.

The WhereNet system used over determination and diversity to combat the effects of multipath. Time, space and frequency spreading were used. Antennas had spaced diversity pairs of helical antennas. Circular polarization was used on both tag and receive antennas. Multiple tag sub-blinks were transmitted and averaged. Eight antennas were used indoors per space. Multiple antennas sets were identified and used for triangulation, results were compared and location determined. DSSS provided both time and frequency diversity. The WhereNet system had a rich set of algorithms, which mirrored its maturity.

The A/D and DSPs were expensive and contributed to the high system cost. Moore's Law may be in effect because of the largely silicon and digital nature of the system. Cost of the expensive digital components should reduce by 1/2 each 18 months. A/D bit - speed product, however, doubles every 10 years. Tag prices are limited by the cost of the application specific integrated circuit (ASIC), lithium battery, and injected molded plastic case.

UWB. The MSSI UWB system operated like a pulse radar system in reverse. It measured time only, and used wide bandwidth for time resolution. It used analog signal detection with On-Off Keying (OOK). Detected signals were digitally synchronized, errors detected and time measured. The MSSI UWB system had no processing gain other than error detection.

The MSSI UWB peak signal was above the noise level. Higher peak power was used, +24 dBm, and exceeded FCC Part 15 Subpart F rules [8], although the average power was below Part 15 limits. The MSSI system also had a very wide intermediate frequency (IF), 500 MHz, providing limited interference rejection. The "L" band was used because it's quietest. Many satellites operate in the "L" band including GPS. The MSSI system operated over the GPS L2 band, thus is not permitted to operate outdoors.

The MSSI system used expensive RF and microwave components. It was simpler than DSSS A/D and DSP but its RF components may require critical adjustment. Its tunnel diode detector was biased at "the top of hill" by a constant false alarm rate (CFAR) bias loop, and was "pushed" over by signals into its trough. Commercial designs do not use tunnel diodes and minimize expensive analog components.

DSSS and UWB Comparison. The UWB system had 8X more instantaneous bandwidth and shorter pulse length than DSSS. UWB used a shorter "ruler" than DSSS. The greater bandwidth and shorter pulse length were the largest measure of UWB's greater accuracy. UWB has greater inherent accuracy.

UWB short pulse length also provided greater multipath immunity. Gaussian impulses have the greatest immunity, but MSSI's wavelet waveform may be more susceptible to multipath. WhereNet DSSS chip codes were 4000 times longer than MSSI UWB wavelets, thus may be more susceptible to multipath. Processing gain may be needed for UWB to reject interference.

2.2   Test Environment

2.2.1   Test Sites

GUL. NFESC's General Use Laboratory (GUL), located at the rear of the Building 1100 was used for preliminary system light off and integration before loading the systems on the SS Curtiss. An open space was cleared in the rear of the GUL and both test systems were setup with the laser surveying and instrumentation systems. Antennas were mounted on tripods, cables prepared and connected. The test sled was constructed and tested there. The initial light off proved essential as all systems experienced failures, which needed to be corrected before placing the systems aboard ship.

SS Curtiss. The test was conducted aboard the SS Curtiss, home ported at Port Hueneme, California. It is an MPF capable ship used by 3rd Marine Air Wing (3rd MAW) for training. The ship is leased through Maritime Administration (MARAD) from American Overseas Marine Corporation. The SS Curtiss has a civilian crew and cost $1.2K/day.

Figures 12 and 13 shows the starboard side and port/aft detail of the SS Curtiss at Wharf 4. The SS Curtiss was berthed "port side to" with the bow facing north. The port quarter Roll On/Roll Off (RO/RO) ramp was lowered to drive a Navy van with delicate electronic equipment aboard. Heavy equipment, e.g., tables, chairs, power cords, tripods, etc. was craned aboard in ISO containers.

The ramp required 2 hours to set up and was adjusted for tides. It needed to be secured each night. Total time was 4 hours, and was accounted for in the schedule. Subsequent loads were done by crane, with equipment loaded and unloaded into 20-foot ISO containers pierside. The crew was exceptionally skilled in loading cargo. It is clear that the crew frequently loaded delicate and fragile avionics.

Test Area. The tests were conducted on the second RO/RO deck. It was the largest deck and had easiest access by ramp and cranes. Figure 14 shows the plan view of the RO/RO deck. The test area was set up and conducted in Holds 5 and 6. Holds 5 and 6 together were 80 feet wide by 100 feet long by 23 feet high. The walls were the straightest and the most space was available.

Figure 15 shows the test area. Hold 6 is closest and Hold 5 is on the other side of the stanchions. The bulkheads are between Holds 5 & 6 and 3 & 4. Hold 1 is in the far distance. Cargo hold hatch covers are above and below. The beams are visible above. The 20-foot ISO container provides scale. Metal is everywhere, with nothing to absorb RF. Amazingly, cell phones and 2m amateur radios worked in the environment.

Figure 16 shows a 3D perspective RO/RO deck cutaway showing Holds 5 and 6 test area. It shows the overhead beams and stanchions (pillars). The bottom of the beams are 15.8 feet above the deck. The beams extended 7 feet up to the overhead deck covers, for 22.8 feet total height to overhead. The stanchions were 16 inches in diameter. Shelves/brackets were located on the side bulkheads 11 feet above deck, every 7.5 feet. The shelves were 1.5 feet wide, 8 inches deep, and had a 1-inch hole in the center. The ArcSecond laser transmitters were placed on the shelves, thus were referenced to the ship, not on tripods.

Figure 17 shows the overall test area setup. Holds 3 and 4 were used for office and storage equipment. ISO containers were placed in Holds 3 and 4 and the office container had built-in alternating current power and lights. Test equipment and instrumentation was set up outside the office container by the opening between Holds 3 & 4 and 5 & 6, to allow viewing test progress and to facilitate communication. USC used Holds 5 and 6 for their tests, but also did propagation tests between Holds 5 & 6 and 3 & 4. They also did tests in and around the USC container.

**Two booms for each of
Holds 2, 3, 4, 5, and 6**

Helo Deck

**Hold 7 and
RO/RO
Ramps**

**Holds
5 and 6**

**Holds
3 and 4**

**Holds
1 and 2**

**SS Curtiss
View of Starboard side**
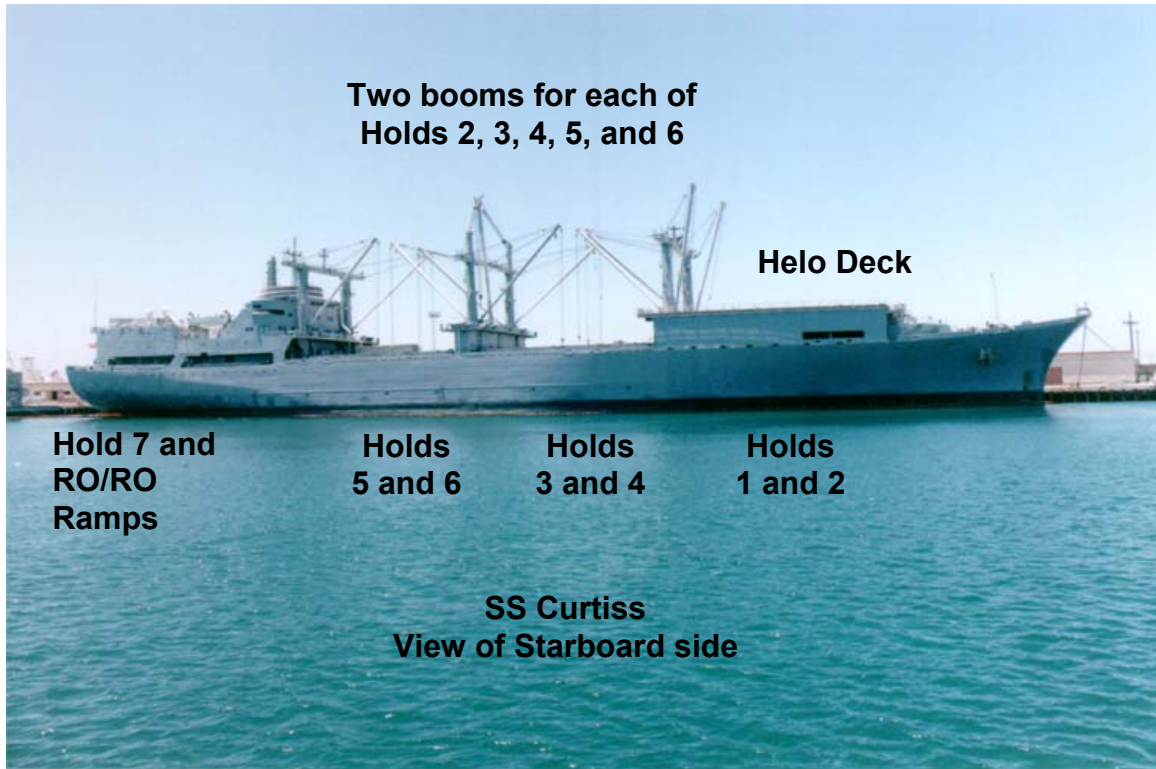
Figure 12. SS Curtiss, starboard side.

**Port Quarter
RO/RO Ramp**

**Stern RO/RO
Ramp**
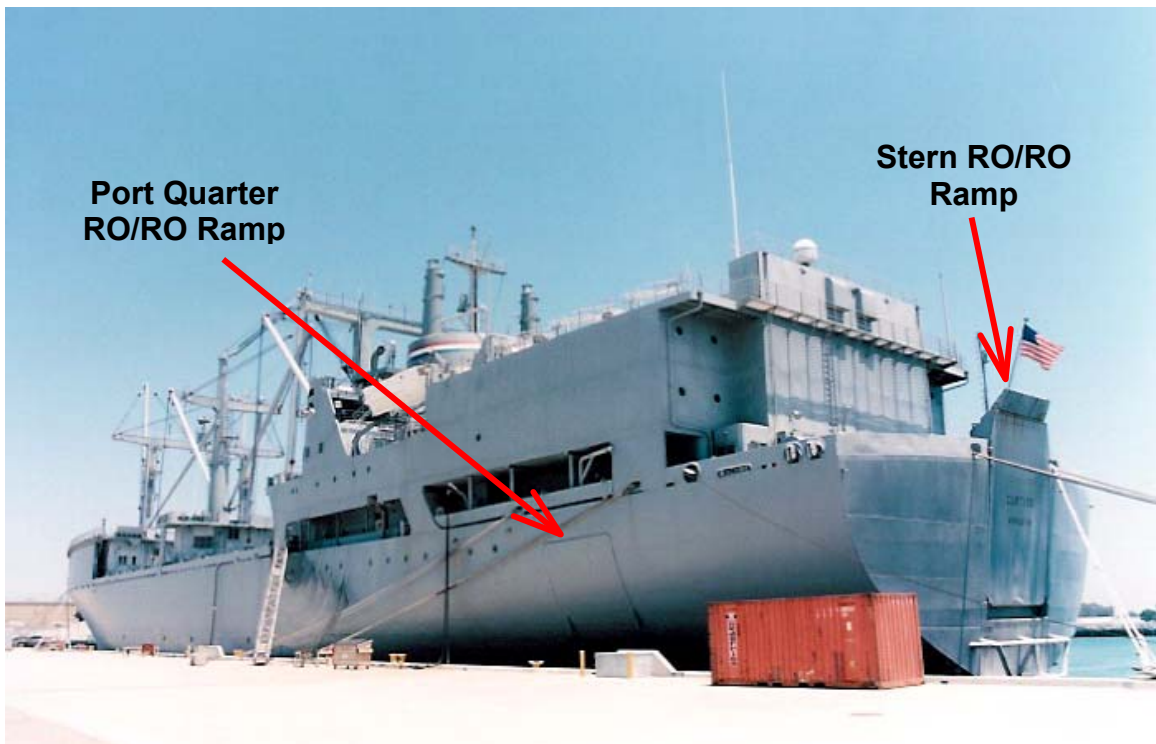
Figure 13. SS Curtiss, port/aft, showing ramps.
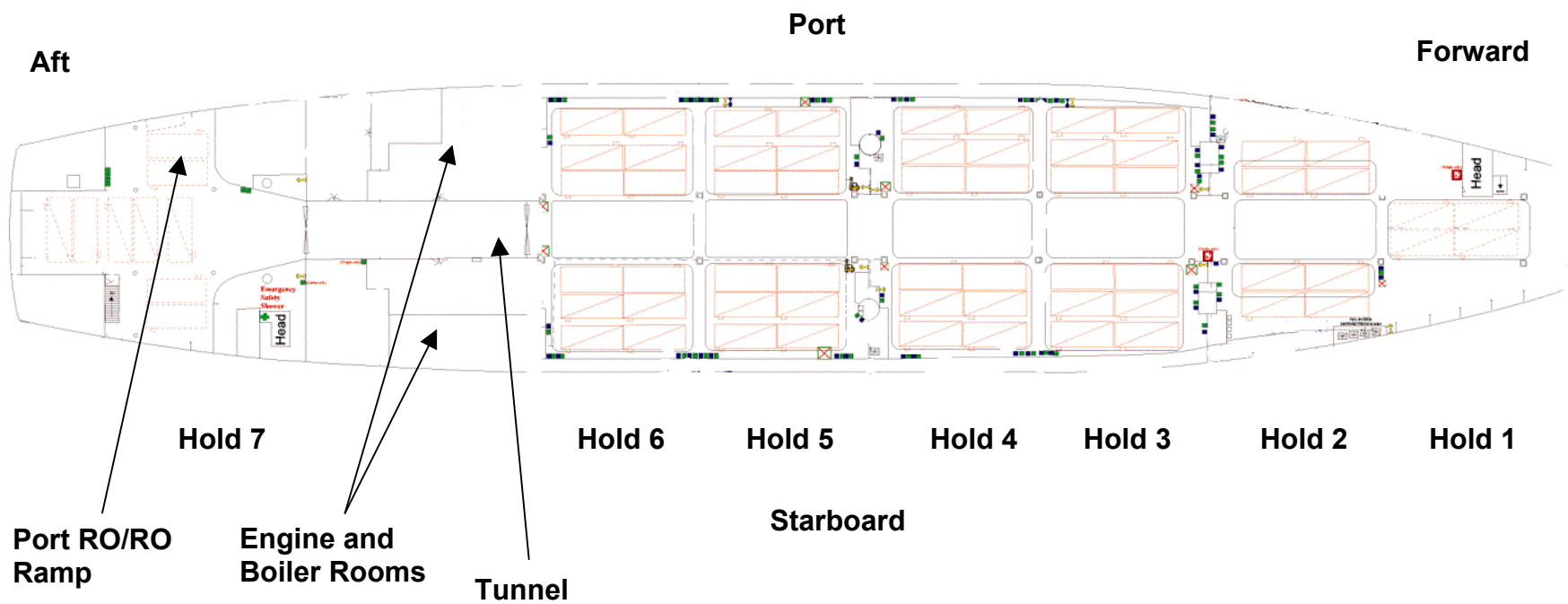
Figure 14. SS Curtiss 2nd RO/RO Deck, top/plan view.

Figure 15. NTAV test area, Cargo Holds 5 and 6, looking forward.
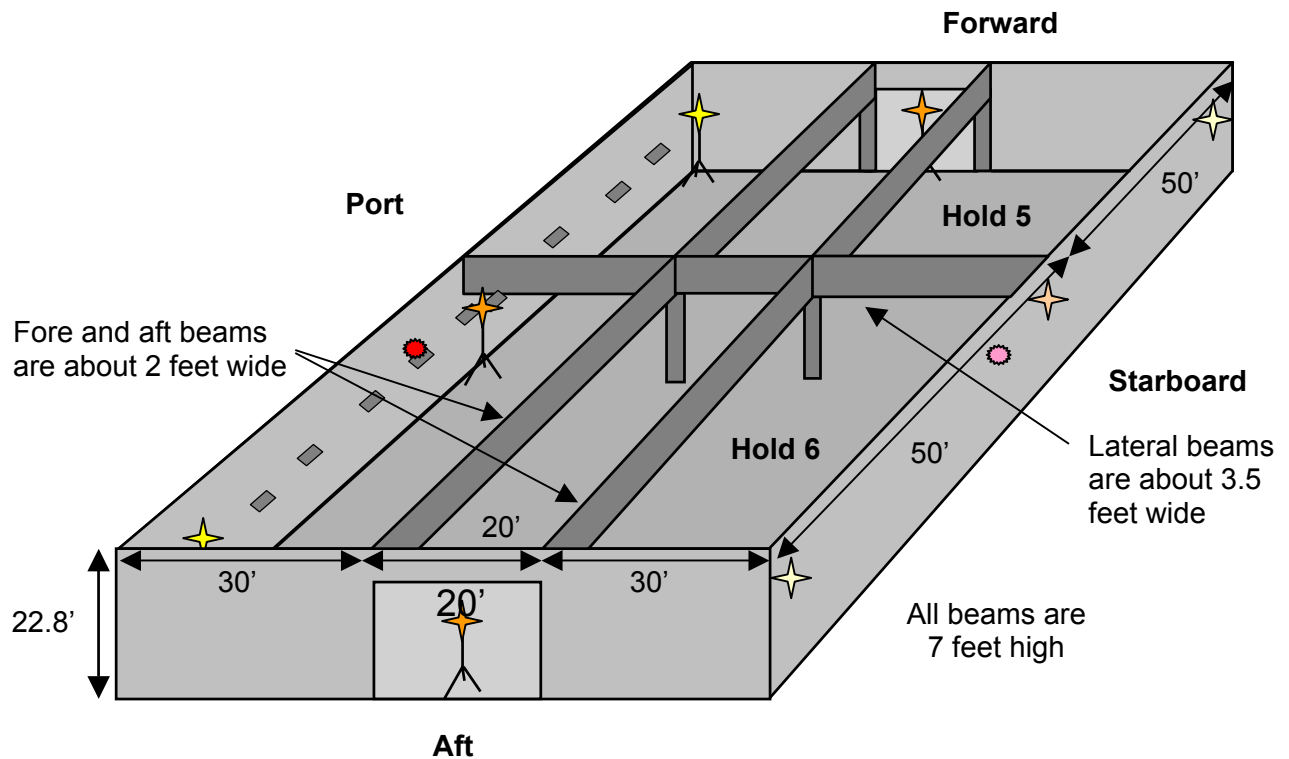
Figure 16. RO/RO deck cutaway of Holds 5 and 6.

Test Space

Office & Storage

Port

Test Space:

30'
20' Aft
30'

Hold 6   Hold 5

50'   50'   10'

Office & Storage:

+ AC & Lights

Office

Shop

Storage

USC

20ft ISO Containers
for Office, Storage,
Equipment & Testing
1 Office, 3 Standard

Hold 4   Hold 3   Fwd

Folding Tables & Chairs
for Open Storage, Tools,
Work Areas, Layout,
Meetings & Food

Starboard

50'   50'
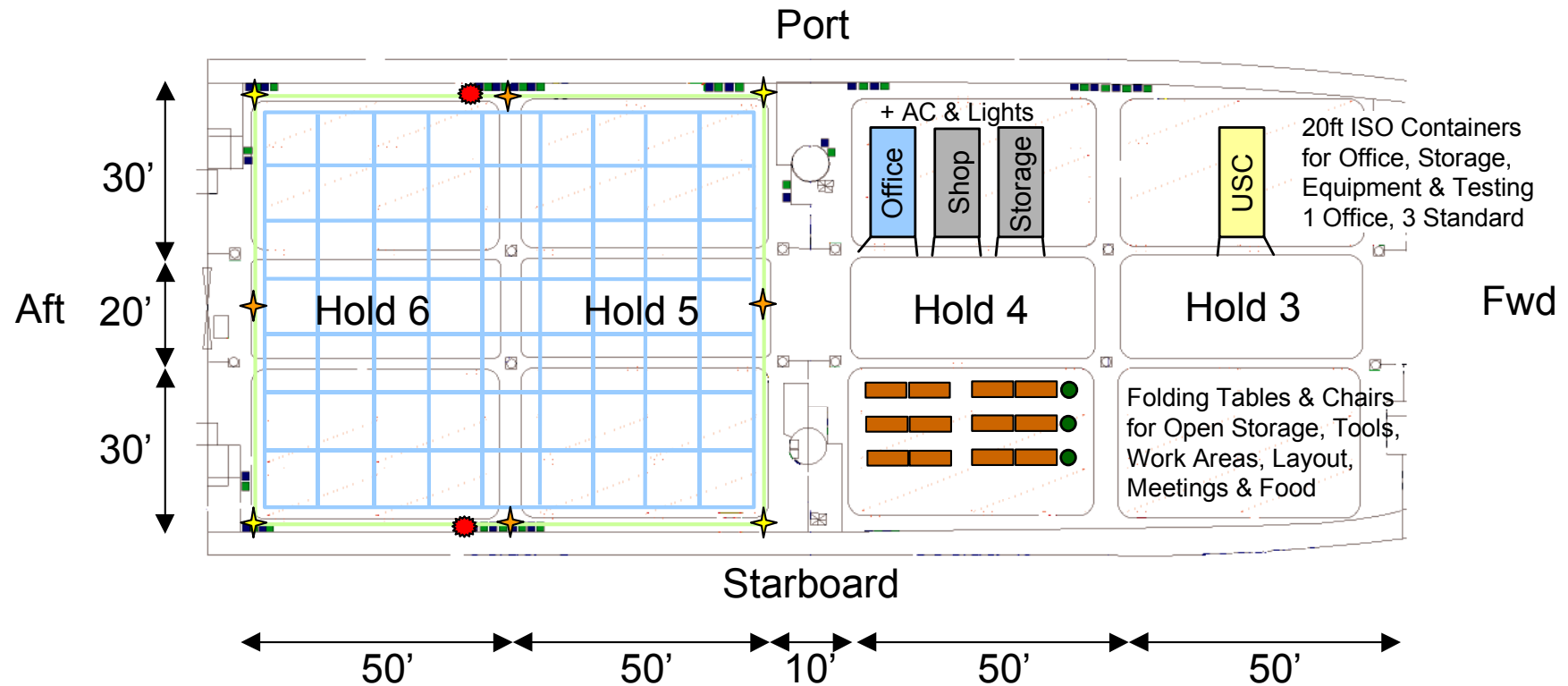
Figure 17. Cargo hold set ups.
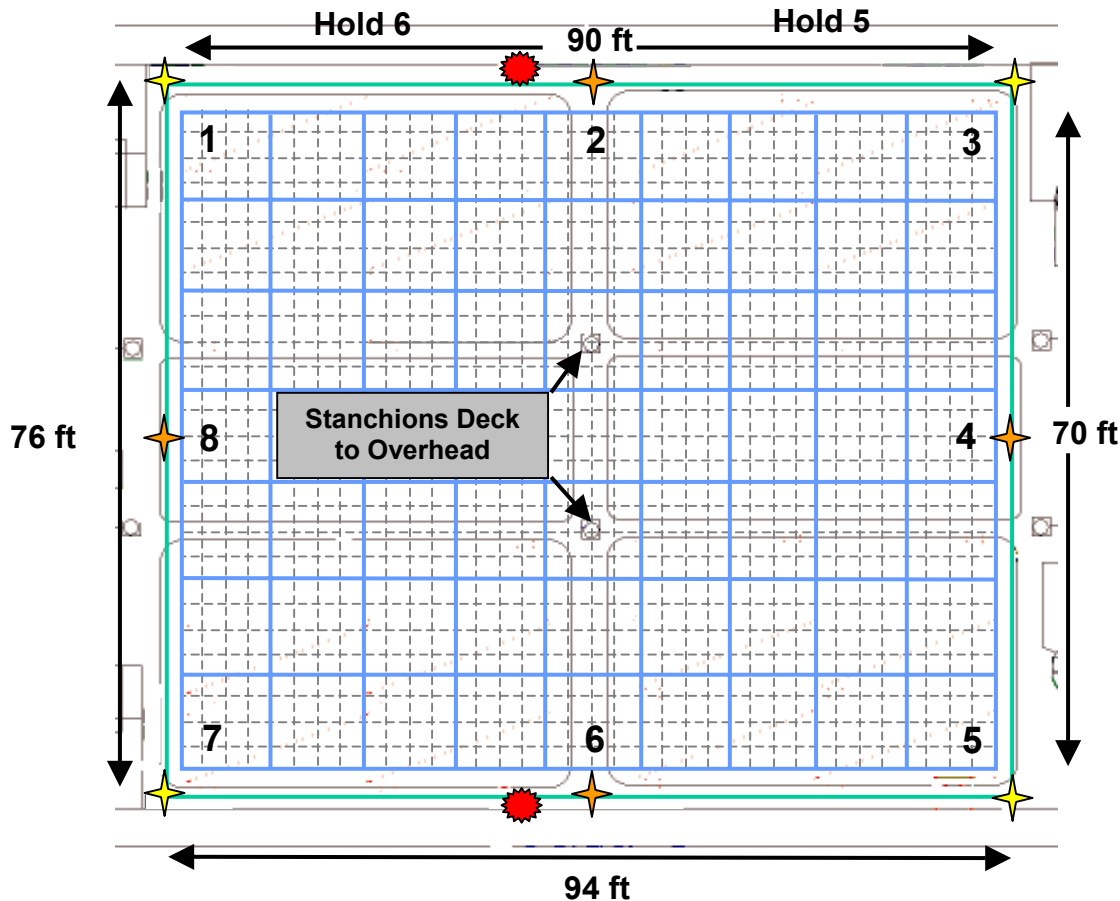
Figure 18. Test box.

Test Box. A Test Box was defined inside Holds 5 and 6. The objective was to provide a calibrated reference grid inside the cargo holds to guide measurements. An ArcSecond Vulcan laser surveying system was used to lay down a grid on the deck of the ship. The Vulcan system's specified accuracy was 1/8-inch over 100 by 100 feet. This grid was used to help navigate the test sled.

Two boxes were defined - an outer calibrated box of 94 feet by 76 feet, and an inner box of 90 feet by 70 feet. The outer box was set with 100-foot tape measures placed near the bulkheads and set square with the laser surveying system. The tape measures provided a reference to lay down chalk lines for the inner box. The inner box was set with chalk lines snapped from the outer box on 10-foot, then 2.5-foot intervals. Yellow gaffers tape was placed on the 10-foot grid, and white gaffers tape was placed on the 2.5-foot grid.

Figure 18 shows the Test Box plan with the inner and outer boxes. The major grid was offset to avoid stanchions and had 80 major intersections. The 2.5-foot minor grid had nearly 1,000 minor intersections. The minor grid was intended for focused investigations to determine error trends near bulkheads and in corners. Only the major grid was used as the test systems were not accurate enough for focused investigations.

One mile of tape was laid on the deck of the ship: about 1/4-mile for the major grid, and about 3/4-mile for the minor grid. Figures 19 through 23 show the final Test Box.

Figure 19. ArcSecond/Lewis & Lewis laser survey party.

Figure 20. Vulcan laser transmitter.

Figure 21. Outer box and inner box corner showing tape measures and chalk lines.
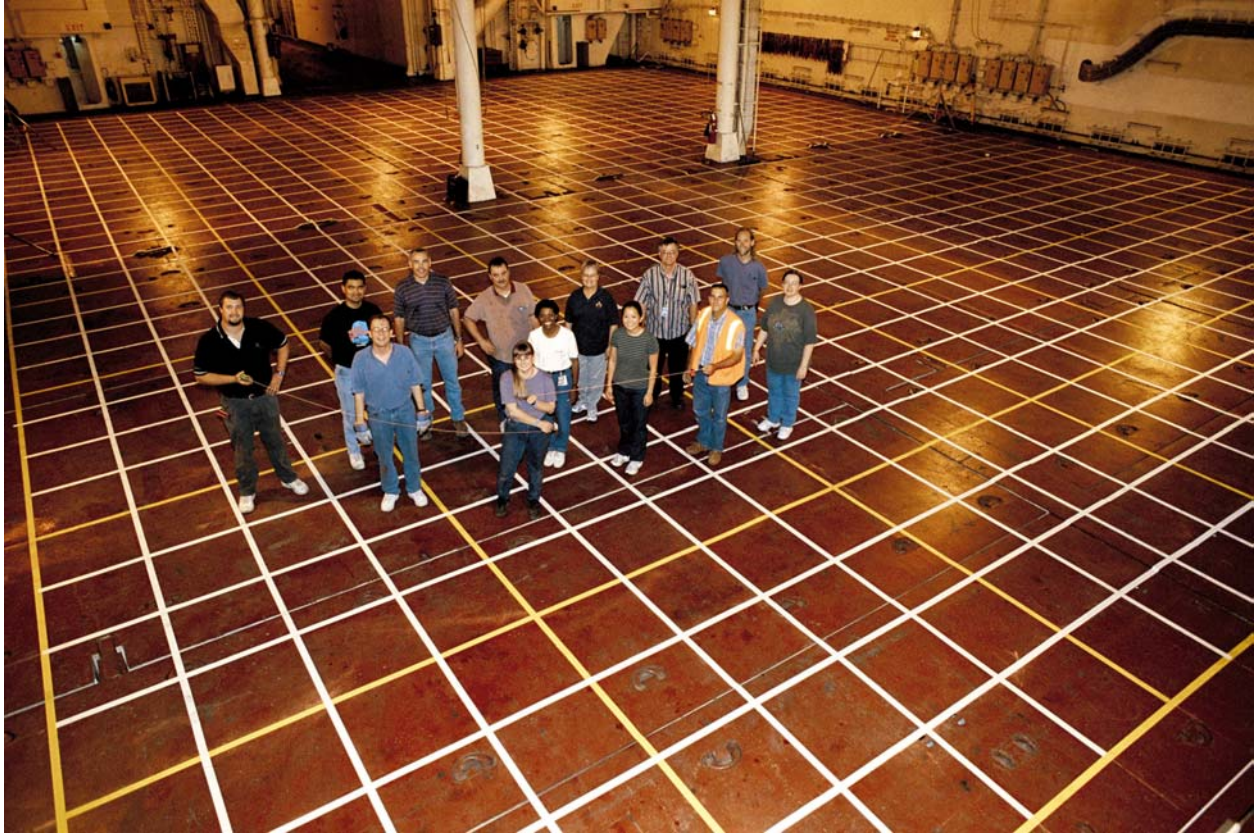
Figure 22. Completed Test Box with NTAV Test Team.

Figure 23. Top view of Test Box, Holds 5 and 6, with test sled, cargo lids open.
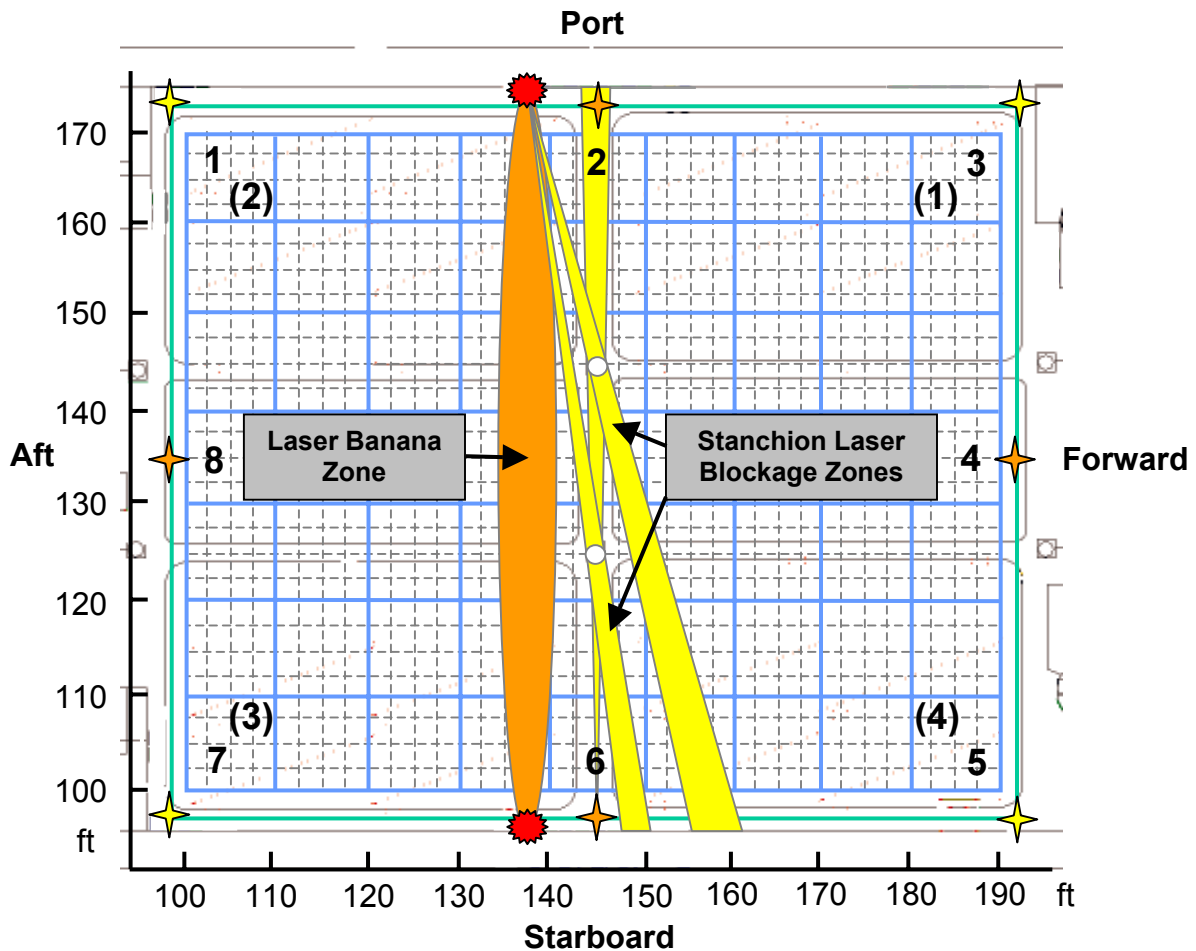
Figure 24. Test Box antenna locations, stanchion laser shadowing, and laser "banana" zone.

Figure 24 shows antenna and laser transmitter locations. Antennas were placed on lighting tripods in the corners and mid-section on each side. The WhereNet and MSSI antennas were stacked one above the other on the corner tripods, Figure 25. WhereNet antennas were placed in the mid-sections, Figure 26. The tripods were extended to place the antenna heights just below the beams.

The antenna locations were measured in three dimensions "X-Y-Z" using the laser surveying system. WhereNet antennas were measured at the bottoms of the two vertical antennas and the center calculated. The MSSI antennas were measured at the front center of the black standoff, near the fat dipole. Figures 27 and 28 show the measurement locations and Table 3 lists the antenna measurements and locations.

The laser transmitters were placed on shelves on the port and starboard bulkheads. The ideal location for the transmitters was the middle shelves, to place stanchion blockage equidistant down the middle of the test box, between two major grid lines. The laser transmitter on the port side could not be placed on the middle shelf due to fire protection lines. It was offset aft 7.5 feet to the next shelf, Figure 29.

Figure 24 shows the stanchion shadowing comparing transmitters centered and offset. During setup, the starboard laser transmitter was also offset 7.5 feet aft, opposite the port transmitter, because of blockage both sides of the center shelf limiting coverage into the near corners, Figure 30. Starboard stanchion blockage mirrored the port blockage. Laser drop outs during test confirmed stanchion blockage zones.

Figure 25. Stacked antennas in corner.

Figure 26. Mid-section antenna.
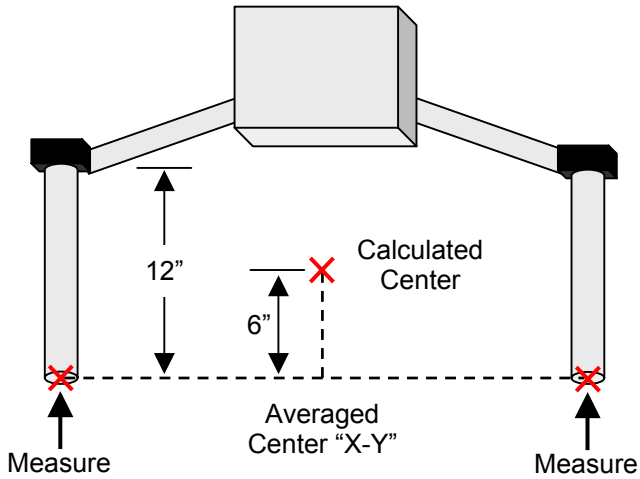
Figure 27. WhereNet antenna measurement locations and calculated position.
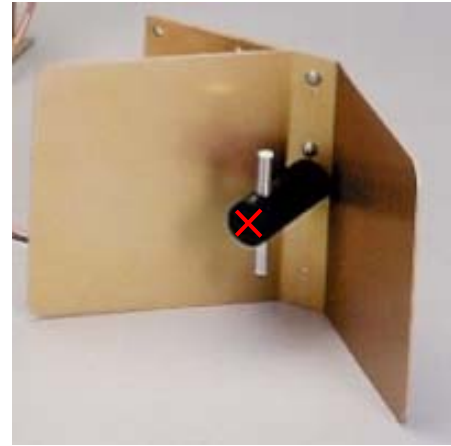
Figure 28. MSSI antenna measurement location.

Table 3. Antenna Locations

Vendor	Antenna Number	Measured Locations (ft)			Calculated Locations (ft)			Notes
		X	Y	Z	X	Y	Z	
WhereNet	1a	-2.92	71.52	10.49	**97.89**	**172.30**	**110.98**	100/170 Corner
	1b	-1.31	73.08	10.46				
	2a	46.36	72.97	10.98	**145.24**	**173.01**	**111.46**	145/170 Port Mid
	2b	44.13	73.04	10.94				
	3a	91.33	69.49	11.60	**191.80**	**168.52**	**112.11**	190,170 Corner
	3b	92.28	67.56	11.61				
	4a	92.27	36.20	12.68	**192.28**	**135.08**	**113.22**	190/135 Fwd Mid
	4b	92.28	33.95	12.75				
	5a	91.39	-0.88	12.17	**192.00**	**100.06**	**112.67**	190/100 Corner
	5b	92.61	1.01	12.17				
	6a	46.12	-2.89	11.75	**144.99**	**97.13**	**112.20**	145/100 Stbd Mid
	6b	43.87	-2.84	11.66				
	7a	-1.67	-3.66	10.63	**97.74**	**97.29**	**111.09**	100/100 Corner
	7b	-2.86	-1.77	10.54				
	8a	-2.23	36.22	11.81	**97.78**	**135.09**	**112.30**	100/135 Aft Mid
	8b	-2.22	33.97	11.79				
	3a	73.6	69.8	12.2	**172.45**	**169.80**	**112.70**	Moved 2nd Week
	3b	71.3	69.8	12.2				
	5a	71.3	0.1	12.8	**172.40**	**100.15**	**113.25**	Moved 2nd Week
	5b	73.5	0.2	12.7				
MSSI	1	91.79	68.20	11.43	**191.79**	**168.20**	**111.43**	190/170
	2	91.71	0.32	12.27	**191.71**	**100.32**	**112.27**	190/100
	3	-2.03	-2.82	10.72	**97.97**	**97.18**	**110.73**	100/100
	4	-2.22	72.01	10.49	**97.78**	**172.01**	**110.49**	100/170

Figure 29. Port laser transmitter.

Figure 30. Starboard laser transmitter

During the tests, a laser "banana" zone was discovered between the two laser transmitters. It was caused by the included angle between the transmitters being too small to accurately calculate the port/starboard "Y" dimension. The "X" axis may have been accurate. The ideal location for the laser transmitters would have been in the middle, to line up both the stanchion blockage zone with the laser "banana" zone. The transmitters could have been mounted center by extending the shelves with plates, mounting the laser transmitters further away from the bulkheads, fire protection lines and other blockage.

Coordinates were offset 100 feet in each dimension to insure negative numbers were not reported. This would cause problems with the test and instrumentation systems. Major, 10 feet, intersections were labeled with "X" and "Y" coordinates, again to help navigation. All measurements were in decimal feet.

Container Load Plan. The second (RO/RO) deck top view, Figure 14, shows the container load plan for the ship. Container outlines are shown in orange. Four containers can also be placed on the amidships center hatches in each hold, the same as Hold 1. The outlines show 20-foot containers.

Figure 31 shows the ship's cross section with operational stowage plan. Containers can be stacked two high in the second (RO/RO) deck. The hatches above the second (RO/RO) deck, Holds 3, 4, 5, and 6, opened to the sky. Containers can be stacked on the main deck topside, with their tops even with the helo deck. The main deck is not enclosed, except under the helo deck, above Holds 1, 2, and 3. Cargo Holds 3, 4, 5, and 6 can hold 32 20-foot containers each, for a total of 64 containers in a compartment.

The Main and third decks were not used for the testing. Main deck hatches over Holds 3, 4, 5, and 6 were opened for the third open space test. Twenty-two containers were loaded in Holds 5 and 6 for the second week container blockage test. The center main deck hatch above Hold 6 could not be opened as a heavy generator was stowed on top.
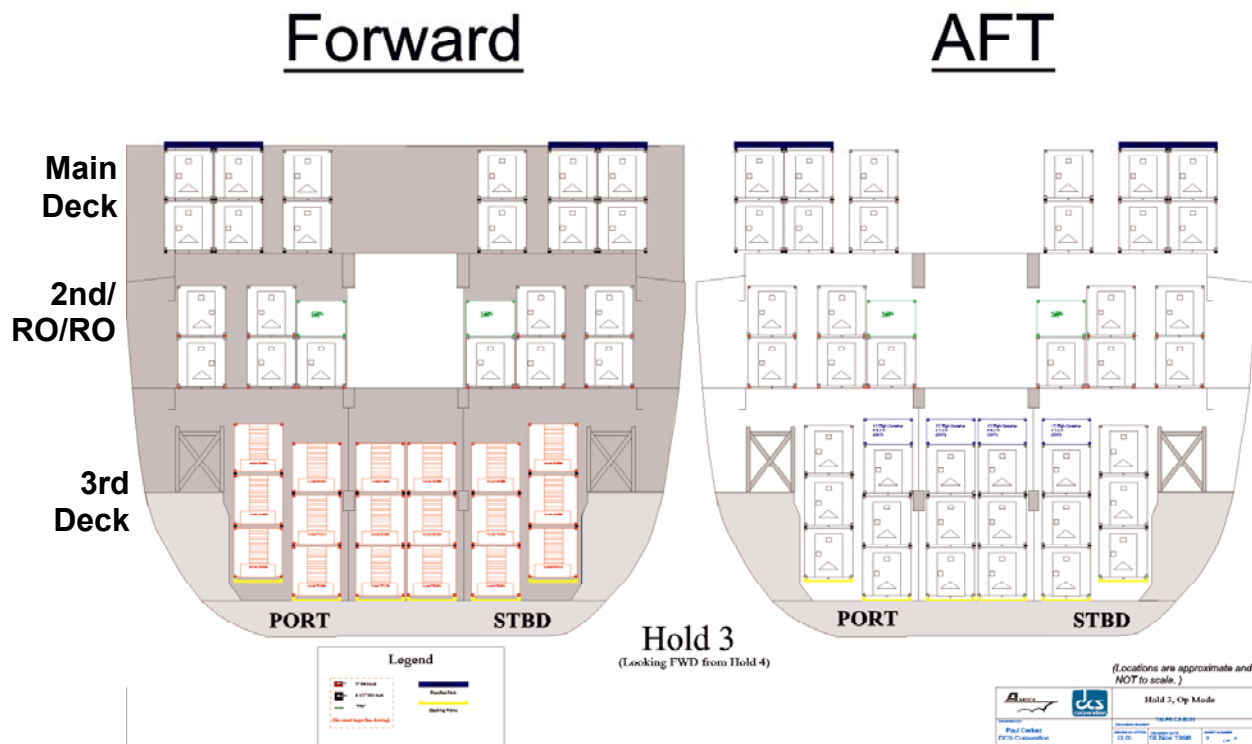
Figure 31. SS Curtiss, cross section, Hold 3, operational container stowage plan.

2.2.2 Test Items

WhereNet. Table 4 lists the WhereNet system test items. One location processor was used with 8 reader processor cards and 8 dual antennas. The older "plastic" antennas were originally planned but WhereNet shipped their improved industrial antennas just before the test began. The industrial antennas had helical antennas and improved RF electronics with greater overload. RG-6U dual coax cable was cut to 300-foot lengths and "F" connectors attached. Cable lengths were measured with a TDR and entered into the WhereNet software.

The WhereNet software was run on a Dell PC with Microsoft NT Server 4.0 and SQL Server 7.0. The Government furnished an AutoCAD.DXF format map of the test box and antenna "X-Y-Z" locations.

Figures 32, 33, 34, and 35 show the major WhereNet test items.

Table 4. WhereNet System Test Items

Category	Vendor	Item	Qty	Description
Hardware	WhereNet	Location Processor Chassis	1	Location processor box with master controller and power supply, PCI PC Bus
		Reader Processor Cards	8	Dual receivers with custom digital processors
		Antennas	8	Dual industrial antennas with helical antennas and improved electronics
		WhereTag "M"	110	ID only, no data
		WhereTag Snap-In Tag Holder	110	Plastic cup to hold tags, used with Velcro tape to attach tags to ISO containers
		Hand-held PC Card	1	PCMCIA Card to set/program tags
		Location Processor Cabinet	1	19" rack, with EtherNet hub and UPS
	Percon	Hand-held Computer Model Falcon 315	1	Used with WhereNet hand-held PC card to set/program tags
	Comm-Scope	Coax Cables, Dual	8	RG-6U, approx 300 ft long each, length measured with TDR
	Thomas & Betts	"F" Coax Connectors	32	Cable TV connectors
		"F" to BNC Adapters	16	Female "F" to male BNC adapters
	Dell	Dell Optiplex PC	1	733MHz PIII, 256 Mb RAM, 2 - 20 GB hard drives, 21-in. monitor 2 – 3 Com EtherNet cards
	APC	Uninterruptible Power Supply	1	Back-UPS Pro, 650 VA, for Dell Computer
Software	Microsoft	NT Server 4.0	1	Service Pack 5
		SQL Server 7.0	1	Service Pack 2
	WhereNet	WhereSoft Locate	1	Version 2.0, auto calibrate tag
		WhereSoft Container	1	Version 2.0
GFI	NFESC	Graphics Map	1	DXF format
	ArcSecond	Antenna Locations	8	Actual, 3D, "X-Y-Z"

Figure 32. WhereNet location processor, reader processor card, and WhereTag "M."

Figure 33. WhereNet dual industrial antenna.

Figure 34. WhereTag "M," internal and external construction.

Figure 35. Percon hand-held computer with WhereNet hand-held PC card.

MSSI. Table 5 lists the MSSI test items. Four receivers with corner antennas were used. A fifth receiver with an omni-directional antenna for "Z" axis measurements was provided, but not used. The fifth receiver was used as a spare to replace a bad receiver. Five tags were used for the open space test. One was used for a reference tag, three were used on the test sled, one was a spare. Seven tags were placed in multiple locations for container blockage testing.

The MSSI software was run on a vendor provided laptop computer running Red Hat 6.2 Linux operating system. An additional RS-232 PCMCIA card was added to the laptop computer to provide a second RS-232 interface to the instrumentation system. The Government provided antenna locations, measured with the laser surveying system. No map was provided as the MSSI software did not have a graphical interface.

All cables were provided with the system and none needed to be prepared. The RS-422 LAN cables were 150 feet long and daisy chained between receivers and to the Base Control Unit. They were long enough to work in the cargo hold. Power extension cords were used to the receiver power supplies.

Figures 36, 37, 38, and 39 show the major MSSI Test Items. The Base Control Unit, a small black box, is not shown. Receiver internal construction is shown.

Table 5. MSSI System Test Items

Category	Vendor	Item	Qty	Description
Hardware	**MSSI**	Receiver	5	"L" Band UWB RF receiver and time measurement
		Antennas, Corner	4	Corner antennas for test box corners
		Antenna	1	Omni-directional antenna: 3D "Z" axis
		Base Control Unit	1	10 MHz master system clock, RS-422 to RS-232 translator
		Tags	7	Fixed ID tags in plastic cups 2 AA batteries
		Receiver Power Supply	5	Power brick + 5-ft extender cord Euro AC cord
		Receiver Antenna Cable	5	18-in. coax cable, type "N" connector
		Base Control Unit Power Supply	1	Small power brick
		RS-422 LAN Cables	5	150 ft, RJ 45, Cat 5 shielded cable
		Mounting Hardware		Various hardware to mount antennas and receivers to tripods
	Panasonic	Laptop Computer	1	450 MHz PIII, 128 Mb RAM, 12 GB HD, 14.1" screen
	Quatech	RS-232 Serial Port	1	PCMCIA RS-232 2nd port for laptop
Software	**Red Hat**	Linux 6.2	1	2.2.14 Kernel
	MSSI	PAG	1	Precision Asset Geolocation Software. Process reads to tag IDs and x-y-z locations
GFI	**ArcSecond**	Antenna Locations	5	Actual, 3D, "X-Y-Z"
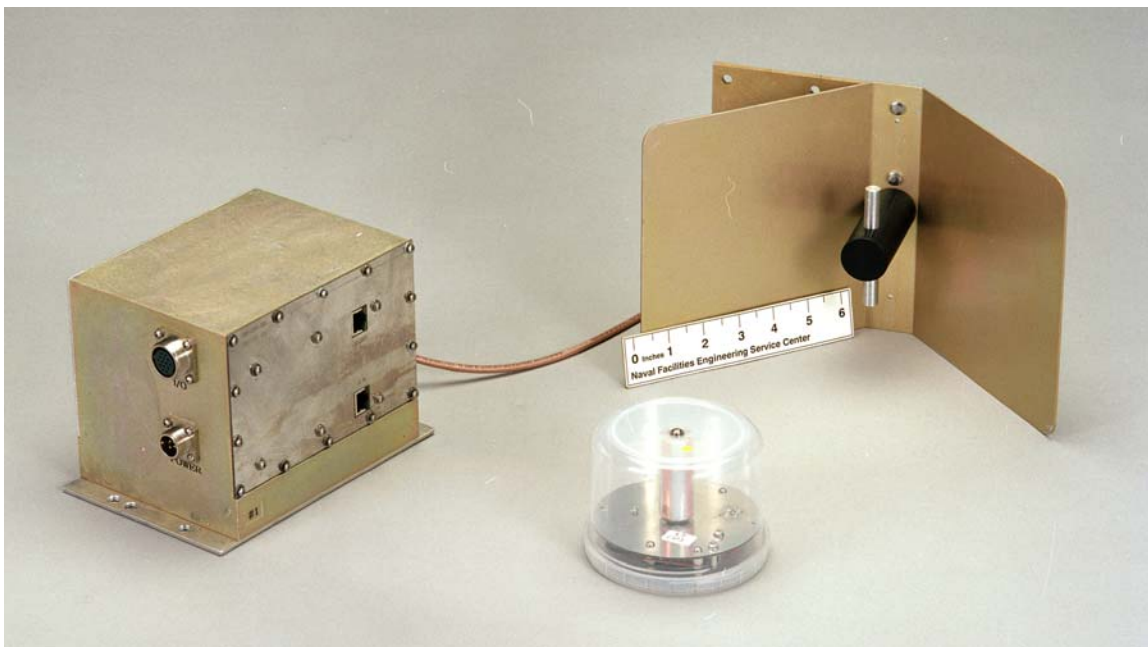
Figure 36. MSSI receiver, corner antenna, and tag.
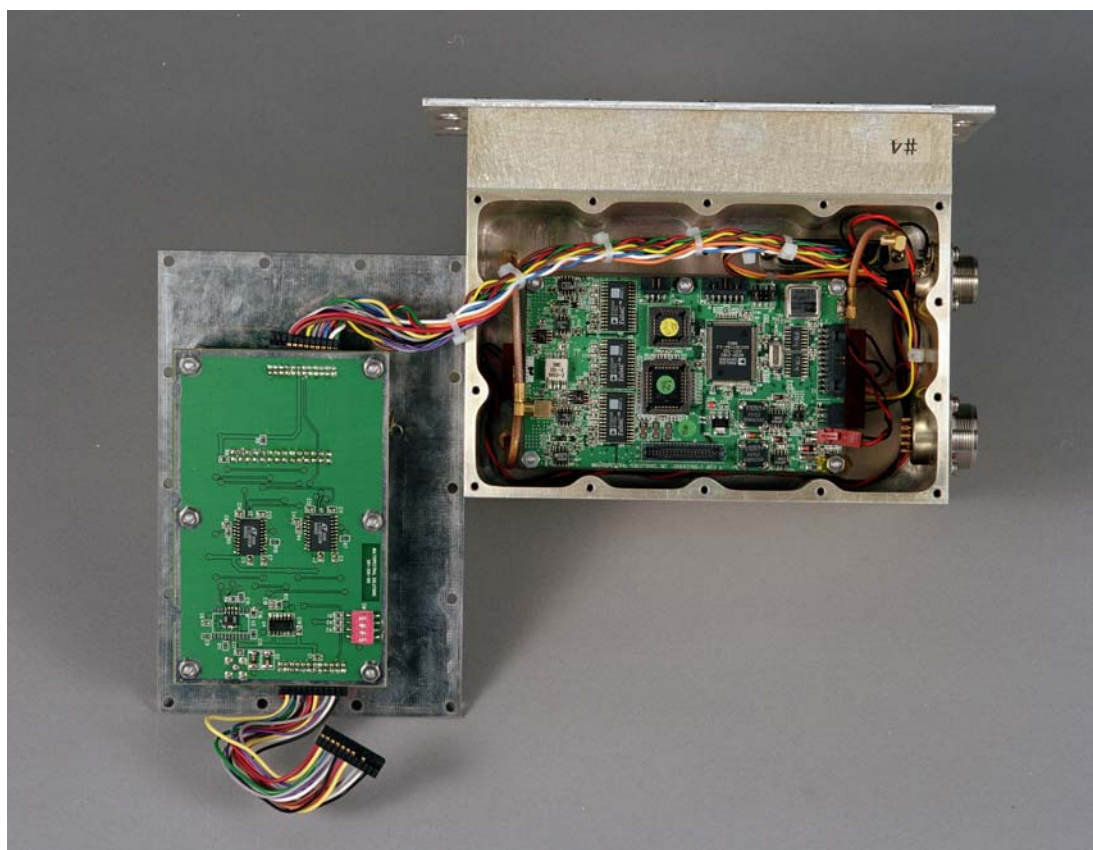
Figure 37. MSSI receiver internal construction, digital compartment:
Cable interface and sync control boards.
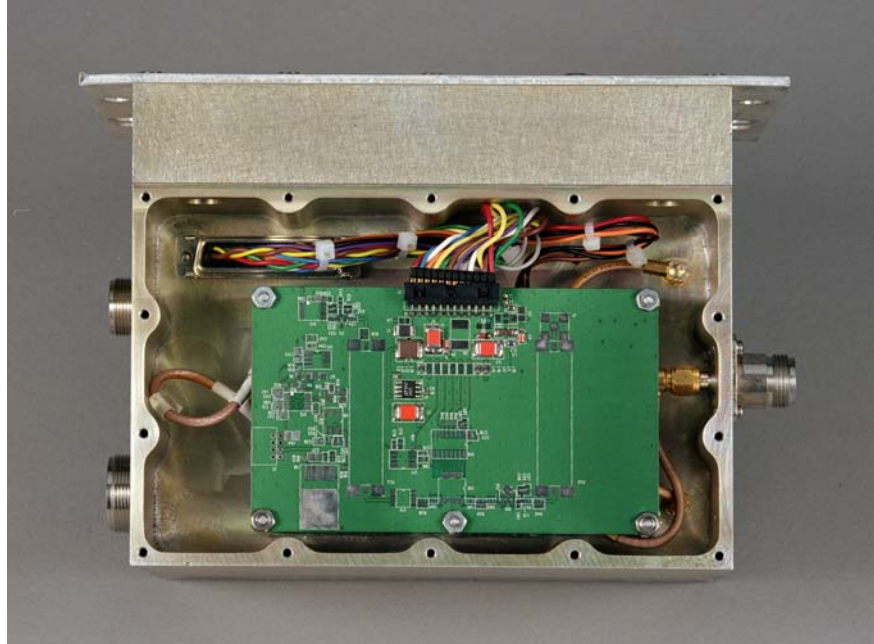
Figure 38. MSSI receiver RF compartment: L-band down converter and variable gain IF.
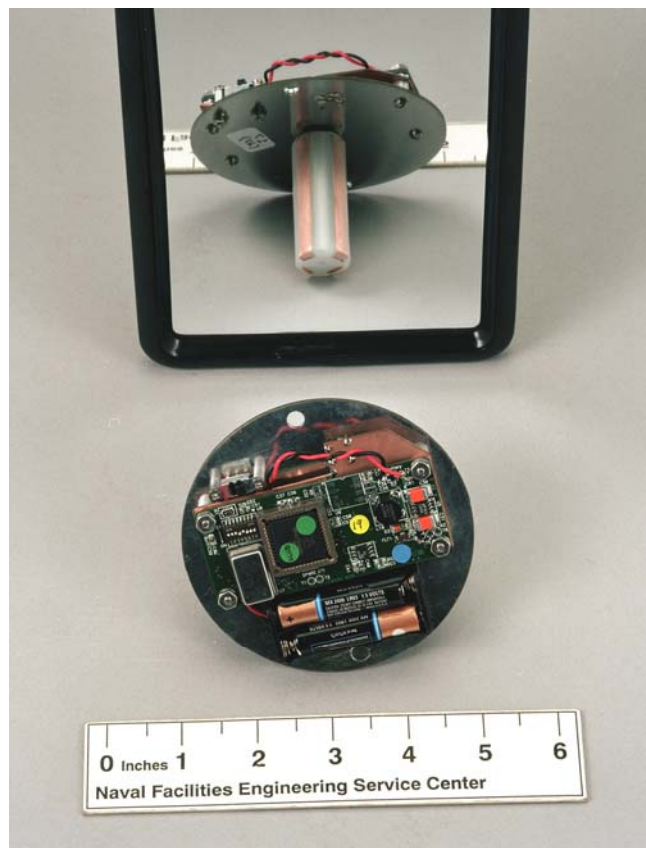
Figure 39. MSSI Tag: Electronics and fat dipole with ground plane.

2.2.3   Other Materials

ArcSecond. Table 6 lists the ArcSecond Vulcan laser surveying system components. One wand and one surveying pole were rented with two transmitters. The wand was used to measure the Test Box grid (Figure 19), antenna locations, and tag locations on containers and vehicles for the second week blockage tests. The surveying pole was mounted on the test sled to measure test sled and tag positions.

The surveying pole used a laser receiver sensor unit screwed to the top of fiberglass surveying poles. Three sections, 1, 2, and 3 feet were provided with the ArcSecond system, and two 3-foot fiberglass pole extensions were used to extend the pole to full height just below the beam. Tags were then mounted on the fiberglass surveying poles at different heights to provide simultaneous measurements. The fiberglass poles provided a non-metallic pole to mount tags, minimizing effect on tag transmissions.

Laser transmitters were mounted on tripods for wand measurements (Figure 20) and on bulkheads for test sled measurements (Figures 29 and 30). System setup was simple. The system did not need to know laser transmitter locations. One reference location (origin) and one axis ("X") were set by placing the tip of the wand/pole in two locations. 3D measurement started after setting the origin and one axis.

The ArcSecond system used a PC Personal Digital Assistant (PDA) to calculate position from the wand and surveying pole laser receivers. The PDA provided a user interface to initialize the system, input pole/tip length, and to provide display of the wand/surveying pole tip position. Both the wand and surveying pole used the PDA. Manual location readings were made from the PDA.

The PDA also provided a RS-232 serial interface to automatically send measurements to another computer. The serial interface worked with an ArcSecond software System Development Kit (SDK) and Dynamic Linked Library (DLL), which read the serial data and made it available to other programs. Fiber-optic RS-232 line drivers were used to extend the serial interface from the PDA to the instrumentation system from the test sled.

Figures 40, 41, 42, and 43 show the major ArcSecond components.

Table 6. ArcSecond System Test Items

Category	Vendor	Item	Qty	Description
Hardware	**ArcSecond Vulcan**	Laser Transmitters	2	Includes batteries, case, and charger
		Receiver – Wand Unit	1	Includes processor, Pocket PC, and batteries
		Receiver – Sensor Pole Mount	1	Includes connection & processing box, Pocket PC, batteries
		Pole Sections & Tip	3	1-, 2-, & 3-ft sections and pole tip
		Cables & Adapters	--	Receiver – processor – Pocket PC – extender, 9-25 Pin RS-232 adapters
	Lewis & Lewis	Pole Sections	2	3-ft pole sections
		Survey Tripods	2	Topcon, for laser transmitters
	Black Box	Fiber-Optic Line Driver	2	RS-232, P/N MD940AMST
		Fiber-Optic Cable P/N EFN2002A	200 ft	Rugged, 62.5 Micron, with ST connectors installed
	Duracell	6 V Lantern Batteries	2	Alligator clips to 1/8" mini phone plug for Fiber-optic line driver
Software	**ArcSecond**	SDK Software	2	Win32 DLL and sample C++ Code

Figure 40. ArcSecond Vulcan laser transmitters and battery pack.

Figure 41. ArcSecond Vulcan Receiver – Wand unit and Pocket PC.

Figure 42. ArcSecond Vulcan Receiver – Sensor, pole mount, with accessories.
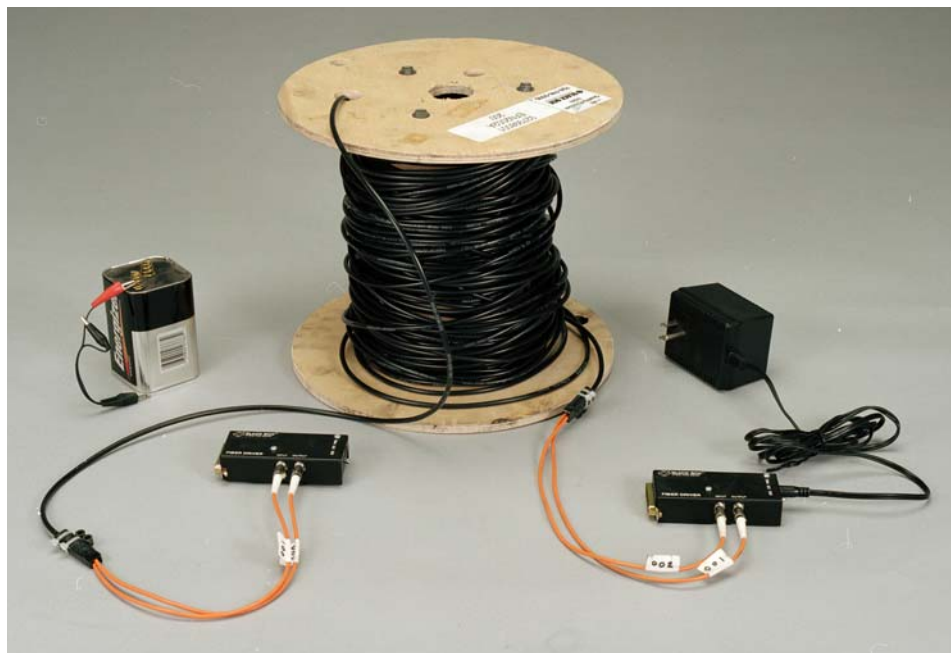
Figure 43. RS-232 fiber-optic line drivers, fiber-optic cable, adapters, and battery.

Test Sled. A Test Sled was constructed to move the surveying pole and tags around the Test Box. The primary concern was safety for the ArcSecond Receiver. The surveying pole was 14 feet long and difficult to handle and keep vertical. The sled also provided stability during measurements. The top of the pole was level with the laser transmitters on the bulkhead shelves.

The pole was mounted on a heavy aluminum cart with large pneumatic tires for easy movement over the irregular ship deck. A piece of 3/4-inch plywood was attached to the cart with C clamps. Non-metallic guy wires were constructed of 1-inch nylon webbing with quick releases and metal turnbuckles were used for fine adjustment. The pole had an integral bubble level.

Tags were mounted at approximately 4, 8, and 11 feet above the deck. The pole just touched the bottom of the beams and was shortened by removing the top 1-foot pole extension. The top tags were then moved down to the 2-foot section, approximately 10 feet above the deck. Tags were mounted facing the same direction, forward for "X" measurement and starboard for "Y" measurement.

Figure 44 shows the Test Sled design and Figure 45 shows the completed Test Sled.
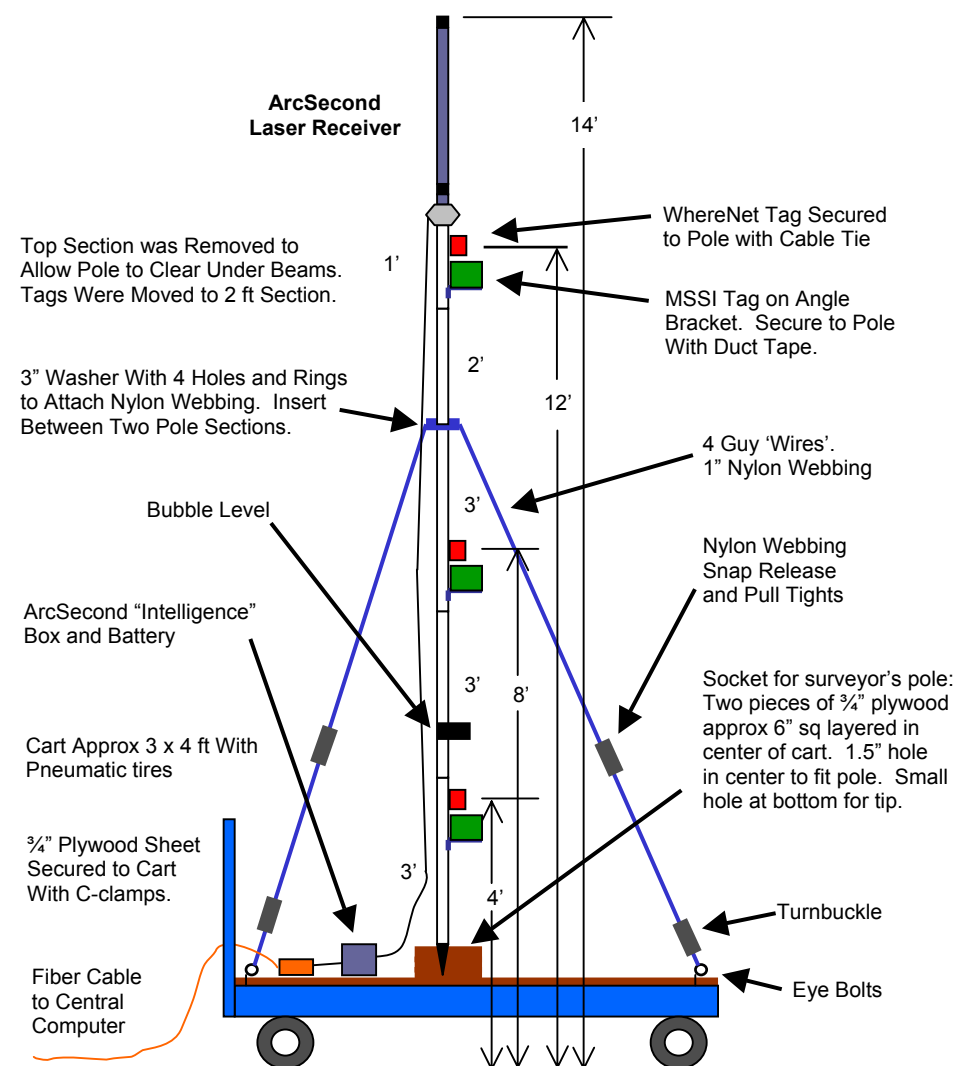
Figure 44. Test Sled design.

2-28

Figure 45. Completed Test Sled.

2.2.4   Test System Architecture

Figure 46 shows the overall test system architecture with the two test systems and laser surveying system mounted on the test sled. All three systems operated simultaneously and measured tag and sled location.

Each system operated at a different frequency and did not interfere with each other. ArcSecond was concerned that the tags might interfere with the sensitive electronics in the laser receiver, but no interference was found between the tags and the laser receiver. High-pressure sodium arc lamps in the cargo holds interfered with the ArcSecond receiver when close to the lights and they were turned off. It was not certain whether the interference was optical, RF, or magnetic from their ballasts.

All systems were wireless to the test sled except the ArcSecond system. Its readings were sent down a fiber-optic cable from the test sled to the instrumentation system. The fiber-optic cable minimized RF interference to the laser system to the test system RF receivers, compared to a copper cable.

Each system processed its own data and fed it to an instrumentation system. The WhereNet system could store and graphically display its data, but the MSSI system and ArcSecond system could not store nor graphically display their data. The instrumentation system provided essential functions for the MSSI and ArcSecond systems. The objective was to record all readings automatically and in real time, eliminating error and providing the ability to take 1000s of measurements. Measurements would be recorded at the same time, providing easy means to correlate, in time, laser readings with tag reports.

2.2.5   Instrumentation System

Environmental System Research Institute (ESRI) developed an instrumentation system to capture data from the three systems: ArcSecond, MSSI, and WhereNet. It was based on two ESRI products: ArcView Geographic Information System (GIS) and Tracking Analyst. They provided the ability to capture and display streams of position data on 2D maps, complementing the MSSI and ArcSecond systems. Data streams were interfaced and recorded with ESRI developed Avenue scripts and custom "C" routines, and displayed using ArcView and Tracking Analyst. Table 7 lists the instrumentation system components and Figure 47 shows the instrumentation system software architecture.

Table 7. ESRI Instrumentation System Components

Category	Vendor	Item	Qty	Description
Hardware	HP	NetServer LH3 Computer	1	Dual P II / 400 MHz, 256 MB RAM, (1) 4 GB and (2) 18 GB hard drives
	APC	Uninterruptable Power Supply (UPS)	1	Back-UPS Pro, 650 VA, for HP computer
Software	ESRI	ArcView GIS	1	Version 3.2
		Tracking Analyst	1	Version 1.0
		Custom Interface Routines	--	Avenue Scripts: MSSI serial RS-232 C++ Routines: ArcSecond DLL WhereNet SQL
	Microsoft	Microsoft Office	1	Excel spreadsheet
		Visual Studio, C++	1	Version 6.0
		NT Server 4.0	1	Service Pack 6
GFI	NFESC	Graphics Map	1	DXF Format

Figure 46. Test system architecture.

Data Interface

New ESRI C++ Routines

NT Operating System & Win 32 API Calls

ArcSecond RS-232 — TAPI → **ArcSec DLL** →

C++ DLL Calls & Sample GUI Set Origin

ArcSecond SDK
MS C++ Visual Studio

Custom Output Routine → **TCP-IP**

WhereNet EtherNet — TCP-IP ← Winsock →

ODBC Calls C++ Routine

WhereNet SQL 7.0 Server Database

Outer Event Loop
Cycles and Scans for Data
From ArcSecond and
WhereNet ODBC Calls and
Passes to Tracking Analyst

MSSI RS-232 — TAPI — **RS-232** →

Tracking Analyst
Direct Stream from MSSI
Configuration Files

Data to Graphics

ESRI Tracking Analyst

Data Streams to Multiple Tracks

RS-232 & ASCII Log File Input

MSSI   RS-232 Direct Stream

Multiple Themes: Multiple Tags

Track / Test Notes Annotations:

Data Entry Screen
on Primary Display
Attached to Data
Points for Notes

Master Log File
ASCII, All Data
Written Here
for Data Reduction

MS Excel
Annotations &
Post Experiment
Data Reduction

Map Display

ESRI ArcView

Tracks

Master Graphics Database
Forward & Reverse Playback
Tagged Data Attributes

All Data in Decimal Feet

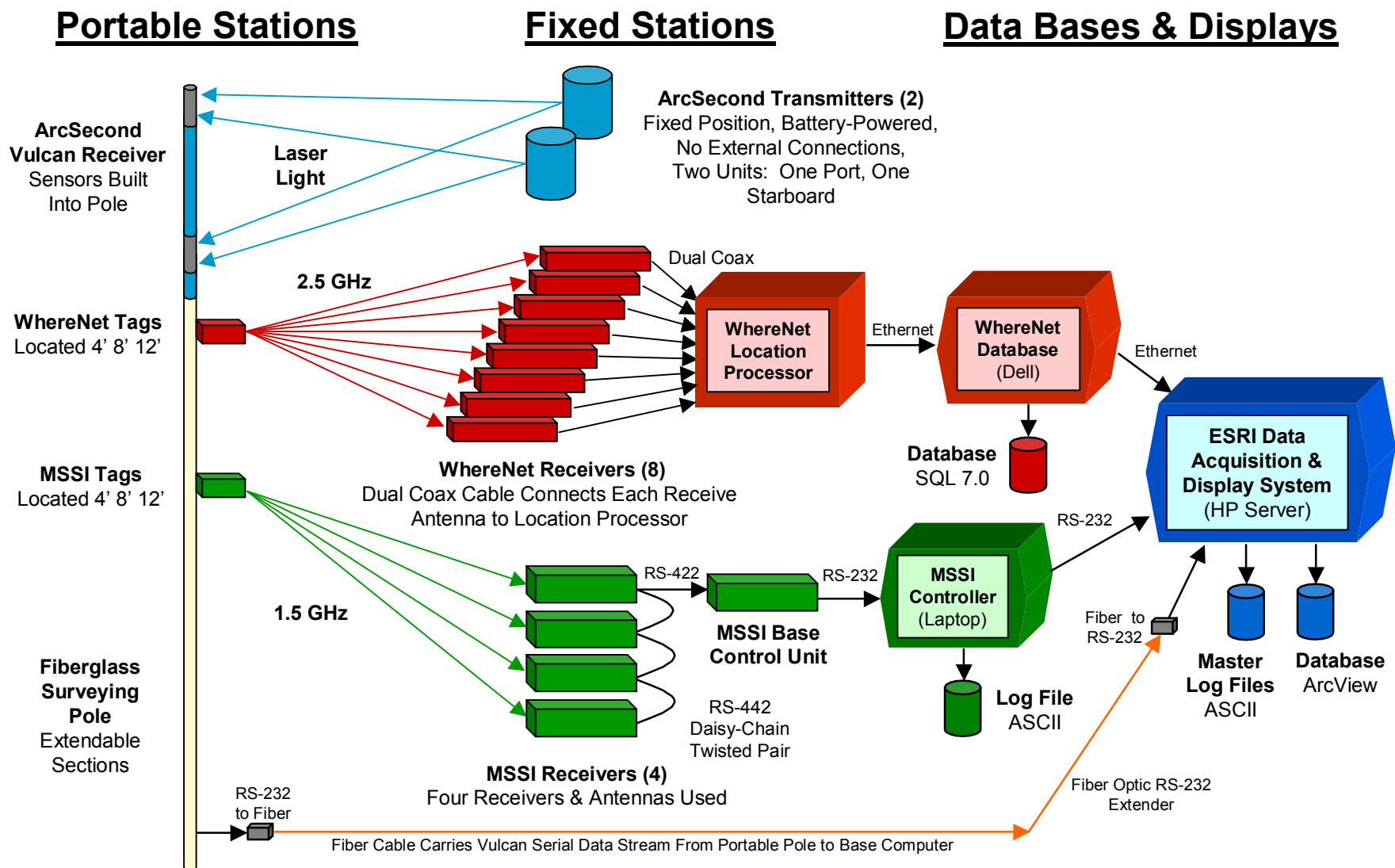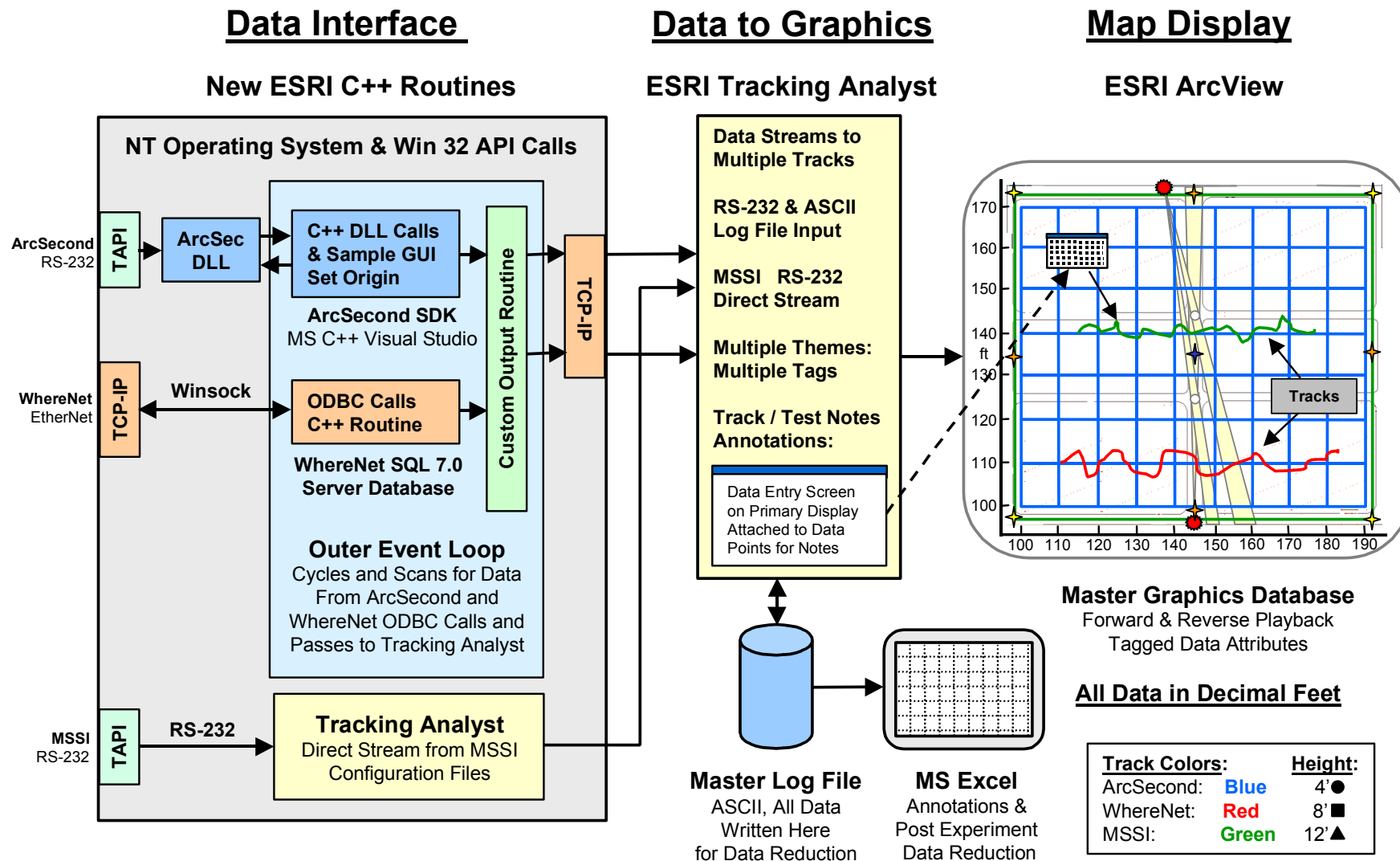| Track Colors:		Height:
ArcSecond:	**Blue**	4'●
WhereNet:	**Red**	8'■
MSSI:	**Green**	12'▲

Figure 47. Instrumentation system software architecture.

<u>Hardware and Software Interfaces</u>. The ESRI instrumentation system had three main components:

- Data Interface
- Data to Graphics Conversion and Recording
- Graphics Display and Databases

The data interface provided interfaces to each of the systems, receiving input in their native formats. The received data was converted to a consistent format and written into linear ASCII log files for archival storage and post data reduction. Data was then sent to the ESRI ArcView GIS system for near real time display. The objective was to merge all three inputs into one display to observe test progress, and guide focused investigations.

ArcSecond provided a Windows Dynamic Linked Library (DLL) and example C++ code to receive readings from the laser surveying system. It worked through a RS-232 serial port, which was extended by fiber-optic line drivers to the Pocket PC running matching ArcSecond software. The C++ routines provided calls to the DLL to access laser readings. The ArcSecond system was easy to work with, with mature drivers and sample software, which was compiled into the ESRI custom C++ routines.

WhereNet provided sample C++ routines to directly access streaming data from their interface manager. It acted much as a serial interface, but through a Transmission Control Protocol/Internet Protocol (TCP-IP) socket. This is the preferred approach by most of their customers as they have their own databases and did not want to use the Microsoft SQL server. We did not successfully make the streaming interface work and instead worked with SQL queries to the WhereNet database.

The MSSI system worked directly into ESRI tracking analyst through its streaming serial interface. ESRI wrote custom Avenue scripts to match incoming data formats. MSSI made a small change to their data formats to match the Avenue formats. This was the easiest interface as ESRI tracking analyst had native RS-232 streaming capability. MSSI provided both raw and averaged reports for each tag.

The ArcSecond and WhereNet routines were wrapped into an overall custom C++ program. It took the Arcsecond and WhereNet inputs and outputted them to Tracking Analyst in its formats. Tracking analyst received the three streams and wrote the inputs to log files and to ArcView. A capability to input and record notes to the log file was added for annotating the log files with test phases and immediate observations, e.g., system resets and test pauses. Tag reports were stored as separate themes.

Arcview provided the ability to selectively display individual tags as themes, and tracking analyst provided the ability to selectively view periods of times and as tracks with connected points. Tracks did not prove useful, cluttering the display with lines resulting from system pops and jumps. The 2D map display provided a powerful tool to watch test progress. The WhereNet system had similar capability.

Mary Canfield, NFESC, lead the instrumentation team. Figure 48 shows the ESRI instrumentation System and Figure 49 shows the instrumentation team with NFESC, ESRI, MSSI, and WhereNet.

<u>Objective</u>. The primary objective of the instrumentation system was to capture all data electronically. It would be done automatically and without human error.   The immediate objective was the visual interpretation of accuracy and trends, and to guide focused investigations in high error areas expected around corners and bulkheads. Instrumentation also helped determine system health.

Figures 50 and 51 show results from earlier MSSI tests with their transceiver system. They trace a path, although the ship test differs significantly. We expected similar results with tag reports visibly tracking sled movement and the grid. Actual results were significantly different.

Figure 48. ESRI instrumentation system.

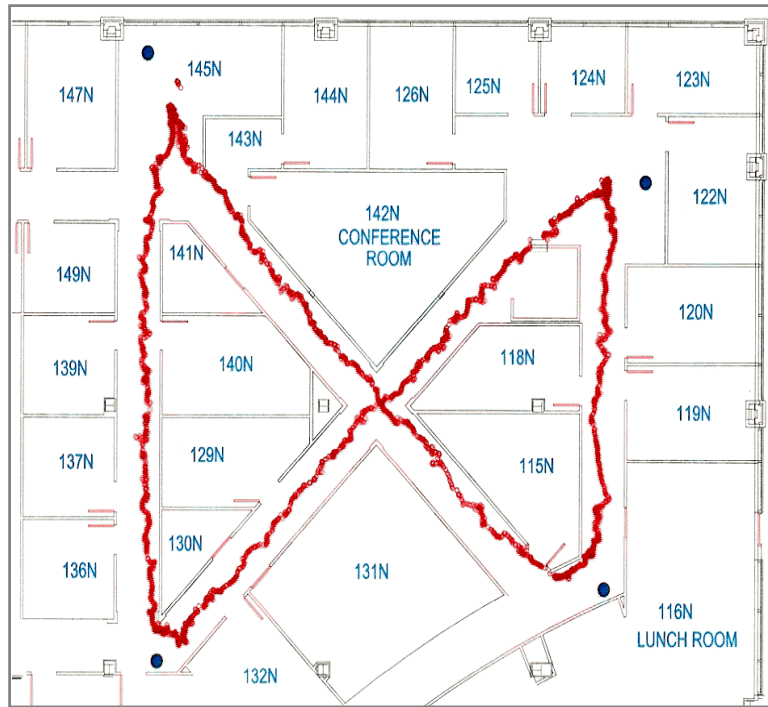Figure 49. Instrumentation Team (right to left): NFESC, ESRI, MSSI, and WhereNet.

Figure 50. MSSI tracks inside office spaces, transceiver system.
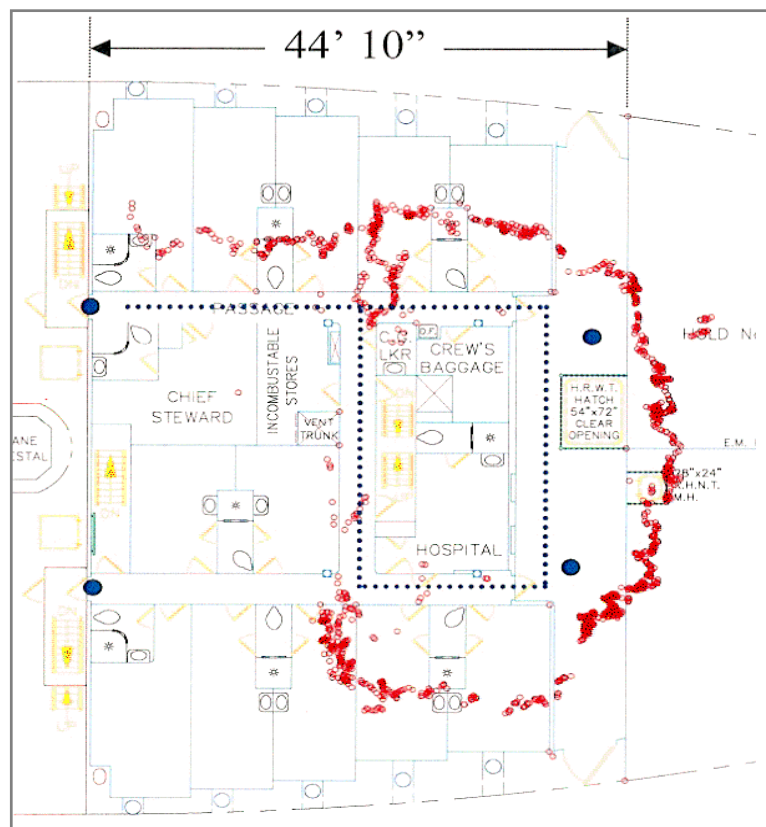(Used with permission from MSSI.)

Figure 51. MSSI tracks inside ship, transceiver system.
(Used with permission from MSSI.)

2.3   Test Identification

2.3.1   General Test Conditions

The test was divided into two primary phases: open space tests and container blockage experiments. They both used the same test box, test items and instrumentation system. Both systems were tested at the same time. The first phase was the primary test, and most of the effort was devoted to it. The second phase was more of an opportunity to use the installed test and instrumentation systems to explore operational issues in a more realistic environment.

The first phase, open space, moved tags around on a sled throughout the test box. The variables were number of antennas (WhereNet) and tag location in three dimensions. The tests had closed overhead hatches, but one test with open hatches was planned. Focused investigations in high error areas (expected around bulkheads and corners) were also planned.

The second phase, blockage, placed tags on containers and vehicles and measured their locations in static settings. The primary variable again was tag location, but added how many containers were in the test box. Vehicle orientation tests were performed at the same time. Tags were placed on the four corners of the vehicles, but the vehicles were not moved.

A third phase by USC was performed to characterize the test environment. They used the same test box, but also performed measurements between major compartments and in a container. USC brought their own equipment and did not use the NTAV test and instrumentation system. Their primary goal was to measure the delay spread, or reverberation character of the open spaces. The single most important measure was reverberation decay time.   USC tests were performed in 1 day at the end of the first week.

2.3.2   Test System Operation

Both test systems and the laser system operated similarly. For the first week, the tags and laser receiver were co-located on the same test sled and moved together over the test box gridlines. The test sled was manually moved, pausing at major 10-foot intersections long enough for all tags to report, figure 23. For the second week test, tags were placed on containers loaded in the test box, Figure 52. The laser surveying system was moved to make manual tag location measurements.

The systems automatically reported their positions concurrently and were automatically recorded by the instrumentation system, Figure 53. Except for the manual sled movement and manual surveying the second week, measurement was fully automatic, with no human input. For the first week, annotations were made at grid intersections to help identify stopping locations for data reduction. Second week laser surveying measurements were manually recorded.

The tags and laser system reported periodically. Tag blink rates were set similarly, WhereNet blink rates were adjustable and 4 seconds is their default. The MSSI blink rate was fixed at 5 seconds. Tag blinks were random to avoid collisions, thus times are approximate. The laser system reported 10 times more frequently than the tags and was periodic. Table 8 lists the tag and laser report rates.

Table 8. Tag and Laser Report Rates

Vendor	Seconds/Blink or Reading
WhereNet	4 sec (approx)
MSSI	5 sec (approx)
ArcSecond	0.5 sec (2/sec)

Figure 52. Second Week Testing: Tags on containers and HMMWVs.
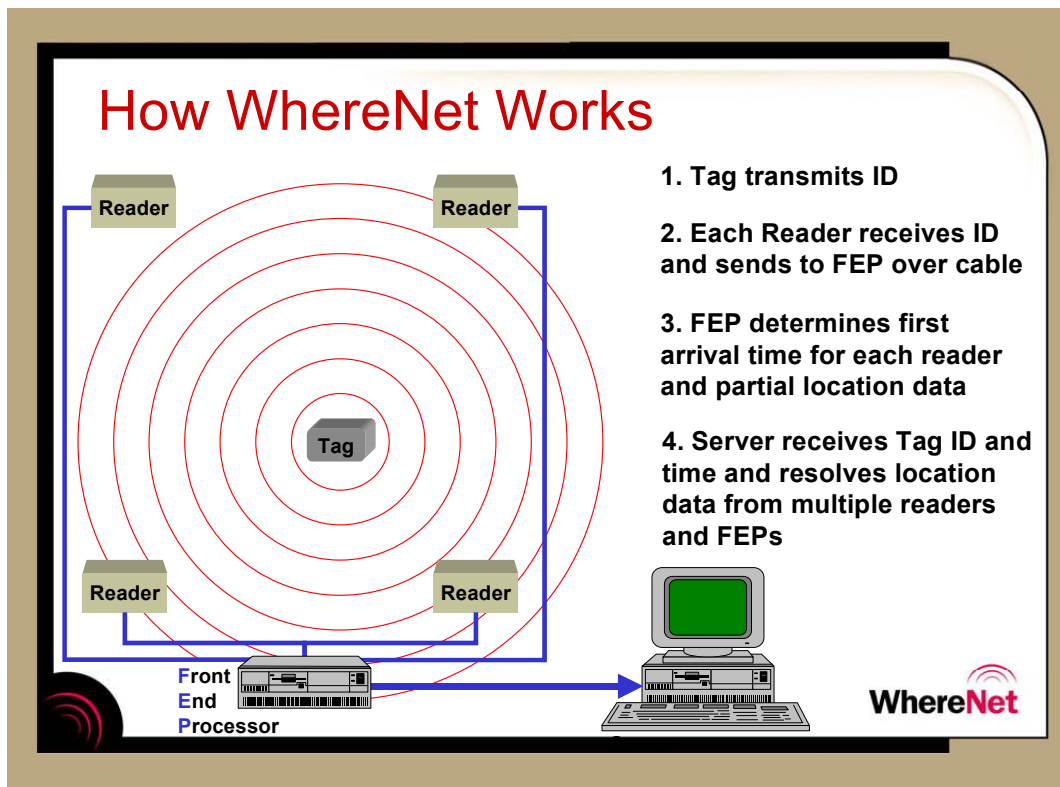
Figure 53. WhereNet automatic tag reports.
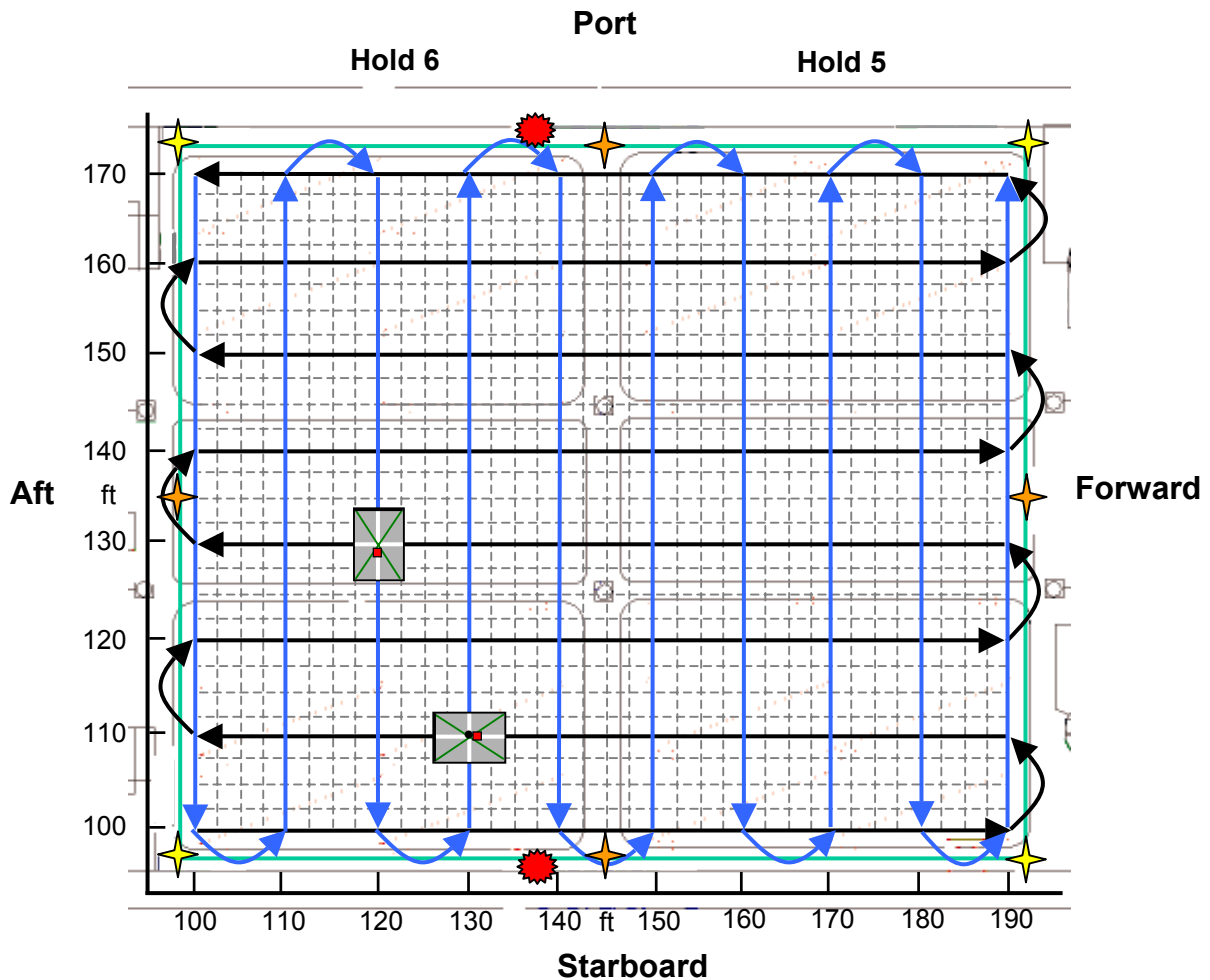
Figure 54. Test sled movement.

2.3.3   Test Procedure

Figure 54 shows the test sled movement pattern for the first week test. The test sled was first moved from aft to forward, back and forth tracing the "X" axis over the major grid. The test started at 100/100 in the aft/starboard corner and moved forward. Sled orientation was maintained so the tags faced forward for a consistent offset. The next row up, the sled moved backward. The "X" row trace stopped at 100/170 in the aft/port corner.

The sled was then turned and traced the "Y" axis. The "Y" axis trace started in the same 100/170 aft/port corner. Sled orientation was maintained so that the tags faced starboard for a consistent offset. The "Y" column trace stopped in the 190/170 forward/port corner. The sled was occasionally backed up and moved to untangle the fiber optic cable around the stanchions.

The sled had "cross hairs" on the bottom to help align the sled to the grid. This was used to help the humans and was not primary determination of sled position. The laser system performed actual position measurements. The sled dwelled at major 10-foot intersections long enough for all of the tags to report. Two men operated the sled and adjusted the pole for vertical position at each intersection.

2.3.4   Error Budget

The ArcSecond laser receiver was mounted at the top of the pole. The sled pole was much longer than specified by ArcSecond, 11- to 12-foot pole extension, resulting in a possible 1/2-inch error at the pole tip. This was mitigated by the vertical alignment of the pole. The error was reduced by the *sin (θ)* of the vertical angle. Perfectly vertical would fully cancel the error, 1 degree would reduce it to 1.75% or 0.01-inch at the pole tip. Comparison tests using the hand-held wand confirmed the calculations.

Tags were assumed vertically aligned above each other. Vertical misalignment caused tags to be horizontally offset from the tip, producing an error. Figure 55 shows vertical misalignment. One degree produced 0.84-inch horizontal error every 4 feet, for 2.5-inch total over 12 feet. The pole was kept within 1 degree.

The ArcSecond PDA software also needed to be modified to allow for the longer pole length. The pole was removed from the test sled and touched to reference index points on the grid to calibrated the sled pole to the grid. Tag heights were set for the pole mounted on the sled. WhereNet assumed a 4-foot tag height.
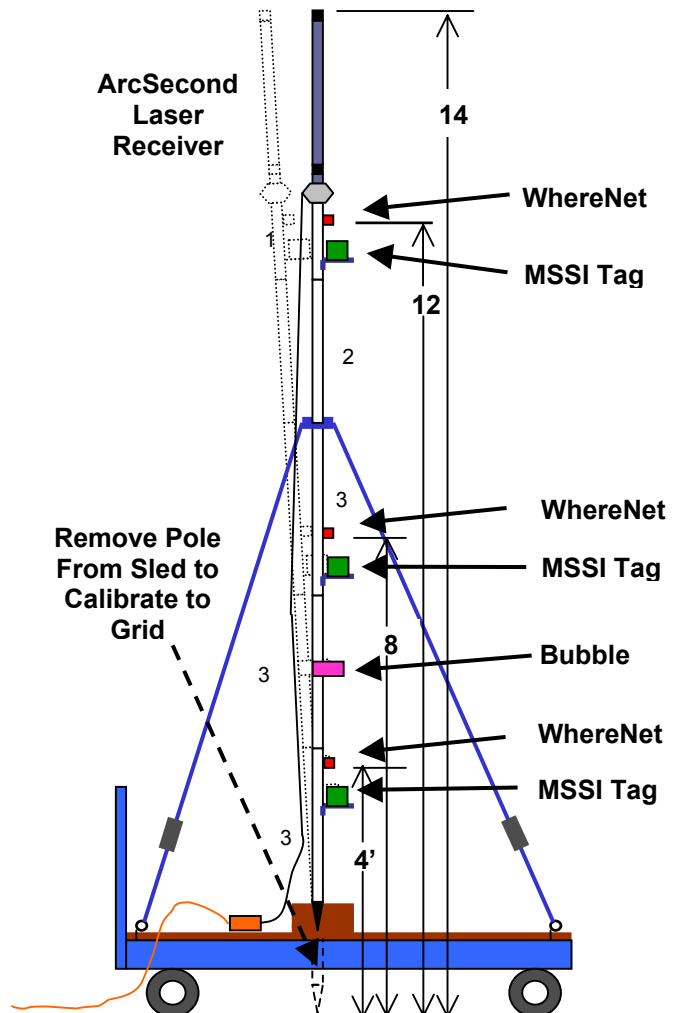

Figure 55. Test sled vertical misalignment.

2-39

2.3.5   Planned Tests

The planned testing was divided into multiple phases. Table 9 provides a summary of the planned and actual tests.

Table 9. Planned and Actual Tests

Major Phase	Hatches	Antennas		Containers & HMMWV	Grid (ft)	Date	
		WhereNet	MSSI			Planned	Actual
Open Space	Closed	4	4	N/A	10	9/27a	9/27p-28a
	Closed	8	4	N/A	10	9/27p	9/28a-p
	Open	8	4	N/A	10	9/28a	N/A
1st Week	Focused Investigation			N/A	2.5	9/28p	N/A
USC	Closed	N/A	N/A	1 in Hold 3	N/A	9/29	9/29
Container Blockage & Vehicle	Closed	8	4	22 / 4	N/A	10/03	10/03
	Closed	8	4	16 / 4	N/A	10/04	10/04
	Focused Investigation			16 / 4	N/A	10/05	10/05

Open Space Tests. The first week testing focused on open space testing for system accuracy measurements and USC's RF environment characterization. The second week testing focused on container blockage and vehicle orientation testing. Open space testing was divided into two comparisons: 4 and 8 WhereNet antennas and closed and open overhead hatches.

The 4 WhereNet/4 MSSI antenna test provided a comparable configuration between WhereNet and MSSI with the same number of antennas. Four antennas was the minimum configuration for operation for both systems. WhereNet experienced frequent partial reads (heard but no location) and a few full dropouts (not heard) with 4 antennas. WhereNet's recommended configuration was 8 antennas per space and the last closed hatch and subsequent tests used 8 WhereNet antennas. WhereNet had consistent reads without dropouts or partial (no location) reads with 8 antennas.

Closed hatches would have the worst case multipath and open hatches would allow RF to escape vertically. One objective was to compare closed and open hatches to see if locations changed or system accuracies improved. The open hatch test was to be run early in the day to take advantage of expected marine layer overcast. The objective was to keep direct sunlight off the ArcSecond system. No problems were found with ArcSecond in direct sunlight. The previous 4 and 8 antenna closed hatch tests continued into the morning of the second day, delaying the open hatch test until the afternoon. The open hatch test was not completed.

Focused investigations on minor grids were planned to look at interesting areas resulting from the first three tests. It was anticipated that errors would increase near bulkheads and in corners, and that focused investigations would be run with finer grid spacing to explore error trends. Focused investigations were not done, as no consistent offsets or trends were discovered during the first three tests.

The test sled paused at 4 locations for extended periods during the 8 WhereNet antenna closed hatch test at various locations within the test box. These were considered focused investigations for convergence analysis for the WhereNet system. WhereNet had fairly random stochastic errors, with data points "bouncing" randomly around within their error circle during measurments. The objective was to average larger data sets to see how accurate the WhereNet system was over a long-term average.

USC setup and ran their tests on Friday, 29 September. We originally planned to do the USC tests on Friday and Saturday, but the ship was not available on Saturday. This required us to compress the schedule and USC was not able to run all of their planned tests. They focused on the essential tests. USC was able to run five open space tests and one container test in 1 day.

Figure 56 shows the planned open space tests. The time for each test allowed for the time to move and pause the test sled at each major intersection. The grid had 80 major intersections and 1 minute was allowed for each stop, for a total of 1 hour 20 minutes. The grid was traced in both the "X" and "Y" directions, for a total of 2 hours 40 min per test. The path length for the sled was about 1/4-mile. This limited the total number of major tests to two per day.

SS Curtiss Planned Open Space Test Schedule																
Phase	Open Space								Focused Investigation							
Day	Wed 9/27								Thurs 9/28							
Hour	8	9	10	11	12	13	14	15	8	9	10	11	12	13	14	15
Major Vertices, 10 ft Closed Hatches																
System Turn On	▬															
4 Corner Antennas		▬	▬	▬												
8 Antennas					▬	▬	▬									
Secure Equipment							▬									
Major Vertices, 10 ft Open Hatchs																
System Turn On									▬							
8 Antennas										▬	▬	▬				
Minor Vertices, 2.5 ft Closed Hatches																
8 Antennas													▬	▬	▬	
Secure Equipment																▬

Figure 56. Planned open space test schedule.

The first test with 4 WhereNet and 4 MSSI antennas had various technical and system problems. The ship started a scheduled generator test at 10 AM, knocking all of the computers off line. It took a while to get everything working again. The first test was rerun in the afternoon of the first day.

The first test took longer than planned, extending into the morning of the next day. The sled pole was more difficult to keep vertical than expected. Subsequent tests went faster than planned, with greater experience handling the sled and instrumentation. After the first test, paths were run in less than an hour, less than 2 hours total for both "X" and "Y" paths.

Container Blockage Tests. The second week testing focused on container blockage and vehicle orientation testing. Overhead hatches were closed for worst-case multipath. Both systems operated with their maximum antenna configurations of 8 WhereNet and 4 MSSI antennas. Blockage testing was divided into two comparisons: double-high and single-high containers. Vehicle orientation tests ran concurrently with the container tests. Four WhereNet tags were placed on each HMMWV, on the four corners. The HMMWV were not reoriented during the tests.

Figures 57, 58, 59, 60, and 61 show the container load locations and configurations. Containers were placed in normal stowage positions in two rows in the middle the cargo hold, leaving clear space around the stack of containers. This allowed the antennas to view the stack without containers immediately in front, blocking view. This gave the systems a chance of success in reading and locating outside facing tags.

An aisle was created between the container stacks, providing an area blocked from direct view of the antennas for double high stacks. The two missing containers in the double stack allowed some of the tags inside the aisle to be seen by facing antennas. Single-high containers allowed antennas to look over containers and see tags facing them. Tags facing away could not be directly seen, but could be seen by reflections in the facing containers.

Containers were first stacked two high with container doors facing outward. Two of the containers in the middle of the top layer could not be placed, reducing the total containers to 22 instead of 24. The center aft overhead hatch over Hold 6 could not be opened as a large heavy generator sat on top of the hatches and could not be moved. One day was required to load 22 containers.

Tags were placed on the containers and tag locations measured the second day. Four WhereNet tags were placed on each container, two on each end, on the doors and the backs, 88 tags total. Velcro tape was used to mount the WhereNet tag cups and tags were placed in the cups. Tags were oriented with the logo and serial number at the top. MSSI tags were placed vertically on top of containers and HMMWV.

Figure 62 shows a plan view of container and tag locations with reference numbers. Figures 63 and 64 show and elevation and front and rear faces of the first row of containers with container and tag locations. Table 10 lists WhereNet tag locations and Table 11 lists MSSI tag locations. Figure 52 shows tags installed on container doors and HMMWV and measurement with the ArcSecond system. Figure 65 shows tags installed on containers in the aisle.

Tests were automatically run by the WhereNet system at 1600 PST after leaving the ship for the day. About 50,000 records, or about 1-hour of data was automatically recorded with 500 to 900 reports per tag. Two MSSI tests, morning and afternoon, were run and recorded during each day. The top layer of containers was removed on the third day and the containers and tags placed outside the ship on the wharf. The WhereNet system again automatically ran measurements at 1600 PST and recorded 50,000 records. Two additional MSSI tests were run on the third day, morning and afternoon.

Focused investigations were run the third and fourth day. WhereNet tags were placed on top of the single stacked containers and read more accurately. WhereNet tags were then placed on the sides at container top edges and also read more accurately than on sides. Optimum tag location was on top, but is not practical because of container stacking, and potential damage to tags. An MSSI tag was changed from vertical to horizontal orientation, and reported location changed markedly, Figure 65.

Two WhereNet forward corner antennas, Nos. 3 and 5, were moved aft from the corners to change them from co-linear alignment on the forward wall, to staggered in both dimensions, Table 3. Tags on the forward most container faces and HMMWV then read more accurately in the "X" axis.
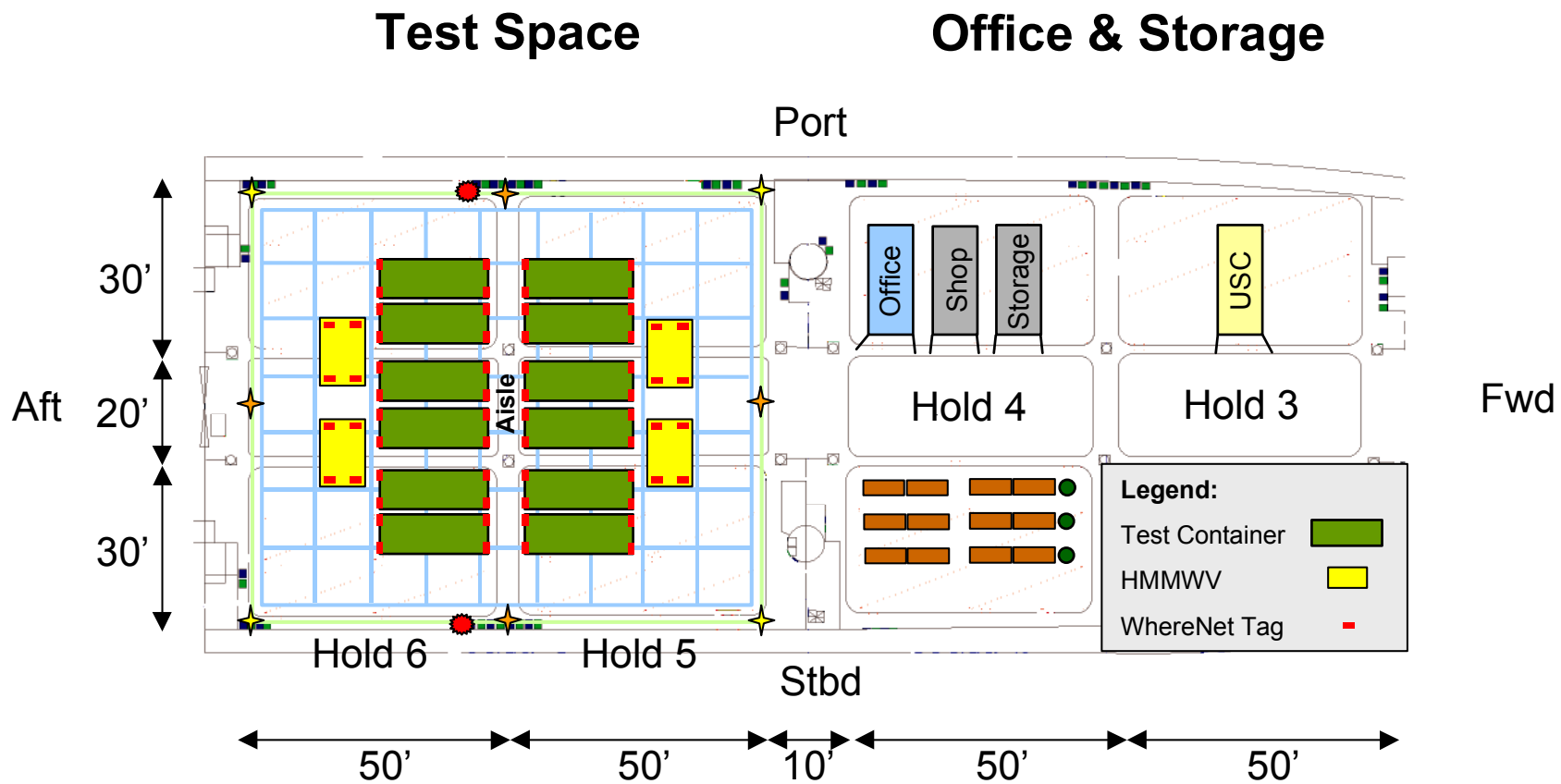
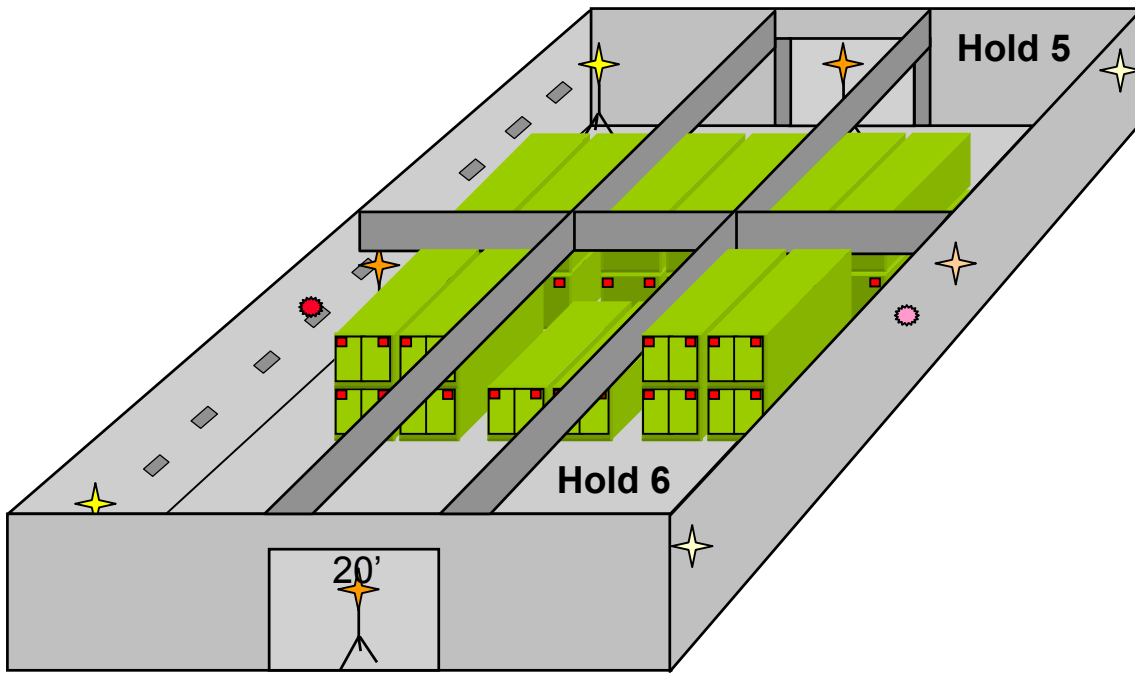Figure 57. Container and HMMWV set ups with tag locations.

Figure 58. Double-high stacked containers (22) with tag locations (88).
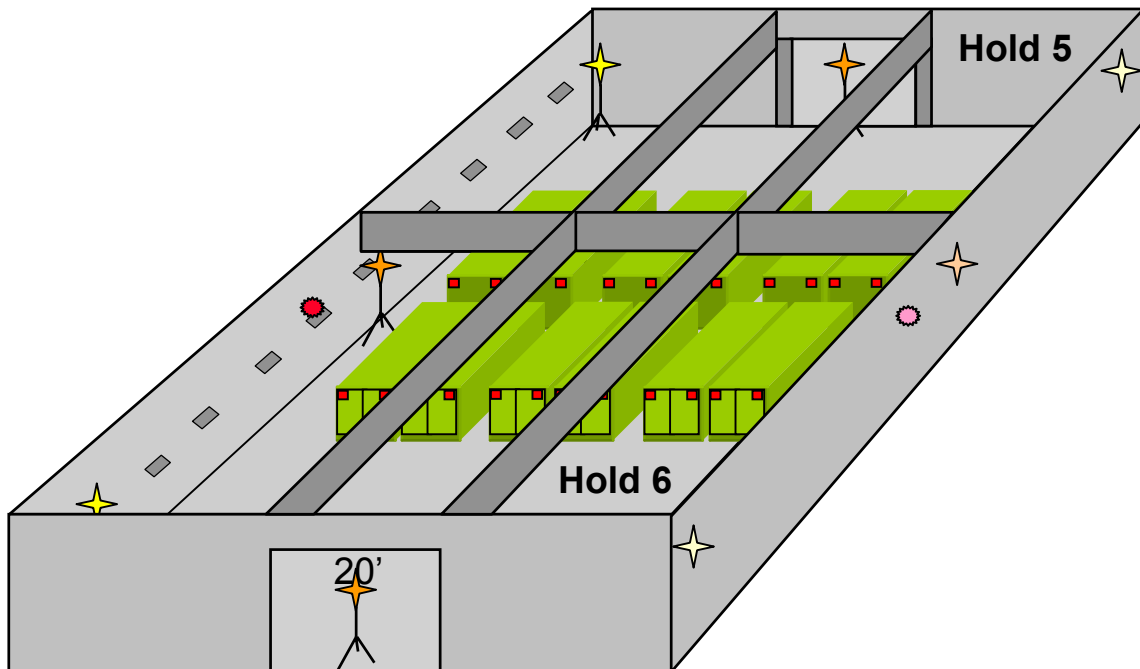

Figure 59. Single-high containers (12) with tag locations (48).

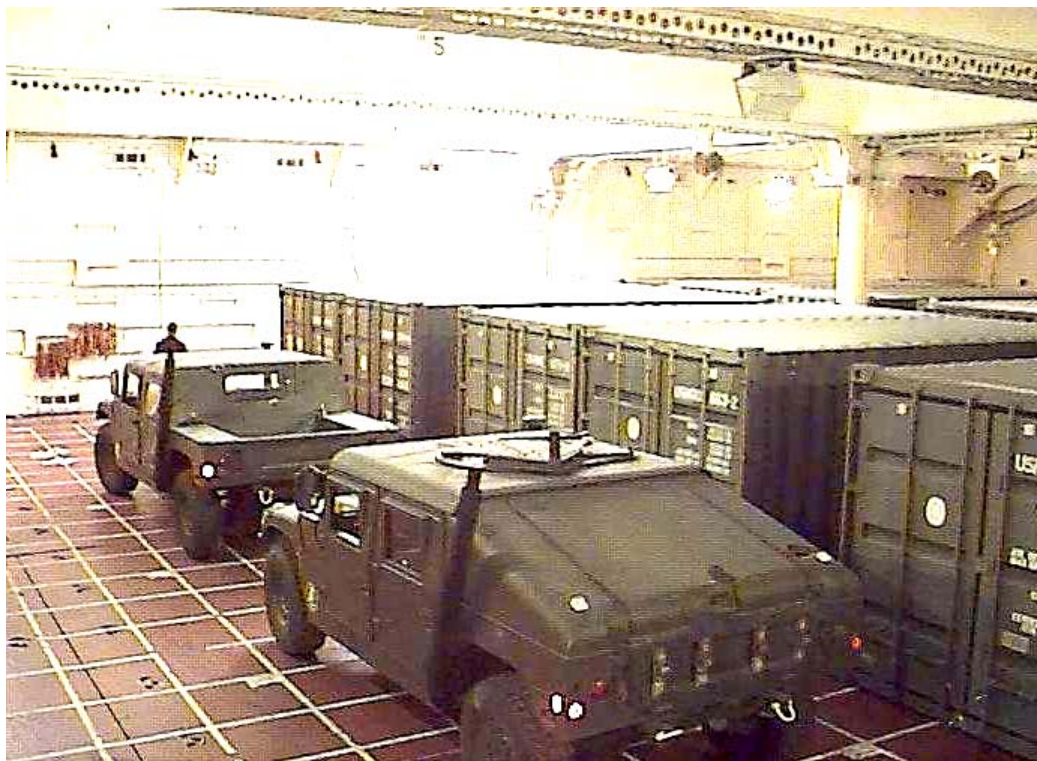Figure 60. Double-high container stack and HMMWV.

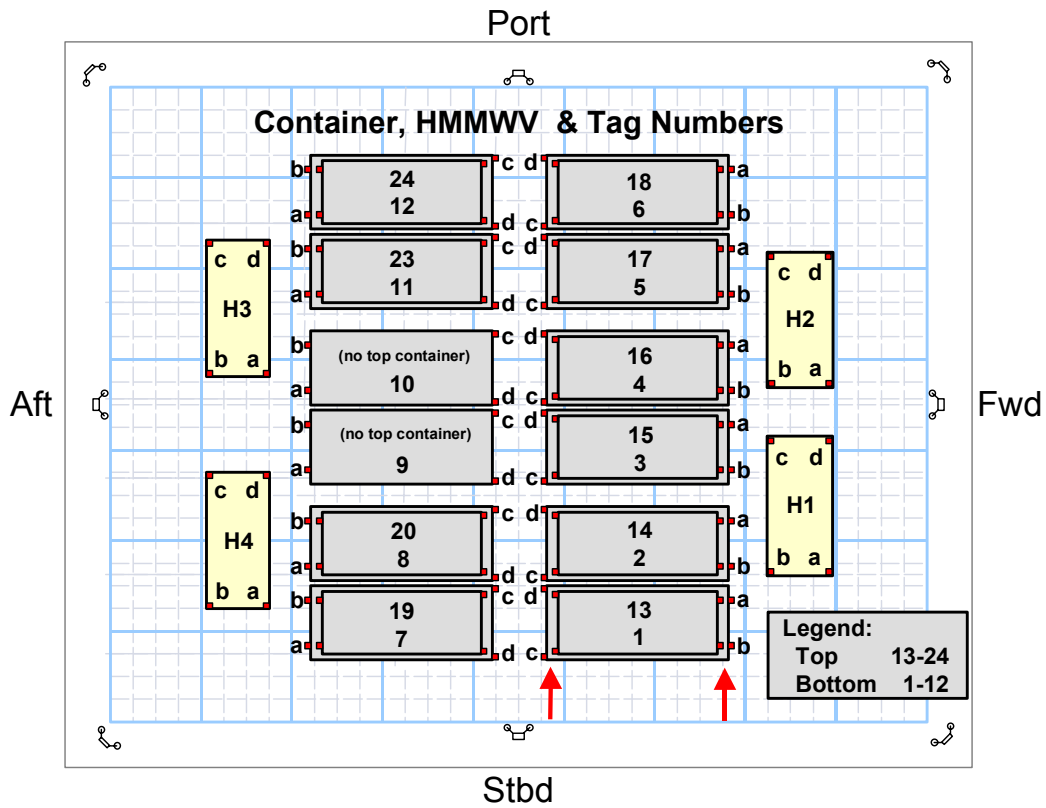Figure 61. Single-high container stack and HMMWV.

Port

Container, HMMWV & Tag Numbers

Aft

Fwd

b	24 / 12	c d	18 / 6 a
a		d c	b

H3 (c d / b a)

b	23 / 11	c d	17 / 5 a
a		d c	b

H2 (c d / b a)

b	(no top container) 10	c d	16 / 4 a
a		d c	b

b	(no top container) 9	c d	15 / 3 a
a		d c	b

H4 (c d / b a)

H1 (c d / b a)

b	20 / 8	c d	14 / 2 a
a		d c	b

b	19 / 7	c d	13 / 1 a
a		d c	b

Legend:
Top   13-24
Bottom   1-12

Stbd

Figure 62. Plan View: Container, HMMWV, and tag locations and numbers.

Front Looking Aft   **ArcSecond Laser Transmitter**   7ft

b a 13	b a 14	b a 15	b a 16	b a 17	b a 18
b a 1	b a 2	b a 3	b a 4	b a 5	b a 6

15ft 10in / 11ft

70 ft
80 ft
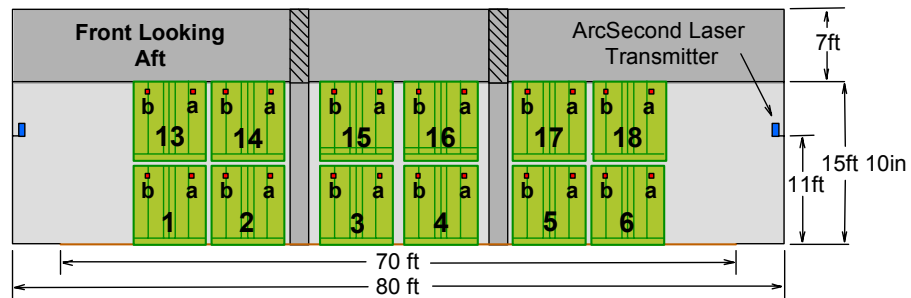
Figure 63. Elevation View: Forward face containers and tag locations.

Aisle Looking Fwd   **ArcSecond Laser Transmitter**   7ft

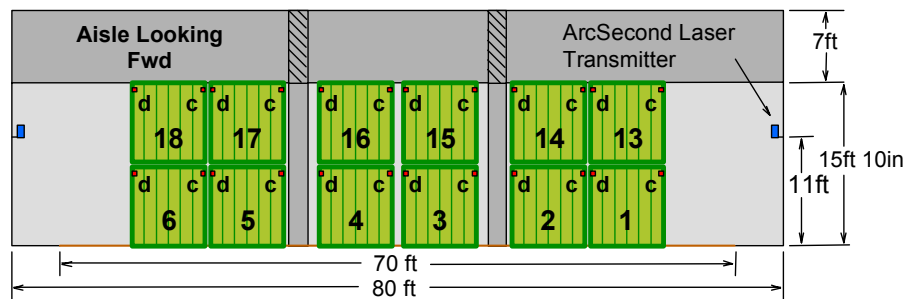| d c 18	d c 17	d c 16	d c 15	d c 14	d c 13
d c 6	d c 5	d c 4	d c 3	d c 2	d c 1

15ft 10in / 11ft

70 ft
80 ft

Figure 64. Elevation View: Inside face containers and tag locations.

Table 10. WhereNet Tag Locations and Containers

Tag Number	Tag ID	Measured Locations (ft)			Tag Number	Tag ID	Measured Locations (ft)		
		X	Y	Z			X	Y	Z
1a	111949	167.8	113.5	107.6	13a	67306	167.8	113.5	115.4
1b	112122	167.7	108.3	107.1	13b	67313	167.8	108.1	115.4
1c	105849	148.0	107.3	107.3	13c	115943	148.0	107.3	115.5
1d	112043	148.1	114.7	107.2	13d	115955	148.1	114.7	115.5
2a	67335	167.9	121.9	107.0	14a	67274	167.9	121.9	115.1
2b	67338	167.9	116.6	107.1	14b	67293	167.9	116.8	115.4
2c	122290	148.2	115.4	107.4	14c	67296	148.2	115.4	115.5
2d	112061	148.2	122.9	107.3	14d	67336	148.2	122.9	115.5
3a	115985	167.7	133.1	107.1	15a	67343	167.7	133.0	115.4
3b	115986	167.6	128.2	107.0	15b	111912	167.6	128.2	115.4
3c	120533	147.9	127.2	107.3	15c	112003	147.9	127.2	115.5
3d	120536	148.0	134.5	107.2	15d	112365	148.0	134.5	115.0
4a	120516	167.6	141.4	107.0	16a	67331	167.6	141.4	115.3
4b	120519	167.6	136.5	107.0	16b	67334	167.6	136.6	115.3
4c	120537	147.9	135.2	107.3	16c	67357	147.9	135.2	115.5
4d	120542	147.9	142.7	107.3	16d	115995	147.9	142.7	115.5
5a	120094	167.6	151.7	107.0	17a	120090	167.6	153.2	115.3
5b	120092	167.7	148.3	107.0	17b	120526	167.7	148.0	115.3
5c	120096	147.9	146.9	107.2	17c	120529	147.9	146.9	115.5
5d	120103	147.9	154.3	107.1	17d	120552	147.9	154.3	115.5
6a	67354	167.8	161.9	107.0	18a	120065	167.8	161.6	115.4
6b	120085	167.8	156.4	107.0	18b	120075	167.8	156.6	115.4
6c	115956	148.0	155.1	107.2	18c	120080	148.0	155.1	115.5
6d	115969	148.0	162.6	107.4	18d	120088	148.0	162.6	115.5
7a	115333	122.4	108.3	107.1	19a	67350	122.4	108.0	115.0
7b	120527	122.4	113.3	107.1	19b	67369	122.4	113.8	114.8
7c	120544	142.1	114.7	107.3	19c	120106	142.1	114.7	115.5
7d	120553	142.2	107.2	107.2	19d	120109	142.2	107.2	115.5
8a	68133	122.4	116.7	107.1	20a	115952	122.4	116.7	114.9
8b	120522	122.4	121.8	107.1	20b	120097	122.4	121.8	114.8
8c	120540	142.1	123.1	107.2	20c	120098	142.1	123.1	115.5
8d	68108	142.2	115.7	107.2	20d	120102	142.2	115.7	115.5
9a	67363	122.3	128.0	107.1	21				
9b	120523	122.3	133.1	107.1	21				
9c	120528	142.0	134.4	107.2	21				
9d	120531	142.0	126.9	107.2	21				
10a	120052	122.3	136.5	107.1	22				
10b	120104	122.3	141.6	107.1	22				
10c	120111	142.0	142.8	107.2	22				
10d	122243	142.0	135.4	107.3	22				
11a	120112	122.2	148.2	107.1	23a	120072	122.2	148.1	115.4
11b	122249	122.2	153.2	107.1	23b	120082	122.2	153.2	115.4
11c	122254	141.9	154.4	107.2	23c	120084	141.9	154.4	115.5
11d	122281	141.9	147.0	107.1	23d	120105	141.9	147.0	115.5
12a	115899	122.3	156.6	107.1	24a	120057	122.3	156.3	115.4
12b	115919	122.3	161.6	107.1	24b	120064	122.3	161.5	115.4
12c	115981	142.0	163.0	107.2	24c	120076	142.0	163.0	115.5
12d	116001	142.0	155.5	107.2	24d	122252	142.0	155.5	115.5

Table 10. WhereNet Tag Locations and HMMWV (continued)

Tag Number	Tag ID	Measured Locations (ft)			Tag Number	Tag ID	Measured Locations (ft)		
		X	Y	Z			X	Y	Z
H1a	120532	179.1	116.9	103.8	H3a	68090	117.2	139.0	103.7
H1b	120534	173.0	116.7	103.8	H3b	69307	111.1	138.8	103.7
H1c	120545	173.0	131.0	104.3	H3c	120117	110.9	152.2	104.9
H1d	120551	178.9	130.6	104.3	H3d	122320	116.7	152.4	104.9
H2a	68089	178.9	137.7	103.7	H4a	115926	117.6	113.3	103.6
H2b	122248	174.7	137.4	103.7	H4b	115977	110.6	116.5	104.9
H2c	122323	172.8	151.1	105.0	H4c	112074	111.5	126.7	104.9
H2d	122330	178.7	151.4	104.9	H4d	112348	117.4	126.8	104.9

Table 11. MSSI Tag Locations, Containers, and HMMWVs

Test Number	Tag ID	Measured Locations (ft)		
		X	Y	Z
A	77	178.5	121.5	108.0
	201	142.0	127.5	105.0
B	41	112.5	150.0	105.0
	77	178.5	121.5	105.0
	161	167.5	160.0	116.5
	167	142.0	156.0	116.5
	201	122.5	130.0	108.0
C	13	168.0	160.2	108.0
	41	111.9	147.9	105.0
	77	178.5	121.5	105.0
	167	148.0	135.8	108.0
	201	122.4	130.4	108.0
D	13	168.0	160.2	108.0
	41	111.9	147.9	105.0
	77	178.5	121.5	105.0
	167	148.0	135.8	108.0
	201	122.4	130.4	108.0

Figure 65. WhereNet tags and horizontally polarized MSSI tag inside aisle.

This page left blank.

3.0   DATA REDUCTION AND ANALYSES

3.1   Objectives

The objectives of the data reduction for the first week were to answer the three primary questions:

- Did the test systems work in an all-metal shipboard environment?
- Were there dead zones and dropouts resulting from multipath?
- What were the resulting accuracies?

The first question was answered aboard ship during the testing, both systems worked in empty cargo holds. The next two questions were the primary focus of the data reduction effort.

The objectives of the data reduction for the second week were to answer two questions:

- What were the effects of blockage by containers?
- What were the optimum tag and antenna locations?

Initial observations aboard the ship during testing indicated reduced accuracy with containers. Limited experiments with different tag locations and orientations, and moving antennas from co-linear alignment on the forward wall, were tried and appeared to improve accuracy.

Data reduction for the first week was more difficult by needing to correlate reported tag positions with the reference laser system. Data sets were relatively small due to using only three tags per system. Both MSSI and WhereNet datasets had approximately 2,000 to 5,000 records each for each test. Data reduction for the second week was simpler as tag locations were relatively static, and did not need to be correlated to laser measurements. The second week WhereNet data had a large number of data points due to the larger number of tags (104 versus 6). WhereNet data sets had 50,000 records for each test.

The primary output was graphical plots. It was the most effective means of presenting and "reducing" the data as trends became visually apparent. 2D map plots were used during the tests to look for trends and consistent offsets to direct focused investigations. None were found during tests.   Trends, however, emerged out of data reduction.

3.2   Data Sets

The data reduction was limited to the available recorded data sets. Unprocessed receiver data from both systems was not recorded, and was not available. The recorded data and analyses follow each system's internal location processing algorithms and system outputs. The MSSI system provided both raw time-stamped and running average tag reports. Total system accuracy, with both system hardware and software was evaluated.

The first three open space data sets were used for analyses. Test 1, "X" axis traverse, was the first complete run. It crossed the laser "banana" zone thus had greater reference error. It was filtered to only include stops at intersections. Tests 2 and 3 traversed the "Y" axis and avoided the "banana" zone and had better reference error. Tests 2 and 3 provided matched sets of tests to compare 4 and 8 WhereNet antennas.

The second week data was limited to each day's data snapshots. WhereNet snapshots were taken at 1600, and MSSI snapshots were taken in the morning and afternoon of each day.

3.3   Approach

3.3.1   Empty Cargo Hold, 1st Week

The technical approach for the data reduction for the empty cargo hold first week testing was:

- Gather data into data sets
- Filter data into groups
- Correlate valid tag reports with laser data
- Calculate differences and perform statistical analyses
- Display data in an easy to interpret fashion
- Investigate trends, error character, and convergence

Gather Data: The data was gathered, merged, identified, and organized. The data from all three sources (ArcSecond, MSSI, and WhereNet) was merged into ArcView and Excel data sets. ArcSecond and MSSI data were already merged as they were input through the ESRI data instrumentation routines. Both ArcSecond and MSSI data existed in both ASCII and ArcView formats. WhereNet data was merged with the ArcSecond data to create its data set. WhereNet data was in MS SQL Server 7.0 format and extracted Excel spreadsheets and merged in Excel. WhereNet data in Excel was then imported into ArcView.

Both ArcView and Excel formats were used for different filtering and plotting processes. Excel's format was the most portable between the various systems, including MS SQL 7.0 used by WhereNet. Excel was used for filtering, correlation, statistical analyses, and plots. ArcView/Tracking Analyst was used for 2D map plotting and presentation. It also visually aided the filtering process.

Filter Data: The second step was to filter and identify data points into the following categories:

MSSI and WhereNet Data:

- Missing Data (report expected and not received, i.e., drop outs)
- Incomplete Reports (heard but no location)
- Range Clips (MSSI)
- System Instability/Failure Data (MSSI)
- Good Data (within 20 feet)
- Pops and Jumps (greater than 20 feet)

Laser Data:

- Good Reference Laser Data
- Missing Data (caused by stanchion blockage, dead batteries, system resets, and cables)
- Banana Zone (incorrect "Y" axis reading between transmitters)
- Static Test Sled (for convergence analysis)

Automated processes were used as much as possible to filter the data. Automated filters identified missing data, incomplete reports, and range clips because of their easy rules. Missing tag reports were manually filled in. Manual review and marking was needed for groups of data, particularly system instability/failure.

Missing tag report data was identified by calculating the time difference between tag reports and sorting by time difference. Longer than average durations indicated missing tag reports. The differences between tag reports were plotted on histograms to determine the number and period of dropouts. Dropouts showed up as "harmonics" in the plots. Partial dropouts (heard but no location) were easy to identify and correlate with laser reports as they had a time stamp. Both full and partial dropouts occurred with 4 WhereNet antennas, and no full and a few partial dropouts occurred with 8 WhereNet antennas.

The MSSI system had frequent system problems, requiring system reset approximately every 10 minutes. Unstable system data was identified visually, using ArcView plots, as the data usually clumped in one area. MSSI system restart was also noted in the ESRI log file and notes. MSSI also had numerous pops and jumps, well outside the majority of errors. MSSI also clipped the out of range data to the test box limits (Test 1), then to the ship hull boundary (Test 2). MSSI clips were discarded from analyses. The objective was to separate MSSI system problems from environmental factors.

Automated Filters:

- Missing Data (report expected and not received in time window, i.e., drop outs)
- Incomplete Reports (heard but no location, WhereNet)
- Pops and Jumps (MSSI: $\geq$ 20 feet)
- Range Clips (MSSI)
- Missing Laser Data (caused by stanchion blockage, resets, batteries)

Manually Filter:

- System Instability/Failure Data (MSSI)
- Laser Banana Zone (incorrect: "Y" axis reading between transmitters)
- Static Test Sled (for convergence analysis)

The laser data likewise needed to be filtered. Missing data caused by stanchion blockage prevented correlation with the other systems, requiring their matching data points to be discarded from analyses. Missing laser data was easy to identify with very large reported numbers. The "banana" zone was treated much the same as a (MSSI) system instability and was visually identified in ArcView. The "banana" zone "X" coordinate may have had high accuracy, whereas the "Y" coordinate clearly had error. The "banana" zone was largely avoided by using only "Y" axis traverses for analyses.

Offsets were calculated to adjust and align the data between the three systems. The MSSI system reported time 3 hours off Eastern Standard Time (EST) for the other two systems Pacific Standard Time (PST). Minutes and seconds were set within a second. ArcSecond time offsets were also calculated from ESRI time and renormalized.

Tags were also mounted on the test sled pole providing a consistent offset. The WhereNet tags were mounted immediately upon the pole with about 1-inch offset, well within its accuracy. The MSSI tags were mounted horizontally, with vertical antenna polarization, on "L" brackets with approximately 3 to 4 inches offset from the center of the pole, possibly significant. Tags were always oriented forward for "X" axis grid traces (positive/add), and starboard for "Y" axis grid traces (negative/subtract).

Offsets:

- MSSI Time (3-hour difference from ArcSecond and WhereNet, EST versus PST)
- Tag Mounting on Test Sled Pole (MSSI angle brackets)

Correlation. Time was the primary correlation factor. Time was used to align the data into sub-sets of datapoints that were closest to the nearest reference laser point. This was simplified by the frequent and rapid reporting of the laser system, approximately 8 to 10 times more frequent than tag reports. The final objective was spatial correlation to the laser system, providing the ability to calculate tag reported position error.

Data was sorted by time to group tag reports close to laser reports. The ESRI instrumentation system recorded time to one second resolution. MSSI and WhereNet reported time to one second resolution. The laser system reported two times a second. One second resolution increased correlation uncertainty during test sled movement, but was not an issue for static test sled periods (at major intersections).

The laser system experienced drop outs cause by stanchion blockage, "banana" zone uncertainty, and hardware problems (batteries and cables). Tag reports were correlated with good laser reports, and tag data associated with missing or inaccurate laser datapoints was identified, and discarded from analyses. The closest laser report and the closest bracketing pair of laser reports were identified with each tag report. The closest laser report was used for difference calculation.

Correlation:

- Tag Data Aligned with Valid Laser Data
- Tag Data Aligned with Blocked or "Banana" Laser Data
- Discarded Tag Data (no valid laser data)

Difference: Spatial difference is the primary result of the system measurements and calculations. It provides the basis for answering the third and primary question:

- What were the resulting accuracies?

Spatial difference was calculated in the following ways:

Difference Calculations:

- "X" and "Y" Axis (cartesian)
- Distance (euclidean)
- By Tag Height

"X and "Y" axis differences were calculated by subtracting tag reported position from actual tag location, equation (1). "X" and "Y" differences could be positive or negative. Separating "X' and "Y" terms allowed analyzing errors in each axis looking for trends. Difference was computed for each tag report.

$$Difference_{(x,y)} = TagReport_{(x,y)} - LaserPosition_{(x,y)} \qquad (1)$$

Distance was calculated by right angle triangle hypotenuse of the "X" and "Y" terms, Equation (2). Distance was always positive. Distance was computed for each tag report.

$$Distance = \sqrt{Difference(x)^2 + Difference(y)^2} \qquad (2)$$

Height, i.e., "Z" axis, was not measured by the tag systems. MSSI was capable of measuring 3D, but the fifth "Z" axis receiver was not set up. WhereNet assumed a 4-foot tag height for its calculations, and MSSI assumed 0 foot for its calculations. Algorithms for both systems considered height in their calculations, and height has an effect on calculated position, particularly close to antennas. Tags were placed at 4-, 8-, and 11-foot heights on the test sled. Humans carried items approximately 4 feet high above floor level. Tags placed on containers were approximately 8 feet and 16 feet high.

Difference was used to calculate accuracy and to look for trends in the reported errors. Histogram plots of difference and distance indicated offsets and the randomness of the errors. Difference plots over time, following sled movement, indicated error trends.

Statistical Analyses. Statistical analyses were performed on the difference data to develop accuracy. Accuracy included only good data. Drop outs, partial reads, range clips, pops and jumps, system instability and failure data were not included in accuracy calculations. Drop outs, partial reads, and pops and jumps were counted and compared total counts to determine tag read reliability.

Common statistical measures were made over datasets including:

- Tag Read Reliability

  - Total Blinks Heard (MSSI/WhereNet)
  - Total Laser Correlated Blinks Heard (MSSI/WhereNet)

  - Number of Range Clips (MSSI)
  - Number of Pops and Jumps (MSSI)
  - Valid Data Points (MSSI "*n*")

  - Partial Reads (WhereNet)
  - Drop Outs (WhereNet)
  - Valid Data Points (WhereNet "*n*")
  - Percentage Good Reads, Partial Reads, and Drop Outs

- Tag Reported Position

  - "X" Average Offset
  - "Y" Average Offset

  - "X" Standard Deviation
  - "Y" Standard Deviation

  - Total Standard Deviation

- Error

  - Average Error
  - Root-Mean-Squared (RMS) Error
  - Time Averaged Error (static tag position)

Tag read reliability was calculated by counting the total number of laser correlated tag reports in each filtered group. The purpose was to establish "*n*" for the statistical calculations. MSSI range clips, and pops and jumps may have been caused by one antenna receiving signal, or false triggers, and calculating a position. MSSI's algorithms may have been not advanced enough to know when not to calculate. MSSI clips and pops and jumps may be similar to WhereNet partial reads and were considered the same.

Tag blink, read reliability, good data "n" for statistical analyses, and percentage of good reads were calculated by Equations (3) to (9).

$$TotalBlinksHeard = \sum Blinks \qquad (3)$$

$$TotalCorrelatedBlinks = TotalBlinksHeard - \sum MissingLaserData \qquad (4)$$

$$n = MSSIValidPoints = TotalCorrelatedBlinks - (Clips + Pops \& Jumps) \qquad (5)$$

$$n = WNetValidPoints = TotalCorrelatedBlinks - (PartialReads + DropOuts) \qquad (6)$$

$$WNetGoodReads\% = \frac{PositionReports}{Total\,BlinksHeard + DropOuts} \times 100\% \qquad (7)$$

$$WNetPartialReads\% = \frac{PartialReads}{Total\,BlinksHeard} \times 100\% \qquad (8)$$

$$WNetDropOuts\% = \frac{DropOuts}{Total\,BlinksHeard + DropOuts} \times 100\% \qquad (9)$$

Offset was computed for each axis. It was used to look for biases or consistent offsets in reported position. It was part of the trend analyses. Offsets showed consistent errors in calculations or possibly tag mounting offset. The MSSI system may have been accurate enough to see the tag mounting offset. Offset was computed by averaging the "X" and "Y" axis differences over the datasets, Equation (10).

$$AvgOffset_{(x,y)} = \frac{1}{n} \sum_{n=1}^{n} Difference(n)_{(x,y)} \qquad (10)$$

Standard deviation of the reported positions was calculated to look for differences, Equation (11). Standard deviation indicates the uncertainty or "fuzzyness" of the readings. It was used for both "X" and "Y" axis, and was referenced to the average location of readings, to remove offsets.

$$StdDev_{(x,y)} = \sqrt{\frac{1}{n} \sum_{n=1}^{n} (TagReport(n)_{(x,y)} - AvgOffset_{(x,y)})^2} \qquad (11)$$

Total standard deviation was also calculated, Equation (12). It is much like RMS Error, but does not include offsets.

$$TotalStdDev = \sqrt{\frac{1}{n}\sum_{n=1}^{n}\left((TagRpt(n)_{(x)} - AvgOffset_{(x)})^2 + (TagRpt(n)_{(y)} - AvgOffset_{(y)})^2\right)} \quad (12)$$

Average error was computed by the sum of the error distances divided by the number of data points, Equation (13). It equally weighs all errors.

$$AvgError = \frac{1}{n}\sum_{n=1}^{n}Distance(n) \quad (13)$$

RMS is the most commonly used measurement of error. It is used to specify the accuracy of GPS and other geolocation systems. It defines the error band with 67% of the readings for Gaussian distributions, one standard deviation, Equation (14).

$$RMS\,Error = \sqrt{\frac{1}{n}\sum_{n=1}^{n}Distance(n)^2} \quad (14)$$

Time Averaged Error analyses were performed on data during static cart periods. The Test Sled stopped in four locations during Test 3 near the center of the test box. The Test Sled also dwelled for long periods in corners prior to tests. Corners were not used as they had the greatest errors.

The objective was to see if a large number of static position readings would increase accuracy. Both WhereNet and MSSI had random errors in their readings, with WhereNet exhibiting the greatest variation. Tag reports were averaged over the periods of test sled stops and compared with laser position, Equations (15), (16), and (17). This was much like the Average Offset, except it was in one location, rather than over the whole test box.

$$TimeAvgReport_{(x,y)} = \left(\frac{1}{n}\sum_{n=1}^{n}TagReport(n)_{(x,y)}\right) \quad (15)$$

$$TimeAvgError_{(x,y)} = TagAvgReport_{(x,y)} - LaserPosistion_{(x,y)} \quad (16)$$

$$TotalTimeAvgError = \sqrt{TimeAvgError(x)^2 + TimeAvgError(y)^2} \quad (17)$$

3.3.2   Container Blockage, Second Week

The technical approach for the data reduction for the container blockage second week testing was similar to the first week testing:

- Gather data into data sets
- Filter data into groups
- Correlate tag datasets with laser data
- Calculate differences and perform statistical analyses
- Display data in an easy to interpret fashion
- Investigate trends and error character

The second week data reduction was easier than the first week, as individual tag reports did not need to be correlated with laser reports as the test sled moved. Tags were in static positions on containers and HMMWV, and did not move during the tests. Only one tag laser position was needed, and was measured by hand using the laser surveying system. All of the remaining measurements were fully automated by the WhereNet system.

Gather Data: WhereNet automatically recorded and saved snapshots of the previous 50,000 tag records at 2400 hours Greenwich Mean Time (GMT). Because of setting the computer clock to GMT, the backup was performed at 1600 PST. A total of four snapshots were taken, one at the end of each day.

The first day did not include all of the tags on the double-stacked containers and HMMWV, because they had not all been placed and measured. The second day had all of the tags and was used for the double high stack test. The top layer of containers was removed the third day and was used for single layer of container analyses. Most of the containers were removed by the fourth day and were not used.

The WhereNet datasets were in SQL 7.0 database format and contained all information for tag reports over the previous period. The SQL 7.0 database formats were converted and saved to ASCII delimited files using Microsoft Access. Each test, and then each tag, was saved into individual ASCII files on a Linux computer. Each file contained approximately 400 to 900 tag reports depending on whether two or one layers of containers were present.

Filter Data. Data filtering was easier than the open space tests. The WhereNet system was stable and did not experience the system instabilities, clips, and jumps and pops of the MSSI system. No laser blockage or banana zones needed to be accounted for. Data was separated into full (with "X-Y" position) and partial (no "X-Y" position) groups. Full drop outs were not analyzed as the number of reports and number of partial reads provided enough information to determine tag read reliability.

Correlation. Correlation was easy as only one tag location laser measurement was used for analyses with its data set. No individual tag report to individual laser report correlation was needed, tags did not move. Table 10 lists the measured tag locations used for correlation.

The laser surveying system transmitters were removed from the bulkheads and placed on tripods for most measurements. The tripods were moved around the space to get tags within view. The laser transmitters were even placed above the open overhead hatches, looking down on the containers.

Some of the tags could not be measured by the surveying system, and then were measured by tape measure from the grid on the floor. Tape measurements were estimated to be accurate within 1/2-foot, well within the accuracy of the WhereNet system.

Calculation. UNIX AWK scripts were written and used to process the datasets for statistical analyses. Calculations included:

- Tag Read Reliability

    - Total Blinks Heard
    - Number of Positions Reported
    - % Position/Blink

- Tag Reported Position

    - "X" Position Average
    - "Y" Position Average

    - "X" Standard Deviation
    - "Y" Standard Deviation

    - Total Standard Deviation

- Error

    - Average Error
    - RMS Error

Tag read reliability was calculated by counting the total number of tag reports in each data set. The double high container stack had more tags and fewer reports per tag were included in the 50,000 record set. The average number of reports for the double stack was 360 to 510. Tags reported randomly and did not have the same number of blinks. The single-high stack had fewer tags, thus more reports per tag were included. The average number of reports for a single high stack was 820 to 910.

Some tags had fewer reports than most and fewer reliable reads. One tag had a much lower blink rate (32 sec/blink) and was consistent between all tests. Another tag did not report during any tests. It may have not been turned on.

Tag blink and read reliability were calculated by Equations (18), (19), and (20).

$$TotalNumberBlinksHeard = \sum Blinks \tag{18}$$

$$TotalPositionsReported = \sum PositionReports \tag{19}$$

$$TagBlink\% = \frac{Total\,Positions\,Reported}{Total\,Number\,Blinks\,Heard} \times 100\% \tag{20}$$

Reported tag positions were averaged for both "X" and "Y" axis, Equation (21). This greatly simplified location error calculations.

$$AvgPosition_{(x,y)} = \frac{1}{n}\sum_{n=1}^{n} Position(n)_{(x,y)} \tag{21}$$

Standard deviation of the reported positions were calculated to look for differences due to multipath, Equation (22). Standard deviation indicates the uncertainty or "fuzzyness" of the readings. It was used for both "X" and "Y" axis, and was referenced to the average location of readings, to remove offsets.

$$StdDev_{(x,y)} = \sqrt{\frac{1}{n}\sum_{n=1}^{n}(TagReport(n)_{(x,y)} - AvgPosistion_{(x,y)})^2} \tag{22}$$

Standard deviation more heavily weighs larger errors by first squaring them, summing, then taking the square root. It also provides a standard measure for Gaussian "bell curve" distributions. The error distributions for both systems were bell like curves. The first standard deviation computes the error band with 67% of the data points. Total standard deviation was calculated, Equation (23). It gives a sense for the total error without the effects of offset.

$$TotalStdDev = \sqrt{\frac{1}{n}\sum_{n=1}^{n}\left((TagRpt(n)_{(x)} - AvgPos_{(x)})^2 + (TagRpt(n)_{(y)} - AvgPos_{(y)})^2\right)} \tag{23}$$

Average error was the distance between the reported position and the actual position, Equation (24).

$$AvgError = \sqrt{(AvgPos_{(x)} - LaserPos_{(x)})^2 + (AvgPos_{(y)} - LaserPos_{(y)})^2} \tag{24}$$

RMS again was calculated as the most common measurement of error, Equation (25). It is basically the same calculation as standard deviation, except it is referenced to actual location rather than the average location of the readings. RMS can be greater than standard deviation because of offsets.

$$RMSError = \sqrt{\frac{1}{n}\sum_{n=1}^{n}(TagRpt(n)_{(x)} - LaserPos_{(x)})^2 + (TagRpt(n)_{(y)} - LaserPos_{(y)})^2} \tag{25}$$

4.0   TEST RESULTS

Both tabular and graphic plots were the primary output of the data reduction. Tabular results included standard statistical factors, and graphical results included 2D maps, sequence plots and histograms to identify trends. Tabular results and histograms were calculated using Microsoft Excel and 2D maps were created with ESRI ArcView and tracking analyst.

4.1   First Week Open Space

4.1.1   Tabular Results

Tables 12 and 13 summarize the data reduction from the three tests by vendor, test, and tag. They provide the overall accuracy over the test box for each test and tag. They answer the second and third questions of whether the systems experience dropouts or dead zones, and how accurate are the systems. They also answer the fifth question of how many antennas are needed in an open space for the WhereNet system. The MSSI system always had four antennas thus was not a factor.

The MSSI system experienced considerable instability, and required restarting approximately every 10 minutes. This produced a large number of gaps in the data. The system also "clipped" data, initially at the test box boundaries for Test 1, and then 5 feet outside the test box for Tests 2 and 3. More clips are evident for Test 1 with the clip boundaries set at the test box dimensions, and fewer clips with the clip boundaries moved further out. The system also experienced frequent jumps and pops that were not clipped, and those over 20 feet were filtered. The unstable/restart, clipped and jump/pop data was filtered out, and the final MSSI data set was sparse. This prevented determining MSSI dropouts and dead zones.

MSSI tags had limited battery life on the order of hours, and tags were changed between tests and during Test 2. Tag 178 was changed to tag 77 data during Test 2 and was treated as the same tag at the same pole position. Tag 77 continued into Test 3. Tag 161 was changed to tag 13 for Test 3.

MSSI Test 1 had the most attention, but the clipped data preclude its being used for reported accuracy. MSSI Test 2 is the most realistic, with the clip boundaries moved further out, no laser banana zone, and has the greatest percentage of good reads. It also has the same sled movement pattern as Test 3. Test 2 was used for MSSI reported accuracy. MSSI Test 3 had the least attention and the greatest instability and worst accuracy. It however showed the promise of the system's inherent capability and accuracy in the last quarter of the test for tag 77, with reported position closely following the sled, with only a few pops.

The WhereNet system was far more stable and all tag readings are included. The WhereNet system did not consistently locate tags with only four antennas in a ship. It required 8 antennas for reliable reads. With four antennas, most reads were partial, without position. It also experienced a few full dropouts. With 8 antennas, only a few partial reads and no full dropouts were recorded. WhereNet 114391 blinked every 16 seconds versus 4 seconds and has fewer reports, it is not due to dropouts. Test Tag 3 provides the best accuracy data for WhereNet and is used for its reported accuracy.

The MSSI system was more accurate than the WhereNet system. The MSSI system had little or no significant offset, and standard deviation closely matched RMS error. The WhereNet system had significant offset, increasing RMS error over standard deviation. MSSI's accuracy was limited by the residual pops below 20 feet. It did not average multiple readings as the WhereNet system, and that hurt its overall accuracy. MSSI accuracy was greater than its resolution of 2 feet. WhereNet's accuracy was close to its measurement resolution of 5.5 feet. MSSI's averaged RMS accuracy was 2 to 5 feet, and WhereNet averaged RMS accuracy was 6 feet.

Table 12. MSSI Open Space Accuracy

Test No.	Tag No.	Blinks Heard	Corr Pos	MSSI Reads				MSSI Reads %			Avg Offset		Standard Deviation			Error	
				Good	Clips	Pops >20	Total	Good	Clips	Pops >20	X	Y	X	Y	Total	Avg	RMS
1	41	717	574	429	273	15	717	59.8	38.1	2.1	-0.4	0.4	2.4	2.3	3.3	**2.3**	**3.4**
	161	533	426	334	191	8	533	62.7	35.8	1.5	-0.3	0.0	1.7	1.8	2.5	**1.9**	**2.5**
	178	296	240	164	122	10	296	55.4	41.2	3.4	-0.1	0.0	2.9	2.9	4.1	**2.4**	**4.1**
2	41	628	521	544	64	20	628	86.6	10.2	3.2	1.2	0.4	3.1	3.9	5.0	**3.8**	**5.1**
	161	448	368	400	34	14	448	89.2	7.6	3.1	0.2	-0.2	2.4	3.8	4.4	**3.1**	**4.4**
	178 / 77	430	358	387	39	4	430	90.0	10.1	9.1	-0.1	-0.4	2.1	4.4	4.8	**3.3**	**4.8**
3	41	407	354	300	26	81	407	73.7	6.4	20.0	-1.6	1.3	5.5	7.8	9.6	**8.4**	**9.8**
	13	374	319	285	19	70	374	76.2	5.1	18.7	-0.6	0.6	3.9	7.3	8.3	**7.0**	**8.3**
	77	391	338	317	23	51	391	81.1	5.9	13.0	-1.6	-0.3	3.9	7.0	8.0	**6.5**	**8.0**

Table 13. WhereNet Open Space Accuracy

Test No.	Tag No.	Blinks Heard	Corr Pos	WhereNet Reads				WhereNet Reads %			Avg Offset		Standard Deviation			Error	
				Good	Partial	Dropout	Total	Good	Partial	Dropout	X	Y	X	Y	Total	Avg	RMS
1	112074	2170	136	151	2019	12	2182	6.9	92.5	0.5	-2.9	3.8	9.5	8.2	12.5	**10.1**	**13.4**
	112348	2123	64	107	2016	25	2148	5.0	93.9	1.2	1.6	2.4	4.1	6.2	7.4	**6.8**	**7.9**
	114391	658	13	117	541	0	658	17.8	82.2	0.0	-1.8	1.8	6.3	8.9	10.5	**9.6**	**10.8**
2	112074	808	82	107	701	6	814	13.1	86.1	0.7	-1.4	3.0	9.8	13.1	16.3	**11.4**	**16.6**
	112348	1657	50	109	1548	108	1765	6.2	87.7	6.1	2.3	2.3	11.6	16.4	20.0	**14.5**	**20.2**
	114391	433	16	32	401	10	443	7.2	90.5	2.3	1.2	10.2	25.0	16.4	29.0	**23.2**	**30.7**
3	112074	536	462	533	3	0	536	99.4	0.6	0	0.8	2.1	3.8	4.7	6.0	**5.5**	**6.4**
	112348	533	462	531	2	0	533	99.6	0.4	0	1.2	2.5	3.0	4.5	5.4	**5.1**	**5.9**
	114391	156	134	150	6	0	156	96.2	3.8	0	0.8	1.7	3.5	3.8	5.1	**4.4**	**5.4**

4.1.2 WhereNet Convergence Analysis

Table 14 summarizes WhereNet convergence analysis for Test 3. The test sled paused at 4 locations for extended periods (greater than 1 minute) during Test 3. These were considered focused investigations for convergence analysis for the WhereNet system. WhereNet had fairly random stochastic errors, with data points "bouncing" randomly around within their error circle during measurements.

The objective was to see if a large number of static position readings would increase accuracy. Both WhereNet and MSSI had random errors in their readings, with WhereNet exhibiting the greatest variation. Tag reports were averaged over the periods of the test sled stops and compared with laser position. This was much like the Average Offset, except it was in a stable location, rather than over the whole test box.

Four locations were selected, one near a corner, two near the middle, and one on the other side. The test sled also dwelled for long periods in corners prior to tests. Corners were not used for analysis as they had the greatest errors.

Table 14. WhereNet Convergence Analysis

Stop No.	Tag No.	No. of Blinks	Actual Location Averaged		Avg. Reported Location		Average Location Difference			Instantaneous Error	
			X	Y	X	Y	X	Y	Total	Avg	RMS
A	112074	17	110.1	120.0	111.1	120.5	1.0	0.5	**1.1**	**3.2**	**3.8**
	112348	18	110.1	120.0	108.5	112.2	-1.6	-7.8	**8.0**	**8.3**	**8.5**
	114391	6	110.1	120.0	109.0	115.7	-1.1	-4.3	**4.4**	**4.4**	**4.7**
B	112074	15	130.0	130.1	130.0	128.7	0.0	-1.4	**1.4**	**3.9**	**4.5**
	112348	14	130.0	130.1	130.3	129.0	0.3	-1.1	**1.2**	**2.0**	**2.2**
	114391	5	130.0	130.1	130.6	124.6	0.6	-5.5	**5.6**	**5.8**	**6.2**
C	112074	13	130.1	150.0	132.4	146.8	2.3	-3.2	**3.9**	**4.9**	**5.4**
	112348	12	130.1	150.0	127.7	147.8	-2.4	-2.2	**3.3**	**3.7**	**4.3**
	114391	4	130.1	150.0	129.2	150.5	-0.9	0.5	**1.0**	**3.2**	**3.5**
D	112074	21	170.0	120.0	169.6	117.0	-0.4	-3.0	**3.0**	**3.4**	**4.1**
	112348	22	170.0	120.0	171.5	117.5	1.5	-2.5	**2.9**	**3.5**	**3.7**
	114391	6	170.0	120.0	170.0	116.8	0.0	-3.2	**3.2**	**3.2**	**3.3**

Average Location Difference was better than Average Instantaneous Error in all but one of the cases, where it was the same. Improvement ranged from 4 to 68 % with an average improvement of 21% over Instantaneous Error.

Stop No. A, tag 112348 had much larger difference and error (8 feet) than the rest. "Y" axis offset accounted for most of the error. This may have been due to a strong multipath reflection. "Y" axis offset also accounted for most of the error in 50% of the cases. Later analyses (Section 5.1.4) identified the cause of the pronounced "Y" axis error as antenna mirror images in bulkheads.

The Average Location Difference average was 4.3 ft, better than system resolution of 5.5 feet. The WhereNet system averaged 4 sub-blinks for each reading. Further averaging multiple readings improved WhereNet Accuracy. Similar improvement would be expected for the MSSI system.

4.1.3 Plots

First week: Open space plot types include:

- Data & Correlation

    - Laser Track (used for correlation)
    - 2D Scatter Plots (colored dots and symbols for tags)
    - Tracks (connected lines between laser and tag reports)
    - Correlated Tracks (interspersed tag reports with laser data connected with lines)

- Error

    - 2D "X-Y" Difference Plots (by blinks)

    - Error Plots (by blinks)
    - Error Histograms

    - Difference Plots (by blinks "X" and "Y" axis)
    - Difference Histograms ("X" and "Y" axis)

- Dropouts

    - Blink Frequency Histograms (used for full drop-out analyses, WhereNet only)

2D Maps: Laser tracks were plotted in ArcView on the test box reference grid to locate "banana" zone and stanchion drop out areas. This was used to filter data to exclude stanchion blockage and "banana" zone laser reports from analyses. Laser tracks were included in other 2D plots as a reference for correlation.

2D scatter plots placed separated data sets and groups on different layers, which were then selectively displayed. The ability to selectively show data sets was used to minimize the data presented to help look for error trends and character. Plots were made over selected time periods to match test starts and stops. Separate plots were made for each vendor. Plots with all tags, and then by individual tags were made. Scatter plots provided a sense for the distribution and evenness of tag reports. Voids, clumping, offsets and convergence became readily apparent.

Tracks were used on MSSI data sets to see if the system traced the grid together with the laser system. It was hoped that if obviously erroneously wrong data (e.g., MSSI system instability, gross pops and jumps, and clips representing data outside of the test box) were removed from the tracks, they would present some discernable grid pattern. This is what was done during the test for data reduction and presentation. The wide variation in reported tag positions, and errors, however, limited usefulness of this approach. The last third of MSSI Tests 2 and 3, tag 77, however, showed the sled following the grid.

Correlated tracks were constructed for WhereNet by interspersing reported tag positions with actual laser positions into one data set. They visually correlated tag reports to actual test sled position. Tracks followed laser position, then "jumped" to tag reports. Lines were drawn from immediately preceding and following laser reports each side of tag reports. Tracks between laser points usually closely followed the reference grid. Tag reports appeared as a "pop and jump" off the laser track, connected by lines to the tag report. This display indicated the types, magnitude and direction of errors, based on location in the test box. Reported position was always away from corners.

Statistical Plots: 2D "X-Y" difference plots were constructed to show the symmetry of difference. They showed offset and overall shape of errors in both dimensions. Data points were connected by lines and they looked like "fuzz balls." The core of the fuzz balls were largely round or oval and differences between "X" and "Y" error distributions, offsets, and pops and jumps were clearly evident.

Error plots were constructed by plotting the distance between reported position and actual position over chronological tag sequence. It combined the "X" and "Y" difference plots with a single measure. Error was always positive. They clearly showed pops and jumps.

Error histograms were plotted to show the distribution of errors. It combined the "X" and "Y" difference plots with a single measure. They gave visual representation for the average and RMS error calculations. The error histograms had log normal distributions. They were the most important plots as they showed overall error.

Difference plots for "X" and "Y" axis were constructed by plotting the difference between reported position and actual position over chronological tag sequence. Difference could be positive or negative. They clearly showed offset, error randomness and pops and jumps. These plots indicated change in error and trends as the test sled moved over each axis in the test box. They showed a clear error trend for WhereNet in the "Y" axis as the sled moved.

Difference histograms for "X" and "Y" axis were plotted to show the distribution of errors. They gave visual representation to the standard deviation calculations. They showed the shape of the distribution and offset. Pops and jumps also showed up as being far from the normal distribution. They also showed offsets and difference between "X" and "Y" axis errors. The difference histograms had bell shaped curves. WhereNet Tests 1 and 2 do not have "X" and "Y"axis histograms as the reads were very sparse and mainly in corners.

WhereNet blink frequency histograms showed the interval between blinks and were used for full drop-out analyses. Primary tag blinks were clustered as large peaks around the average blink rate +/- 1 to 2 seconds. Smaller peaks located at harmonics of the average blink rate indicated missed blinks, or dropouts. Second harmonics were totaled and were multiplied by one for single dropouts. Third harmonics were likewise totaled and multiplied by two for double dropouts, and so on.

Tables 15 lists the first week open space plots.

Table 15. First Week Open Space Plots

Vendor	Test	Figure No.					
ArcSecond	1-3	66 - 68	Tag No.				
MSSI	--		41	161	13	178	77
	1	69 - 93	70 - 77	78 - 85	--	86 - 93	--
	2	94 – 118	95 - 102	103 - 110	--	111 - 118	
	3	119 - 143	120 - 127	--	128 - 135	--	136 - 143
WhereNet	--		112074	112348	114391	--	--
	1	144 - 165	145 - 151	152 - 158	159 - 165	--	--
	2	166 - 187	167 - 173	174 - 180	181 - 187	--	--
	3	188 - 215	189 - 197	198 - 206	207 - 215	--	--

4.1.4 First Week Open Space Figures

4.1.4.1 <u>ArcSecond Sled Plots</u>. Figures 66 through 68 show the ArcSecond plots for the test sled movement for Tests 1 through 3, respectively. The test sled traversed the "X" axis for Test 1 and traversed the "Y" axis for both Tests 2 and 3. The sled passed through the banana zone for Test 1, and skirted the "banana" zone for Tests 2 and 3. The banana zone is clearly visible in Test 1 between "X" axis location 130 to140 feet over the whole "Y" axis. The banana zone increased error in that region. Tests 2 and 3 were not subject to the same error and are considered better runs. They also traversed the same direction and provided equal comparison.

Stanchion blockage is also visible between "X" axis location 150 to 160 feet near the outside edges. It lined up closely with the expected pattern, both bottom and top. Stanchion blockage is most visible along "X" axis location 150 feet for Tests 2 and 3.

Sled movement in corners and turning to cross back and forth is visible in all three plots. The sled could not reach into the forward corners due to the antenna tripods being closer to the grid. Sled movement in the center to untangle the fiber optic cable around stanchions is visible in all Figures 66, 67, and 68.

The sled closely followed the grid in all three tests. Improvement in handling the sled and tracing the grid is visible from Tests 1, 2 and 3. The only system that closely traced the grid was the ArcSecond laser system. Close agreement between the grid and the ArcSecond plots provides great confidence in the laser reference system. All of the map plots include the grid and sled movement for reference.
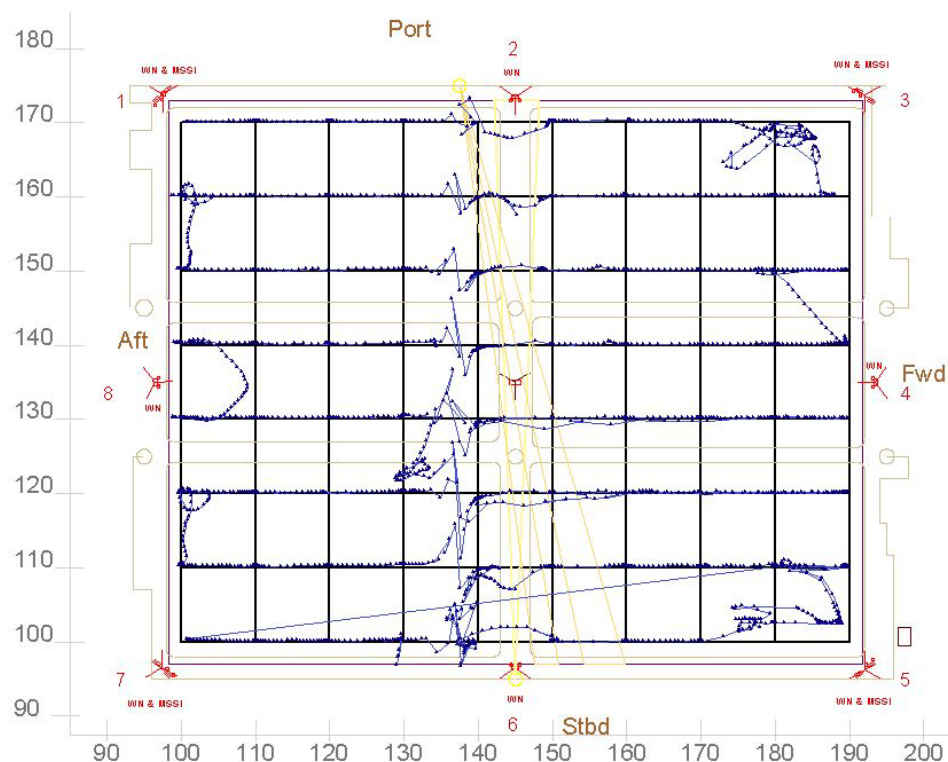
Figure 66. Open space Test 1 ArcSecond "X" axis traverse
with laser "banana" zone on grid.
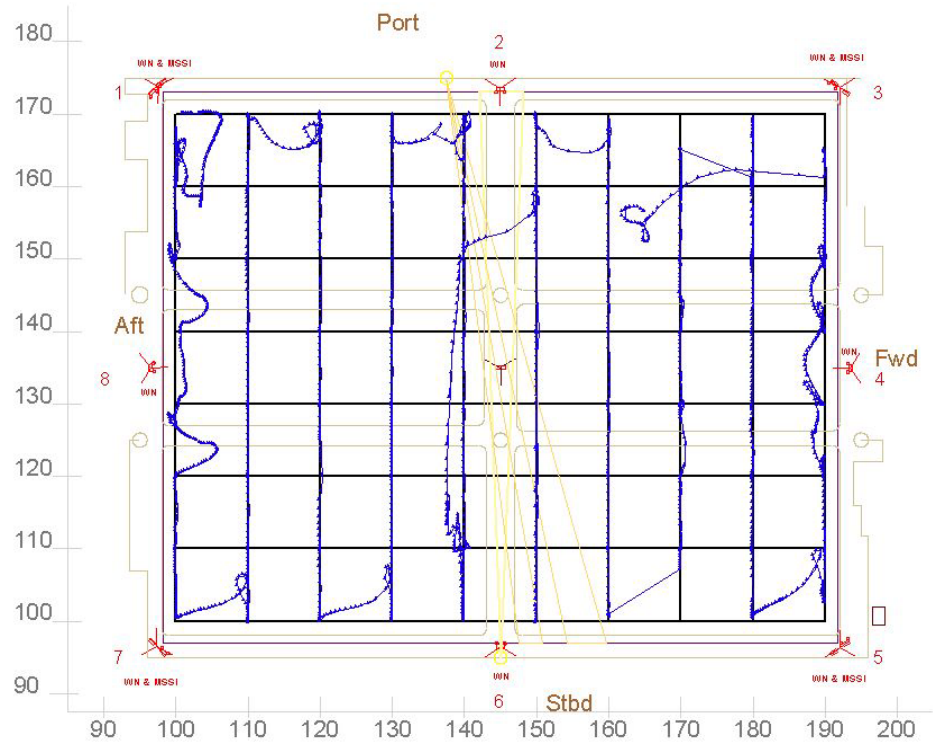
Figure 67. Open space Test 2 ArcSecond "Y" axis traverse on grid.
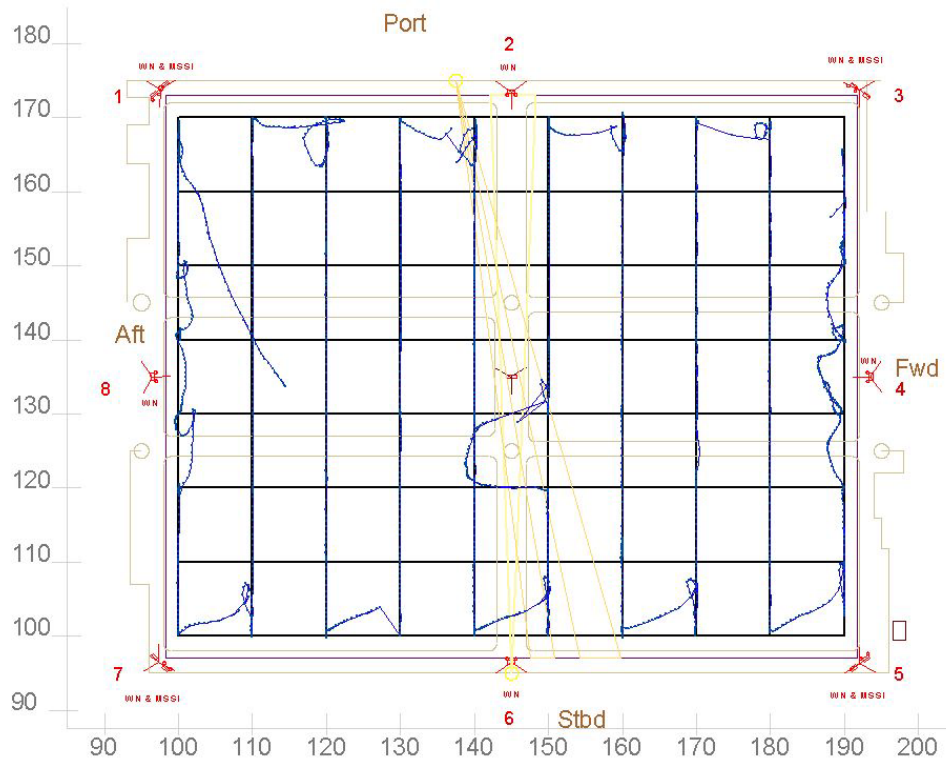
Figure 68. Open space Test 3 ArcSecond "Y" axis traverse on grid.

4.1.4.2 MSSI Plots. MSSI data reduction was done first and is presented first. Table 16 lists the MSSI figures:

Table 16. MSSI Test Result Figures

Test No.	Description	Figure No.					
	Tag No:	All	41	161	13	178	77
1	2D Scatter Plot	69	70	78	--	86	--
	2D "X-Y" Difference	--	71	79	--	87	--
	Error vs Blinks	--	72	80	--	88	--
	Error Histogram	--	73	81	--	89	--
	"X" Difference vs Blinks	--	74	82	--	90	--
	"X" Difference Histogram	--	75	83	--	91	--
	"Y" Difference vs Blinks	--	76	84	--	92	--
	"Y" Difference Histogram	--	77	85	--	93	--
	Blink Frequency Histogram	--	--	--	--	--	--
2	2D Scatter Plot	94	95	103	--	111	
	2D "X-Y" Difference vs Blinks	--	96	104	--	112	
	Error vs Blinks	--	97	105	--	113	
	Error Histogram	--	98	106	--	114	
	"X" Difference vs Blinks	--	99	107	--	115	
	"X" Difference Histogram	--	100	108	--	116	
	"Y" Difference vs Blinks	--	101	109	--	117	
	"Y" Difference Histogram	--	102	110	--	118	
	Blink Frequency Histogram	--	--	--	--	--	--
3	2D Scatter Plot	119	120	--	128	--	136
	"X-Y" Difference vs Blinks	--	121	--	129	--	137
	Error vs Blinks	--	122	--	130	--	138
	Error Histogram	--	123	--	131	--	139
	"X" Difference vs Blinks	--	124	--	132	--	140
	"X" Difference Histogram	--	125	--	133	--	141
	"Y" Difference vs Blinks	--	126	--	134	--	142
	"Y" Difference Histogram	--	127	--	135	--	143
	Blink Frequency Histogram	--	--	--	--	--	--

"X-Y," "X," and "Y" Difference versus Blink plots include all correlated positions, even clips. 2D Scatter plots, Error, and "X" and "Y" Difference histograms do not include clips. Clips were not included in statistical calculations. No Blink Frequency histograms were done for MSSI as the data was too sparse for drop-out analysis. They were only done for WhereNet.

The 2D Scatter and "X-Y" Difference plots showed most of the pops and jumps were diagonal the same direction. This may have been due to filtering clips, which would have removed pops & jumps more perpendicular to the test box sides. Only the pops and jumps that fit in the test box, often diagonal between corners were left.

Test 3 shows the both the worst and best system performance. The first portion shows clumping resulting from inattention and not resetting the system when needed. Clumping and instability are readily apparent. The last quarter of the test shows the MSSI system at its best, with tag reports following the grid closely, with occasional pops and jumps. This is what we had hoped to see during the testing.
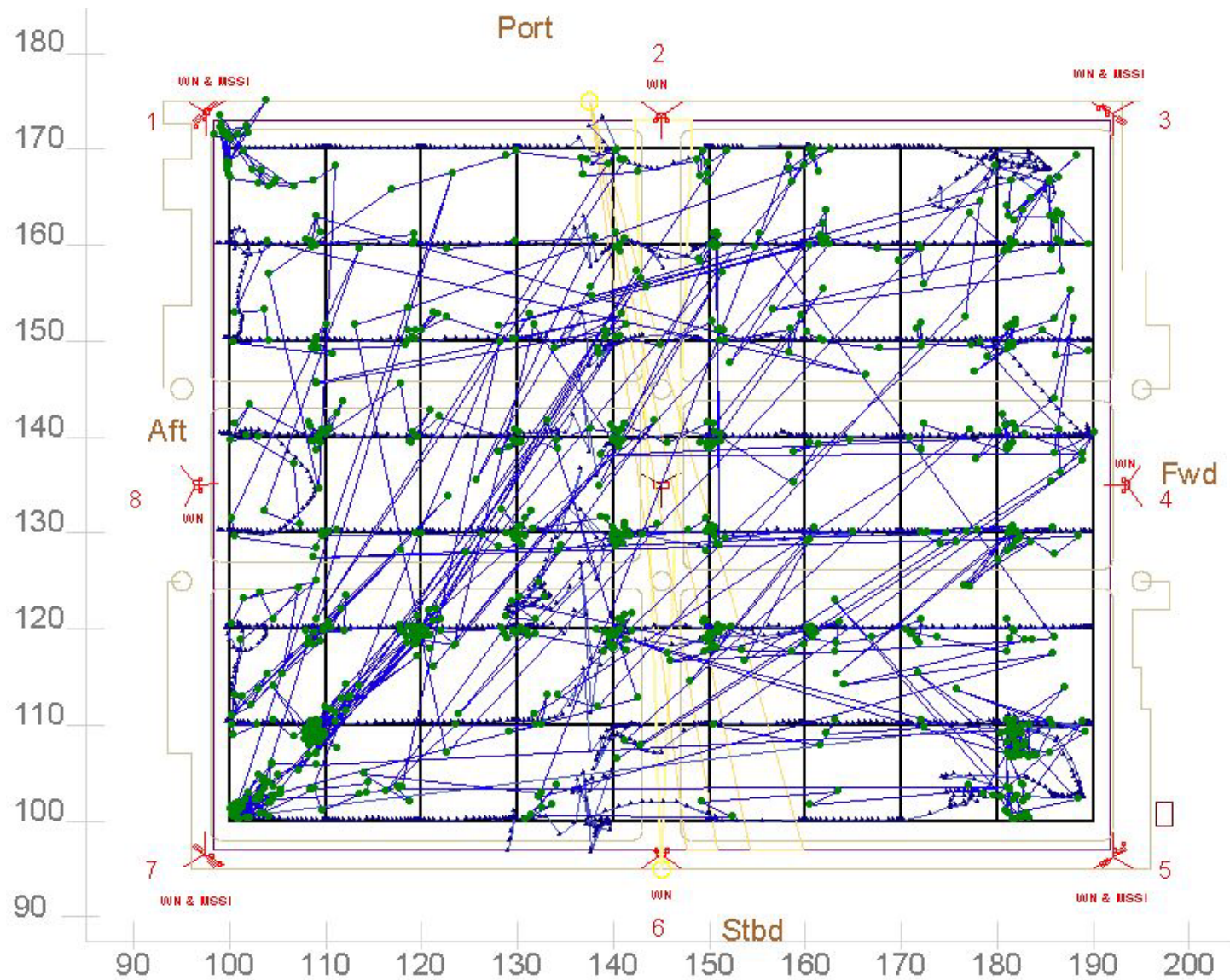
Figure 69. MSSI Test 1: All tag reported positions with tracks.
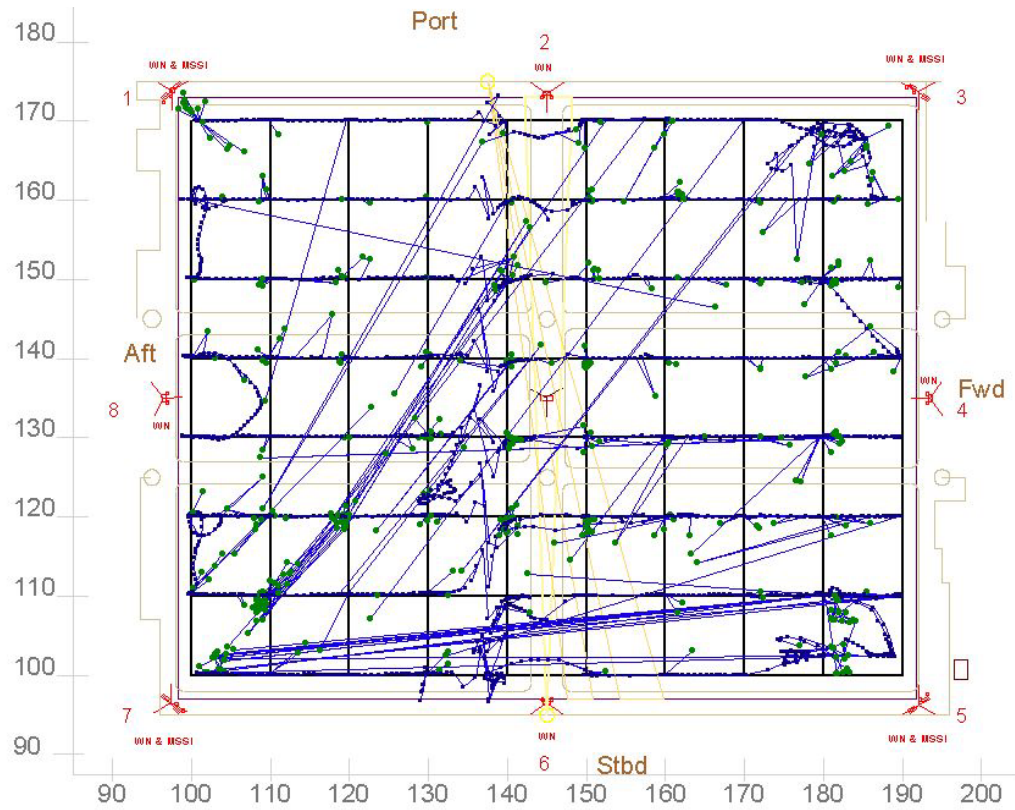
Figure 70. MSSI Test 1, Tag 41: Reported and correlated positions.
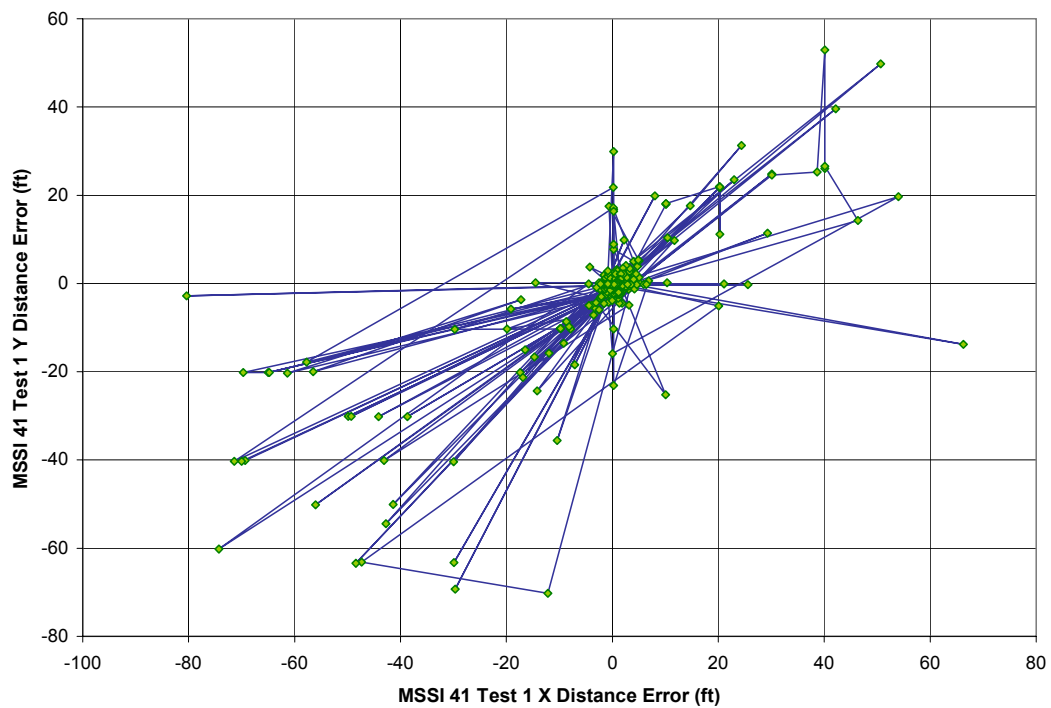
Figure 71. MSSI Test 1, Tag 41: "X-Y" difference versus blink.
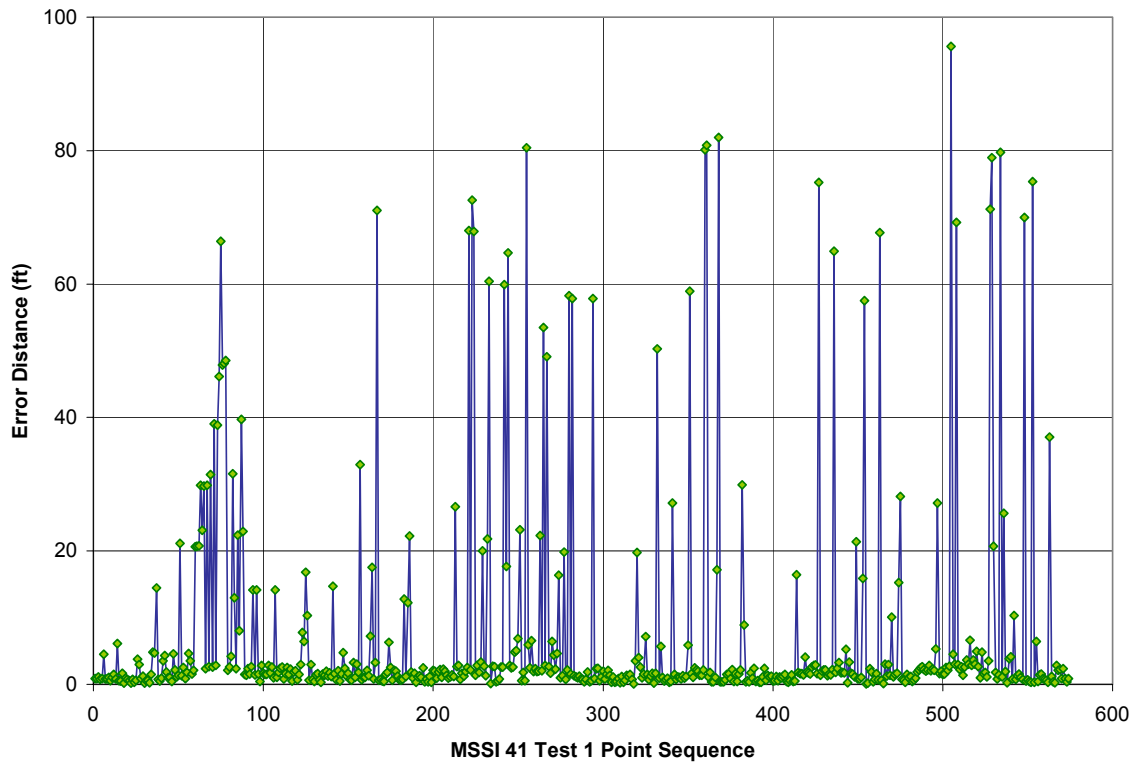
Figure 72. MSSI, Test 1, Tag 41: - Error versus blink.
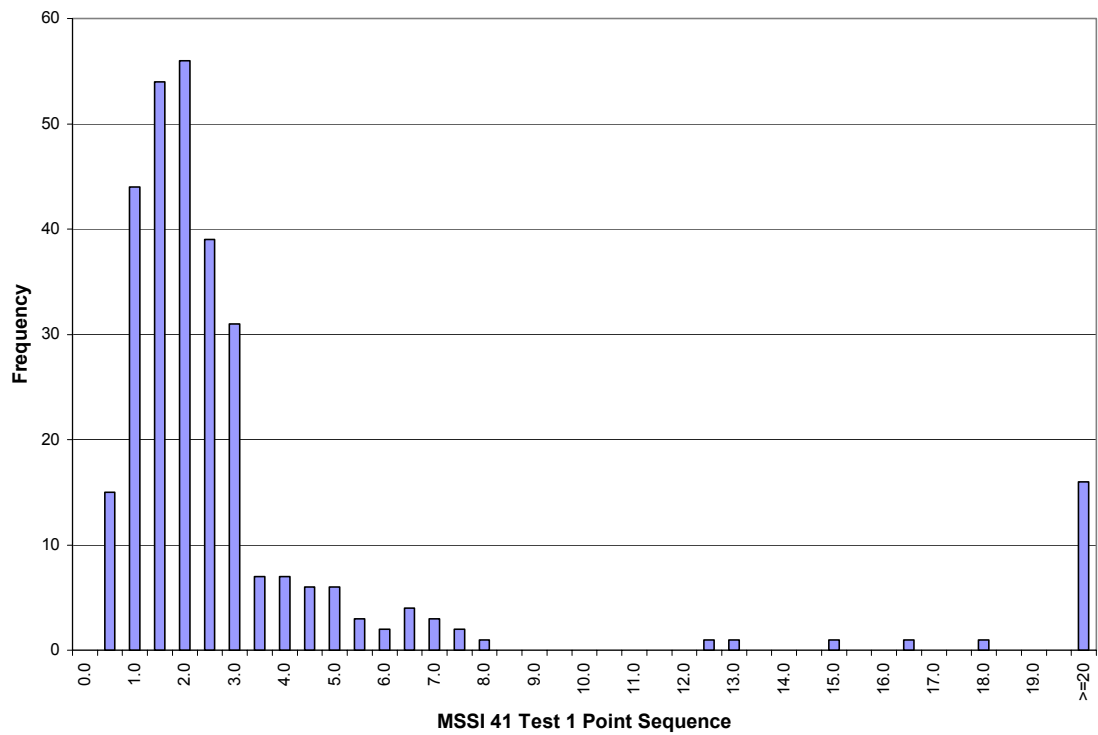

Figure 73. MSSI Test 1, Tag 41: Error histogram.
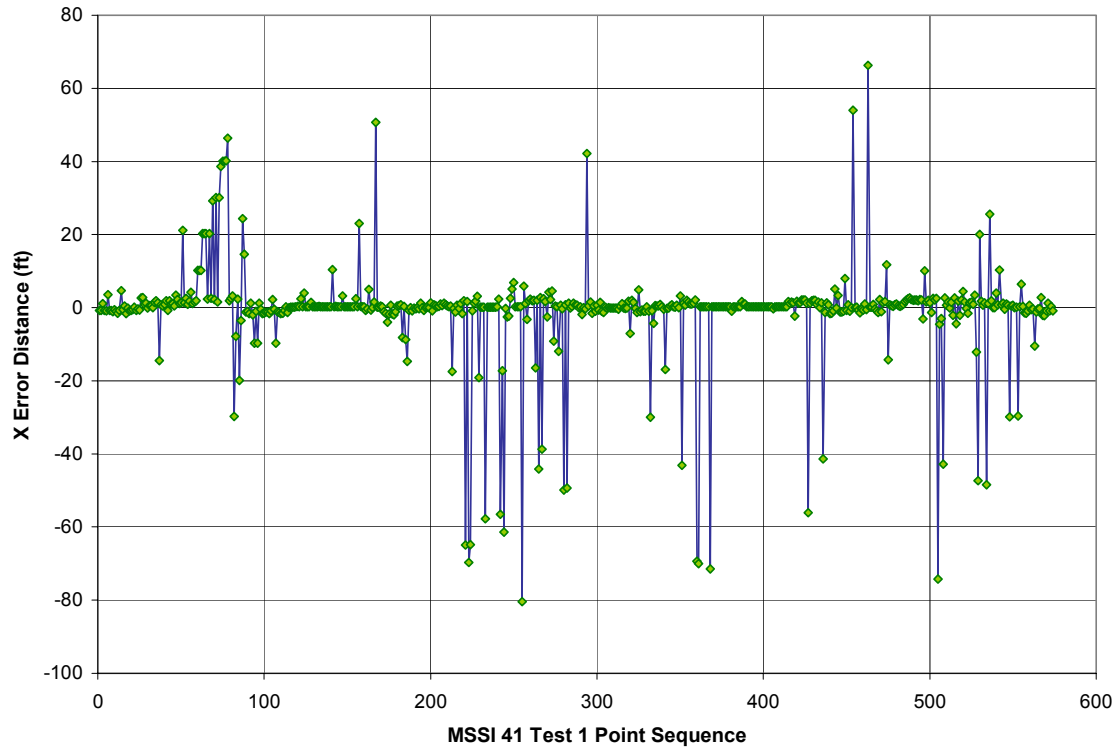
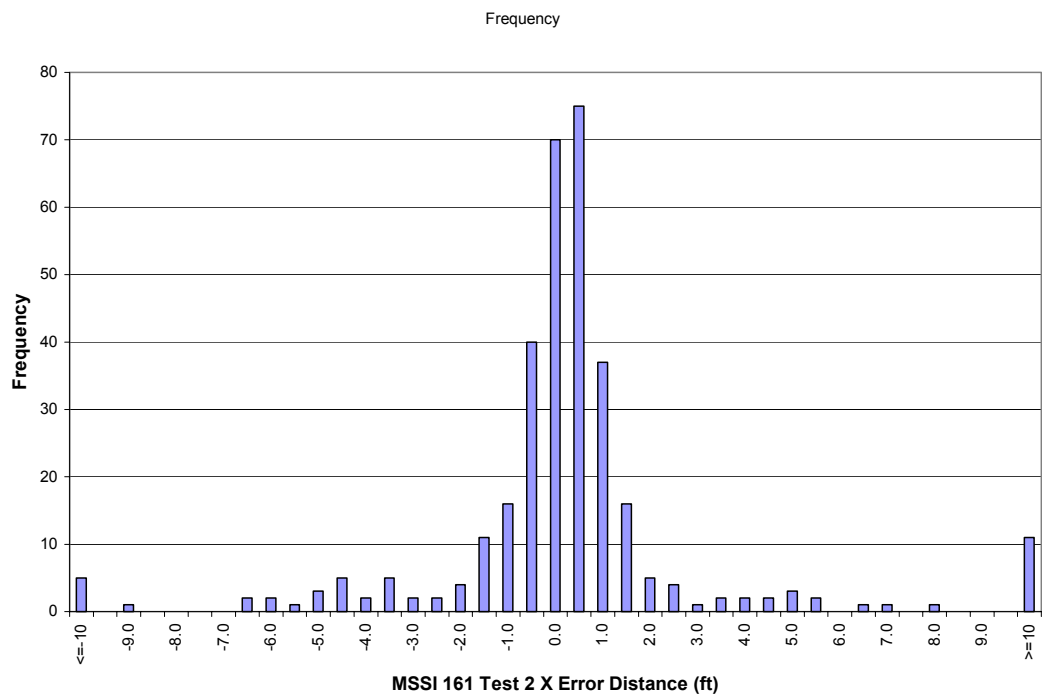Figure 74. MSSI Test 1, Tag 41: "X" difference versus blink.
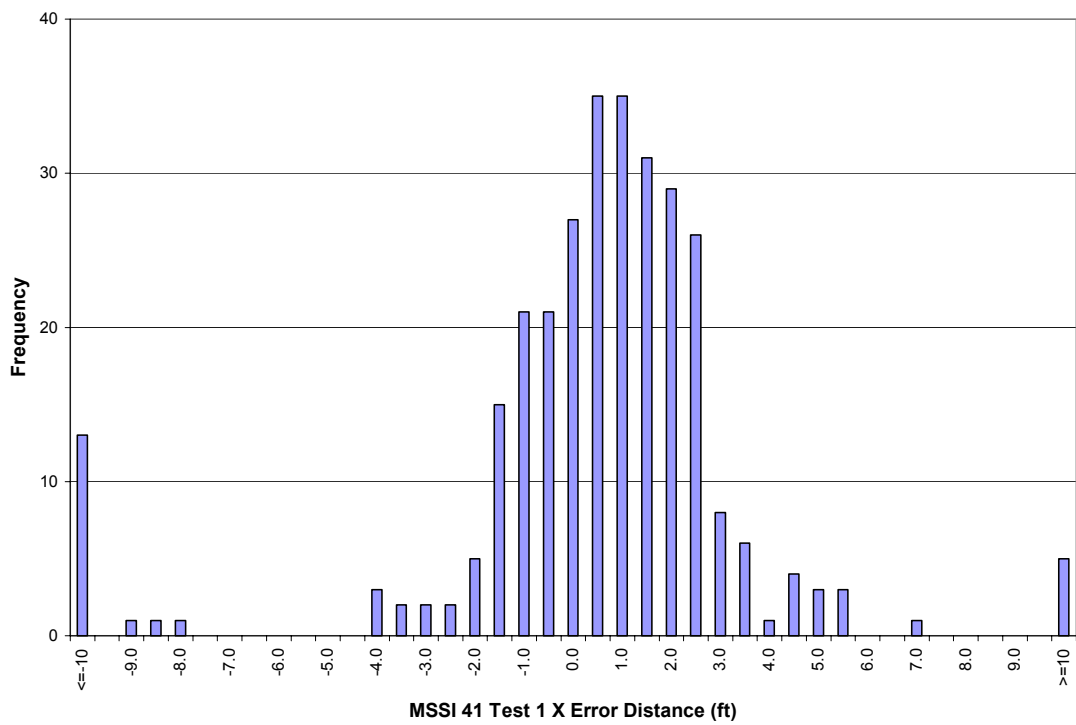
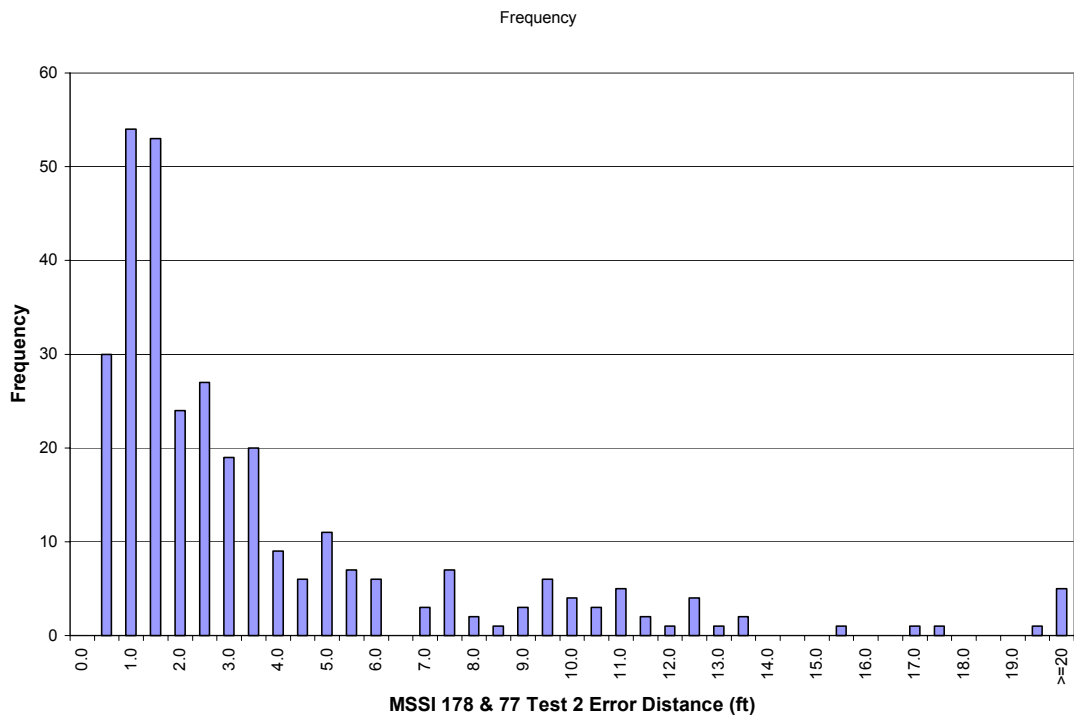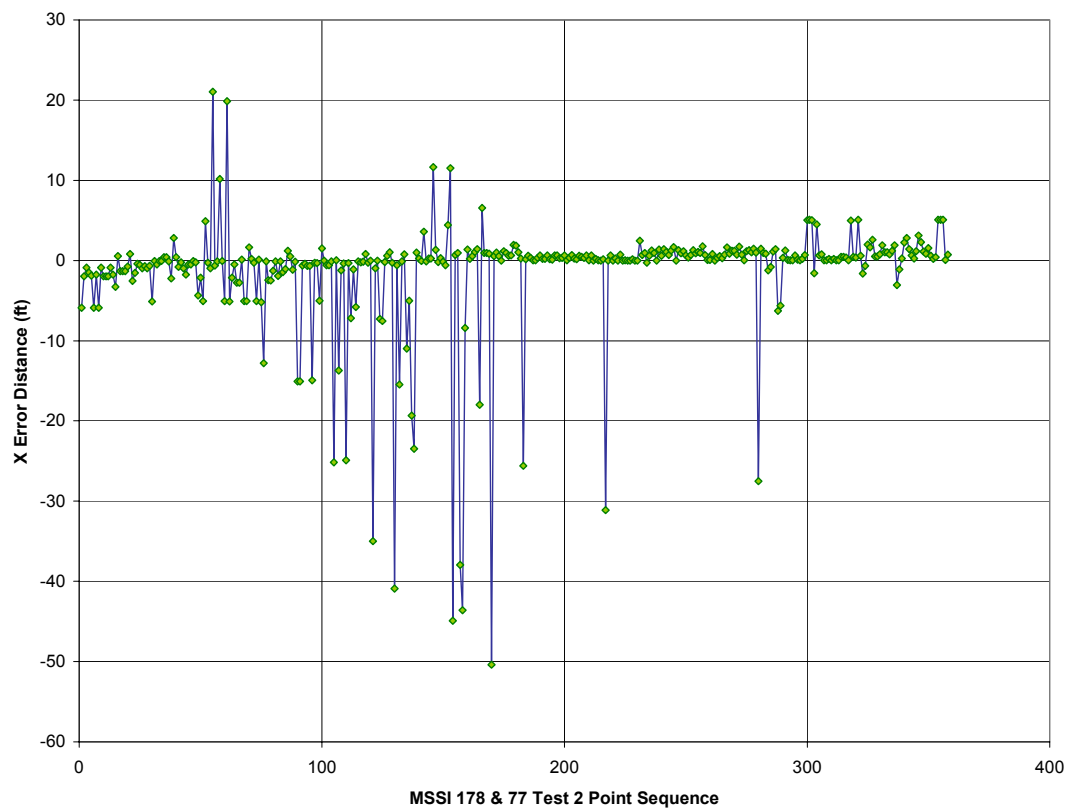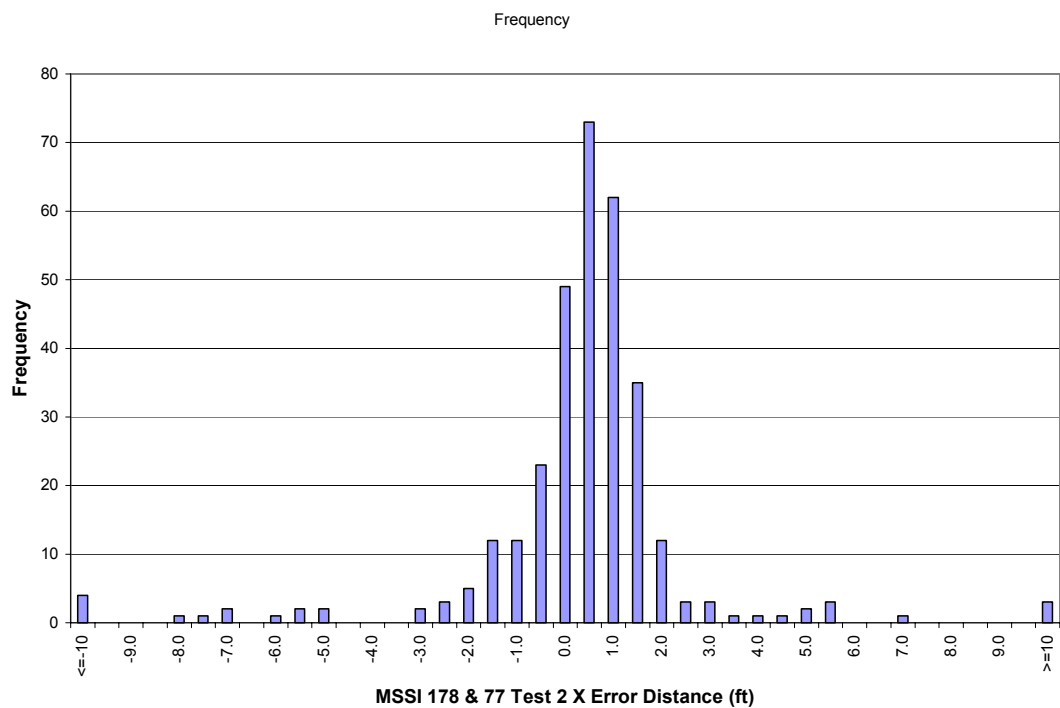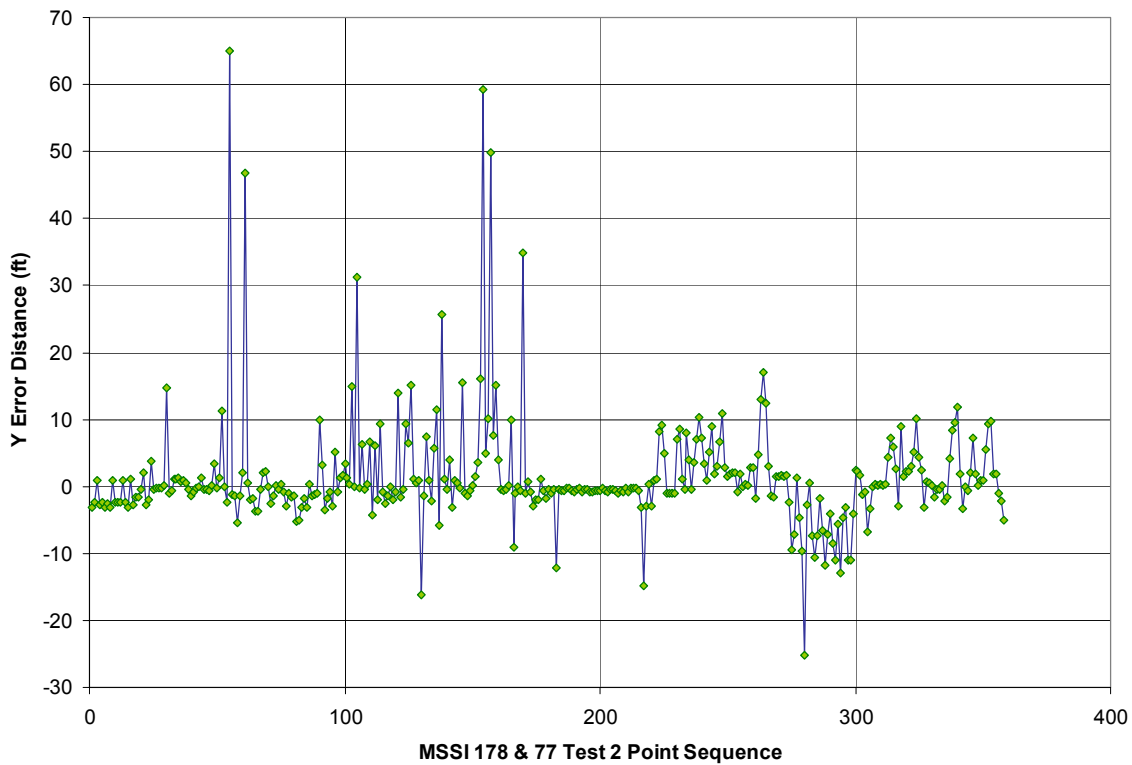Figure 75. MSSI Test 1, Tag 41: "X" difference histogram.
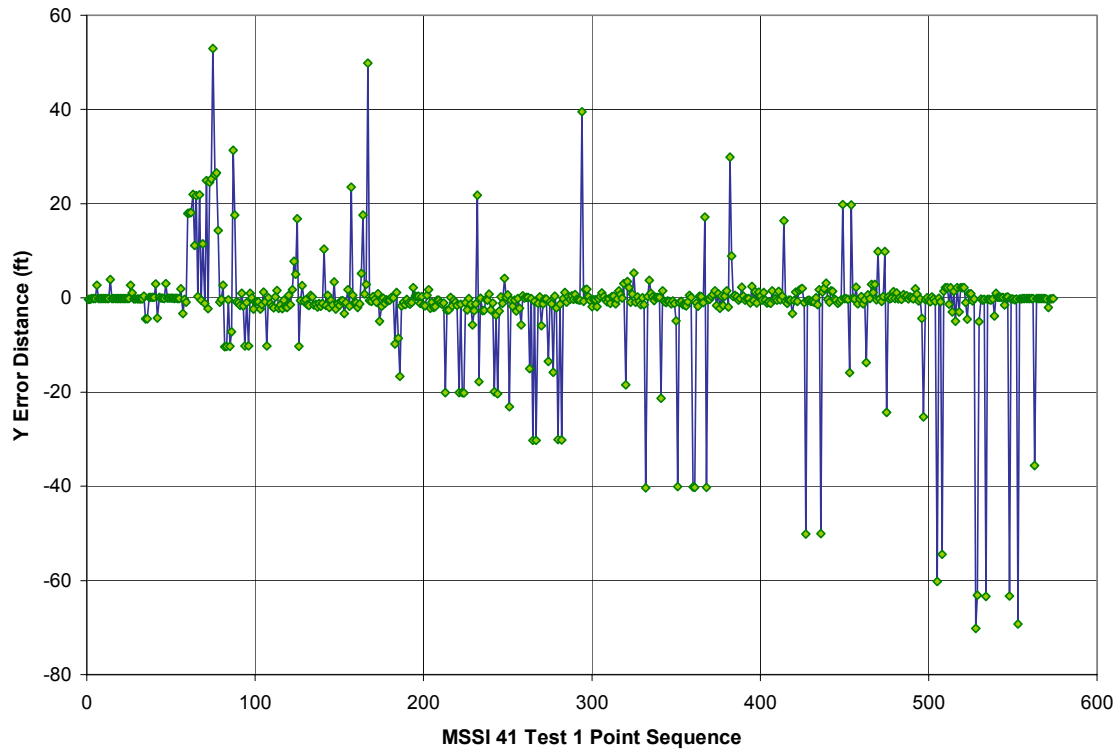
Figure 76. MSSI Test 1, Tag 41: "Y" difference versus blink.
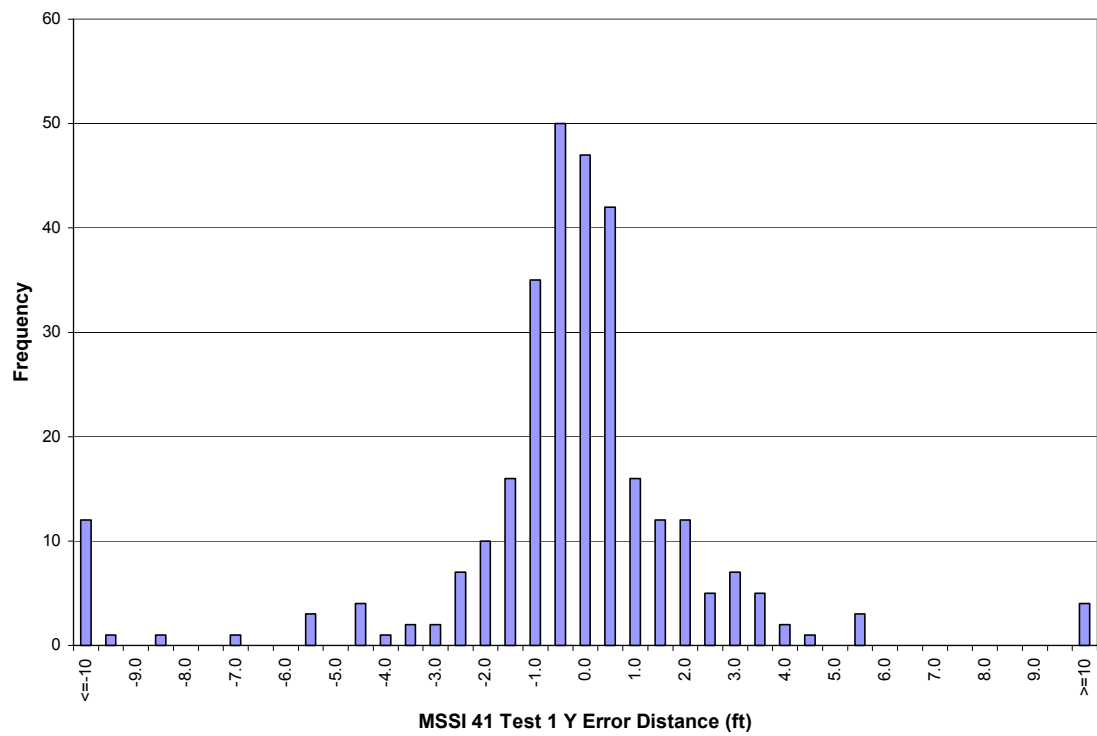
Figure 77. MSSI Test 1, Tag 41: "Y" difference histogram.
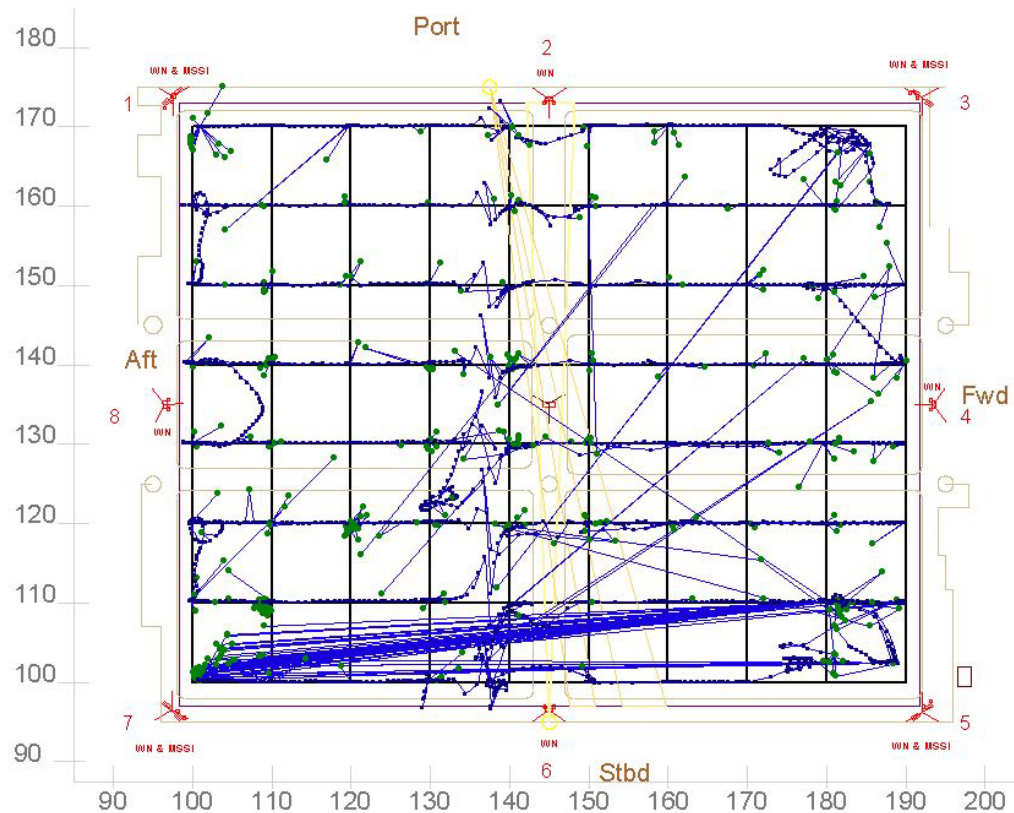
Figure 78. MSSI Test 1, Tag 161: Reported and correlated positions.
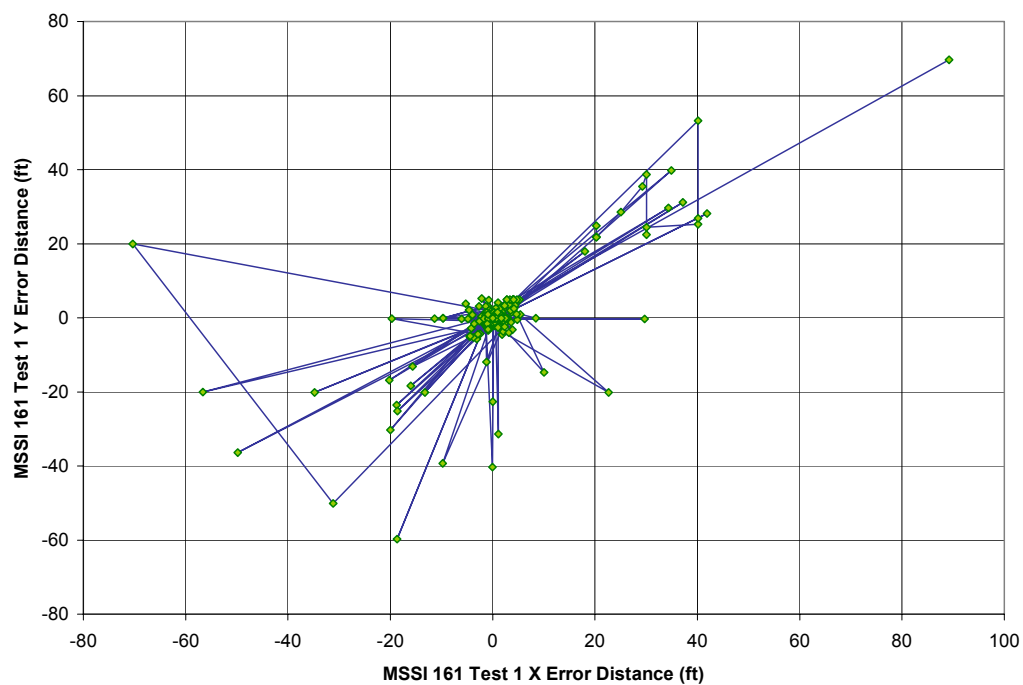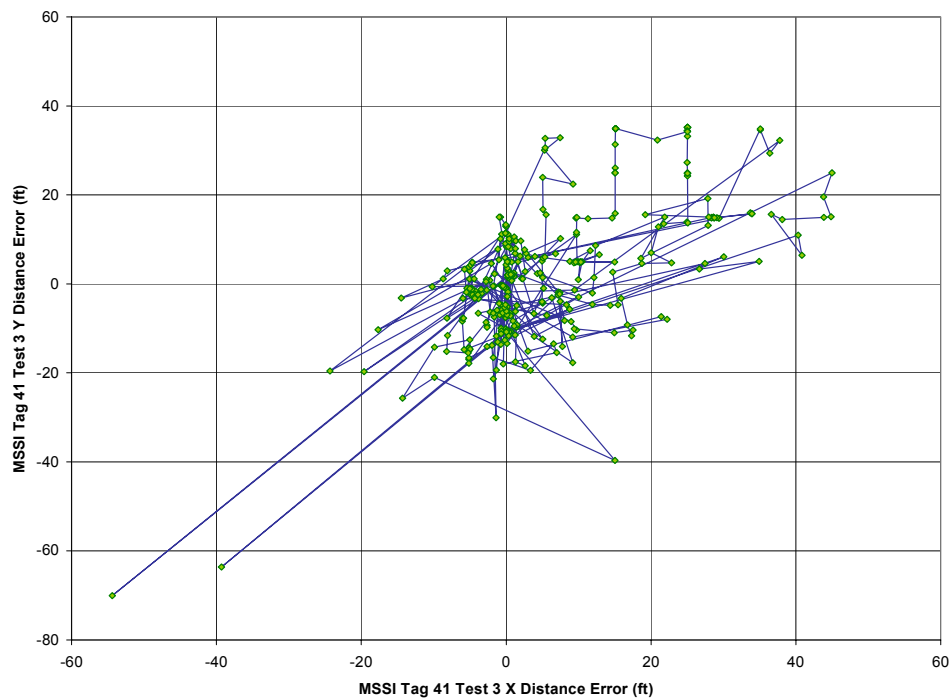

Figure 79. MSSI Test 1, Tag 161: "X-Y" difference versus blink.

4-14
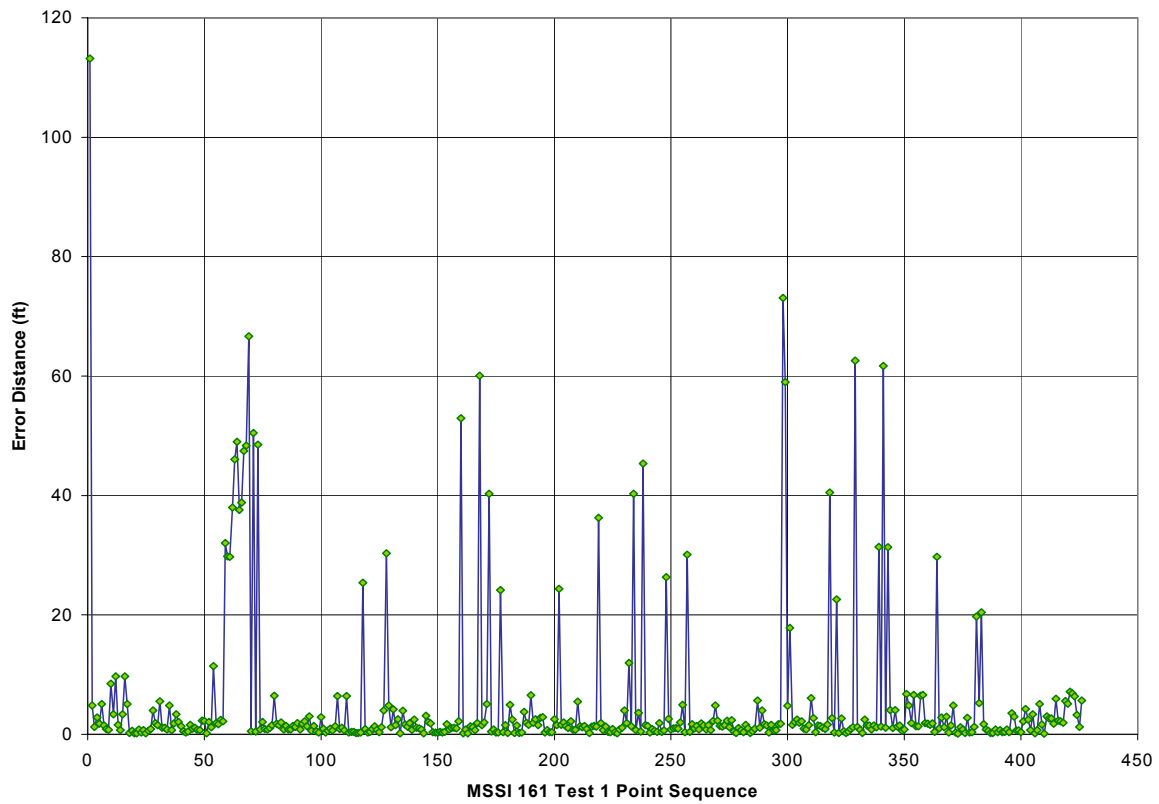
Figure 80. MSSI Test 1, Tag 161: Error versus blink.
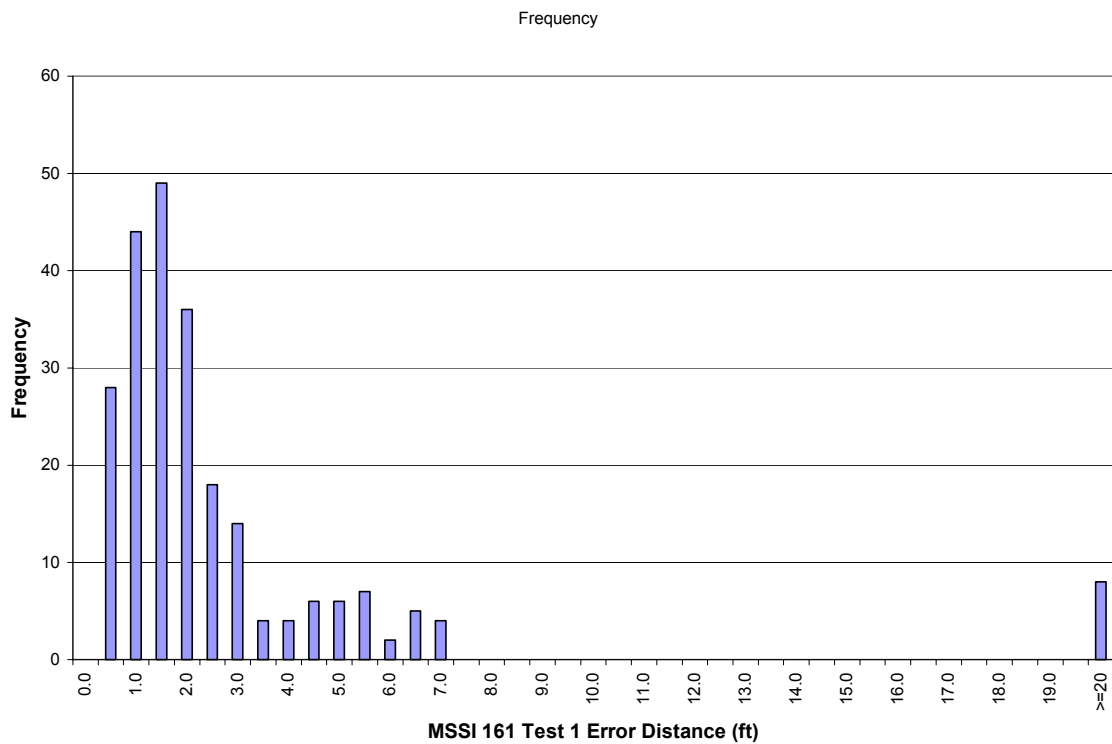
Figure 81. MSSI Test 1, Tag 161: Error histogram.
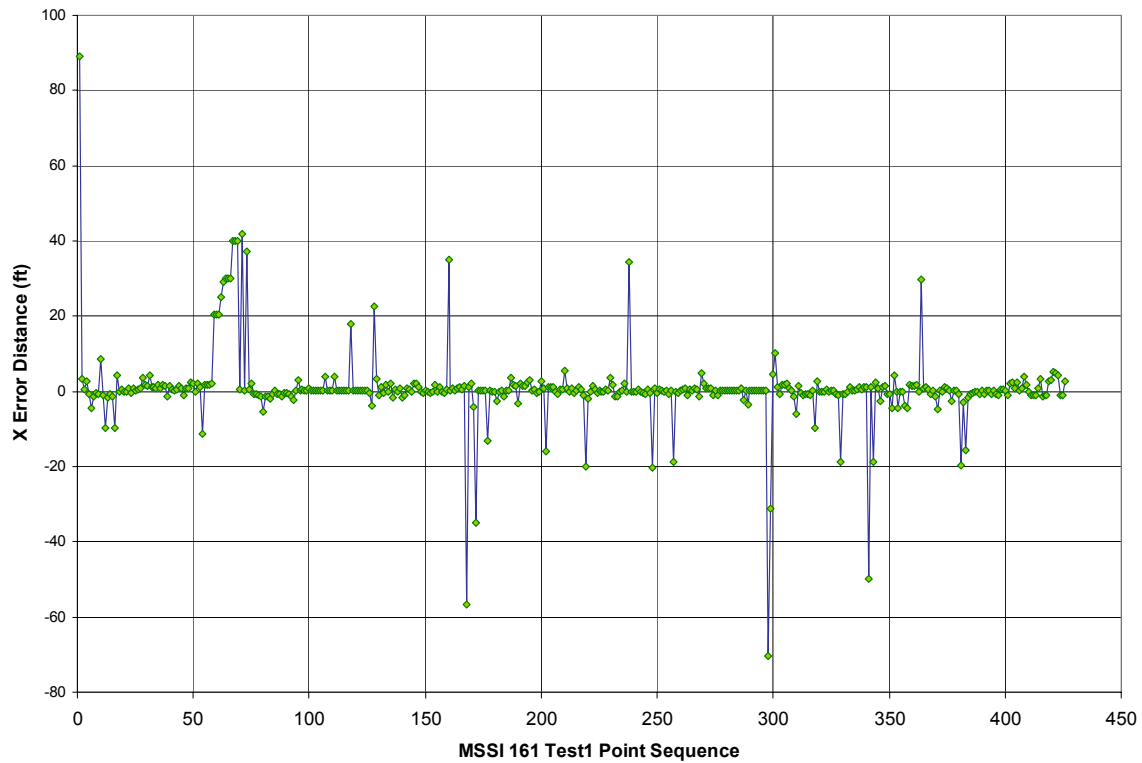
Figure 82. MSSI Test 1, Tag 161: "X" difference versus blink.
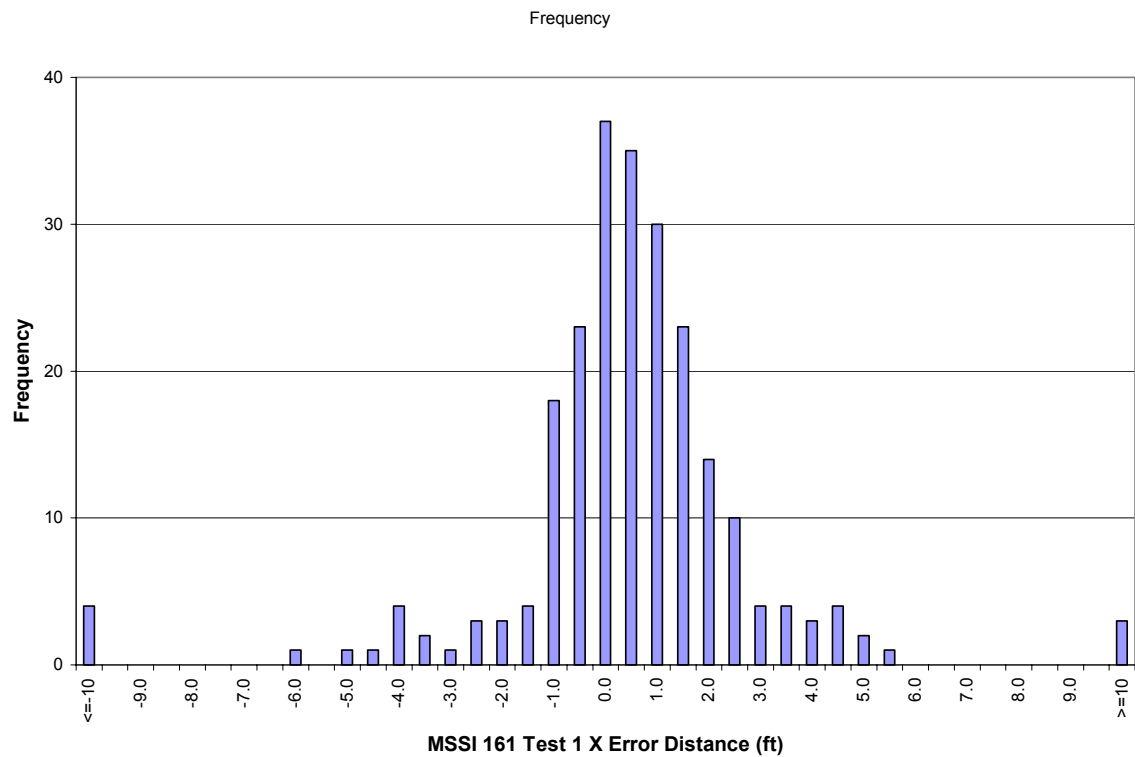
Figure 83. MSSI Test 1, Tag 161: "X" difference histogram.
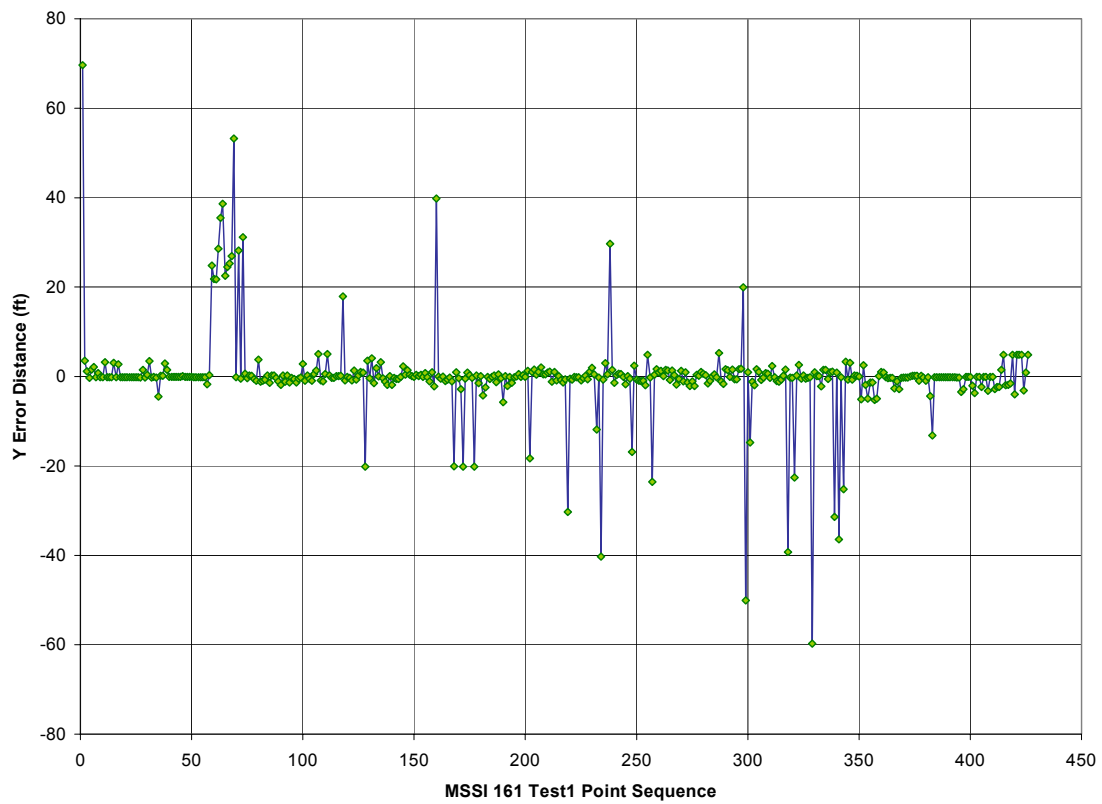
Figure 84. MSSI Test 1, Tag 161: "Y" difference versus blink.
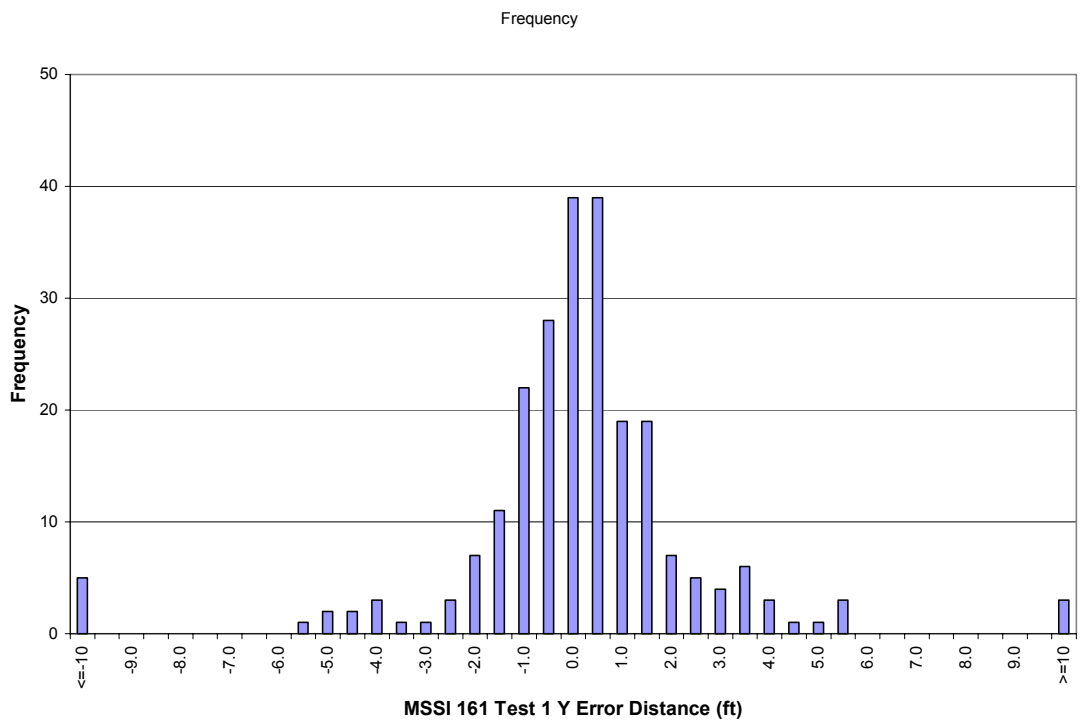
Figure 85. MSSI Test 1, Tag 161: "Y" difference histogram.
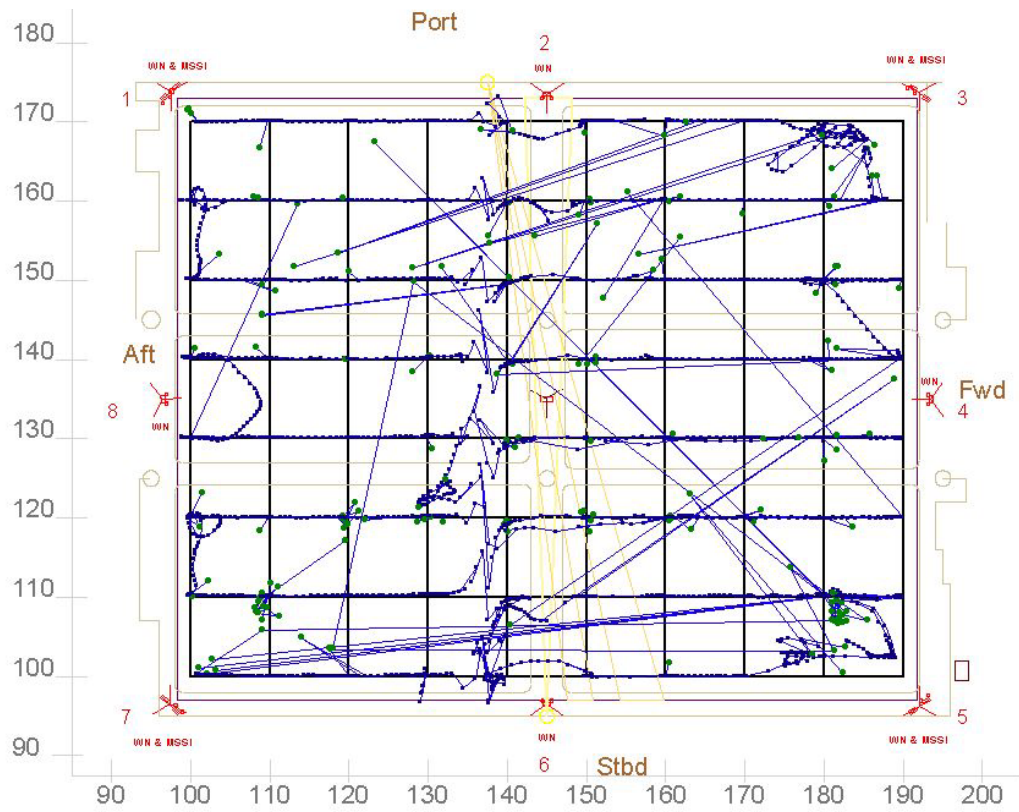
Figure 86. MSSI Test 1, Tag 178: Reported and correlated positions.
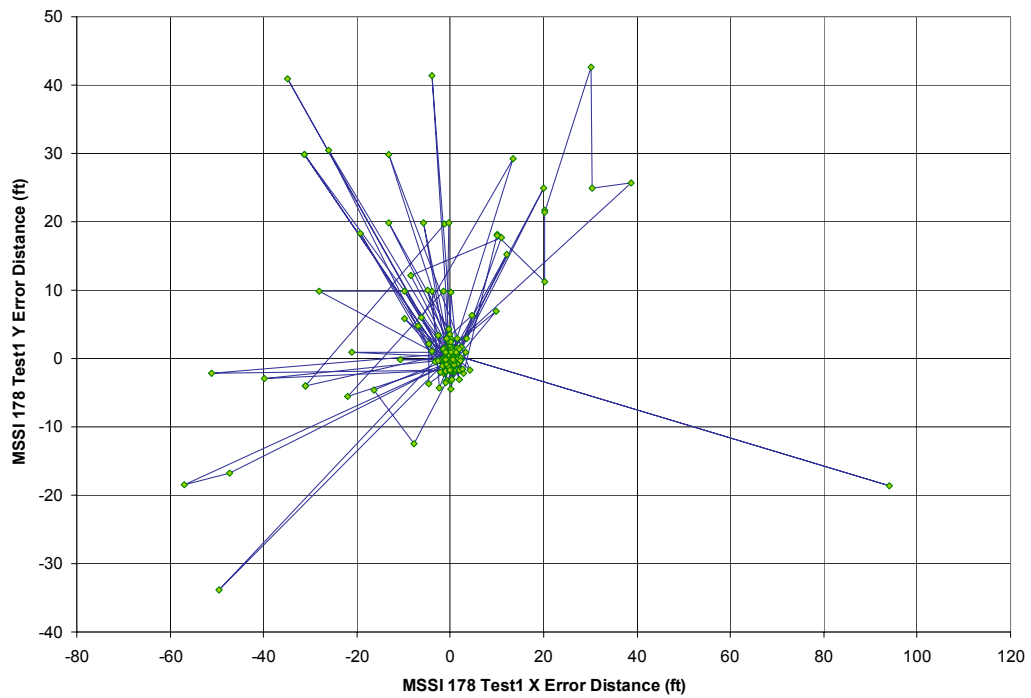
Figure 87. MSSI Test 1, Tag 178: "X-Y" difference versus blink.
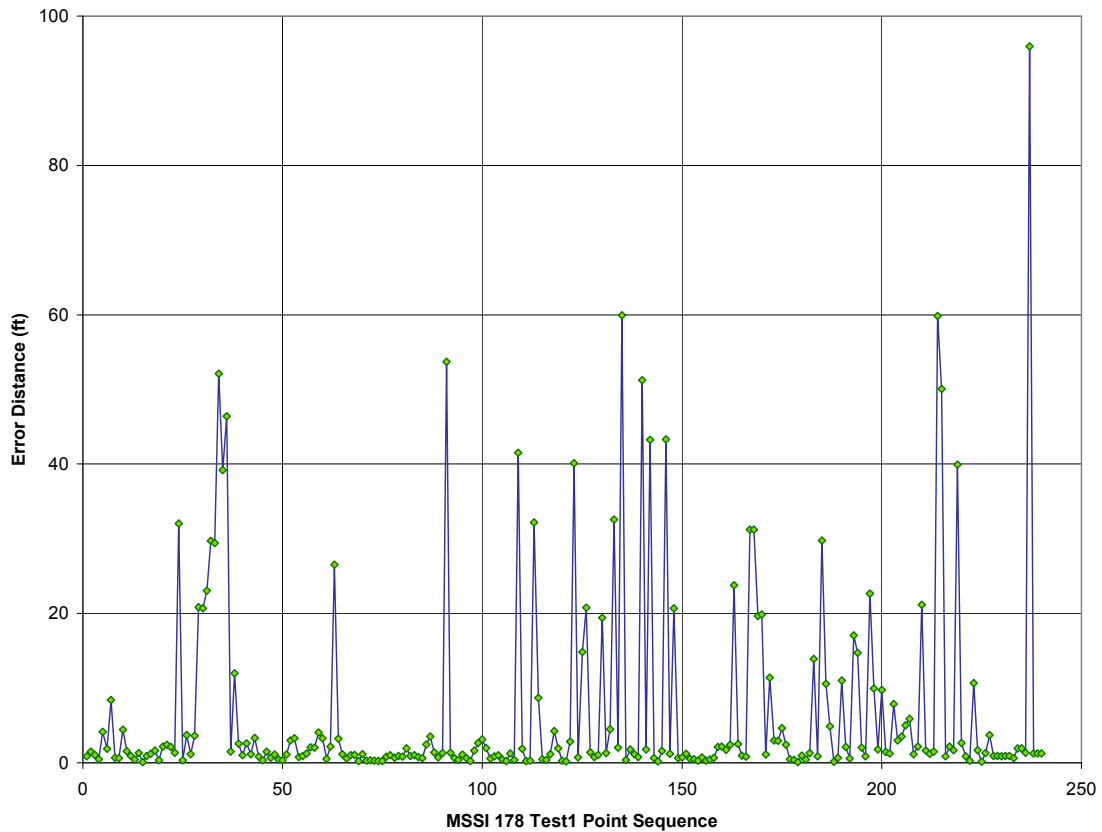
Figure 88. MSSI Test 1, Tag 178: Error versus blink.
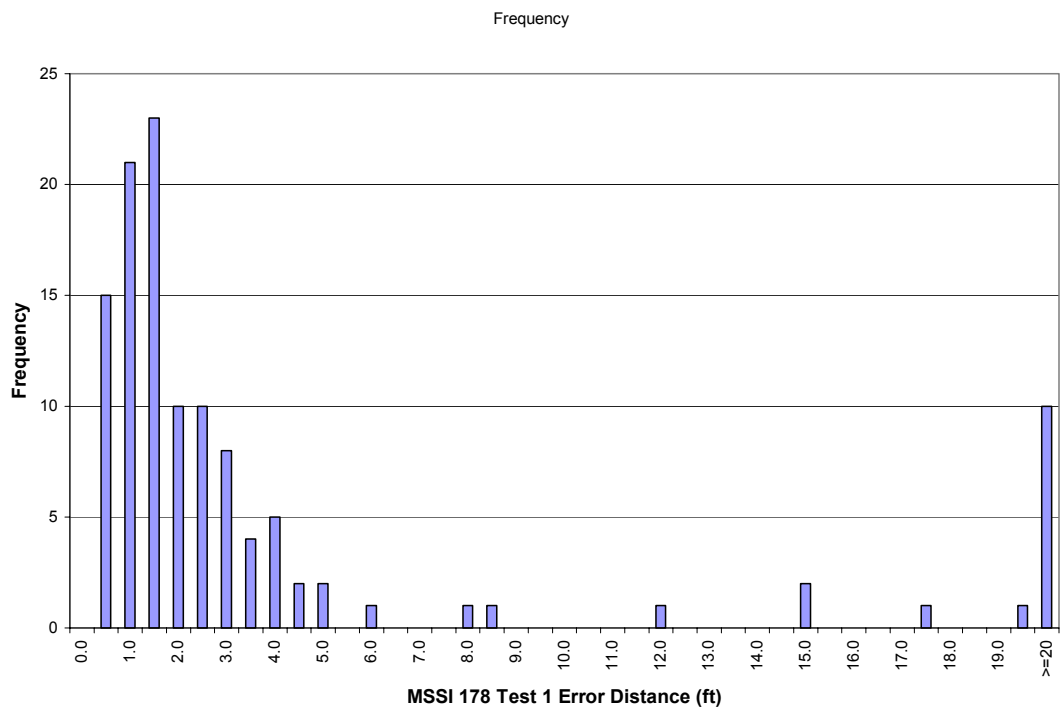

Figure 89. MSSI Test 1, Tag 178: Error histogram.
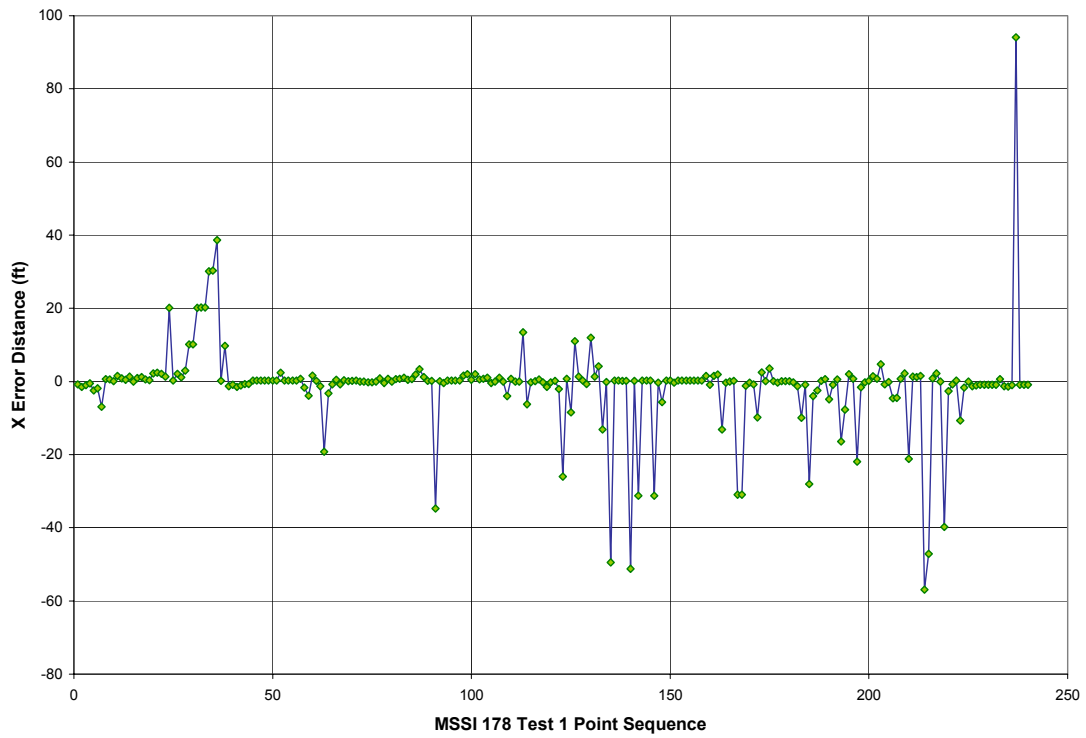
Figure 90. MSSI Test 1, Tag 178: "X" difference versus blink.
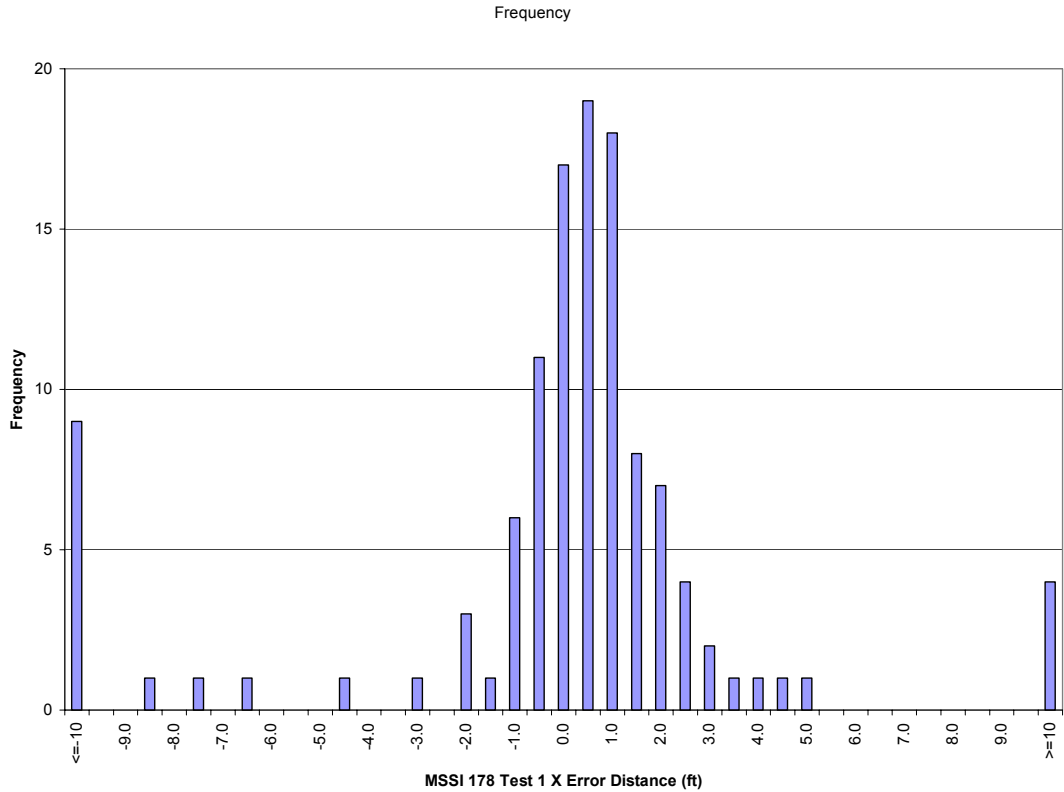
Figure 91. MSSI Test 1, Tag 178: "X" difference histogram.
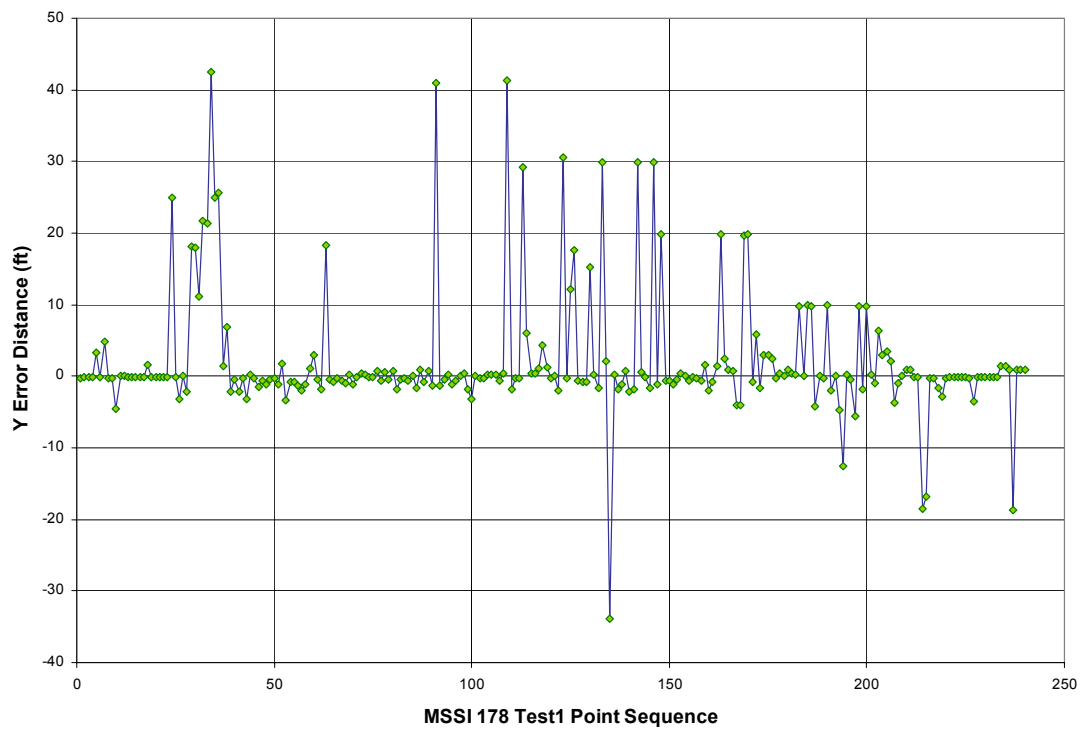
Figure 92. MSSI Test 1, Tag 178: "Y" difference versus blink.
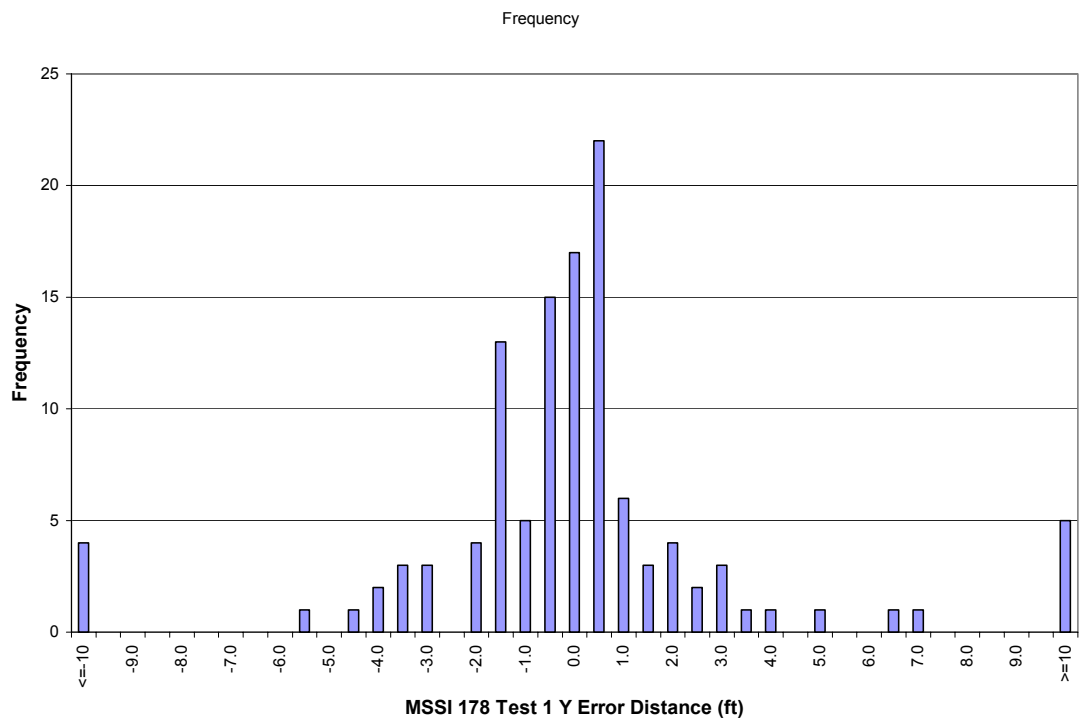
Figure 93. MSSI Test 1, Tag 178: "Y" difference histogram.
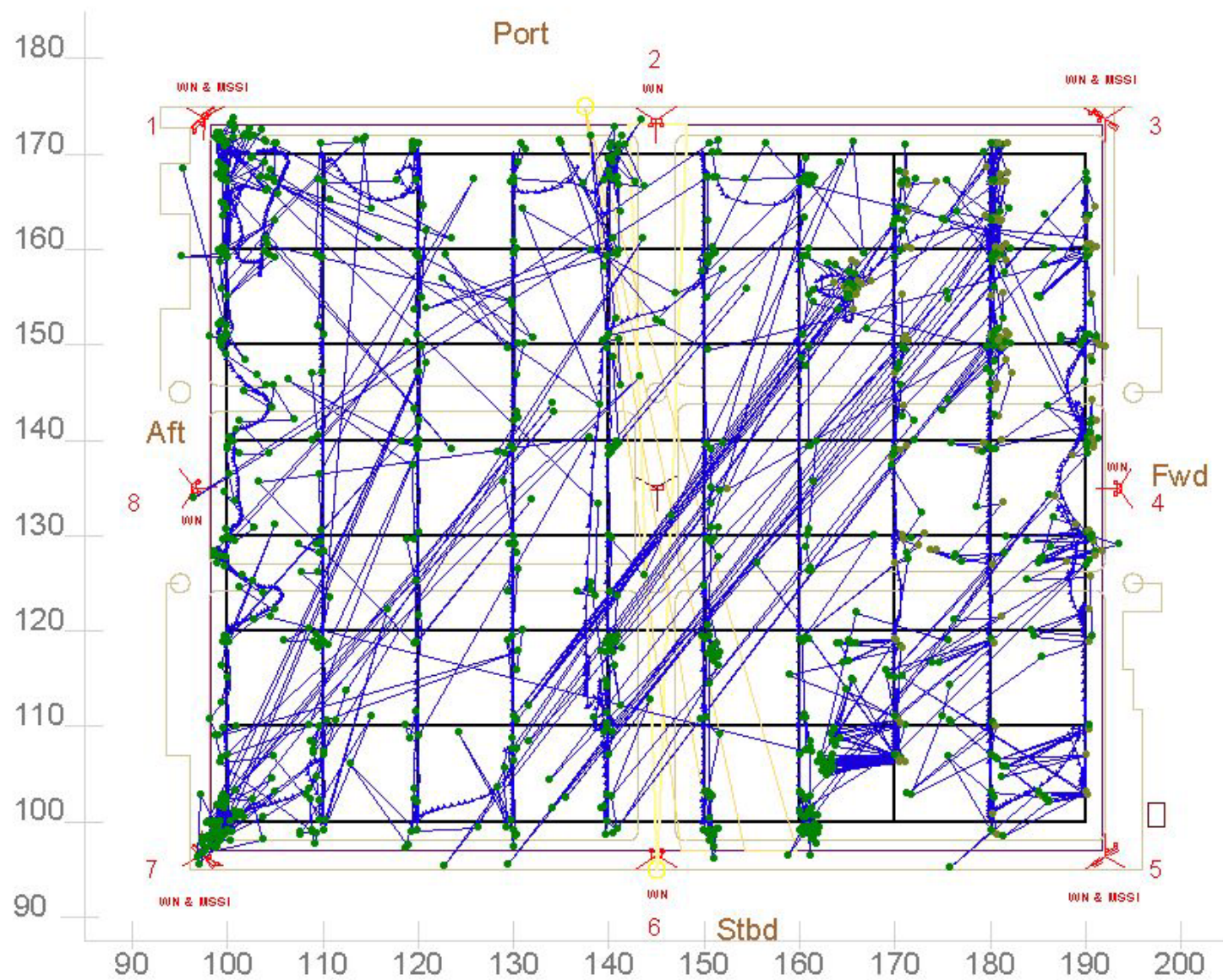
Figure 94. MSSI Test 2: All tag reported positions with tracks.
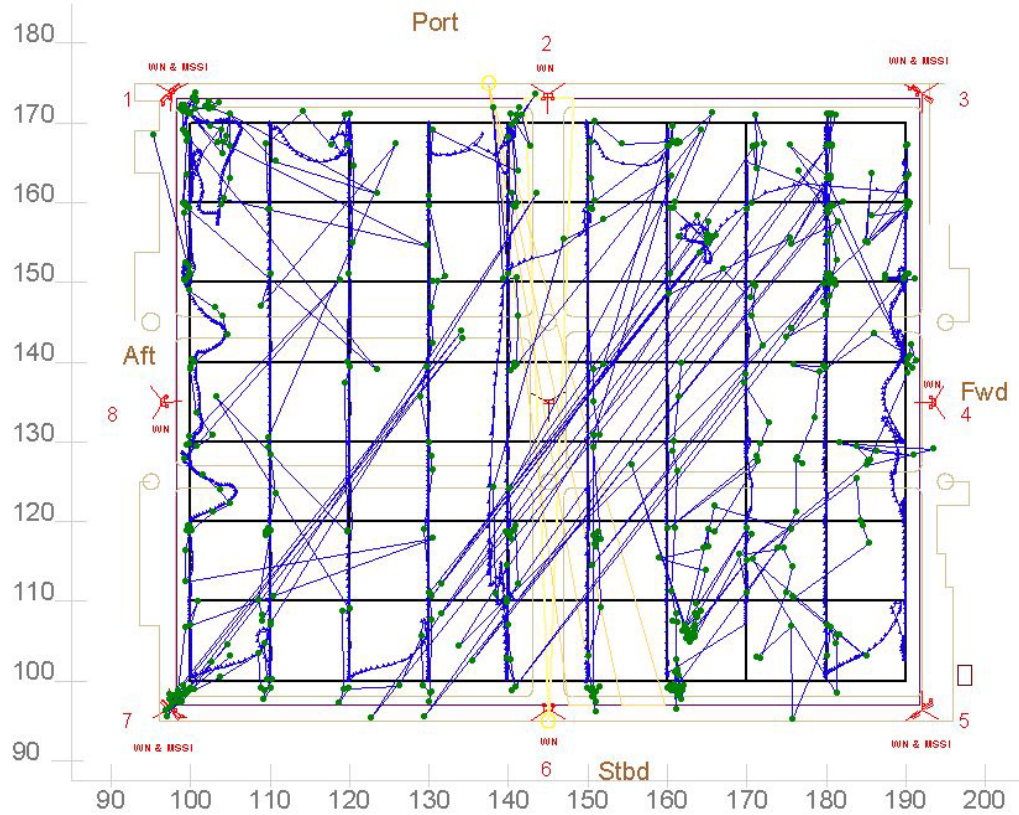
Figure 95. MSSI Test 2, Tag 41: Reported positions with tracks.
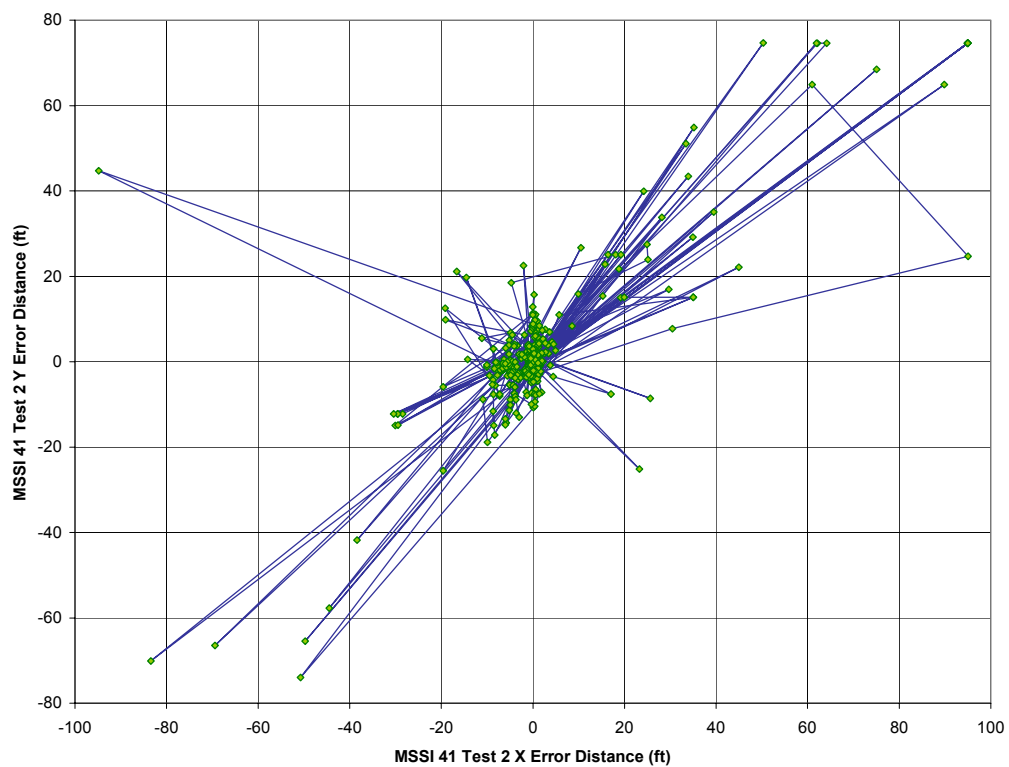
Figure 96. MSSI Test 2, Tag 41: "X-Y" difference versus blink.
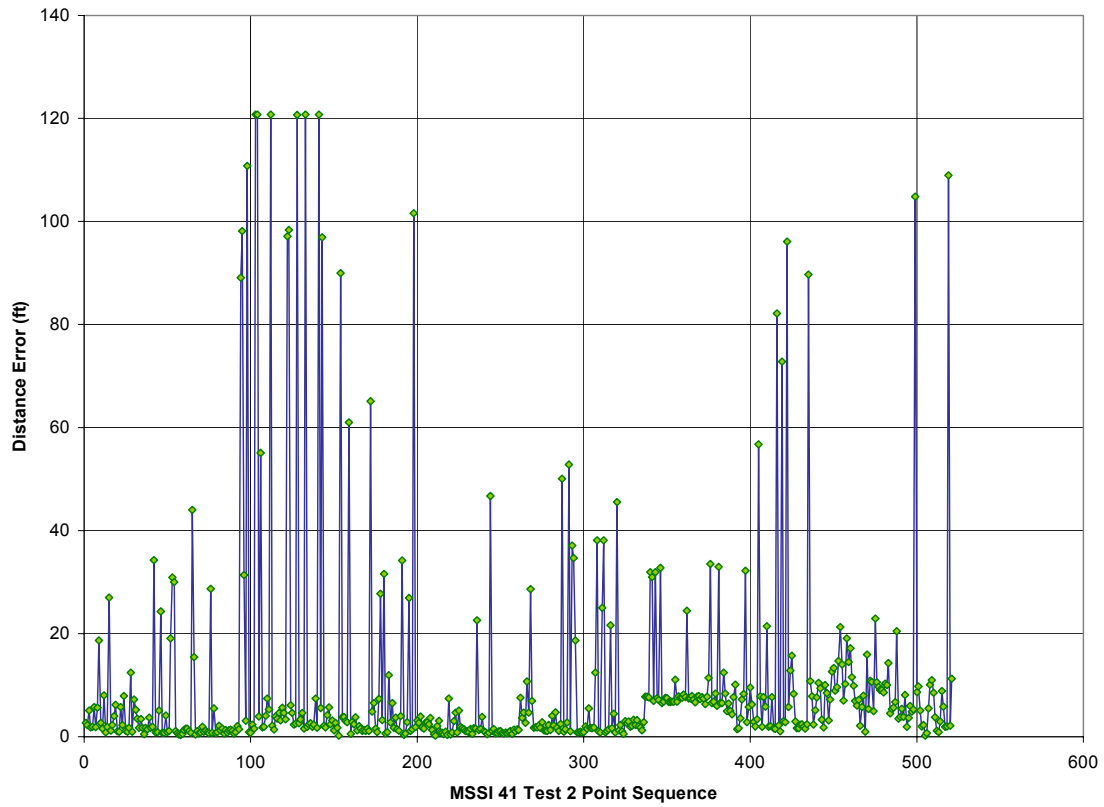
Figure 97. MSSI Test 2, Tag 41: Error versus blink.
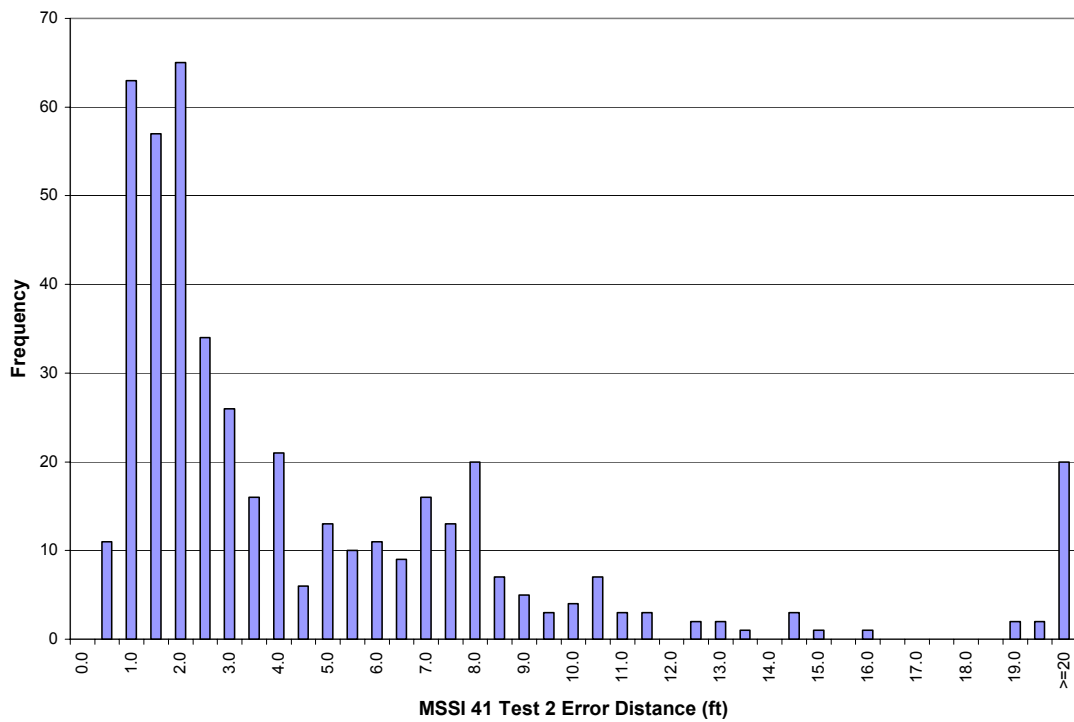
Figure 98. MSSI Test 2, Tag 41: Error histogram.
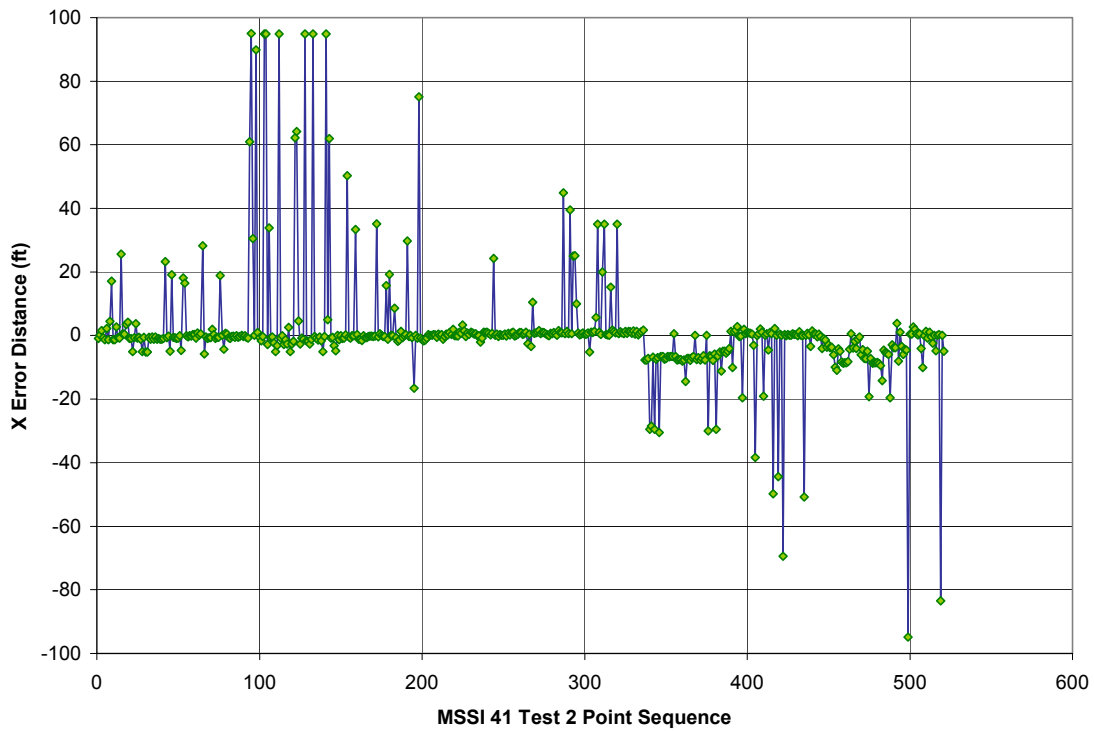
Figure 99. MSSI Test 2, Tag 41: "X" difference versus blink.
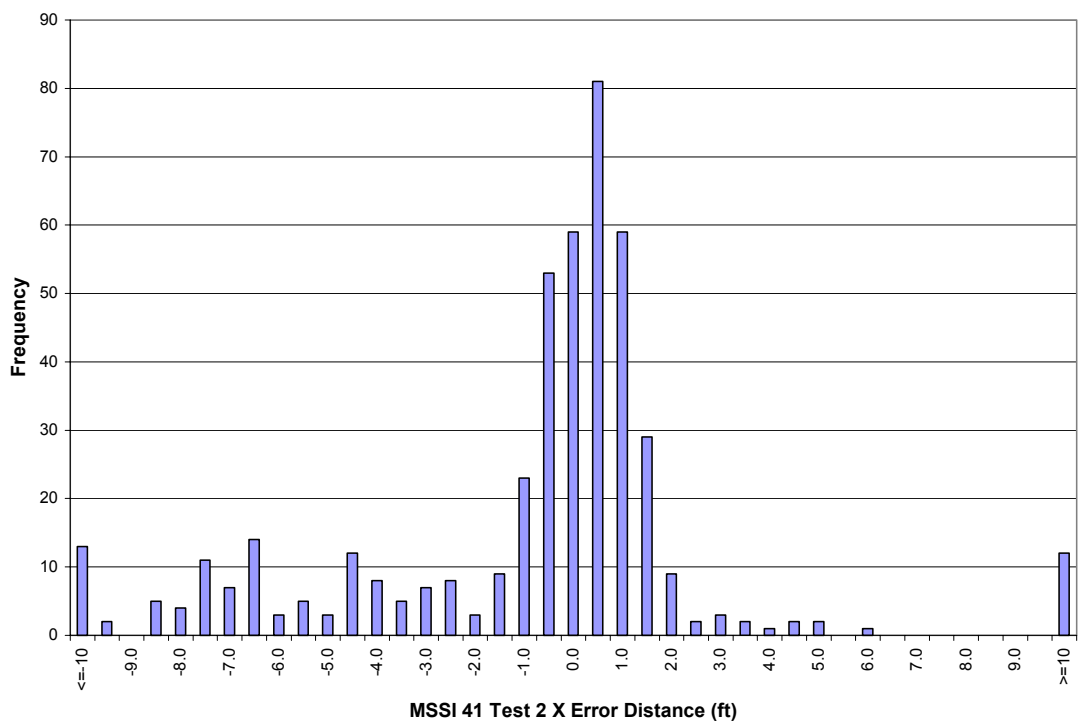
Figure 100. MSSI Test 2, Tag 41: "X" difference histogram.
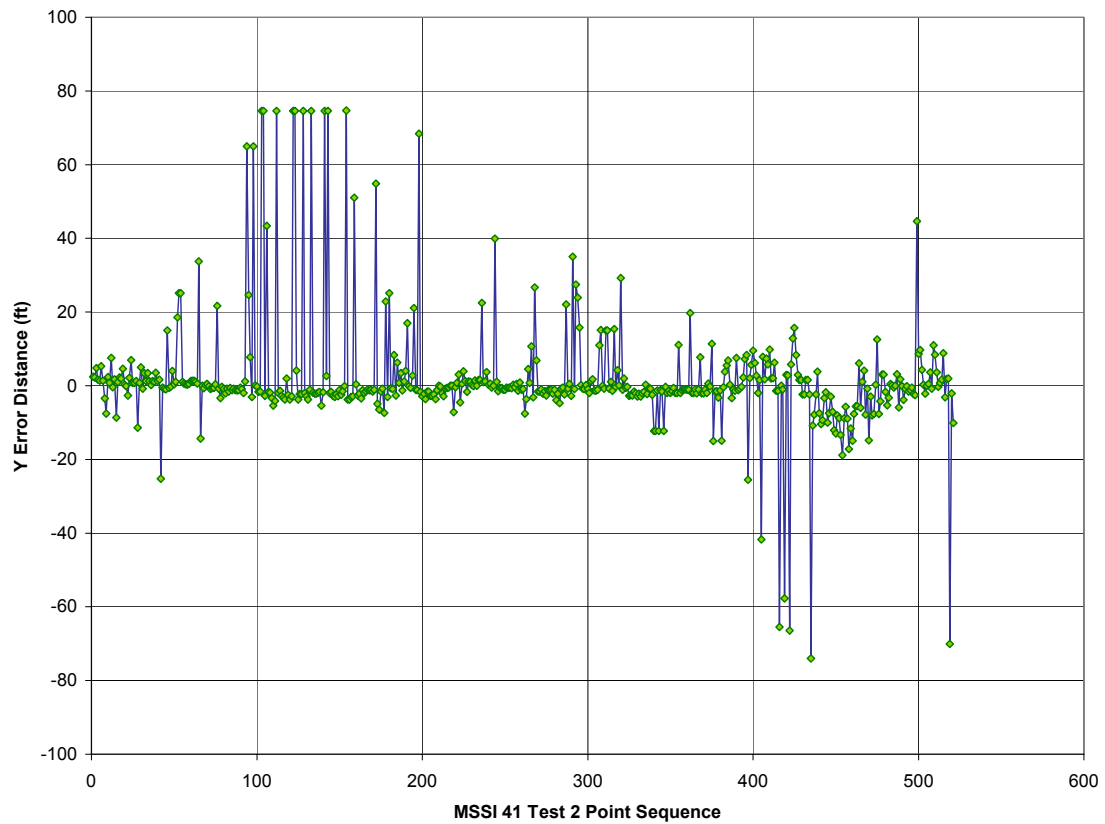
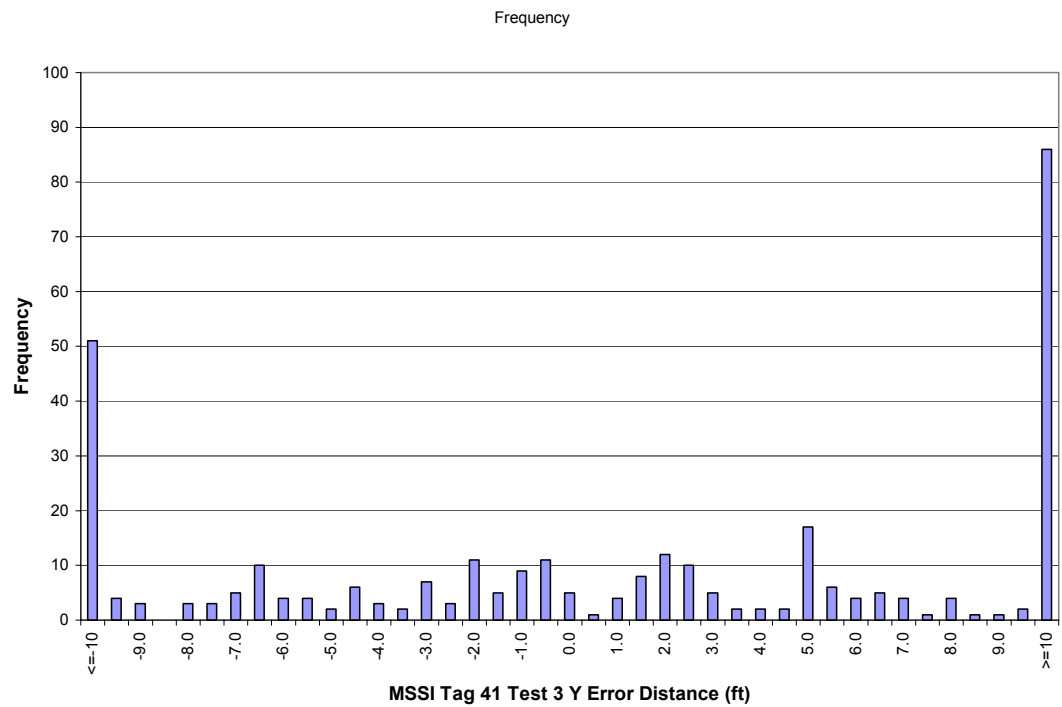Figure 101. MSSI Test 2, Tag 41: "Y" difference versus blink.
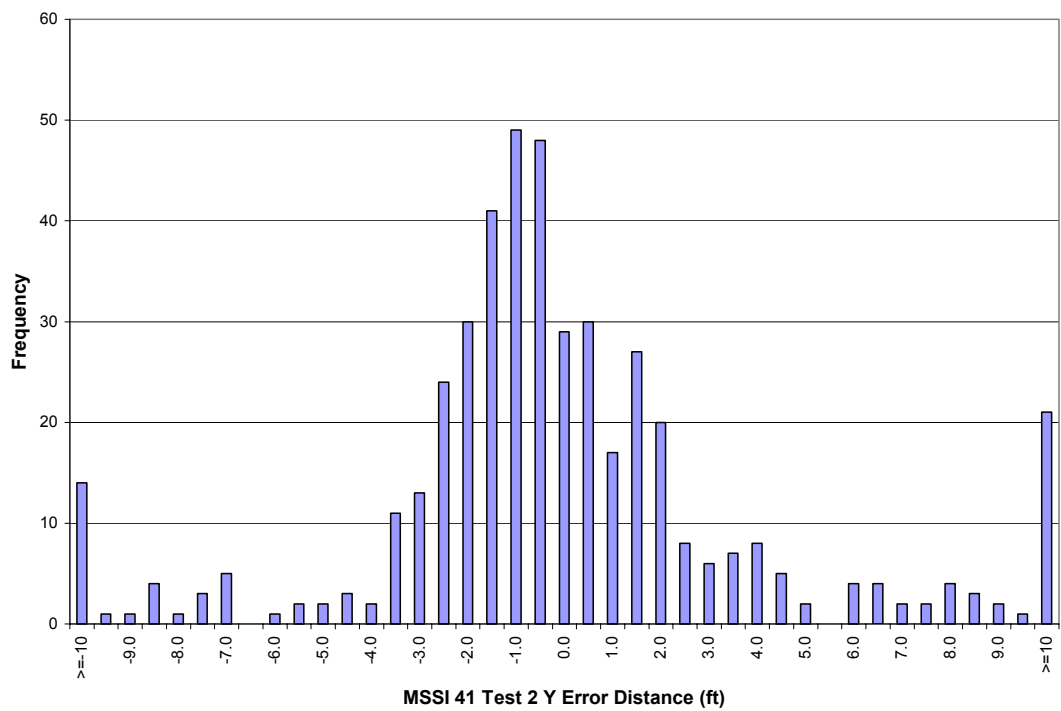
Figure 102. MSSI Test 2, Tag 41: "Y" difference histogram.
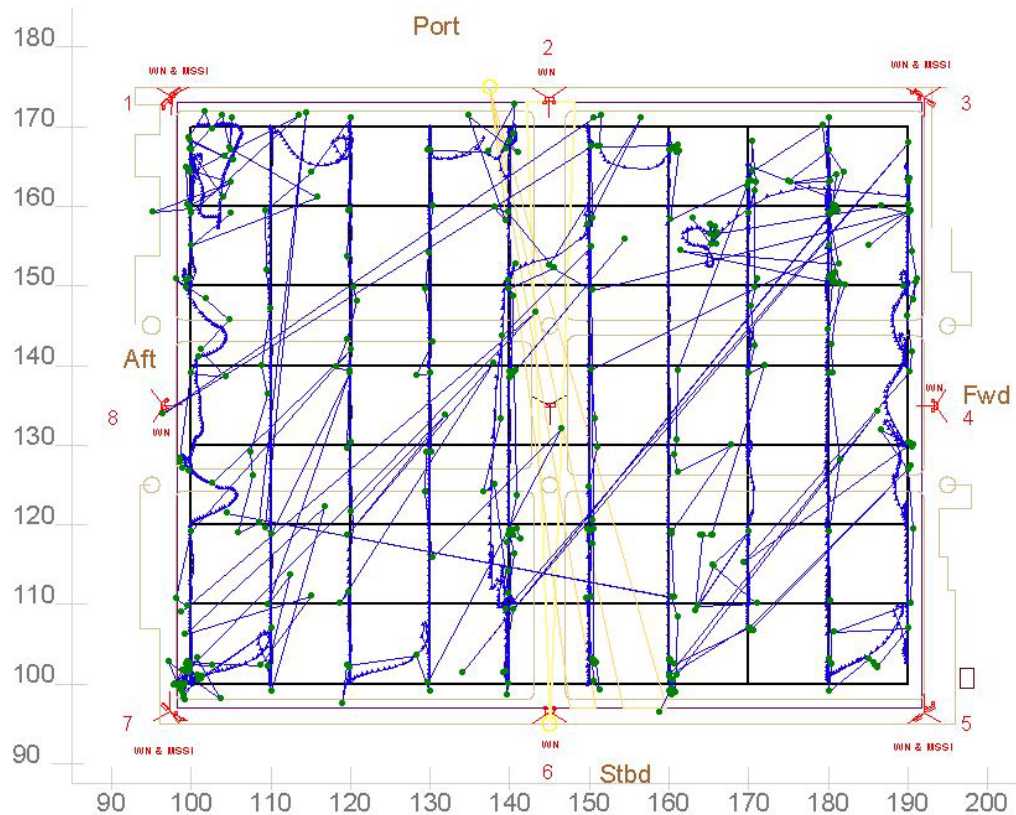
Figure 103. MSSI Test 2, Tag 161: Reported and positions with tracks
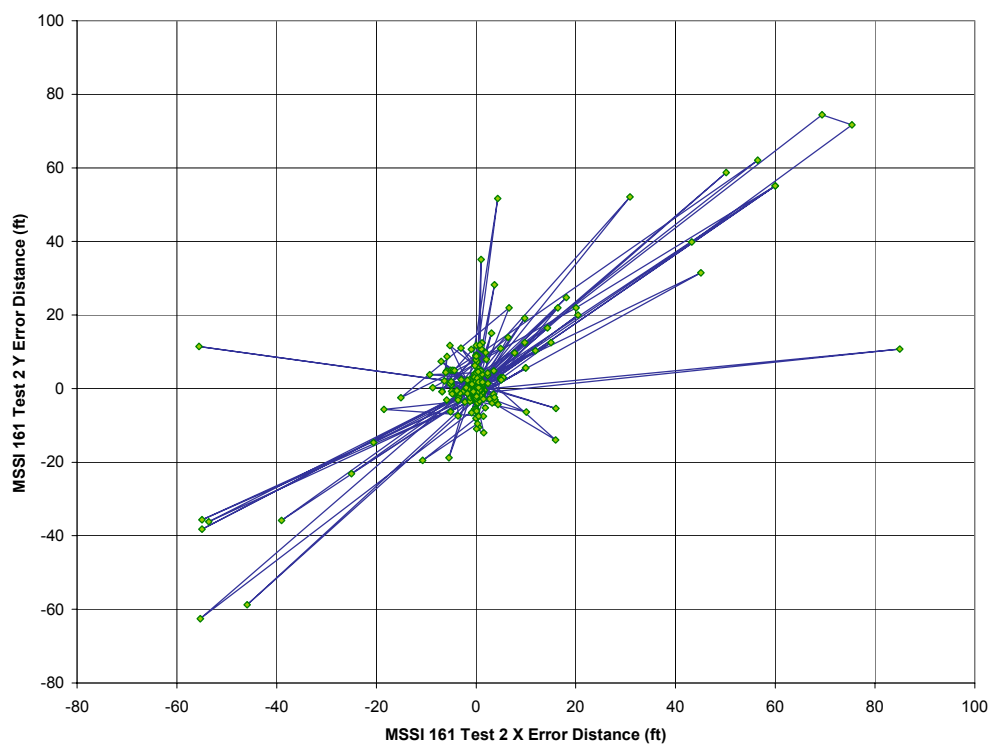
Figure 104. MSSI Test 2, Tag 161: "X-Y" difference versus blink.
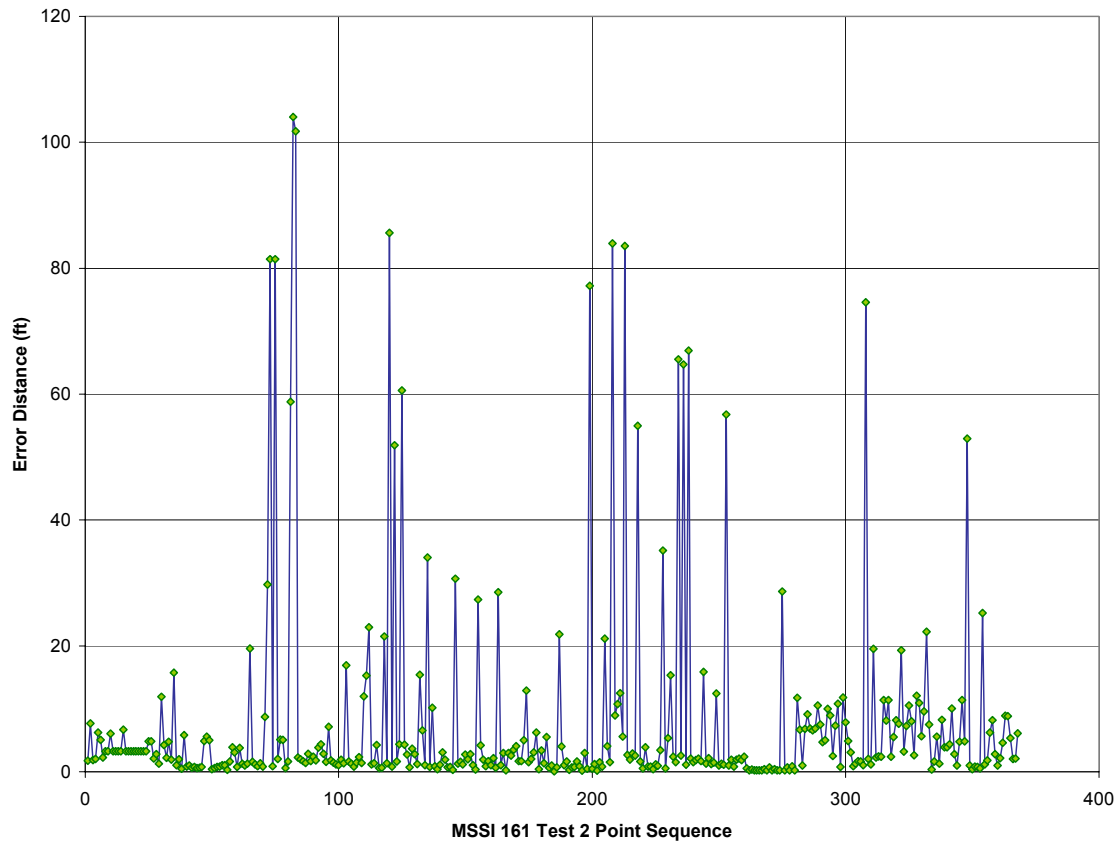
Figure 105. MSSI Test 2, Tag 161: Error versus blink.
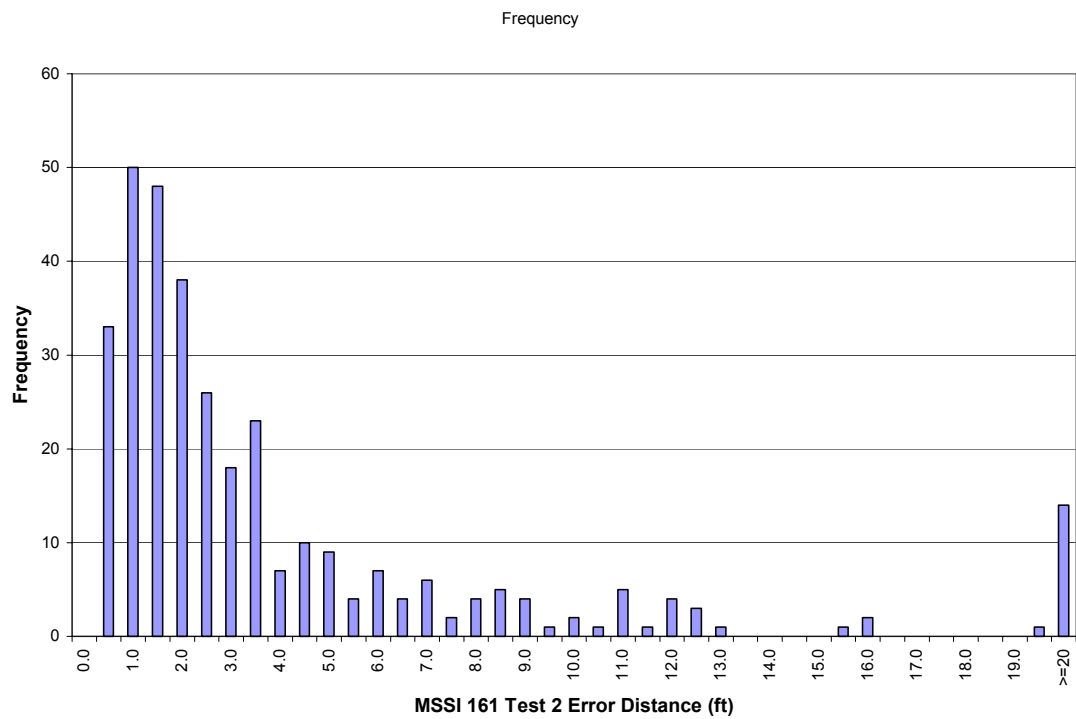
Figure 106. MSSI Test 2, Tag 161: Error histogram.
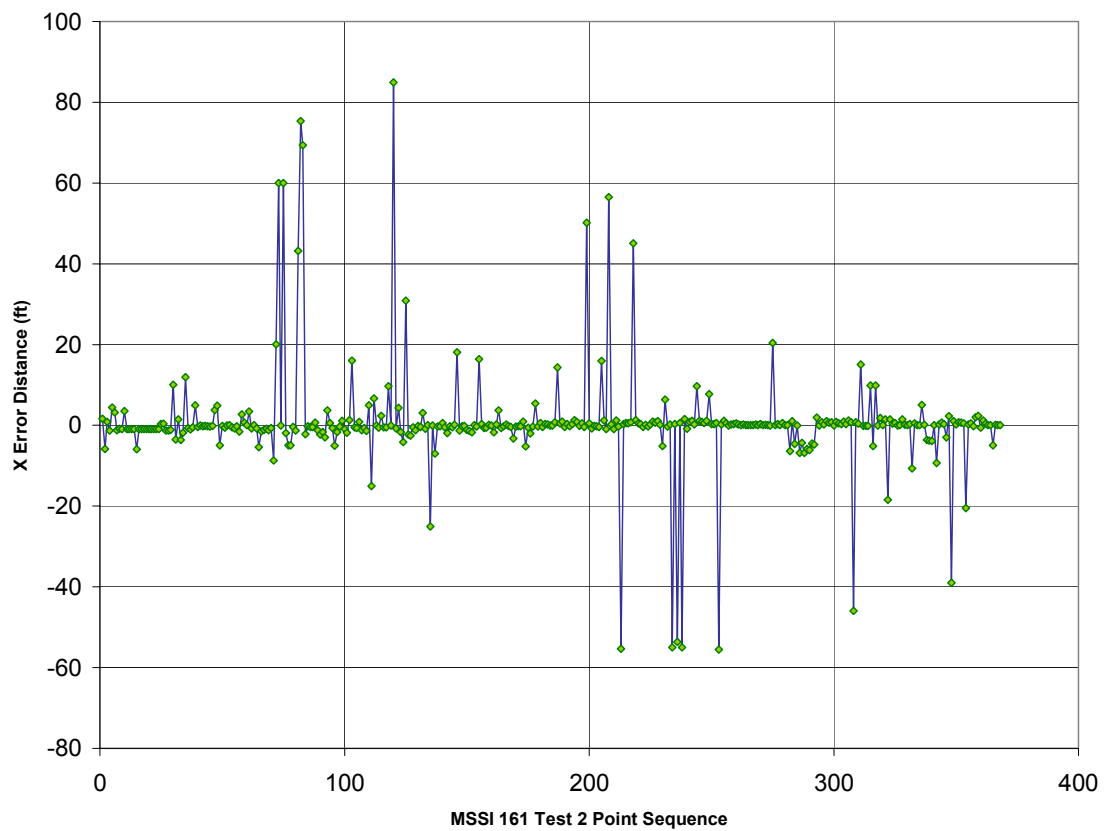
Figure 107. MSSI Test 2, Tag 161: "X" difference versus blink.

Figure 108. MSSI Test 2, Tag 161: "X" difference histogram.
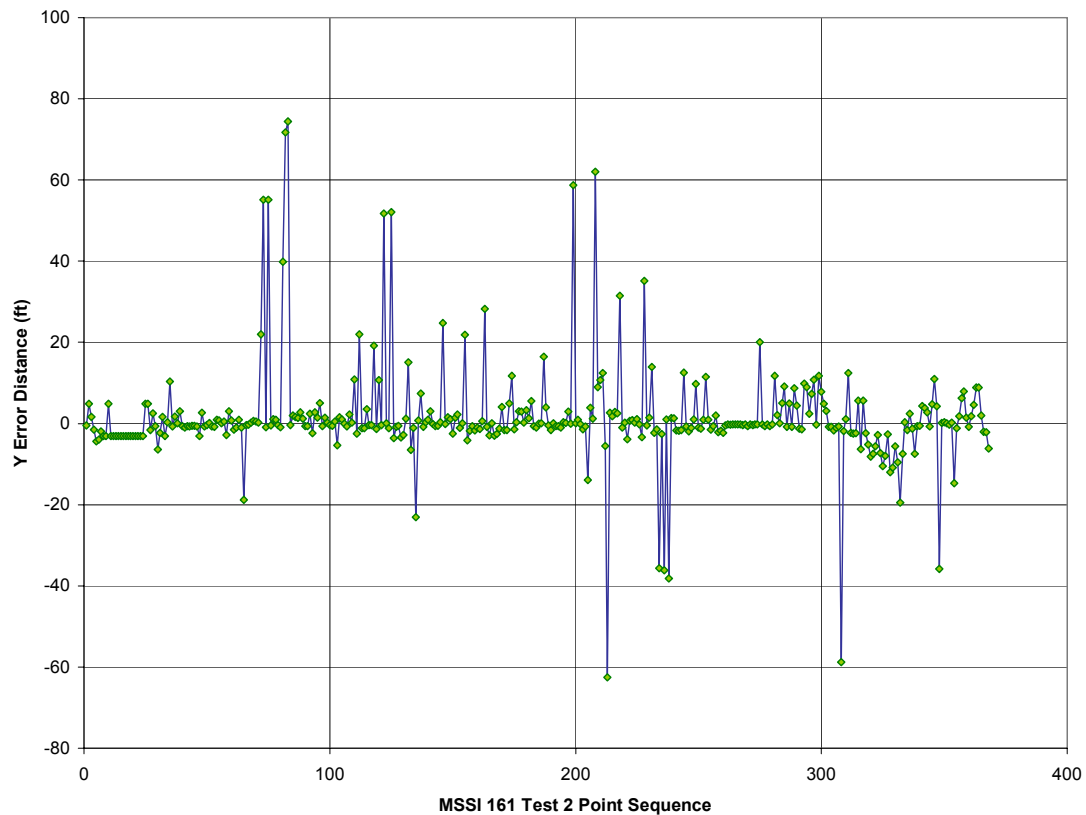
Figure 109. MSSI Test 2, Tag 161: "Y" difference versus blink.
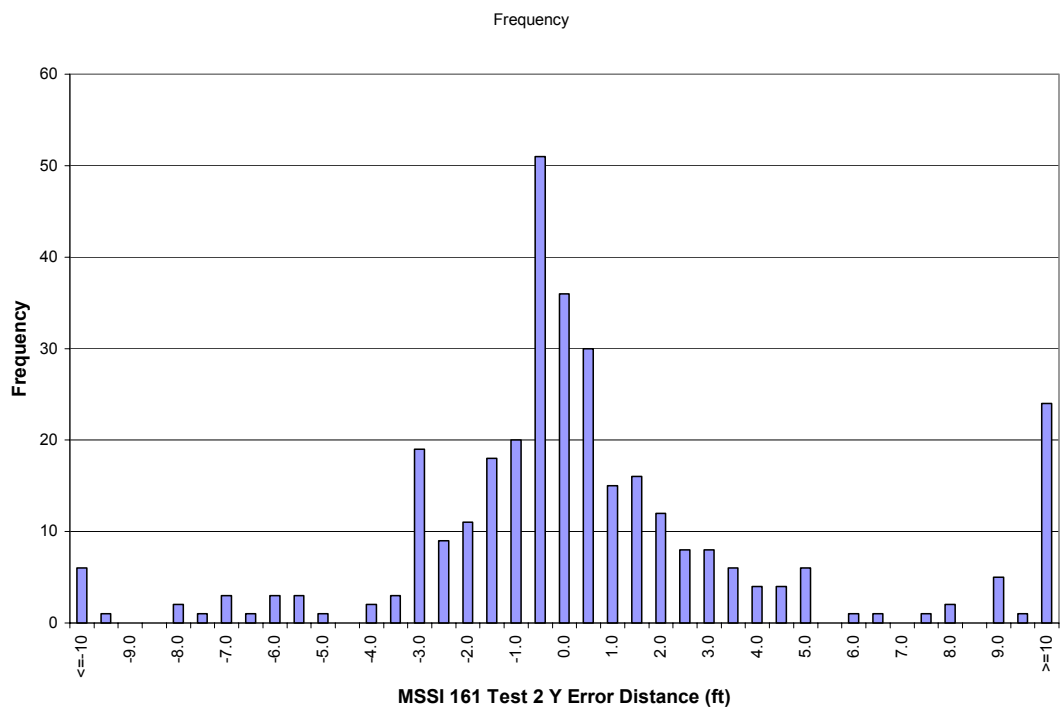
Figure 110. MSSI Test 2, Tag 161: "Y" difference histogram.
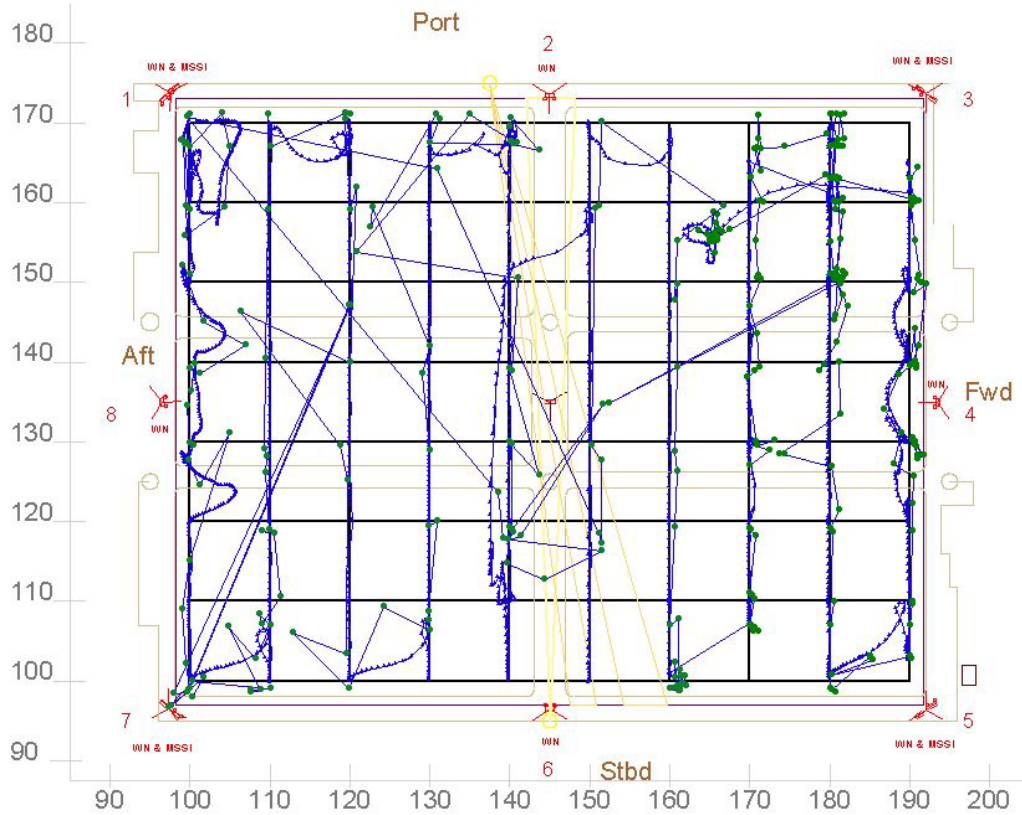
Figure 111.   MSSI Test 2, Tag 178/77: Reported and positions with tracks.
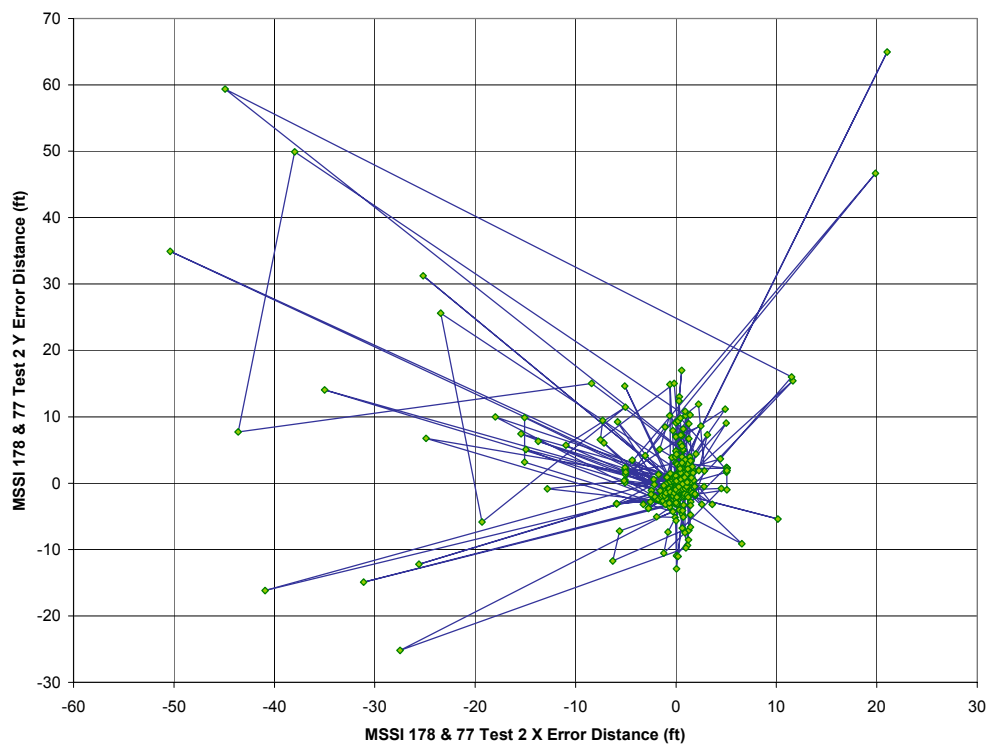
Figure 112. MSSI Test 2, Tag 178/77: "X-Y" difference versus blink .
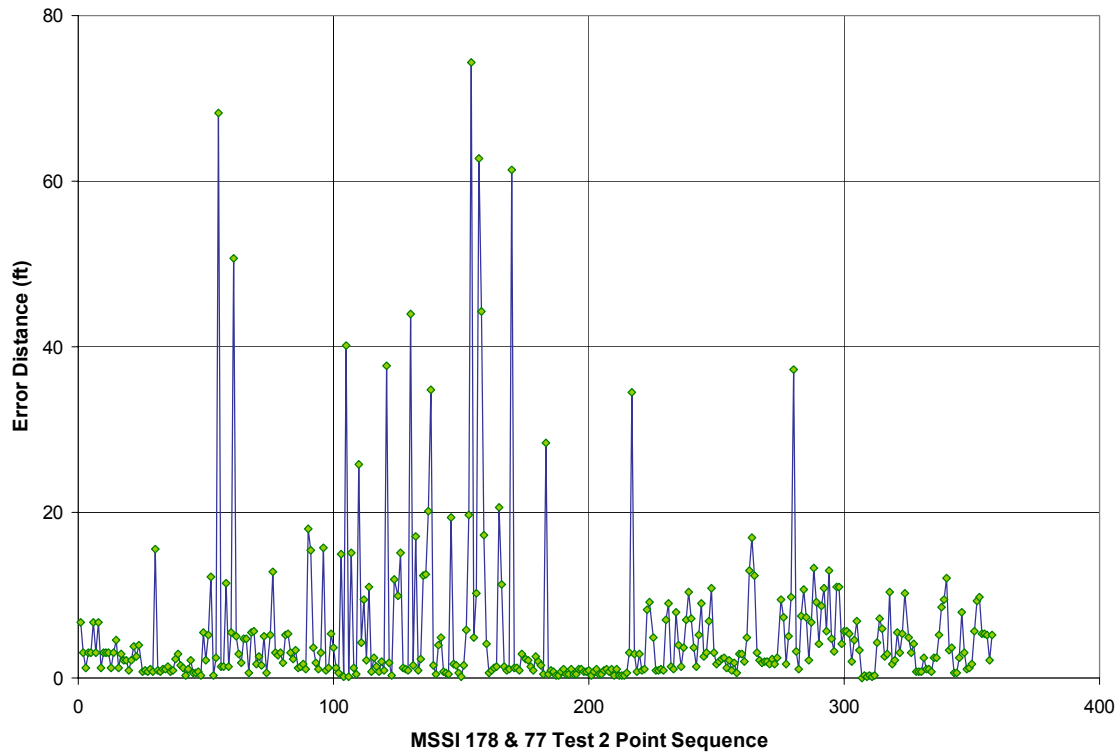
Figure 113. MSSI Test 2, Tag 178/77: Error versus blink.

Figure 114. MSSI Test 2, Tag 178/77: Error histogram.

Figure 115. MSSI Test 2, Tag 178/77: "X" difference versus blink.

Figure 116. MSSI Test 2, Tag 178/77: "X" difference histogram.

Figure 117. MSSI Test 2, Tag 178/77: "Y" difference versus blink.
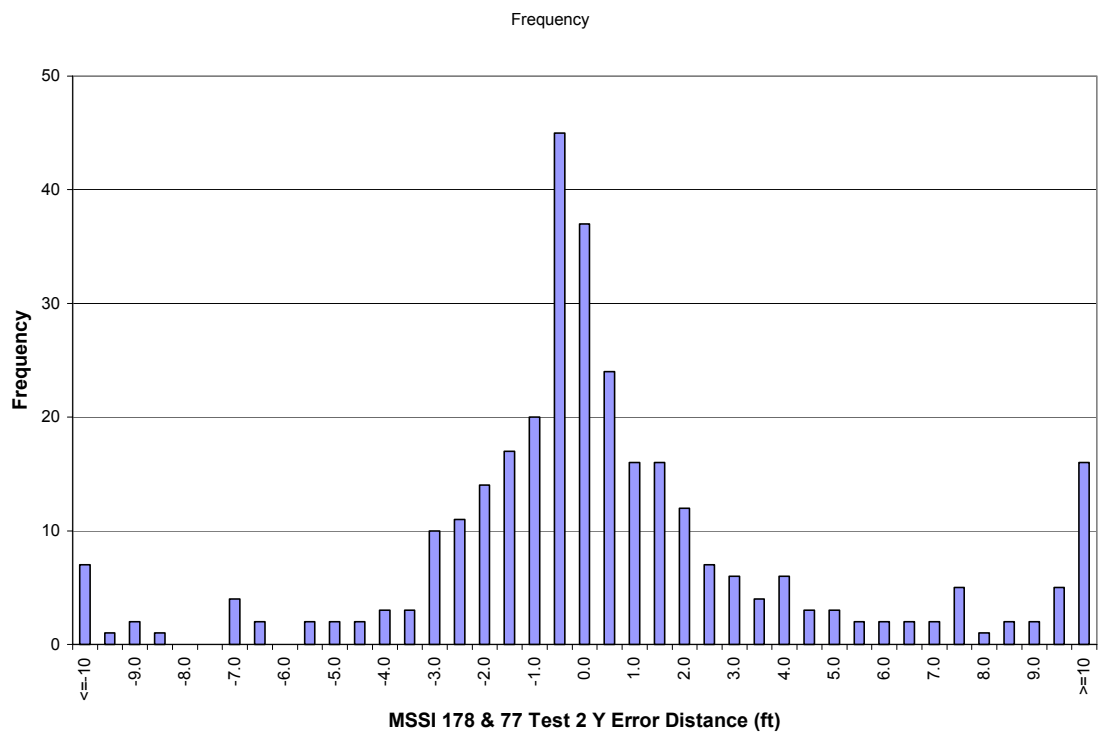
Figure 118. MSSI Test 2, Tag 178/77: "Y" difference histogram.
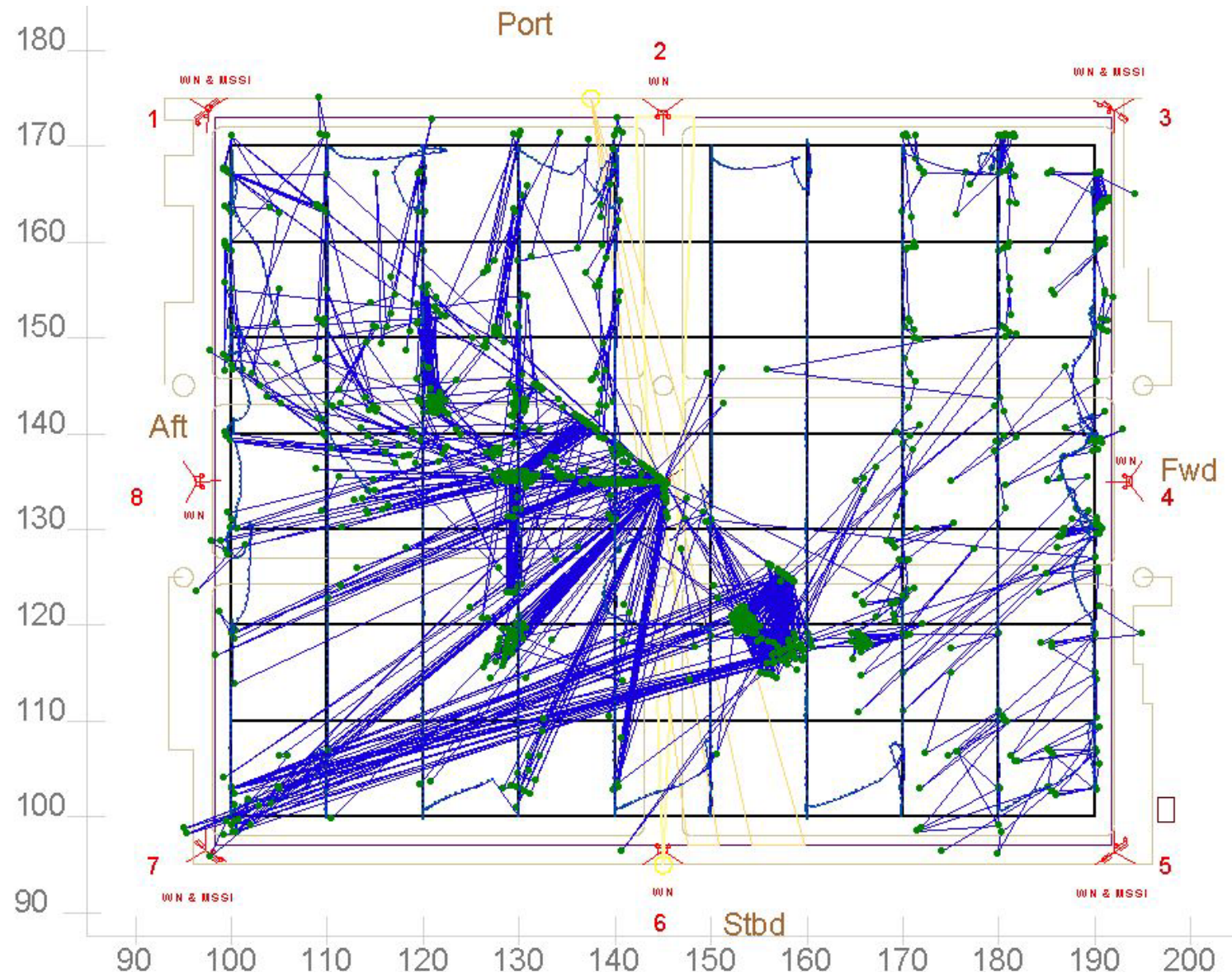
Figure 119. MSSI Test 3: All tag reported positions with tracks.
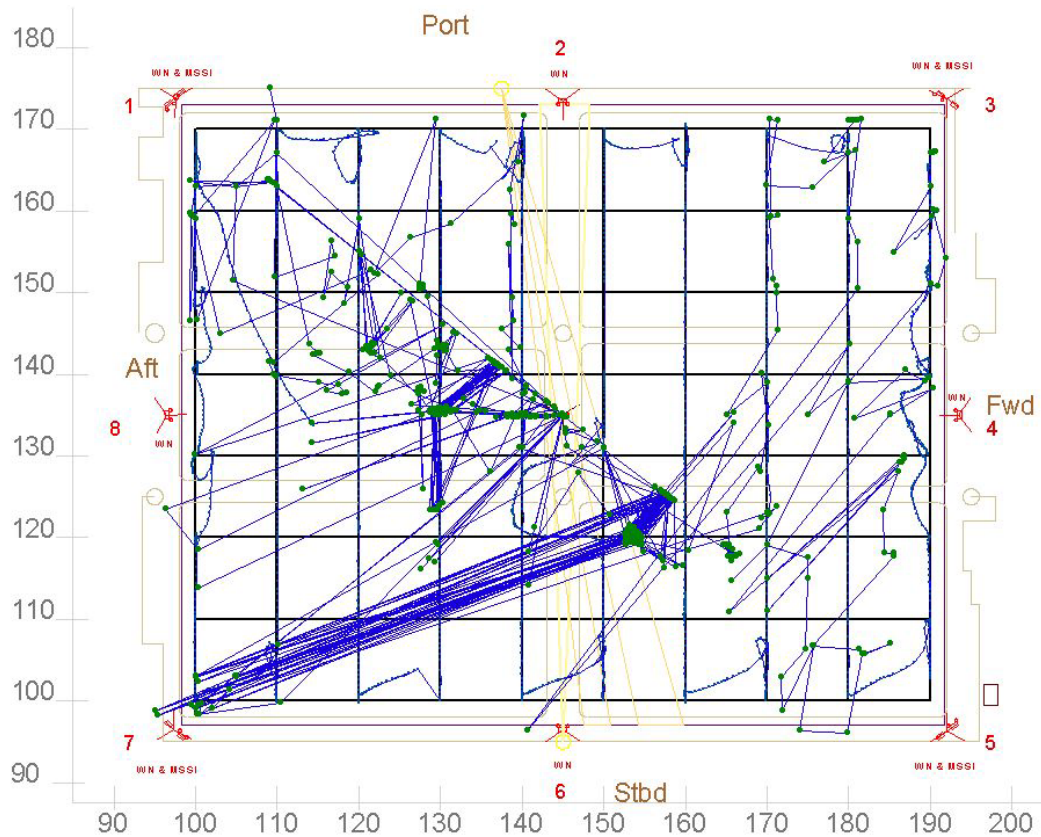
Figure 120. MSSI Test 3, Tag 41: Reported positions with tracks.

Figure 121. MSSI Test 3, Tag 41: "X-Y" difference versus blink.
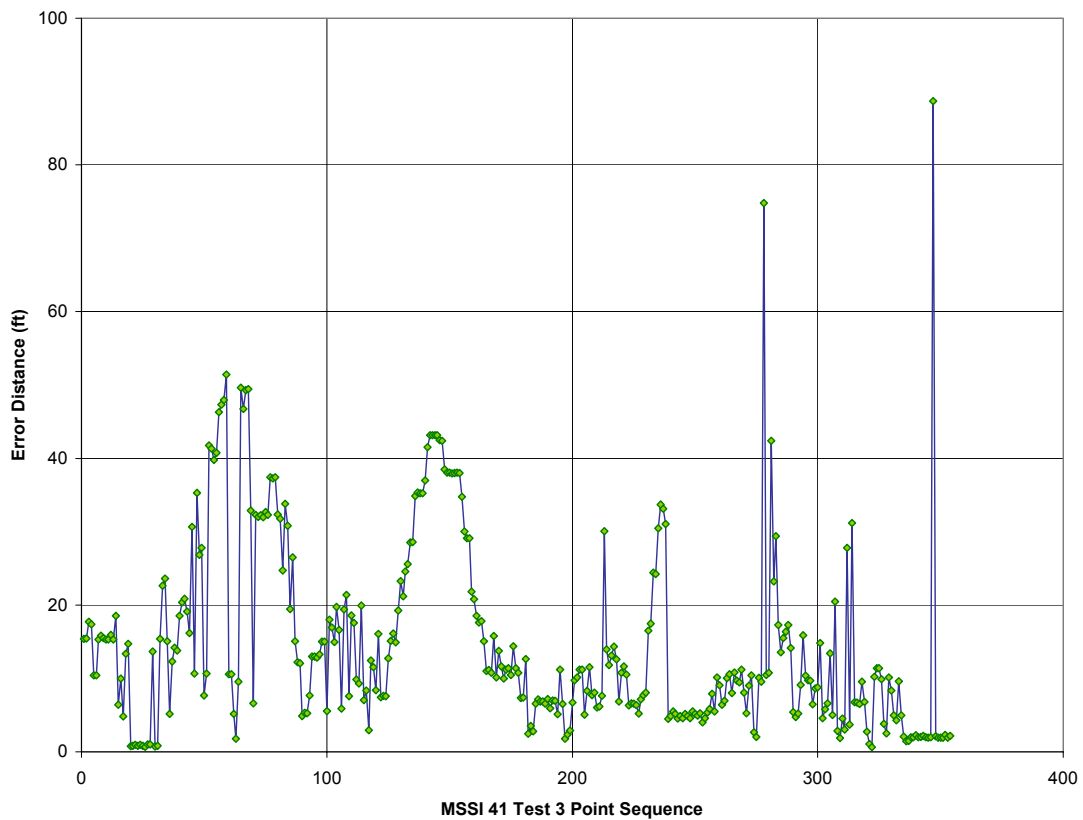
Figure 122. MSSI Test 3, Tag 41: Error versus blink.
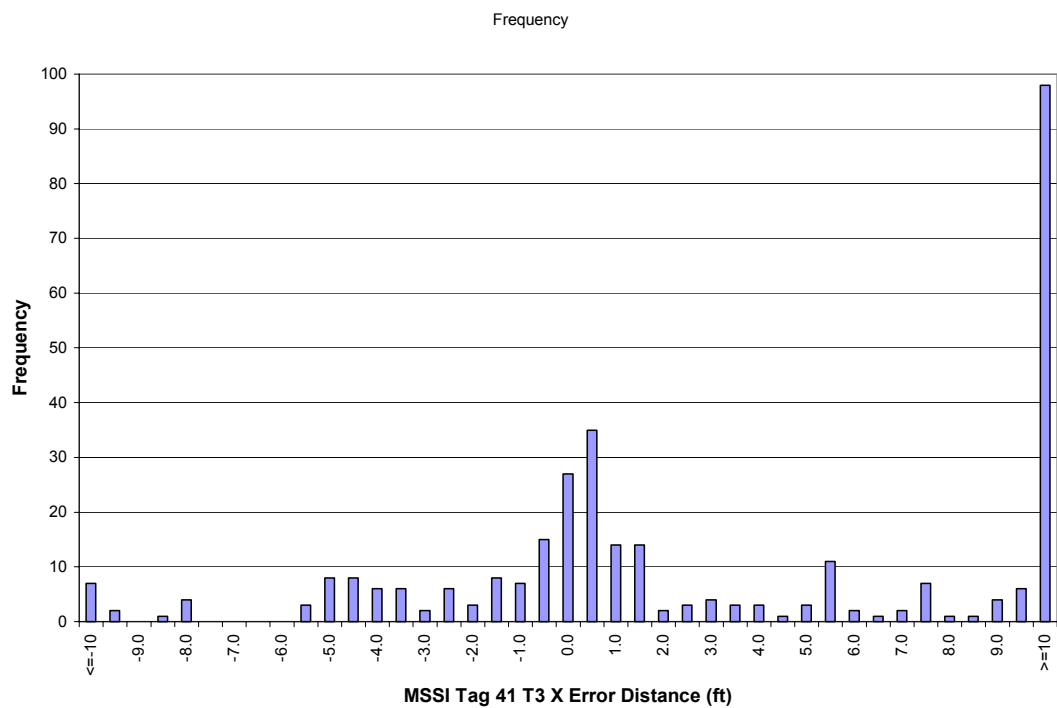
Figure 123. MSSI Test 3, Tag 41: Error histogram.
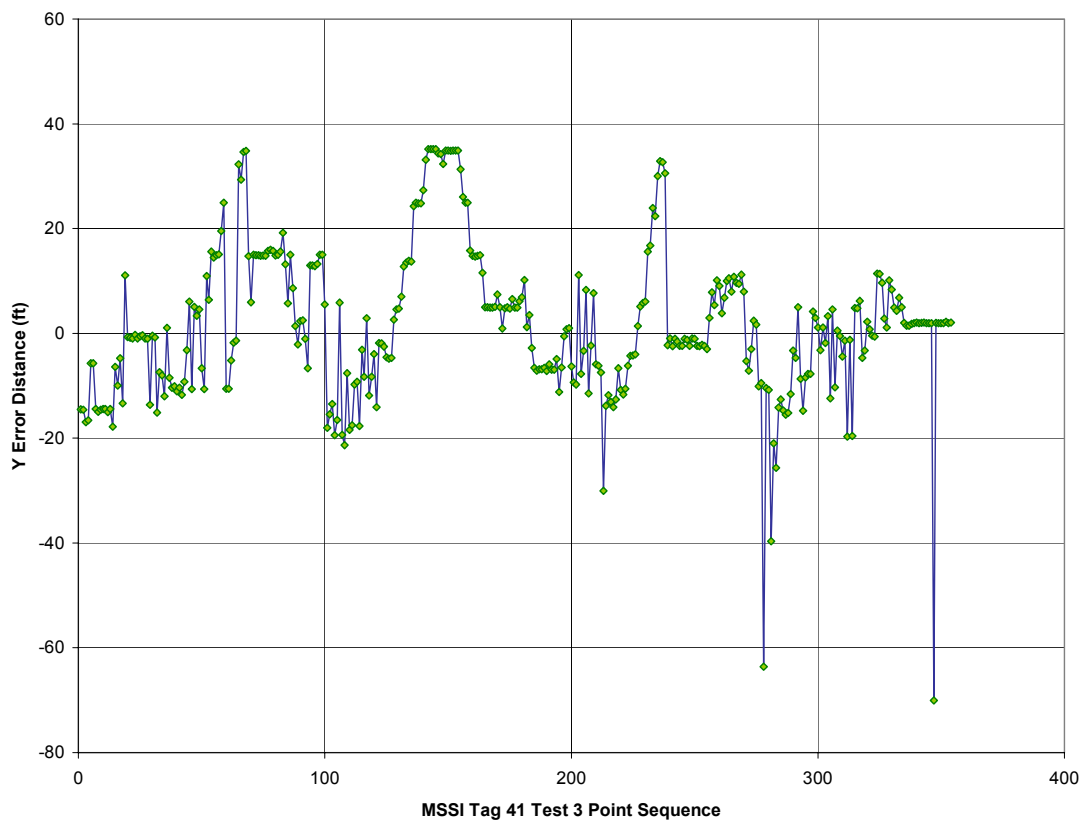
Figure 124. MSSI Test 3, Tag 41, "X" difference versus blink.
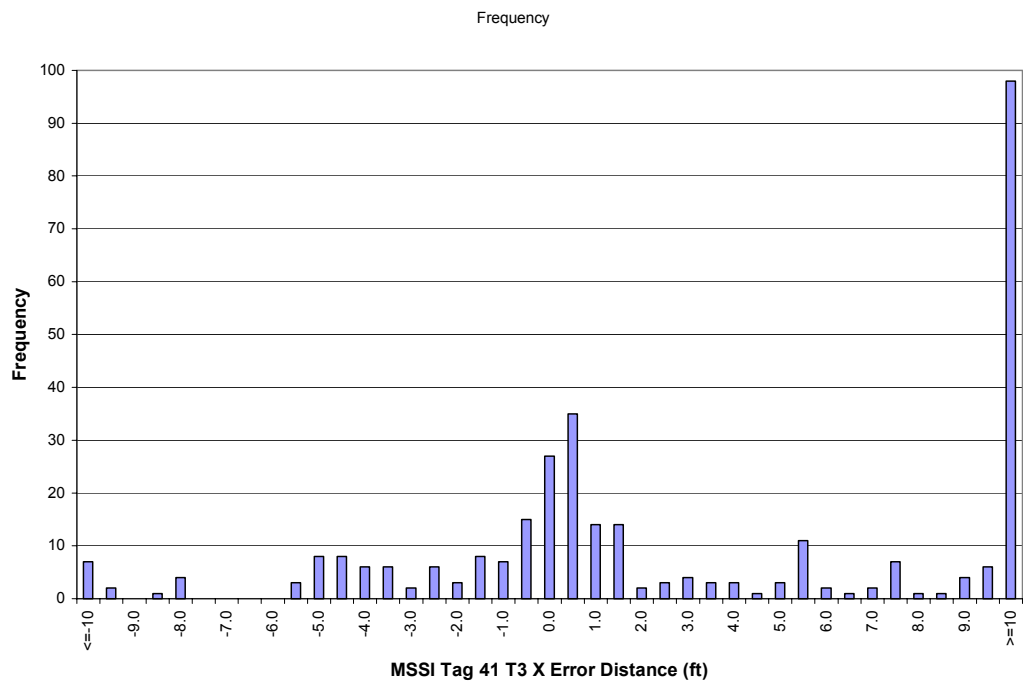
Figure 125. MSSI Test 3, Tag 41: "X" difference histogram.
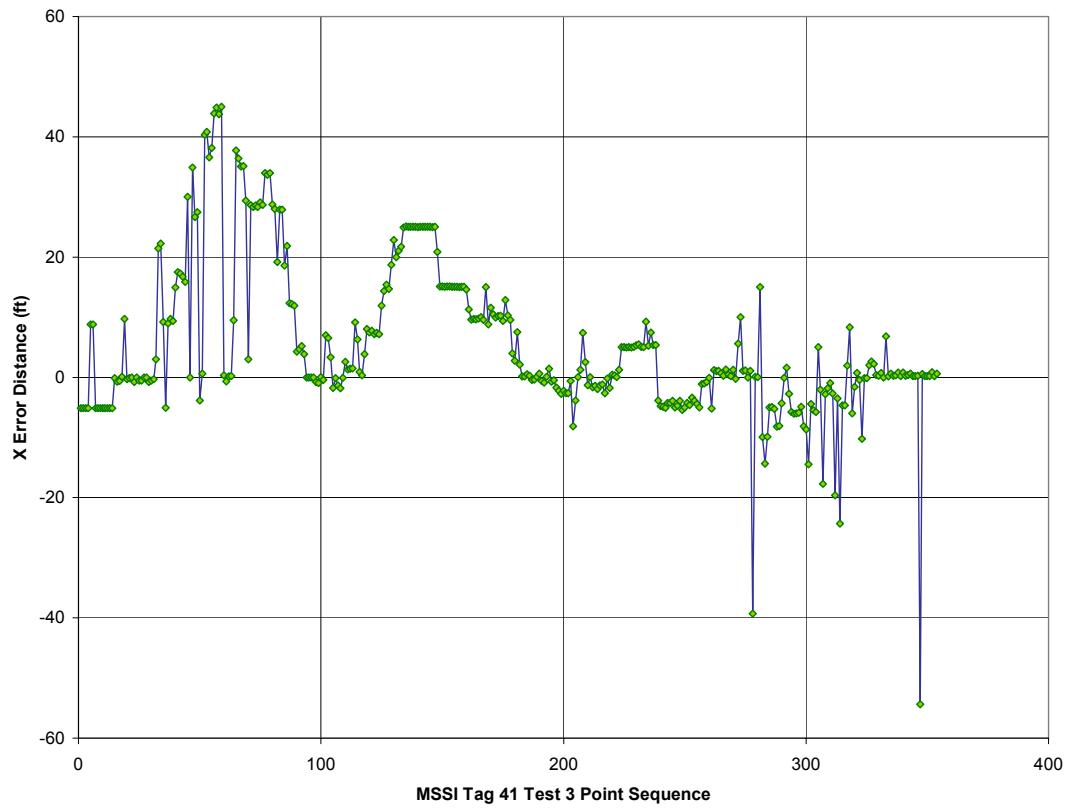
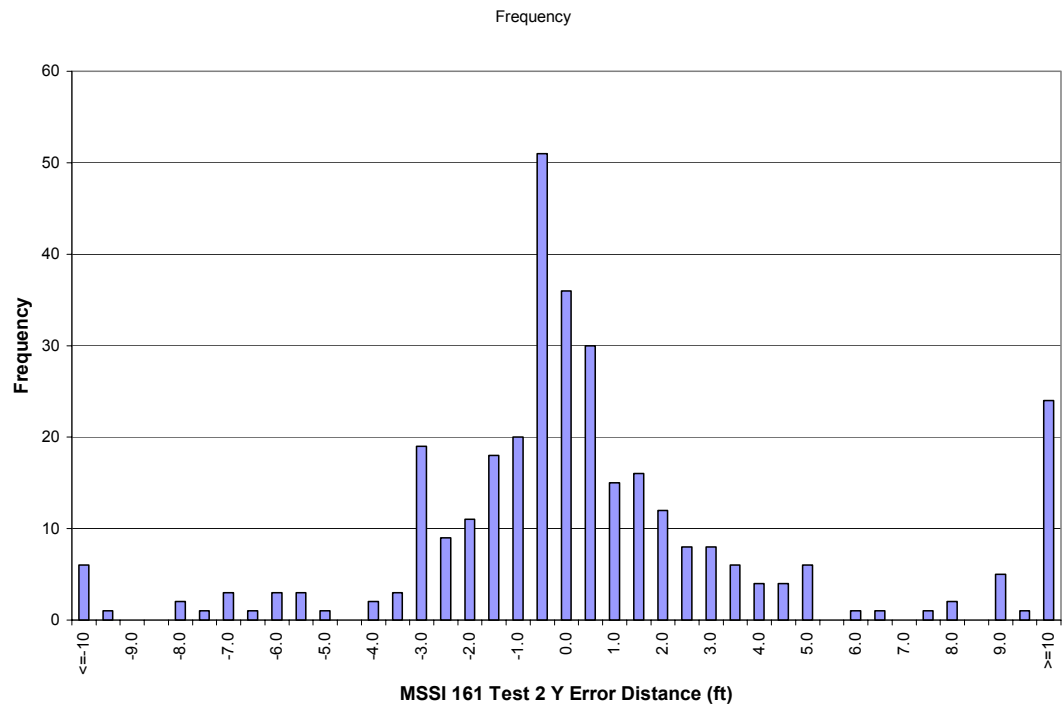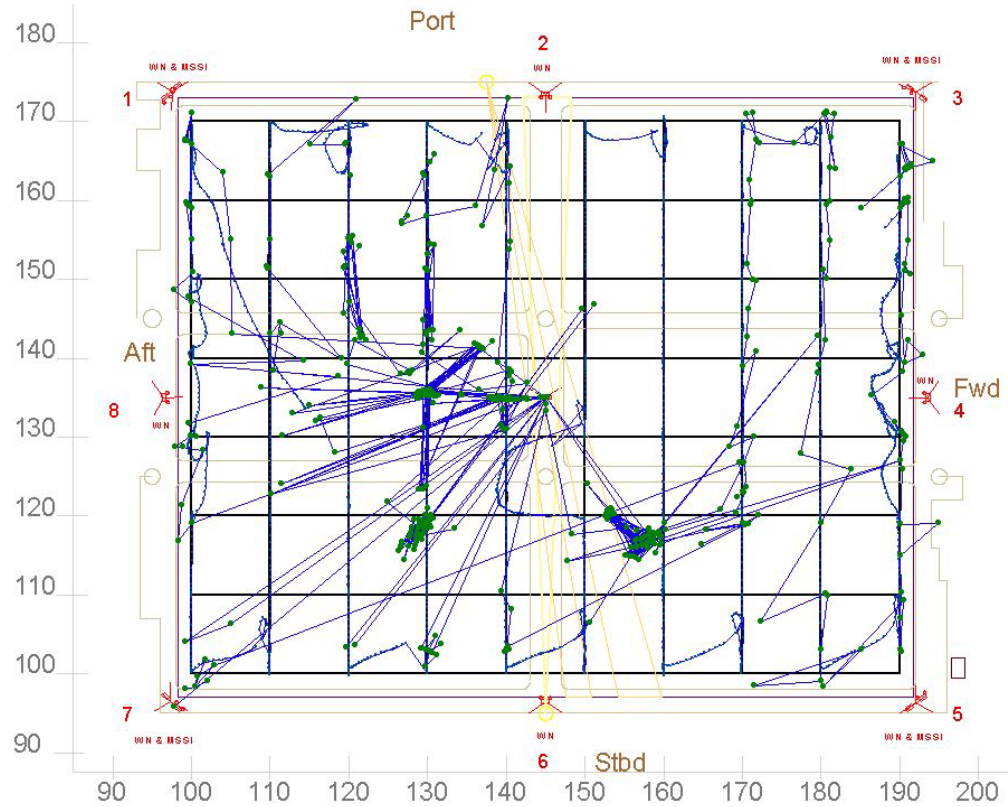Figure 126. MSSI Test 3, Tag 41: "Y" difference versus blink.

Figure 127. MSSI Test 3, Tag 41: "Y" difference histogram.
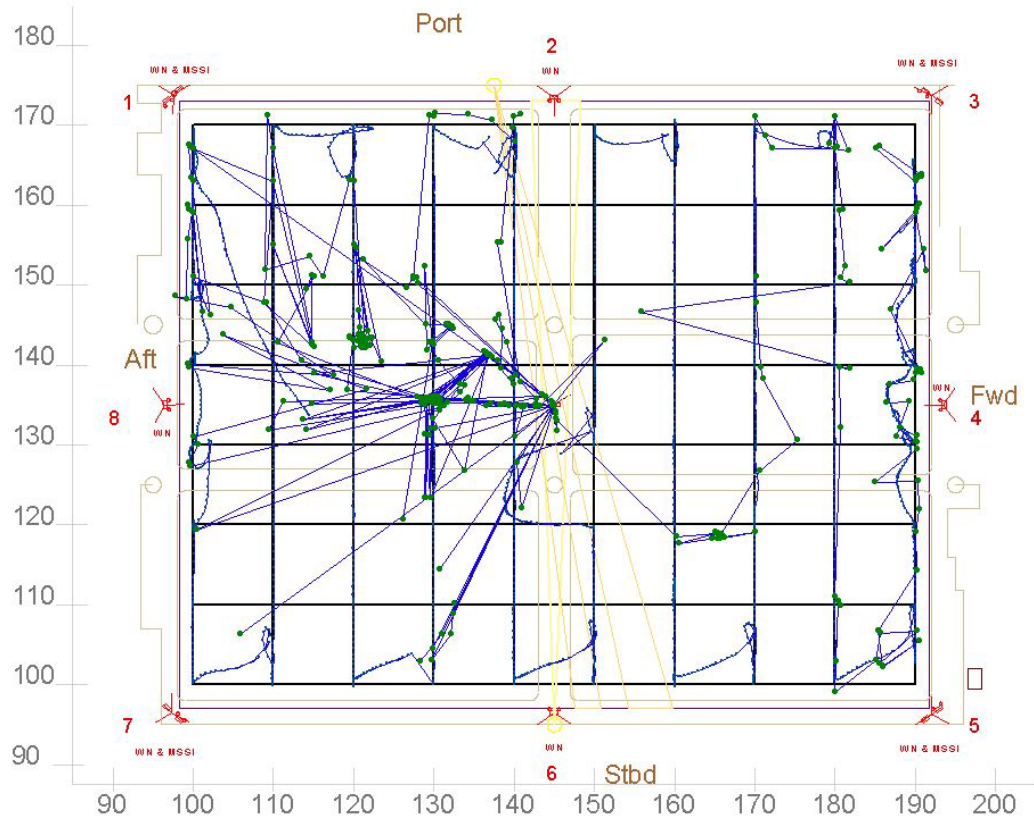
Figure 128. MSSI Test 3, Tag 13: Reported positions with tracks.
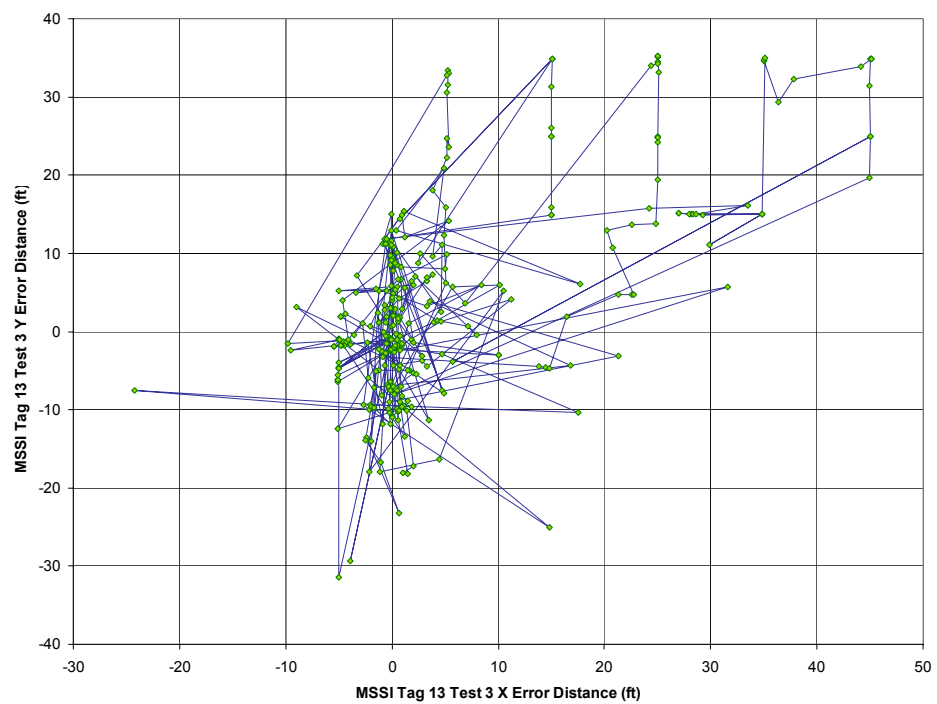
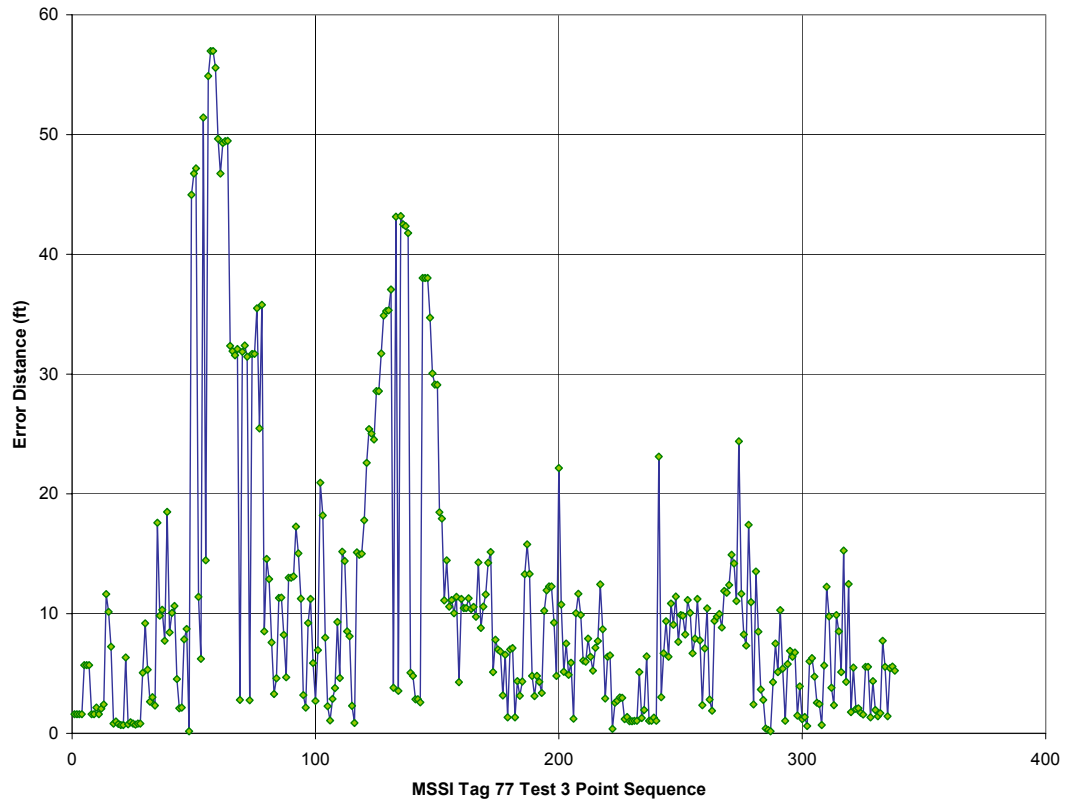Figure 129. MSSI Test 3, Tag 13: "X-Y" difference versus blink.
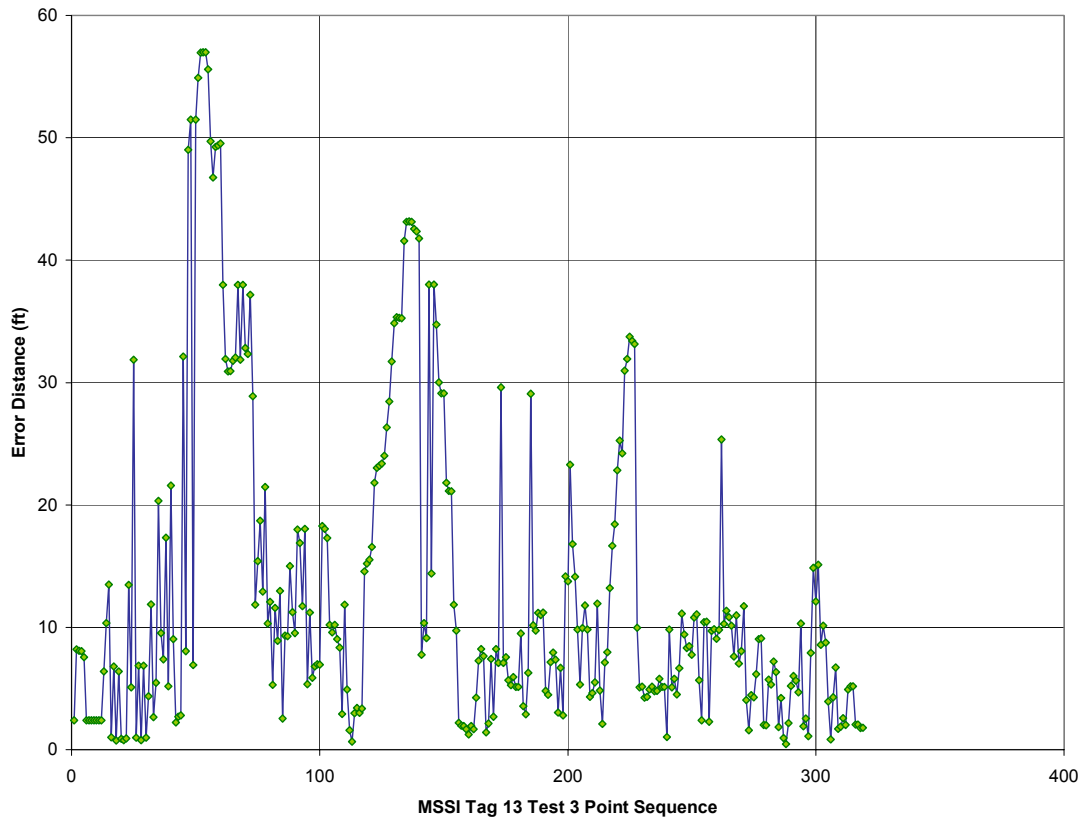
Figure 130. MSSI Test 3, Tag 13: Error versus blink.
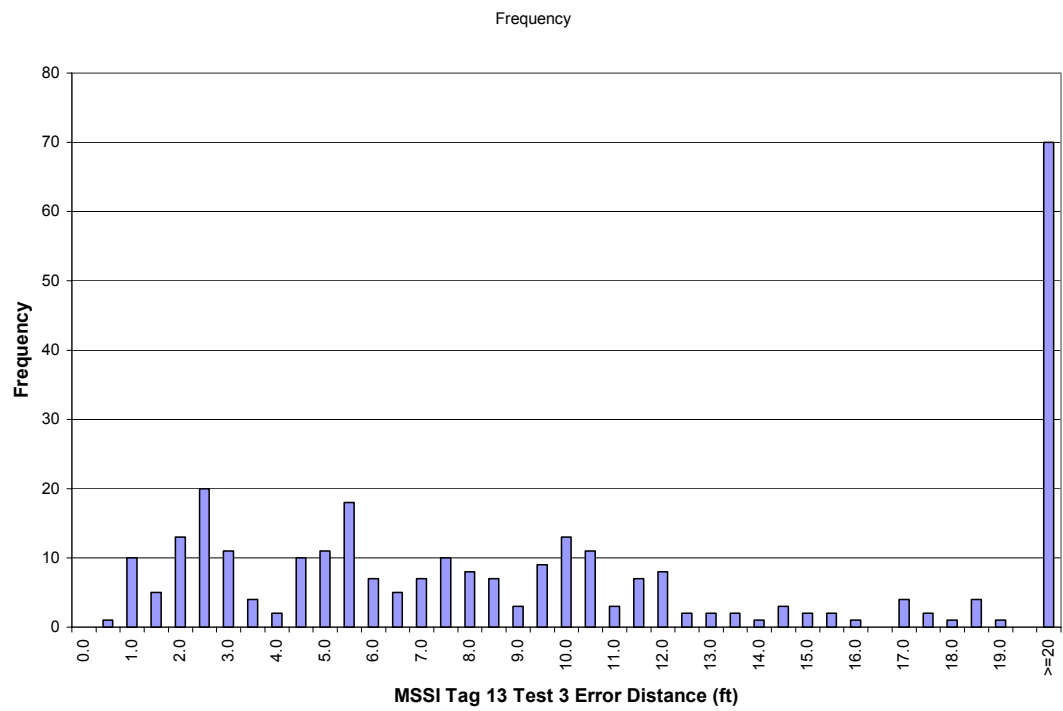
Figure 131. MSSI Test 3, Tag 13: Error histogram.
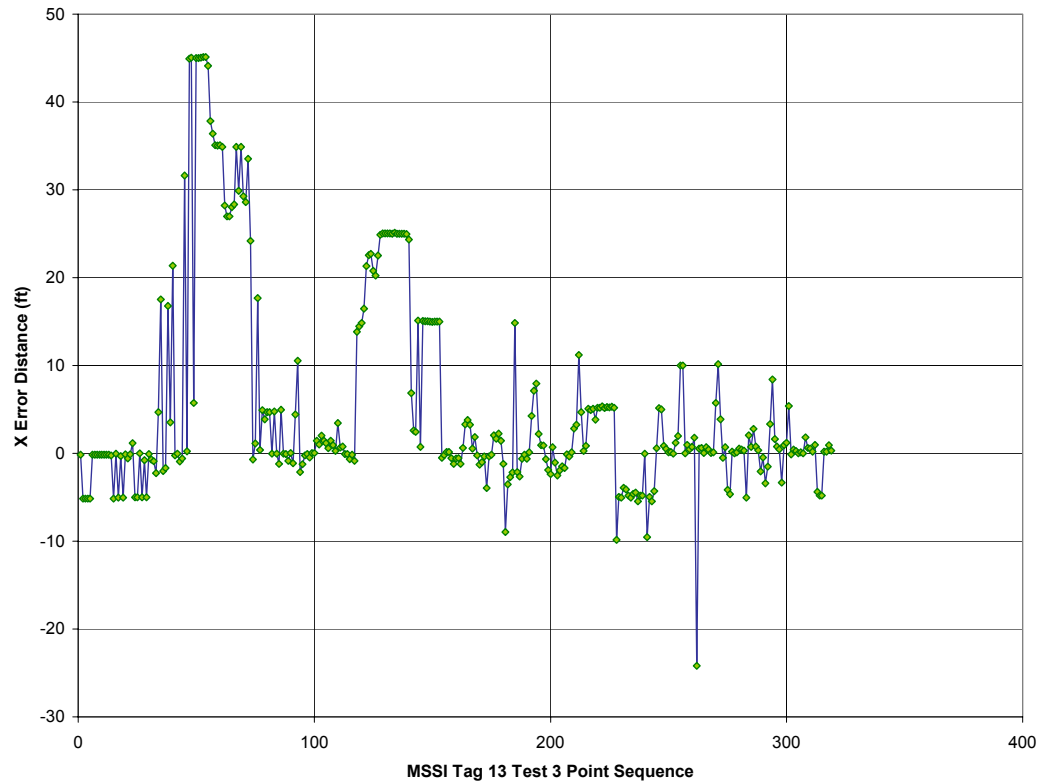
Figure 132. MSSI Test 3, Tag 13: "X" difference versus blink.
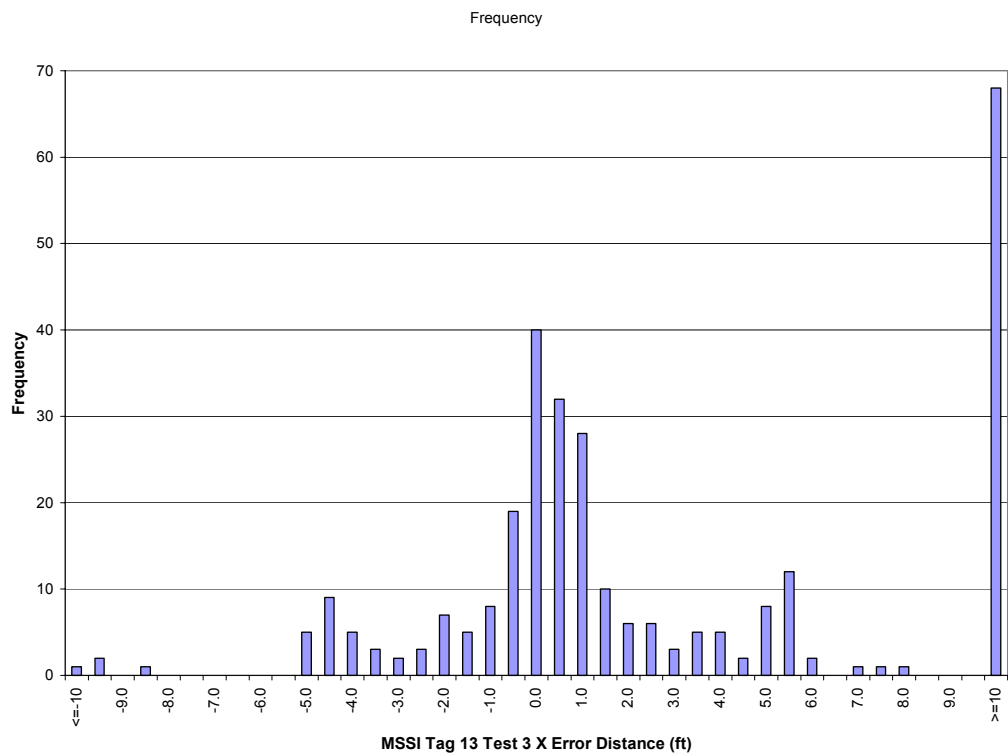
Figure 133. MSSI Test 3, Tag 13: "X" difference histogram.
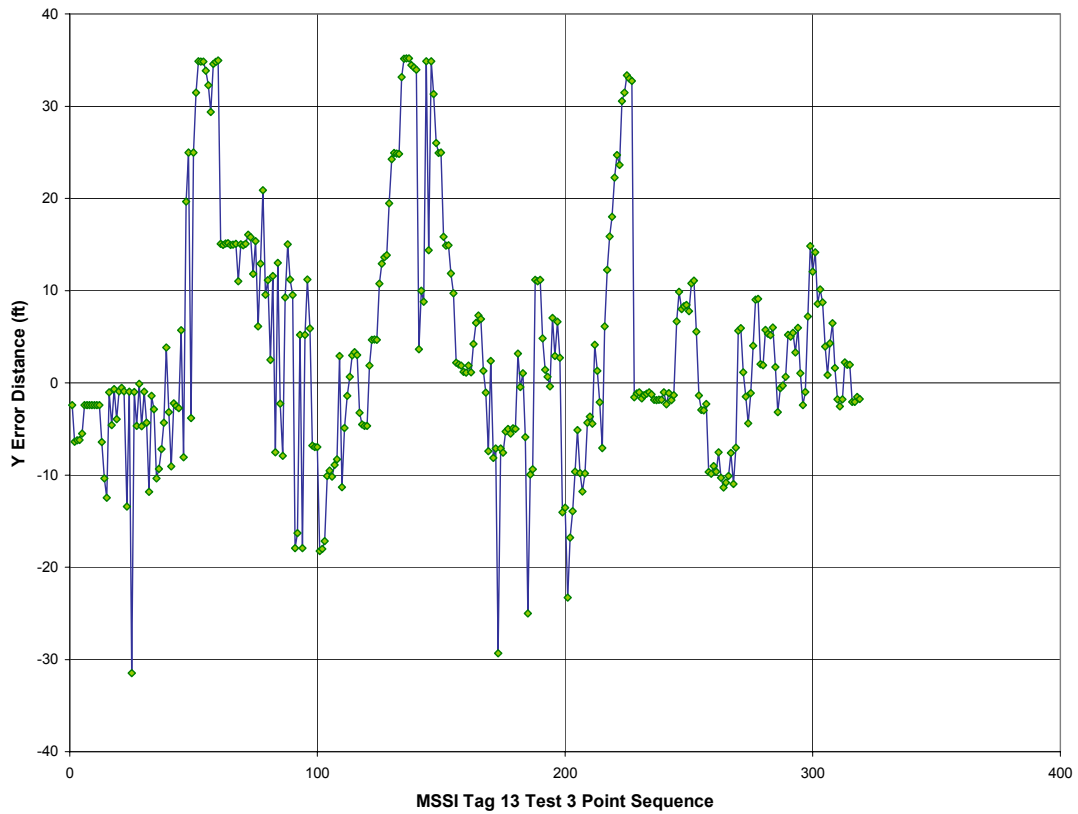
Figure 134. MSSI Test 3, Tag 13: "Y" difference versus blink.

Figure 135. MSSI Test 3, Tag 13: "Y" difference histogram.

4-43

Figure 136. MSSI Test 3, Tag 77: Reported positions with tracks.
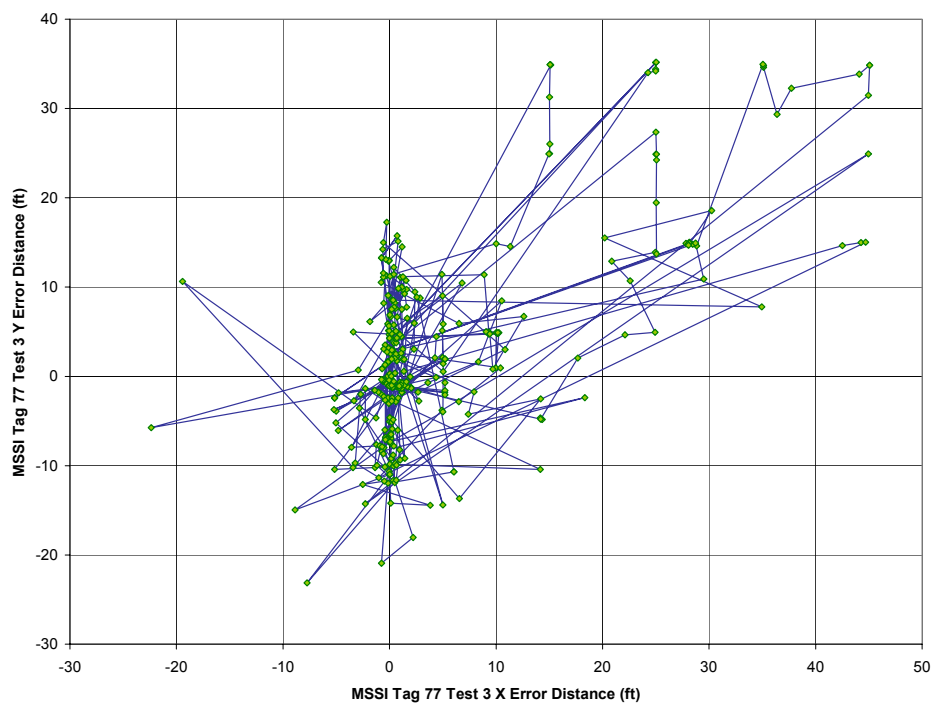
Figure 137. MSSI Test 3, Tag 77: "X-Y" difference versus blink
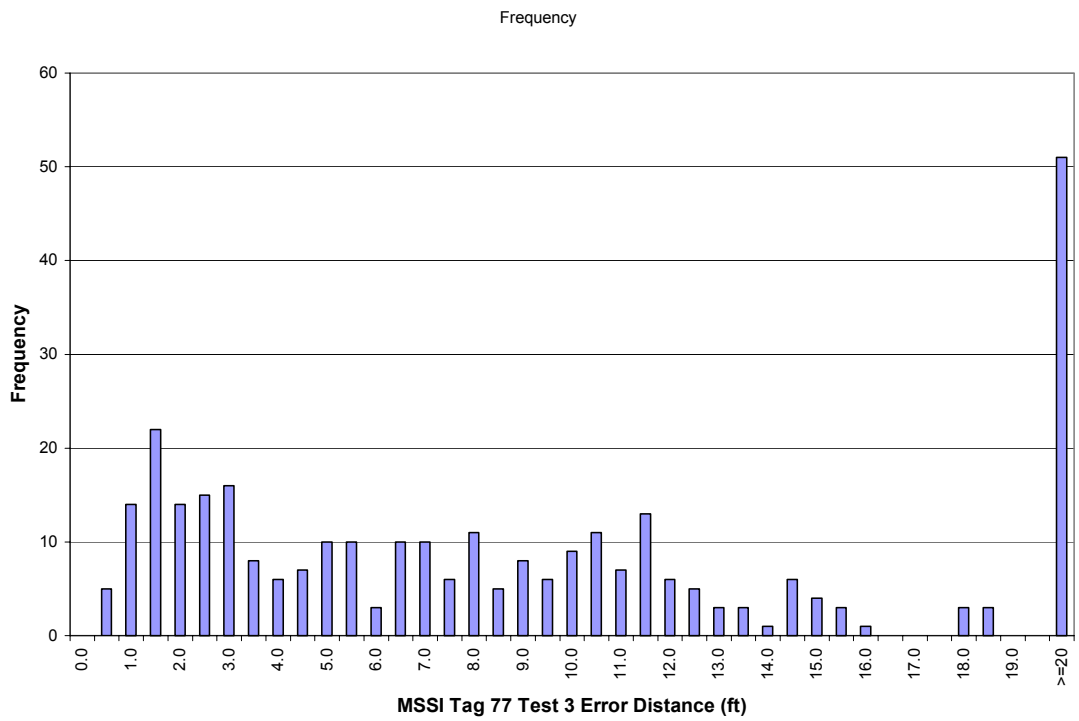
Figure 138. MSSI Test 3, Tag 77: Error versus blink.
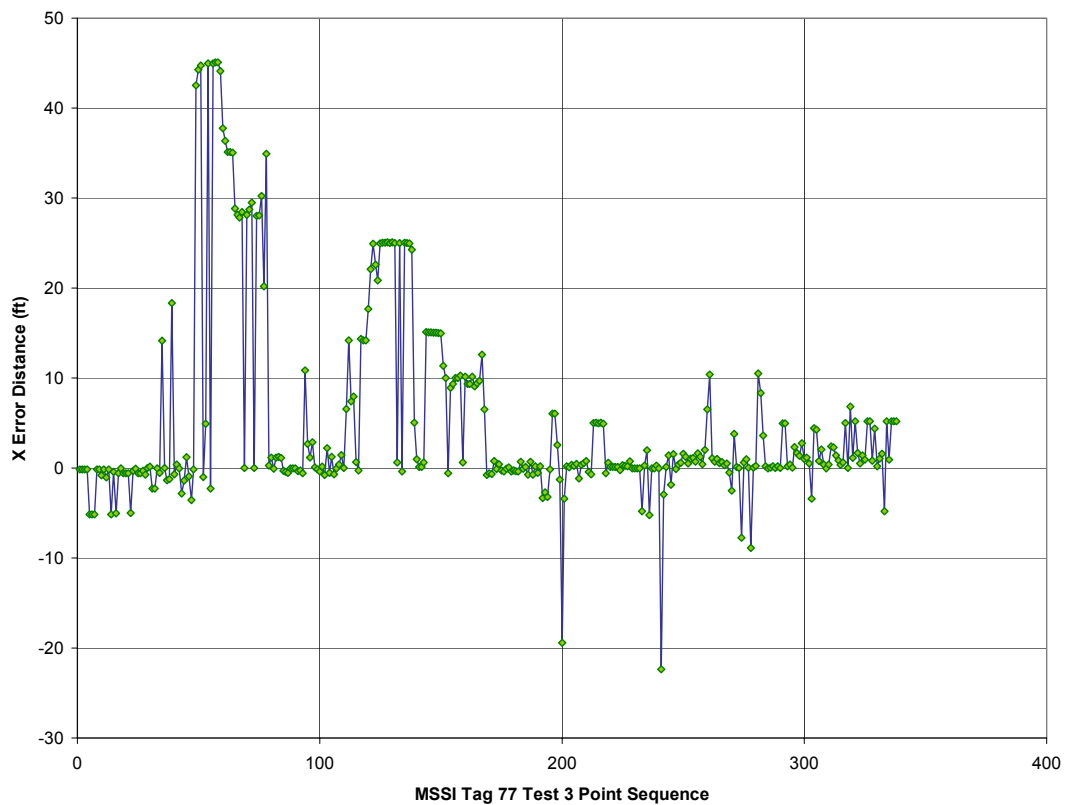

Figure 139. MSSI Test 3, Tag 77: Error histogram.

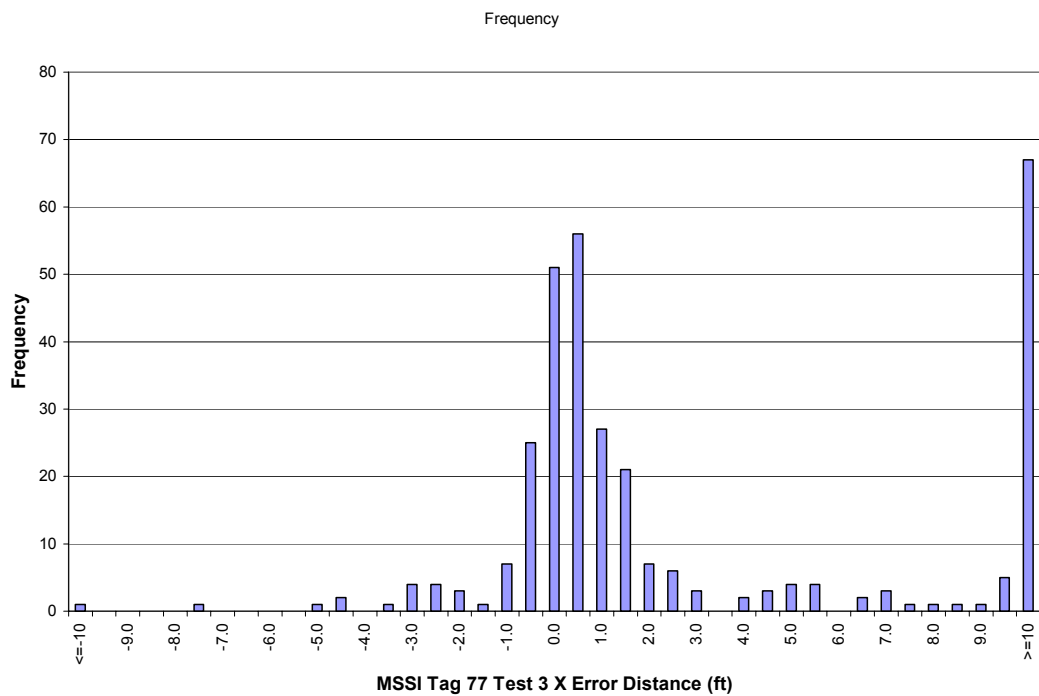Figure 140. MSSI Test 3, Tag 77: "X" difference versus blink.

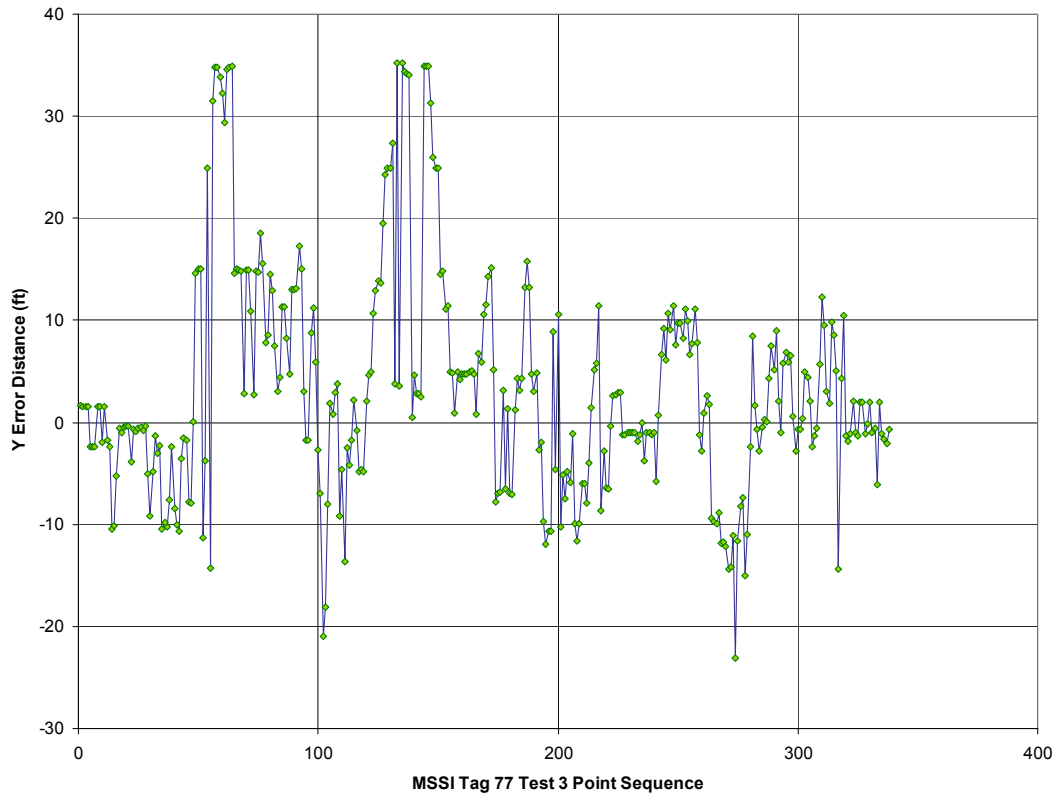Figure 141. MSSI Test 3, Tag 77: "X" difference histogram.

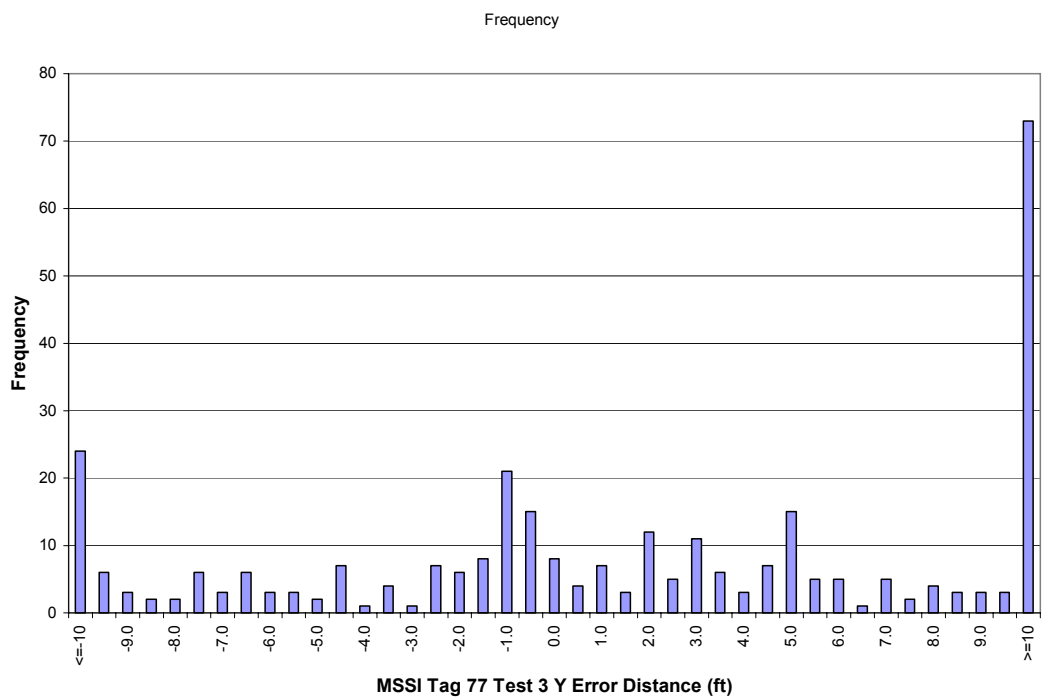Figure 142. MSSI Test 3, Tag 77: "Y" difference versus blink.

Figure 143. MSSI Test 3, Tag 77: "Y" difference histogram.

4.1.4.3 WhereNet Plots: WhereNet data reduction was performed second and is presented second. Table 17 lists the WhereNet test figures:

Table 17. WhereNet Test Result Figures

Test No.	Description	Figure			
	Tag No:	All	112074	112348	114391
1	2D Scatter Plot	144	145	152	159
	2D "X-Y" Difference	--	146	153	160
	Error vs Blinks	--	147	154	161
	Error Histogram	--	148	155	162
	"X" Difference vs Blinks	--	149	156	163
	"X" Difference Histogram	--	--	--	--
	"Y" Difference vs Blinks	--	150	157	164
	"Y" Difference Histogram	--	--	--	--
	Blink Frequency Histogram	--	151	158	165
2	2D Scatter Plot	166	167	174	181
	2D "X-Y" Difference vs Blinks	--	168	175	182
	Error vs Blinks	--	169	176	183
	Error Histogram	--	170	177	184
	"X" Difference vs Blinks	--	171	178	185
	"X" Difference Histogram	--	--	--	--
	"Y" Difference vs Blinks	--	172	179	186
	"Y" Difference Histogram	--	--	--	--
	Blink Frequency Histogram	--	173	180	187
3	2D Scatter Plot	188	189	198	207
	2D "X-Y" Difference vs Blinks	--	190	199	208
	Error vs Blinks	--	191	200	209
	Error Histogram	--	192	201	210
	"X" Difference vs Blinks	--	193	202	211
	"X" Difference Histogram	--	194	203	212
	"Y" Difference vs Blinks	--	195	204	213
	"Y" Difference Histogram	--	196	205	214
	Blink Frequency Histogram	--	197	206	215

All reported tag positions are included in the plots, no filtering was performed. The plots include all correlated positions. "X" and "Y" difference histograms were not done for Tests 1 and 2 because of the sparsity of data, with predominant clumping in corners. Blink frequency histograms were done for full drop-out analyses. Tests 1 and 2 had full drop-outs, none were observed in Test 3 with 8 antennas.

Most reported positions with four antennas were in corners or along the starboard bulkhead. Tag reports with 8 antennas were fairly evenly distributed throughout the test box. Tag reports were always away from corners and often away from bulkheads. Tag reports were made even along the bulkheads with 8 antennas (analog systems have difficulty here).   An offset towards starboard is apparent and shows up in the 2D Scatter plots, 2D "X-Y" Difference plots, and "Y" axis difference plots and histograms.

The "Y" axis difference in Test 3 moved back and forth with sled movement, encompassing the same number of cycles. The "Y" axis difference data was smoothed with a "cosine" filter and plotted to see the underlying pattern. Figures 195, 204, and 213 show the pattern. It is strongest towards the ends and is easiest to see in Figure 213. It also caused a broadening in the "Y" axis difference histograms.
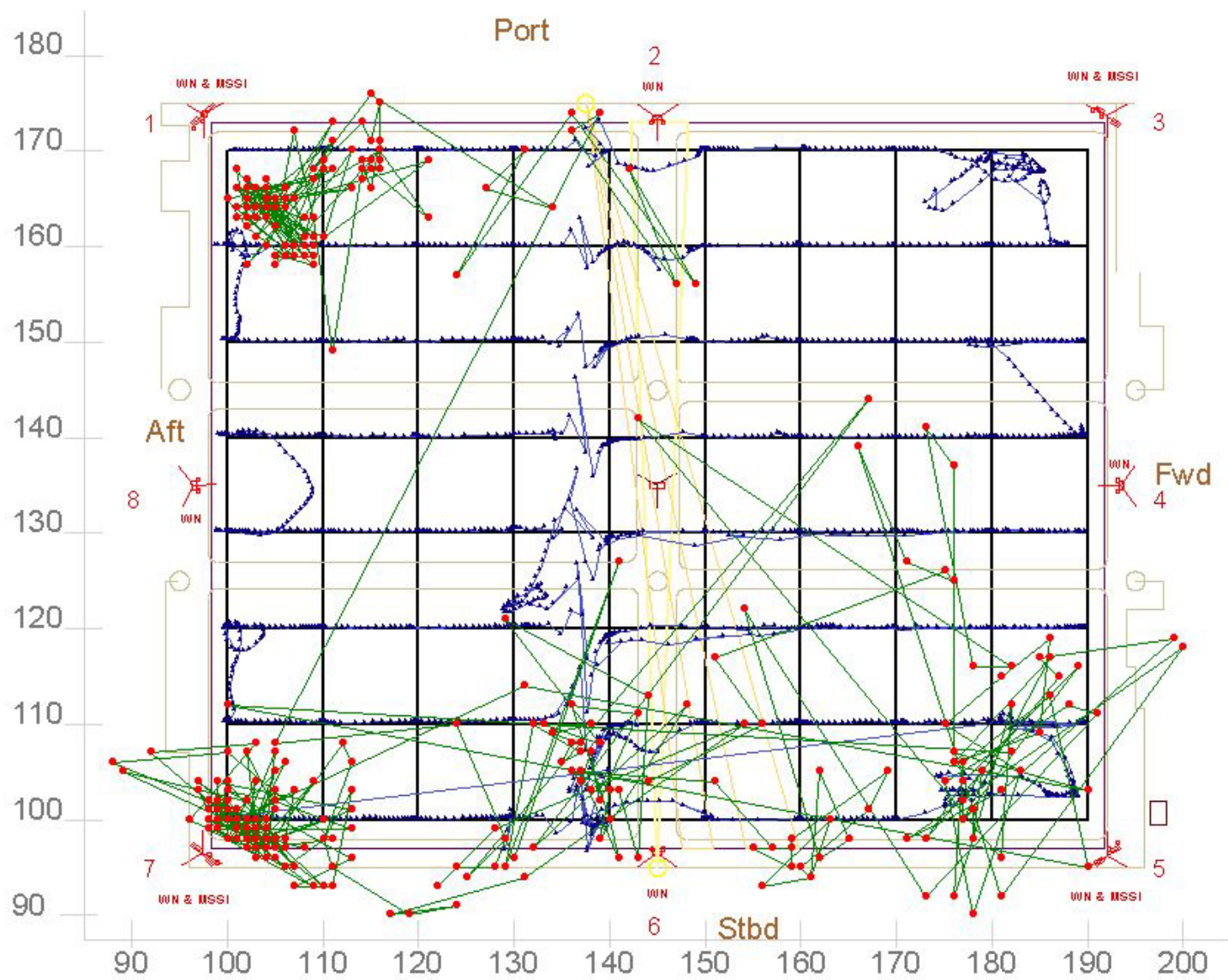
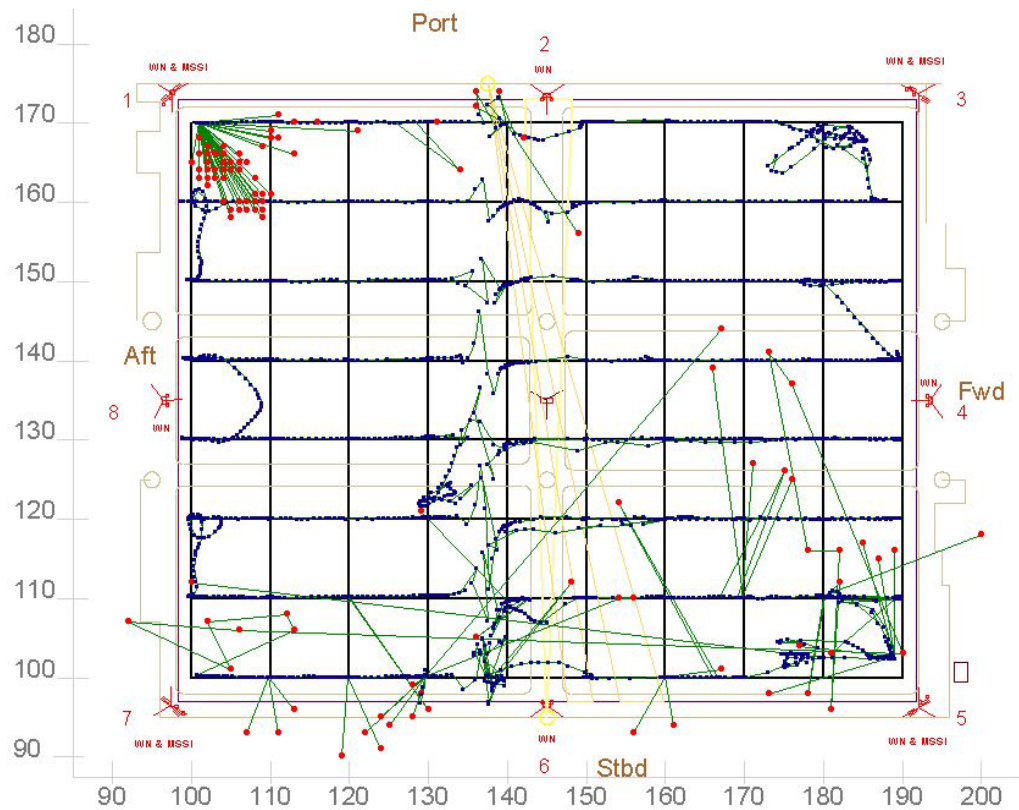Figure 144. WhereNet Test 1: All tag reported positions with tracks.

Figure 145. WhereNet Test 1, Tag 112074: Reported and correlated positions.
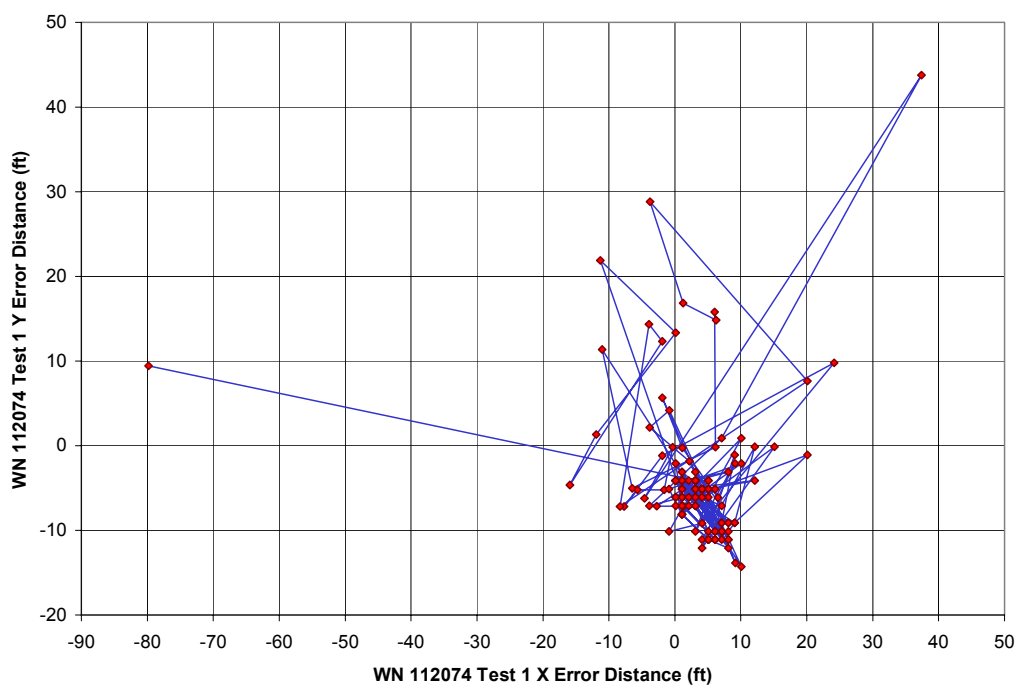

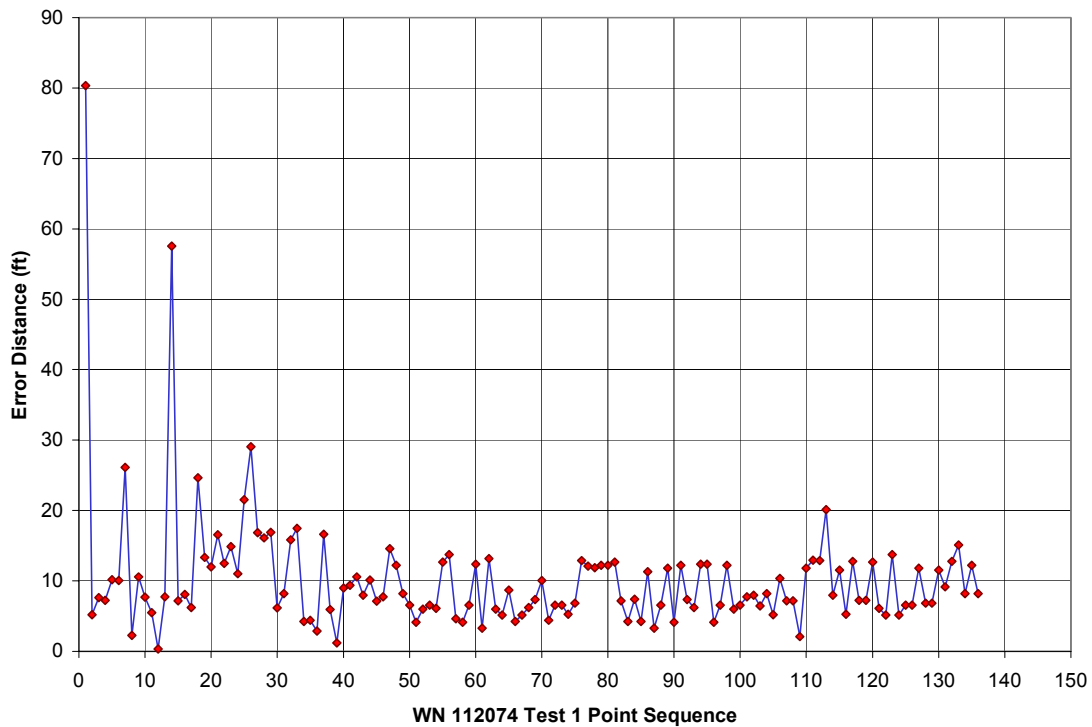Figure 146. WhereNet Test 1, Tag 112074: "X-Y" difference versus blink.

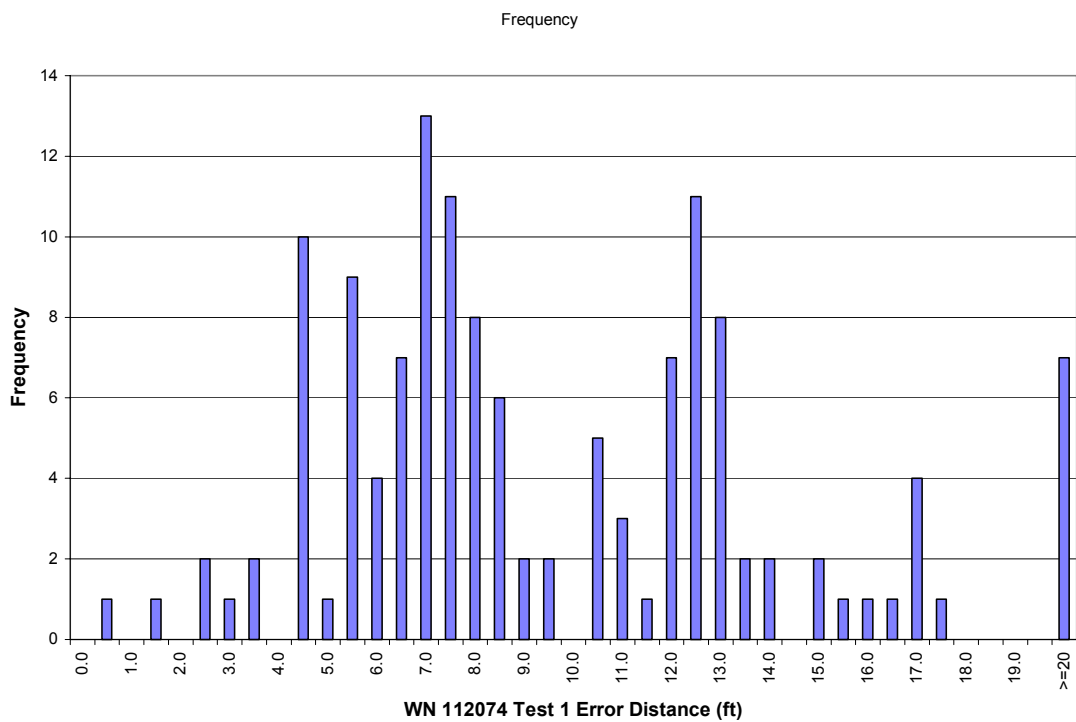Figure 147. WhereNet Test 1, Tag 112074: Error versus blink.

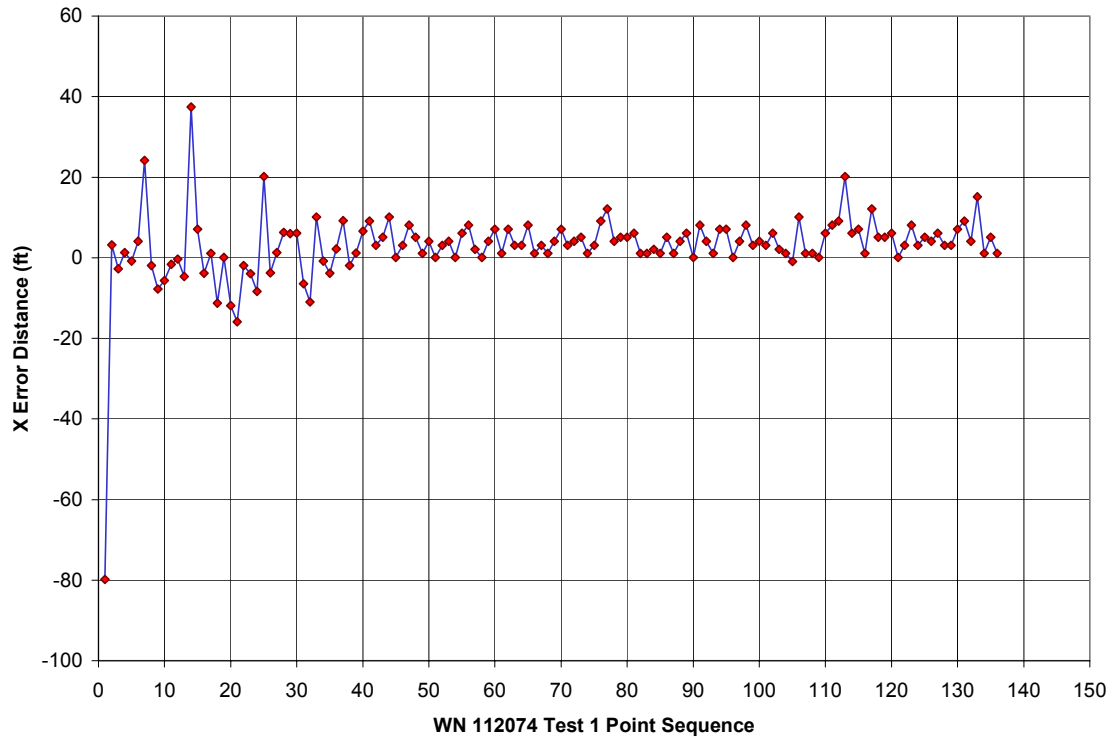Figure 148. WhereNet Test 1, Tag 112074: Error histogram.

Figure 149. WhereNet Test 1, Tag 112074: "X" difference versus blink.
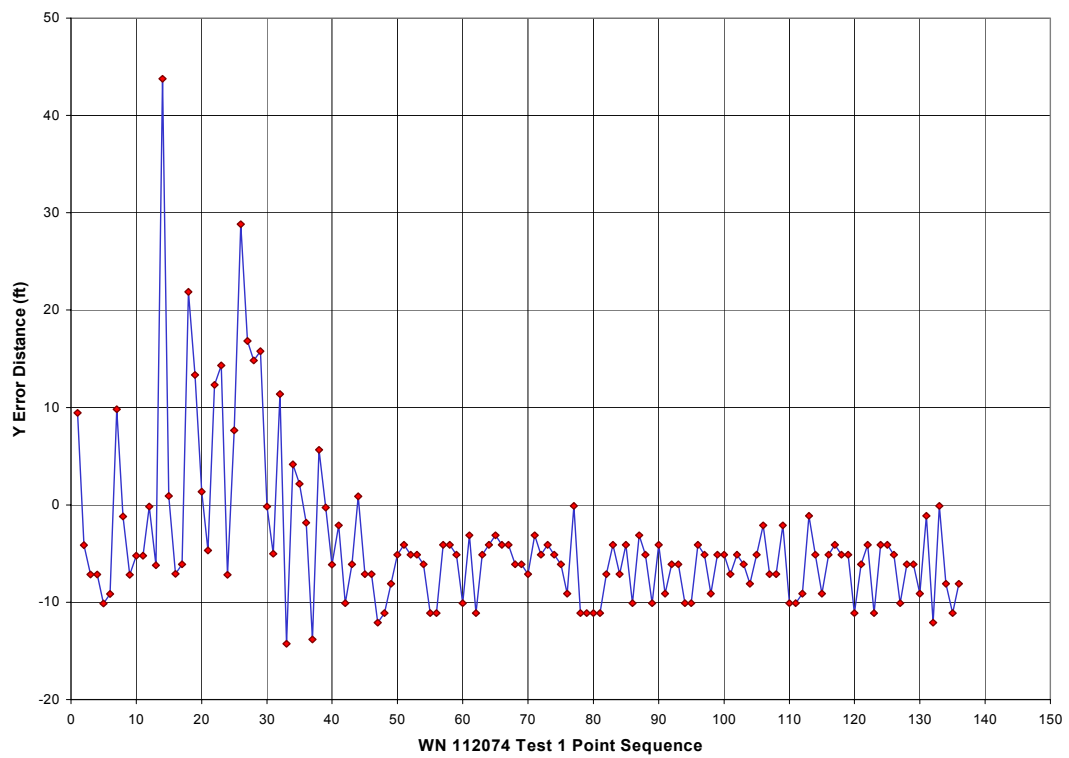

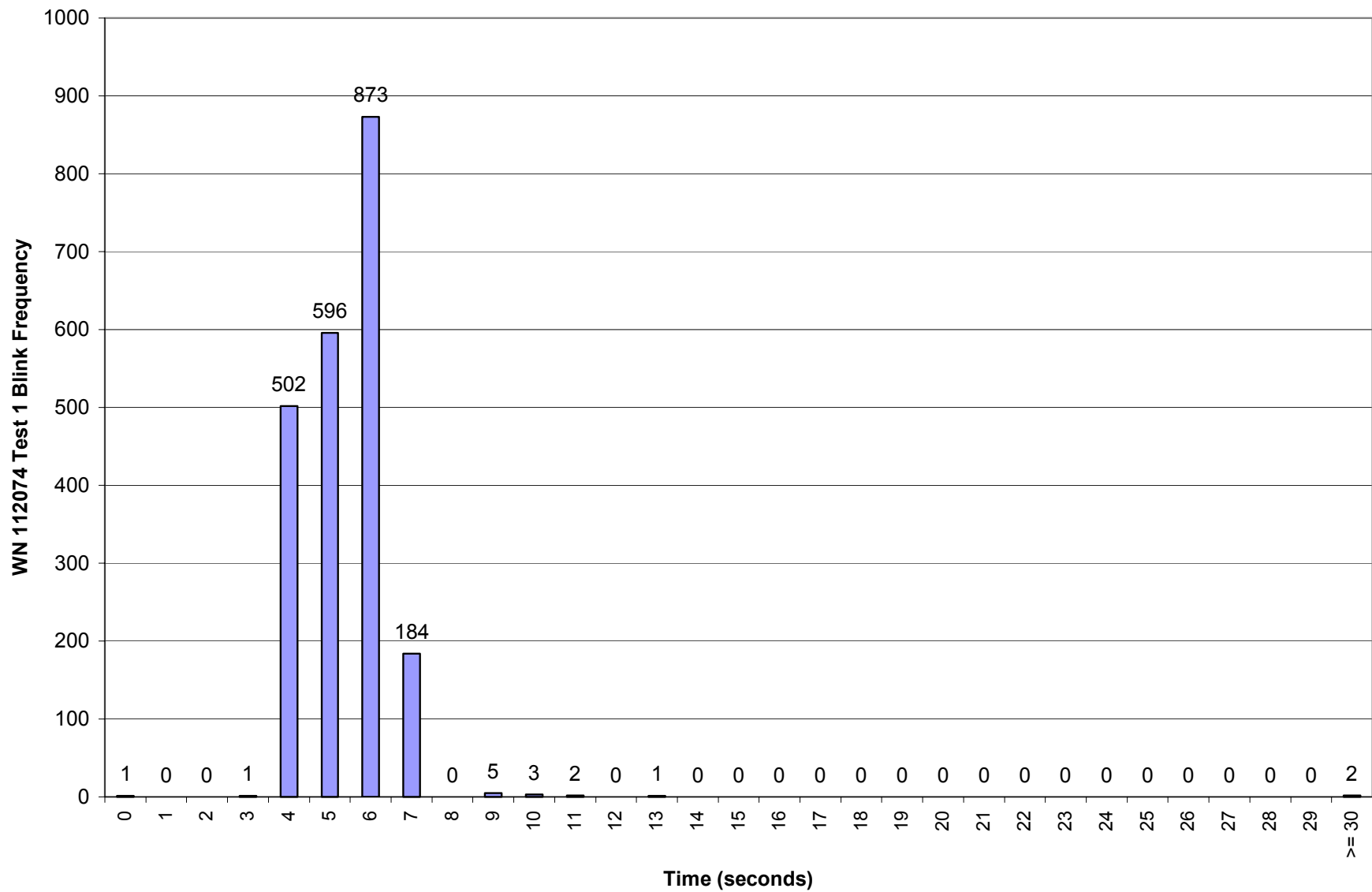Figure 150. WhereNet Test 1, Tag 112074: "Y" difference versus blink.

Figure 151. WhereNet Test 1, Tag 112074: Blink frequency histogram.

Figure 152. WhereNet Test 1, Tag 112348: Reported and correlated positions.

Figure 153. WhereNet Test 1, Tag 112348: "X-Y" difference versus blink.
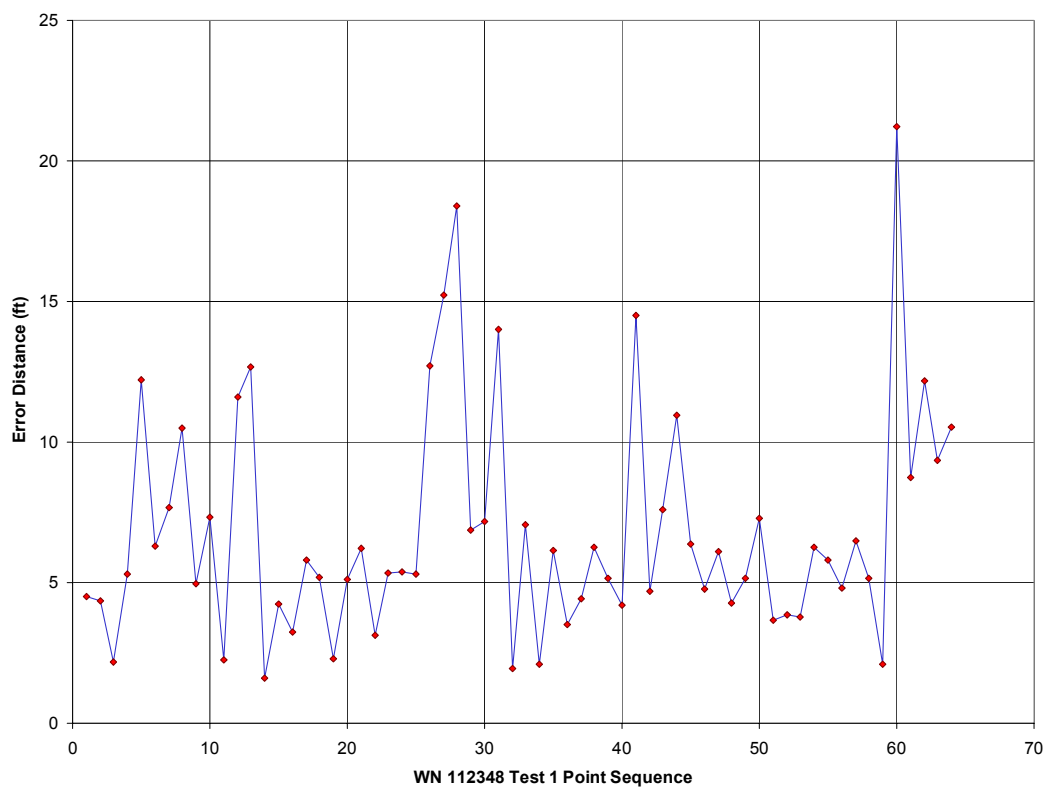
Figure 154. WhereNet Test 1, Tag 112348: Error versus blink.
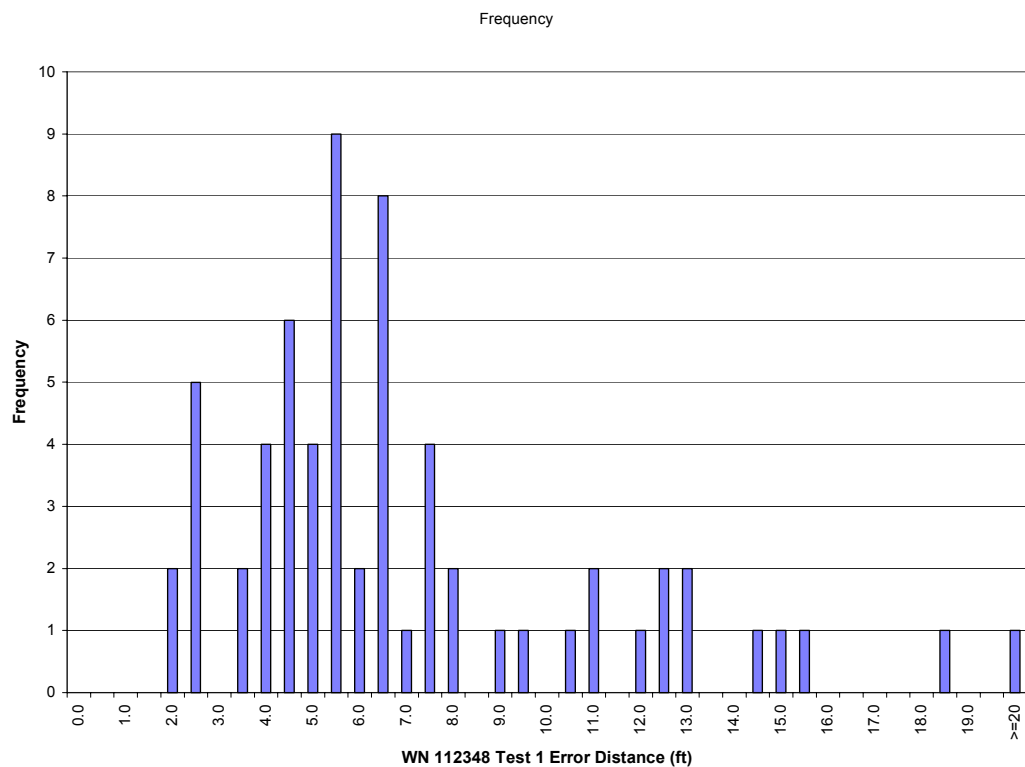
Figure 155. WhereNet Test 1, Tag 112348: Error histogram.

Figure 156. WhereNet Test 1, Tag 112348: "X" difference versus blink.

Figure 157. WhereNet Test 1, Tag 112348: "Y" difference versus blink.

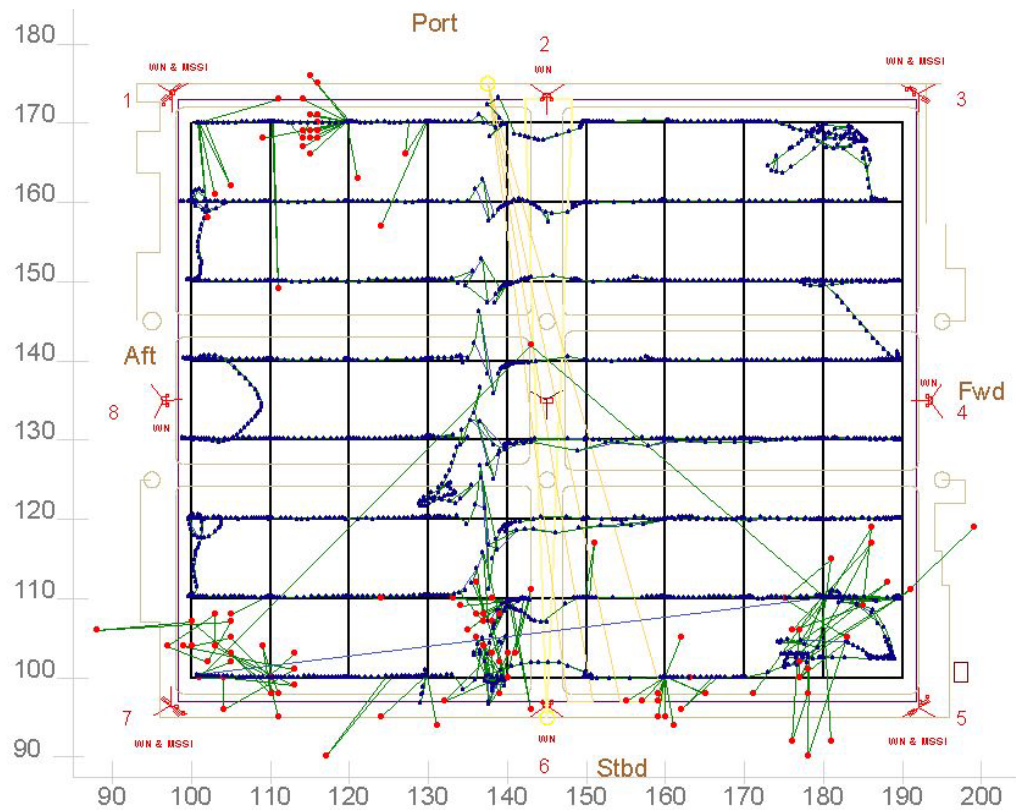Figure 158. WhereNet Test 1, Tag 112348: Blink frequency histogram.

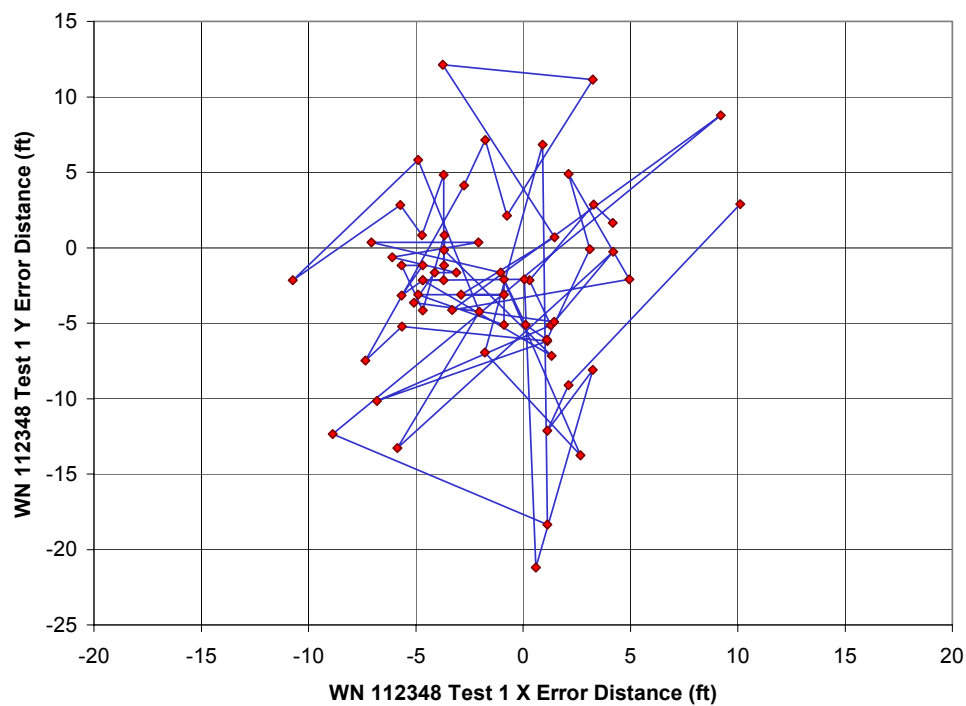Figure 159. WhereNet Test 1, Tag 114391: Reported and correlated positions.

Figure 160. WhereNet Test 1, Tag 114391: "X-Y" difference versus blink.

Figure 161. WhereNet Test 1, Tag 114391: Error versus blink.

Figure 162. WhereNet Test 1, Tag 114391: Error histogram.

Figure 163. WhereNet Test 1, Tag 114391: "X" difference versus blink.

Figure 164. WhereNet Test 1, Tag 114391: "Y" difference versus blink.
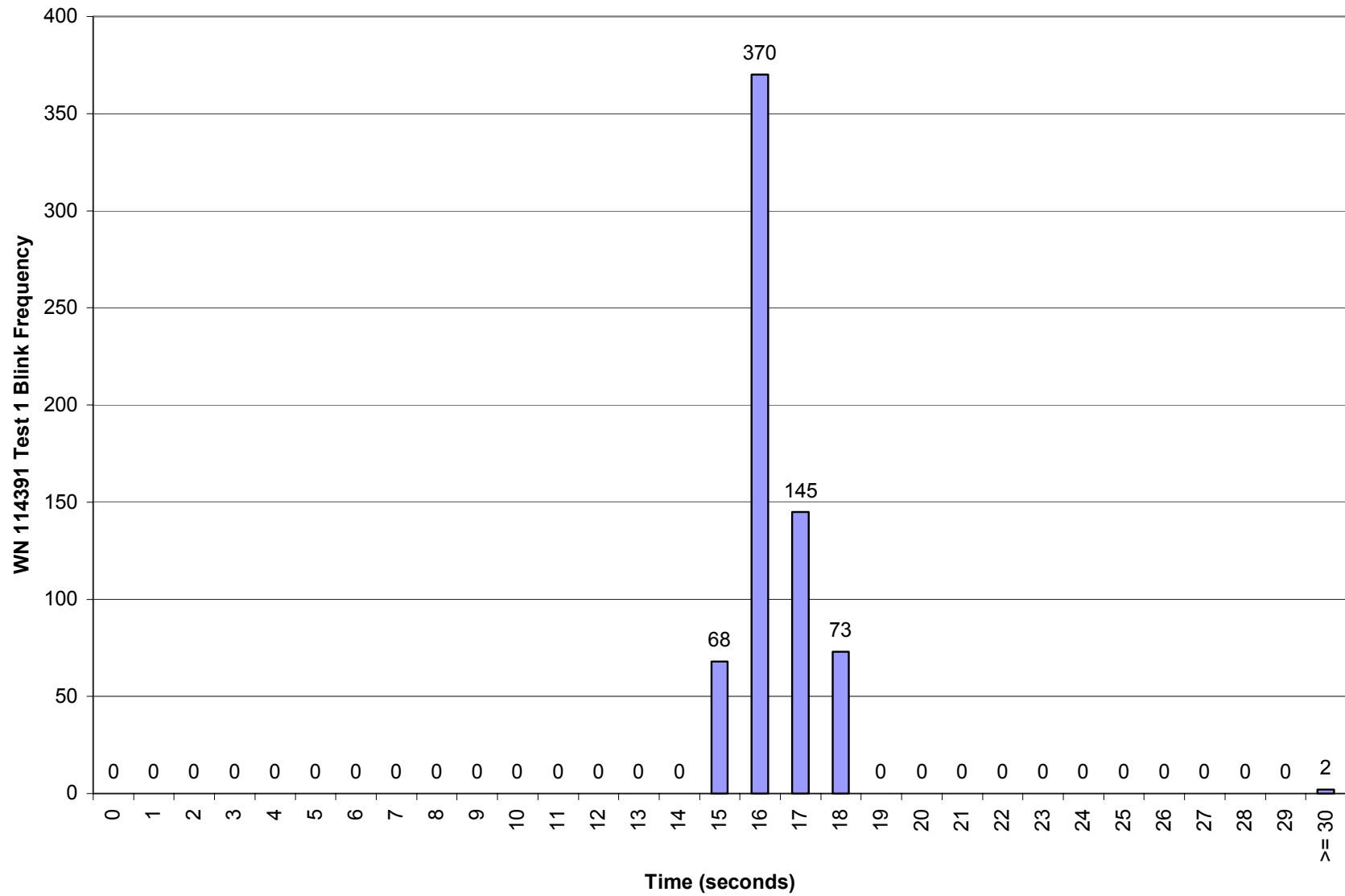
Figure 165. WhereNet Test 1, Tag 114391: Blink frequency histogram.
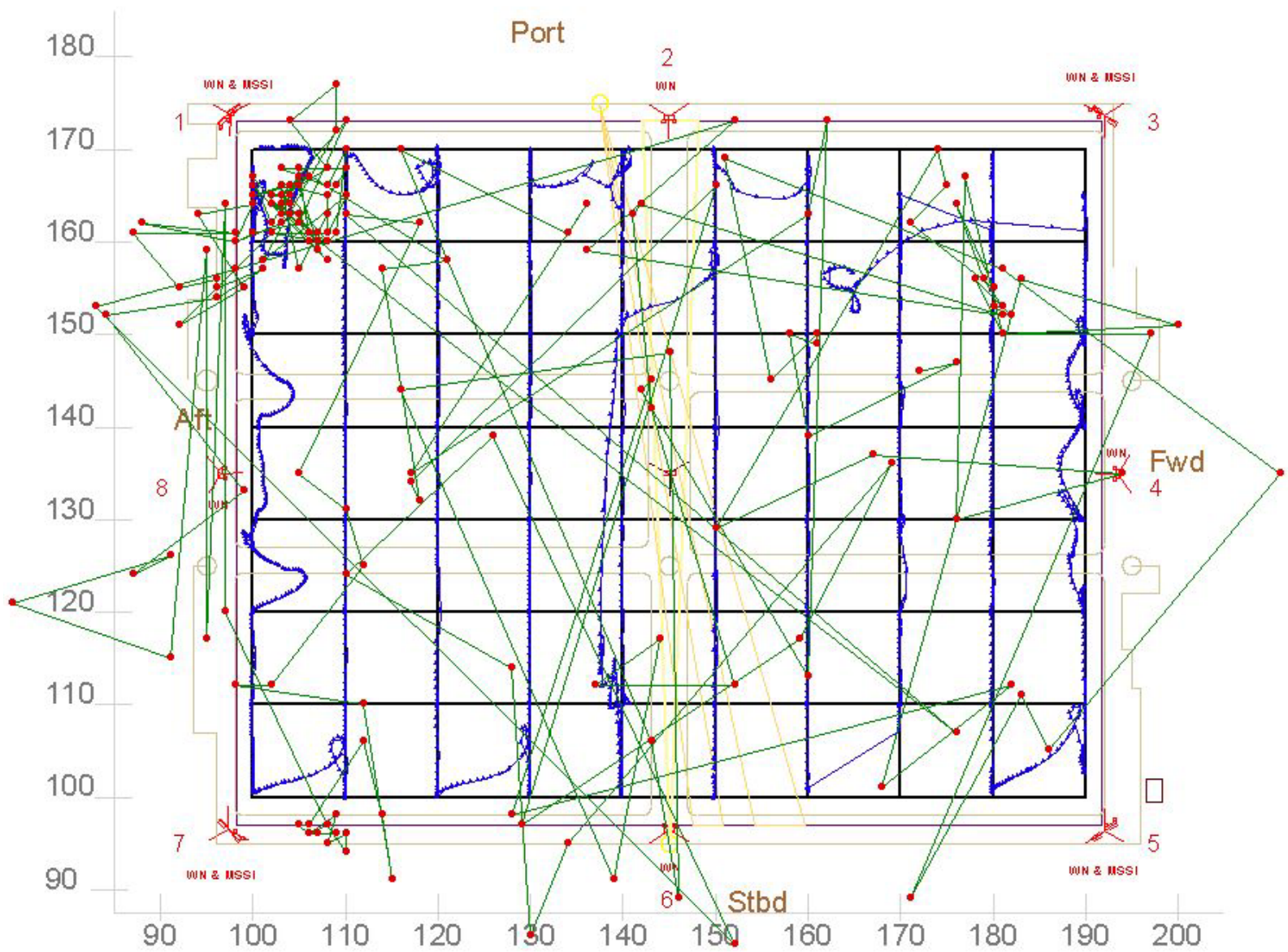
Figure 166. WhereNet Test 2: All tag reported positions with tracks.
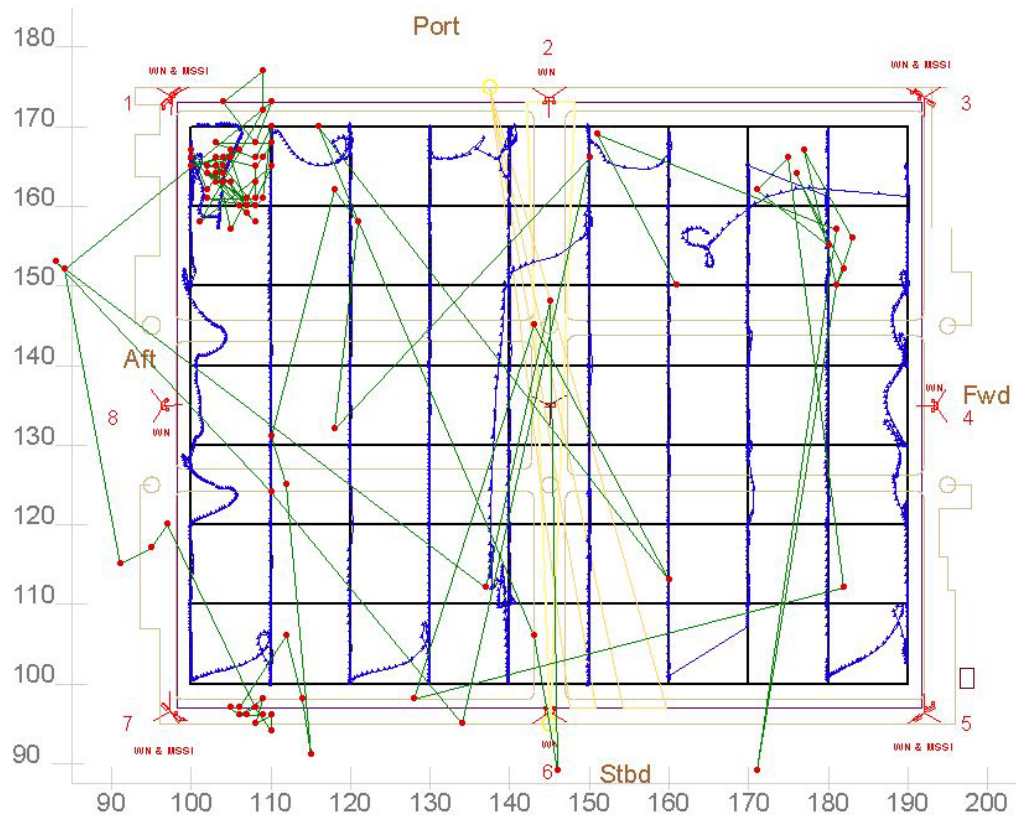
Figure 167. WhereNet Test 2, Tag 112074: Reported positions with tracks.
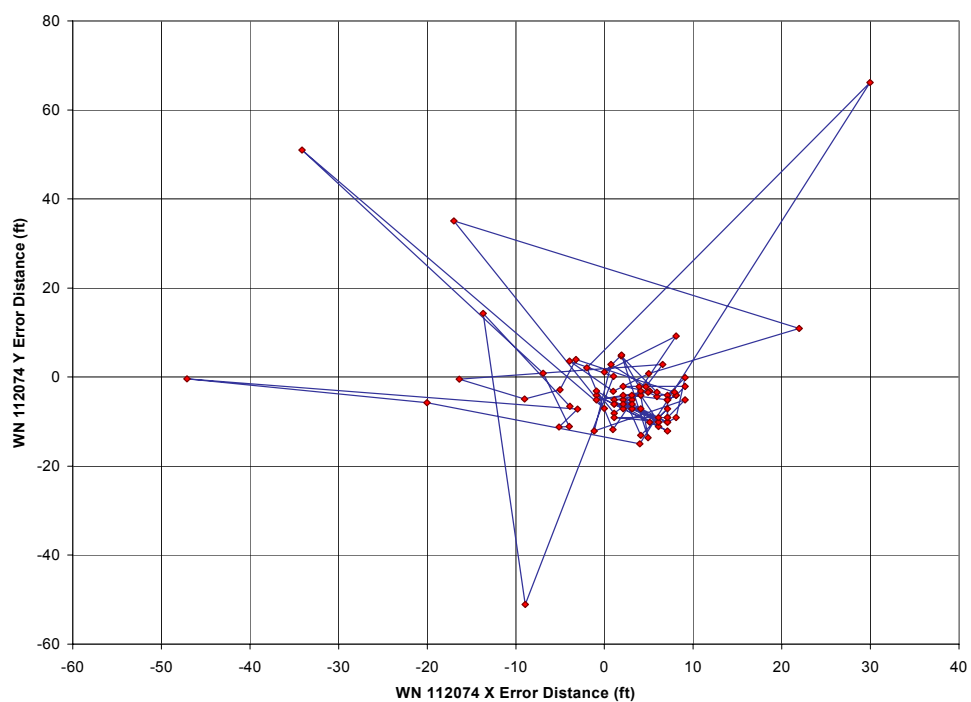
Figure 168. WhereNet Test 2, Tag 112074: "X-Y" difference versus blink.
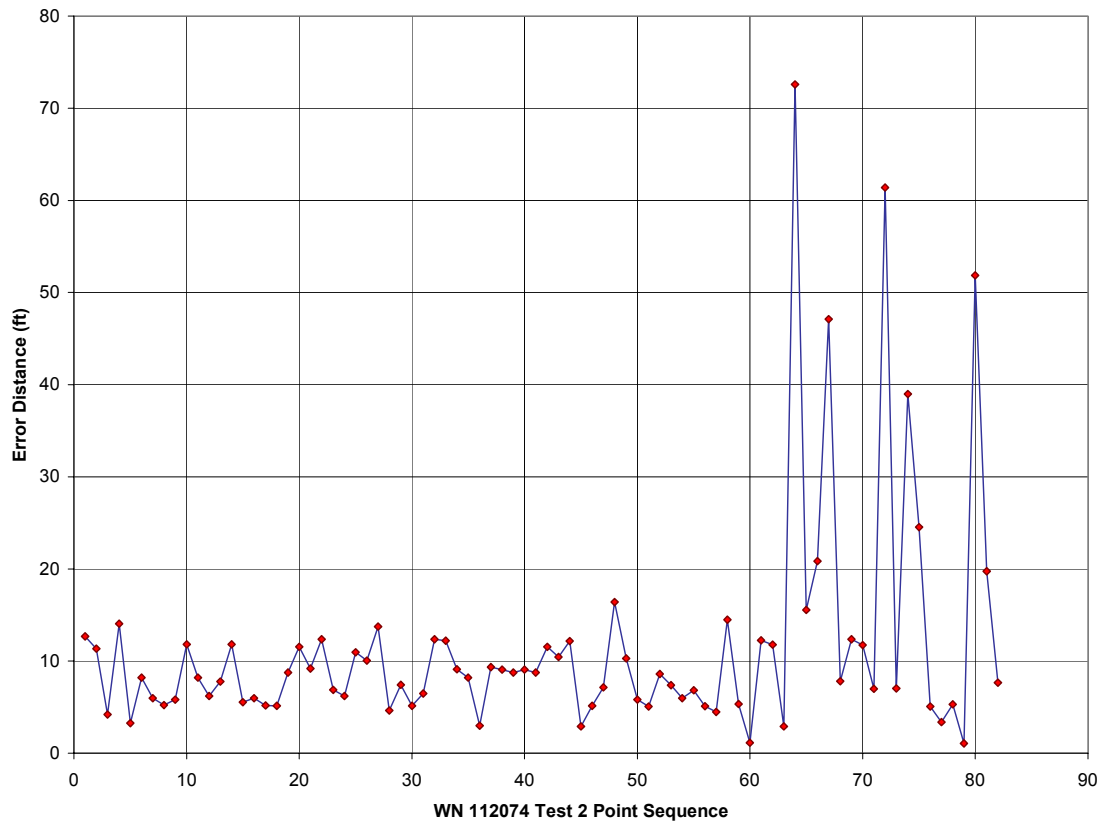
Figure 169. WhereNet Test 2, Tag 112074: Error versus blink.
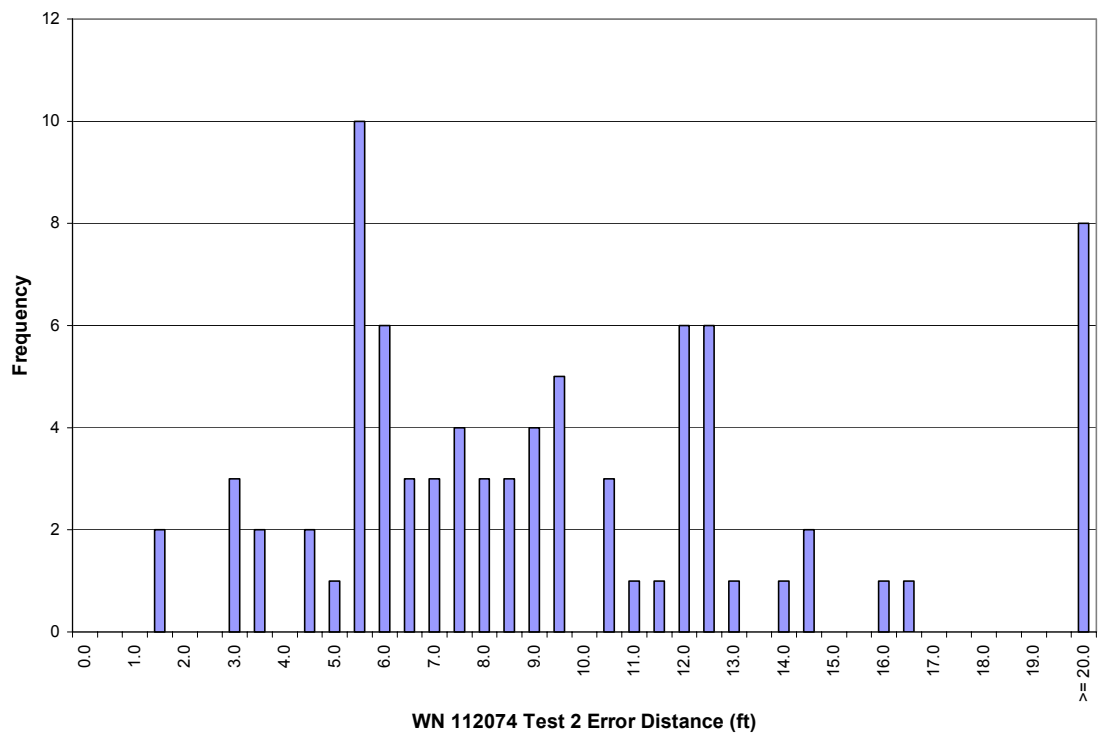
Figure 170. WhereNet Test 2, Tag 112074: Error histogram.
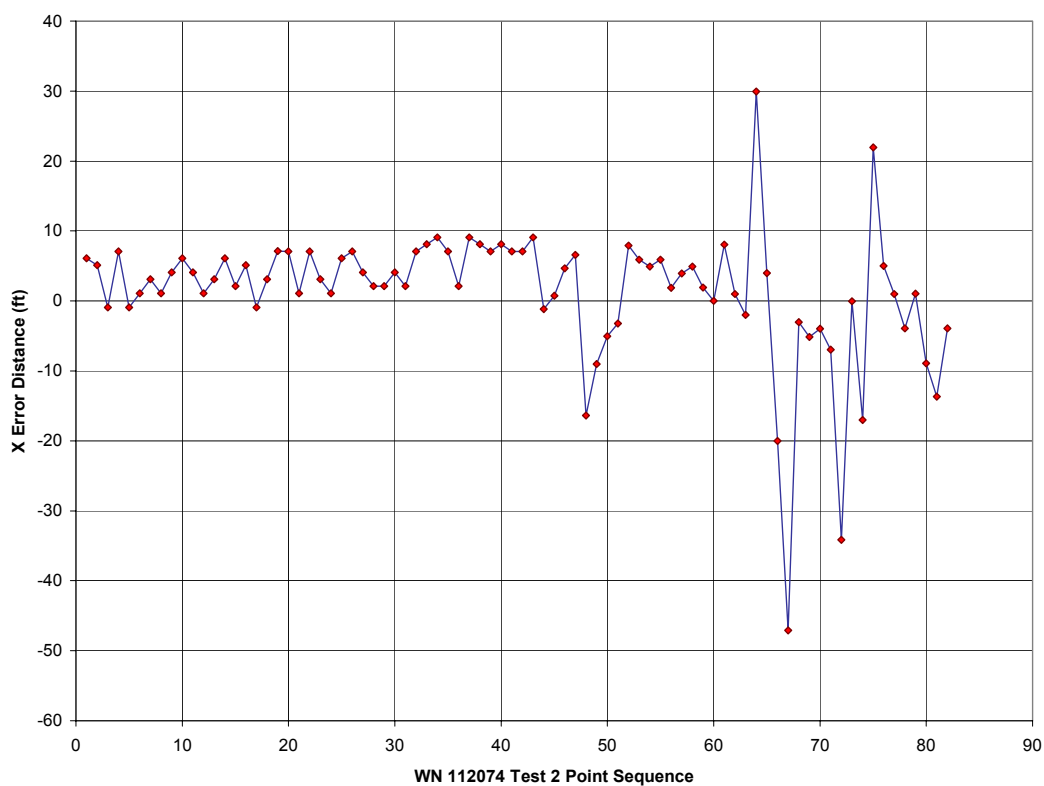
Figure 171. WhereNet Test 2, Tag 112074: " X" difference versus blink.
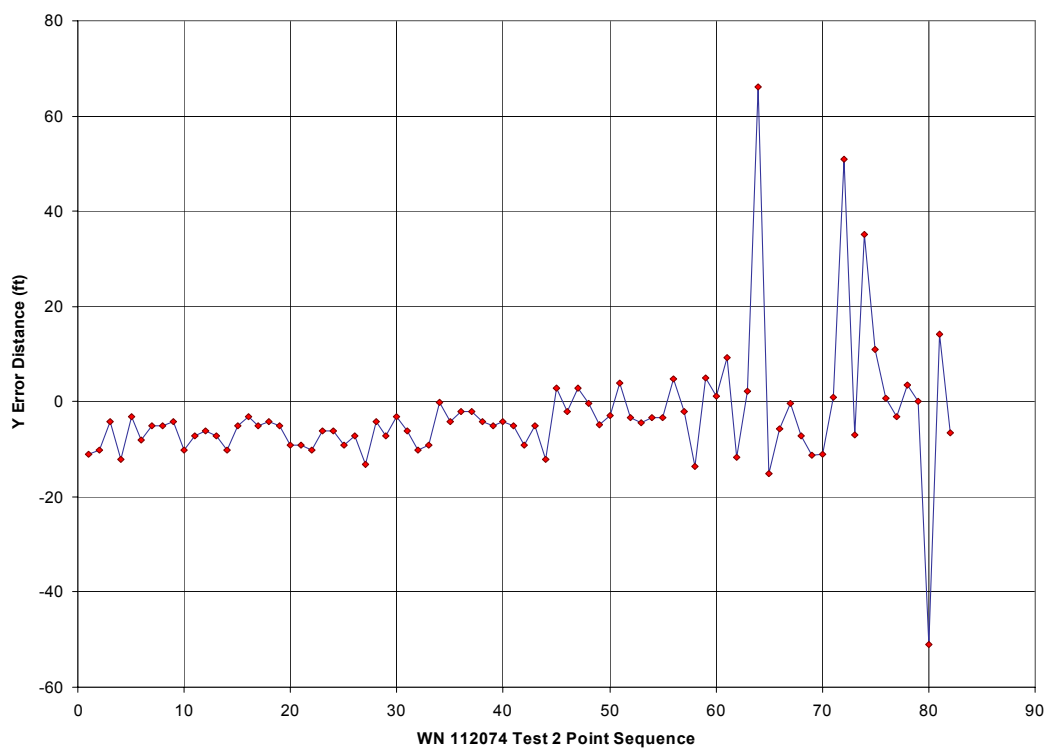
Figure 172. WhereNet Test 2, Tag 112074: "Y" difference versus blink

.

4-65
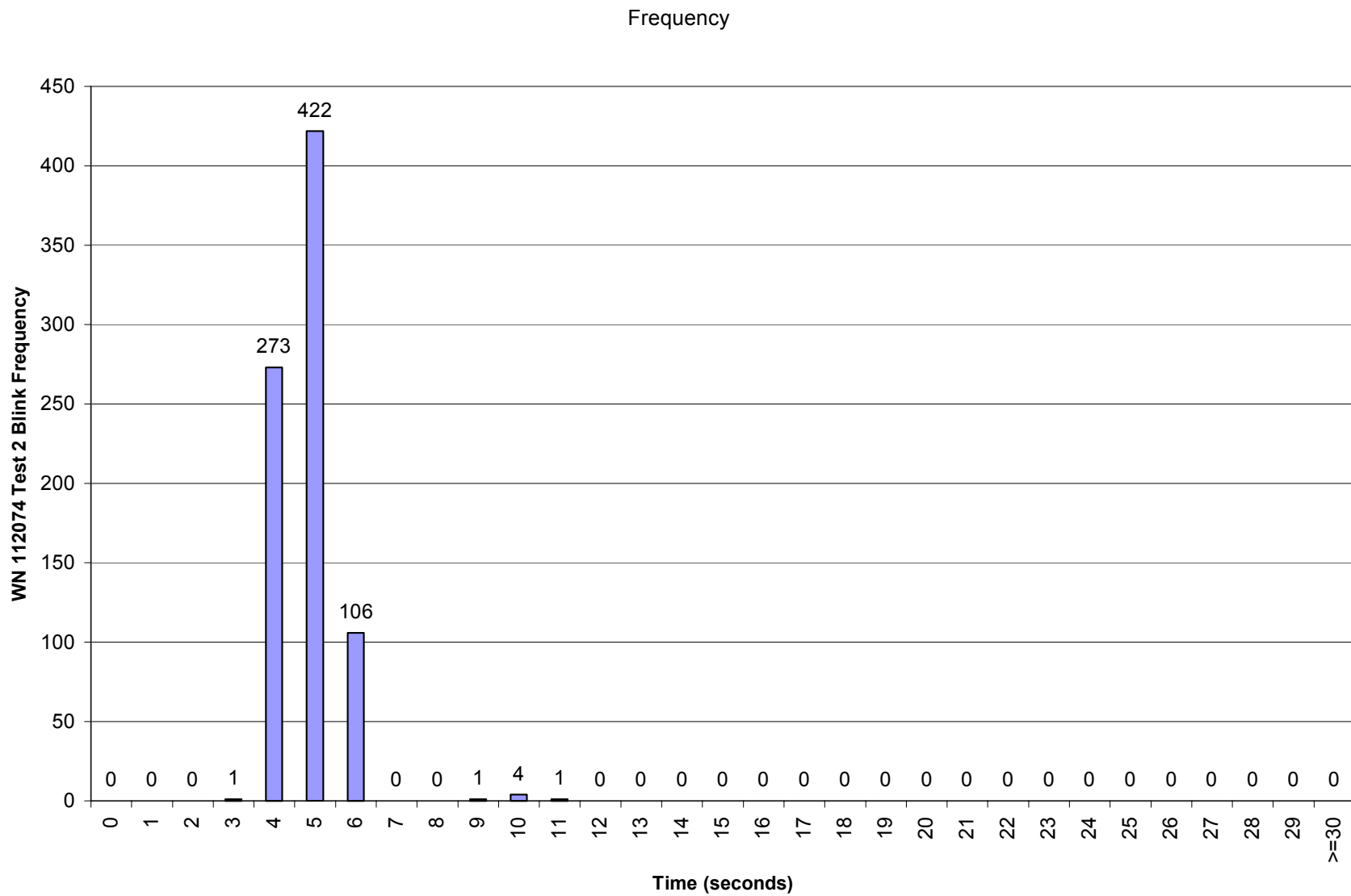
Frequency

Figure 173. WhereNet Test 2, Tag 112074: Blink frequency histogram.
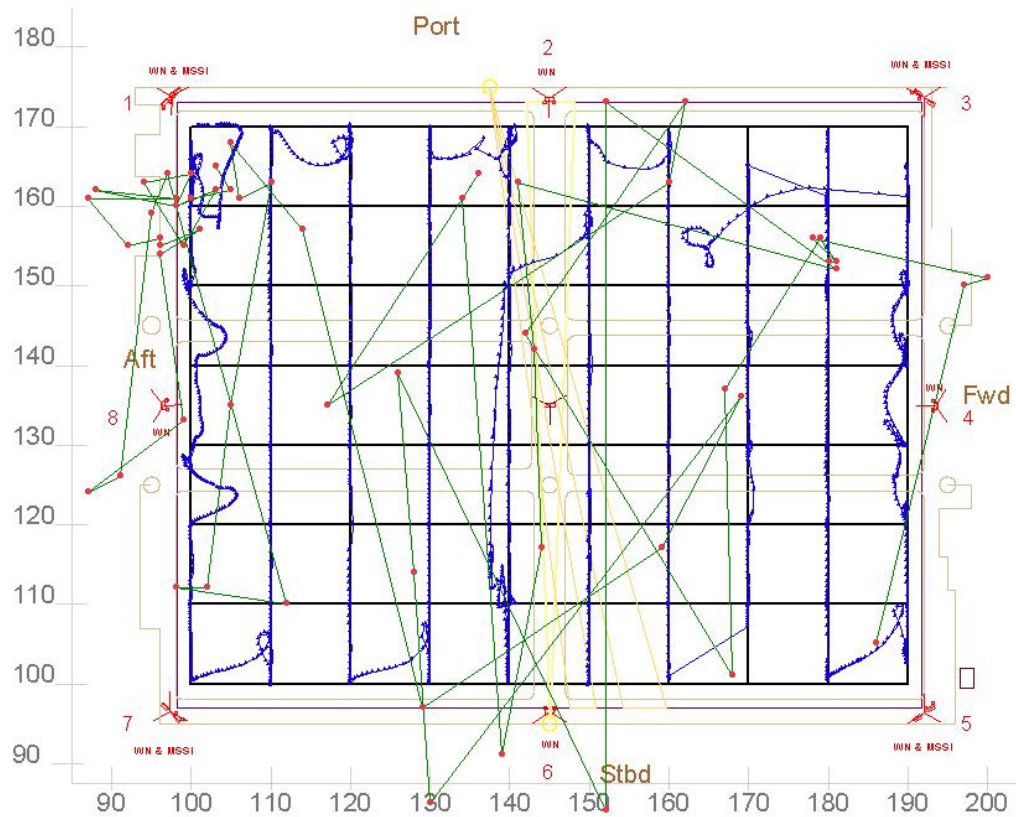
Figure 174. WhereNet Test 2, Tag 112348 reported positions with tracks.
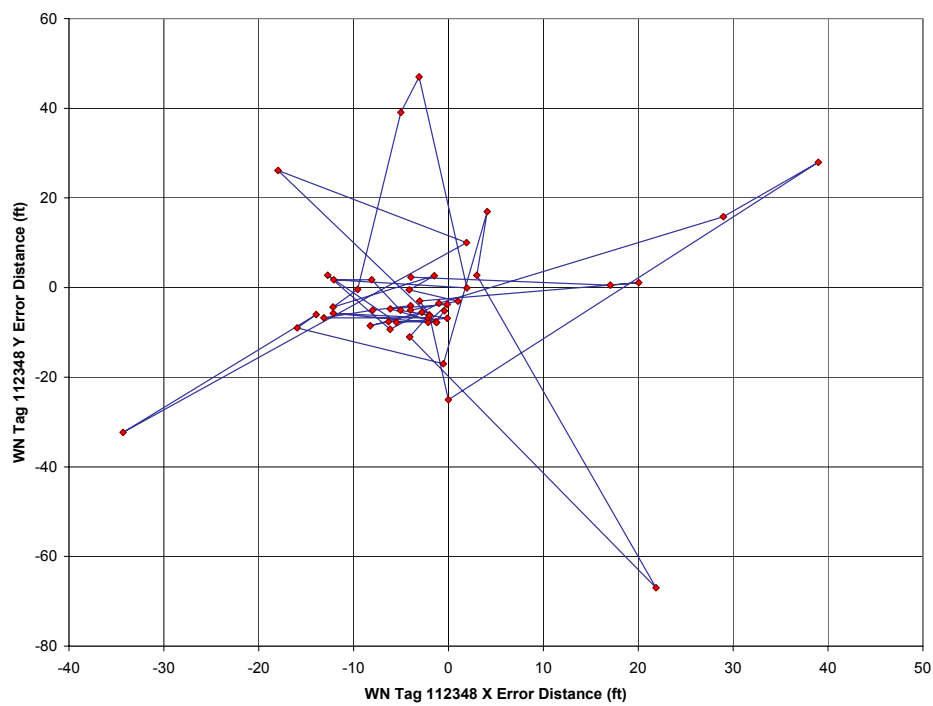
Figure 175. WhereNet Test 2, Tag 112348: "X-Y" difference versus blink.

4-67
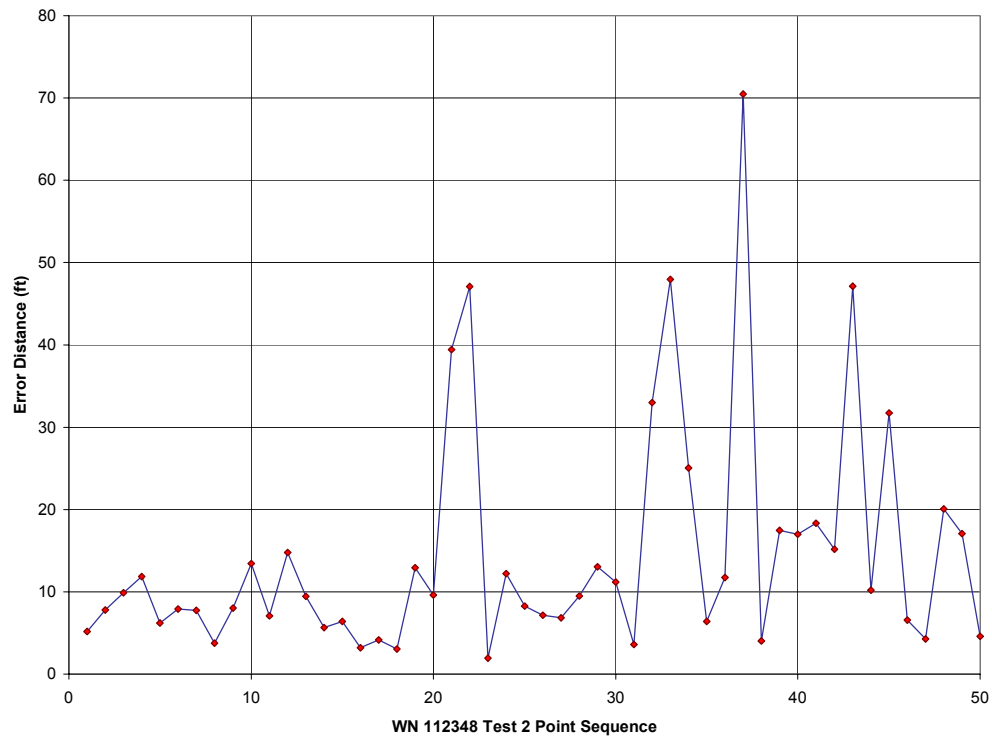
Figure 176. WhereNet Test 2, Tag 112348 error versus blink.
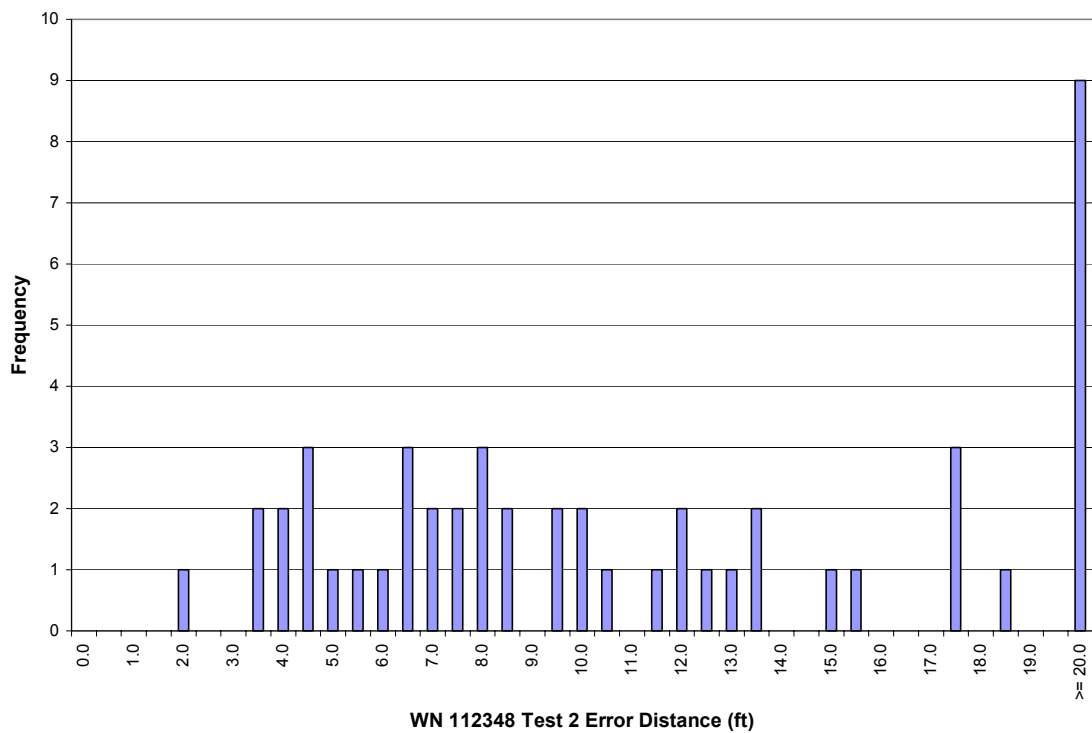
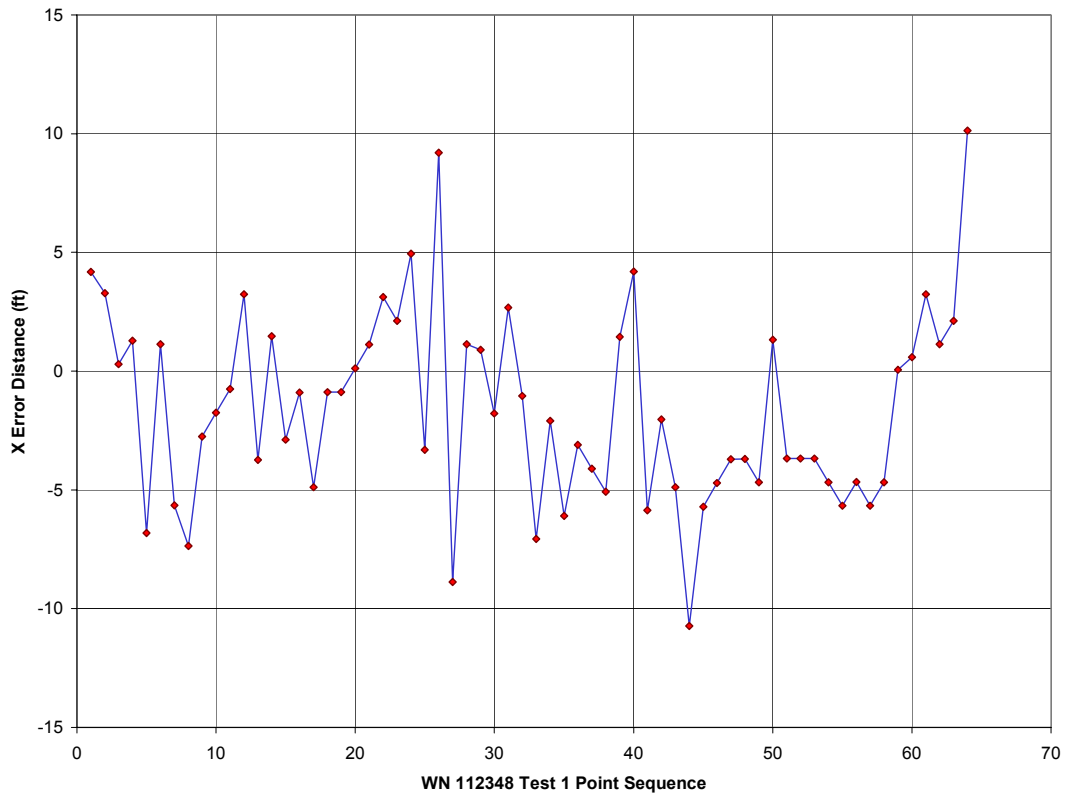

Figure 177. WhereNet Test 2, Tag 112348: Error histogram.

4-68
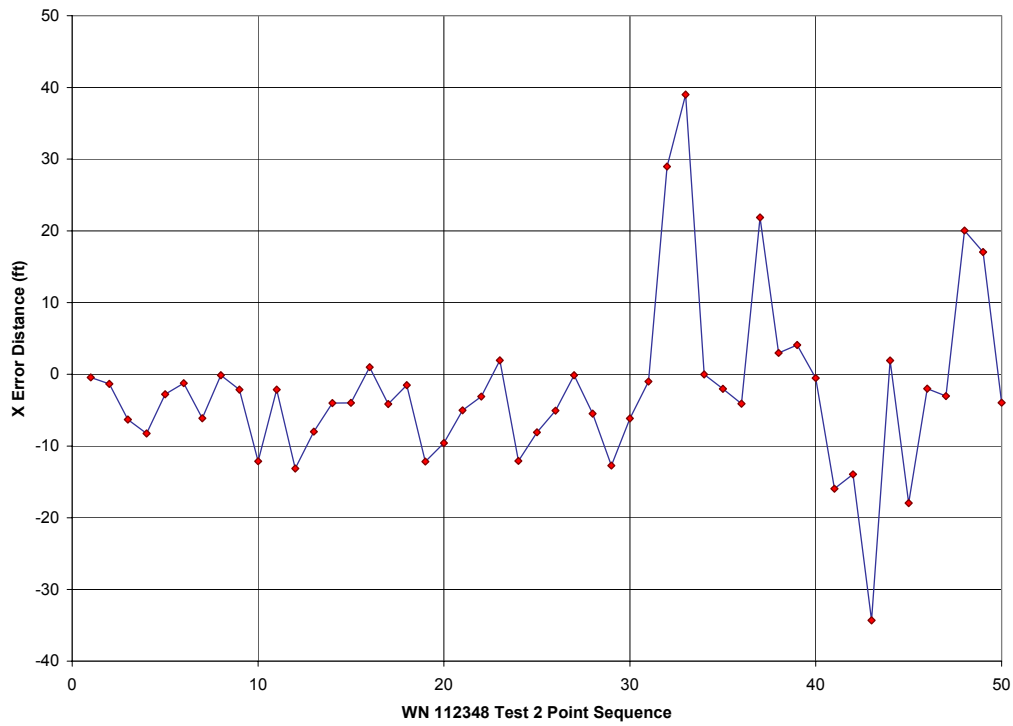
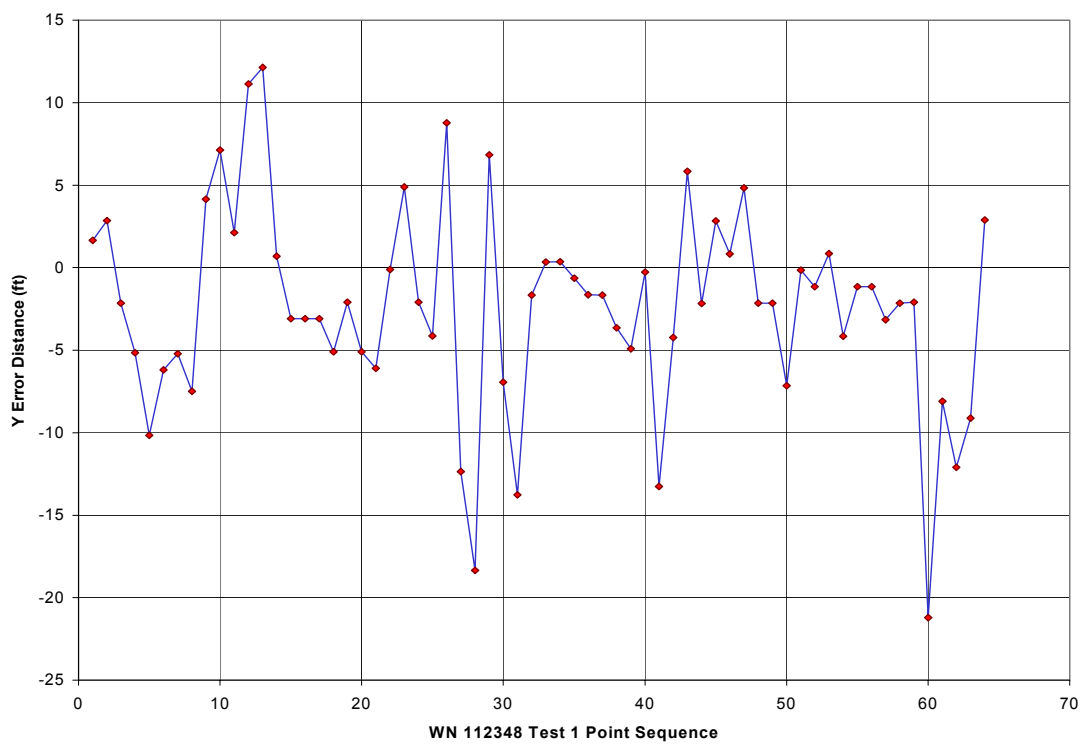Figure 178. WhereNet Test 2, Tag 112348: " X" difference versus blink.
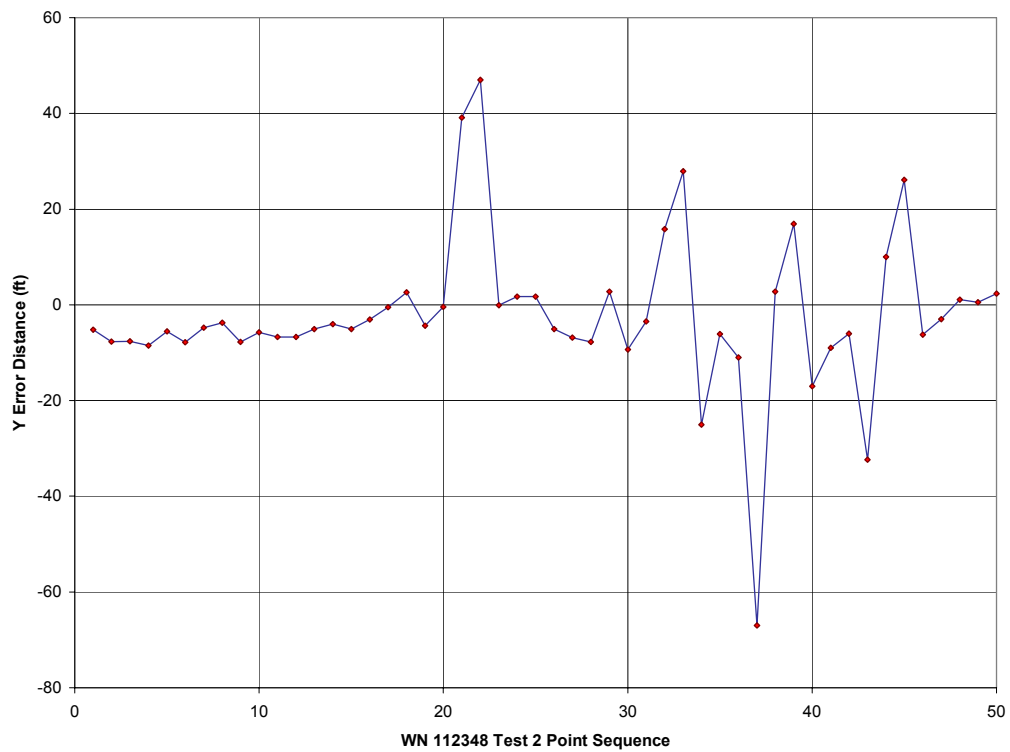
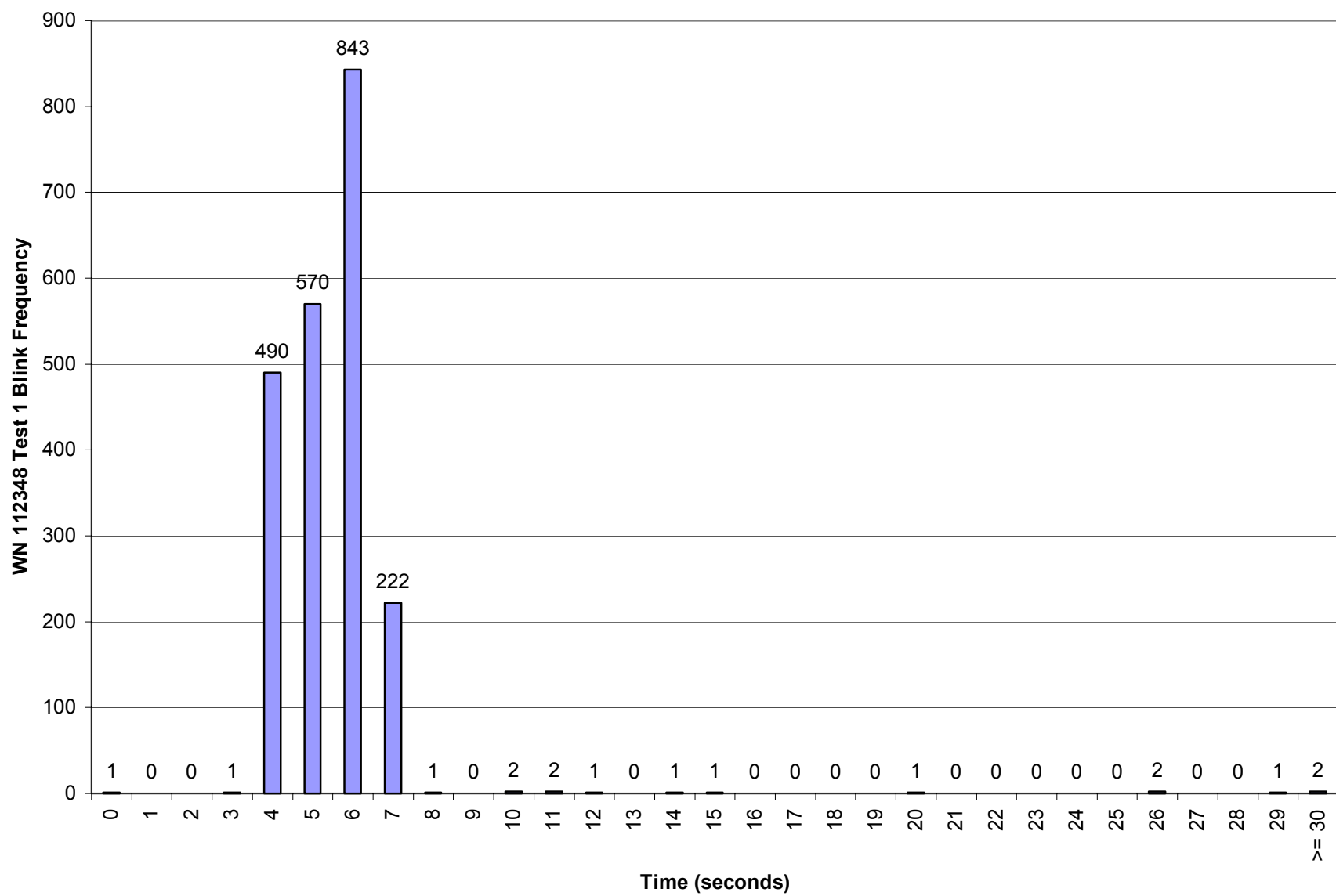Figure 179. WhereNet Test 2, Tag 112348: "Y" difference versus blink
.
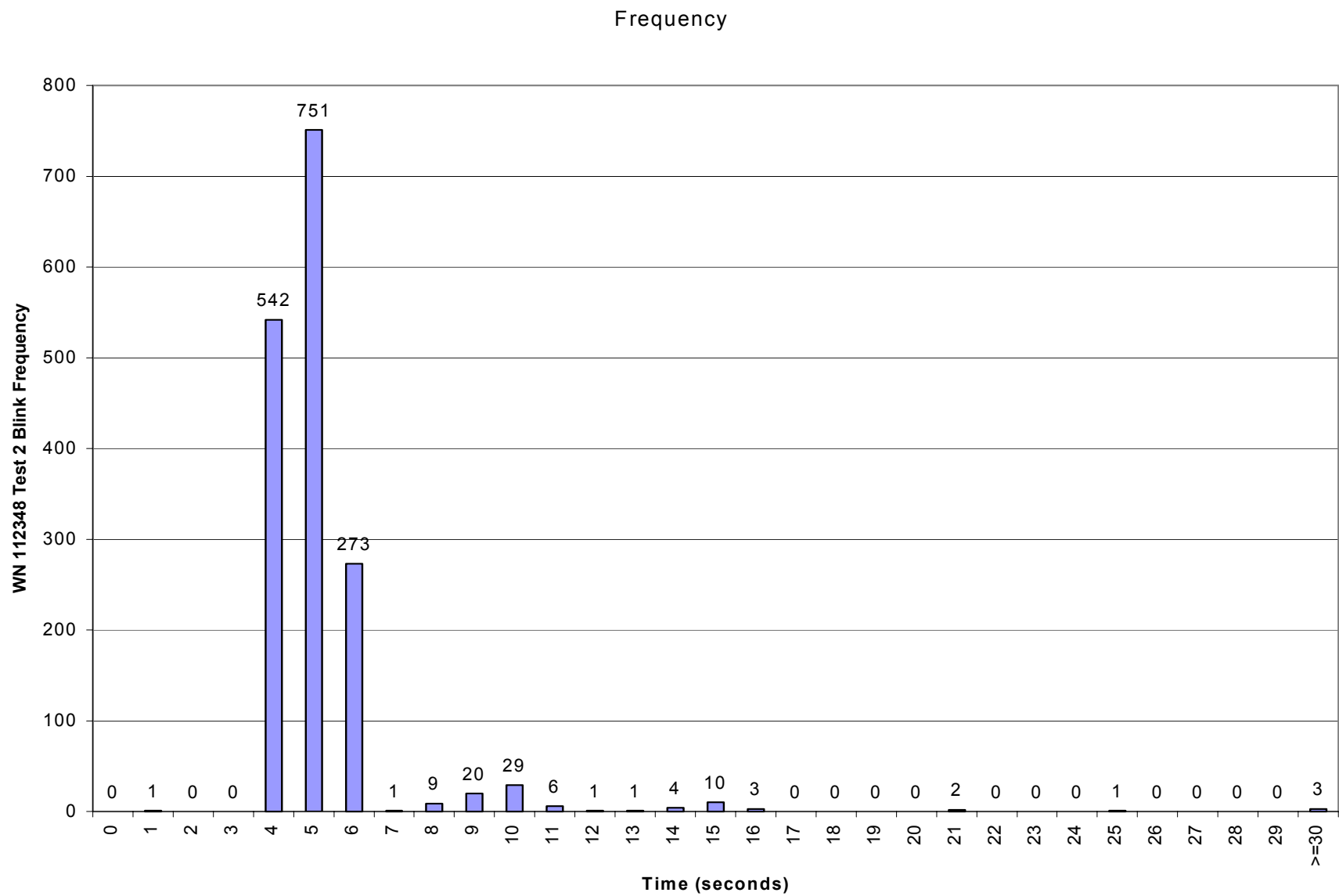
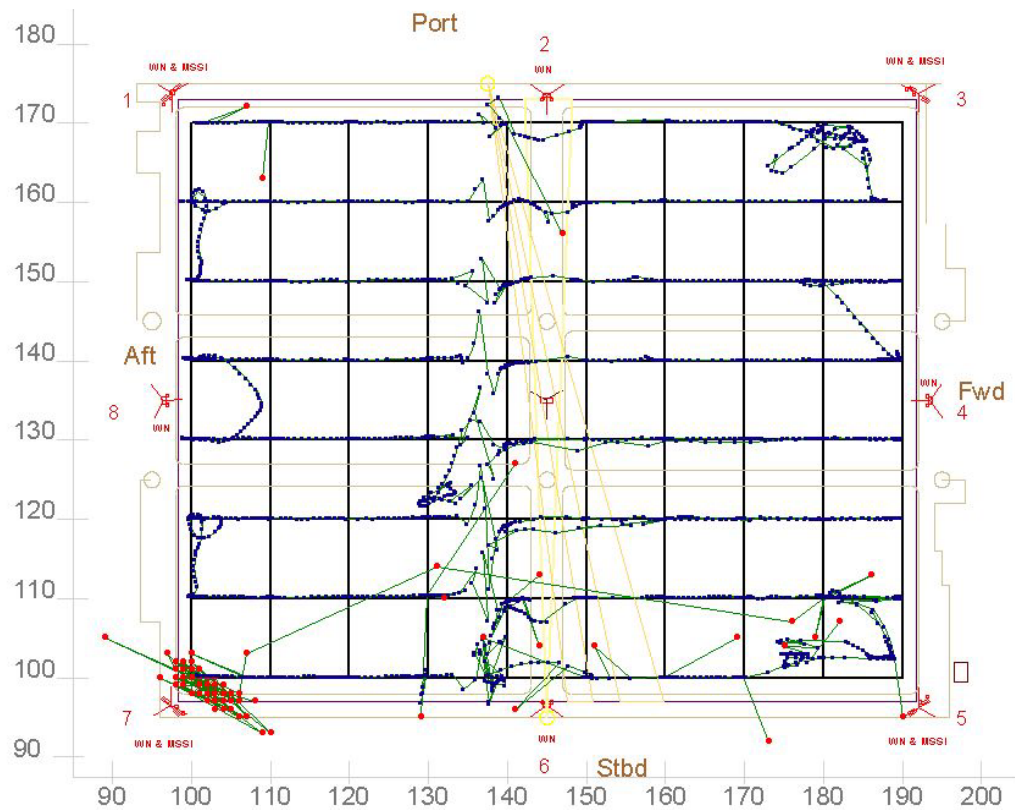Figure 180. WhereNet Test 2, Tag 112348: Blink frequency histogram.
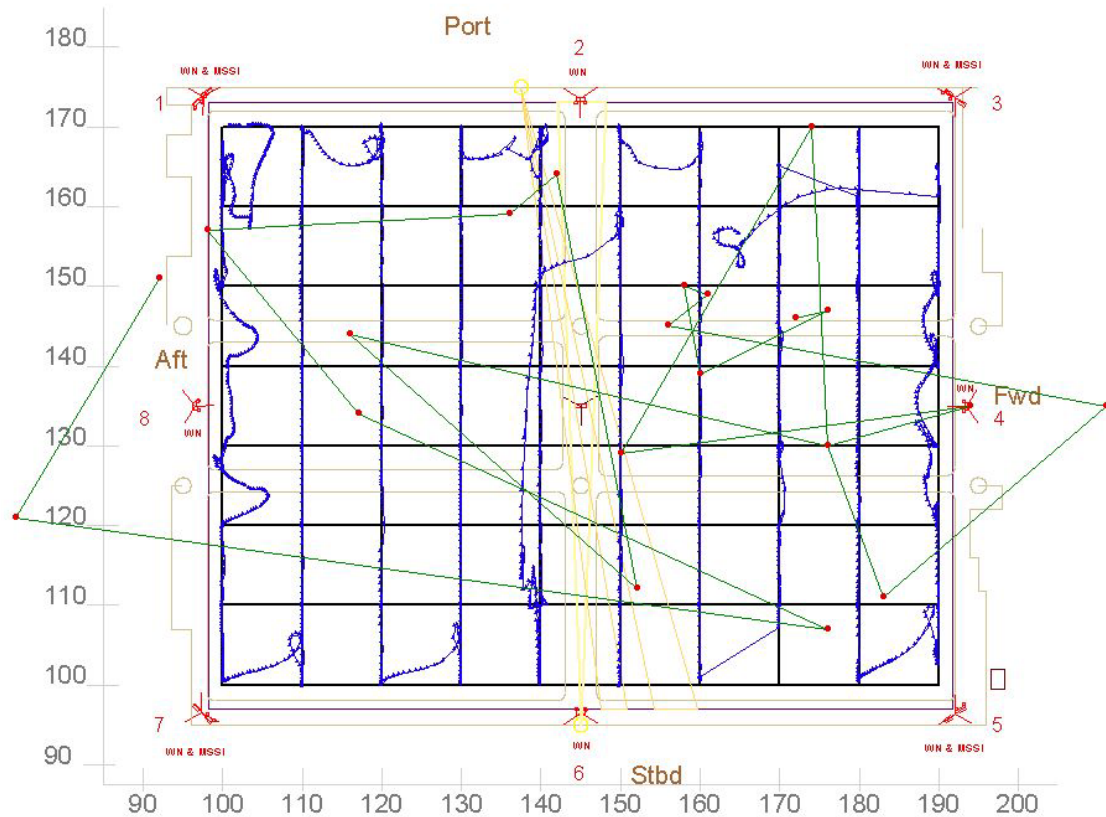
Figure 181. WhereNet Test 2, Tag 114391: Reported positions with tracks.
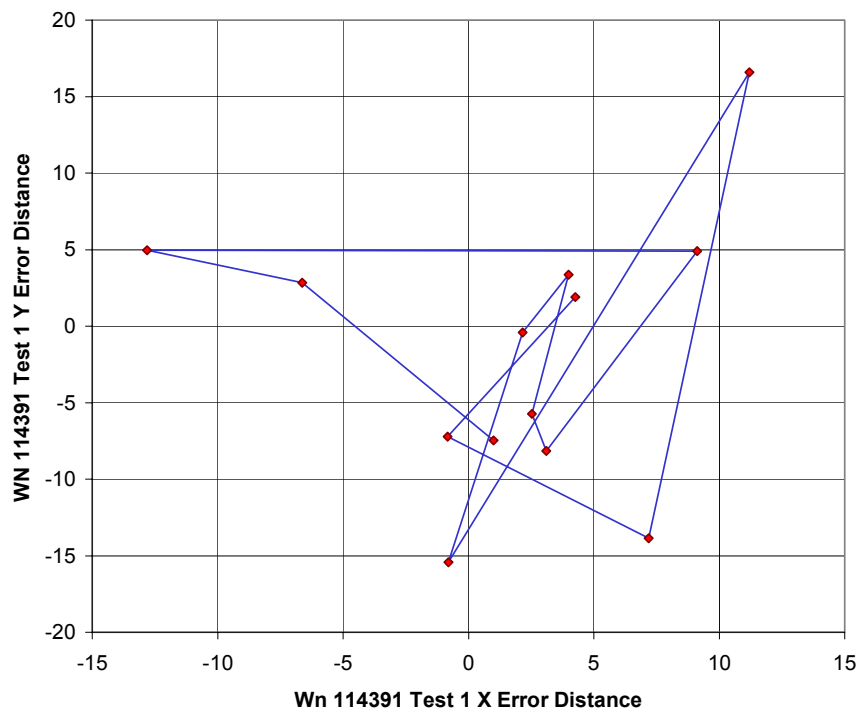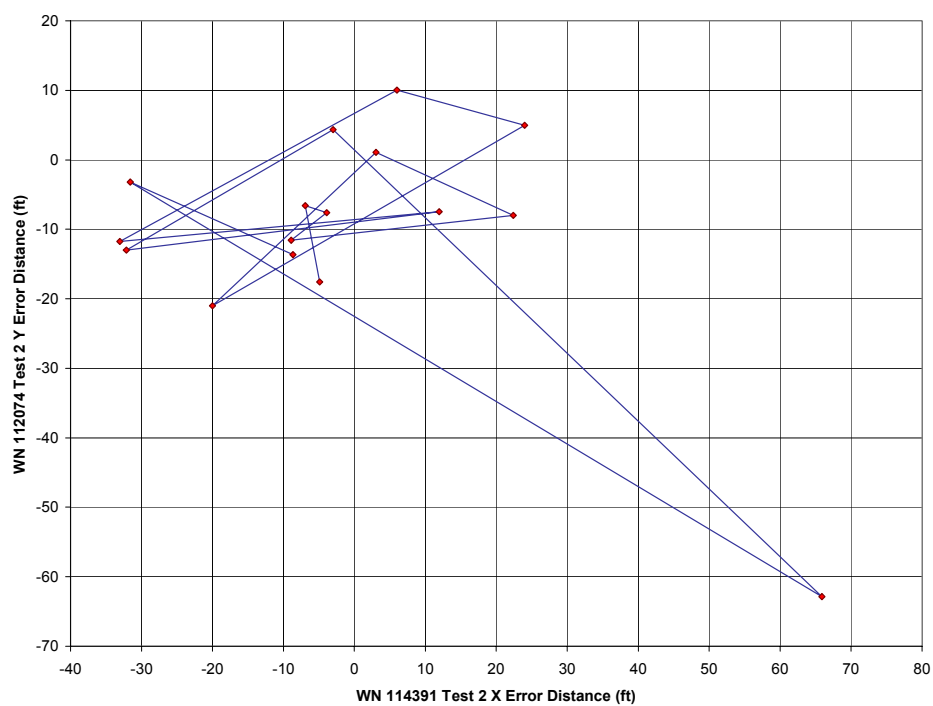

Figure 182. WhereNet Test 2, Tag 114391: "X-Y" difference versus blink.
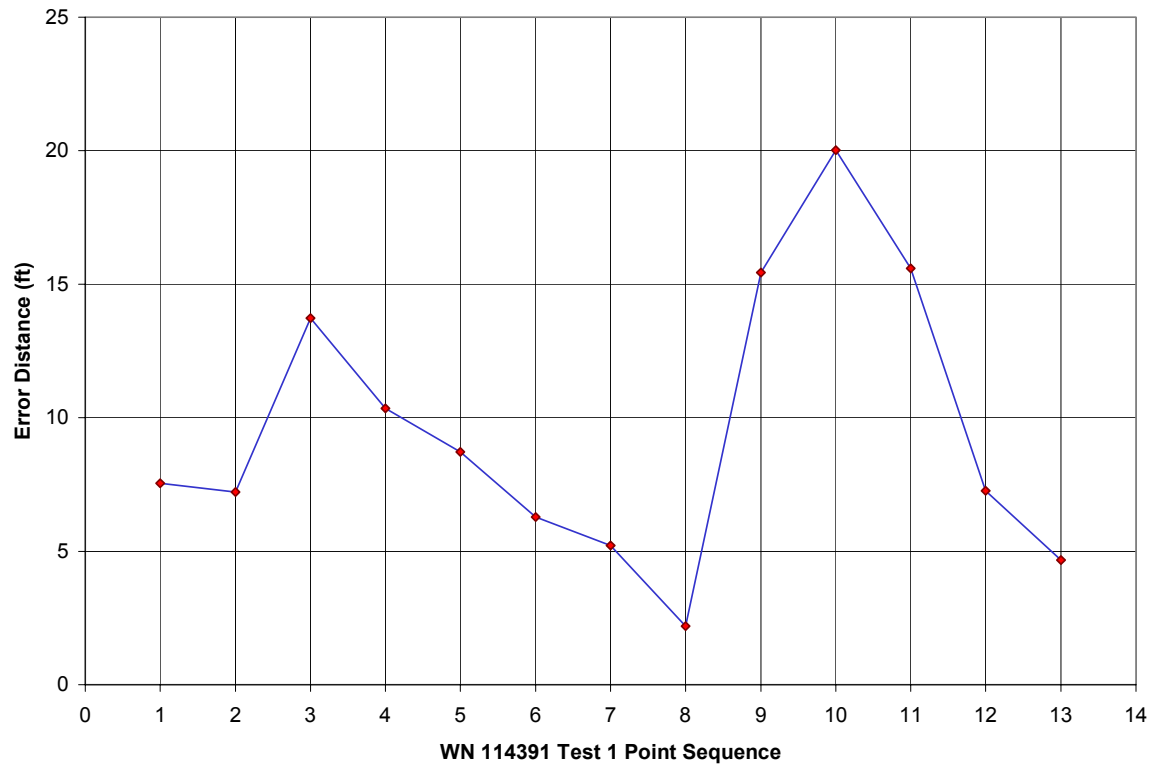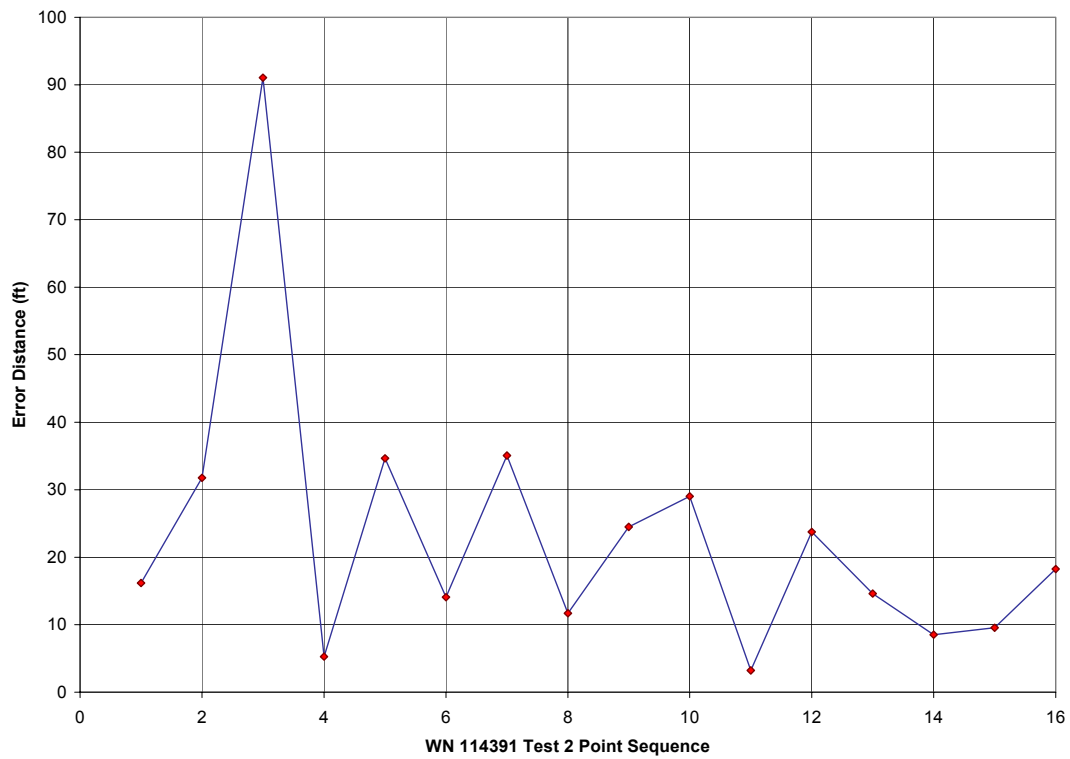
Figure 183. WhereNet Test 2, Tag 114391: Error versus blink.

Figure 184. WhereNet Test 2, Tag 114391: Error histogram.

Figure 185. WhereNet Test 2, Tag 114391: "X" difference versus blink.

Figure 186. WhereNet Test 2, Tag 114391: "Y" difference versus blink.

Figure 187. WhereNet Test 2, Tag 114391: Blink frequency histogram.
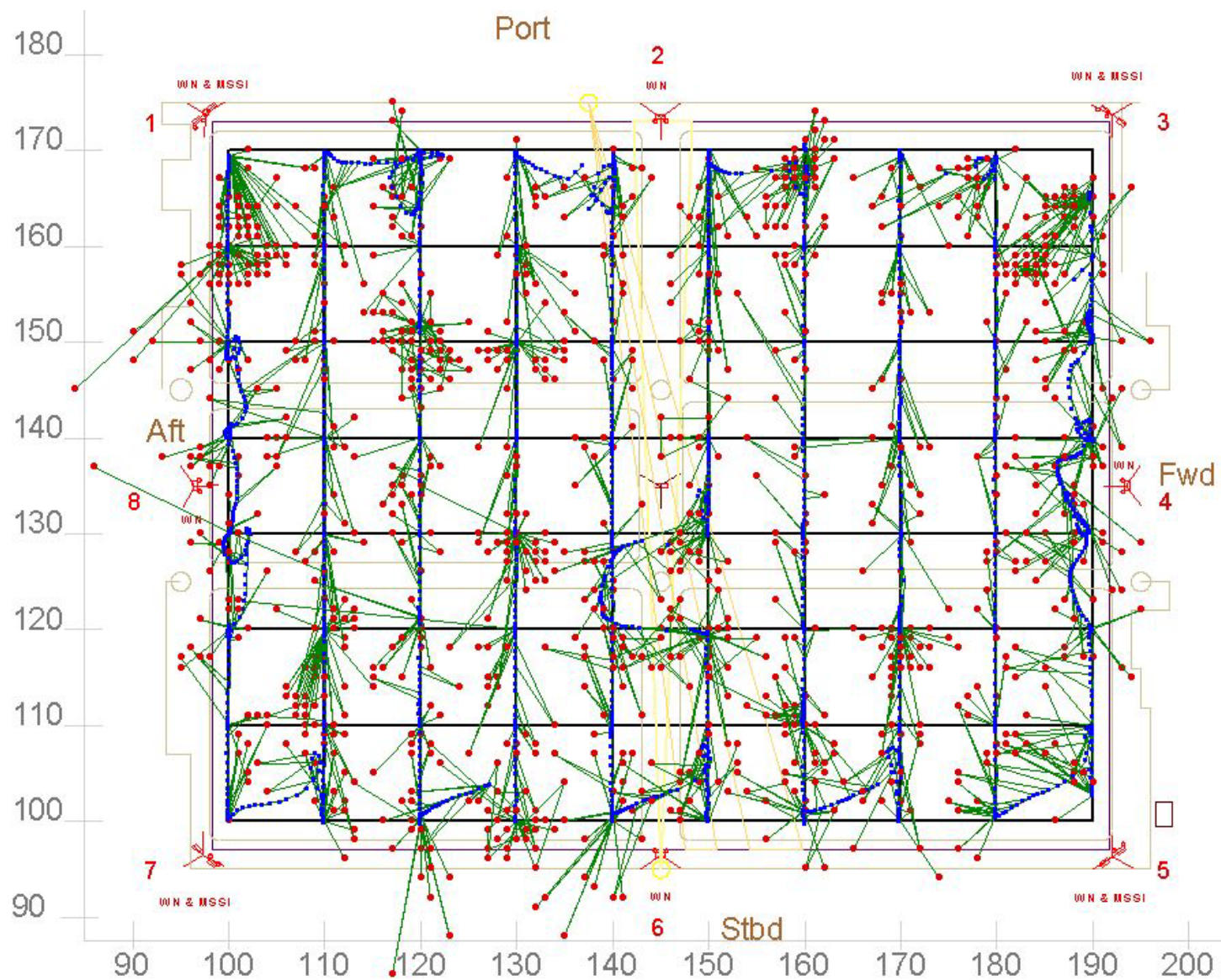
Figure 188. WhereNet Test 3: All tag reported and correlated positions.
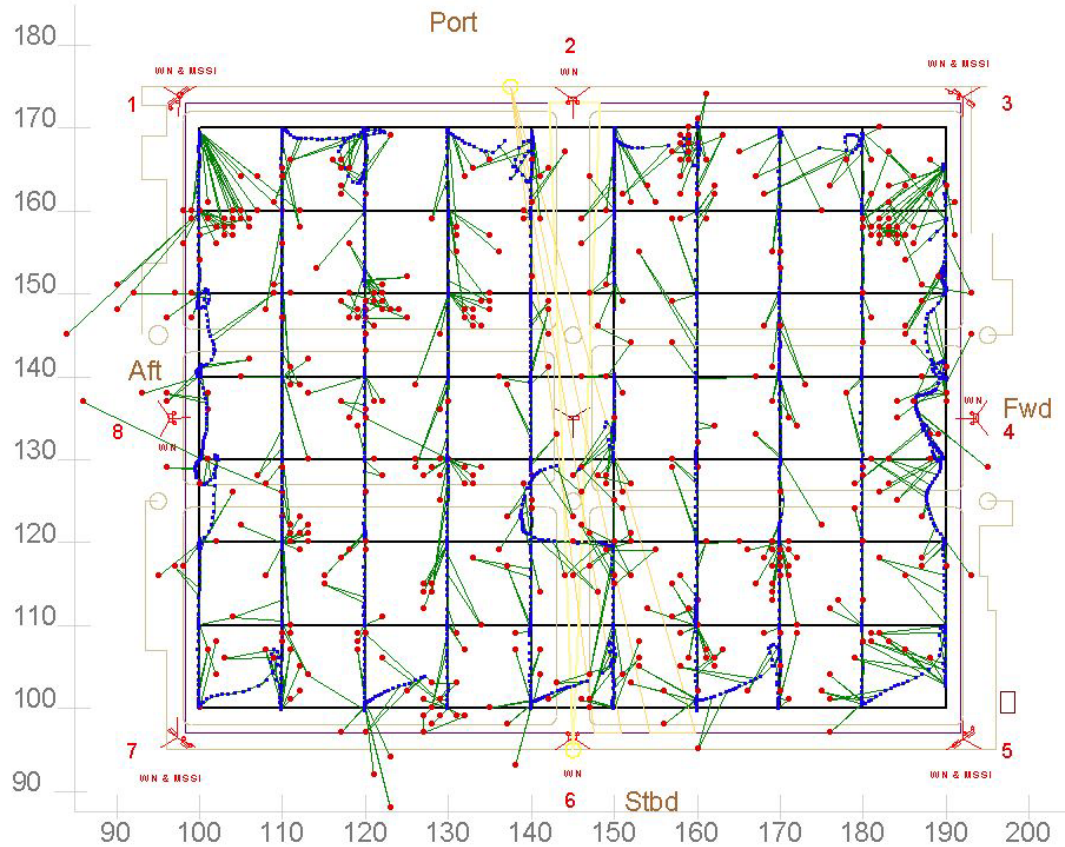
Figure 189. WhereNet Test 3, Tag 112074: Reported and correlated positions.
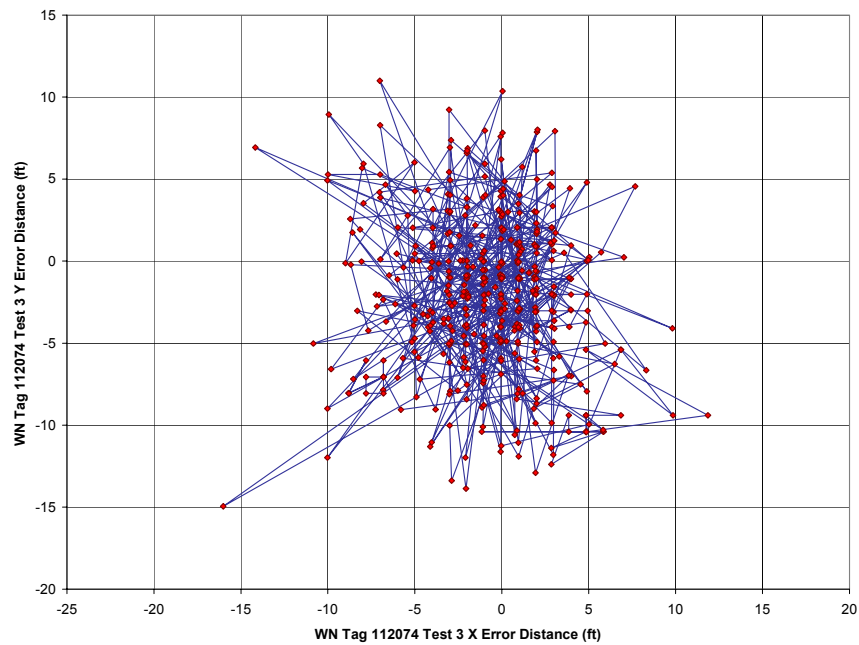
Figure 190. WhereNet Test 3, Tag 112074: "X-Y" difference versus blink.
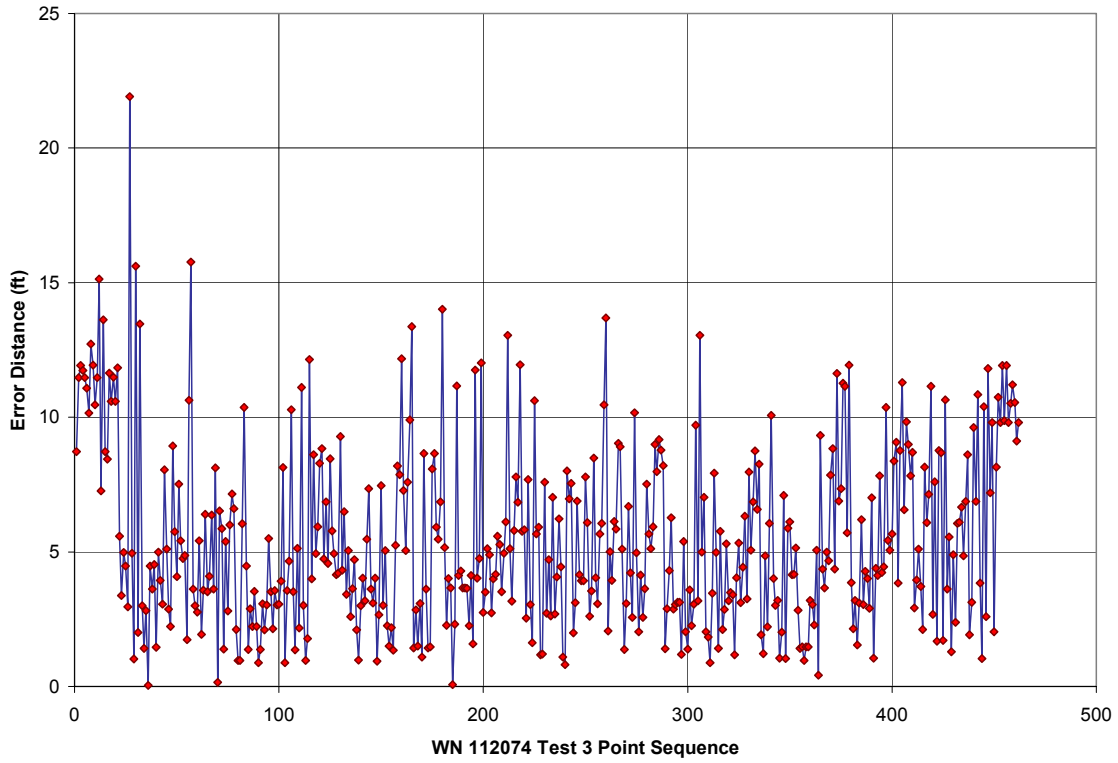
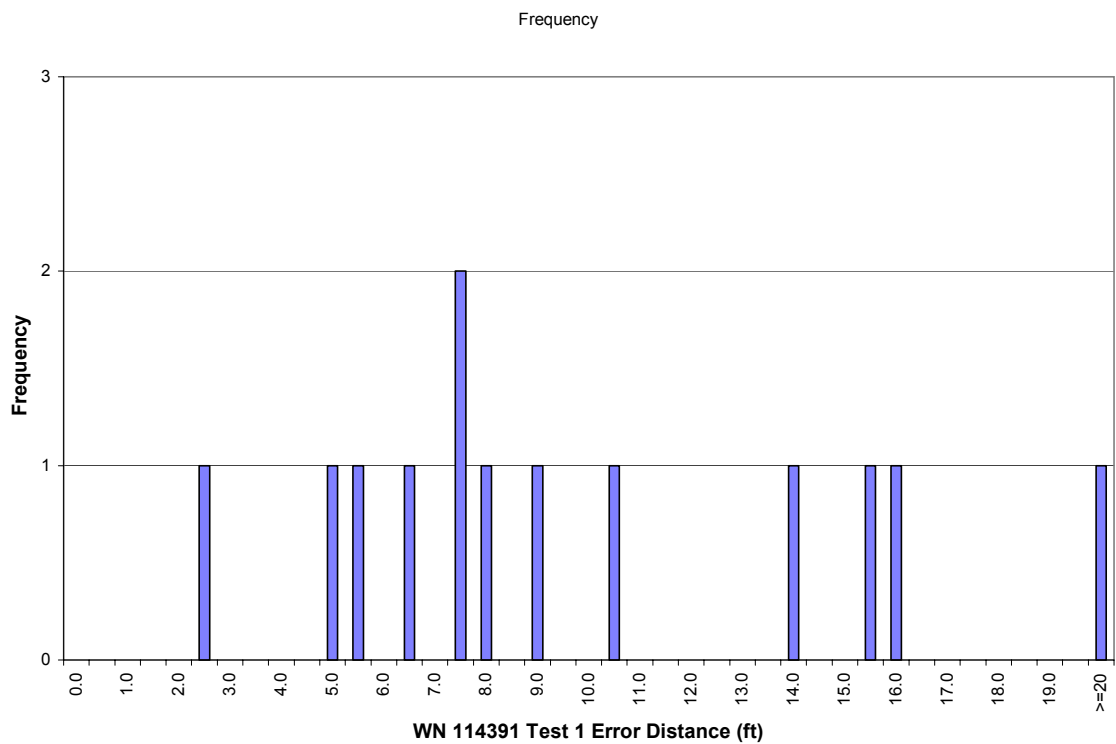Figure 191. WhereNet Test 3, Tag 112074: Error versus blink.
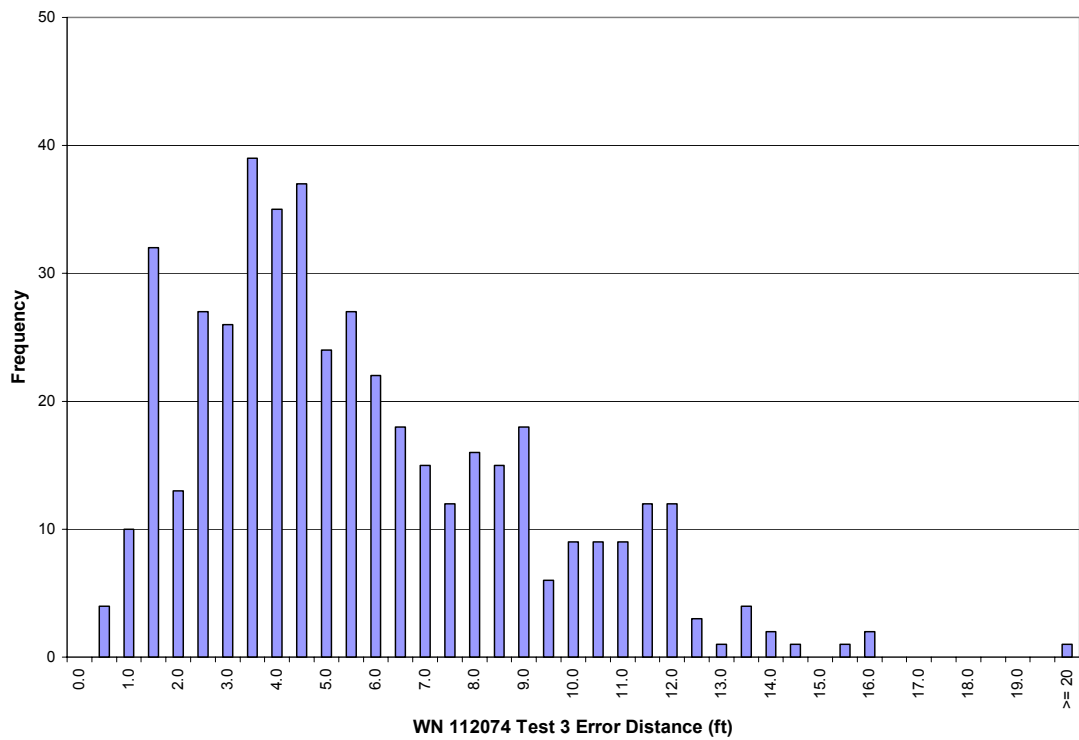
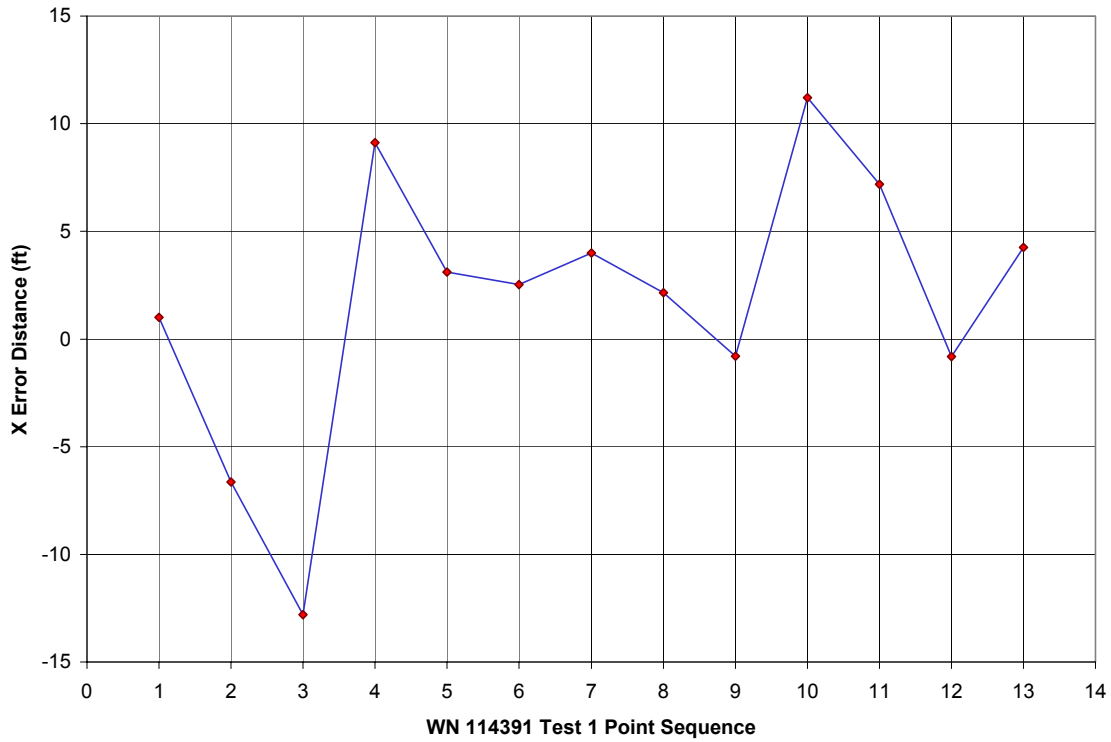Figure 192. WhereNet Test 3, Tag 112074: Error histogram.
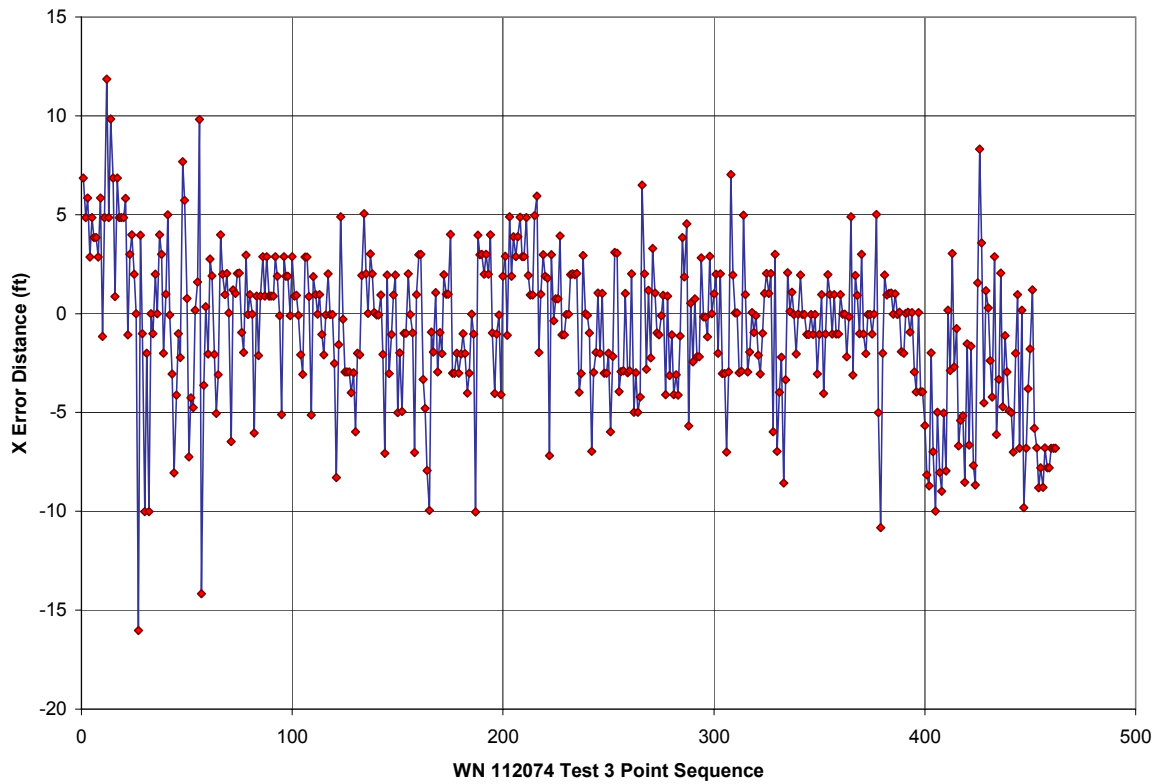
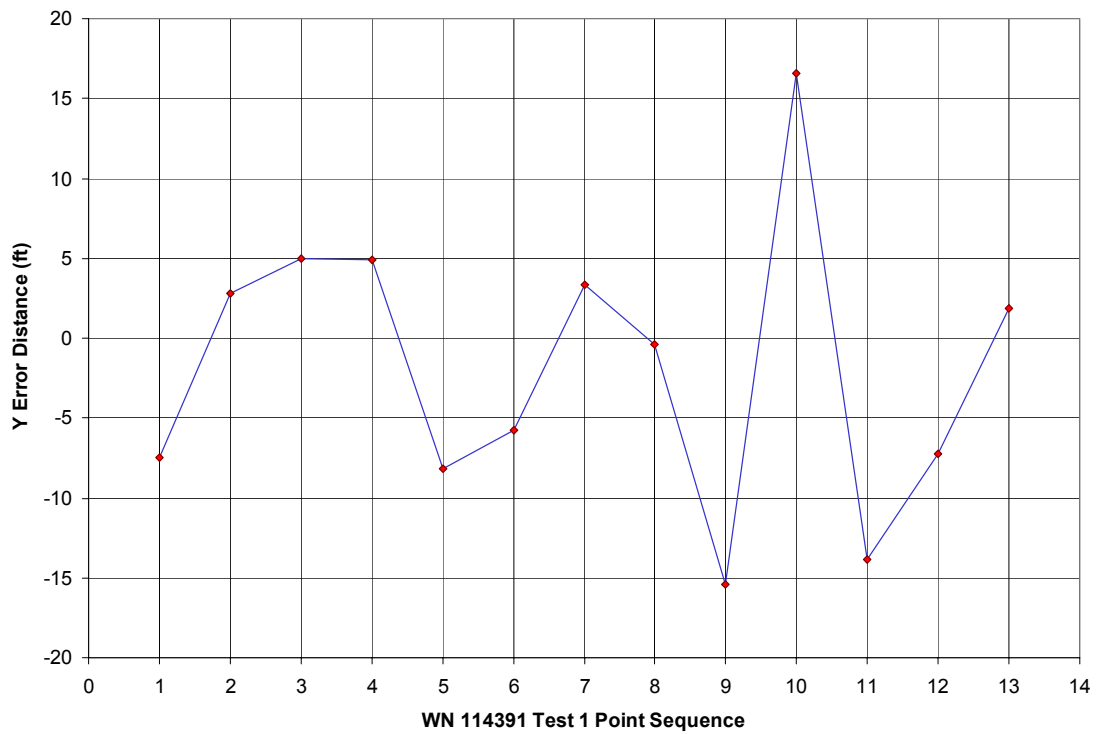Figure 193. WhereNet Test 3, Tag 112074: "X" difference versus blink.
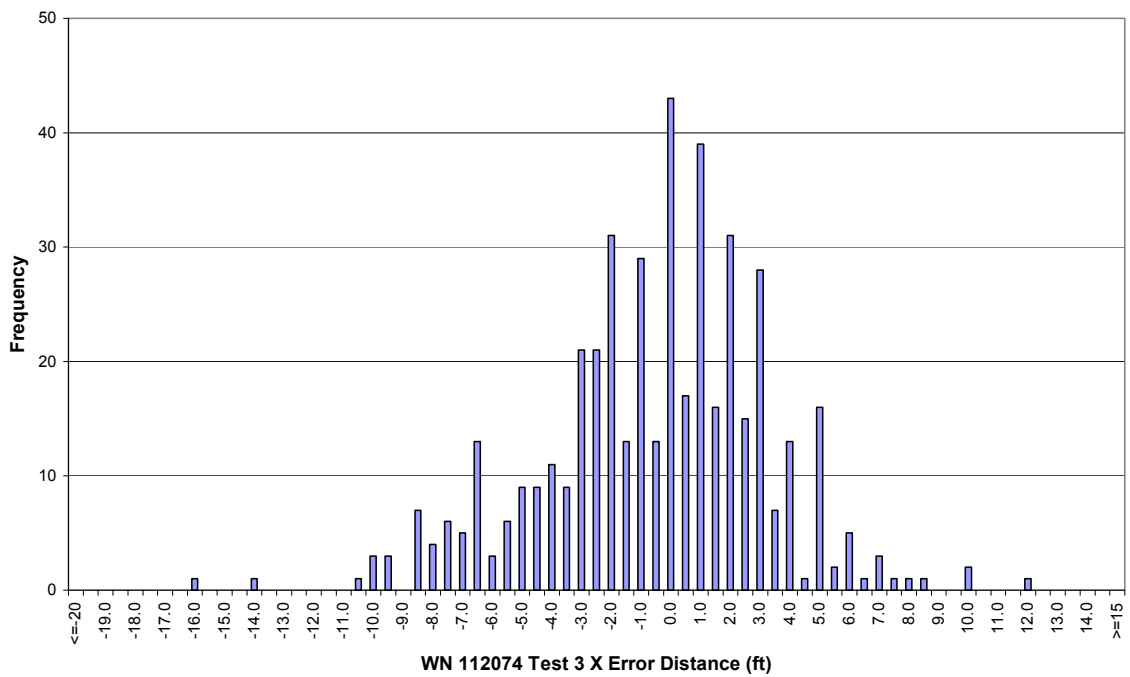
Figure 194. WhereNet Test 3, Tag 112074: "X" difference histogram.
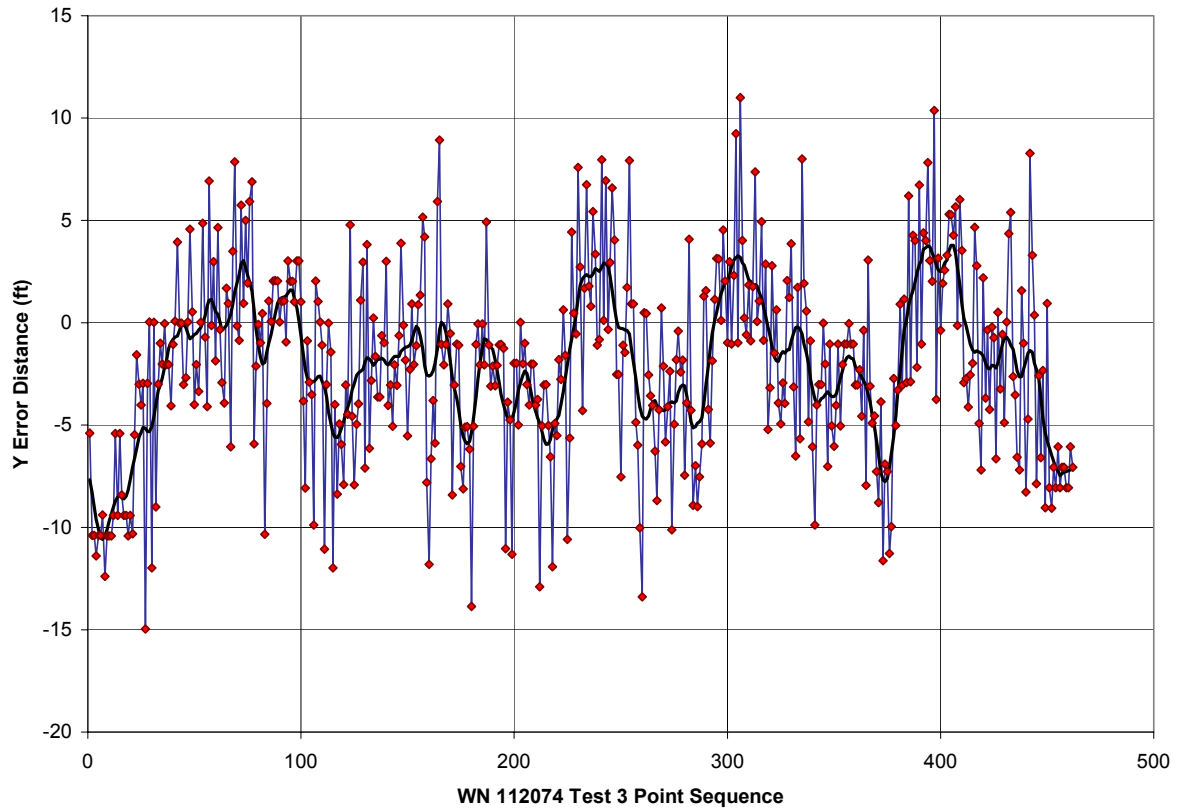
Figure 195. WhereNet Test 3, Tag 112074: "Y" difference versus blink.
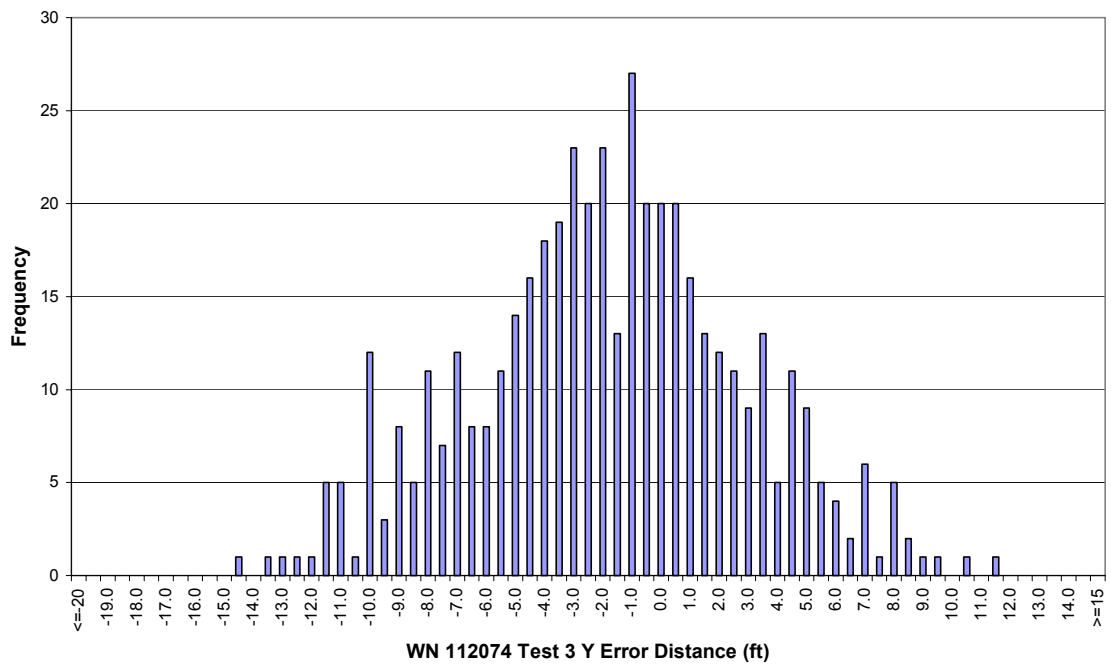
Figure 196. WhereNet Test 3, Tag 112074: "Y" difference histogram.

4-79
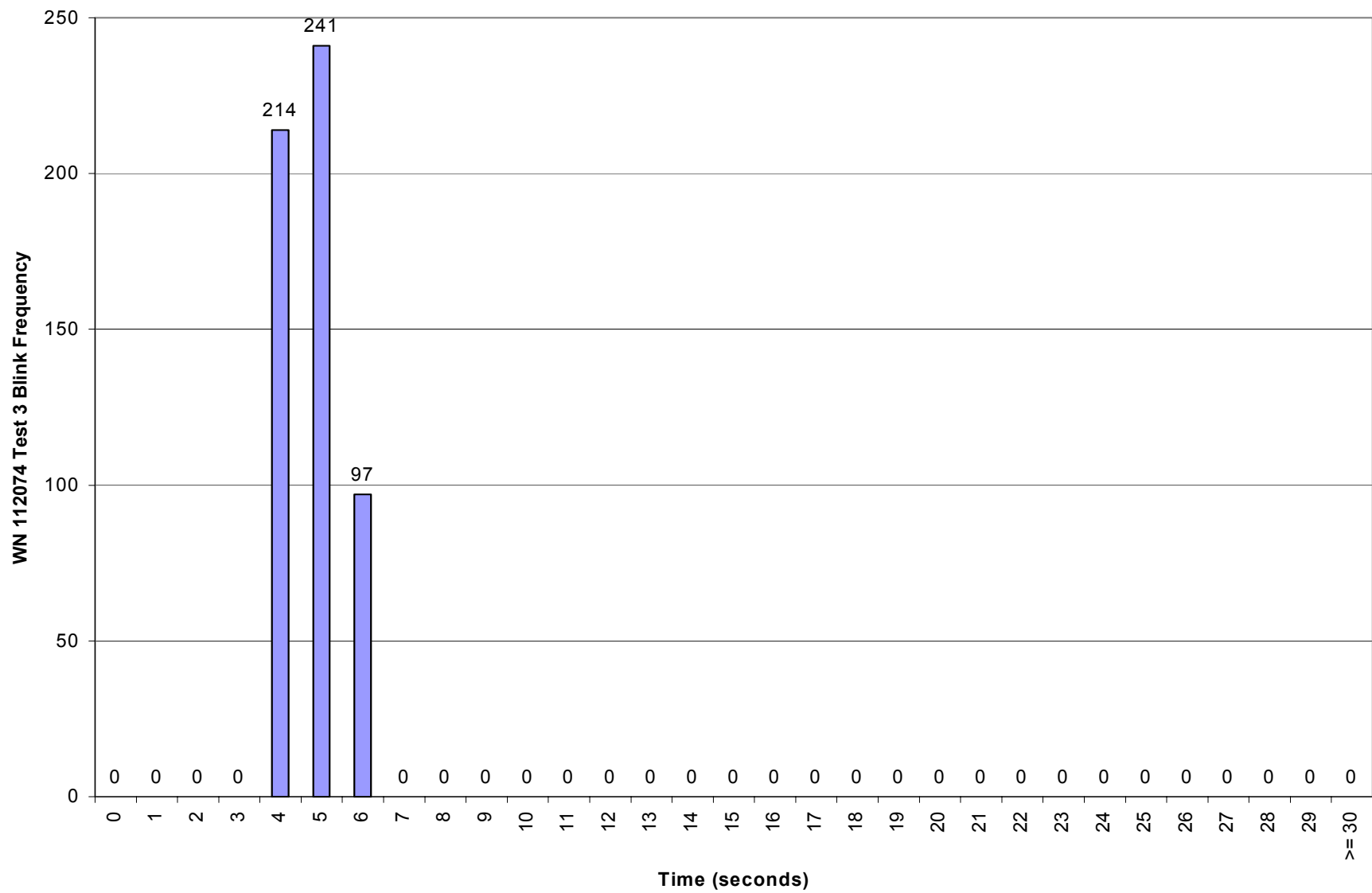
Figure 197. WhereNet Test 3, Tag 112074: Blink frequency histogram.
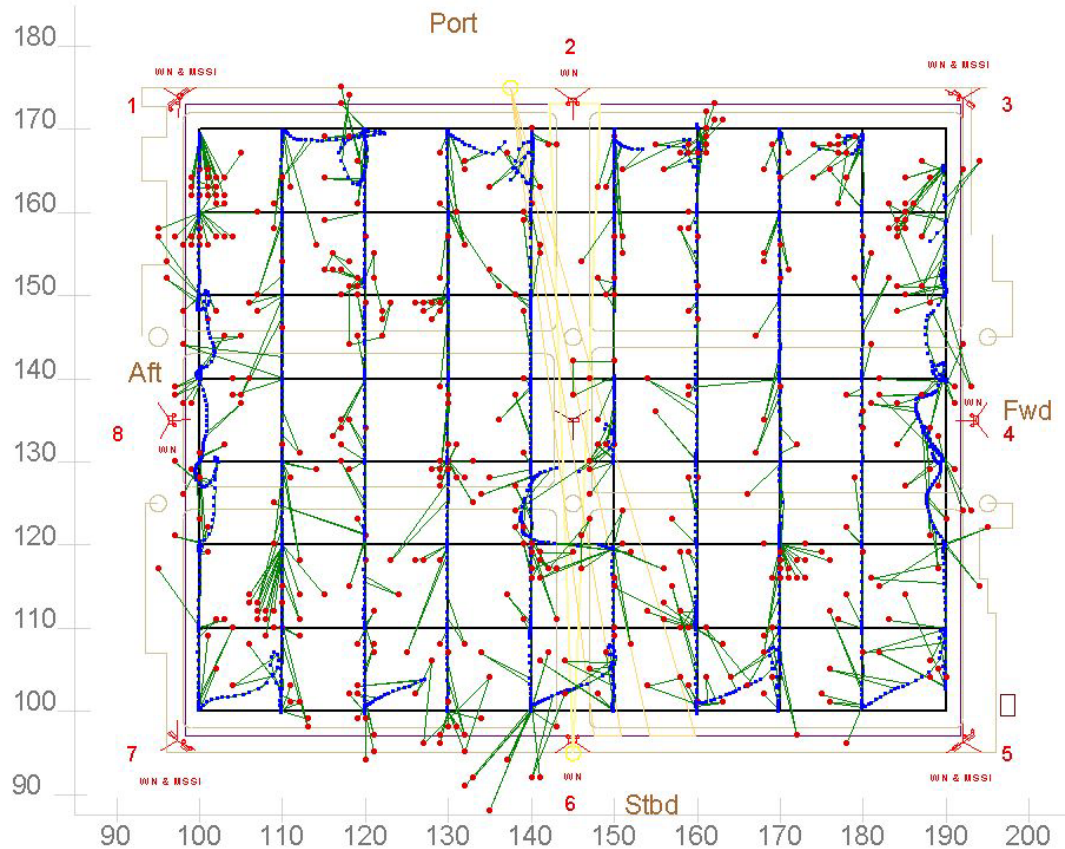
Figure 198. WhereNet Test 3, Tag 112348: Reported and correlated positions.
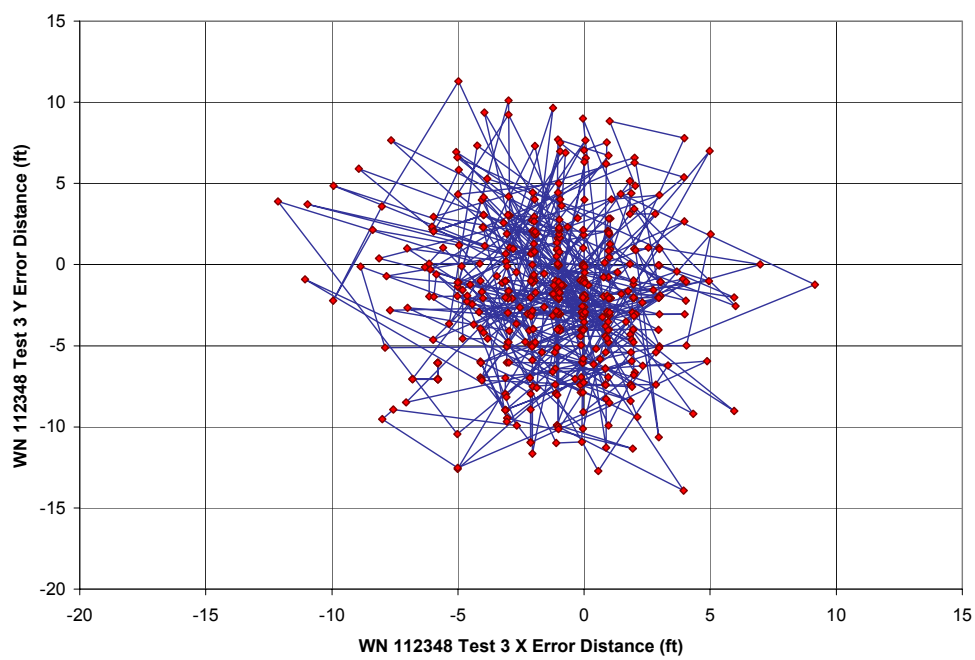
Figure 199. WhereNet Test 3, Tag 112348: "X-Y" difference versus blink.
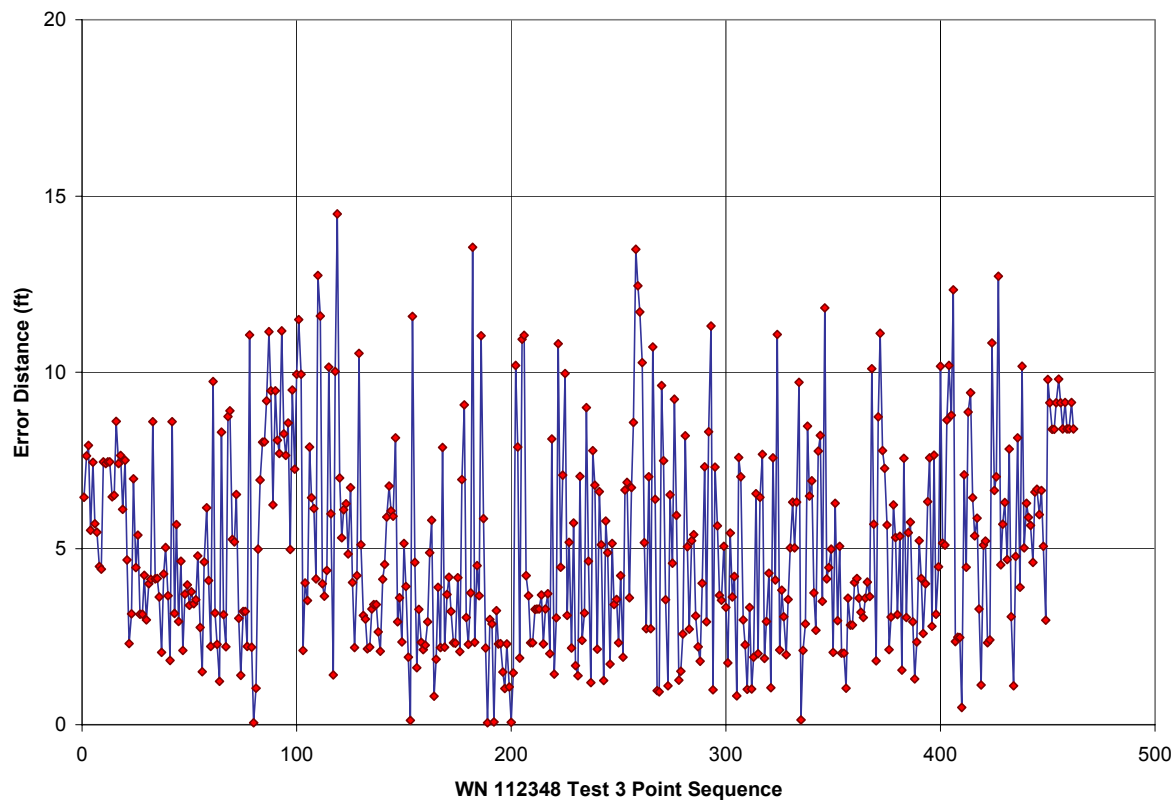
Figure 200. WhereNet Test 3, Tag 112348: Error versus blink.
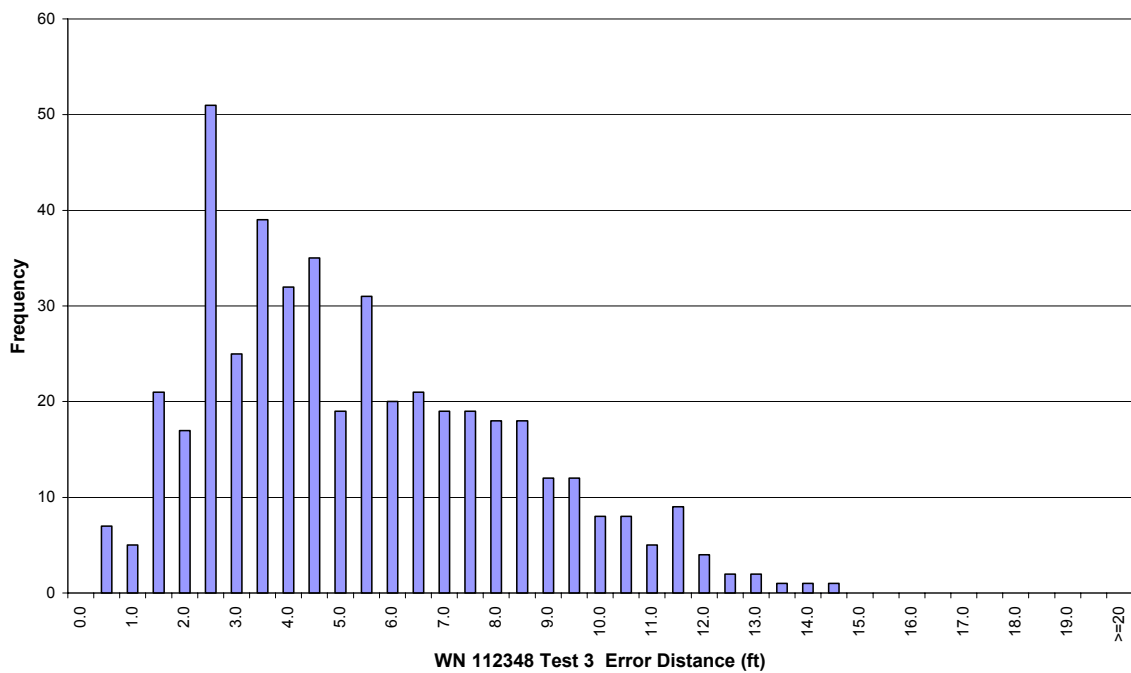
Figure 201. WhereNet Test 3, Tag 112348: Error histogram.
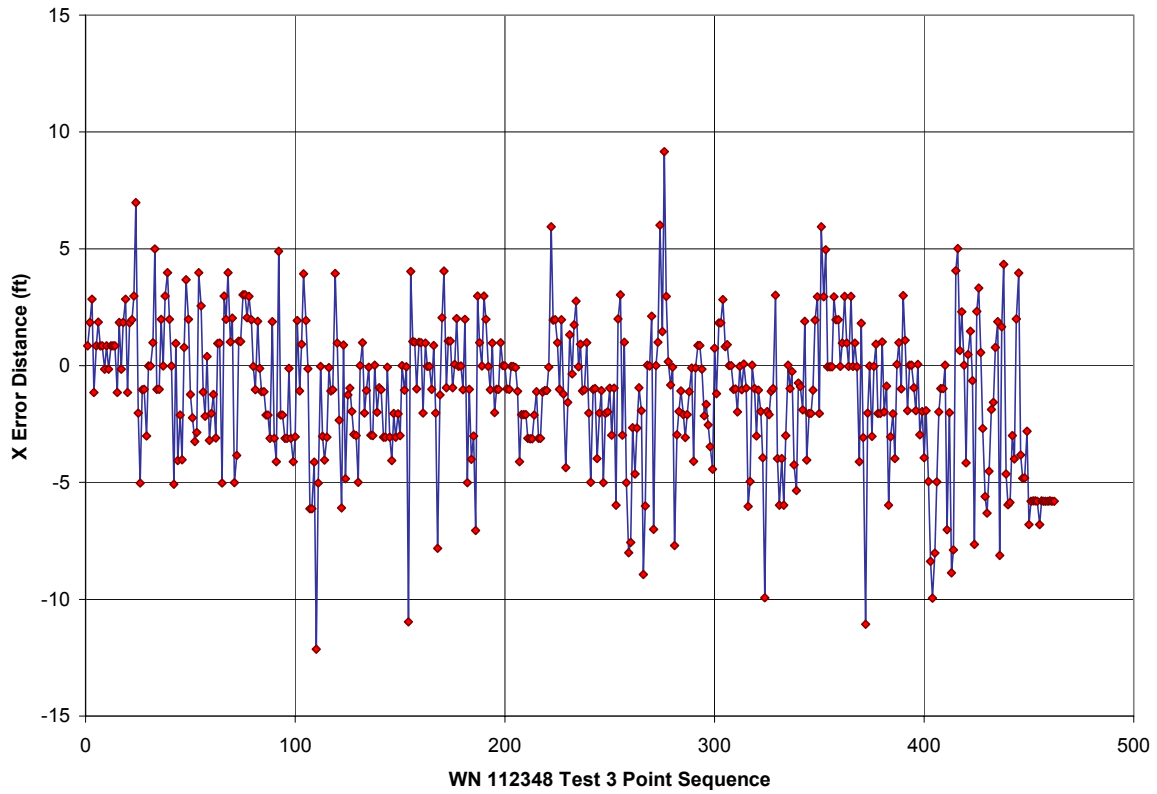
Figure 202. WhereNet Test 3, Tag 112348: "X" difference versus blink.
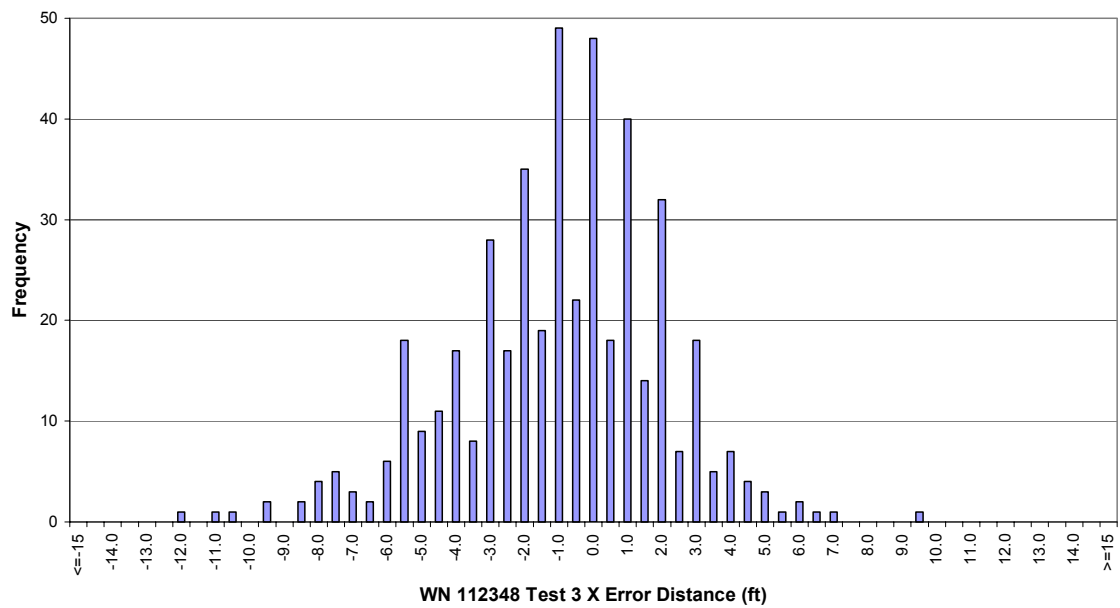
Figure 203. WhereNet Test 3, Tag 112348: "X" difference histogram.
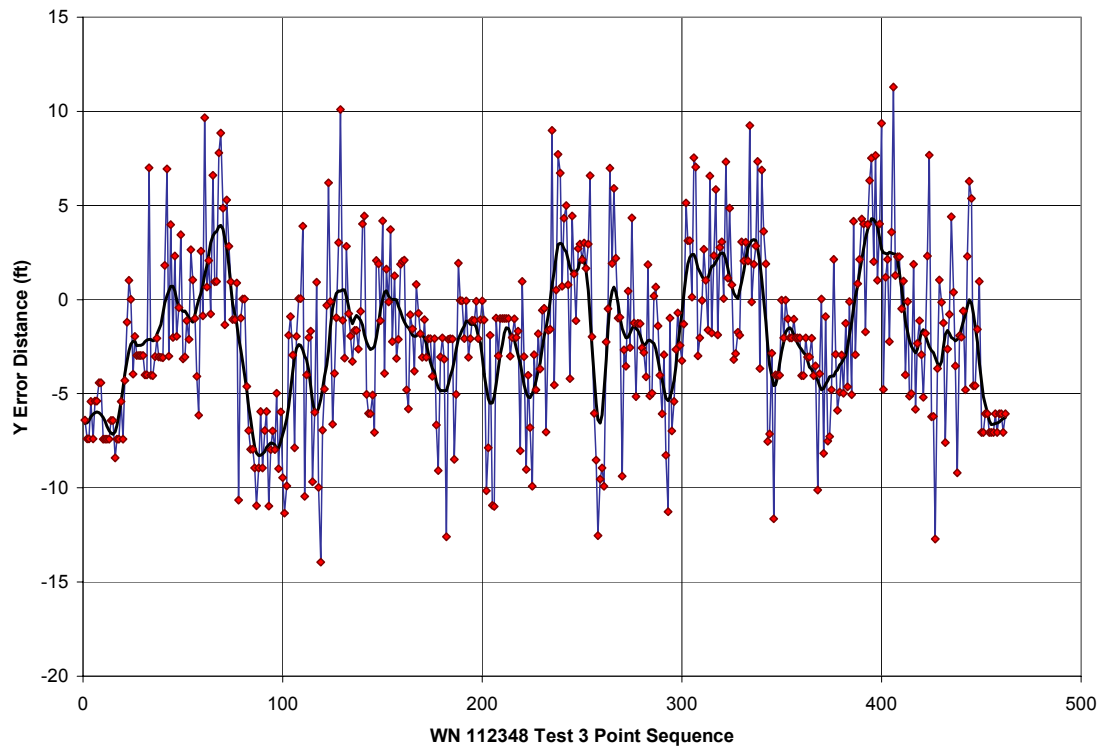
Figure 204. WhereNet Test 3, Tag 112348: "Y" difference versus blink.
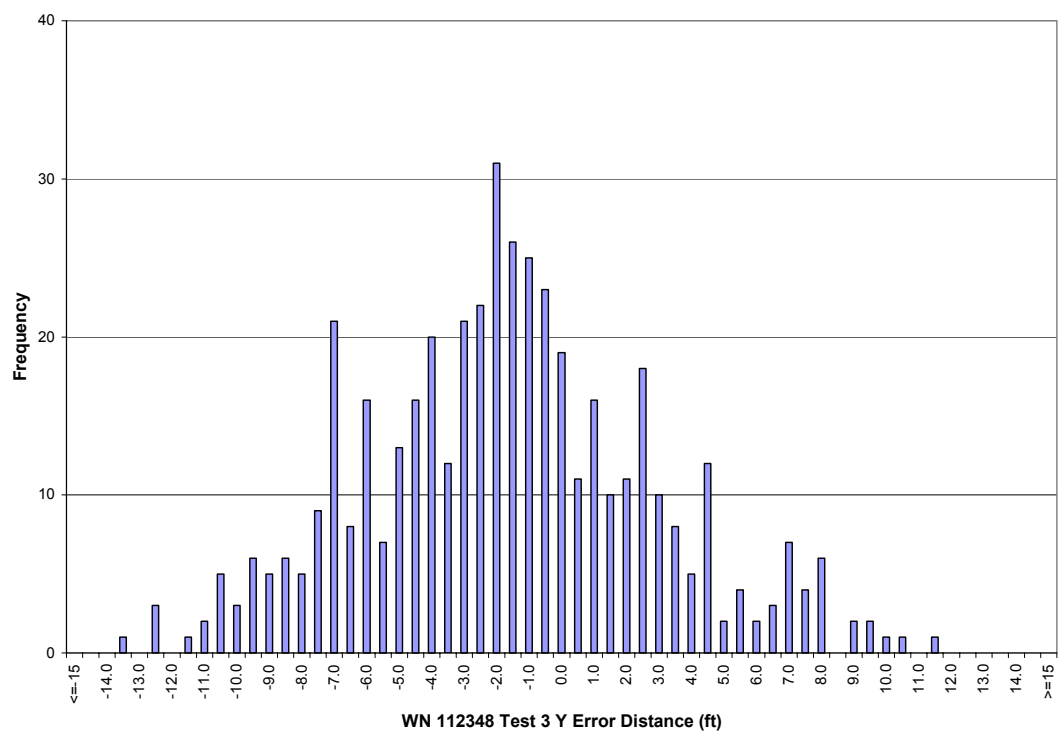
Figure 205. WhereNet Test 3, Tag 112348: "Y" difference histogram.
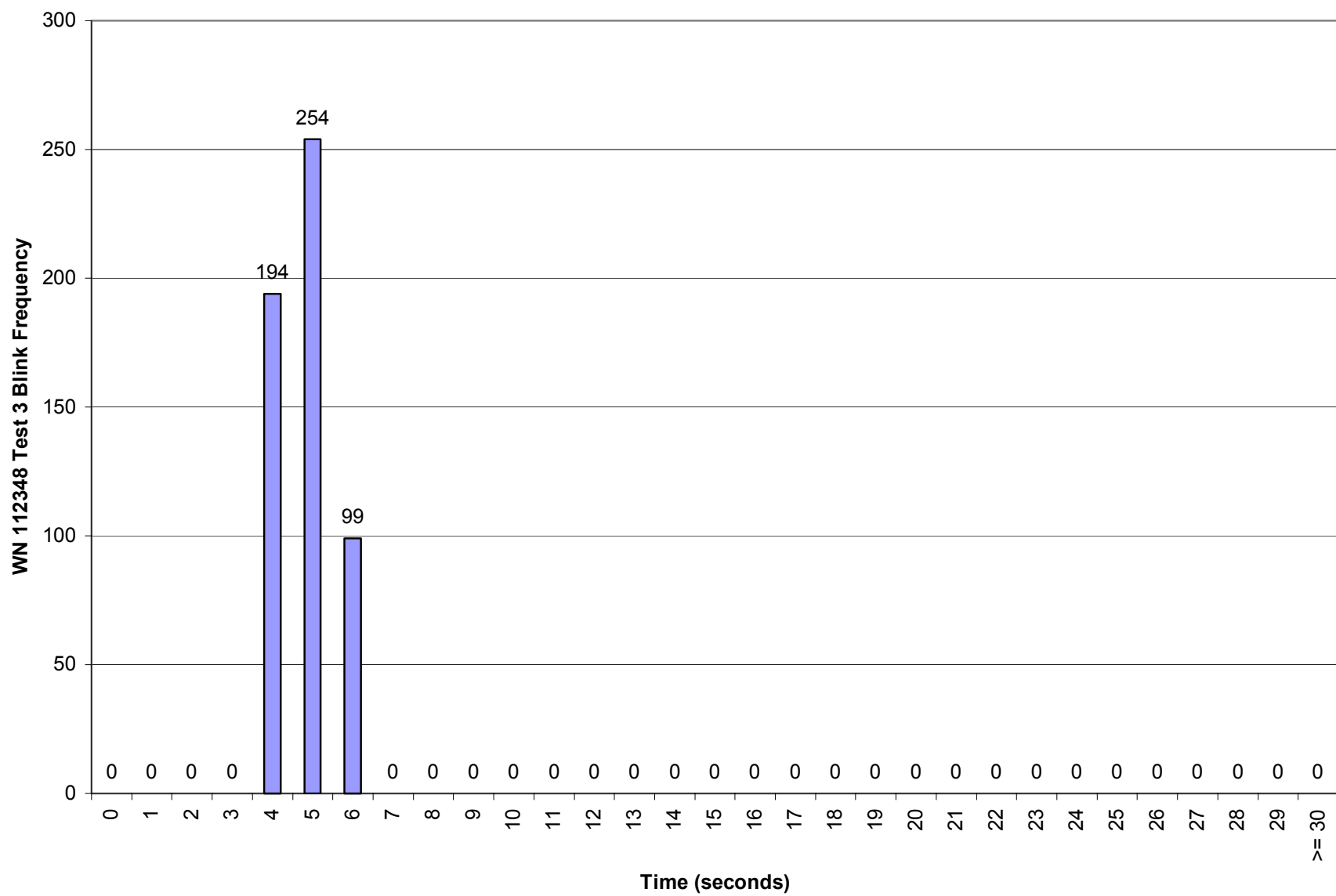
Figure 206. WhereNet Test 3, Tag 112348: Blink frequency histogram.
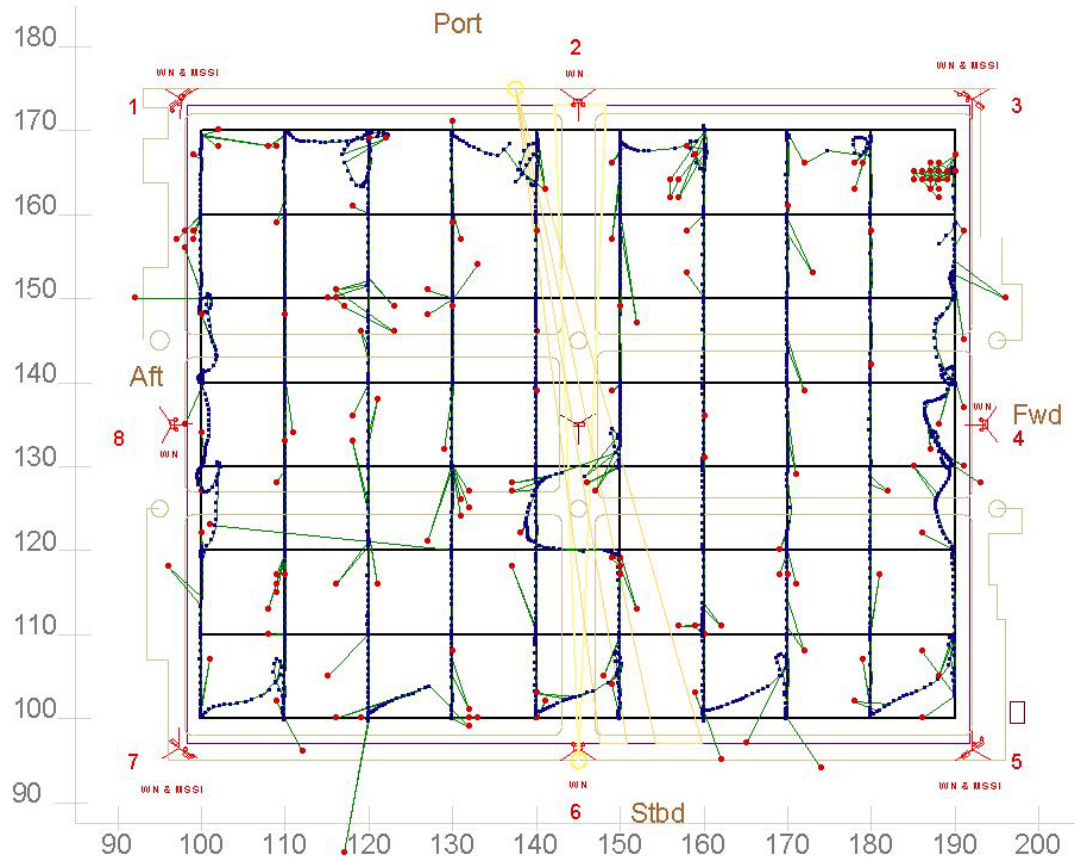
Figure 207. WhereNet Test 3, Tag 114391: Reported and correlated positions.
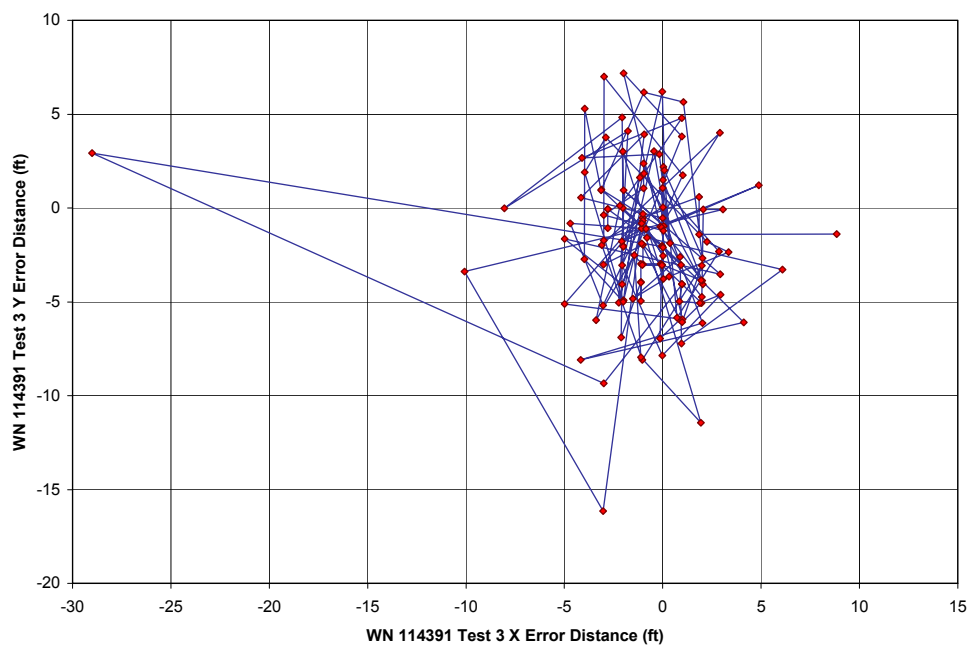

Figure 208. WhereNet Test 3, Tag 114391: "X-Y" difference versus blink.
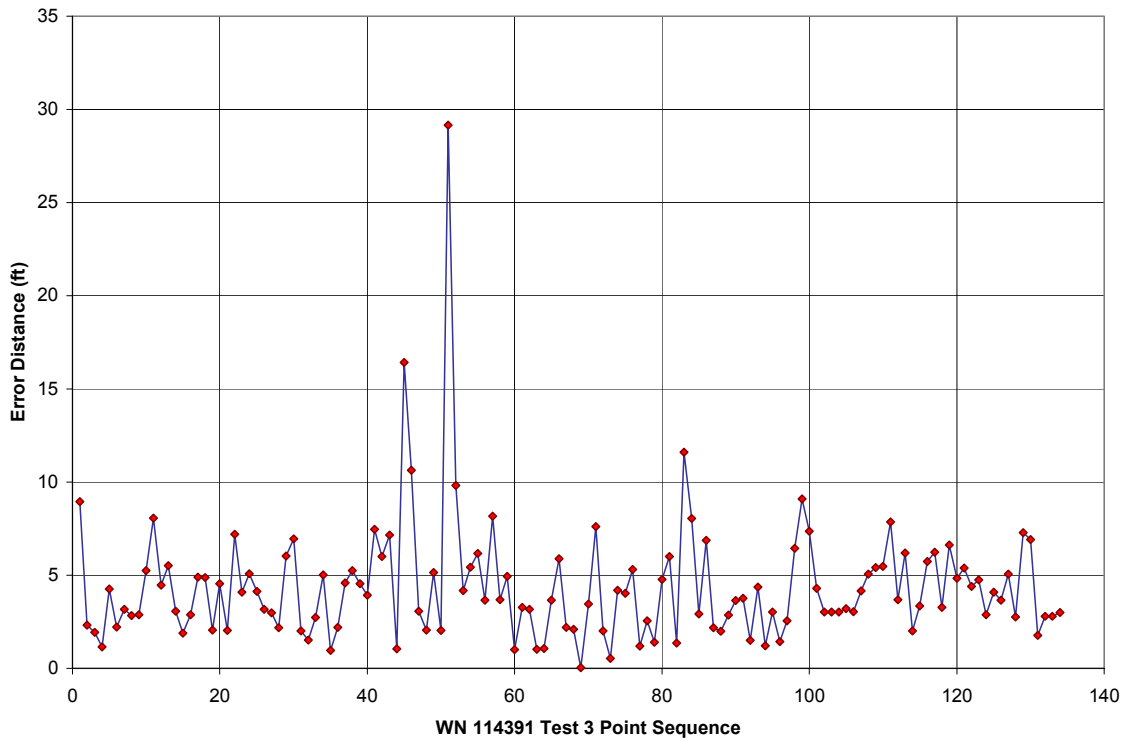
Figure 209. WhereNet Test 3, Tag 114391: Error versus blink.
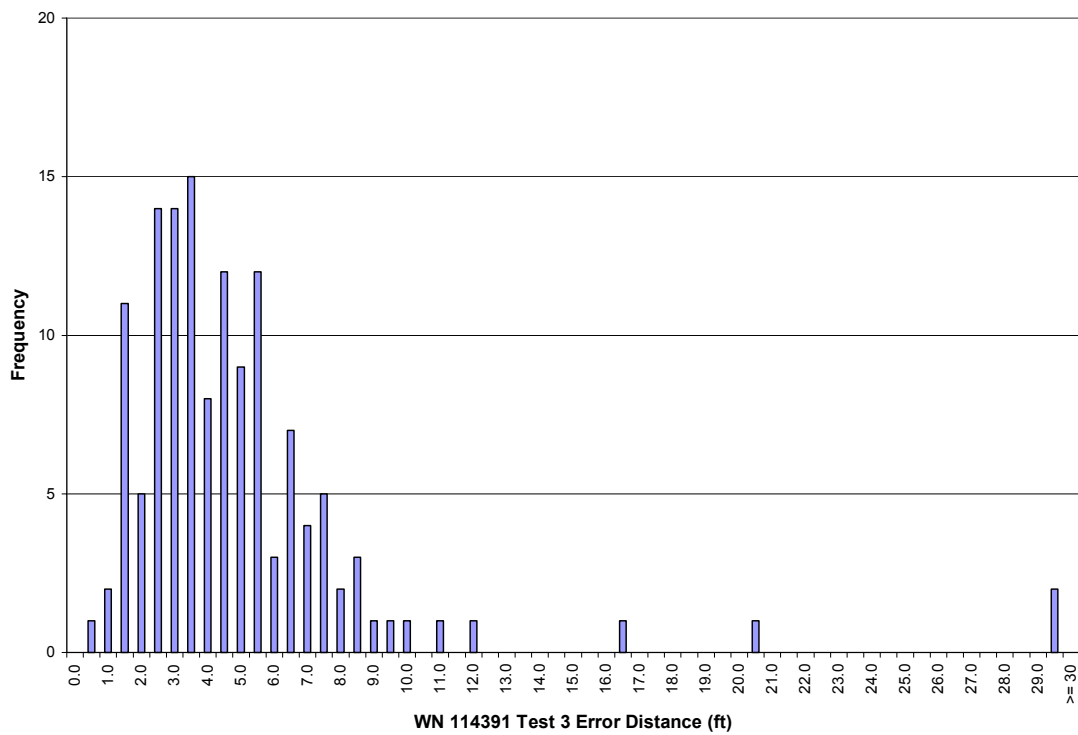
Figure 210. WhereNet Test 3, Tag 114391: Error histogram.
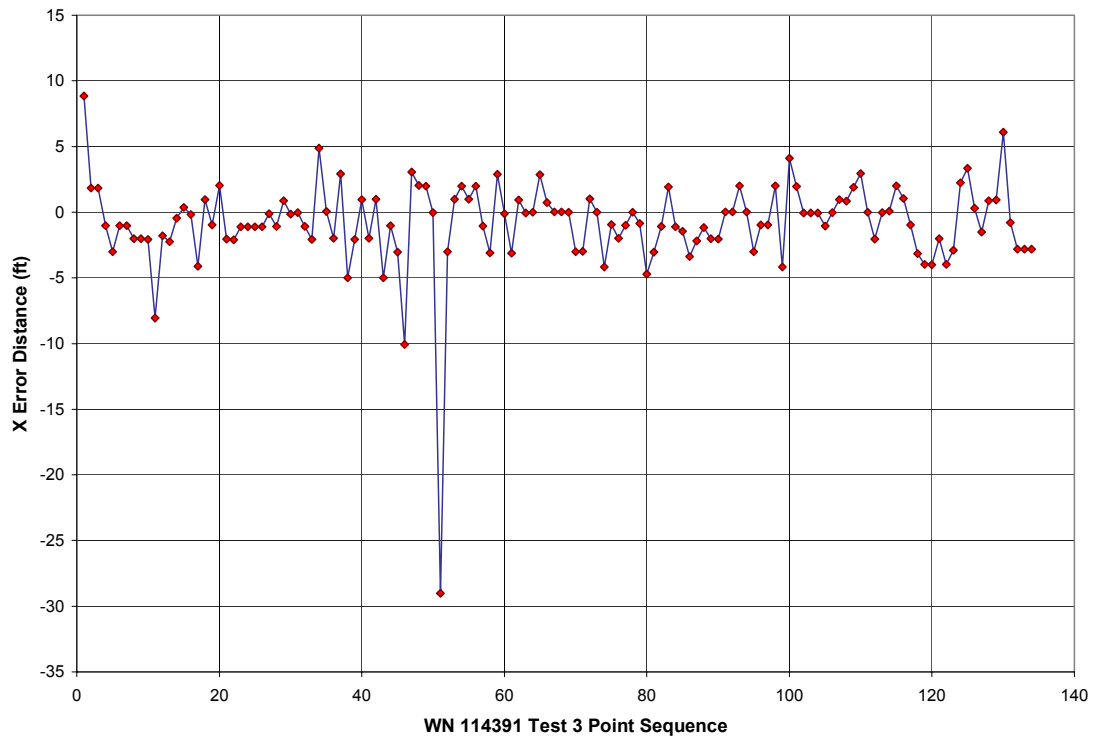
Figure 211. WhereNet Test 3, Tag 114391: "X" difference versus blink.
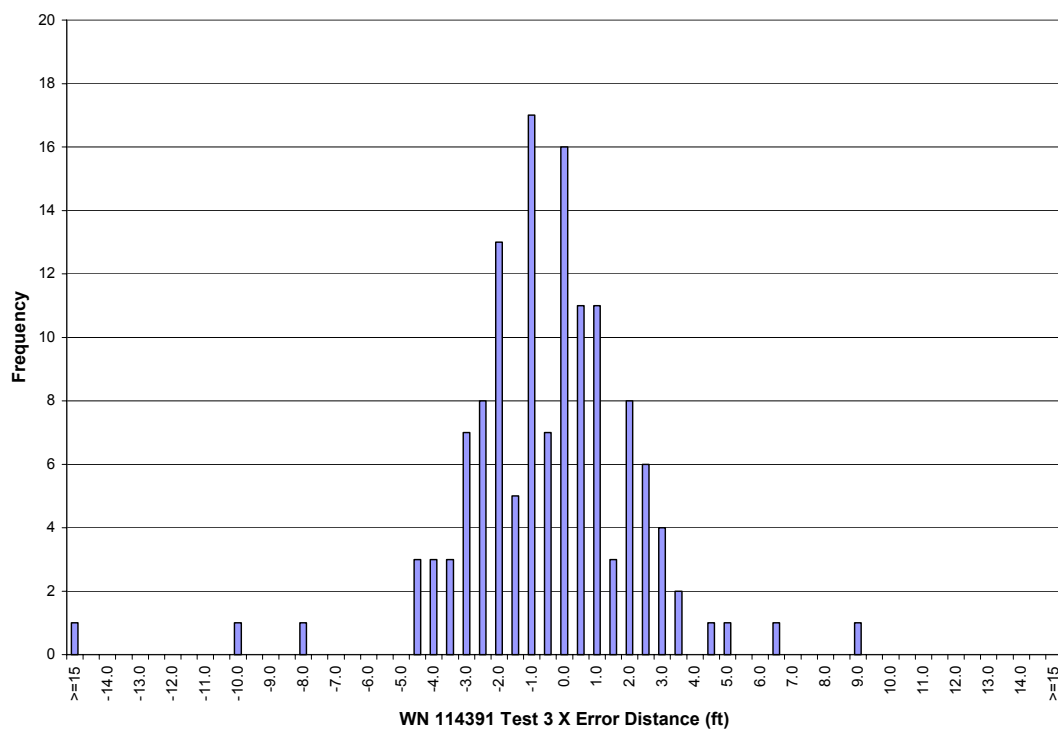
Figure 212. WhereNet Test 3, Tag 114391: "X" difference histogram.
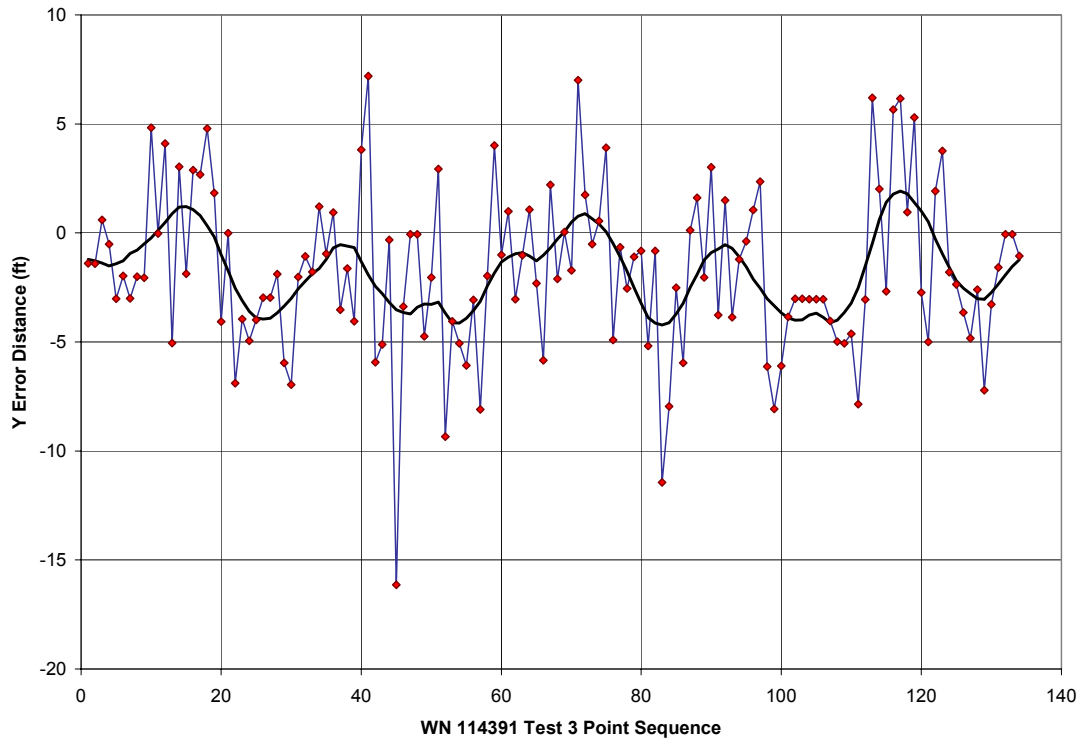
Figure 213. WhereNet Test 3, Tag 114391: "Y" difference versus blink.
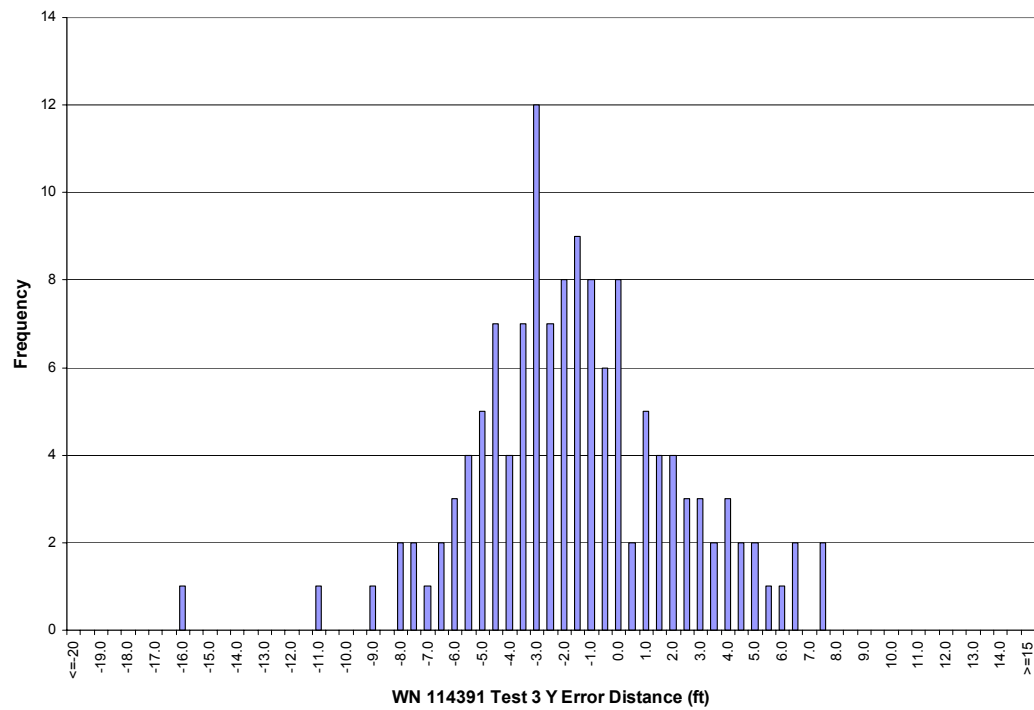
Figure 214. WhereNet Test 3, Tag 114391: "Y" difference histogram.
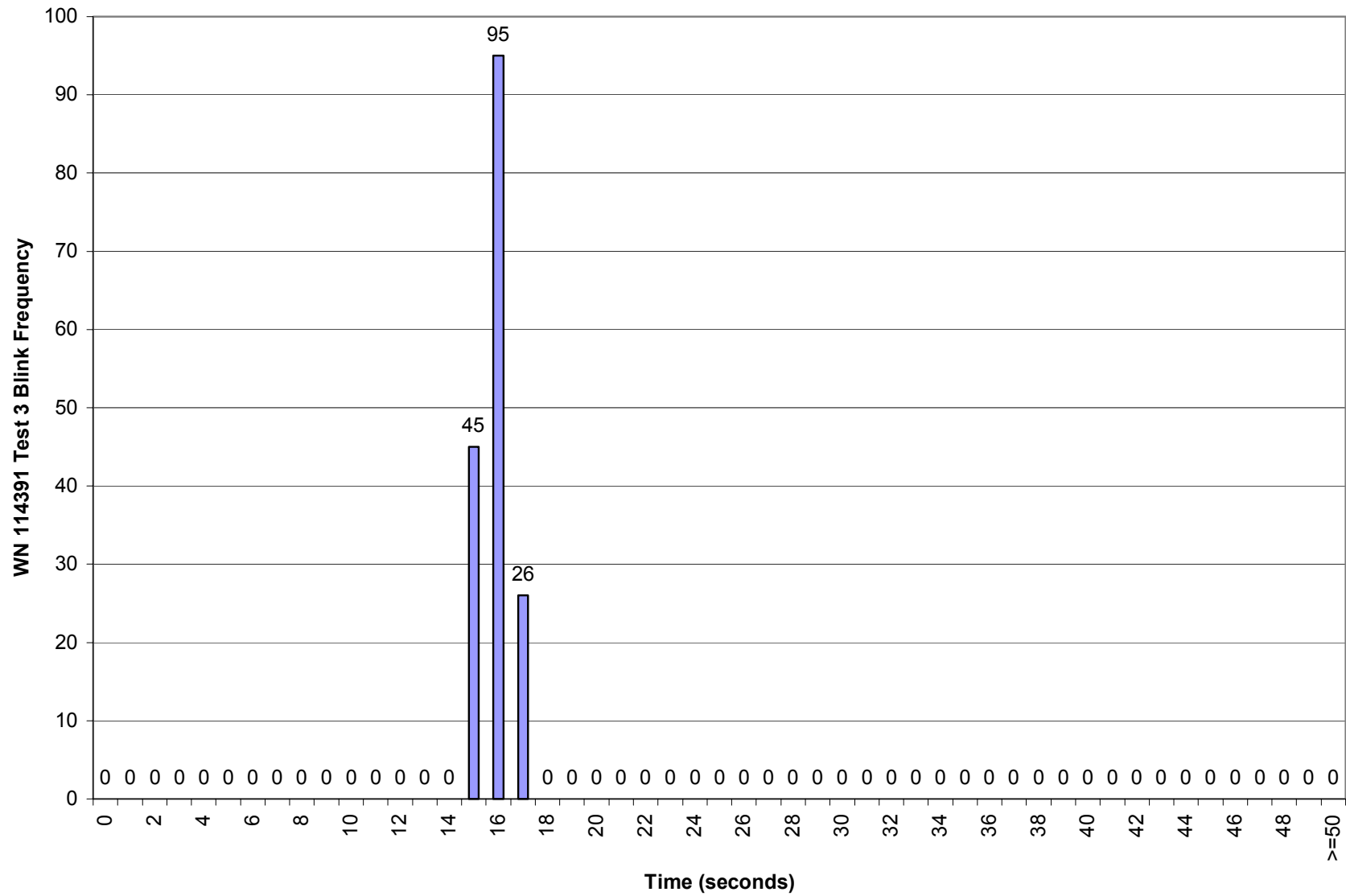
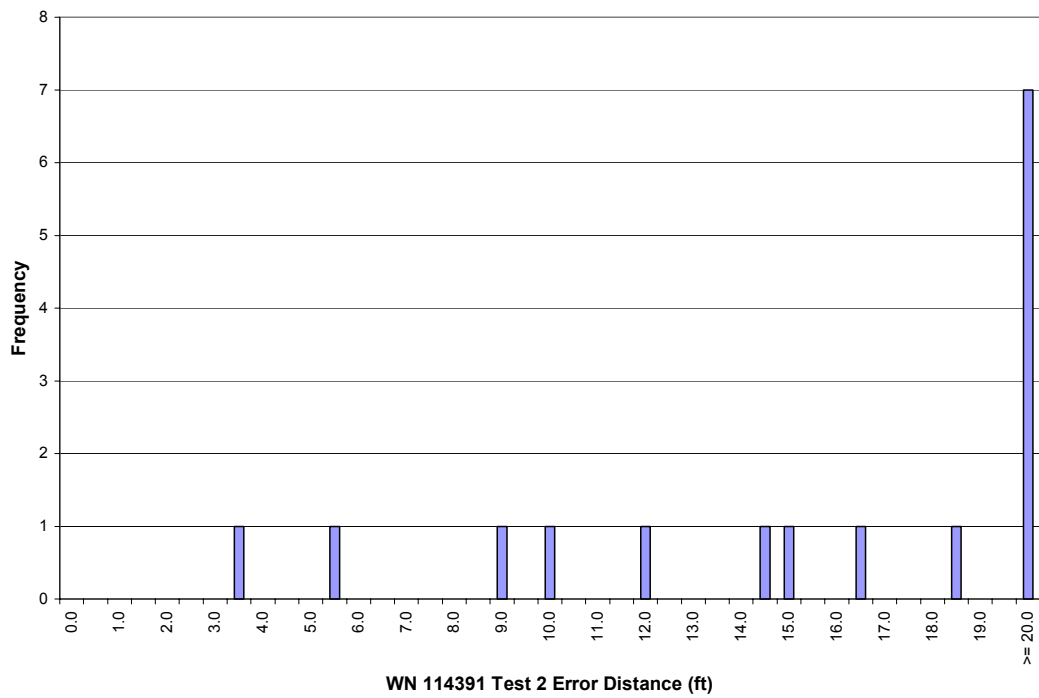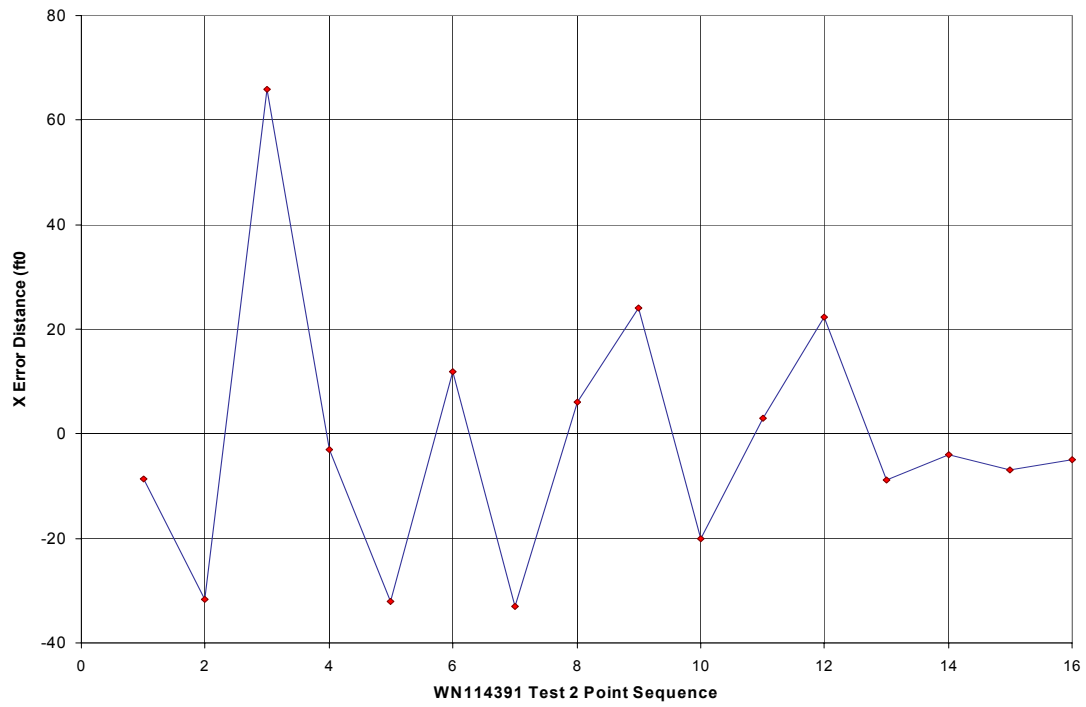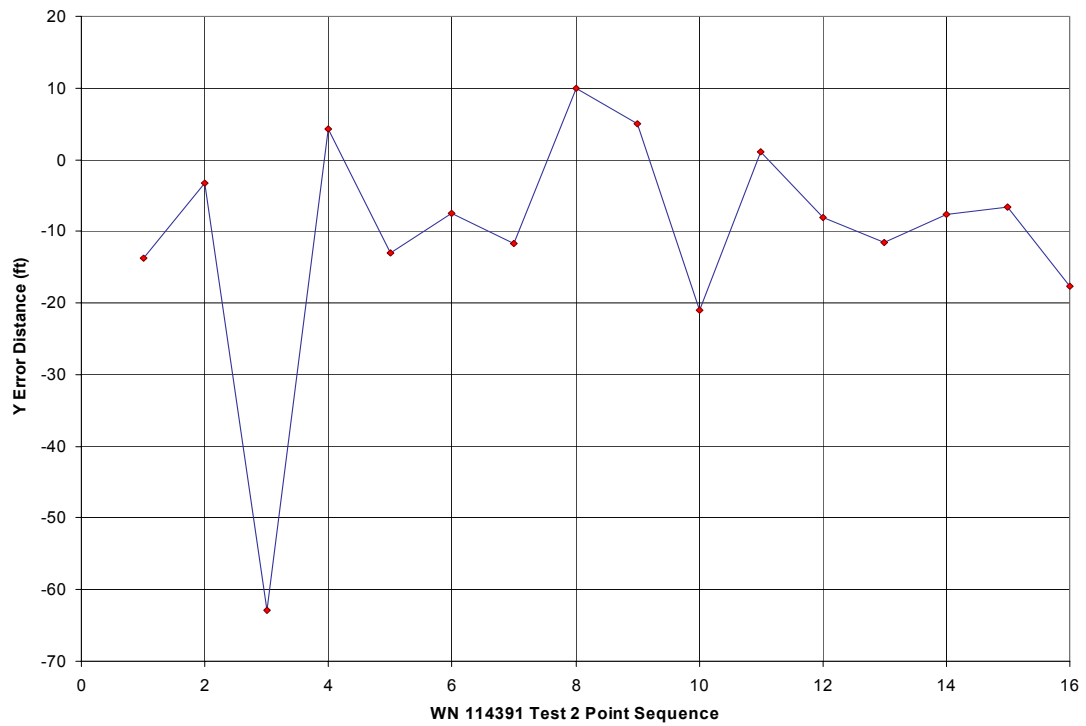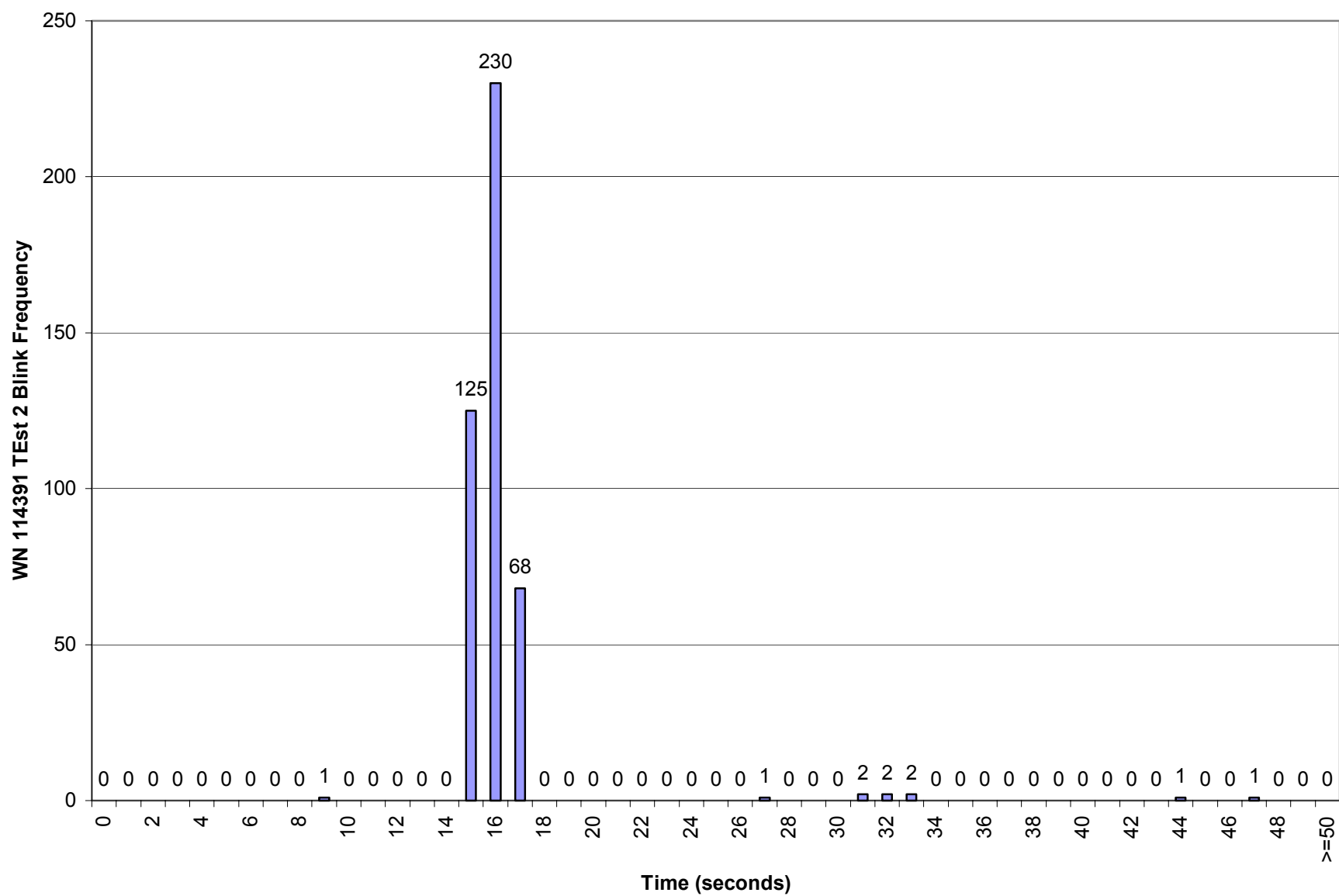Figure 215. WhereNet Test 3, Tag 114391: Blink frequency histogram.

4.2 2nd Week Container Blockage

4.2.1 WhereNet:

Tabular Results: Tables 18 through 22 summarize the WhereNet data reduction for single, then double-high containers. They answer the fourth question about effects of blockage. Tables 18 through 20 list tags on containers, and Tables 21 and 22 list tags on HMMWVS. Table values are color coded to ease interpretation. Blue is best, green -- good, yellow -- caution, orange -- marginal, and red -- failure.

First-order tag signal receipt blockage effects are indicated by the first three color coded columns, summarizing the number of blinks heard and positions reported. They indicate both received signal strength, number of antennas receiving, and multipath effects. Tag 2c had a lower blink rate of 16 seconds and was accounted for, and Tag 11a appears to have been turned off, with no reads for both single and double-high containers.

Blockage affected the number of blinks heard and positions reported.   Positions/Blinks (%) was the most sensitive measurement. Single and double-high containers showed a marked difference. Tag reads were less reliable with single-high versus double-high containers. This is completely opposite of what was expected.

Standard statistical factors are indicated in the second and third colored columns. Standard Deviation indicates the "fuzzyness" of error, and may indicate multipath effects. Significant asymmetry between "X" and "Y" standard deviation were noted for some tags and positions. Average and RMS error was the final metric. It included offset, possibly caused by reflections causing tags to appear elsewhere. Error proved to be the most sensitive measure of blockage effects.

Graphic Plots: Figures 216 through 221 show the color-coded tabular results by tag location. The figures follow the sequence of the color-coded columns in the tables, starting with read reliability, standard deviation, and then accuracy. Single-high containers are on top, then double high stacks below. HMMWVS are shown on the same figures.

Clear patterns and trends emerged in the figures. The WhereNet system was less accurate with single-high containers than double-high containers. Most surprisingly, it was most accurate in the aisleway formed between the double-high stacked containers (Figure 221).   The system appears to geo-locate with only two antennas on opposite ends of the aisleway. This indicates the WhereNet system has the ability to bi-laterate with only two antennas. WhereNet confirmed software version 2.0 tested had bi-lateration.

The reduction of overall accuracy with single-high containers may be caused by increased reflections, multipath and partial blockage by single-high containers. A possible explanation is that tag images may be reflected by opposite containers for some antennas, but blocked for others, producing confusing patterns. This was prevented by complete blockage by double high containers for all but two antennas.

Tag locations and reported locations for HMMWV mounted tags are shown in Figures 220 and 221. Tag location largely appears in the zone between the three closest antennas on the forward and aft bulkheads. The antennas did not have geographical dispersion to measure the "X"axis. The forward corner antennas were moved aft, even with the forward container faces at the end of the second week, to provide geographical dispersion. Localization accuracy improved in the "X"axis, with the reported tag positions aligned with HMMWV position (Figure 220, forward).

More antennas are needed to adequately cover the tested load pattern.

Table 18. WhereNet Accuracy, Single-High Stacked Containers

Tag No.	Blinks Heard	Positions Reported	Positions / Blinks %	Avg Location		Standard Deviation			Actual Location		Error		Comment
				X	Y	X	Y	Total	X	Y	Avg	RMS	
1a	0	0	N/A	0.0	0.0	N/A	N/A	N/A	167.8	113.5	N/A	N/A	no reports
1b	852	10	1%	179.1	106.9	6.7	8.6	10.9	167.7	108.3	11.5	16.3	
1c	899	899	100%	140.9	103.8	2.5	5.3	5.8	148.0	107.3	7.9	9.8	
1d	0	0	N/A	0.0	0.0	N/A	N/A	N/A	148.1	114.0	N/A	N/A	no reports
2a	249	0	0%	0.0	0.0	N/A	N/A	N/A	167.9	121.9	N/A	N/A	no reports
2b	0	0	N/A	0.0	0.0	N/A	N/A	N/A	167.9	116.6	N/A	N/A	no reports
2c	127	127	100%	145.8	106.3	5.8	4.1	7.1	148.2	115.4	9.4	11.8	blink 32 sec
2d	846	0	0%	0.0	0.0	N/A	N/A	N/A	148.2	122.9	N/A	N/A	no reports
3a	882	882	100%	171.0	133.8	2.7	1.6	3.1	167.7	133.1	3.4	4.6	
3b	900	397	44%	172.7	120.0	6.1	12.0	13.5	167.6	128.2	9.7	16.6	
3c	875	853	97%	146.7	125.2	7.9	4.1	8.9	147.9	127.2	2.3	9.2	
3d	389	2	1%	185.0	130.5	0.0	4.9	4.9	148.0	134.5	37.2	52.9	2 reports
4a	743	9	1%	186.2	135.4	3.0	5.9	6.6	167.6	141.4	19.6	21.8	
4b	871	871	100%	169.3	134.9	2.9	1.3	3.2	167.6	136.5	2.3	3.9	
4c	889	889	100%	148.7	137.0	4.4	1.9	4.8	147.9	135.2	2.0	5.2	
4d	712	1	0%	183.0	137.0	N/A	N/A	N/A	147.9	142.7	35.6	N/A	1 report
5a	871	12	1%	175.8	129.7	8.7	5.3	10.2	167.6	151.7	23.5	26.6	
5b	871	359	41%	185.6	147.6	4.6	4.7	6.5	167.7	148.3	17.9	19.1	
5c	876	875	100%	152.7	154.6	2.7	3.0	4.0	147.9	146.9	9.1	10.0	
5d	804	3	0%	179.0	140.7	9.2	4.5	10.2	147.9	154.3	34.0	42.8	
6a	869	1	0%	190.0	134.0	N/A	N/A	N/A	167.8	161.9	35.7	N/A	1 report
6b	867	276	32%	186.6	161.8	3.9	5.2	6.5	167.8	156.4	19.6	20.7	
6c	878	67	8%	143.5	167.1	8.8	9.9	13.3	148.0	155.1	12.9	18.5	
6d	905	6	1%	170.3	141.0	17.2	16.6	23.9	148.0	162.6	31.1	41.6	
7a	898	895	100%	107.4	109.6	3.1	2.0	3.7	122.4	108.3	15.1	15.5	
7b	888	205	23%	166.5	133.3	11.8	5.2	12.9	122.4	113.3	48.4	50.2	
7c	616	1	0%	155.0	144.0	N/A	N/A	N/A	142.1	114.7	32.0	N/A	1 report
7d	878	692	79%	148.4	101.6	3.8	7.8	8.7	142.2	107.2	8.3	12.1	
8a	882	881	100%	100.8	120.4	6.1	1.9	6.4	122.4	116.7	21.9	22.8	
8b	871	2	0%	145.0	116.0	12.7	19.8	23.5	122.4	121.8	23.3	40.5	2 reports
8c	864	117	14%	126.2	130.9	28.8	14.1	32.0	142.1	123.1	17.8	36.7	
8d	879	863	98%	152.5	109.7	4.0	4.9	6.4	142.2	115.7	11.9	13.5	
9a	894	894	100%	110.0	128.7	4.8	0.9	4.9	122.3	128.0	12.3	13.3	
9b	848	147	17%	176.7	135.9	8.1	5.6	9.9	122.3	133.1	54.5	55.6	
9c	880	13	1%	149.2	141.6	22.9	15.1	27.4	142.0	134.4	10.2	29.4	
9d	897	893	100%	149.8	118.7	8.2	4.0	9.1	142.0	126.9	11.3	14.5	
10a	873	826	95%	87.9	135.0	7.7	3.5	8.5	122.3	136.5	34.4	35.5	out of box
10b	875	875	100%	123.3	132.1	1.1	2.1	2.4	122.3	141.6	9.5	9.8	
10c	884	884	100%	136.2	128.9	10.0	13.9	17.1	142.0	142.8	15.1	22.8	
10d	877	876	100%	153.8	130.1	3.6	1.6	3.9	142.0	135.4	12.9	13.5	
11a	0	0	N/A	0.0	0.0	N/A	N/A	N/A	122.2	148.2	N/A	N/A	dead tag
11b	895	895	100%	146.8	124.7	2.0	1.8	2.7	122.2	153.2	37.6	37.7	
11c	826	2	0%	163.5	132.0	21.9	0.0	21.9	141.9	154.4	31.1	49.2	2 reports
11d	873	873	100%	140.0	142.4	1.8	1.4	2.2	141.9	147.0	5.0	5.5	
12a	874	652	75%	91.6	151.3	8.2	1.9	8.4	122.3	156.6	31.1	32.3	out of box
12b	888	888	100%	145.2	152.9	3.0	4.2	5.1	122.3	161.6	24.6	25.1	
12c	859	1	0%	126.0	140.0	N/A	N/A	N/A	142.0	163.0	28.0	N/A	1 report
12d	878	878	100%	155.6	148.6	2.2	2.3	3.2	142.0	155.5	15.2	15.6	

Legends:

>810	(>90%)	>90%
450-810	(50-90%)	50-90%
90-450	(10-50%)	10-50%
<90	(<10%)	<10%
No Blinks		No Calc

<5 ft	<5 ft	<5 ft
5-10 ft	5-10 ft	5-10 ft
10-20 ft	10-20 ft	10-20 ft
>20 ft	>20 ft	>20 ft
No Calc	No Calc	No Calc

<10 ft	<10 ft
10-20 ft	10-20 ft
20-30 ft	20-30 ft
>30 ft	>30 ft
No Calc	No Calc

Table 19. WhereNet Accuracy, Double-High Stacked Containers, Bottom Layer

Tag No.	Blinks Heard	Positions Reported	Positions / Blinks %	Avg Location		Standard Deviation			Actual Location		Error		Comment
				X	Y	X	Y	Total	X	Y	Avg	RMS	
1a	361	264	73%	191.5	116.8	6.3	5.1	8.1	167.8	113.5	23.9	25.3	out of box
1b	477	477	100%	171.1	108.3	2.4	2.7	3.6	167.7	108.3	3.4	5.0	
1c	502	502	100%	143.8	106.9	0.9	1.4	1.6	148.0	107.3	4.2	4.5	
1d	394	394	100%	142.3	114.7	5.4	2.2	5.8	148.1	114.7	5.8	8.2	
2a	493	462	94%	200.2	120.7	5.3	1.7	5.6	167.9	121.9	32.3	32.8	out of box
2b	388	348	90%	198.5	122.7	7.2	1.8	7.4	167.9	116.6	31.2	32.1	out of box
2c	71	67	94%	143.0	119.4	2.9	3.7	4.7	148.2	115.4	6.6	8.1	blink 32 sec
2d	481	481	100%	142.0	121.9	3.0	1.8	3.5	148.2	122.9	6.3	7.2	
3a	400	400	100%	190.4	141.2	5.9	1.5	6.1	167.7	133.1	24.1	24.9	edge of box
3b	501	499	100%	178.5	130.9	5.9	1.4	6.1	167.6	128.2	11.2	12.8	
3c	494	494	100%	142.7	124.9	2.4	1.5	2.9	147.9	127.2	5.7	6.4	
3d	466	466	100%	137.6	133.0	2.8	1.2	3.0	148.0	134.5	10.5	11.0	
4a	495	491	99%	180.9	145.2	8.3	4.7	9.5	167.6	141.4	13.9	16.8	
4b	394	389	99%	182.1	134.6	3.3	1.3	3.5	167.6	136.5	14.6	15.1	
4c	503	503	100%	139.6	128.2	5.3	1.7	5.5	147.9	135.2	10.9	12.2	
4d	492	492	100%	141.5	142.9	1.2	1.4	1.9	147.9	142.7	6.4	6.6	
5a	0	0	NA	0.0	0.0	N/A	N/A	N/A	167.6	151.7	N/A	N/A	
5b	496	464	94%	190.2	149.3	9.2	2.4	9.5	167.7	148.3	22.5	24.5	out of box
5c	497	497	100%	140.6	150.5	5.4	3.3	6.3	147.9	146.9	8.1	10.3	
5d	487	141	29%	148.8	157.8	8.9	8.4	12.2	147.9	154.3	3.6	12.7	
6a	489	146	30%	194.8	154.7	2.1	1.0	2.4	167.8	161.9	28.0	28.2	out of box
6b	481	454	94%	206.8	144.2	7.0	1.7	7.2	167.8	156.4	40.9	41.6	out of box
6c	503	394	78%	139.6	162.7	7.3	6.1	9.5	148.0	155.1	11.3	14.8	
6d	512	512	100%	141.7	155.5	0.7	1.0	1.2	148.0	162.6	9.5	9.6	
7a	505	380	75%	102.2	109.6	7.7	2.9	8.3	122.4	108.3	20.2	21.9	edge of box
7b	504	503	100%	114.8	115.6	5.1	0.8	5.2	122.4	113.3	7.9	9.5	
7c	490	490	100%	140.0	111.4	2.5	2.3	3.4	142.1	114.7	3.9	5.2	
7d	501	497	99%	141.1	103.2	2.7	4.6	5.3	142.2	107.2	4.1	6.7	
8a	501	495	99%	88.3	122.1	3.2	2.2	3.8	122.4	116.7	34.5	34.8	out of box
8b	489	488	100%	94.1	120.7	7.1	2.0	7.4	122.4	121.8	28.3	29.3	out of box
8c	490	490	100%	140.8	120.4	3.2	1.6	3.6	142.1	123.1	2.9	4.6	
8d	497	102	21%	143.6	117.0	10.0	9.0	13.5	142.2	115.7	1.9	13.6	
9a	502	436	87%	91.2	130.0	8.2	1.1	8.2	122.3	128.0	31.2	32.3	out of box
9b	497	99	20%	83.2	134.1	12.3	4.0	12.9	122.3	133.1	39.2	41.4	out of box
9c	499	496	99%	158.0	128.2	7.5	3.9	8.5	142.0	134.4	17.2	19.2	
9d	503	503	100%	146.2	121.2	1.0	3.8	3.9	142.0	126.9	7.0	8.0	
10a	490	162	33%	84.6	131.3	10.7	4.4	11.5	122.3	136.5	38.0	39.8	out of box
10b	498	416	84%	87.5	141.8	11.5	1.2	11.5	122.3	141.6	34.8	36.7	out of box
10c	499	499	100%	122.8	142.3	6.4	3.0	7.1	142.0	142.8	19.2	20.5	
10d	492	492	100%	147.2	127.1	3.3	2.0	3.9	142.0	135.4	9.8	10.5	
11a	0	0	NA	0.0	0.0	N/A	N/A	N/A	122.2	148.2	N/A	N/A	dead tag
11b	506	216	43%	108.4	151.0	7.2	2.0	7.5	122.2	153.2	14.0	15.9	
11c	487	486	100%	143.9	147.1	2.7	2.7	3.8	141.9	154.4	7.5	8.4	
11d	494	494	100%	139.9	143.1	2.9	2.8	4.1	141.9	147.0	4.4	6.0	
12a	494	18	4%	90.4	152.3	21.6	4.2	22.0	122.3	156.6	32.2	39.8	out of box
12b	503	502	100%	103.8	154.3	6.1	0.8	6.1	122.3	161.6	19.9	20.8	
12c	498	496	100%	146.3	163.4	1.8	2.4	3.0	142.0	163.0	4.3	5.2	
12d	500	499	100%	146.0	141.1	3.5	2.6	4.4	142.0	155.5	15.0	15.6	

Legends:

>450	(>90%)	>90%
250-450	(50-90%)	50-90%
50-250	(10-50%)	10-50%
<50	(<10%)	<10%
No Blinks		No Calc

<5 ft	<5 ft	<5 ft
5-10 ft	5-10 ft	5-10 ft
10-20 ft	10-20 ft	10-20 ft
>20 ft	>20 ft	>20 ft
No Calc	No Calc	No Calc

<10 ft	<10 ft
10-20 ft	10-20 ft
20-30 ft	20-30 ft
>30 ft	>30 ft
No Calc	No Calc

Table 20. WhereNet Accuracy, Double-High Stacked Containers, Top Layer

Tag No.	Blinks Heard	Positions Reported	Positions / Blinks %	Avg Location		Standard Deviation			Actual Location		Error		Comment
				X	Y	X	Y	Total	X	Y	Avg	RMS	
13a	483	479	99%	194.9	115.7	2.2	0.7	2.3	167.8	113.5	27.2	27.3	out of box
13b	493	491	100%	178.2	109.0	3.3	2.7	4.2	167.8	108.1	10.4	11.3	
13c	501	500	100%	149.5	100.1	3.4	5.8	6.7	148.0	107.3	7.4	10.0	
13d	509	125	25%	150.9	108.8	5.8	6.7	8.8	148.1	114.7	6.6	11.0	
14a	500	27	5%	194.2	115.1	7.4	8.5	11.3	167.9	121.9	27.1	29.9	out of box
14b	498	426	86%	196.7	119.1	5.6	1.6	5.8	167.9	116.8	28.9	29.5	out of box
14c	505	421	83%	140.9	106.0	6.9	4.9	8.5	148.2	115.4	11.9	14.6	
14d	513	513	100%	145.2	119.2	2.6	1.8	3.2	148.2	122.9	4.8	5.7	
15a	487	135	28%	204.4	135.3	6.6	0.8	6.6	167.7	133.0	36.7	37.5	out of box
15b	483	217	45%	201.3	130.1	11.1	1.2	11.2	167.6	128.2	33.8	35.7	out of box
15c	486	486	100%	151.1	128.2	2.0	1.6	2.5	147.9	127.2	3.4	4.2	
15d	498	498	100%	143.5	127.3	2.7	2.2	3.5	148.0	134.5	8.5	9.2	
16a	498	471	95%	180.7	139.8	7.9	1.1	8.0	167.6	141.4	13.2	15.4	
16b	455	276	61%	207.2	136.5	6.6	2.8	7.2	167.6	136.6	39.6	40.4	out of box
16c	492	492	100%	137.0	126.6	4.0	3.1	5.0	147.9	135.2	13.9	14.8	
16d	486	486	100%	150.0	140.3	4.0	1.7	4.4	147.9	142.7	3.2	5.4	
17a	503	119	24%	195.3	154.8	13.2	4.0	13.8	167.6	153.2	27.8	31.1	out of box
17b	483	25	5%	196.2	153.2	8.6	3.1	9.1	167.7	148.0	28.9	30.9	out of box
17c	510	510	100%	138.8	153.5	2.1	1.6	2.7	147.9	146.9	11.3	11.6	
17d	482	439	91%	135.9	160.7	9.0	5.6	10.6	147.9	154.3	13.6	17.2	
18a	493	382	77%	187.6	160.1	4.3	1.3	4.6	167.8	161.6	19.8	20.4	
18b	490	205	42%	195.1	155.1	4.6	3.4	5.7	167.8	156.6	27.3	28.0	out of box
18c	500	474	95%	143.2	165.7	3.8	3.1	4.9	148.0	155.1	11.6	12.6	
18d	500	497	99%	143.5	165.6	1.2	6.1	6.2	148.0	162.6	5.4	8.2	
19a	498	497	100%	119.1	108.9	3.6	1.2	3.8	122.4	108.0	3.4	5.1	
19b	491	491	100%	88.7	118.0	2.5	1.0	2.6	122.4	113.8	34.0	34.1	out of box
19c	510	453	89%	144.5	103.4	5.9	5.3	7.9	142.1	114.7	11.6	14.0	
19d	493	493	100%	145.0	104.9	0.7	3.9	3.9	142.2	107.2	3.7	5.4	
20a	492	492	100%	98.1	121.9	3.5	1.2	3.7	122.4	116.7	24.8	25.1	out of box
20b	503	33	7%	100.0	119.2	14.7	0.9	14.7	122.4	121.8	22.5	27.2	
20c	499	499	100%	148.1	117.5	6.5	5.1	8.3	142.1	123.1	8.2	11.7	
20d	495	122	25%	133.8	110.1	8.9	7.1	11.4	142.2	115.7	10.1	15.2	
21a													
21b													
21c													
21d													
22a													
22b													
22c													
22d													
23a	494	484	98%	91.3	145.4	4.0	2.7	4.8	122.2	148.1	31.0	31.4	out of box
23b	510	143	28%	89.5	154.7	8.6	1.5	8.7	122.2	153.2	32.8	34.0	out of box
23c	505	503	100%	139.6	157.1	3.5	1.8	3.9	141.9	154.4	3.6	5.3	
23d	497	497	100%	137.8	142.4	2.1	1.7	2.7	141.9	147.0	6.2	6.8	
24a	489	479	98%	91.7	152.1	4.6	1.4	4.8	122.3	156.3	30.9	31.3	out of box
24b	491	13	3%	96.4	156.8	12.2	2.0	12.4	122.3	161.5	26.3	30.1	out of box
24c	498	498	100%	144.2	157.2	1.2	2.5	2.8	142.0	163.0	6.2	6.8	
24d	496	364	73%	141.4	159.9	4.0	4.7	6.2	142.0	155.5	4.5	7.6	

Legends:

>450	(>90%)	>90%
250-450	(50-90%)	50-90%
50-250	(10-50%)	10-50%
<50	(<10%)	<10%
No Blinks		No Calc

<5 ft	<5 ft	<5 ft
5-10 ft	5-10 ft	5-10 ft
10-20 ft	10-20 ft	10-20 ft
>20 ft	>20 ft	>20 ft
No Calc	No Calc	No Calc

<10 ft	<10 ft
10-20 ft	10-20 ft
20-30 ft	20-30 ft
>30 ft	>30 ft
No Calc	No Calc

Table 21. WhereNet Accuracy, Single-High Stacked Containers, HMMWVs

Tag No.	Blinks Heard	Positions Reported	Positions / Blinks %	Avg Location		Standard Deviation			Actual Location		Error		Comment
				X	Y	X	Y	Total	X	Y	Avg	RMS	
H1a	879	645	73%	173.0	121.2	4.4	2.8	5.2	179.1	116.9	7.5	9.1	
H1b	853	823	96%	172.9	115.3	2.2	2.8	3.6	173.0	116.7	1.4	3.9	
H1c	877	850	97%	184.9	134.4	3.4	1.7	3.8	173.0	131.0	12.4	13.0	
H1d	878	441	50%	185.2	134.3	5.2	3.7	6.4	178.9	130.6	7.3	9.7	
H2a	834	213	26%	188.8	137.5	4.1	2.3	4.7	178.9	137.7	9.9	11.0	
H2b	874	733	84%	178.9	132.4	4.3	4.6	6.2	174.7	137.4	6.5	9.0	
H2c	885	875	99%	166.8	152.0	5.0	2.2	5.4	172.8	151.1	6.1	8.2	
H2d	879	722	82%	173.0	158.7	7.3	4.9	8.8	178.7	151.4	9.2	12.8	
H3a	882	881	100%	102.5	125.8	4.9	3.0	5.8	117.2	139.0	19.7	20.6	
H3b	872	871	100%	93.5	135.5	6.4	0.7	6.4	111.1	138.8	17.9	19.1	out of box
H3c	890	890	100%	108.3	145.7	2.0	3.3	3.8	110.9	152.2	7.0	8.0	
H3d	883	883	100%	109.1	148.0	3.1	1.4	3.4	116.7	152.4	8.8	9.4	
H4a	872	865	99%	100.7	106.7	3.0	2.7	4.0	117.6	113.3	18.1	18.6	
H4b	875	838	96%	97.0	112.5	3.9	2.5	4.6	110.6	116.5	14.2	14.9	out of box
H4c	852	852	100%	100.2	125.2	3.1	1.1	3.3	111.5	126.7	11.4	11.9	
H4d	844	844	100%	90.7	122.9	6.8	1.8	7.0	117.4	126.8	27.0	27.9	out of box

Legends:

>810	(>90%)	>90%
450-810	(50-90%)	50-90%
90-450	(10-50%)	10-50%
<90	(<10%)	<10%
No Blinks		No Calc

<5 ft	<5 ft	<5 ft
5-10 ft	5-10 ft	5-10 ft
10-20 ft	10-20 ft	10-20 ft
>20 ft	>20 ft	>20 ft
No Calc	No Calc	No Calc

<10 ft	<10 ft
10-20 ft	10-20 ft
20-30 ft	20-30 ft
>30 ft	>30 ft
No Calc	No Calc

Table 22. WhereNet Accuracy, Double-High Stacked Containers, HMMWVs

Tag No.	Blinks Heard	Positions Reported	Positions / Blinks %	Avg Location		Standard Deviation			Actual Location		Error		Comment
				X	Y	X	Y	Total	X	Y	Avg	RMS	
H1a	501	501	100%	178.7	122.8	4.2	1.3	4.4	179.1	116.9	5.9	7.4	
H1b	484	484	100%	188.0	117.3	4.9	3.2	5.8	173.0	116.7	15.0	16.1	
H1c	491	460	94%	194.0	134.3	7.0	4.4	8.3	173.0	131.0	21.3	22.9	out of box
H1d	492	477	97%	191.9	139.5	7.2	3.1	7.8	178.9	130.6	15.7	17.6	out of box
H2a	469	329	70%	199.5	135.1	7.3	3.0	7.9	178.9	137.7	20.8	22.2	out of box
H2b	492	488	99%	184.1	140.2	8.2	2.7	8.7	174.7	137.4	9.9	13.1	
H2c	497	486	98%	191.9	149.5	5.9	1.3	6.0	172.8	151.1	19.2	20.1	out of box
H2d	495	495	100%	179.7	162.4	3.0	3.0	4.2	178.7	151.4	11.0	11.8	
H3a	500	475	95%	92.5	127.8	6.7	3.7	7.6	117.2	139.0	27.1	28.2	out of box
H3b	490	361	74%	86.2	133.9	7.2	1.1	7.3	111.1	138.8	25.4	26.5	out of box
H3c	503	475	94%	102.3	149.6	5.8	1.4	6.0	110.9	152.2	9.0	10.8	
H3d	500	500	100%	103.7	148.6	2.9	1.0	3.0	116.7	152.4	13.5	13.9	
H4a	494	494	100%	107.2	106.2	2.6	2.7	3.8	117.6	113.3	12.6	13.1	
H4b	501	441	88%	94.9	116.0	4.3	5.5	7.0	110.6	116.5	15.7	17.2	out of box
H4c	483	483	100%	90.8	124.3	4.7	1.1	4.8	111.5	126.7	20.8	21.4	out of box
H4d	481	481	100%	102.1	125.0	3.9	1.3	4.1	117.4	126.8	15.4	15.9	

Legends:

>450	(>90%)	>90%
250-450	(50-90%)	50-90%
50-250	(10-50%)	10-50%
<50	(<10%)	<10%
No Blinks		No Calc

<5 ft	<5 ft	<5 ft
5-10 ft	5-10 ft	5-10 ft
10-20 ft	10-20 ft	10-20 ft
>20 ft	>20 ft	>20 ft
No Calc	No Calc	No Calc

<10 ft	<10 ft
10-20 ft	10-20 ft
20-30 ft	20-30 ft
>30 ft	>30 ft
No Calc	No Calc

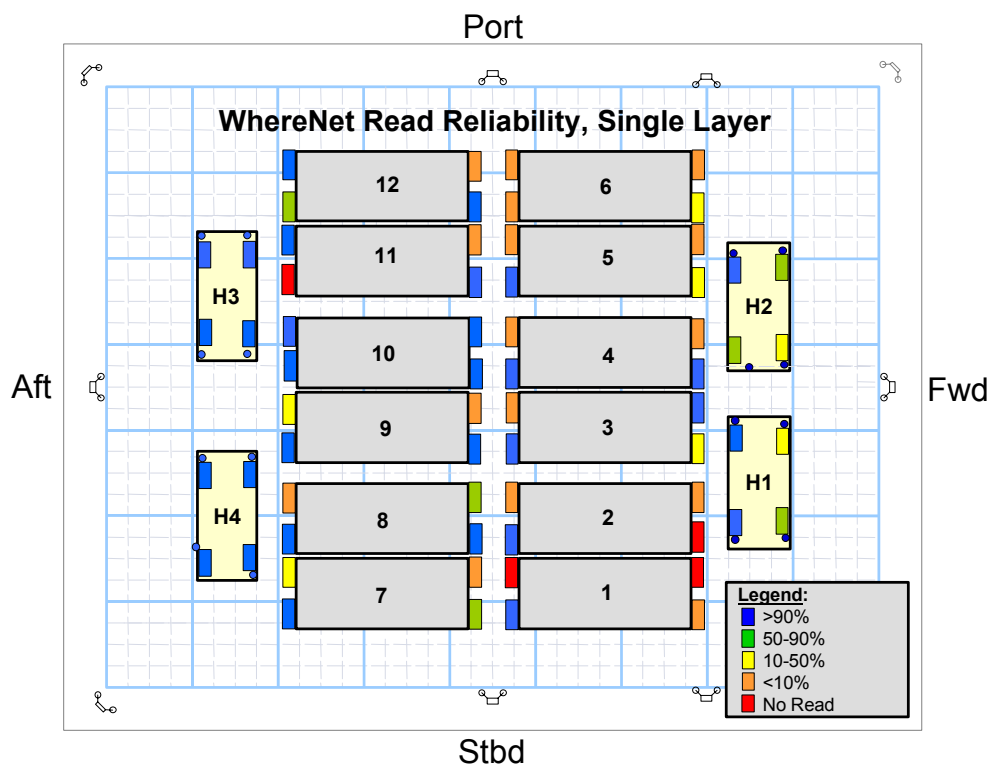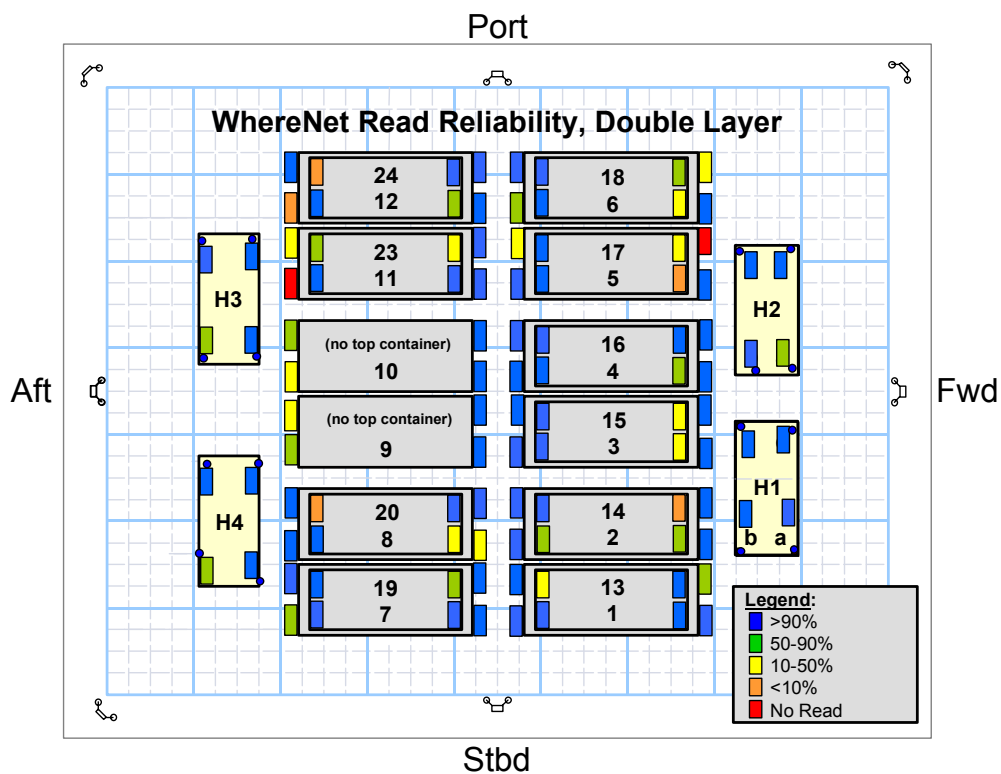Figure 216. WhereNet read reliability for single layer of containers.

Figure 217. WhereNet read reliability for double layer of containers.
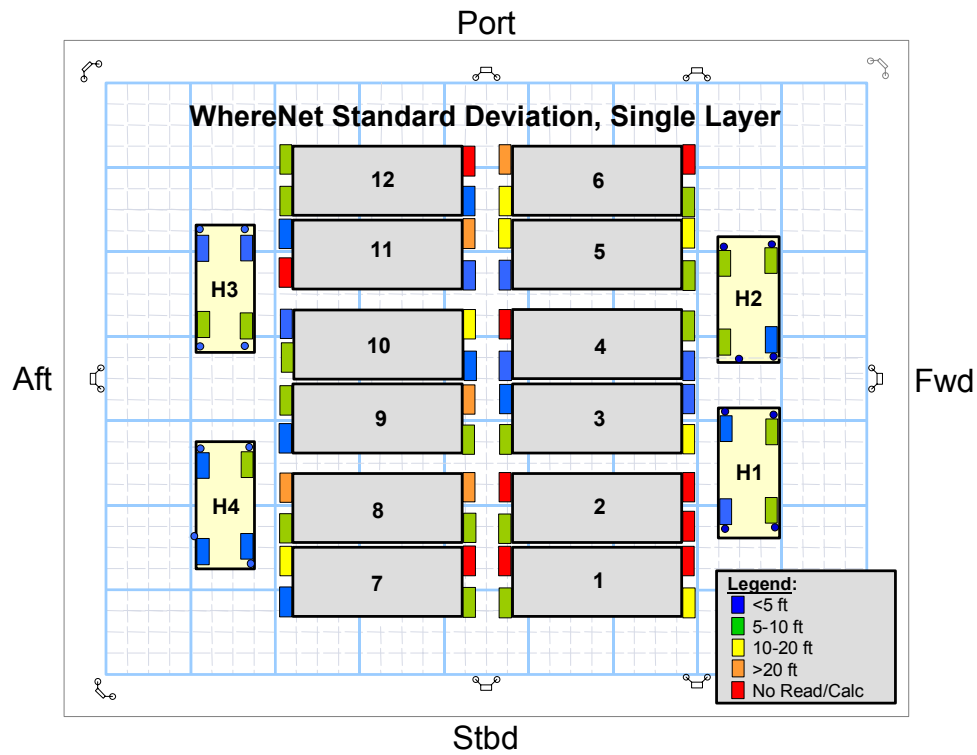
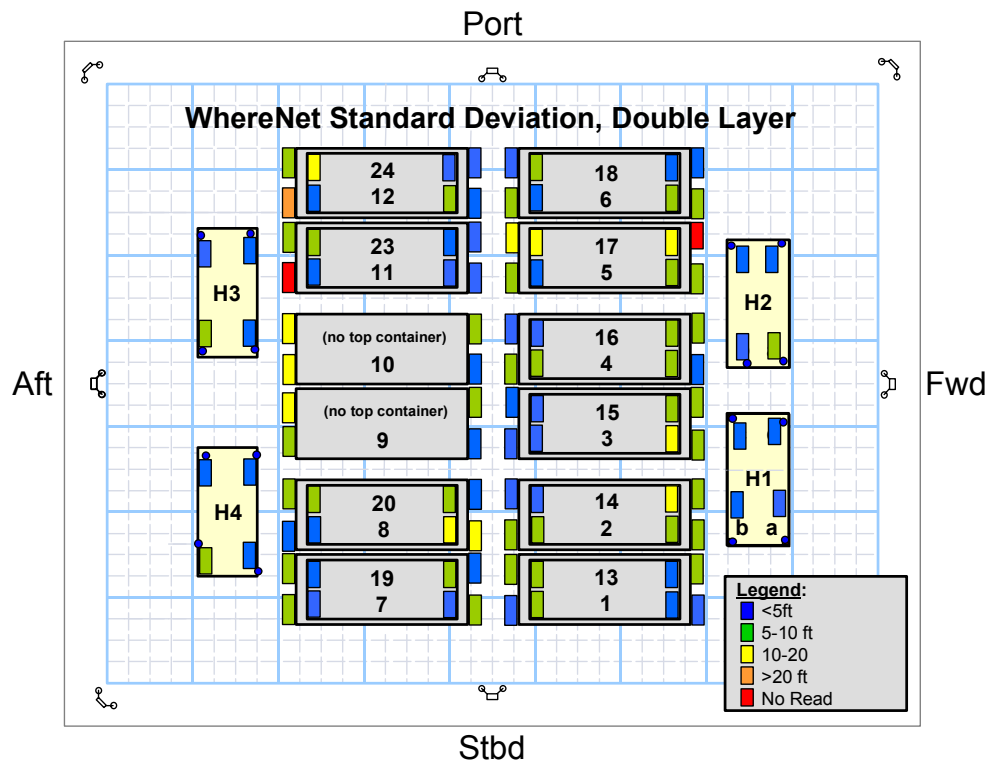Figure 218. WhereNet standard deviation for single layer of containers.

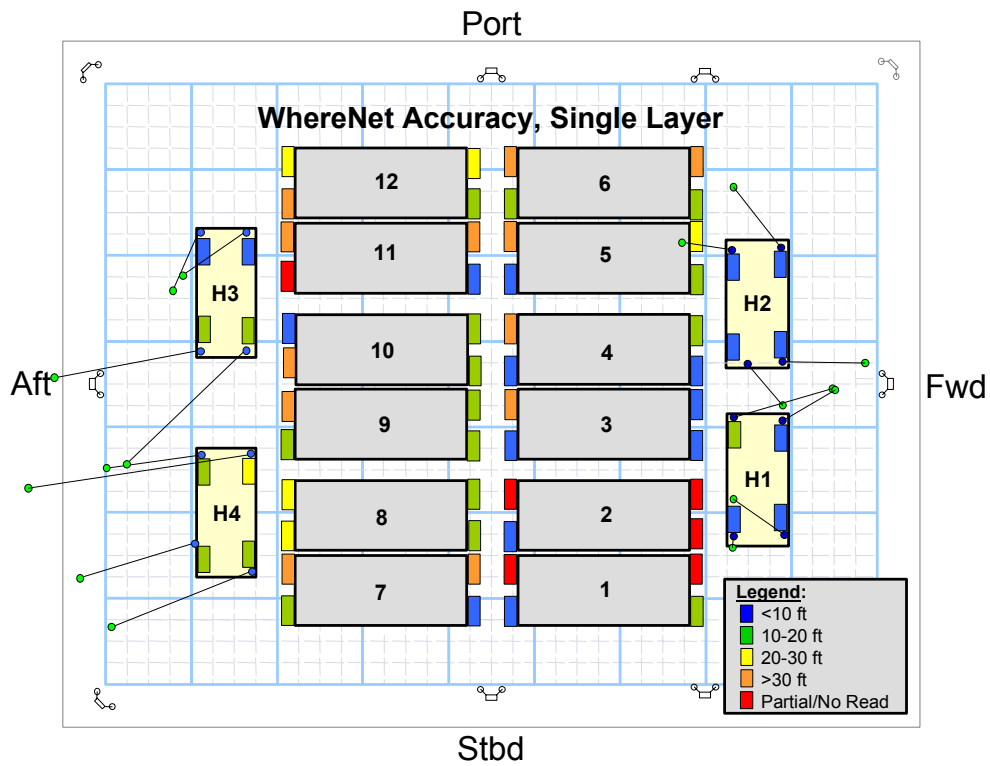Figure 219. WhereNet standard deviation for double layer of containers.

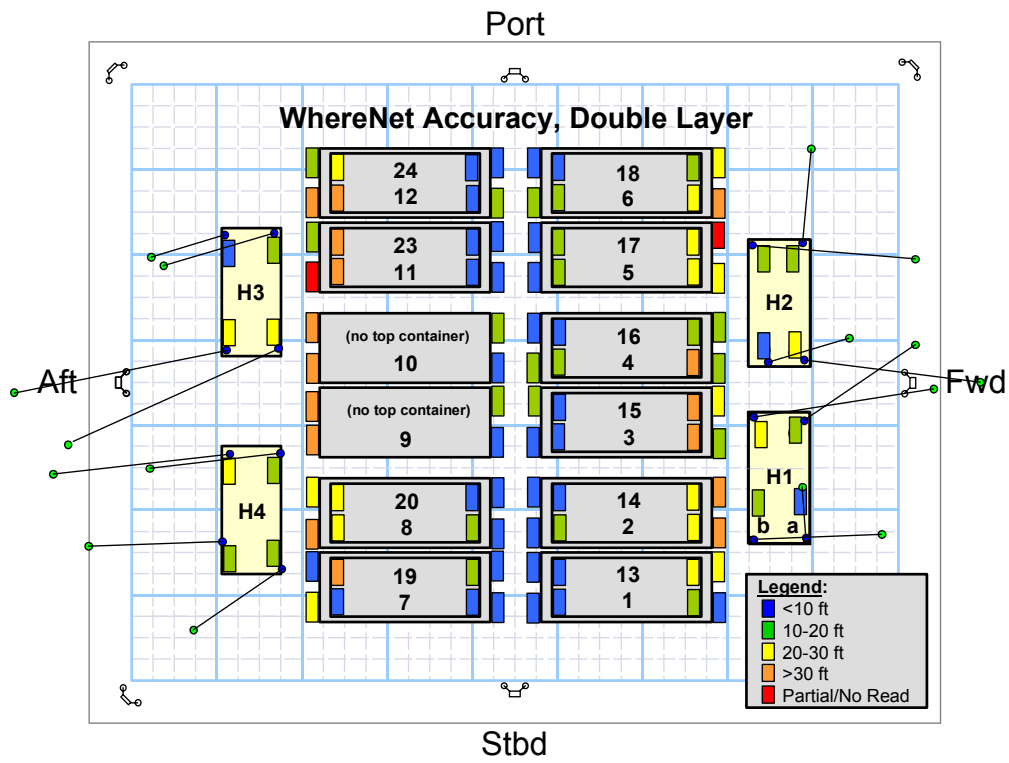Figure 220. WhereNet accuracy for single layer of containers.

Figure 221. WhereNet accuracy for double layer of containers.

4.2.2 MSSI:

Tabular Results: Table 23 summarizes the MSSI data reduction for double then single-high containers. It answers the fourth question about effects of blockage.

Tags were placed on top of containers with the antennas oriented vertically. Tags on top of double-high containers were above the bottom of beams, and clear view to the antennas was blocked. Tags on top of single-high containers were in clear view of all antennas, with no obstructions. Container tops are not the optimum location for mounting tags.

Accuracy was worse for double-high containers than single-high containers. Average and RMS accuracy for double-high containers was between 8 and 15 feet. Average and RMS accuracy for single high containers was between 2 and 4 feet. The single-high container test can be considered to be similar to the open space test, without blockage, but with static tag locations.

The MSSI system in Tests "B" and "C" was largely unstable, with significant numbers of clips, resulting from not resetting the system as needed. Tests "A" and "D" had the fewest number of clips, and the system was reset as needed. They provided the best data for double and single-high containers.

Clipped data was filtered out of analyses and not plotted. Only data left in the test box boundaries was considered. Tag 201 consistently had the fewest number of clips.

Graphic Plots: Figures 222 through 226 show the tag reports without clips. Figures 222, 223, and 224 show tests with double-high containers with tags in different locations. Figures 225 and 226 show tests with single-high containers. Two tests were conducted each day, one in the morning (AM), and the other in the afternoon (PM).

Test A, Tag 201 appeared to read close to the tag location in the center of the container stack, Figure 222. The two aft antennas had fairly clear line of sight to the tag as the aft center containers were only single-high. The forward antennas were blocked from view. Apparently three out of four antennas got a fix on the tag to locate it. UWB signals may have diffracted around corners and propagated between containers to a forward antenna. Figure 223 shows the possible UWB propagation paths.

Test A, Tag 77 was located on a HMMWV and was blocked from the aft antennas and could only be read directly by the two forward antennas, Figure 222. Apparent tag location was between the two forward antennas. This may have been caused by bi-lateration as with WhereNet, or may have been caused by additional time delays around containers to aft antennas, making it appear further away.

Test B shows an unstable system without resets. Most of the data points were clips and not plotted. With clips included, each tag's reports appeared as a large "cloud," and made interpretation difficult. Tag 201 data was largely not clipped and shows the nature of the clouds.

Test C shows the MSSI system after reset, with readings close to tags, then becoming progressively unstable. Most of the final data points were clips and are not shown.

Test D shows the MSSI system on its best behavior, with resets as needed. Tag reports clustered near tag locations, with occasional pops. Tags 201 and 167 in the center reported very close to actual position. Reported positions of Tags 41, 13, and 77 further away from center "leaned" towards the outside.

UWB signals may have propagated well around and between containers. UWB may require fewer antennas to work around blockage and multipath.   More testing is needed to confirm.

Table 23, MSSI Container Blockage Accuracy

| Test No.	Tag No.	Blinks Heard	MSSI Reads				MSSI Reads %			Avg Offset		Standard Deviation			Error	
			Good	Clips	Pops >20	Total	Good	Clips	Pops >20	X	Y	X	Y	Total	Avg	RMS
A	77	91	58	30	3	91	64.4	33.3	3.3	9.1	6.7	2.3	1.2	2.6	11.5	11.6
	201	51	44	5	2	51	86.3	9.8	3.9	-0.6	1.4	5.3	5.1	7.3	8.1	11.1
B	41	88	60	16	12	88	68.2	18.2	13.6	-2.0	-4.0	7.8	1.7	8.0	8.1	9.1
	77	836	19	817	0	836	2.3	97.7	0.0	4.8	9.3	5.4	3.3	6.3	11.9	12.1
	161	409	172	231	6	409	42.1	56.5	1.5	13.6	2.3	3.5	6.6	7.5	15.5	15.7
	167	94	39	52	3	94	41.5	55.3	3.2	-5.2	4.7	3.9	7.2	8.1	10.4	10.6
	201	1004	529	104	371	1004	52.7	10.4	37.0	-2.4	2.5	10.0	5.3	11.4	10.5	11.9
C	13	1214	216	742	256	1214	17.8	61.1	21.1	0.7	-2.2	1.2	1.5	1.9	2.7	3.0
	41	288	214	68	6	288	74.3	23.6	20.8	-1.2	-0.2	1.1	1.4	1.8	1.5	2.1
	77	1164	97	1065	2	1164	8.3	91.5	0.2	2.4	-2.5	0.8	0.5	0.9	3.5	3.6
	167	575	208	351	16	575	36.2	61.0	2.8	0.8	-1.7	1.0	1.2	1.6	2.1	2.4
	201	152	138	11	3	152	90.8	7.2	2.0	-3.0	-3.7	4.2	2.7	5.0	5.4	7.0
D	13	383	379	4	0	383	99.0	1.0	0.0	1.2	0.0	1.3	1.7	2.1	1.8	2.4
	41	222	218	3	1	222	98.2	1.4	0.5	-1.6	0.6	0.7	1.0	1.2	1.9	2.1
	77	351	350	1	0	351	99.7	0.3	0.0	2.6	-0.3	0.6	0.7	0.9	2.7	2.8
	167	209	208	0	1	209	99.5	0.0	0.5	1.1	0.7	1.0	1.4	1.7	1.5	2.1
	201	98	93	4	1	98	94.9	4.1	1.0	0.2	0.1	3.1	2.2	3.8	1.8	3.8
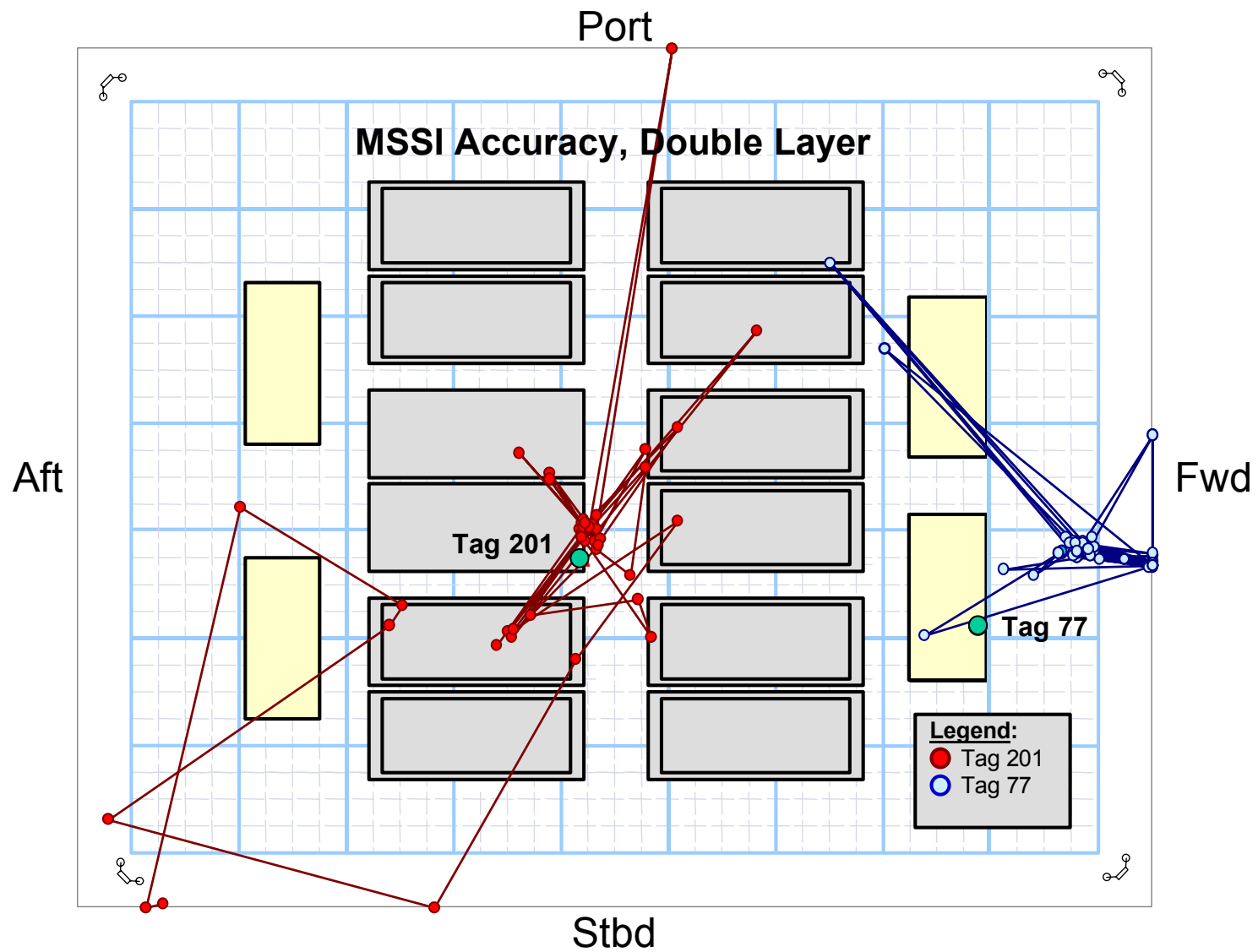
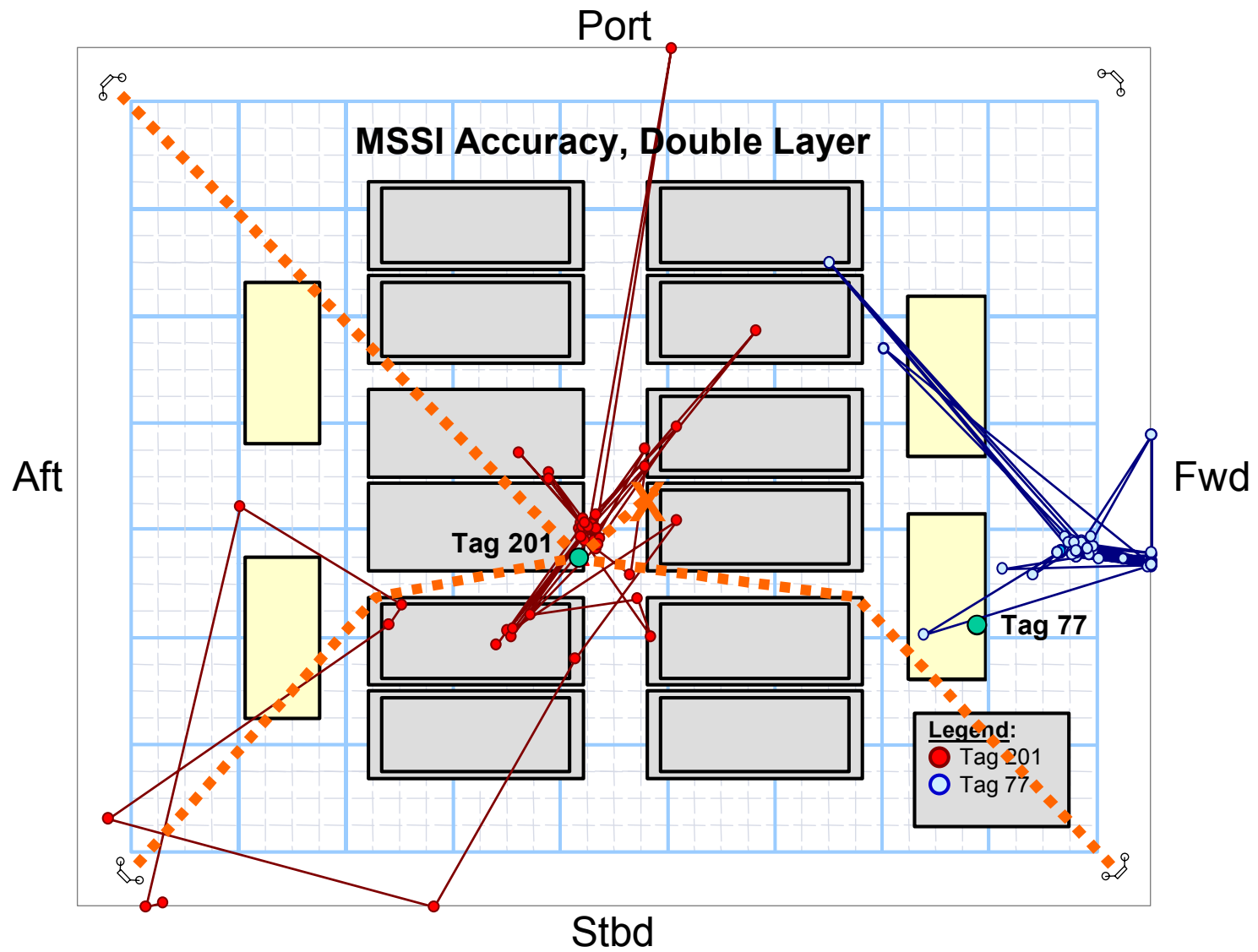Figure 222. MSSI Accuracy for double layer of containers, Test A (AM).

Figure 223. MSSI for double layer of containers, Test A (AM), Propagation and Diffraction.
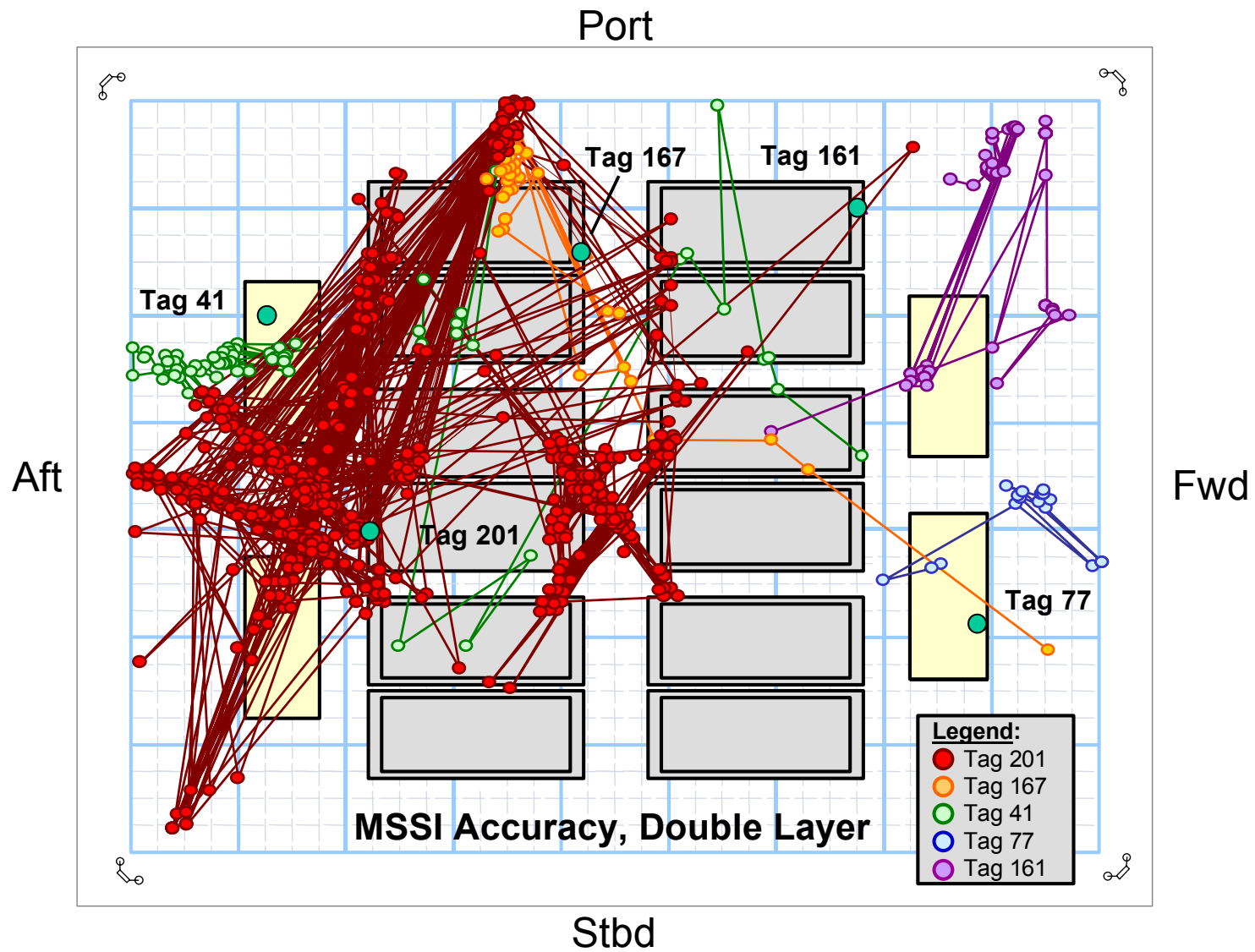
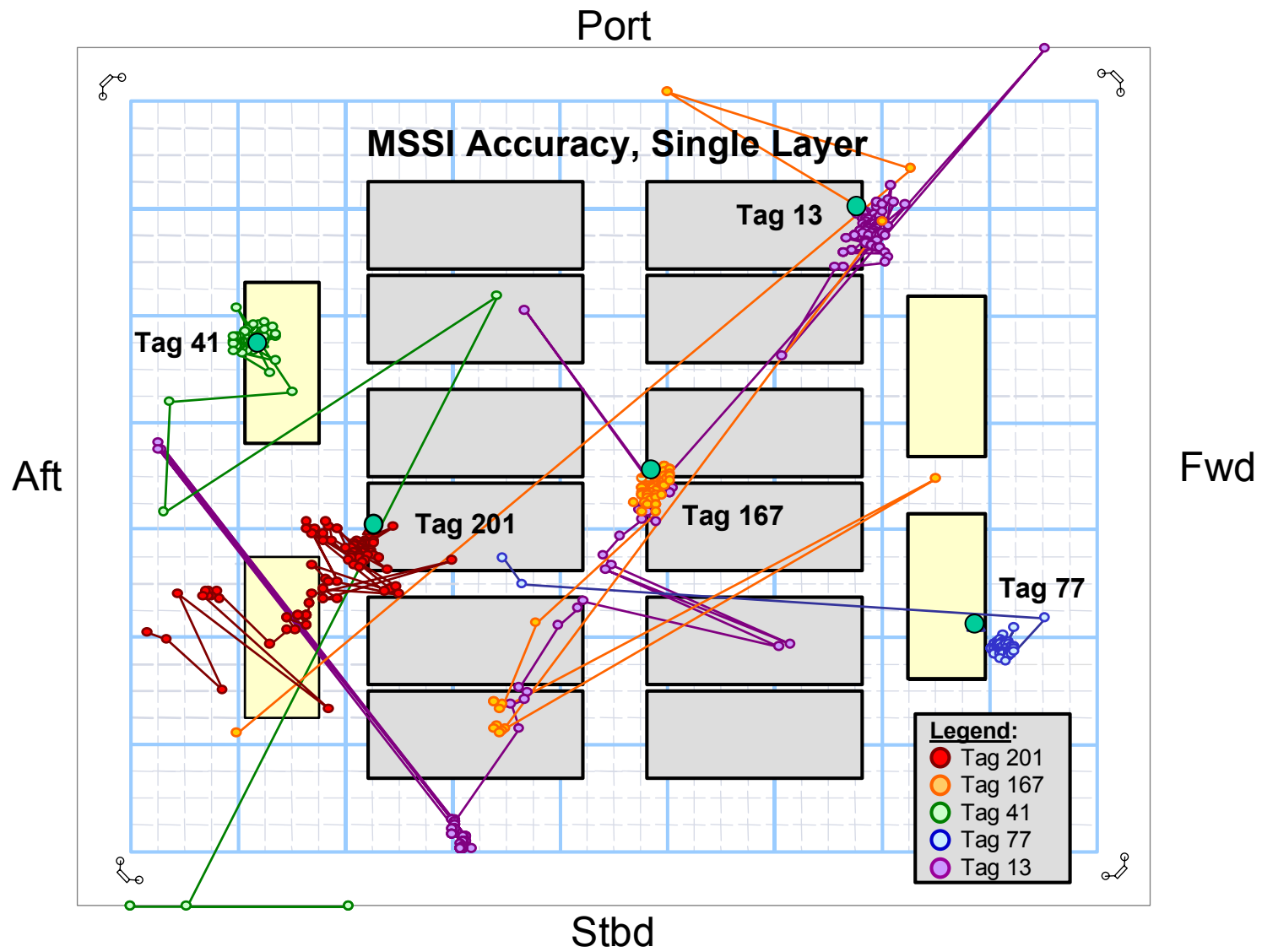Figure 224. MSSI accuracy for double layer of containers, Test B (PM).

Figure 225. MSSI accuracy for single layer of containers, Test C (AM).
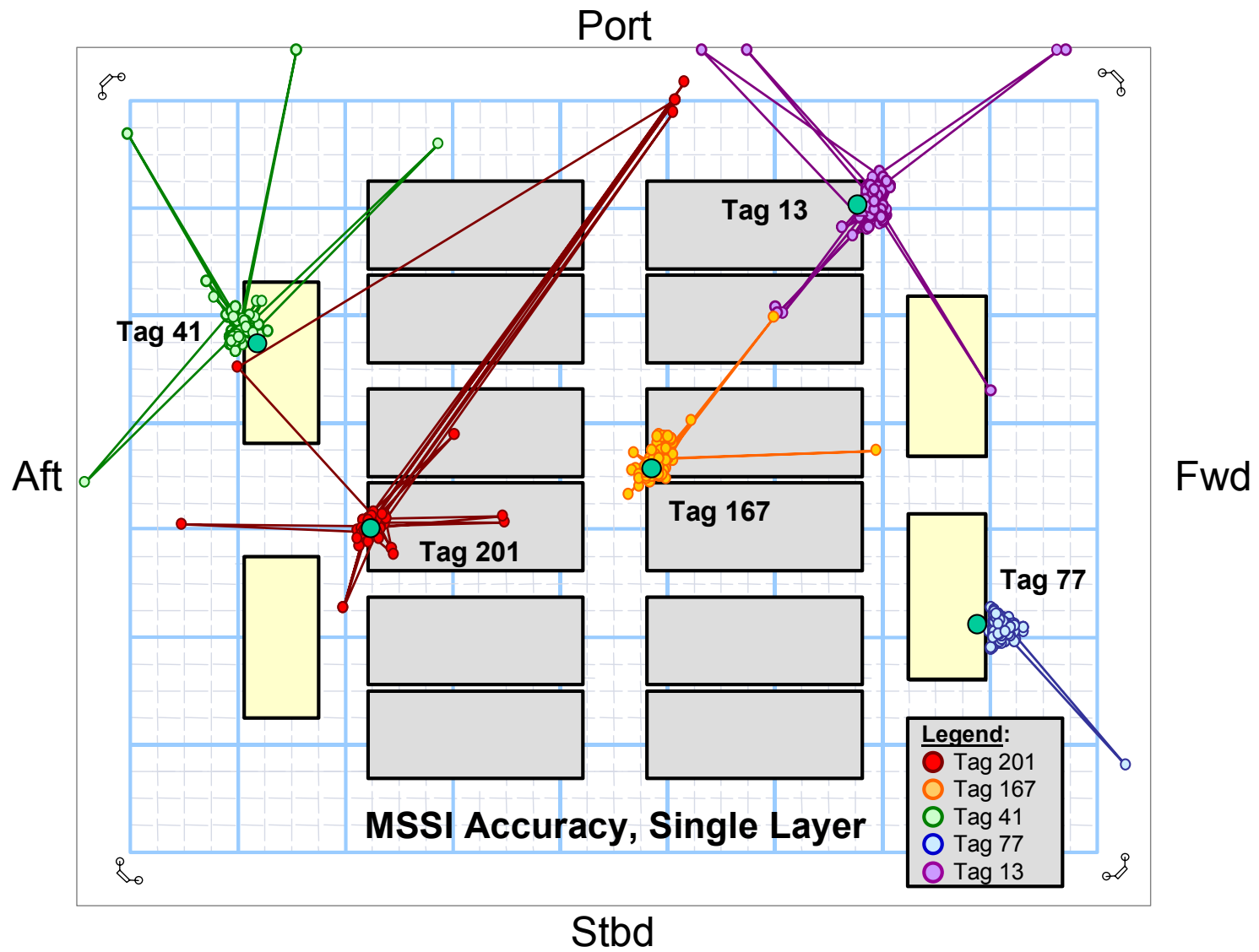
Figure 226. MSSI accuracy for single layer of containers, Test D (PM).

This page left blank

5.0 FINDINGS

Two state-of-the-art PAL technologies, DSSS and UWB, were tested aboard the SS Curtis in Port Hueneme. Both open space accuracy and container blockage tests were performed in two consecutive weeks. The shipboard testing answered, or addressed, five primary questions:

- Do DSSS and UWB work in shipboard environments?
- Do they have dropouts and dead zones resulting from multipath?
- What are the resulting accuracies?

- What are the effects of blockage by containers?
- What are the optimum tag and antenna locations?

5.1 First Week, Open Space

5.1.1 Does it Work on a Ship?

The first question was answered aboard ship during the testing. Both systems worked well in empty cargo holds, able to read near bulkheads and in corners. This was a substantial improvement over earlier analog RFID systems, which do not work well in ships. Wireless Mountain, a major RFID distributor, tested surveyed analog PAL systems on a ship, and found they had major dropouts and misreads near bulkheads and in corners. They also cannot discriminate tags in different cargo holds because of RF leakage between cargo holds. Analog systems cannot accurately localize tags in cargo holds. The answer to "Does it work in a ship?" question for digital PAL systems was not known for certain before the test.

5.1.2 Dropouts and Dead Zones

The second question, dropouts, was also answered during the test. The DSSS system had mainly partial reads and dozens of full dropouts with a minimum set of four antennas in the open space. The recommended configuration of 8 antennas worked well, with few partial dropouts and no full dropouts in the open space. No dead zones near bulkheads and corners were evident as with analog.

The UWB system did not experience dropouts with four antennas. It did, however, have frequent out-of-scale reports (pops and jumps), which may have been due to CFAR bias loops triggering tunnel diodes, or received UWB wavelets pushing tunnel diodes in and out of troughs, leaving them near tops (no read), causing erroneous readings. Location algorithms may have then attempted to calculate position. Clips, pops and jumps were considered partial reads for data analyses. The DSSS system had more mature algorithms, and reported a partial reads without location when not enough antennas heard a signal.

5.1.3 Accuracy

The third question, accuracy, was the focus of data reduction. Both systems worked within vendor advertised/estimated accuracy in the empty cargo holds. The DSSS system specified 10-foot accuracy for 67% of reads (one standard deviation). The UWB vendor estimated accuracy to a few feet in a ship. The RMS (67%) accuracy of the systems in their optimum configurations were:

DSSS / WhereNet   6 feet

UWB / MSSI   2 to 5 feet

The DSSS system had an average offset of 1-foot in the "X" axis and 2 feet in the "Y" axis. The UWB system did not have significant offset in either axis.

5.1.4 Antenna Locations

A surprising finding was DSSS system "Y" axis error was greater than the "X" axis, and followed tag location over the Y axis (Figures 195, 204, and 213). The error also changed based on tag height. This phenomenon did not appear for the "X" axis. The error made the tag location appear further inside, or the antennas to appear further outside. The UWB system did not have this error.

The difference between "X" and "Y" axis was that the DSSS center "X" axis antennas did not have bulkheads immediately behind them to produce reflections, but had an opening or tunnel behind them, Figure 227. The center "Y" axis antennas had bulkheads immediately behind them. The bulkheads created virtual images of antennas behind the "Y" axis antennas, causing the antennas to appear further outside the test box for some readings, Figure 228. Corners caused three virtual images of the antennas.

The DSSS system used circularly polarized, omni-directional antennas that equally received reflected signals from both front and rear. Depending on the multipath, received signals could be received stronger from the front, or the rear, changing the apparent location of the antenna. The UWB system used corner antennas that did not receive from the sides or rear, thus did not have the same problem. A different type of antenna is needed for the DSSS system aboard ships.

Options to address reflections include different antennas or RF absorbent material behind antennas to reduce reflections. Directional or flush mounted antennas can be used near bulkheads and in corners. Patch antennas are a possible candidate for flush-mounted antennas. They are relatively thin, can be mounted on metal surfaces, and provide omni-directional pattern with circular polarization.

5.2   Second Week, Container Blockage

5.2.1 Accuracy

Both the DSSS and UWB systems had reduced accuracy during the second week container blockage experiments. This was expected by the vendors, as line-of-sight to antennas was blocked by containers. Fewer readings were taken with the UWB system due to the small number of tags, but accuracy degraded to about 10 feet with double-high containers. Single-high container's accuracy was about 3 feet.

The DSSS system tags along outside container faces were viewed by only 2 or 3 co-linear antennas, allowing position to be determined only in one dimension. HMMWV tag reported positions appeared largely on the axis between the antennas. Corner antennas were then moved from co-linear alignment to provide spatial diversity in both axis. HMMWV tag read accuracy improved with reported positions closer to the HMMWV's center axis.

Reduced accuracy for DSSS system tags on containers may have been also caused by tag reflections in nearby surfaces. For single-high containers, antennas could look over containers and see tags inside the aisleway between the containers. The antennas could only see tags facing them, not facing away. The antennas, however, may have seen reflections of the facing away tags in opposite container faces. This would cause tags to appear further away from their locations for those antennas, increasing error.

Tags were placed on top of containers for the single container tests, and both systems read locations more accurately than when they were placed on faces. Placing tags on top of containers so that antennas have direct line of sight to tags is optimum for RF. It is not optimum for tag physical survivability.

Ray tracing analysis may prove useful in analyzing blockage and reflections for a complex reflective environment. Ray tracing analyses can be used to optimally select antenna locations and types.
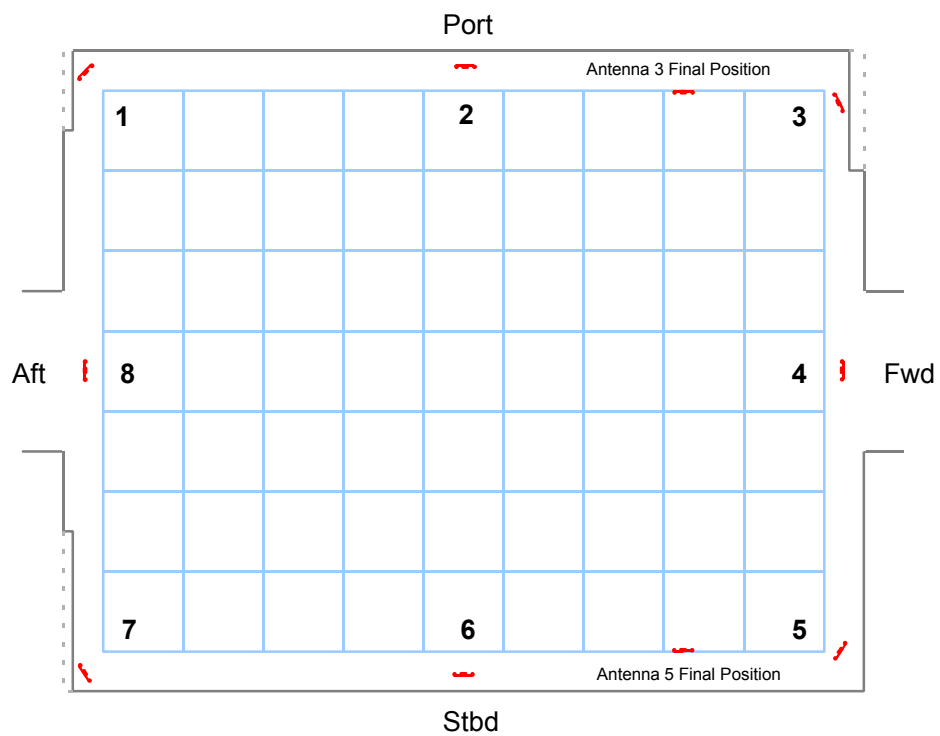
Figure 227. Antenna locations showing tunnels behind aft and forward center antennas
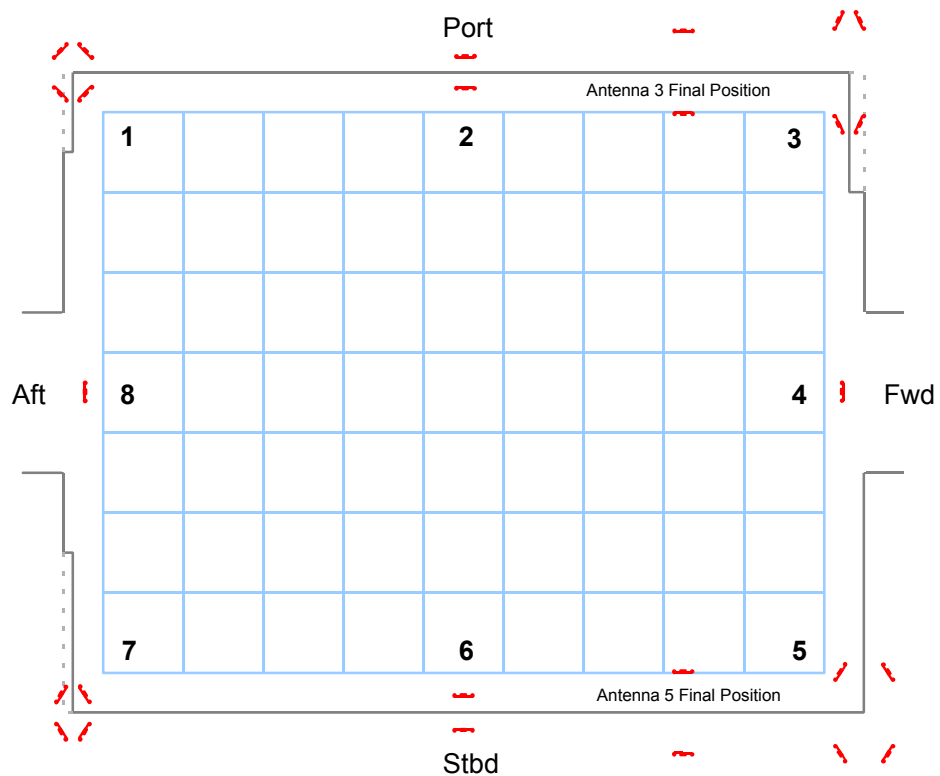

Figure 228. Antennas with virtual images.

5.2.2 Algorithms

Another surprising finding was that the DSSS system accuracy increased in the aisleway between the double-high stacked containers. This may have been due to the DSSS system bi-laterating with only 2 antennas at opposite ends of the aisle. The DSSS system normally tri-laterates with sets of 3 antennas to determine location in "X-Y" axis. The containers stacked higher than the antennas may have forced the system to bi-laterate, as only 2 antennas both sides of the aisle could hear the tags.

Algorithms need to include bi-lateration for aisleways, corridors, and passageways. Ships are usually stowed with firelanes between cargo and containers. Bi-lateration can also help with partially stacked containers, as containers are placed in established positions, thus tags location in one axis between two antennas is usually known. Antennas can then be placed to read tags along faces in one axis, mitigating reflections from opposite containers. Bi-lateration sets need to be included, assuming containers, cargo, and tags are roughly aligned between pairs of antennas.

Using generalized 2D position locations algorithms with multiple sets of tri-laterating antennas may not be ideal in a high multipath shipboard environment. Quad-lateration for 3D may also be needed to differentiate tags in cargo holds on different decks. Progressive stacking algorithms may be needed to support cases where tags are completely blocked by other stacked cargo, and are not visible down aisleways or fire lanes. The algorithms would remember the last recorded position of a tag. The DSSS system has the capability for reporting tags it can no longer hear, which can be extended for stacking.

The UWB system needs more mature algorithms to determine when to calculate based on the number of antennas that hear a tag report to minimize dropouts and pops and jumps. Pops and jumps seemed to be spurious and relatively isolated events. An "olympic" scoring algorithm that throws out the high and low and averages the rest may be useful to identify and isolate pops and jumps. The DSSS system uses four sub-blinks and averages them to one reading.

The UWB system likewise could benefit from improved bi-and tri-lateration algorithms found in the DSSS system. It may prove useful to integrate both systems, using UWB for increased accuracy, and the COTS DSSS system for mature algorithms, databases, and user interfaces.

5.2.3 Dropouts and Antenna Locations

Dropouts and standard deviations were greater for single- than double-high containers. These metrics indicate reflections and multipath were worse with partial blockage than full blockage. This indicates needing more antennas and receivers. This may be impractical with the relatively high cost of both the DSSS and UWB systems.

Twelve antennas, adding 2 more per each along port and starboard sides, are needed to provide bi-lateration along container faces, and spatial diversity for breakbulk and major end items, Figure 229. Nineteen antennas are needed for an optimum antenna configuration with antennas placed mid-section along bottoms of beams, Figure 230. Hardware cost for 19 antennas and receivers would be $80 to 90K before installation, which may double the cost. The SS Curtiss requires between 70 to 120 antennas, totaling $300 to $500K for hardware, or $500K to $1M installed.

A new LHD ship has 75 compartments. Assuming 15 antennas per compartment, and including ramps and elevators, a total of 1,200 antennas would be needed. Hardware cost would be on the order of $5M, or $10 to $12M installed as part of a SHIPALT. This may not be feasible, although it may pay for itself in time saved during intense operations. A less expensive alternative is needed, and was investigated as part of the NTAV program. It may provide a 1 to 2 order of magnitude cost reduction.
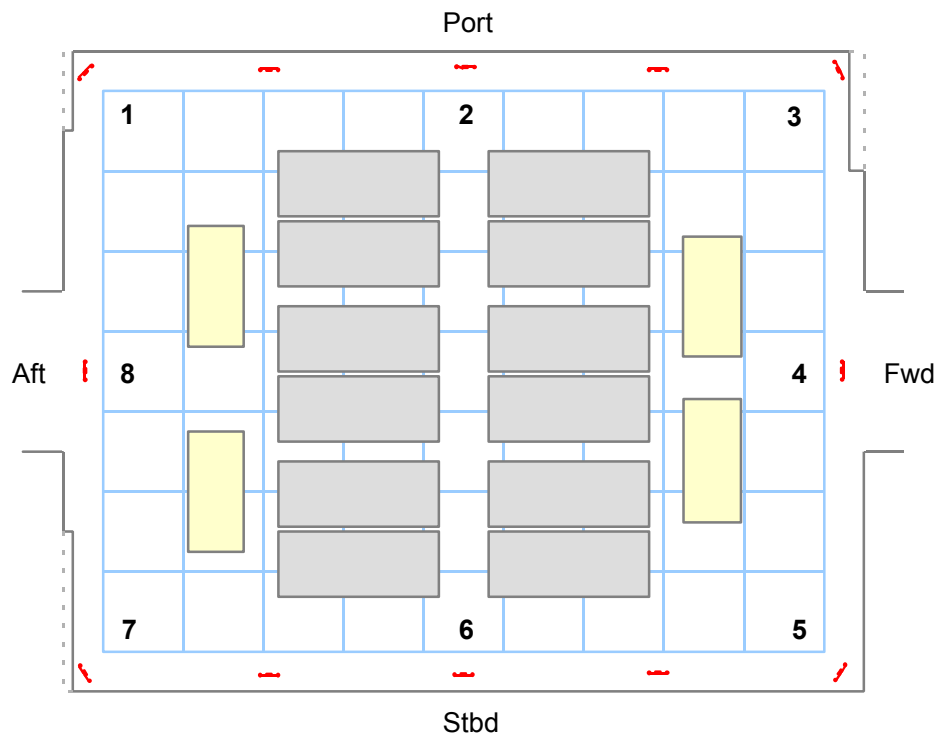
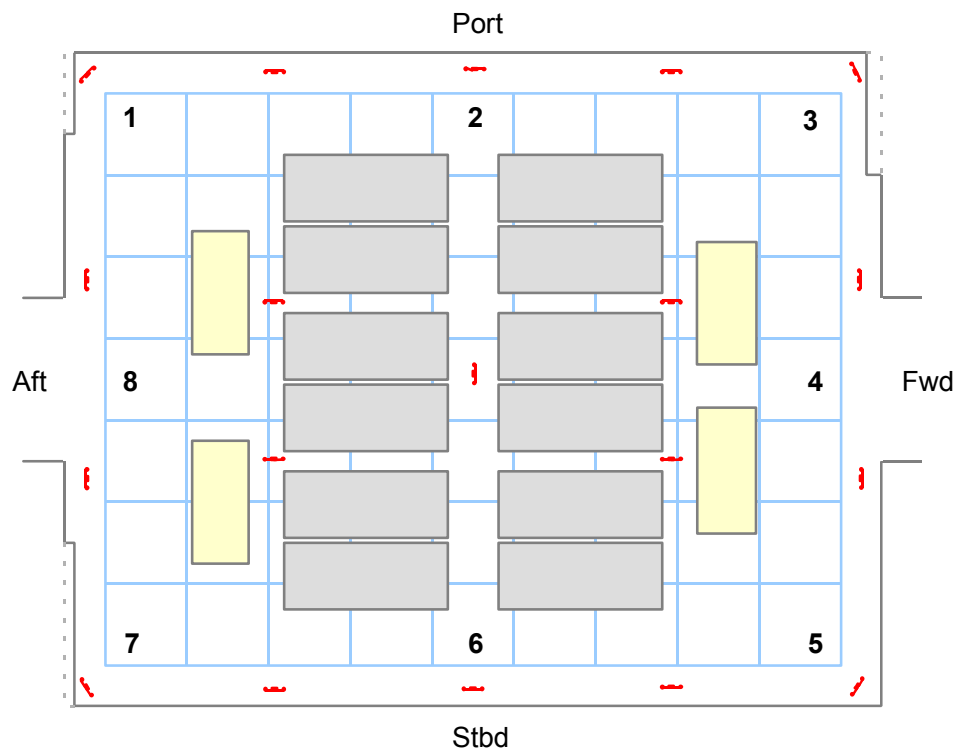Figure 229. Minimum additional antennas for test load .

Figure 230. Optimum antenna configuration for cargo hold.

This page left blank.

6.0 CONCLUSIONS

Ships present an adverse and difficult RF environment and best available PAL technologies need further development and testing. The tested COTS DSSS system was mature and stable, but did not have sufficient accuracy to determine vehicle orientation. The tested UWB system may have enough accuracy to determine vehicle orientation, but was unstable, had immature algorithms, and required additional engineering to make it suitable for commercial production and use. It is also violated FCC rules and was not approved for operation. A newer commercial version of the UWB system was released July 2003 and addresses these issues [11]. Both systems are expensive and could be cost prohibitive to use aboard ships.

Commercial developers will not likely develop shipboard capable systems on their own because market is too small. The general rule of thumb for Ventura Capital (VC) investment is a market size of $1B or more. Additional Government investment is needed to help address the key critical issues so that they can be incorporated into COTS systems that can be later procured for shipboard applications. WhereNet is a successful example of this business model. Their system derived from initial DOE investment into the fundamental technology, taking it from theory to application, and was later commercialized with VC investment. It is now being used in the automotive manufacturing industry.

The FCC issued a First Report and Order (R&O) on Part 15 operation of UWB on April 22, 2002 [8]. Key application areas included imaging, vehicular radars, and short-range communications and measurement. Asset visibility is not expressly allowed, but asset visibility is on the FCC's list of UWB applications [9] [10]. UWB PAL systems should be developed and tested that follow Part 15 rules to prove the viability of the technology and application.

The primary key for commercial success of PAL systems is accuracy. The often-heard benchmark accuracy figure is 1-foot, and was confirmed by Intel Corp. as 1- to 3-foot cube [12]. Markets will substantially open, to possibly $1B, once this milestone is met. Additional bandwidth is needed to achieve increased accuracy and the FCC opened over 7.5 GHz for Part 15 unlicensed UWB operation. This is 125 times more than the available 60 MHz in the 2.45 GHz ISM II band used by WhereNet, and 18 times greater than the 400 MHz used by MSSI. This will make the 1-foot accuracy a ready possibility.

Cost is still the primary driving factor. Readers for most commercial digital systems are on the order of a few to several $K. Ships will require more readers than office or industrial environments because of blockage, reflections and multipath. Reader costs are prohibitive for most applications, unless the assets are large and have high value (automobile or aircraft parts). Most digital system tags cost about $25 to $35 each. This is far from the <$1 threshold mentioned by most customers for broad application. Most tag cost reduction is being focused in passive tag technologies, which do not require localization. Much lower cost is required.

DARPA invested in UWB localizer and networking technologies. It promises much higher accuracy (1-inch) and substantial cost reduction. The tags themselves become the readers and network, eliminating wired infrastructure. The opportunity is eliminating pre-installed infrastructure and costs, allowing PAL system to be rapidly and opportunistically deployed ships, black or gray bottom. Assuming tag cost on the order of $50, tag readers will be two orders magnitude less expensive than available COTS DSSS and UWB systems. Fewer readers will be needed as the tags themselves will cooperatively range, only needing a few reference tags in known locations. It will also potentially solve blockage problems. No wires are needed and tags can be easily replaced for maintenance.

DARPA's UWB technology could also solve AM, the "Holy Grail" of logistics. It may be possible to solve the $3B loss during Desert Storm and provide a truly hands off logistics tracking capability requested by warfighters. Commercial follow-on is likely. Appendix B describes the technology.

This page left blank

7.0 RECOMMENDATIONS

Three focus areas have been identified for future work. They derive from results and findings from the NTAV shipboard testing and understandings of the phenomenology and system performance factors. The three primary investment areas are:

- Accuracy and Performance Improvement
- Shipboard Environment/Testing/Modeling and Simulation
- Cost Reduction

7.1 Accuracy and Performance Improvement

The first investment area, accuracy and performance improvement, addresses improvements to COTS technology to make it applicable for shipboard environments, and advancing the emerging UWB technology towards commercialization. Three sub-areas have been identified for development:

- Algorithms
- "C" Band UWB
- Hybrid COTS/UWB
- Long Range COTS/UWB

Algorithms. Algorithm development is applicable to any localization technology, whether DSSS or UWB. Any system must pretty much do the same things after they hear tags and measure arrival times. Algorithm development for shipboard applications include:

- Bi-Lateration for Aisleway/Passageway/Container Faces
- Quad-Lateration for 3D
- Path Blockage and Reflection Recognition and Mitigation
- Optimum Antenna Set Selection
- Progressive Stacking/Blockage

"C" Band UWB. MSSI released a commercial "C" Band PAL system July 2003 [11]. The system operates at 6.35 GHz and is approved by the FCC. It has much smaller tags, "golf ball" size, and longer battery life (3+ years). It could be tested in a shipboard environment.

Hybrid COTS/UWB. Another approach is to create a UWB DSSS PAL system using >500 Mhz bandwidth for 1-foot accuracy. Recent hardware advances can be applied to achieve 10X bandwidth and processing power needed for UWB DSSS. Mature COTS can be levered to speed development. A 10X version of the newly approved ANSI T-20 Committee, BSR INCITS 371.1 – 2.4 GHz RTLS Air Interface Protocol standard can be used [13]. IEEE 802.15.3a, Wireless Personal Area Network (WPAN) proposed OFDM waveform, and IEEE 802.15.4a WPAN-LR (low-data rate) developing UWB waveforms may also be used. Development and testing can help IEEE 802.15.4 efforts.

- Merge Mature COTS with Emerging UWB
- Stability/Maturity/Algorithms plus Higher Accuracy
- ANSI/IEEE/ISO Standardization

Long Range COTS/UWB. A longer range UWB RTLS (10 miles) can be developed by modifying a COTS RTLS system to operate in the military UHF band (225 to 400 MHz). The wide bandwidth would result in a large fractional bandwidth, thus UWB. It would be a licensed system for military/government use only. It could track containers and major end items in ports using minimum infrastructure.

7.2 Shipboard Environment/Testing/Modeling and Simulation

The second investment area, shipboard environment/testing/modeling and simulation, focuses on the shipboard RF environment itself. Three sub-areas have been identified for development:

- Antenna Types and Locations
- Loaded Ship Configuration Testing
- Modeling and Simulation

<u>Antenna Types and Locations</u>. Antenna types will focus on virtual image reduction. Surface mount antennas including patch and other types of antennas and multiple polarization UWB antennas will be identified and tested. Alternate antenna locations will be also investigated to mitigate virtual images, and optimize signal blockage and reflections. The optimum number of antennas and locations will be investigated for different cargo holds and cargo stow locations for different MPF and LHD ships.

<u>Loaded Ship Configuration Testing</u>. Shipboard testing should be performed aboard loaded MPF and LHD ships. Improved COTS and UWB PAL systems will be installed on ships and improvements in algorithms tested with different loaded configurations. Different antenna types and locations will likewise be tested. This testing is expected to be expensive as coordination with Space and Naval Warfare Systems Command (SPAWAR) Systems Center (SSC) is needed for installations aboard ships.

<u>Modeling and Simulation</u>. A related effort will be performed in modeling and simulation for the shipboard RF environment. Virtual source ray tracing analyses will be performed to check sight lines from/to tags and antennas, checking for blockage and reflections. Shipboard metal surfaces, including decks, bulkheads, overheads, beams, etc. together with containers, will be treated as mirrors.

Animated visualizations will be created showing tag blinks and their reflections. Tags and their reflections will appear to scintillate throughout the space. DSSS and UWB RF waveforms will be superimposed on the blinks and summed, showing the summation effects of multipath. These simulations will be used to investigate optimum antenna placement and types.

Ray tracing analyses will be correlated with delay-spread measurements to validate the models. Other RF models used for cell-phone antenna placement in urban areas and aboard ship may also be tried.

7.3 Cost Reduction

The third investment area, Cost Reduction, focuses on dramatic cost reduction and capability improvement possible with the DARPA developed UWB localizer technology. It presents the greatest possibility for capability improvement, combining all facets of asset visibility into one architecture and system. It potentially provides the biggest bang for buck of all technologies. It depends on DARPA reaching a major milestone in localizer capability to work up to 30 meters.

Once the milestone is reached, the localizers would be tested in a shipboard environment, much the same as the other systems. If successful, it would follow the path of the other systems, with algorithm development and testing on loaded ships, and possibly aircraft carriers. Testing and validation of Autonomous Manifesting in containers would complete its capabilities.

We expect parallel commercial development with the technology once the localization milestone is reached. Localizers will need asset visibility and tag memory capabilities to be added to make them commercially viable. UWB localizer technology is furthest out, but provides the greatest potential and a possible transition of DARPA technology by ONR. Appendix B describes the technology and testing.

8.0 REFERENCES

1.   GAO Report B-246015, "Operation Desert Storm: Transportation and Distribution of Equipment and Supplies in Southwest Asia," 26 Dec 1991.

2.   Navy-Marine Corps White Paper, "...From the Sea," Article NNS 130, Navy News Service (NavNews 048/92), 6 October 1992

3.   Navy-Marine Corps White Paper, "Forward...From the Sea," Navy Office of Information, http://www.navy.mil, 9 November 1994

4.   Marine Corps Capstone Concept Paper," Operational Maneuver from the Sea," Marine Corps Combat Development Command, Quantico, Virginia, 4 January 1996

5.   Marine Corps Concept Paper, "Ship-To-Objective Maneuver," Marine Corps Combat Development Command, Quantico, Virginia, 25 July 1997

6.   Marine Corps Capstone Concept, "Expeditionary Maneuver Warfare," Supplement, Marine Corps Gazette, February 2002

7.   Gunderson, S.J, "Naval Total Asset Visibility: Application of Ultra Wide Band Location Systems for Precision Asset Location and Autonomous Manifesting," Briefing at ONR Workshop on Ultrawide-band Communications, Berkeley Wireless Research Center, Berkeley, California, 17 May 2000.

8.   First Report and Order, "Revision of Part 15 of the Commission's Rules Regarding Ultra-Wideband Transmission Systems, ET Docket 98-153," Federal Communications Commission, Washington D.C., Adopted: February 14, 2002, Released: April 22, 2002.

9.   Keynote Address, Gallagher, M.D., Deputy Assistant Secretary for Communication and Information, U.S. Department of Commerce, 2002 International Symposium on Advanced Radio Technologies, Institute of Telecommunication Sciences (ITS)/Nationa1 Institute of Standards and Technology (NIST), Boulder, Colorado, 4 March 2002.

10.   Keynote Address, "Walk DON'T Run -The First Step in Authorizing Ultra- Wideband Technology," Thomas, E.J., Chief, Office of Engineering and Technology, Federal Communications Commission (FCC), Institute of Electrical and Electronic Engineers (IEEE) Conference on Ultra Wideband Systems and Technology (UWBST) 2002, Baltimore, Maryland, 21-23 May 2002.

11.   Fontana, R.J., Richley, R., Barney, J., "Commercialization of an Ultra Wideband Precision Asset Location System," Proceedings, Institute of Electrical and Electronic Engineers (IEEE) Conference on Ultra Wideband Systems and Technologies (UWBST) 2003, Reston, Virginia, November 2003.

12.   Personal Communication, Leeper, D.G., Chief Technical Officer, Wireless Technologies, Intel Corporation, at UWBST 2002, Baltimore, Maryland, 22 May 2002.

13.   American National Standard for Information Technology – Real Time Locating Systems (RTLS) Part 1: 2.4-GHz Air Interface Protocol, BSR INCITS 371.1, American National Standards Institute, Inc. (ANSI), New York, NY, 2003.

14.   Fleming, R.A. and Kushner, C.E., "Technological Solutions to Autonomous Cargo Manifesting," Program Progress Report No.1, Aether Wire & Location, Nicasio, California, 6 February 2001.

15.   Schantz, H.G. and Fullerton, L., "The Diamond Dipole: A Gaussian Impulse Antenna," 2001 IEEE APS Symposium and USNC/URSI National Radio Science Meeting, Boston, Massachusetts, 8 July 2001.

16.   Fleming, R.A., Kushner, C.E, Killian, A.J.," Technological Solutions to Autonomous Cargo Manifesting - Additional Requirement," Aether Wire & Location, Nicasio, California, 22 October 2001.

Appendix A

USC Shipboard Environment Characterization

The University of Southern California (USC) UltRa Lab conducted shipboard RF environment characterization of the SS Curtiss immediately following the first week open space tests. Tests were not performed during the second week with containers. Dr. Robert Scholtz led the team of professors and students. The test provided an excellent opportunity for USC to perform channel measurements in a ship. They were funded by ONR Code 313 Marine Corps 6.1 research grant.

Four primary tests were run:

- Pulse Response with Sampling Oscilloscope
- Transfer Function with Network Analyzer
- Pulse Response with a UWB Test Radio
- Interference Check with Spectrum Analyzer

The pulse response with sampling scope test was straightforward, operating similar to container tests conducted by AetherWire at the Port of Oakland [14] and Appendix B. A low-powered pulser was connected to an UWB diamond dipole antenna [15] to radiate impulses. Synch reference was provided by coax cable to the sampling oscilloscope. Measurements were made with a 20 G sample/sec sampling oscilloscope connected to a pre-amplifier and matching diamond dipole antenna. Figure A-1 shows the pulse generator and oscilloscope equipment configuration.

The sampling scope had limited memory, thus many readings needed to be spliced together to form a composite picture, lengthening time required for measurement and limiting the number of tests that could be made. The sampling oscilloscope had high background noise, limiting noise floor, preventing measurement to -20 dB. Averaging was not used due to the long measurement times.

The network analyzer was used to improve noise floor. It measured the channel frequency and phase response and the result was Fourier transformed into the time domain. It had 40 to 50 dB lower noise floor than the digital sampling oscilloscope. Ship's high pressure sodium arc lamps were turned off, as they raised the noise floor 6 dB. Figure A-2 shows the network analyzer test equipment configuration.

The UWB test radios were Time Domain PulsON™ Application Demonstrator (PAD). They operated in pairs, one transmitting and the other receiving. They were used for channel measurements and sampled the environmental response, much the same as a pulse generator/sampling oscilloscope. They did not need a synchronization cable between units, they were able to automatically synchronize between themselves from received pulses. Samples were sent to a connected laptop PC. No pictures were taken of the PADs and no data was made available. Time Domain provided the units to USC under non-disclosure.

A spectrum analyzer was used to measure interference from shipboard radios and radars.

UWB diamond dipole antennas were used for all tests. They are like "bow-tie" antennas, with broad response, but have the "fat" side connected inside resulting in a diamond appearance. The PADs have smaller diamond dipole antennas, and the oscilloscope and network analyzer measurements used larger antennas with -3 dB response from 700 MHz to 1.8 GHz. Figures A-3 and A-4 show a test setup in holds 5 and 6. Figures A-5 thru A-7 show the measurement equipment, measurements and data processing equipment.
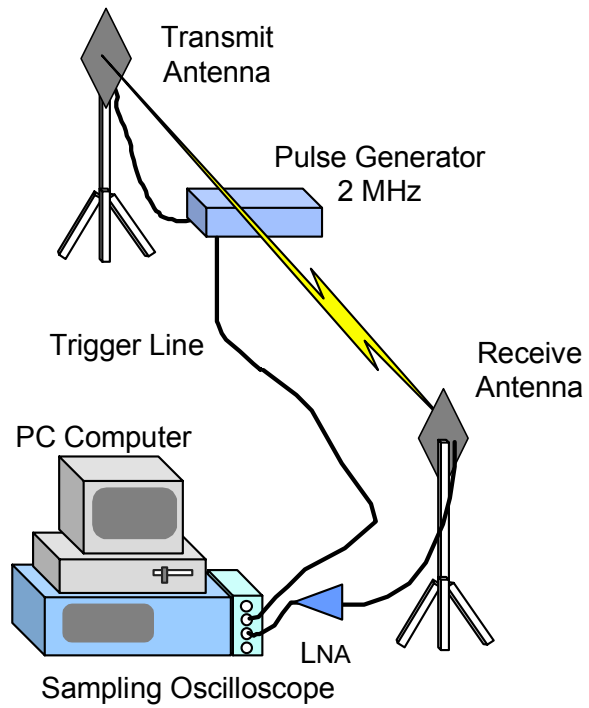
Figure A-1. USC pulse generator and sampling oscilloscope test equipment.
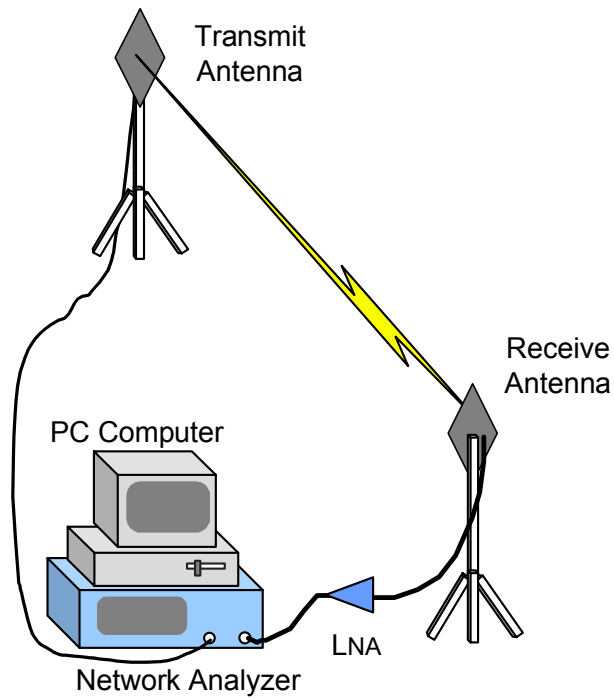

Figure A-2. USC network analyzer test equipment.

Figure A-3. USC test equipment setup in SS Curtiss Holds 5 and 6, looking port forward.
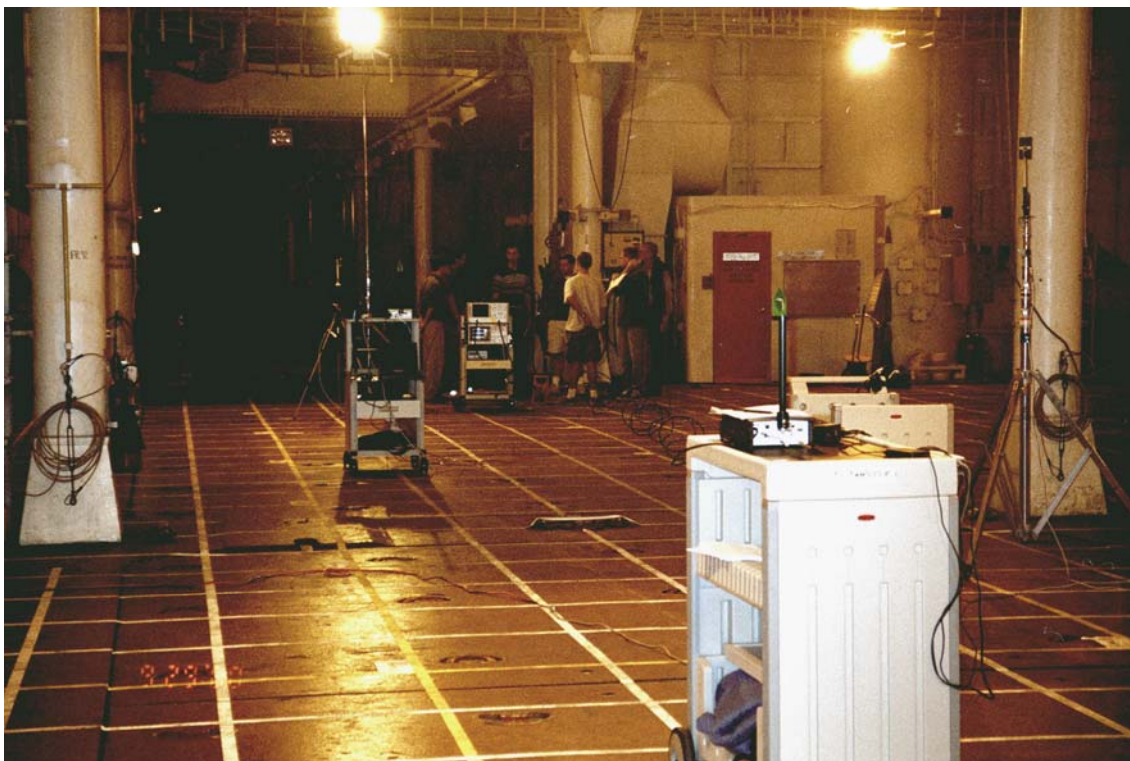

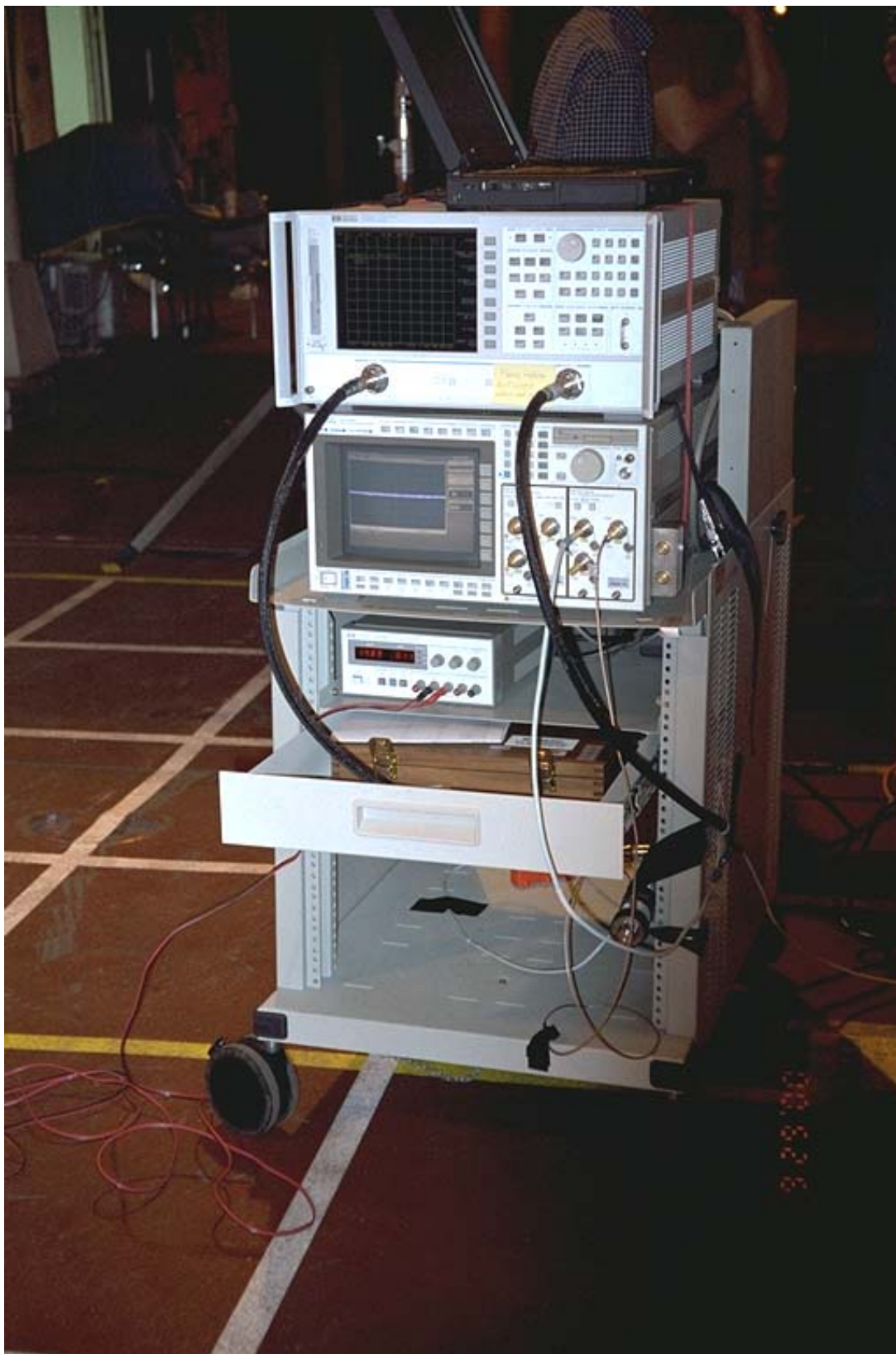Figure A-4. USC test equipment setup in SS Curtiss Holds 5 and 6, looking forward.

Figure A-5. USC network analyzer and sampling oscilloscope.

Figure A-6. USC team taking measurements.

Figure A-7. USC team processing measurements with PC and MATLAB.

Five different channel measurement tests were made with antennas in different locations, each with sampling oscilloscope and network analyzer. Figures A-8 through A-12 show the test configurations. The transmit antenna is the triangle and the receive antenna is the circle.
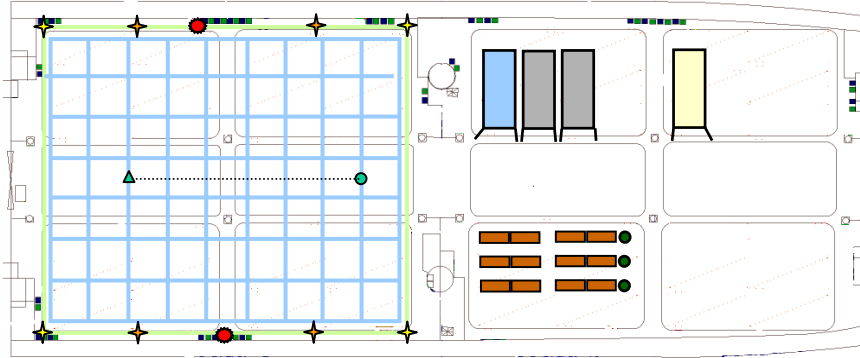
Figure A-8. Test 1 Configuration: 60-foot distance, down the middle.
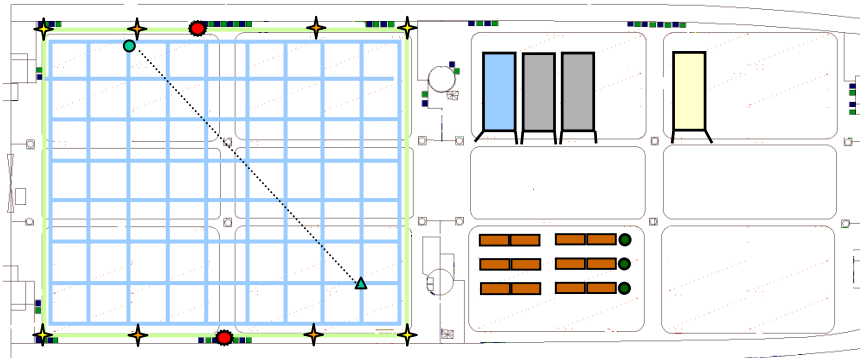
Figure A-9. Test 2 Configuration: 85-foot Distance, through a stanchion.
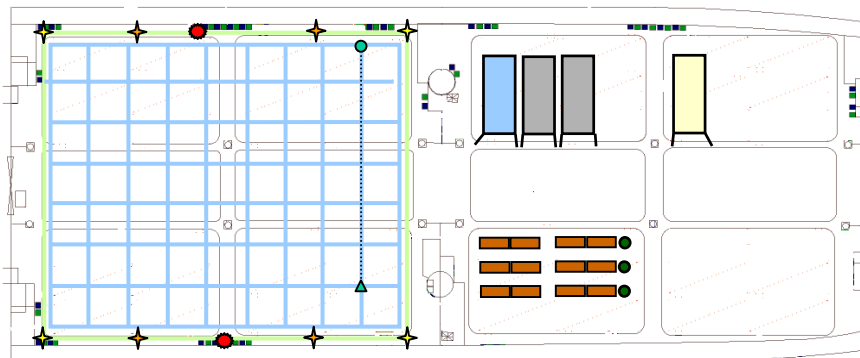
Figure A-10. Test 3 Configuration: 60-foot distance, to a corner.
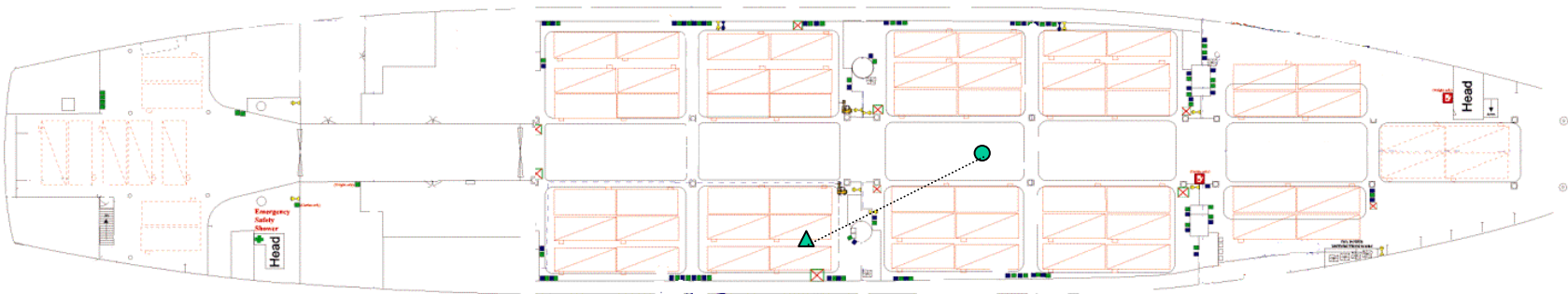
Figure A-11. Test 4 Configuration – 60-foot distance between two compartments and blocked by a bulkhead.
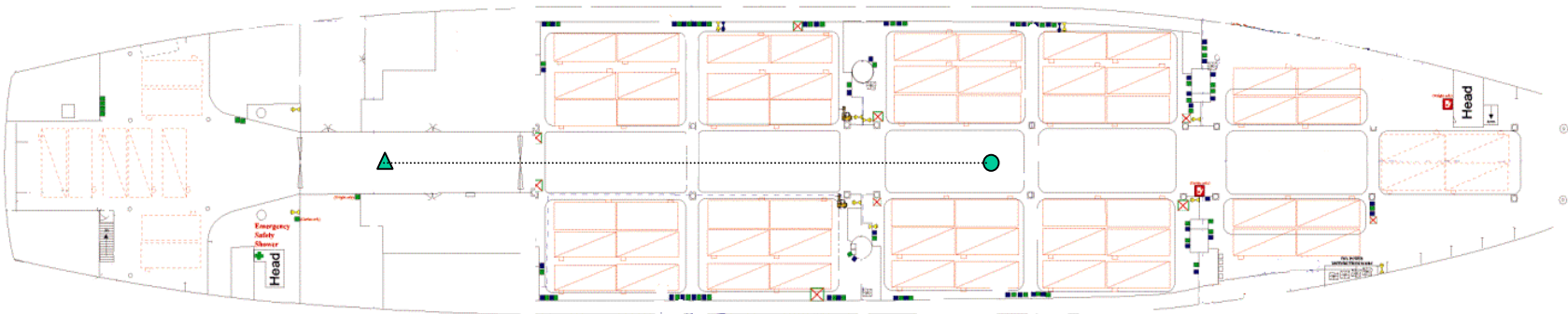
Figure A-12. Test 5 Configuration, 200-foot distance between two compartments and tunnel in direct line of sight.

A-7

Figures A-13 through A-17 show the sampling scope test results. Test 1 included 4 µsec of data. Data did not start at 0 µsec and decay times must be adjusted to account for the time offset. The high noise floor of the sampling oscilloscope of -6 dB masked the final decay to -20 dB, the normal delay spread figure. The -6 dB point was reached at about 1 µsec. The balance of tests included only 2 µsec of data, reducing time to take measurements. Decay time to -20 dB is estimated to be 2-3 µsec.
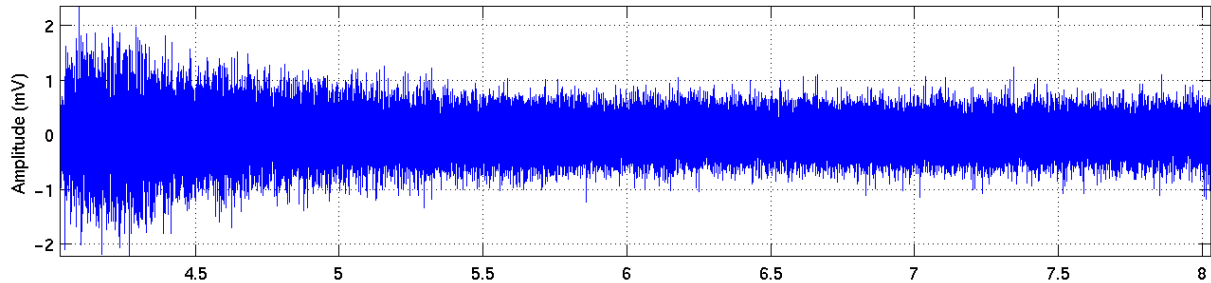
Figure A-13. Test 1 decay, sampling oscilloscope.
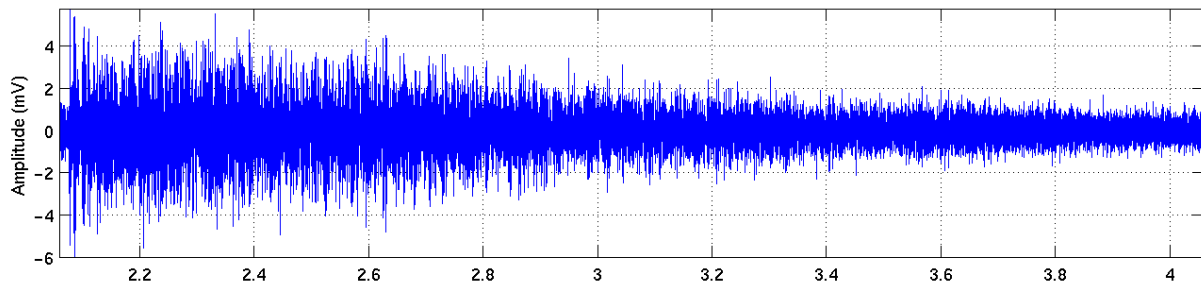
Figure A-14. Test 2 decay, sampling oscilloscope.
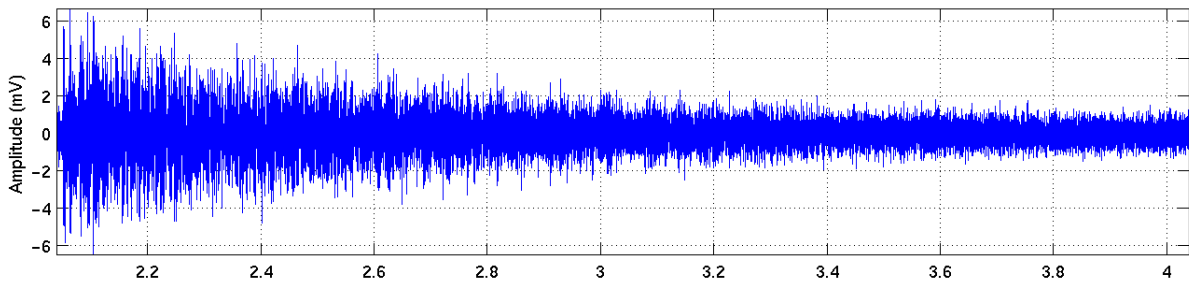
Figure A-15. Test 3 decay, sampling oscilloscope.
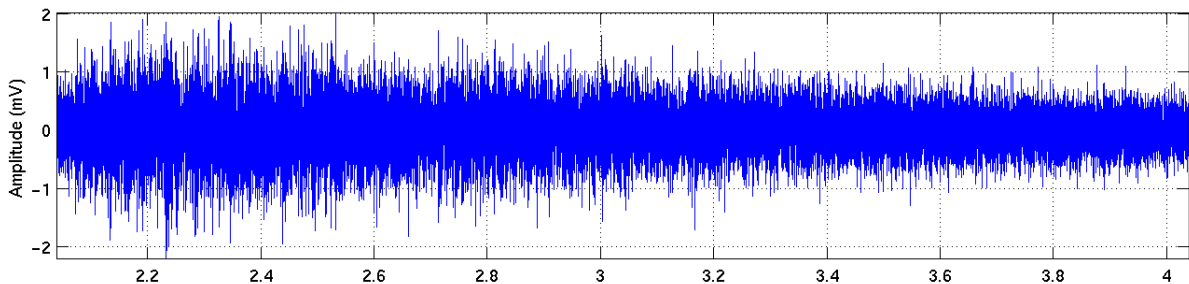
Figure A-16. Test 4 decay, sampling oscilloscope.

Test 4 shows no initial pulse, it was blocked by the bulkhead, and a slow ramp up of reverberation. Reverberation may have coupled between the two compartments through the opening, producing a double integration of energy.
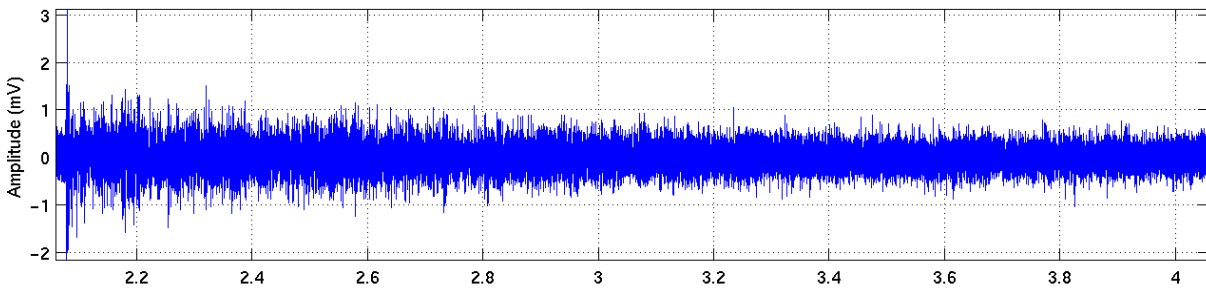

Figure A-17. Test 5 decay, sampling oscilloscope.

Test 5 shows the initial direct impulse is much higher than the overall reverberation. This may be caused by the direct line of sight filtering caused by the tunnel, providing little energy to the intervening compartment for reverberation.

Figures A-18 through A-21 shows the network analyzer measurements and Inverse Fast Fourier Transform (IFFT) for Tests 3 and 5. The network analyzer took 3,200 measurements at 1 MHz steps.
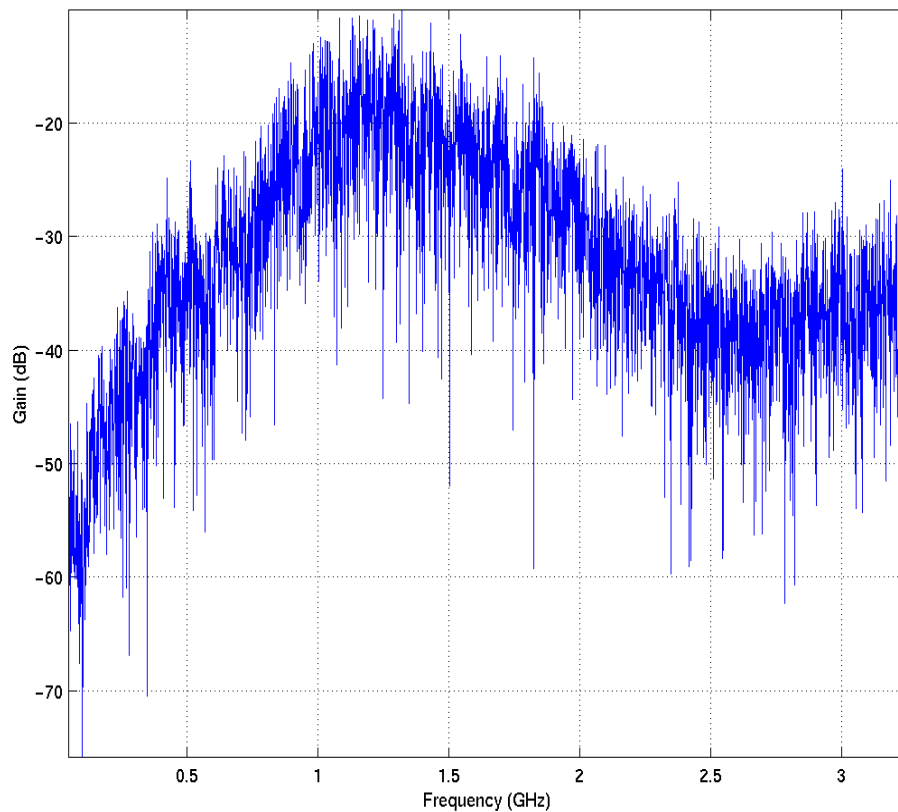

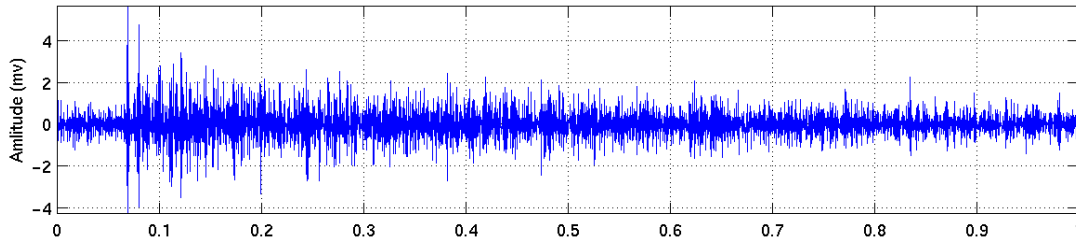Figure A-18. Test 3 amplitude measurement, network analyzer.

Figure A-19. Test 3 IFFT time response, network analyzer.

Figure A-18, Test 3 amplitude, the magnitude of the envelope of amplitude measurement is largely the square of the antenna responses. -6 dB responses correspond to each antenna's -3dB response. Multipath nulls are visible in the amplitude plot, extending up to 30 to 40 dB below average.

Figure A-19, Test 3 IFFT, shows the initial impulse delayed by 60 nsec, corresponding to 60-foot antenna separation. This provides excellent confirmation of the network analyzer/IFFT measurement technique.

Figure A-20, Test 5 amplitude, multipath nulls are visible in the amplitude plot, extending up to 30 to 40 dB below average.
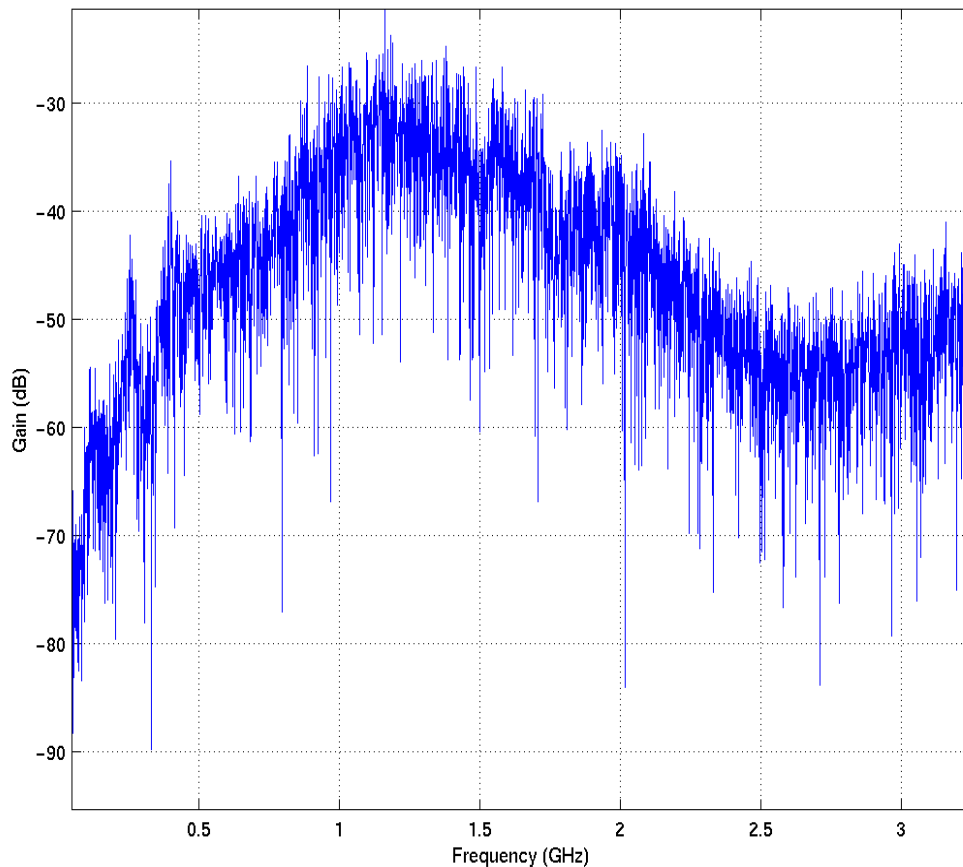

Figure A-20. Test 5 amplitude measurement, network analyzer.

Figure A-21, Test 5 IFFT, shows the initial impulse delayed by 210 μsec, corresponding to the 200-foot antenna separation. This again provides excellent confirmation of the network analyzer/IFFT measurement technique.
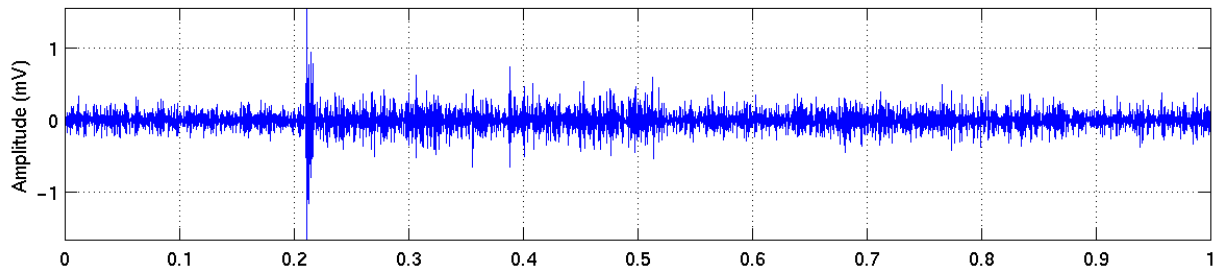

Figure A-21. Test 3 IFFT time response, network analyzer.

Figure A-22 shows a spectral measurement of a shipboard 10 GHz X-band search radar signal through a UWB antenna, made in the enclosed cargo bay of the USS Curtiss. The spectrum analyzer resolution bandwidth was 300 kHz, with *max hold* feature ON. Instantaneous or average measurements did not show significant energy. Peak measurements were required for the radar. Ship's radar emissions leaked into the closed cargo holds.
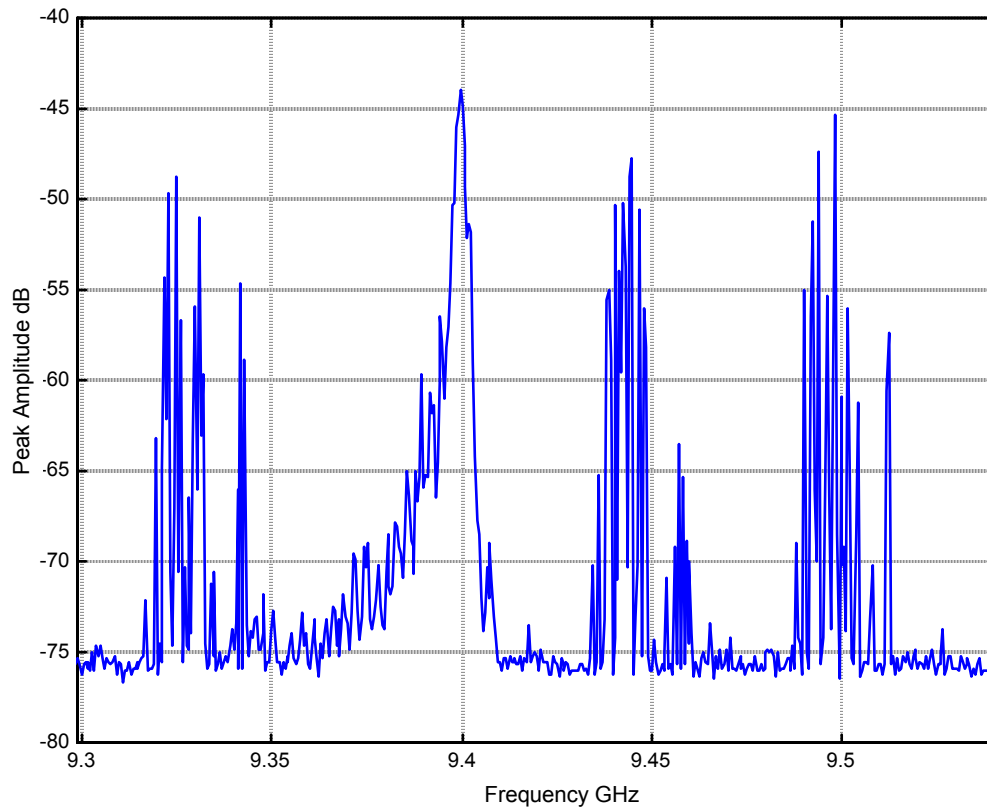

Figure A-22. Radar interference measurement, spectrum analyzer.

The scope data was auto-correlated to look for internal structure, indicating possible resonances. Figure A-23 shows a sample of oscilloscope sampled data and Figures A-24 through A-26 show the auto-correlation.   The auto-correlation showed the antenna impulse responses and no resonances. The passband of the test setup was likely too high to excite the ship's compartment cavity resonances.
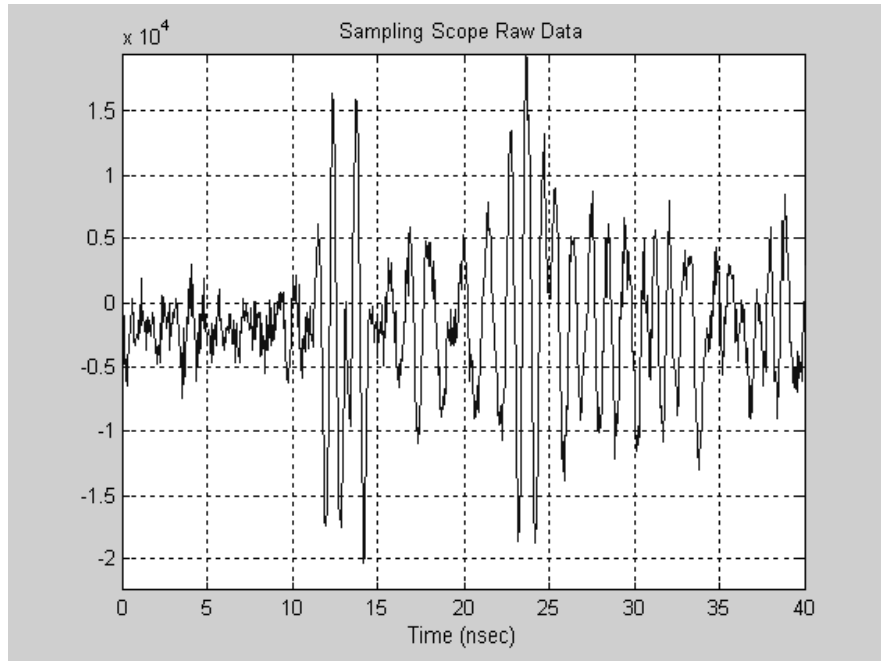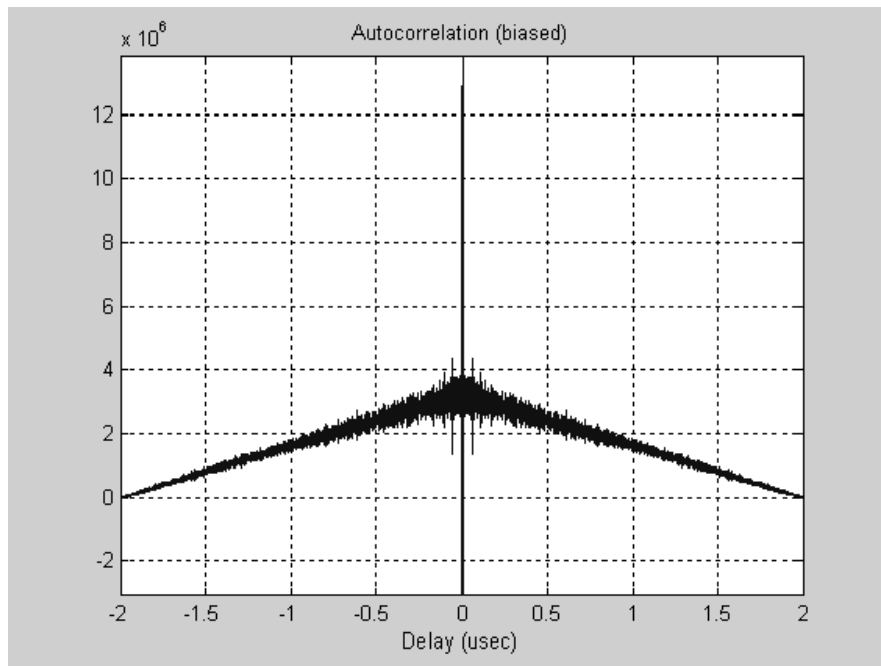

Figure A-23. Sampling scope raw data.
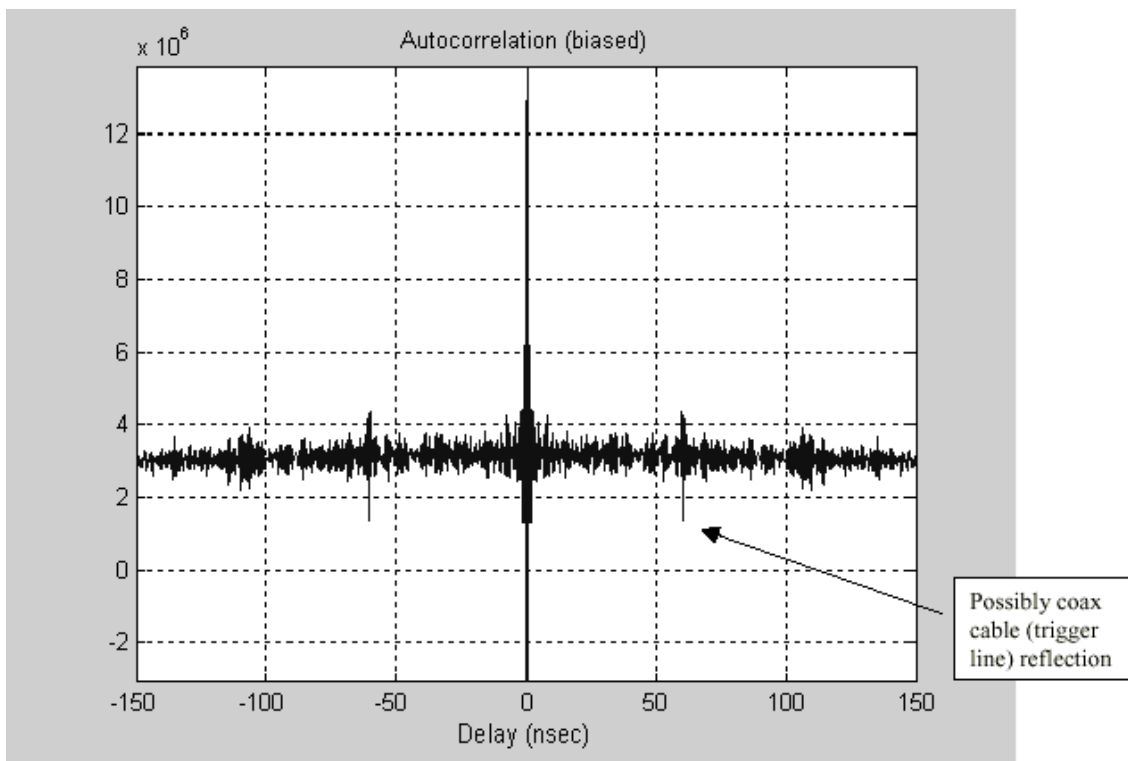

Figure A-24. Self auto-correlation, ± 2 μsec.
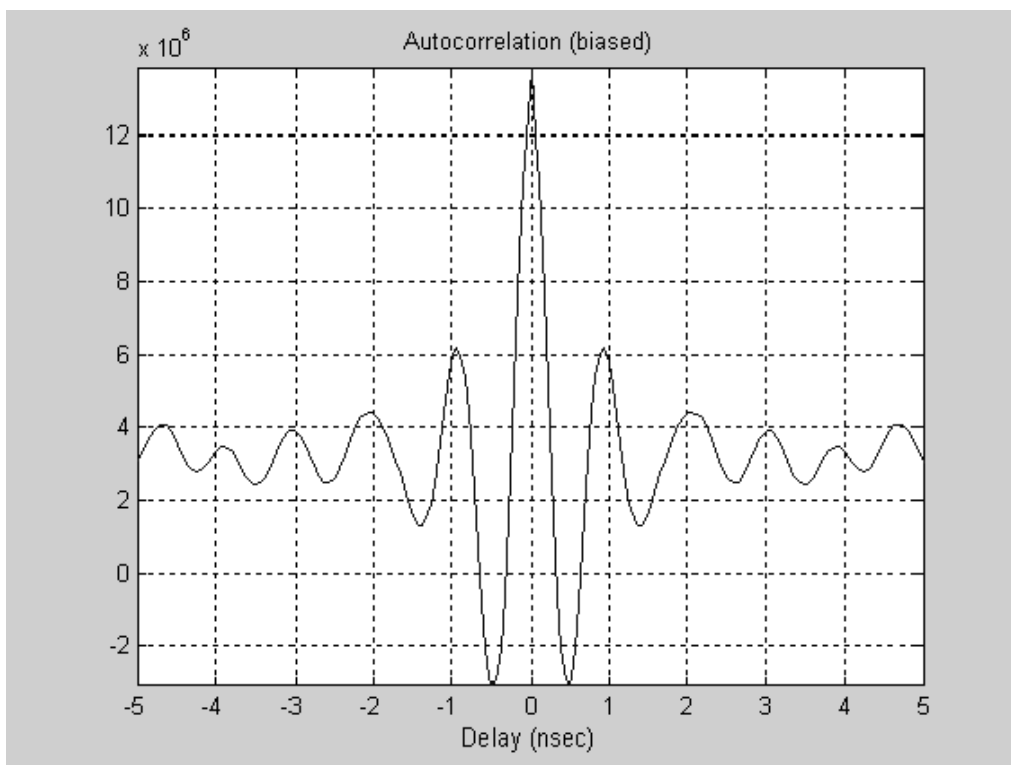
Figure A-25. Self auto-correlation, ± 150 µsec.

Figure A-26. Self auto-correlation, ± 5 µsec.

CONCLUSION

The SS Curtiss had very long delay spreads, approximately 1 µsec to -6 dB, and estimated 2-3 µsec at -20 dB. This is approximately 10 – 300 times longer than 10 to 300 nsec typical of office and industrial environments. It is also longer than 0.5 to 1 µsec typical for ISO containers [14], Appendix B. The WhereNet DSSS system was designed to operate up to 1 µsec delay spread. The ship exceeded that.

Multipath nulls were measured between 30 to 40 dB using a network analyzer. They would greatly affect narrow-band systems causing dropouts. The multipath nulls had some effect on the DSSS system with 60-MHz spread, particularly with 4 antennas; and little effect on the UWB system with 400-MHz instantaneous bandwidth.

The ship's 10 GHz "X" band radar leaked into the compartments, but was higher in frequency than the test systems. Ship navigational radars also operated at 3.1 GHz, close to, but still above the 2.45 GHz ISM II frequency band used by the DSSS WhereNet system. 3.1 GHz is the lower frequency bound for FCC Part 15 Subpart F unlicensed UWB "C" band operation.

Ships present a challenging RF environment with long delay spreads and deep multipath nulls. It is amazing that either of the tested PAL systems worked aboard the ship. The RF environment may explain some of the difficulty the WhereNet DSSS system had with dropouts with 4 antennas; and the MSSI UWB system had with out-of-scale readings, and pops and jumps.

Figure A-27 shows the USC team in front of the SS Curtiss.

Figure A-27. USC team in front of the SS Curtiss.

Appendix B

Autonomous Manifesting

Background. During Desert Shield/Desert Storm, 40,000 ISO containers were shipped into the theater. 25,000 of those containers were opened to determine their contents as paper manifests were inaccurate or lost.   The lack of confidence in the logistics system resulted in 2-3x over shipment, and with misplaced and lost materiel, resulted in losses totaling $3 billion per GAO Report B-246015, Dec 1991 [1].

Following Desert Storm, the ability to automatically manifest containers was identified.   The objective was to tag items, place them in ISO containers, and after doors were closed, the containers would automatically read the tagged items and update their electronic manifest. This would enable warfighters to rapidly load and unload containers without cumbersome and error prone manual inventory procedures. Warfighters could then concentrate on the fight.

After Desert Storm, DoD and commercial efforts began to develop Radio Frequency Identification (RFID) to automatically manifest containers and provide remotely readable electronic manifests. Various approaches were tried including portal readers with bar codes, passive RFID, magnetic loops, acoustics, and other methods. All of these failed for various reasons and were not commercialized. (If they worked, they would now be pervasive).

The most common proposed and tried approach was to use a barcode/passive RFID interrogator at a container door to read tagged items as they are loaded and unloaded. The primary failure of this approach is knowing whether items entered or exited through the door. It cannot be known for certain whether an item is inside or outside, just that it passed by. Items outside the container, near the front door, also can cause erroneous readings.

Another operational failure of the portal approach is needing to manually scan bar-coded items as they enter/leave requiring additional handling. Passive RFID readers are expensive, sometimes more expensive than the container itself ($3,000). Passive RFID tag and reader costs continue to decrease and this approach may become viable in the future. The need to reliably measure whether an item entered or exited a container is still required for this approach to work reliably and to be accepted.

The second common approach is to bound interrogation inside a container after the container doors are closed. This is complicated by tightly stuffing the containers (Figure B-1) producing blockage and preventing reliable reads.   A passive RFID system can be used to scan the contents of the container after stuffing, just before the door is closed. This eliminates the logic problem of knowing whether items are inside or outside the container. Passive RFID readers do not have enough range to reliably read tags from the front to the rear of the container (usually 40 ft, but up to 53 ft). Very high reader power levels (10W) are needed

Figure B-1. Tightly stuffed container.

to overcome tag orientation, multi-path nulls, and blockage. Battery powered passive tags can increase range and/or reduce reader power level, but increase tag cost.

NFESC Autonomous Manifesting Test: NFESC conducted autonomous manifesting tests under the Marine Corps Systems Command (MARCORSYSCOM) Advanced Warfighting Technology (AWT) sponsorship in November 1994 in Port Hueneme. These tests used a Savi RFID system operating in UHF bands of 315 and 433 MHz. Empty containers were placed in a row side-by-side on trailer chassis, such that the containers were elevated above ground, Figure B-2. Hand-held interrogators were placed inside the containers to simulate a dedicated container reader. RFID tags were installed on empty cardboard boxes, the tagged boxes placed in the containers, and the doors shut. The objective was to uniquely read the tagged boxes in the containers and to manifest the contents of each container.
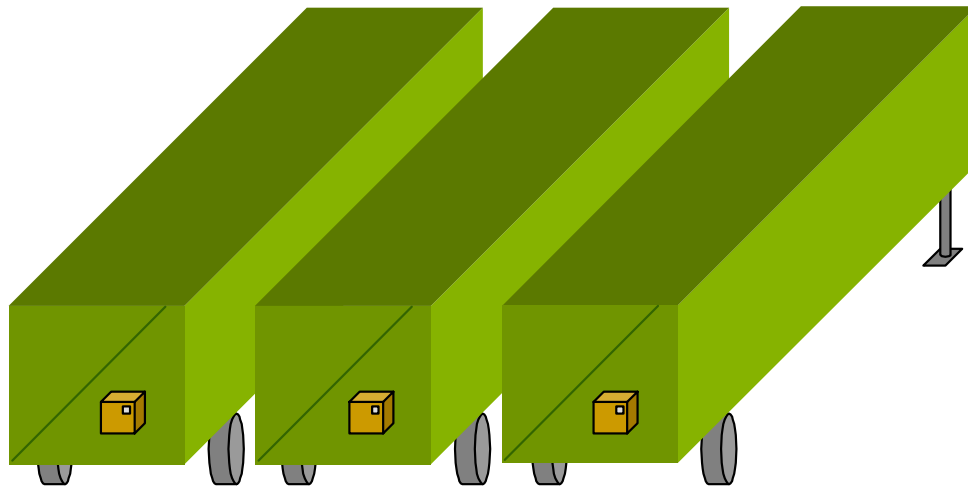

Figure B-2. Adjacent containers on trailer chassis.
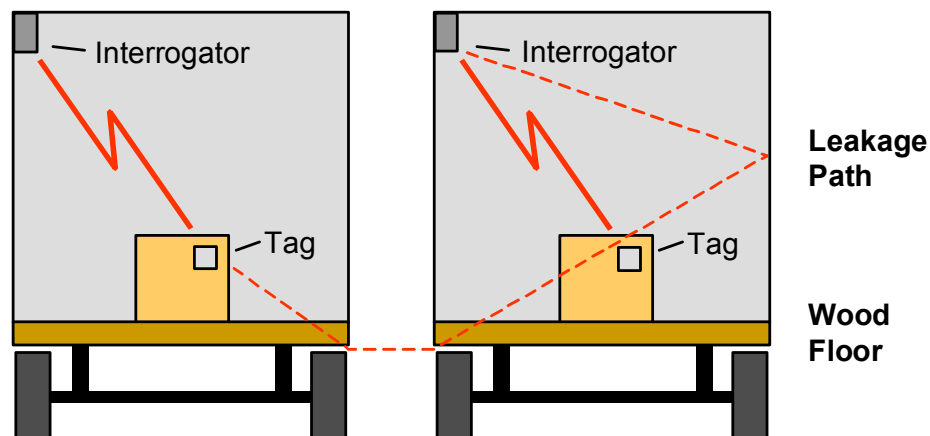

Figure B-3. Adjacent containers and RF leakage through wood floors.

All of the tags were read, however, tags in adjacent containers were likewise read. Interrogators could not discriminate tags inside or outside containers, or in adjacent containers. ISO containers have wood floors and the radio frequency (RF) leaked through the floors into adjacent containers, Figure B-3. The signals were attenuated between containers, but were still strong enough to be read. Tags were read as far as 2-3 containers down. Closing the container doors did not bound the interrogation as hoped. Other approaches were tried including acoustics, magnetics, and higher RF frequencies. Each had its own limitations and problems. Autonomous manifesting needs a way to limit interrogation to a container.

Naval Total Asset Visibility: The Office of Naval Research (ONR) funded the Naval Total Asset Visibility (NTAV) project to address deficiencies in current automatic identification technologies (AIT) for seabasing. The objective of seabasing is to provide selective offload and just-in-time delivery directly to inserted forces without logistics buildup ashore. Automatic tracking is needed to speed locating items aboard ships. The goal is to be able to identify a specific item, on a specific pallet, in a specific container, and in a specific storeroom.

NTAV focused on next generation RFID systems with the ability to localize.   The objective was to locate items aboard ships within 1-foot. Current state-of-the-art of commercial Real Time Location Systems (RTLS) was 5-10 foot accuracy due to limited bandwidth in unlicensed bands. This is adequate to locate containers and major end items (vehicles), but is not adequate to locate a box or pallet without uncertainty. 1-foot resolution is the most heard accuracy benchmark for warehousing and manufacturing.

Ultra-Wideband (UWB): Ultra-Wideband (UWB) was identified as a potential technology to achieve greater accuracy using greater bandwidth.   The FCC opened over 7.5 GHz of bandwidth for unlicensed UWB operation on February 14, 2002.   Greater accuracy is now possible because of greater available bandwidth. 1-foot accuracy can be readily achieved with 500-MHz minimum bandwidth specified by the FCC from 3.1 to 10.6 GHz.

During our technology survey, we learned of DARPA investment in UWB localizers being developed by Aether Wire and Location, Inc. Their objective was to develop cooperative ranging localizers with 3D localization with 1-cm accuracy and 30-m range for virtual reality. The localizers also would have ad-hoc networking, able to self organize networks and to relay information between localizers. The localizers are a transceiver based localization system with receiver and transmitter in each unit, unlike beacon systems with use a transmitter tag with a set of receivers. The localizers were targeted to become single chip designs, and were presently two custom chip designs with supporting circuitry. Figure B-4 shows the fourth generation localizer available in 2000 and figure B-5 shows the fifth generation localizer available in 2002.

Figure B-4. Fourth generation localizer (actual size).   Figure B-5. Fifth generation localizer.

Autonomous Manifesting Hypothesis: We realized high accuracy localization on the order of inches may be able to solve the container autonomous manifesting problem. It may be possible to know if tagged items are inside or outside a container by knowing its location. Localizers would form a reduced scale version of a Precision Asset Location (PAL) system within a container. The required range would be 10's of feet, 10 times smaller than a ship, and the required accuracy would be 10 times less, or about an inch. Location knowledge would effectively bound interrogation.

Single chip self-networking localizers would allow that tags themselves to become the reader/ interrogators and overcome cargo blockage in containers. No dedicated expensive reader/interrogators would be needed nor permanently installed. Single chip designs would reduce tag costs to acceptable levels and potentially follow Moore's Law. Figure B-6 shows a notional concept for localizer installation in a container and on tagged items.

Autonomous Manifesting Concept

Reference Localizers

Tagged Items

Self Networking / Ranging Localizers Form Ad-Hoc Localizing Network for Tag Locations
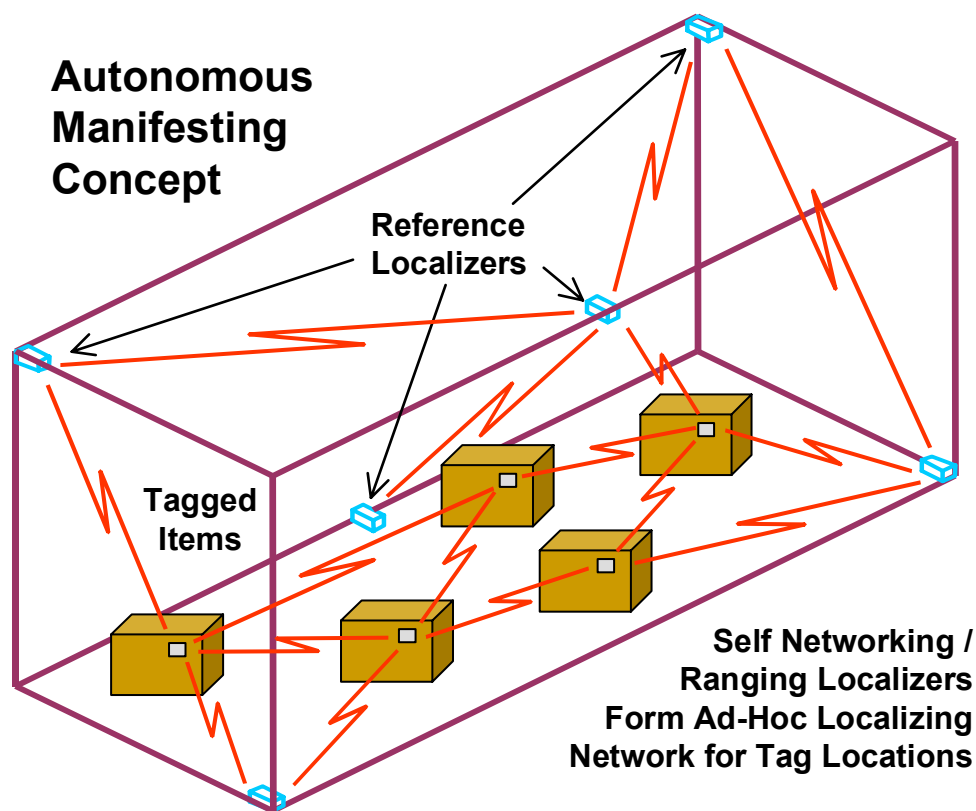
Figure B-6. Autonomous manifesting localizer Installation in containers and on tagged items.

We contacted the Dr. Norm Whitaker, DARPA Program Manager of the Warfighter Visualization Program. We discussed our logistics application and he agreed to its military and commercial payoff and significance. We requested permission to test the Aether Wire localizers for Autonomous Manifesting in our NTAV program.   He agreed and Aether Wire responded to our Broad Area Announcement (BAA). Aether Wire proposed testing the container RF environment to see if localizers would work in containers. The localizers were not ready to be directly tested in containers as they were still in development.

Berkeley Wireless Research Center UWB Workshop: We presented the Autonomous Manifesting with UWB localizers concept at ONR Workshop on Ultrawideband Communications at the Berkeley Wireless Research Center, Berkeley, California, 17 May 2000, sponsored by Dr. Jim Freebersyser, ONR Code 313. This was the first public presentation of the Autonomous Manifesting with UWB concept [7].

Port of Oakland Container RF Characterization: Aether Wire and the Naval Facilities Engineering Service Center (NFESC) conducted an initial RF characterization of ISO containers at the Port of Oakland on 25 May 2000. The tests were conducted at the Hawk Transportation facility underneath the I-80 freeway interchange near the tollbooths to the city of San Francisco. Figure B-7 shows the test site layout showing container locations and types. Figures B-8 and B-9 show the stacked container configurations.

Figure B-8. 2x2 stacked containers.

Figure B-7. Port of Oakland container layout.   Figure B-9. Side-by-side containers on trailers.

The 2x2 stacked and side-by-side containers were standard 40-ft ISO containers with corrugated steel sides and wood floors with steel supports.   The 2x2 stack was used for RF multipath and inter-container leakage measurement on ground and stacked. The side-by-side containers were used RF leakage tests through the wood floors to repeat the earlier Savi tests. A refrigerated container (reefer) was also used for RF multi-path tests. It had corrugated aluminum walls and an extruded aluminum floor with I-beam like rails to allow air return across the floor. It presented the worst case multipath test with metal surfaces on all six faces. A composite container was not located for the tests and was not used.

The 2x2 stacked containers faced east towards the City of Oakland. The side-by-side containers on trailers and the refrigerated container faced west towards San Francisco across the Bay. Television towers on top of Twin Peaks were clearly visible and radiated directly into the side-by-side containers. Orientation towards San Francisco and the television towers was significant as measured background interference levels were much higher in the west facing containers. This affected leakage measurements between containers as background noise levels were similar to leakage levels and averaging was required to minimize background noise from San Francisco. Background noise was not a problem with east facing 2x2 stacked containers for leakage measurements.

Test Equipment: Container RF measurements were made using UWB impulses and capturing with a 10 Gsample/sec digitizing oscilloscope. A fast high-amplitude pulse generator drove a Transverse Electro-Magnetic (TEM) horn antenna with -3dB response from 100 MHz to 8 GHz. A like TEM horn antenna was connected to the digitizing oscilloscope either directly, or through broadband amplifiers for inter-container leakage measurements.   The digitizing oscilloscope was synchronized to the pulse generator via a custom fiber optic cable to minimize radio frequency interference (RFI) propagating down a metallic cable. The pulse generator was likewise run off a battery through an uninterruptible power supply (UPS) to eliminate conducted interference through power cables.   The digitizing oscilloscope was operated off a portable 120VAC power generator through an isolation transformer.

Table A-1 lists the test equipment and Figures B-10 through B-13 show the test equipment and setup.

Table A-1. Test Equipment

| Vendor	Item	Qty	Description
Picosecond Pulse Labs	Model 2600 Turbo Pulse Generator	1	45 V at 300 psec Rise Time and 600 psec Fall Time
Tektronix	TDS 694C Digital Oscilloscope	1	10 Gsample/sec, 3 GHz Bandwidth Real-time Digitizing Oscilloscope
Farr Research	Model TEM-01-100 TEM Horn Antenna	2	100 MHz – 8 GHz, -3 dB
Mini-Circuits	Model ZJL-3G Broadband RF Amplifier	1 1	19 dB Gain, 20 MHz – 3 GHz, +/- 2.2 dB
APC	Uninterruptable Power Supply (UPS)	1	Back-UPS Pro, 650 VA, for Pulse Generator
Aether Wire	Fiber Optic Sync Cable	1	Custom
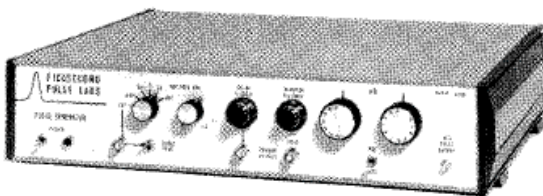
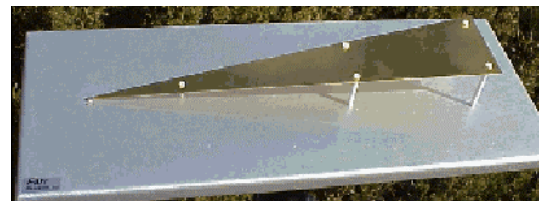Figure B-10. Picosecond pulse generator.

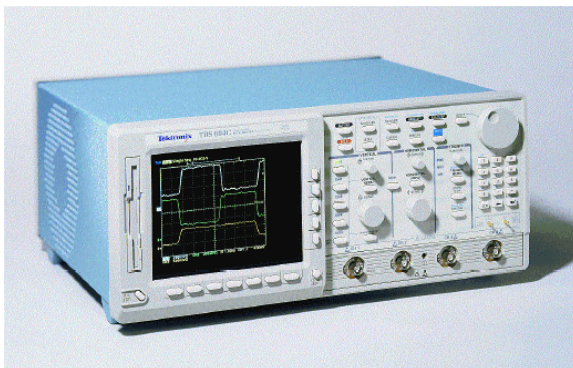Figure B-11. Farr Research TEM horn antenna.

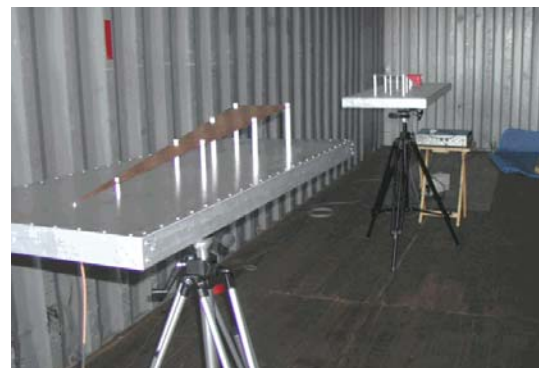Figure B-12. Tektronix digitizing oscilloscope.

Figure B-13. Typical test setup.

Figure B-14 shows free-air response outdoors of the test setup. The pulse generator was connected to a TEM horn. It was pointed at the second TEM horn connected to the digitizing oscilloscope. The resulting waveform is a double differentiated Gaussian impulse. The waveform is nearly theoretical with a large center peak and two lower negative peaks. The approximate 800 psec period indicates a 1.2 GHz center frequency.
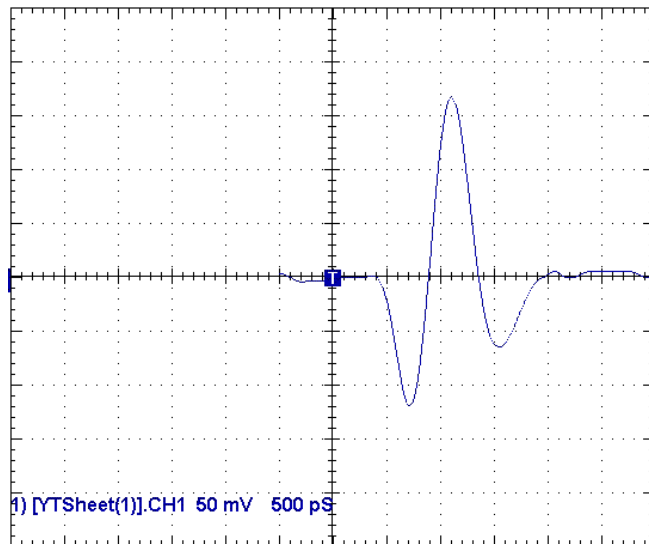

1) [YTSheet(1)].CH1 50 mV   500 pS

Figure B-14. Free-air time response of test setup, 500 psec/div.

Figure B-15 shows the background interference spectrum in a open container facing westward towards San Francisco. The large spikes on the left are broadcast VHF FM and VHF/UHF TV stations, and analog cellular <1 GHz. The small spikes on the right are PCS cellular telephones centered around 1.9 GHz. Background interference was very strong and averaging was used to reduce its effect for inter-container RF leakage measurements. Figure B-16 shows the effect of measurement before averaging and after averaging 100 samples. Effective reduction of interference is 20 dB, or 10 times.

1) [YTSheet(1)].CH1 10 dB   200 MHz

4) [YTSheet(1)].CH1 10 mV   5 nS
2) [YTSheet(1)].CH1 10 mV   5 nS

Waveform 1 With Averaging (100x)
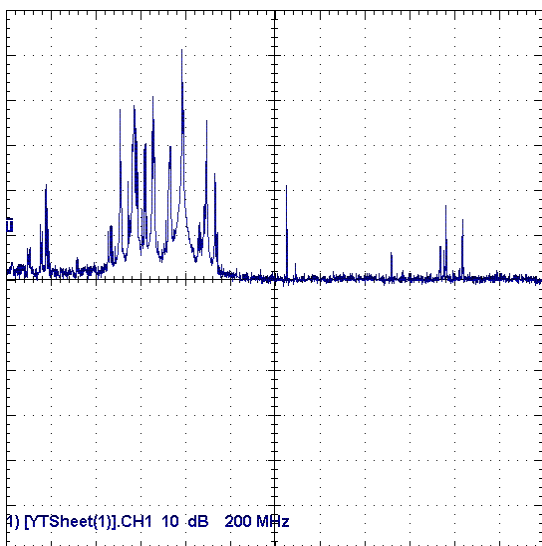Waveform 2 Without Averaging

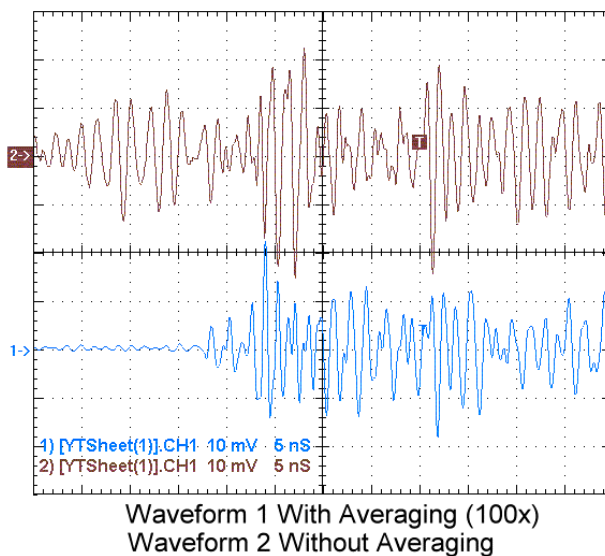Figure B-15. Background interference frequency spectrum, 0-2.4 GHz.

Figure B-16. Background interference plus signal and signal alone after averaging.

B-7

Test Setup and Procedure: Multipath and leakage measurements were made in different container configurations. Tests were performed with doors open/closed, and various antenna locations and orientations. Table B-2 provides an overview of the tests. Figures B-17 through B-19 show example tests.

Table B-2. Test Summary

Container	Test	Description
2x2 Stack	Multipath	Container on Ground
		Stacked Container on Top
	Leakage	Containers on Ground
		Stacked Containers on Top
		Top to Bottom Container
		Outside Into Top Container
Side-by-Side	Multipath	Container on Trailer Chassis
	Leakage	Containers on Trailer Chassis
	Interference	Container on Trailer Chassis
Refrigerated	Multipath	Container on Ground

Figure B-17. 2x2 container test setup.

Figure B-18. Side-by-side container leakage test.

Figure B-19. Refrigerated container multipath test.

Test Results: Measured multipath inside containers was much worse than expected. The textbook predicted about 50 nsec reverberation decay time. The longest decay time was 1,000 nsec to 10% (-20 dB) of its peak amplitude inside the refrigerated container. Antenna location and orientation did change decay times. Figure B-20 shows the measured reverberation decay inside the refrigerated container with the doors closed and the antennas at opposite ends, 29-feet apart.
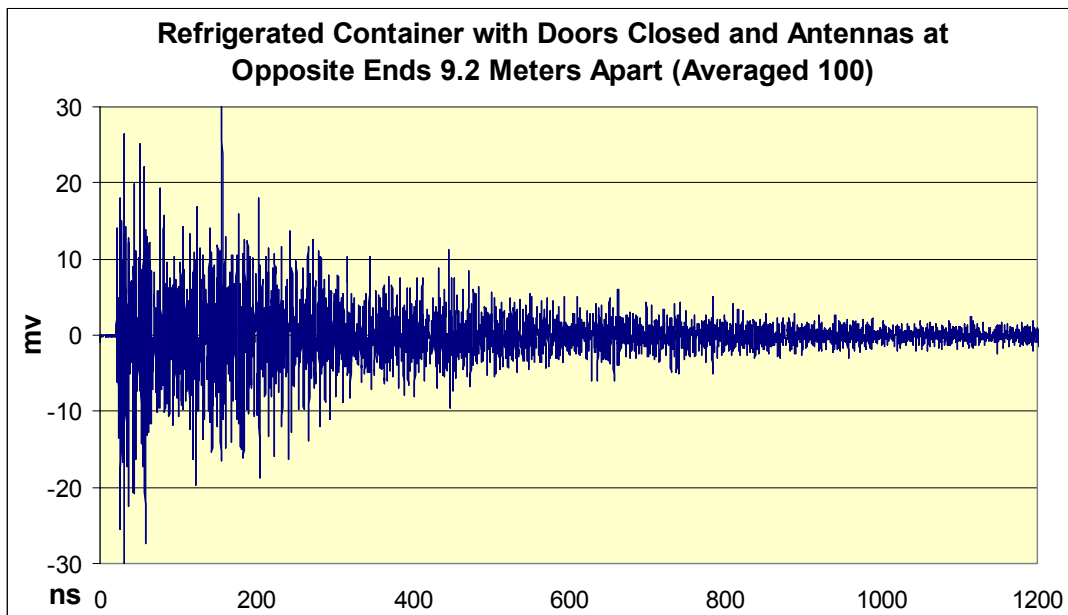
Figure B-20. Refrigerated container reverberation, doors closed, antennas opposite ends.

Figure B-21 shows RF leakage between side-by-side containers on truck trailers. Leakage is 20-30 dB lower than internal reverberation. The leakage waveform looks much like internal reverberation.
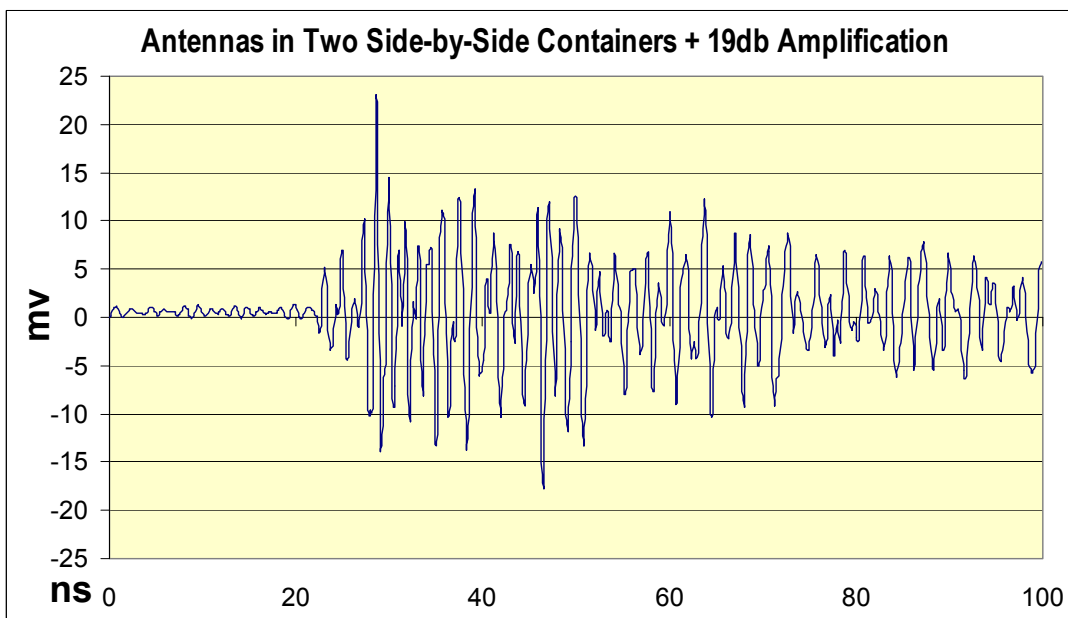
Figure B-21. RF leakage waveform between side-by-side containers on trailers.

Eureka!!!:   During data reduction, Aether Wire convolved the measured container delay spreads with their doublet waveform, and found the reverberation nearly disappeared. The first reaction was "Oh, That's funny."[1] Further checks found the phenomenon was correct. The majority of the energy in the delay spread is resonances and were nearly cancelled by the Aether Wire doublet waveform. They slowed their fourth generation localizers down from 5 nsec to 7 nsec due to problems with early localizer chips, which fortunately coincided the doublet notches with the container resonances.

Figure B-22 shows an expanded start of a received waveform. Distinct multipath reflections are visible for the first 40 nsec, then the waveform turns into a decaying oscillation with the appearance of beat frequencies causing sinusoidal amplitude variation.   Figure B-23 shows the Fourier transform frequency spectrum of the same waveform. Regularly spaced peaks are visible in the spectrum with an overall downward slope with increasing frequency.
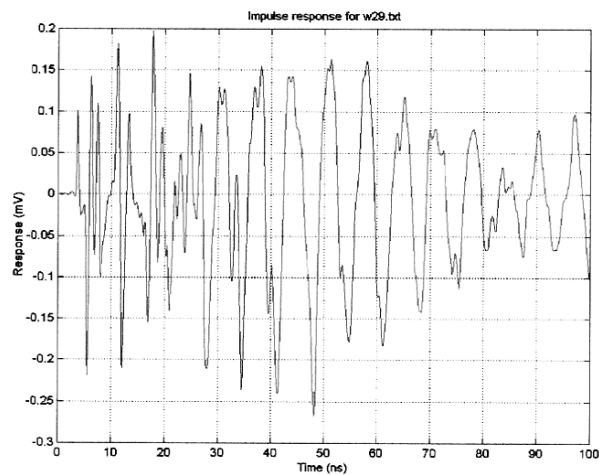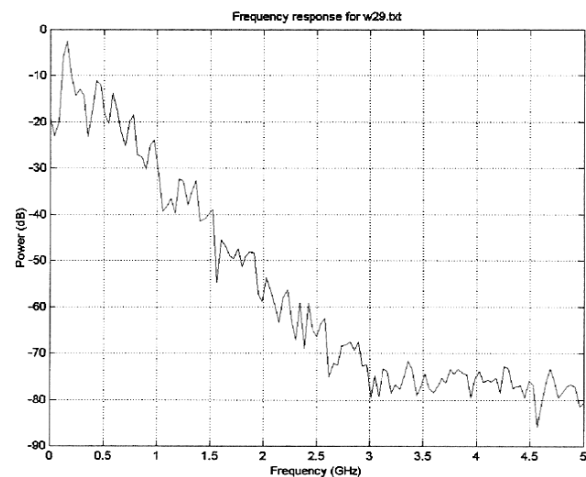

Figure B-22. Early impulse response.
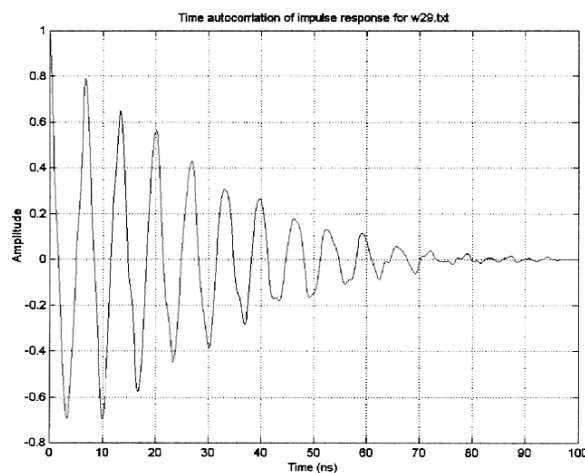

Figure B-23. Frequency response.

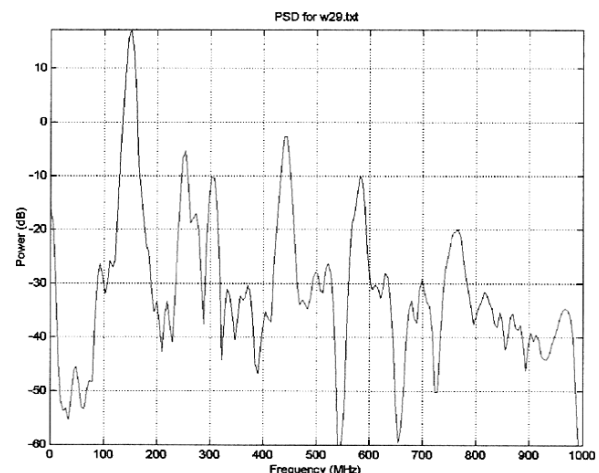Figure B-24. Time auto-correlated response.

Figure B-25. Power spectral density.

---

[1] "The most exciting phrase to hear in science, the one that heralds new discoveries, is not "Eureka!" (I found it!) but "That's funny..."" -- Issac Asimov

The waveform was then time auto-correlated with itself to reveal internal structure, Figure B-24. The internal waveform is a damped sinusoid with 7 nsec duration (same as the Aether Wire doublet) and decays within 80 nsec, close to the earlier textbook estimate. Figure B-25 shows the Fourier transform frequency spectrum of the autocorrelated waveform (power spectral density, PSD). Resonances appear at 150, 300, 450, and 600 MHz, or harmonics of a fundamental. The primary resonance of 150 MHz and 6.5 nsec period coincides roughly with the primary horizontal and vertical dimensions of the container of 8 feet or 8 nsec. Another peak at 250 MHz with 4 nsec period is likewise apparent.

Figure B-26 shows standing waves. Metal surfaces provide electrical shorts resulting in minimums. Closed standing waves are integral multiples of 1/2 waves. The wood floor provides an open end with a maximum, and supports 1/4 standing waves. Harmonics are odd series, 1/4, 3/4 much as an open pipe.
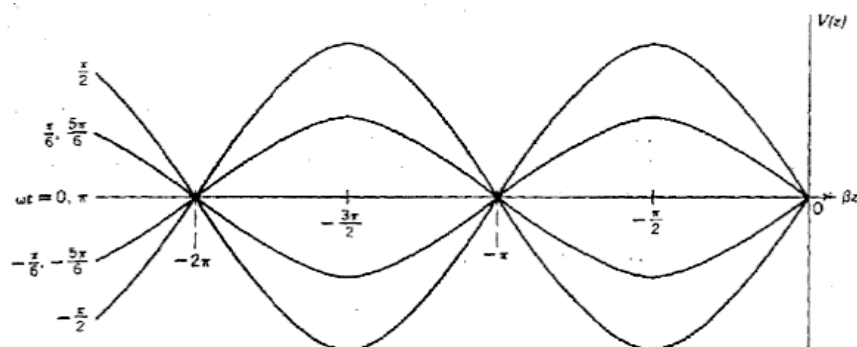

Figure B-26. Standing waves.

The big question is what keeps the containers ringing so long (80 nsec versus 1,000 nsec to -20 dB)? Figure B-27 shows the spectrum over a 10 μsec window. Several closely spaced peaks are apparent, with 138 MHz and 149 MHz the strongest. The closely spaced peaks may be due to the side-wall corrugations providing different spacings, thus producing closely spaced resonances. The effect may be like the sympathetic resonance used in pianos to extend ring using three closely tuned strings per note. If strings are tuned to the same frequency, the ring damps out quickly. Subsequent testing showed the close peak are evenly spaced at 10MHz and were related to the pulse generator 100 ns impulse spacing.
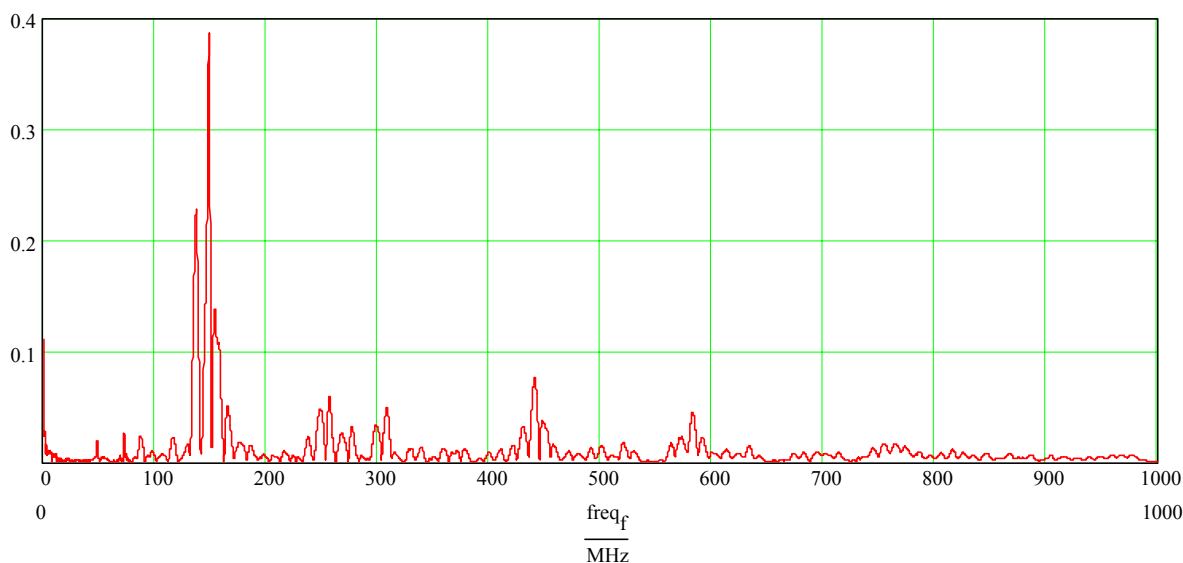

Figure B-27. Spectrum (over 10 μsec), ISO container on top of trailer chassis, transmit antenna at rear and receive antenna mid-container with 12-foot separation.

B-12

Figure B-28 shows the spectrum of the resonances with four different container configurations. The top trace is a container on asphalt, the second is a container stacked on top of another container, the third is a container on a trailer, that the last is the refrigerated container on the ground. Steel containers had the most pronounced resonances. The refrigerated container had the least pronounced resonance, but the longest delay spread. This may have been due to the closely spaced extruded I-beams across the floor acting as a Hemholtz resonator/absorber and/or diffuser. The refrigerated container walls were also aluminum, thus non-magnetic without magnetic hysteresis and losses.
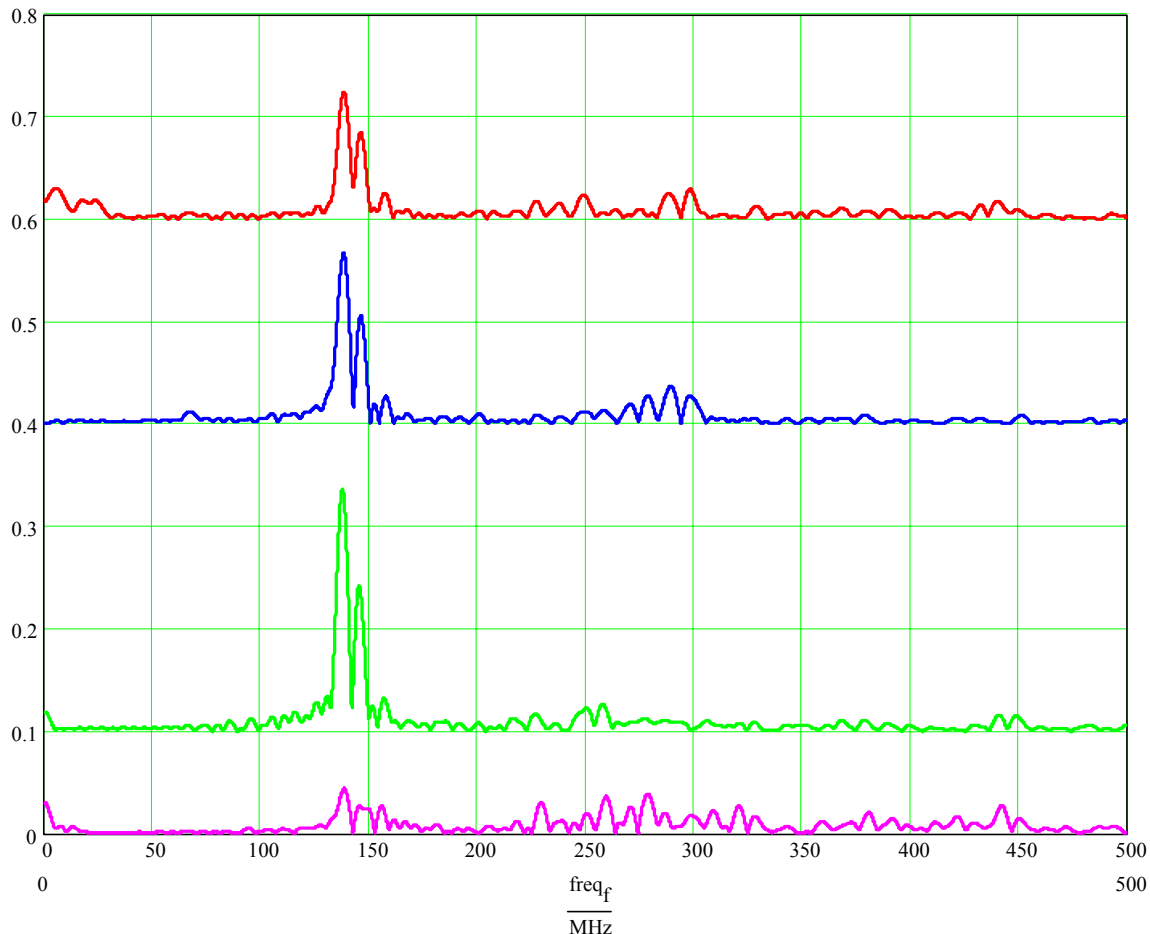

Figure B-28. Spectrum for four container configurations: on asphalt, stacked on top of another container, on chassis trailer, and refrigerated dontainer on asphalt.

Figures B-29 through B-34 show different doublet spacings and resulting radiated spectrums with notches. Frequency spacing between the notches changes with the doublet time spacing, thus the notches can be tuned by changing doublet spacing. The objective is to line up notches with resonance peaks. Tunable localizers will be needed to adjust themselves for empty and stuffed containers as resonance frequencies are expected to change with container dimensions, construction and loaded cargo dielectric properties. Aether Wire included tunable notches in their next generation localizer design for DARPA.

Cancellation of container resonances by doublets needed to be empirically confirmed by testing. NFESC proposed and ONR approved additional work for testing to confirm the cancellation hypothesis. This led to Phase II of the Autonomous Manifesting tests.
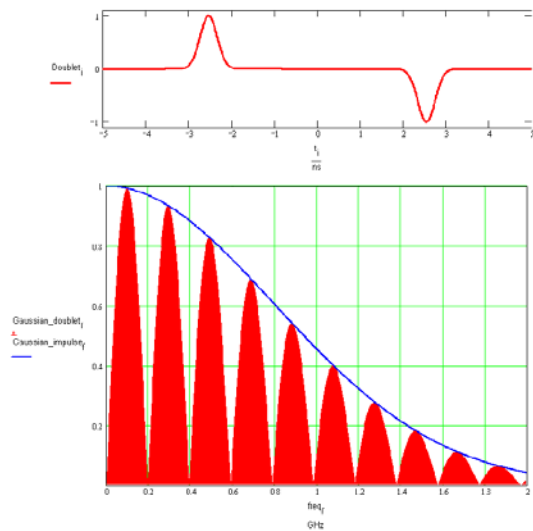
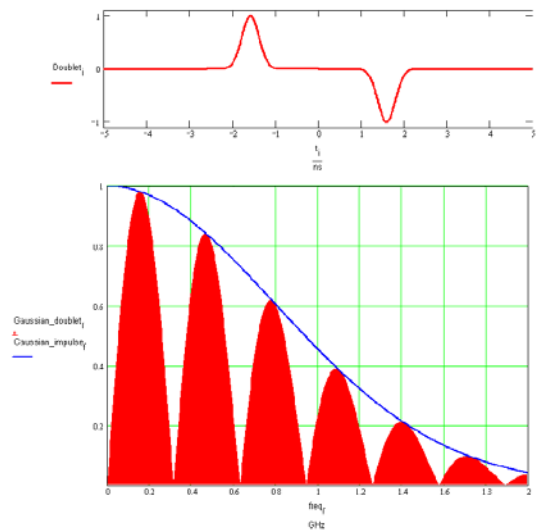Figure B-29. 5.0 nsec doublet spacing.

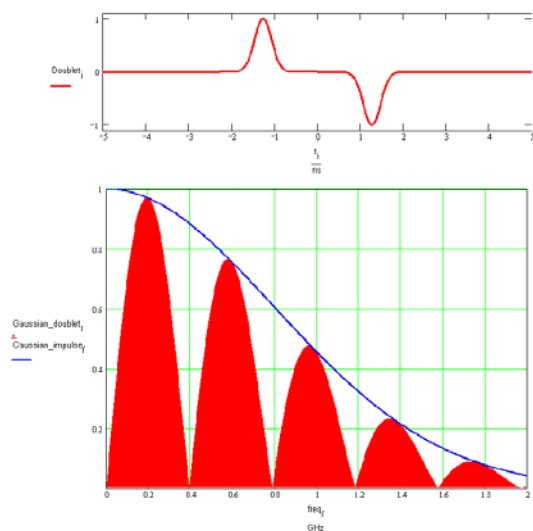

Figure B-30. 3.0 nsec doublet spacing.

Figure B-31. 2.5 nsec doublet spacing.
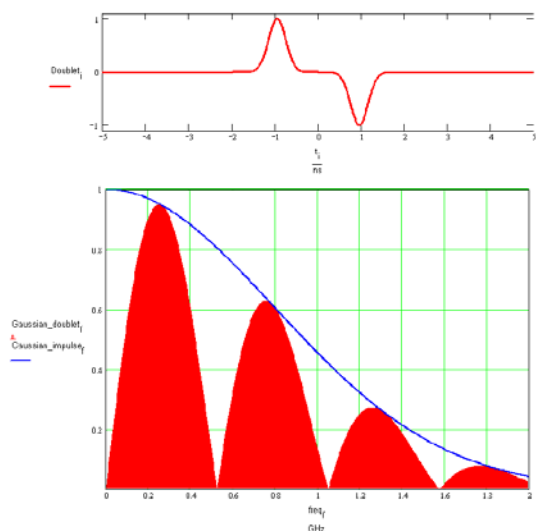

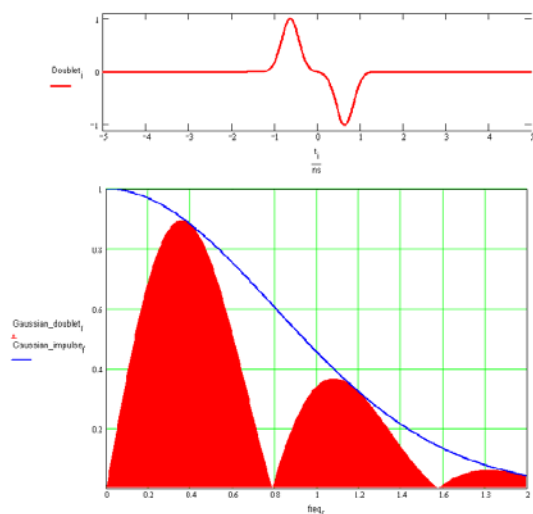Figure B-32. 2.0 nsec doublet spacing.

Figure B-33. 1.2 nsec doublet spacing.
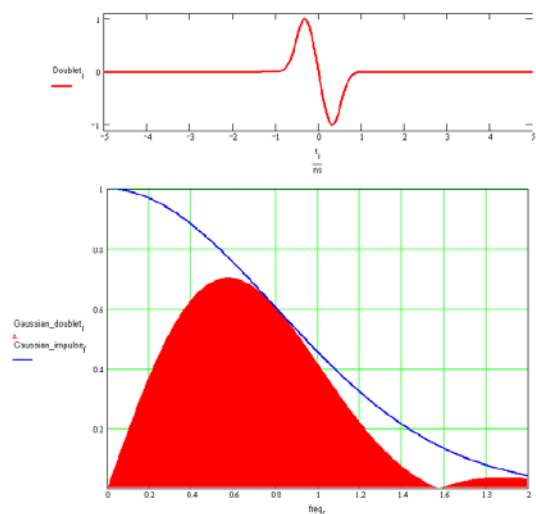

Figure B-34. 0.6 nsec doublet spacing.

B-14

<u>Phase II Empirical Container Testing</u>: NFESC tasked Aether Wire to perform empirical tests to confirm the container resonance hypothesis and the ability of doublets to cancel resonances. Objectives for the testing included:

1. Test and validate the findings resulting from initial data reduction of the Port of Oakland tests and simulation to verify Aether Wire doublets minimize standing waves in ISO containers.

2. Measure and plot standing wave behavior within ISO containers.

3. Perform additional empirical testing in an ISO container to verify Aether Wire localizers ability to localize and communicate within ISO containers.

Aether Wire purchased and installed a 40-foot steel ISO container with a wood floor on site for testing. It was elevated about 6-inches above ground on concrete footings. Figure B-35 shows the installed ISO container.

Figure B-35. Installed ISO container.

Test equipment was the same as the Port of Oakland initial test with pulse generator, two TEM horn antennas, broadband amplifier, digitizing oscilloscope, and fiber optic synchronizing cable. Figure B-36 shows a test setup inside the container.

Two localizers were added: a fourth generation localizer (Gen 4) and a fifth generation localizer (Gen 5) antenna retrofitted on Gen 4, Figures B-36 and B-37. They were used as transmitters to generate actual doublet waveforms to excite the container. The Gen 4 transmitter antenna is the largest, and the Gen 5 transmitter antenna is the smaller square antenna standing vertically off the printed circuit board. Localizer receivers were not complete thus not used. TEM horn receive antenna and oscilloscope were used for these tests.

Figure B-36. Test setup inside ISO container with Gen 4 transmit antenna and TEM receive antenna.
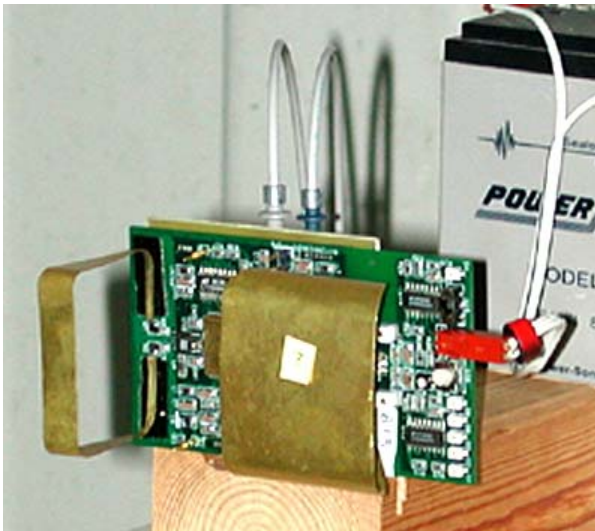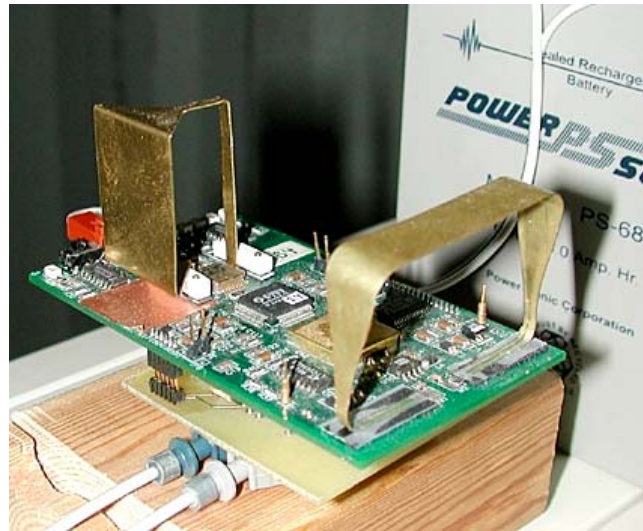

Figure B-37. Gen 4 localizer.

Figure B-38. Gen 5 localizer antenna on Gen 4.

The localizers were operated off battery and fed the fiber optic synchronizing cable through a special interface board. The localizers were configured using a laptop computer, which also displayed received and doublet waveform symbol correlation.

Test Procedure: The primary Port of Oakland test was repeated to confirm prior observations and establish confidence in the test setup. The transmit TEM antenna was set up in the center rear of the container and the receive TEM antenna was set up in the center of the container 12 feet away. Pulse generator output was set at 14.2V peak with 300-psec rise time and 600-psec fall time with 100-nsec separation. The effective rise and fall times were 0.5 nsec and 1.0 nsec.

Figure B-39 shows the raw data and the auto-correlated waveforms. Figure B-40 shows the Fourier transform spectrum of the auto-correlated waveform, or the PSD. Resonances are clearly apparent, with 138 MHz being the dominant resonance as before. Lower resonances at 69 and 87 MHz are also evident. The resonance at 69 MHz is 1/2 the dominant resonance of 138 MHz, thus may be the 2nd harmonic. The amplitude of the 69 MHz peak is reduced by antenna low frequency roll-off and may be equal or greater than the 138 MHz peak. The 87 MHz resonance is approximately 1/3 the 250 MHz peak observed in the earlier Port of Oakland measurements, Figure B-25, and 1/4 of the 350 MHz resonance in Figure B-40. A very low peak at 46 MHz is 1/3 of the 138 MHz peak and may be related.
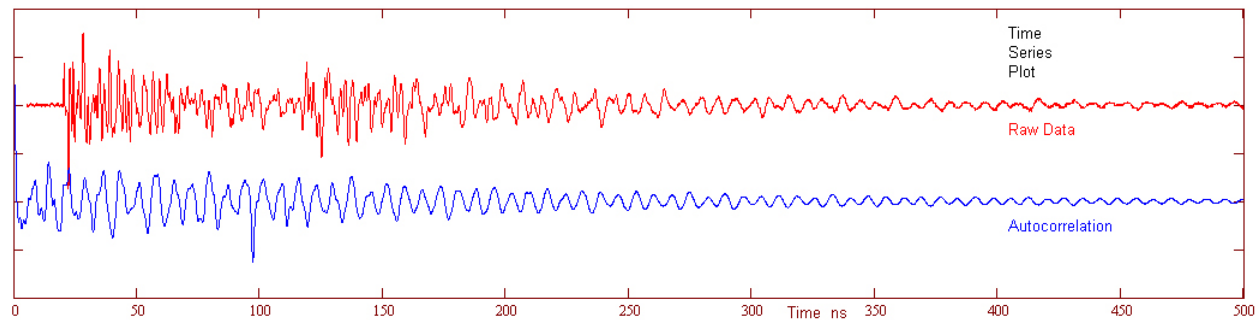

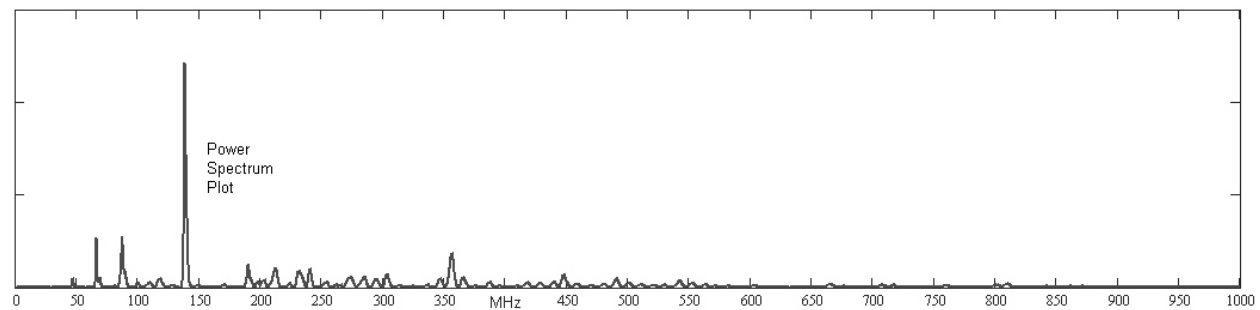Figure B-39. Raw and auto-correlated time waveforms, mid-container.

Figure B-40. Power spectral density, mid-container.

Additional measurements were made at the same distance middle of the container, but with different horizontal and vertical displacements, Figures B-41 to B-43. Resonance frequencies and magnitudes changed with location as would be expected from the standing wave hypothesis. The dominant frequencies are related to horizontal and vertical container dimensions, with 69 MHz and 138 MHz being the strongest.

Assuming 69 MHz is the 1/2 standing wave, and 138 MHz is the full standing wave, the period is 7 nsec, or 7 ft at the speed of light, i.e. close to internal horizontal and vertical dimensions. This period coincides with the fortunate selection of 7 nsec for doublet spacing and canceling resonance.   A 14 nsec doublet spacing would cancel both 69 MHz and 138 MHz.
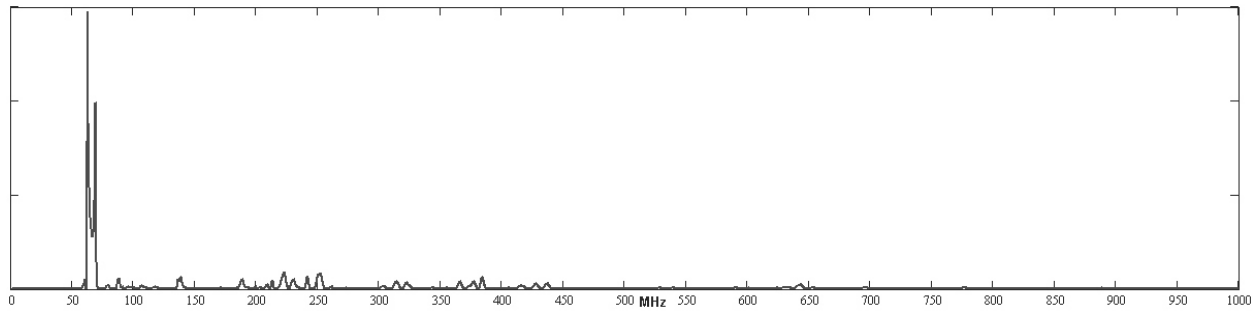
Figure B-41. Power spectral density in container, receive antenna at Z=41" and X=17".
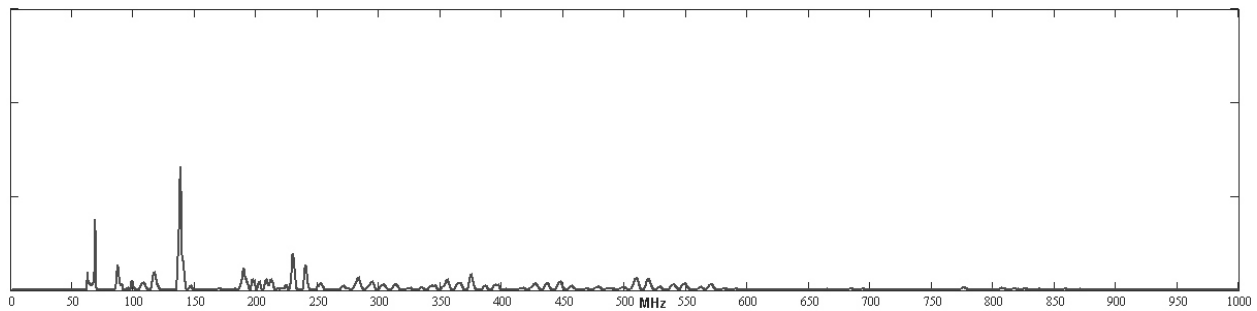

Figure B-42. Power spectral density in container, receive antenna at Z=47" and X=17".
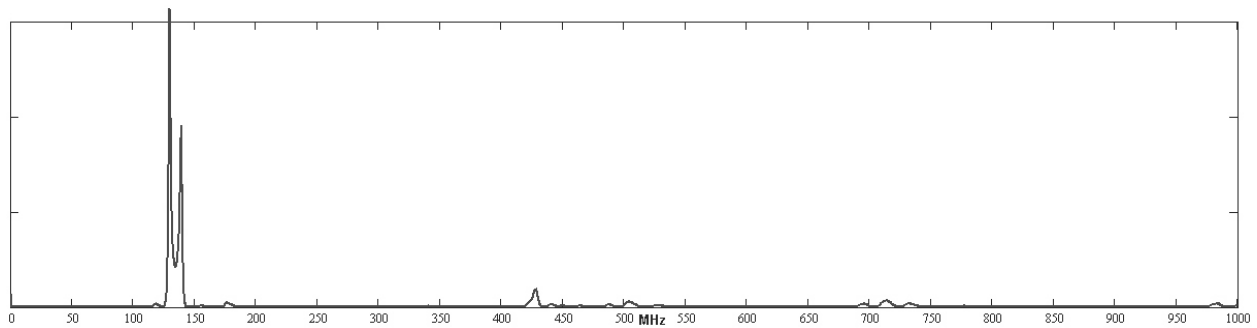

Figure B-43. Power spectral density in container, receive antenna at Z=41"and X=71".
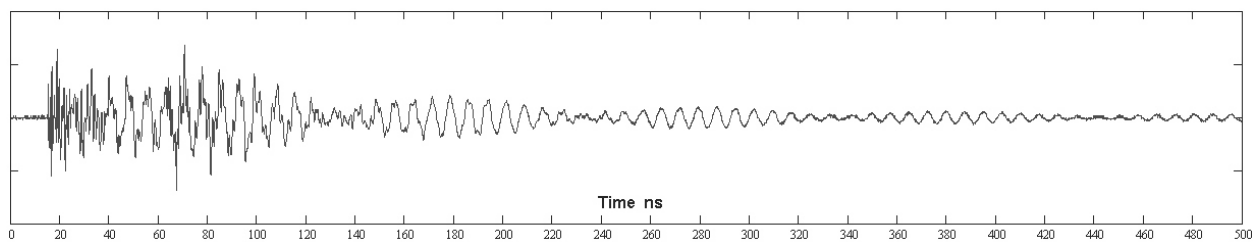
Figure B-44. UWB impulse response of Figure B-43 showing closely spaced beat frequencies.

Closely spaced resonance peaks are apparent in both Figure B-41 and B-43. Figure B-44 shows the impulse time response of Figure B-43. The first 40 nsec has random noise from the impulse. Sinusoidal amplitude variations cause by two closely space beat frequencies are present, confirming earlier observations of closely spaced resonance peaks and the potential of sympathetic resonance extending decay time like a piano or a bell.

Standing Wave Plot: Measurements were then made to plot standing waves across the container. The receive antenna was moved in small increments horizontally across the container at a fixed height of 51-inches. The antenna was moved laterally from wall to wall, 10 to 80-inches. Measurement could not be made at immediately at each wall as the large receive TEM antenna ground plane shorted against the wall. We hoped to use the small Aether Wire large current radiator (LCR) antennas with its receiver to get close to the walls and in corners, but the input amplifiers had stability problems thus could not be used. The receiver stability issues were resolved after testing.

All frequencies from 50 MHz - 1 GHz were simultaneously measured at each location because of impulse excitation and real-time digitizing of the received waveform. Extensive data reduction was performed to generate plots. Figure B-45 shows the PSD from 50-250 MHz for locations from 10 to 80 inches horizontally. Standing waves are clearly evident.
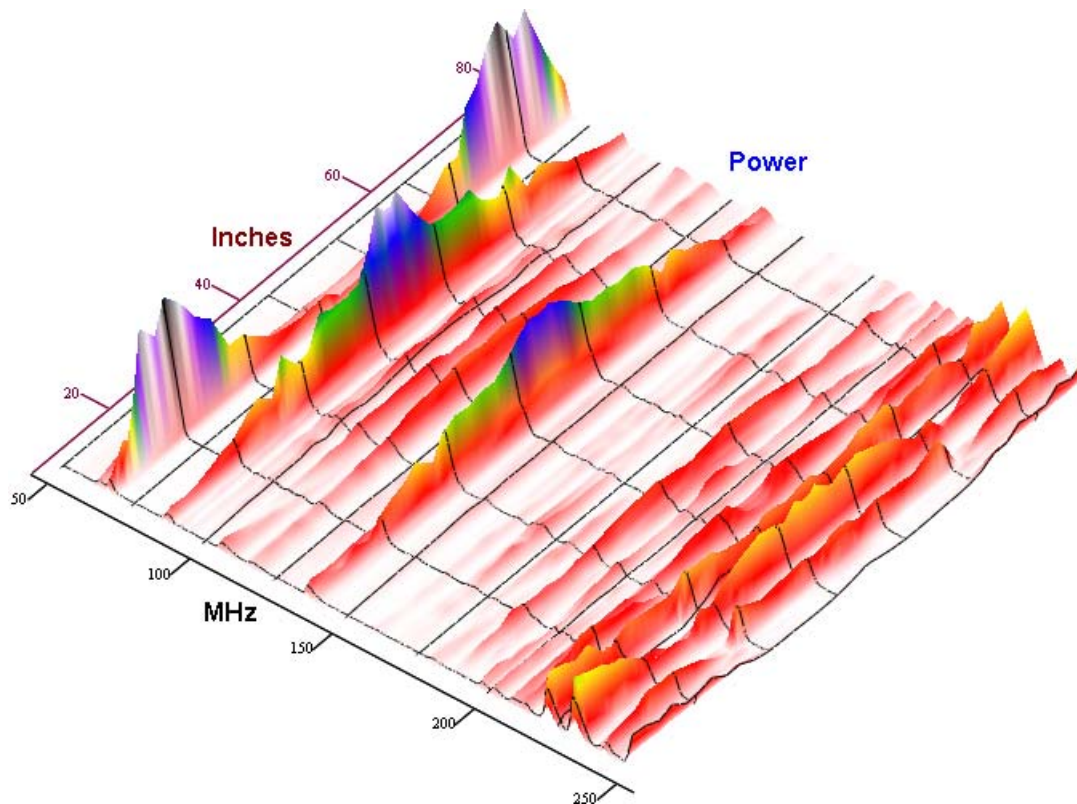

Figure B-45. Power spectral density for container, locations from 10 to 80-inches, 50-250 MHz.

Three large peaks at 68, 87 and 138 MHz have the greatest amplitude. Several smaller peaks occur between 170 and 250 MHz, with standing wave behavior clearest at 230 MHz. The ends of these standing waves may be minima at the wall, but cannot be observed due to the receive antenna not able to approach closer than 10-inches to the walls.

The pattern of the peaks is not quite what was expected. 69 MHz, the lowest resonance frequency has 2 peaks and 138 MHz has 1 peak, quite opposite of what was expected. Some of the standing waves may be vertical, or standing waves set up between horizontal and vertical sides, thus not fully measured by horizontal measurements alone. This plot indicates a very complex RF environment.

Fine structure with nulls every 10 MHz is evident in this plot and previous plots, and is directly related to the 100 nsec spacing between impulses. This was confirmed by changing pulse spacing.

Test Environment Sensitivity: Additional testing was performed to characterize the effect of operator position and door position. Figures B-46 and B-47 show the effect of operator position and door position. The PSDs did not change significantly with operator position. Most surprisingly, PSD did not change much with door position, indicating resonances are not related to the long dimension of the container, but rather the short dimensions.
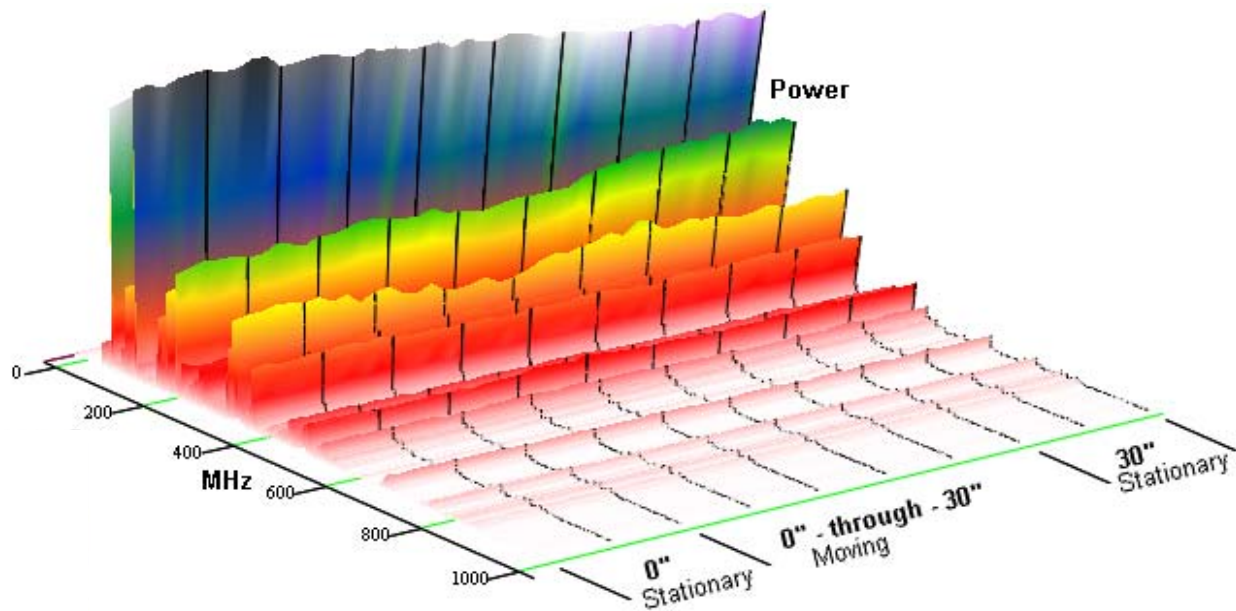

Figure B-46. Power spectral density versus operator position.
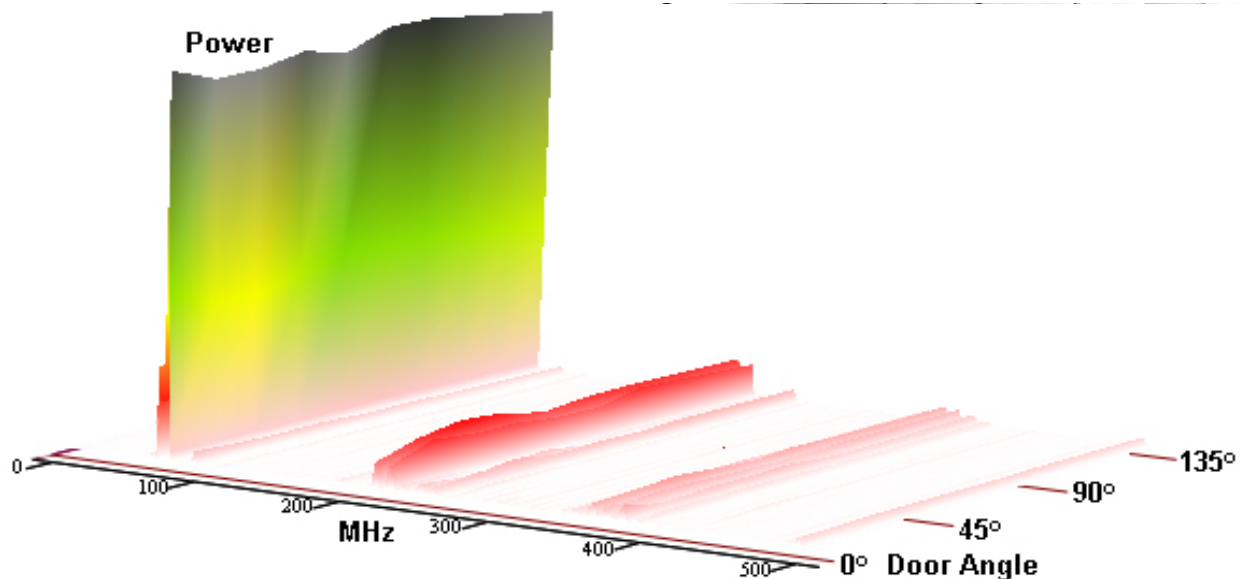
Figure B-47. Power spectral density versus door position.

Optimum Doublet Spacing: Measurements were then performed to identify the optimum doublet spacing to minimize resonances. Doublet spacing was varied from 0.6 nsec to 100 nsec. Figure B-48 shows the PSDs for various doublet spacings. The vertical tick marks on each plot indicate the computed cancellation frequencies. The strongest peak at 138 MHz was cancelled by 7.4 nsec and 14.3 nsec doublet separation, with 14.3 nsec providing the lowest overall peaks.
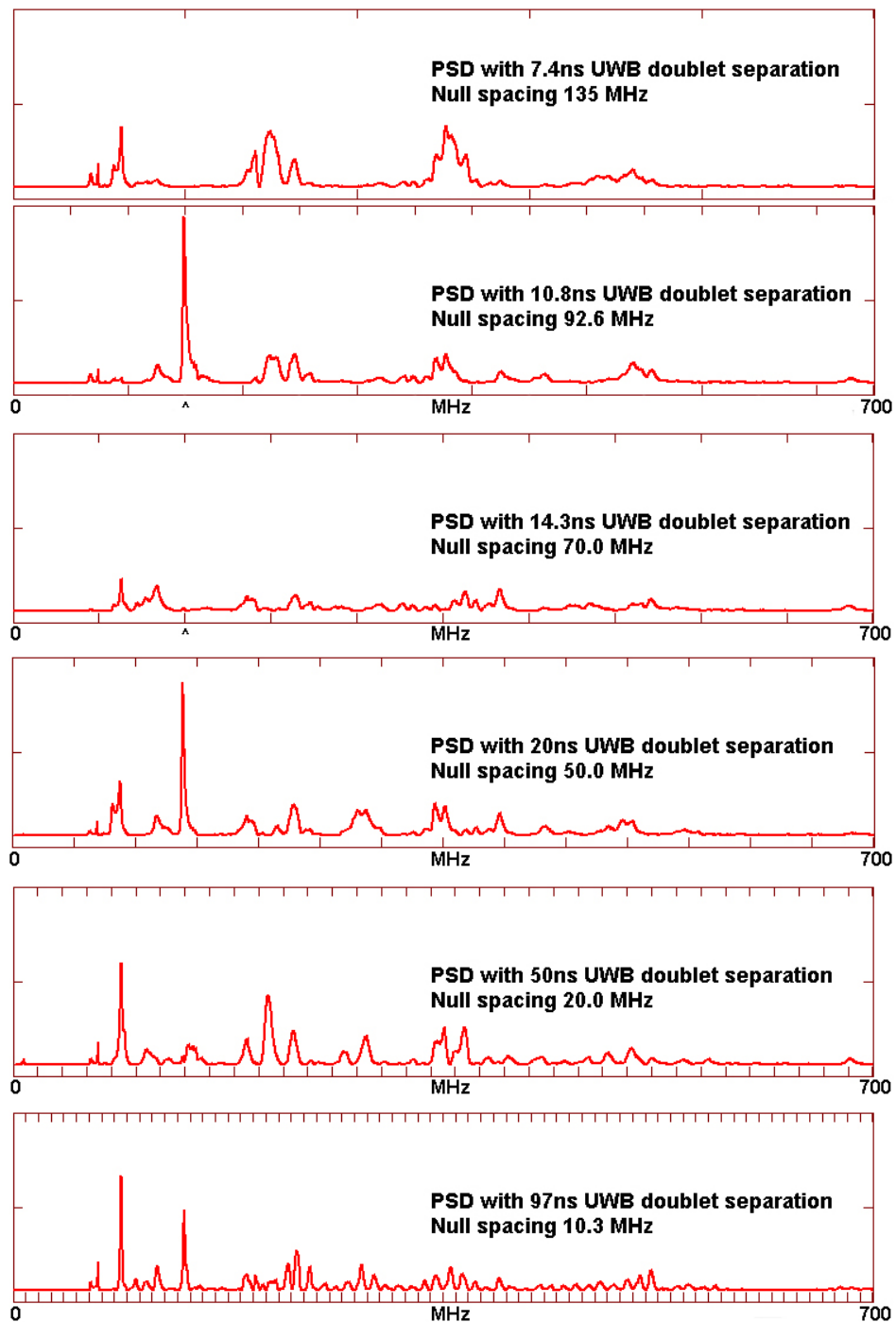
Figure B-48. Power spectral density with various doublet spacings.

Figure B-49 shows the maximum power for each frequency with doublets adjusted from 1 to 66 nsec. The maximum power at peak frequencies with doublet separations from 0-30 nsec is shown in Figure B-50. The Root Mean Square (RMS) sum of the PSDs of frequencies for 0 to 1 GHz is shown in Figure B-51. The minimum total power occurs at 14 nsec. 14 nsec may be the optimum doublet spacing for ISO containers.

Figure B-49. Power spectral density maximum per frequency.

Figure B-50. Power at peak frequencies versus doublet separation.

Figure B-51. Root mean square sum of PSD from 0 – 1 GHZ versus doublet separation.

Gen 4 and Gen 5 Tests: A Gen 4 localizer was then placed in the container and adjusted to transmit 1023-bit Kasami Direct Sequence Spread Spectrum (DSS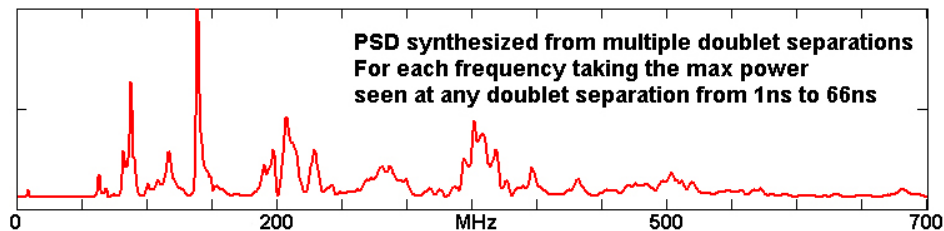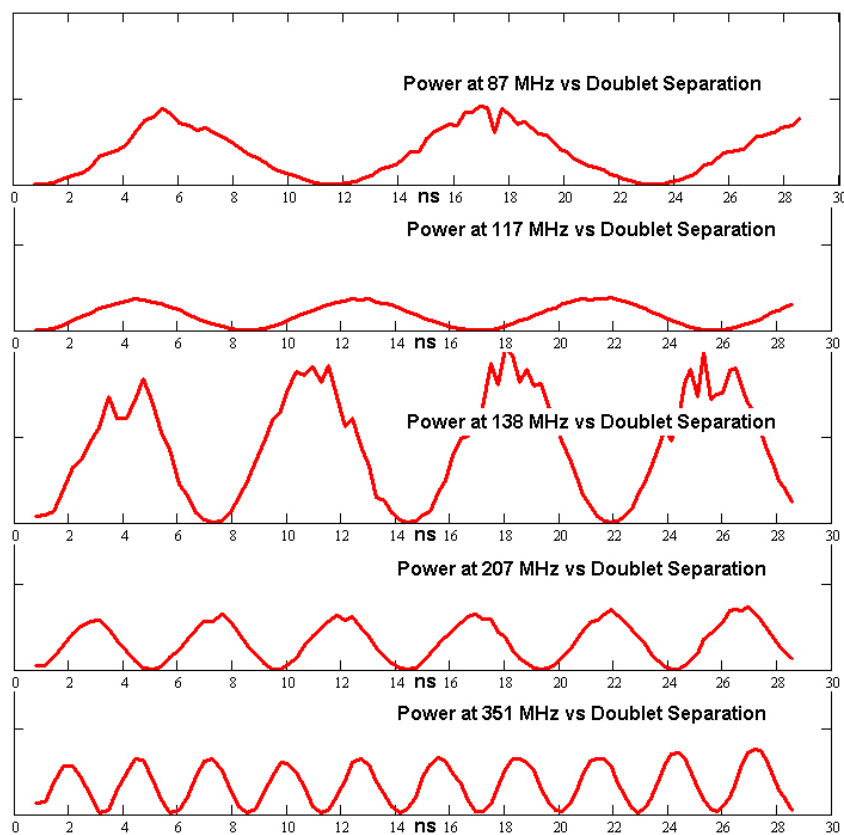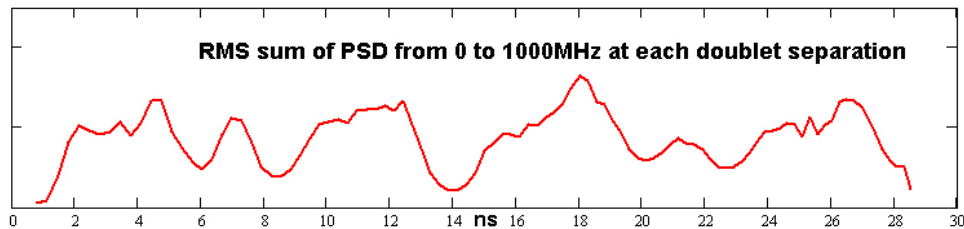S) sequences with 7.25 nsec doublet separation. Figure B-52 shows the PSD of the Gen 4 localizer. As predicted, the peak at 138 MHz is absent. 14.3 nsec doublet separation would additionally cancel the peaks at 207 MHz and 351 MHz. The Gen 4 localizer, however, could not be adjusted to 14 nsec. The hypothesis of doublets canceling container resonances is confirmed.
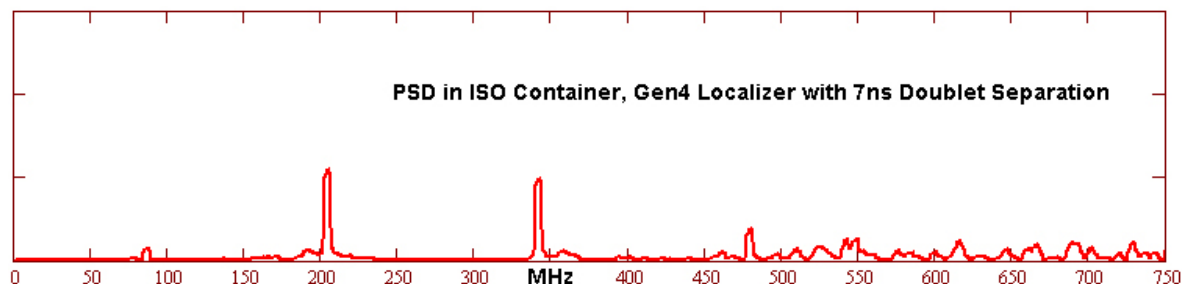
Figure B-52. Power spectral density of Gen 4 localizer with 7 nsec doublet separation in container.

The Gen 5 localizer was not completed in time for testing. A Gen 5 antenna was placed on a Gen 4 localizer to compare responses, Figure B-38. Testing was conducted outdoors comparing both antennas, Figure B-53. Figure B-54 shows the time-amplitude response of the antennas in free space. The Gen 5 antenna shows much less ringing than the Gen 4 antenna.

Figure B-53. Outdoor Gen 4 and Gen 5 antenna testing.
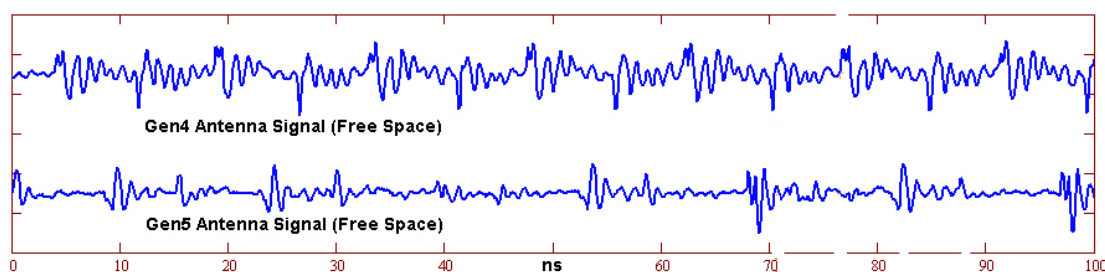
Figure B-54. Time-amplitude response of Gen 4 and Gen 5 antennas, free space.

Figure B-55 shows the free space PSDs with the Gen 4 and Gen 5 antennas on a Gen 4 localizer. The Gen 5 antenna has much fewer spectral peaks to excite container resonances. Figure B-56 shows the comparison of the PSDs for the Gen 4 and Gen 5 antennas in the ISO container. The peaks are much lower for the Gen 5 antenna versus the Gen 4 antenna.

Figure B-55. PSDs of Gen 4 and Gen 5 antennas, free space.

Figure B-56. Power spectral density inside ISO container, Gen 4 and Gen 5 antennas.

Conclusion: The hypothesis of Aether Wire doublets canceling container resonances was confirmed by empirical measurement using a pulse generator and with Aether 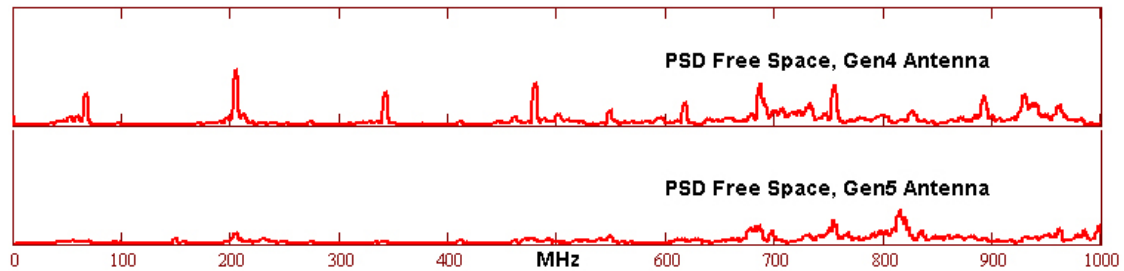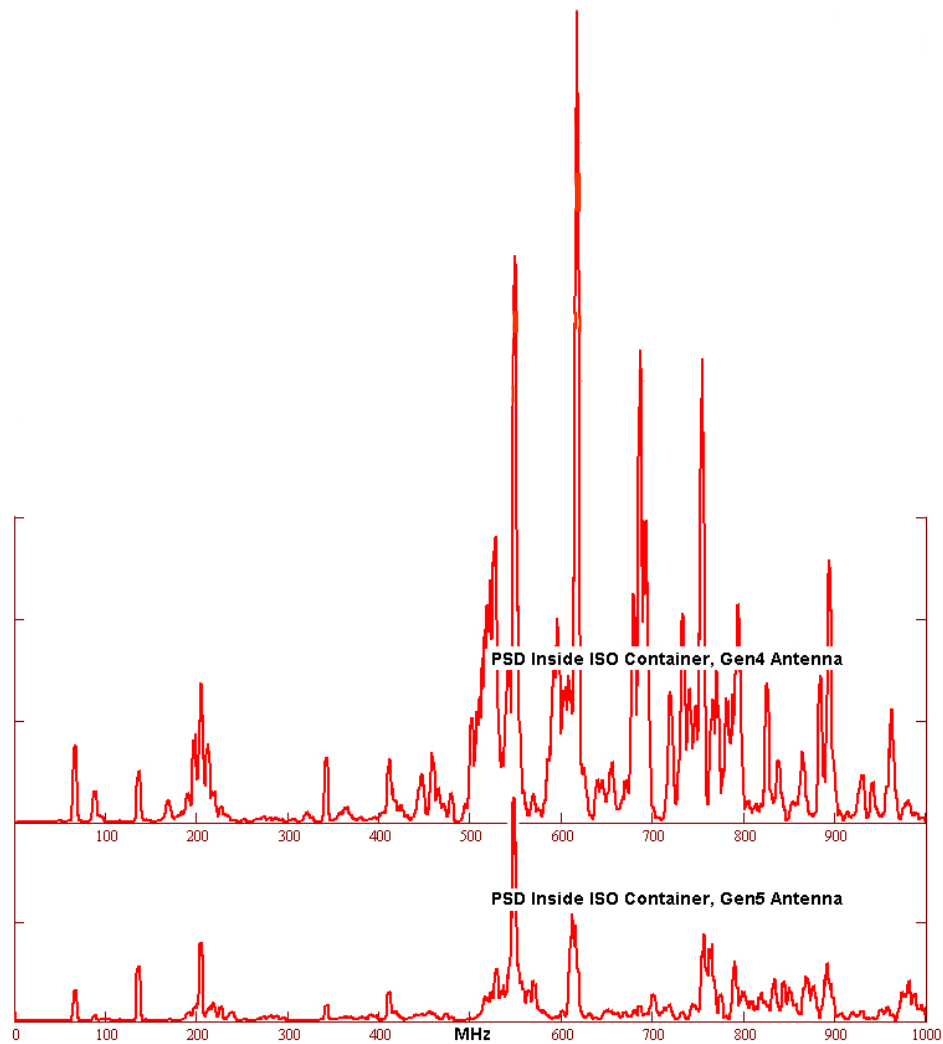Wire Gen 4 localizers. Standing wave phenomenon in the ISO container was plotted on one axis and the standing wave hypothesis was confirmed. Standing wave behavior is more complex than was originally assumed with vertical, horizontal, and compound modes. The long dimension had little effect on resonance.

An optimum doublet spacing of 14 nsec was identified by both empirical measurement and post processing of the test data. 14 nsec cancels both the strong 69 MHz and 138 MHz resonances, with attenuation of the 207 MHz and 350 MHz peaks. The disadvantage of the 14 nsec doublet spacing compare to 7 nsec is the requirement for greater transmitter current, thus power. This can be offset by larger antennas with greater inductance.

Gen 5 localizer development had not progressed far enough to perform testing to verify Aether Wire localizer's ability to localize and communicate within ISO containers. After these tests, Aether Wire continued development and resolved engineering issues with the Gen 5 receivers and further refined antenna design to minimize ringing. Gen 5 localizers now are able to localize in free space up to 30 feet.

Localizer testing in ISO containers continued under private industry funding and Gen 5 localizers were tested again inside the container November 2002. The localizers communicated up to 3 feet inside the container, or within near field. More work still needs to be done to increase range in a container. Aether Wire proposed additional development to progress to single chip design, with improved driver chip. The objective is a coin-sized localizer, suitable for asset tagging and autonomous manifesting.

High precision localizers with resolution and accuracy on the order of a few inches may be a viable approach to achieve autonomous manifesting. The missing ingredient for these systems has been localization.

Infrastructure Reduction: Aether Wire later demonstrated the ability to self network several localizers. Self-networking leads to the potential of localizers being exclusively used within ship holds, and on cargo, to form an ad-hoc networked RTLS. No pre-installed dedicated readers would be needed, saving cost. Localizers would be temporarily placed on bulkheads, forming reference points for tagged cargo. Localizers placed on cargo would be read during stow, and conversely would read adjacent localizers, bypassing blockage. Large numbers of readers would not be needed for tightly stowed spaces as localizer tags would contribute to the network. Localizers would be used inside and outside containers, performing Autonomous Manifesting and RTLS. One architecture is possible, with potential great cost reduction.

This Appendix summarizes two Aether Wire & Location reports: Fleming, R.A., and Cushner, C.E., "Technological Solutions to Autonomous Cargo Manifesting," Program Progress Report No. 1, 6 February 2001, Aether wire and Location, Nicasio, California [14], and Fleming, R.A., Cushner, C.E., Killian, J., "Technological Solutions to Autonomous Cargo Manifesting – Additional Requirement," 22 October 2001, Nicasio, California [16].

Most of the figures in this Appendix were provided by Aether Wire & Location and used with their permission. Additional material and figures were provided by NFESC from briefings: Gunderson, S.J, "Naval Total Asset Visibility: Application of Ultra Wide Band Location Systems for Precision Asset Location and Autonomous Manifesting," ONR Workshop on Ultrawideband Communications, Berkeley Wireless Research Center, Berkeley, California, 17 May 2000 [7].

This page left blank.

Appendix C

Participating Organizations and Personnel

Table C-1. Participating Organizations and Personnel

Organization	Personnel	Title / Role	Test
ArcSecond, Inc. 44880 Falcon Place #100 Dulles, VA 20166 (703) 435-5400	Mr. Edmund Pendelton	Executive Vice President	
	Mr. Sean Beliveau	Construction Applications Manager	●
	Mr. Jeff Skolnick	Director of Application Software	
	Mr. Dan Robbins	Application Software Development	
Environmental Systems Research Institute, Inc. 380 New York Street Redlands, CA 92373-8100 (909) 793-2853	Mr. Mike Quin	Federal Marketing Representative	
	Ms. Diane Shimota	Manager, Implementation Services	
	Ms. Nicky Daaman	Technical Designer	●
	Mr. Chagan Shi	Technical Designer	
Lewis & Lewis Enterprises 1600 Callens Road Ventura, CA 93003 (805) 644-7405	Mr. Tom Lewis	President	
	Mr. Perry Albertson	GPS Operations Manager	●
Maritime Administration (MARAD) **SS Curtiss** 201 Mission St., Suite 2200 San Francisco, CA 94105 (415) 744-3125	Capt. Frank Johnston	MARAD Western Regional Director	
	Mr. Mike Williams	MARAD Representative	●
	Mr. Peter Clark	SS Curtiss, Chief Mate	●
	Mr. Chuck Bowen	SS Curtiss, D/E Maintenance	●
	Mr. Thomas Griffith	SS Curtiss, Chief Engineer	●
	Mr. David Burton	SS Curtiss, 1st A/E	●
	Mr. Rick Cavender	SS Curtiss, 2nd A/E	●
	Mr. Del Mar Tomlin	SS Curtiss, 3rd A/E	●
	Mr. Bob Rush	SS Curtiss, QMELECT	●
	Mr. Ron Drew	SS Curtiss, STWD/CK	●
	Mr. Ken Herzstein	SS Curtiss, GU/DES	●
Multispectral Solutions, Inc. 20300 Century Blvd No. 175 Germantown, MD 20874 (301) 442-8305	Dr. Robert Fontana	President	
	Mr. Rob Mulloy	Vice President	●
	Mr. Jay Knight	Manager, Business Development	
	Mr. Don Perino	Engineer	●
	Mr. Edward Richley	Engineer	●
Naval Facilities Engineering Service Center 1100 23rd Ave Port Hueneme, CA 93043 (805) 982-1262	Mr. Steven Gunderson	Principal Investigator	●
	Ms. Mary Canfield	Instrumentation & Data Redux Lead	●
	Mr. Geoff Dann	Electronic Systems Lead	●
	Mr. Jon Reed	Test Sled	●
	Mr. Ted Gallo	Test Sled	●
	Ms. Karol Scott	Data Reduction & GIS	●
	Mr. Ramon Flores	Project Lead & Test Plan	●
	Mr. Dan McCambridge	Ship Coordination, Seabasing Test	●
	Mr. Sam Oppedisano	Heavy Equipment Coordination	●
	Ms. Jessica Hiraoka	2nd Week Test Design & Execution	●
	Ms. Gladis Aispuro	2nd Week Test Support	●
	Mr. Paul Del Signore	Photographer	●

Table C-1. Participating Organizations and Personnel (continued)

Organization	Personnel	Title / Role	Test
University of Southern California Communication Sciences Institute Dept. of Electrical Engineering - Systems 3740 McClintock Ave., EEB-500 Los Angeles, CA 90089-2565	Dr. Robert Scholtz	Professor & Chair EE Dept	•
	Dr. Keith Chugg	Professor	•
	Mr. Joon-Yong Lee	USC Ship Test Director	•
	Mr. Robert Weaver	Laboratory Director	•
	Mr. Carlos Corrada	Student	•
	Mr. Eric Homier	Student	•
	Mr. Robert Wilson	Student	•
WhereNet, Inc. 2858 De La Cruz Blvd. Santa Clara, CA 95050 (408) 845-8500	Mr. David Wisherd	CEO	
	Mr. George Reis	VP Engineering	
	Mr. David Stryker	VP Software	
	Dr. Robert Boyd	Chief Scientist	•
	Ms. Henrietta Whitty	Project Manager	•
	Mr. Mark Monroe	Field Engineer	•
	Mr. Alex Hamed	Software Engineer	

Table C-2. Participating Organizations and Personnel, Autonomous Manifesting

Organization	Personnel	Title / Role	Test
Aether Wire & Location, Inc. 5950 Lucas Valley Road Nicasio, CA 94946 (415) 662-2055	Dr. Robert Fleming	President / Principal Investigator	1&2
	Ms. Cherie Kushner	Vice Pres / Principal Investigator	1&2
	Mr. Steven Crandall	Hardware Engineer	1&2
	Mr. Joseph Killian	Researcher, Phase 2	2
	Mr. Vincent Coli	Vice President, Marketing	2
	Mr. Gary Roberts	Software Engineer	2
	Mr. Dan Van Winkle	Senior RF Engineer	2
Berkeley Wireless Research Center 2108 Allston Way, Suite 200 Berkeley, CA 94704-1302 (510) 666-3102	Dr. Bob Brodersen	Scientific Co-Director Professor, EECS Dept.	1
	Mr. Ian O'Donnell	Graduate Student	1
Port of Oakland 530 Water Street Oakland, CA 94607 (510) 627-1301	Mr. Ray Boyle	Director of Maritime	1
	Mr. David Adams	Chief Warfinger	1
	Mr. Christopher Peterson	Warfinger	1
Hawk Pacific Corporation 3470 Mt. Diablo Blvd. Ste A-100 Layfayette, CA 94549	Mr. James Frazier	Director	1
	Mr. Jeff Sibley	Operations Manager	1
	Mr. Eric de la Cruz	Fork Lift Operator	1
	Mr. Candy Torres	Fork Lift Operator	1

Note: Test 1, Port of Oakland
          Test 2, Container Resonance